Gating in Neuronal Networks

Mircea Steriade and
Denis Paré

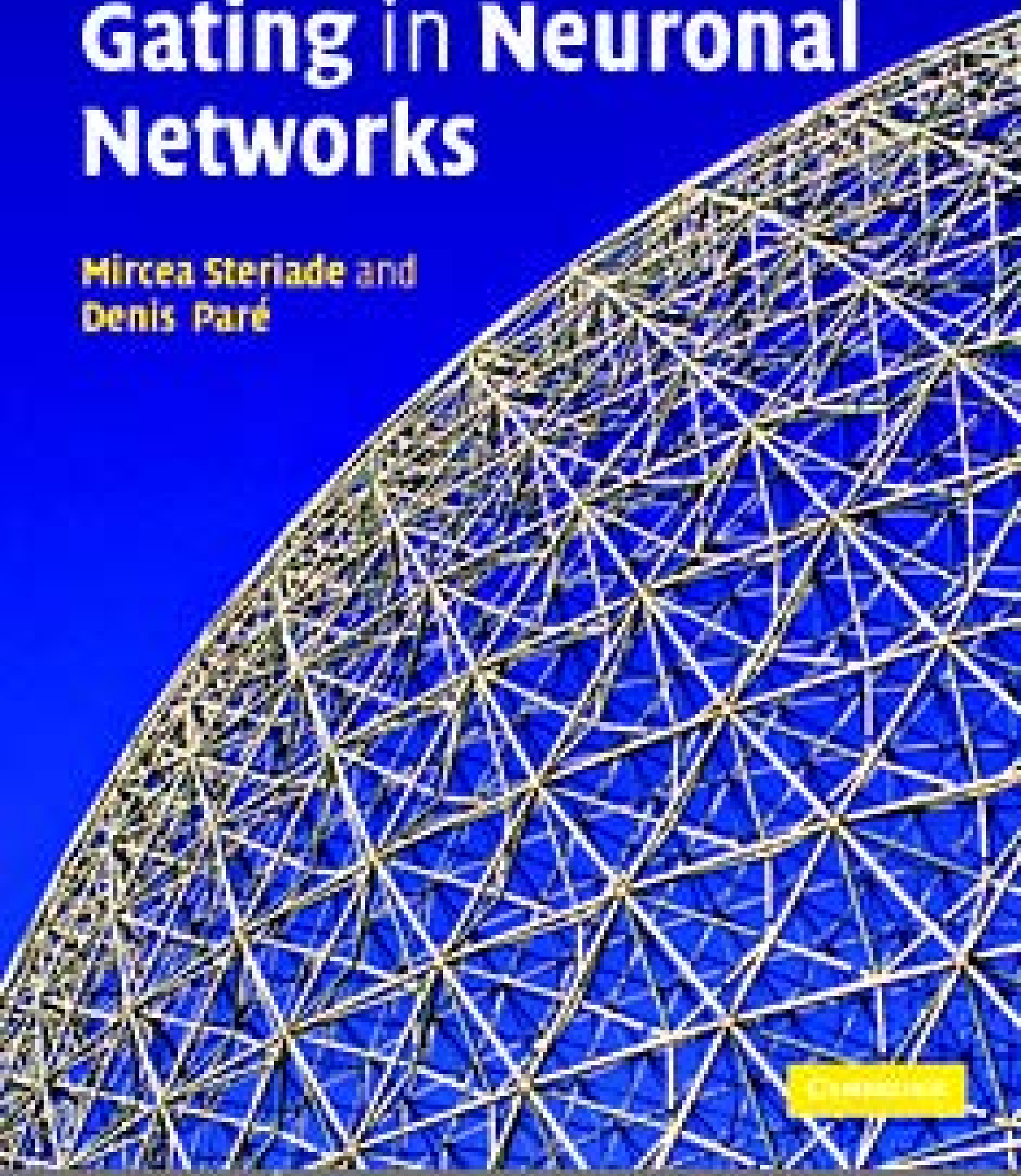

CAMBRIDGE www.cambridge.org/9780521851220

This page intentionally left blank

Gating in Cerebral Networks

The correct functioning of the mammalian brain depends on the integrated activity of myriad neuronal and non-neuronal cells. Throughout, neuronal networks are under the control of neuromodulatory systems. One goal of current neuroscientific research is to elucidate how these systems operate, especially during normal conscious behaviours and processes. Mircea Steriade and Denis Paré describe the neuronal properties and networks that exist within and between the cortex and two important subcortical structures: the thalamus and the amygdala. The authors explore the changes in these properties, covering topics including morphology, electrophysiology, architecture and gating, and comparing regions and systems in both normal and diseased states. This book is aimed at graduates and postdoctoral researchers in neuroscience.

Mircea Steriade held the position of Professor and Head of the Laboratory of Neurophysiology at Laval University, Quebec, from 1968 to 2006.

Denis Paré holds the position of Professor at the Center for Molecular and Behavioral Neuroscience at Rutgers University, New Jersey.

Gating in Cerebral Networks

Mircea Steriade
Denis Paré

CAMBRIDGE
UNIVERSITY PRESS

CAMBRIDGE UNIVERSITY PRESS
Cambridge, New York, Melbourne, Madrid, Cape Town, Singapore, São Paulo

Cambridge University Press
The Edinburgh Building, Cambridge CB2 8RU, UK
Published in the United States of America by Cambridge University Press, New York
www.cambridge.org
Information on this title: www.cambridge.org/9780521851220

First published in print format 2007

ISBN-13 978-0-511-34127-4 eBook (EBL)
ISBN-10 0-511-34127-X eBook (EBL)

ISBN-13 978-0-521-85122-0 hardback
ISBN-10 0-521-85122-X hardback

MS dedicates this book to Donca, Claude and Jacqueline.
DP dedicates this book to Noemi, Julian and Martha.

Sadly, when this book was in the final stages of production, Dr. Mircea Steriade passed away at the age of 81, after a long fight with cancer. Dr. Steriade began writing this book while undergoing chemotherapy, knowing that his was a terminal condition. Mircea Steriade was an extremely energetic man, passionate, uncompromising, forever driven by scientific discovery. He published more than 400 scientific papers during his career and was respected by supporters and competitors alike. I refer the reader to earlier obituaries [1,2] for biographical information.

I met Mircea Steriade in 1985 when I started as a PhD student in his laboratory. To a young graduate student, he was a formidable man who commanded respect. He had an unrivaled knowledge of the scientific literature and knew by heart the references of many classical papers. His culture was not limited to science however as he was an accomplished pianist, a student of history, and an avid reader of French literature. After my post-doctoral training in 1992, I returned to Steriade's Department at University Laval (Quebec City, Canada) as an Assistant Professor. We had adjacent offices and had lunch together every day. Thus, we grew very close and stayed in touch after I left Laval for Rutgers University in 2001. I am deeply indebted to him for he patiently taught me everything he knew about the science trade. More than a mentor however, he was a friend whose support and advice had a decisive influence in my life. Even after 50 years of research in neuroscience, he was still consumed by his work. He would often call me to share his excitement about the latest finding to come out of his laboratory. This is the image of Mircea I cherish most: passionate, enthusiastic, inquisitive, and forever young.

In correcting the proofs of this book, I was reminded of all the knowledge lost with the passing of Mircea Steriade. In writing this, I am reminded of the mentor who taught me so much and of the friend I miss.

Denis Paré

[1] Buzsáki, G., Paré, D. (2006) Mircea Steriade (1924–2006). *Nature Neuroscience* **9**: 713.

[2] Timofeev, I. (2006) Mircea Steriade (1924–2006). *Neuroscience* **142**: 917–920.

Contents

Preface

In neuroscience, the term gating can assume various meanings depending on the level of analysis. At the level of ionic channels, gating refers to the transition between two or more conformational states of channel proteins. At the neuronal or networks level, gating refers to changes in responsiveness and in inhibitory processes during different behavioral states. In both instances, the causative events and their functional consequences can vary widely. This book focuses on gating in the thalamocortical and amygdalocortical systems.

In the *thalamocortical system*, gating was often used to describe the blockade of signal transmission from the external world to the cerebral cortex during disconnected states, such as slow-wave sleep. In this monograph, we also discuss evidence that, despite absence of information from the external world, the behavioural state of slow-wave sleep is associated with the processing of internally generated signals and with synaptic plasticity. We also argue that these events may lead to the consolidation of memory traces acquired during the waking state as well as to a form of consciousness expressed by dreaming mentation. The opening of thalamic gates during brain-active states of waking and REM sleep changes the excitability of cortical neurons and leads to different forms of mentation.

In the *amygdalocortical system*, gating refers to how the transmission of sensory inputs is modulated according to their emotional significance. This process leads to alterations not only in behavioural responsiveness, but also in memory consolidation. In this system, gating can also be used to describe the facilitating effect of emotions on memory. We will therefore present evidence that, via the amygdala, emotional arousal can facilitate memory.

Besides these topics, this book compares the anatomical and physiological organization of two different brain networks: the thalamocortical and amygdalocortical systems. Whereas the thalamocortical system is the gateway for sensory inputs into consciousness, the amygdalocortical system receives highly processed sensory information from the neocortex and uses it to generate affects and modulate memory. Although both systems display unique properties, they are also similar in many ways. In particular, both systems illustrate how neuronal computations arise from complex interactions between the intrinsic properties of constitutive elements and the architecture of the network in which they are inserted. We will show how intrinsic neuronal properties are modulated, and sometimes overwhelmed, by background synaptic activities, which would explain some dissimilarities between data obtained in the intact brain and in some simplified preparations.

Acknowledgements

MS thanks the skilful and creative collaboration of his Ph.D. students and postdoctoral fellows during the past 37 years, since he established the Laboratory of Neurophysiology at Laval University. In particular, he is grateful to the work, during the past two decades, of D. Paré, R. Curró Dossi, D. Contreras, A. Nuñez, F. Amzica, I. Timofeev, D. Neckelmann, F. Grenier, P. Fuentealba, S. Crochet, Y. Cissé and D. Nita. P. Giguère was in charge of the technical development of laboratories. MS also thanks T. J. Sejnowski, M. Bazhenov, A. Destexhe and W. Lytton for their collaboration in combined experimental and computational studies. During all his work in Canada, MS's work was supported by grants from the Medical Research Council of Canada (now Canadian Institutes for Health Research), National Science and Engineering Research Council of Canada, Human Frontier Science Program, and National Institutes of Health of the USA.

DP acknowledges the essential contribution of his graduate and postdoctoral students. In particular, he wishes to underscore the creative involvement of J. Apergis-Schoute, E. Bauer, D. Collins, S. Duvarci, E. Lang, K. Likhtik, M. Martina, R. Paz, J.G. Pelletier, A. Pinto, A. Popescu, S. Royer and R. Samson. He also acknowledges the support of other friends, scientists or otherwise, who helped him during his career. They include S. Charpak, M. De Curtis, P. Giguère, J.F. Paré, G.J. Quirk, Y. Smith and J. Tepper. While in Canada, DP's research was supported by the Medical Research Council and the Natural Sciences and Engineering Research Council. Since in the US, his work is supported by the National Institutes of Health and the National Science Foundation.

Chapter 1

Morphology and electroresponsive properties of thalamic neurons

To discuss gating processes in the thalamus during different normal and pathological conditions (see Chapters 6 and 7), we should first describe the types of neurons and neuronal networks as well as the modulation of intrinsic properties of thalamic neurons by synaptic activities in various behavioural states.

[1] Jones (1997) described different subdivisions of the human thalamus and compared them to nuclear systematizations in earlier morphological studies.

1.1 Nuclear systematization, morphology and immunoreactivity of thalamic cells

Thalamic nuclei can be systematized into sensorimotor (or relay), association, intralaminar, and reticular neuronal aggregates. The term relay indicates that those nuclei, among them visual lateral geniculate (LG), auditory medial geniculate (MG), and somatosensory ventroposterior (VP), transfer to cerebral cortex specific sensory signals arising in the ascending afferent pathway. This does not imply that such nuclei operate as mere relays, as if nothing would change between activities in afferent fibres and in thalamocortical axons. Indeed, the presence of local-circuit inhibitory neurons in various nuclei and the relations that thalamic relay neurons entertain with thalamic reticular (RE) inhibitory neurons, account for integrative processes in thalamic relay nuclei, mainly consisting of response selectivity higher than that recorded at prethalamic levels.

Before discussing the morphology, connections and properties of different neuronal classes in the thalamus, a brief account of the major thalamic nuclei is necessary. Figure 1.1 illustrates the nuclear groups in the cat, a species of choice for the study of many topics discussed in this monograph. The neuronal aggregates include some sensory (LG, VP), motor (ventroanterior, VA; ventrolateral, VL; ventromedial, VM), association (lateral posterior, LP; pulvinar, PUL; mediodorsal, MD), rostral intralaminar (centrolateral, CL; centralis medialis, CeM), and RE nuclei. The anterior nuclear group (anteromedial, AM; anteroventral, AV) is connected to the limbic system. The human thalamus (Jones, 1997)[1] comprises groups of nuclei that are similar to those

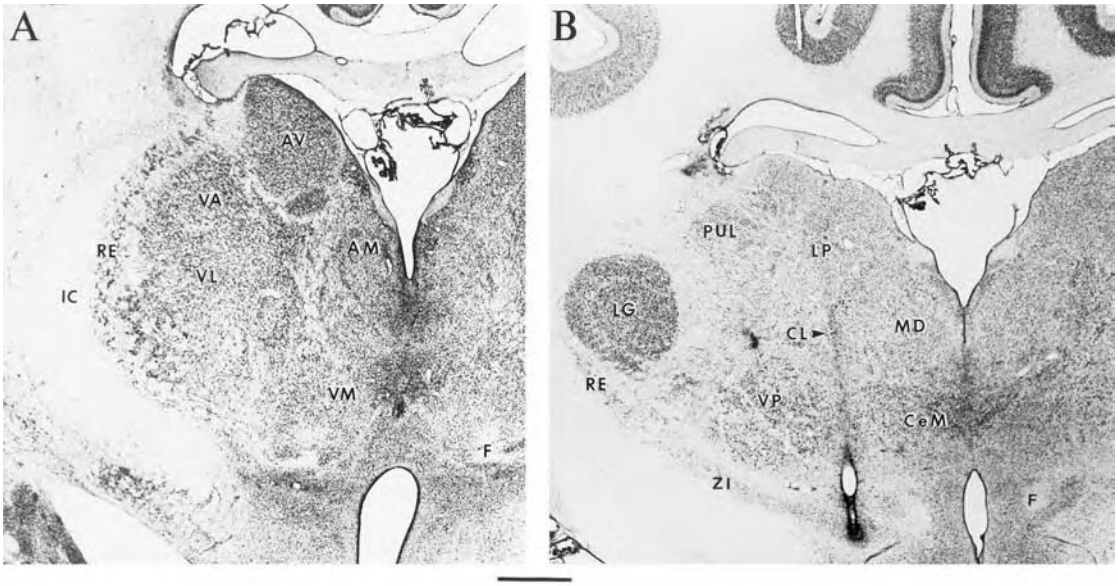

Fig. 1.1 Thalamic nuclei in the cat. Frontal (thionine-stained) sections at A 11 (A) and A 8 (B). Abbreviations: AM and AV, anteromedial and anteroventral nuclei; CeM, central medial nucleus; CL, central lateral nucleus (arrowhead points to a microelectrode track passing through the CL nucleus); F, fornix; IC, internal capsule; LG, lateral geniculate nucleus; LP, lateral posterior nucleus; MD, mediodorsal nucleus; PUL, pulvinar nucleus; RE, reticular nucleus; VA, VL, VM, and VP, ventroanterior, ventrolateral, ventromedial, and ventroposterior nuclei; ZI, zona incerta. Unpublished data by M. Steriade (1981).

previously described in felines and especially in Old World monkeys (Jones, 1985).[2] The sensory (LG, MG, two VP sectors), motor (VA, VL, VM), association (LP, MD), intralaminar (CL, CeM, and centrum medianum, CM), and RE, as well as some other thalamic nuclei are depicted in Figure 1.2.

The three major types of thalamic neurons are (a) those with cortical projections (called relay or thalamocortical, TC); (b) those whose axonal projection does not extend beyond the nucleus in which the soma is located (called local-circuit neurons or interneurons); and (c) those located in the RE nucleus. All TC neurons are glutamatergic and therefore excitatory, whereas both local-circuit and RE neurons use γ-aminobutyric acid (GABA) as neurotransmitter and are therefore inhibitory.

1.1.1 Thalamocortical neurons

Thalamocortical (TC) neurons are bushy (Figure 1.3A) and their variations are linked to soma size, large neurons projecting to middle and deep cortical layers, whereas small neurons project preferentially to superficial layers (Jones, 1985; Steriade *et al.*, 1997). After intracellular staining of one relay neuron, two closely apposed neurons may

[2] In a study focused on intralaminar nuclei of non-human primates, Jones and his colleagues (Hunt *et al.*, 1991) found that GABA-immunoreactive cells in thalamic intralaminar nuclei were only slightly fewer than in principal relay nuclei and assumed that previous reports of their absence or relatively low numbers probably resulted from failure to apply stereometric formulae that reveal the density of neurons per volume of tissue.

[3] In this *in vitro* study, dye-coupling of LG neurons was accompanied in a subset of cells (17%–19%) by spikelets, which survived application of antagonists of fast chemical synaptic transmission and were reversibly blocked by the gap junction blocker carbenoxolone. Spikelets are considered to be the electrophysiological correlate of electrotonic coupling via gap junctions (Perez-Velazquez & Carlen, 2000; see also Destexhe *et al.*, 1994a).

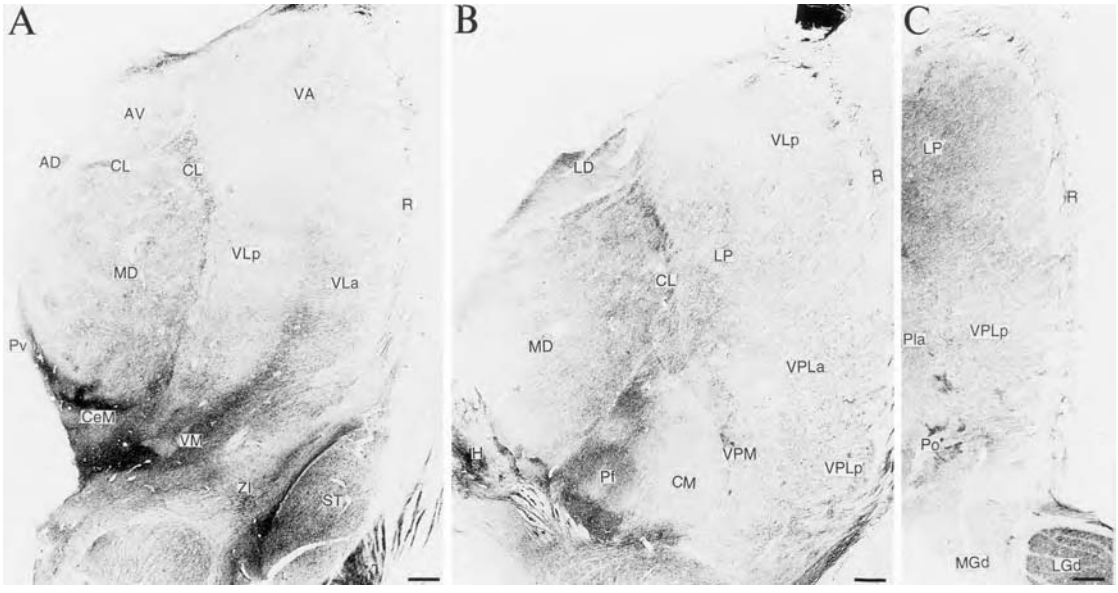

Fig. 1.2 Thalamic nuclei in humans. Frontal sections stained for acetyl cholinesterase. (A–C), three sections from anterior to posterior sites. Bar, 1 mm. Abbreviations (other than those explained in Figure 1.1): AD, anterodorsal nucleus; H, habenula; LD, laterodorsal nucleus; MGd, dorsal part of medial geniculate nucleus; Po and Pli, posterior and inferior pulvinar nuclei; Pv, paraventricular nucleus; R, reticular nucleus; ST, subthalamic nucleus; VLa and VLp, anterior and posterior parts of VL nucleus; VPLa, VPLp and VPM, anterior and posterior parts of lateral VP nucleus, medial VP nucleus. Modified from Jones (1997).

be found (Figure 1.3B); this likely reflects electrotonic coupling, as revealed in cat dorsal LG neurons (Hughes *et al.*, 2002a).[3]

In contrast to earlier hypotheses, which assumed that axonal collaterals of TC neurons contact local interneurons, there are no such intranuclear axonal collaterals in relay nuclei of the dorsal thalamus.[4] The only possible exception is the cat LG, in which axonal collaterals of TC neurons provide inputs to local intralaminar interneurons (Stanford *et al.*, 1983; Cox *et al.*, 2003). Thus, in general, TC neurons can communicate only through intermediary RE or neocortical neurons.

In some TC systems, the differences in soma size of relay neurons are paralleled by large variations in axonal conduction velocities of different types of cortically projecting neurons. For example, in the complex of motor-related nuclei, the antidromic response latencies of VM neurons projecting to cortical areas 4 and 6 are much longer (2.8–3 ms) than the antidromic response latencies of VA–VL neurons to stimulation of the same areas (1.8–2.3 ms) (Steriade, 1995a).[5] Despite variations in travel distances between the somatosensory thalamus and cortex, the latency from the mouse VP to a target cortical neuron is remarkably constant, generally *c.*2 ms (Salami *et al.*, 2003).[6] The highest conduction velocities (40–50 ms^{-1}) among all thalamic relay cells are displayed by a special neuronal class recorded from the large-cell

[4] The absence of intranuclear axonal collaterals in VL, VP and other relay thalamic nuclei, as demonstrated by intracellular staining (Steriade & Deschênes, 1984) and Golgi staining (see Jones, 1985),[2] stands in contrast with earlier hypotheses postulating that such presumed recurrent axonal collaterals would play a role in setting up postinhibitory rebound excitations and rhythmicity of discharges during spindles, by acting on local inhibitory interneurons (Andersen & Andersson, 1968). It is now recognized that sleep spindles are generated by thalamic reticular (RE) neurons and interactions with TC neurons (see Steriade *et al.*, 1985, 1987a).

[5] These differences between the conduction velocities of VM and VL–VA neurons projecting to the motor cortex match the longer latencies of VM responses evoked by stimulation of cerebellar fastigial nucleus (*c.*3 ms), compared with the VA–VL responses evoked by stimulation of cerebellar interpositus or dentate nuclei (1.7 and 2.4 ms, respectively).

[6] The authors calculated the conduction velocity from excitatory postsynaptic currents (EPSCs) in layer IV neurons by stimulating the VP complex and the white matter (WM)

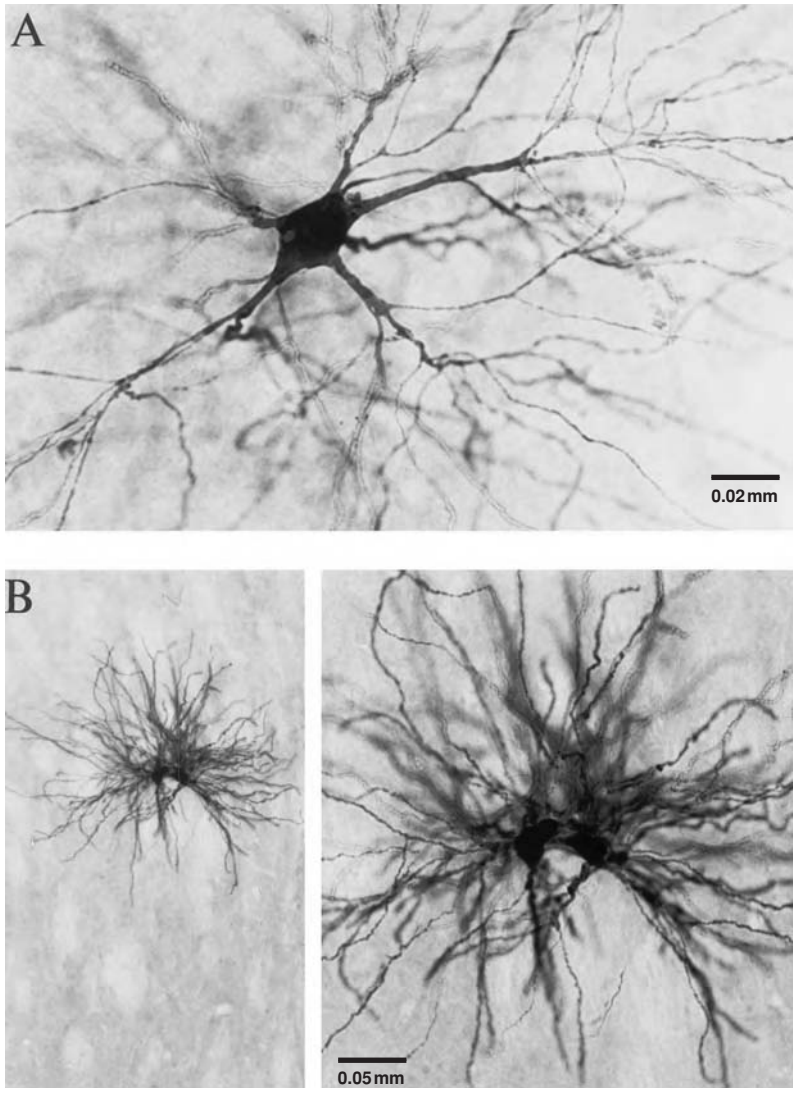

Fig. 1.3 Morphological features of thalamocortical (TC) neurons. (A) Intracellular staining (neurobiotin) of a relay neuron from the ventrolateral (VL) nucleus of the cat. The neuron had a soma 20 μm in diameter with radiating tufted dendrites, characteristic of relay neurons. (B) Two neurons were found close to each other, after one neuron was intracellularly stained (see text). (A) Modified from Contreras & Steriade (1995); (B) unpublished data by D. Contreras & M. Steriade.

[6] (*cont*). in mouse thalamocortical slices. The conduction velocity was found to be 10-fold faster between the thalamus and the WM than from WM to layer IV neurons (despite the fact that the VP–WM path is much longer and more variable in length), this difference being accounted for by the heavily myelinated VP–WM path, compared with the much weaker myelination in the WM–cortex path. Thus, most of the conduction time is spent travelling the intracortical pathway. Other systems, such as the olivocerebellar (Sugihara *et al.*, 1993) and amygdaloperirhinal (Pelletier & Paré, 2002) pathways, similarly show that input timing needs to be within a certain window. These results support the idea that conduction velocities of axons in given systems are adjusted to compensate for variations between the input source and target neurons.

part of the rostral intralaminar nucleus CL, antidromically activated from cortex at latencies of 0.4–0.5 ms (Steriade & Glenn, 1982).

Studies on neuronal immunoreactivity of non-human primates (Hashikawa *et al.*, 1991) showed that parvalbumin-containing neurons in the MG complex prevail in the ventral MG nucleus and project to layer IV of the primary auditory cortex, whereas calbindin-containing neurons prevail in the magnocellular part of the MG complex and project to layer I. In the human thalamus, calretinin immunoreactivity is weak in the geniculate nuclei but strong in the midline and anterior intralaminar nuclei (Fortin *et al.*, 1998).

1.1.2 Local-circuit neurons

Local-circuit GABAergic thalamic interneurons are not always considered in didactic schemes of thalamic circuits because, although they constitute 20%–30% of neurons in all thalamic nuclei of cats and

primates, including intralaminar nuclei (Jones, 1985), as well as in the dorsal LG nucleus of rats, they are virtually absent from other thalamic nuclei of rodents (Steriade *et al.*, 1997). Most slice studies are conducted on rodents, even though local thalamic interneurons may play an important role in the investigated function.

Local interneurons are characterized by their small soma and complex dendrites with *en passage* and terminal swellings. The output of local interneurons arises from axon terminals that form inhibitory synapses onto somata and dendrites of relay neurons but also, importantly, from the dendritic appendages of interneurons that are equipped with presynaptic vesicles, known as F2 terminals (Jones, 1985; Guillery, 1969; Montero, 1986). The latter contact the dendrites of TC neurons and form symmetrical (inhibitory) profiles within the triadic circuitry of synaptic aggregations called glomeruli (see Figure 16 in Steriade, 2001a).

The role of presynaptic dendrites of local interneurons in generating a peculiar type of inhibitory postsynaptic potential (IPSP) is discussed in Section 1.2. Some interneurons may not possess an obvious axon in dorsal thalamic nuclei other than the LG.

1.1.3 Reticular neurons

Reticular (RE) neurons have long dendrites (Figure 1.4), whose secondary and tertiary branches possess vesicle-containing appendages that form synapses on the dendrites of neurons in the same nucleus (Deschênes *et al.*, 1985; Yen *et al.*, 1985). Axoaxonic synapses have also been described in the rat RE nucleus (Pinault *et al.*, 1997). More recently, it was shown in slices maintained *in vitro* that RE neurons of rats and mice are electrically coupled and that electrical synapses require C×36 (Landisman *et al.*, 2002), the predominant type of connexin in gap junction channels (Condorelli *et al.*, 2000; Rash *et al.*, 2000; Venance *et al.*, 2000). The electrophysiological correlates of central neurons coupled by gap junctions are spikelets (Hughes *et al.*, 2002). Experiments *in vivo* on cat RE neurons showed the presence of spikelets during and outside RE cells' oscillatory activity (Fuentealba *et al.*, 2002, 2004a) (Figure 1.5). The spikelets in RE neurons are significantly different from excitatory postsynaptic potentials (EPSPs) and fast prepotentials (FPPs) (Figure 1.6), which are triggered by synaptic mechanisms. The fact that spikelets and EPSPs are different events in RE neurons results from two major features (Fuentealba *et al.*, 2002, 2004a). First, the rising phase in spikelets peaked at *c.*0.5 ms and the decaying phase at *c.*2 ms, whereas the same phases peaked at *c.*1 ms and *c.*4 ms in EPSPs (Figure 1.6A). Second, spikelets were unable to elicit full action potentials, even during states of membrane depolarization close to firing threshold, whereas EPSPs led to cell firing at the same level of depolarization (Figure 1.6B). It is then possible that fast events displaying very short durations, such as spikelets, do not generate full action potentials even if they reach the threshold for spike generation. Spikelets could also be distinguished from fast prepotentials (FPPs), which are usually considered as dendritic spikes triggered by synaptic volleys (Figure 1.6). FPPs are characterized by

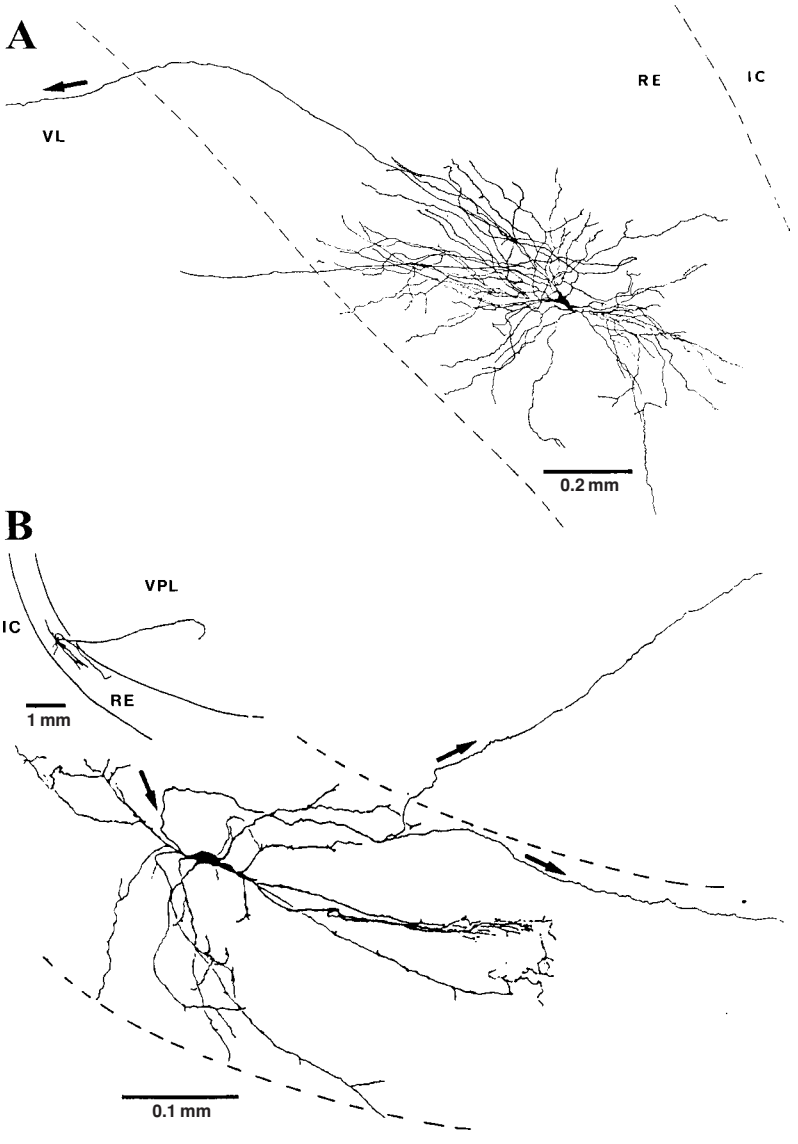

Fig. 1.4 Morphology of intracellularly stained cat thalamic reticular (RE) neurons. (A) RE neuron located in the rostral pole of the nucleus, reconstructed from horizontal sections after intracellular staining. Note the long extent of dendrites and main axonal branch running caudally towards the thalamic ventrolateral (VL) nucleus. (B) Intracellularly injected neuron in the somatosensory sector of the RE nucleus showing, at two different magnifications, the dendritic field extending across the full thickness of the RE nucleus and the axon running to the ventroposterolateral (VPL) nucleus. Modified from (A) Steriade and Deschênes (1984) and (B) Yen *et al.* (1985).

a rapid falling phase and an initiation at *c.*5–6 mV below the usual firing level. These synaptic events are efficiently triggered by corticothalamic volleys. The amplitudes of FPPs are much greater than those of spikelets, and their time-course are also different (see scaled spikelet and FPP in Figure 1.6A). Finally, in contrast to spikelets, FPPs are mainly present during periods of membrane depolarization and are virtually absent at membrane potentials more negative than –70 mV. These results *in vivo* (Fuentealba *et al.*, 2002, 2004a) led to the conclusion that spikelets represent one of the factors that account for the generation of synchronized rhythms, such as spindles, in the isolated thalamic RE nucleus. Experiments *in vitro* led to a similar conclusion (Long *et al.*, 2004).

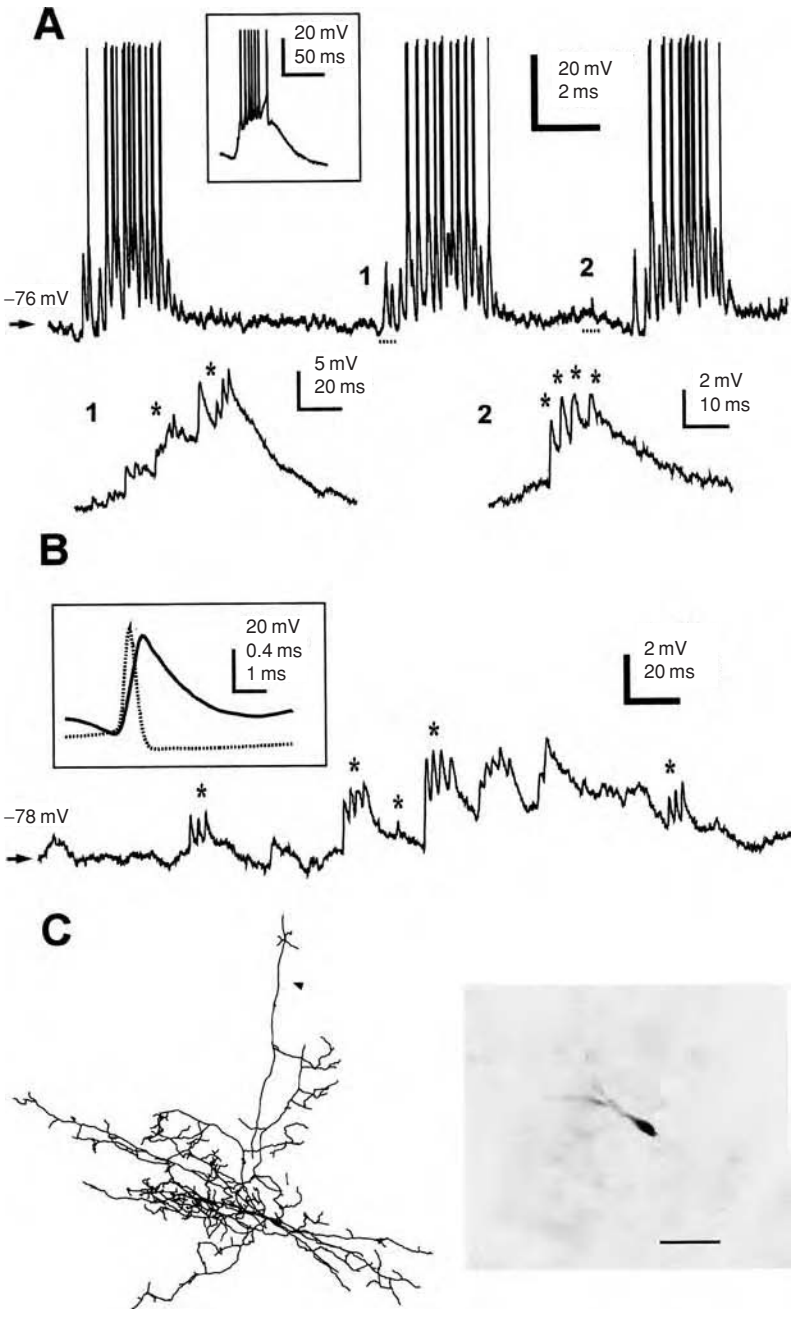

Fig. 1.5 Spikelets during spontaneous activity of cat RE neurons. Barbiturate anaesthesia. (A) Spike-bursts over the depolarizing envelope of spindles. Typical low-threshold spike-burst of RE cell expanded in inset. Epochs marked 1 (at the onset of a spindle sequence) and 2 (during interspindle lull) are expanded below and show spikelets (asterisks), i.e. fast-rising and low-amplitude events occurring in isolation or in clusters. (B) Another RE neuron displaying spikelets (asterisks) occurring in isolation or in clusters. Inset shows the average ($n = 500$) of spikelets (solid line; calibration bar 0.4 mV), scaled with the average ($n = 500$) of full action potentials (dotted line; calibration bar 20 mV). (C) Intracellularly stained (neurobiotin) RE neuron located in the rostrolateral sector of the nucleus. Photograph (right) and reconstruction (left). Arrowhead indicates the axon to the dorsal thalamus. Calibration bar within the photograph, 0.1 mm for RE neuron in the photograph and 0.15 mm for the reconstructed neuron. Modified from Fuentealba *et al.* (2004a).

Thus, contrary to TC neurons, RE neurons form an interconnected network, particularly well suited for the generation of oscillatory activity which can occur even in the isolated RE nucleus (see Chapter 6). The most effective mechanism for generating oscillations within the RE nucleus is probably provided by $GABA_A$-receptor-mediated synapses among RE neurons. Indeed, computational studies showed that RE neurons densely interconnected with

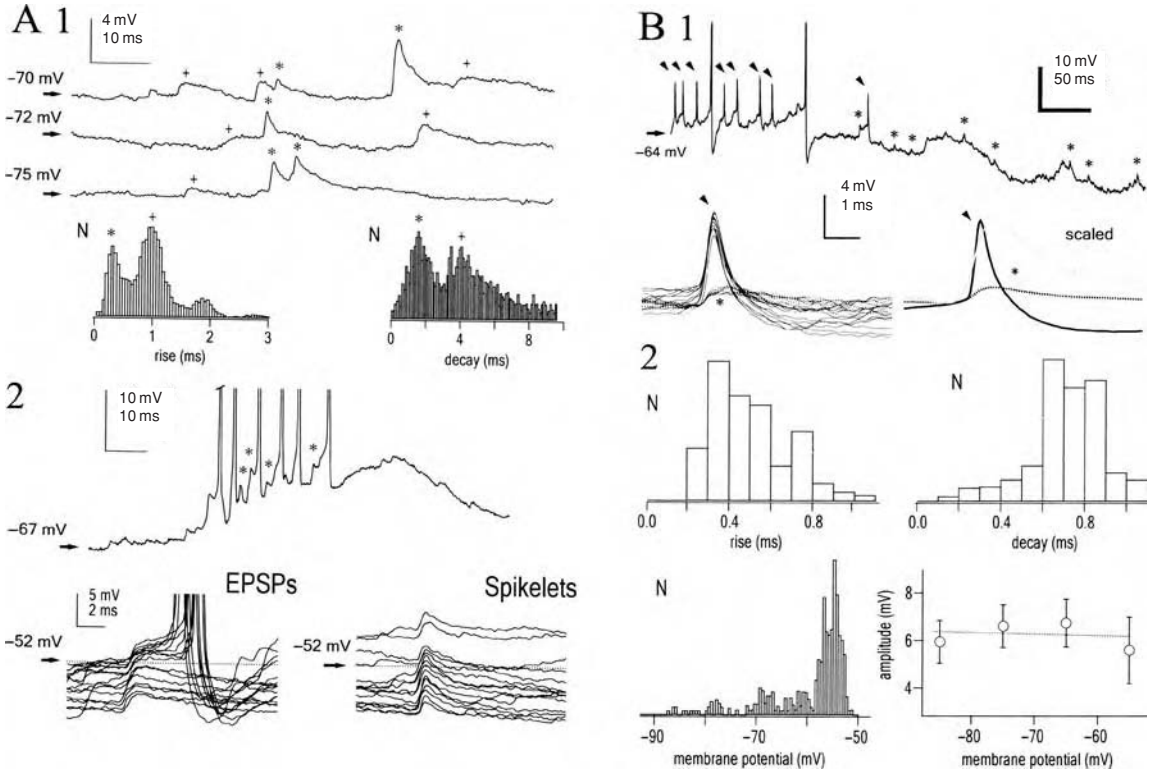

Fig. 1.6 Spikelets and EPSPs as well as FPPs are different types of depolarizing event in cat RE neurons. (A1) Barbiturate anaesthesia. The top three traces, from the same RE neuron, show two types of depolarization: spikelets (*) and EPSPs (+). Below, two histograms show the distribution of the rising and decaying phases (left and right, respectively) in the two types of event. (A2) Ketamine–xylazine anaesthesia in another RE neuron. Spikelets (*) are present during the firing of RE cell (spikes truncated). Note different rising phases in spikelets and some EPSPs that give rise to action potentials. Below, superimposed traces from the same neuron showing EPSPs and spikelets. Modified from Fuentealba *et al.* (2004b). (B) Another RE neuron recorded under ketamine–xylazine anaesthesia. (B1) Top trace displays FPPs (arrowheads) and spikelets (*). Action potentials truncated. Below, superimposition of single events (left) and averages ($n = 100$) showing both FPPs and spikelets (right); the grey trace shows the averaged spikelet scaled ($\times 5$) for comparison. (B2) Upper histograms show the rising and decaying phases (left and right, respectively) of FPPs. Bottom left histogram shows the voltage sensitivity of FPPs. Bottom right histogram shows voltage independency of the amplitude of FPPs. Each point is the average of ten points taken from intervals of 10 mV. Modified from Fuentealba *et al.* (2004a).

$GABA_A$ synapses produced synchronous oscillations within the frequency range of spindles (Destexhe *et al.*, 1994a), as demonstrated by experiments on the isolated RE nucleus (Steriade *et al.*, 1987a). In contrast, networks of model RE neurons fully interconnected through $GABA_B$ synapses failed to synchronize within this frequency range (Fuentealba *et al.*, 2002, 2004a). Experiments *in vitro* similarly showed

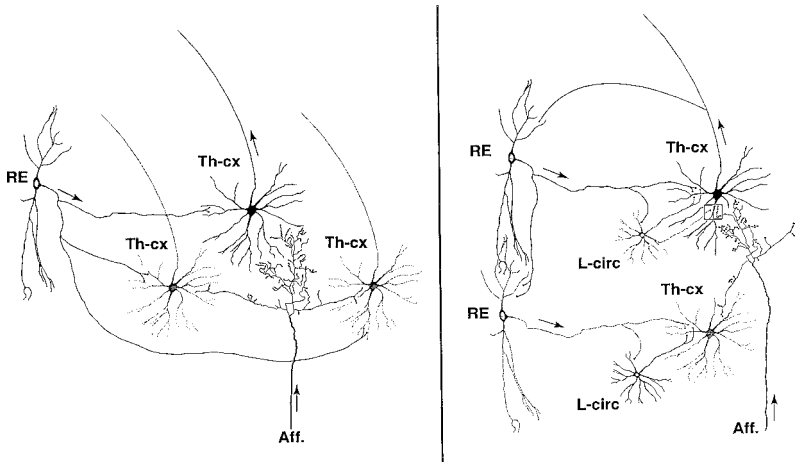

Fig. 1.7 Tentative schemes of operations in synaptic networks involving TC (Th-cx), local-circuit (L-circ), and RE thalamic cells. Left panel does not represent L-circ cells, as is the case of most relay nuclei in rodents. Right panel also depicts L-circ cells, as is the case in felines and primates. *Left panel:* activity in the afferent (Aff) prethalamic axon prevalently excites Th-cx in the centre. The inhibition exerted by the RE neuron is distributed equally to the three Th-cx neurons, but it mainly affects the two cells at the periphery because of the reduced amount of afferent excitation to these cells. *Right panel:* interactions between RE, L-circ and Th-cx neurons. In top Th-cx cell, which receives prevalent excitation from the Aff axon, directly connected RE neurons contribute to further enhancement of this relevant activity by inhibiting the pool of L-circ inhibitory elements (see Steriade *et al.*, 1984a). Simultaneously, the activity in adjacent RE sectors (bottom RE neuron) is suppressed by axonal collateralization and dendrodendritic inhibition among RE neurons (Deschênes *et al.*, 1985; Yen *et al.*, 1985; Pinault *et al.*, 1997). The consequence would be the released activity of target L-circ neurons and inhibition of weakly excited Th-cx neurons in thalamic areas adjacent to the active focus. This operation postulated a mechanism for inhibitory sculpturing in the thalamus. Modified from Steriade (1991), based on experiments by Steriade *et al.*, 1986; scheme kindly redrawn by E. G. Jones.

that rodents express very little $GABA_B$ responses in RE neurons (Ulrich & Huguenard, 1996).[7] Studies using expression of $GABA_B$ receptor gene transcripts in primate thalamus also concluded that there is a low level of $GABA_B$ receptors in the RE nucleus, in contrast with the high density of $GABA_B$ receptors in the dorsal thalamus (Muñoz *et al.*, 1998).

1.2 Intrathalamic and thalamocortical neuronal networks

We will first discuss the intrathalamic relations between TC and GABAergic local-circuit and RE neurons. Next, we will deal with reciprocal connections between TC and neocortical neurons.

[7] In another experimental and modelling study, the same team (Zhang *et al.*, 1997) also placed emphasis on $GABA_A$ receptors in the RE neurons and concluded that their prolonged inhibitory postsynaptic currents (IPSCs) are consistent with studies of spindle synchrony in an interconnected network of RE inhibitory neurons, as previously demonstrated experimentally (Long *et al.*, 2004) and in computational studies (Fuentealba *et al.*, 2002, 2004a). Other experiments, in ferret slices, have shown that $GABA_B$ responses to glutamate applied in the perigeniculate sector of the RE nucleus are also present, since the rebound spike-bursts were blocked by an antagonist of $GABA_B$ receptors (Sanchez-Vives *et al.*, 1997).

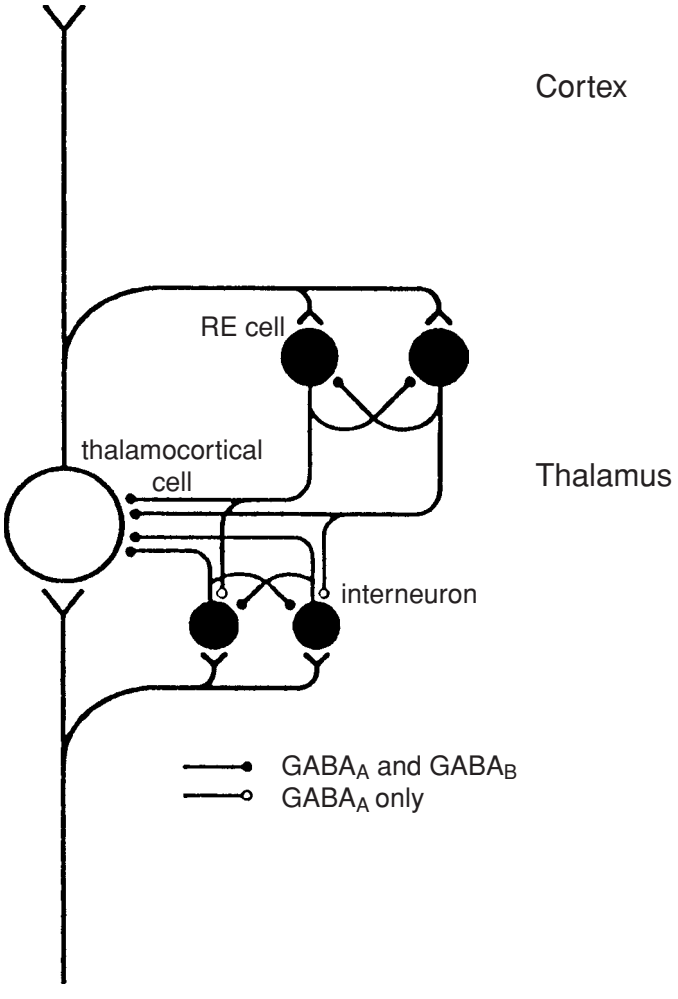

Fig. 1.8 Scheme of intrathalamic circuits, based on intracellular recordings *in vitro* in thalamic slices from rat LG TC cells and local interneurons. Note RE–interneuron inhibition, similar to that postulated in Figure 1.7 and experimental data on other thalamic nuclei *in vivo* (Steriade *et al.*, 1985). Modified from Zhu & Lo (1999).

1.2.1 Intrathalamic neuronal networks

Basically, (a) ascending fibres from specific systems contact both TC and local-circuit neurons (Jones, 1985; Steriade *et al.*, 1997);[8] (b) the axons of the local interneurons contact TC neurons and their presynaptic dendrites contact other interneurons (Jones, 1985; Steriade *et al.*, 1997)[9] (Figure 1.7, right panel); (c) RE neurons project to virtually all TC neurons, with the exception of anterior nuclei of cats (Steriade *et al.*, 1984), as well as to local interneurons[10] (Figure 1.7, right panel; Figure 1.8).

One of the two outputs of local-circuit inhibitory interneurons, which arises from their dendritic appendages generates a peculiar type of IPSP in TC neurons (Paré *et al.*, 1991).[11] This IPSP is the earliest in the sequence of IPSPs, thus preceding the $GABA_{A\text{-}B}$ sequence (Hirsch & Burnod, 1987; Crunelli *et al.*, 1988). To circumvent the possible intervention of inhibitory processes arising in thalamic RE nucleus, the complete sequence of IPSPs in TC neurons was induced by inhibitory local-circuit cells in the anterior nuclei that, in felines, are devoid of

[8] Govindaiah and Cox (2004) used parasagittal slices from rat LG nucleus to preserve the optic tract (OT) input, recorded intracellularly from relay cells and local interneurons, and revealed that OT tetanic stimulation activated metabotropic glutamate receptors (mGluRs) located on presumed presynaptic GABA-containing dendrites of interneurons, which led to increased inhibition in target thalamocortical neurons. Using a series of pharmacological manipulations in the bath, the authors concluded that the increased IPSPs in TC cells were not due to suprathreshold depolarization of the interneurons at the somatic level, but to OT-induced activation of mGluRs that are presumably localized on presynaptic dendrites of LG interneurons. Thus, they hypothesized that synaptic activation of mGluRs on presynaptic dendrites of LG interneurons increases the release of GABA from these dendrites, without influencing the axonal output, and may modulate synaptic transmission at retino-LG synapses, thus representing a focal form of information integration (see also Steriade, 2004a).

[9] See Figure 16 in Steriade (2001a).

[10] About 8%–10% of RE neurons project to local inhibitory interneurons (Liu *et al.*, 1995). Whole-cell recordings in slices of rat LG nucleus showed that stimulation of the thalamic RE

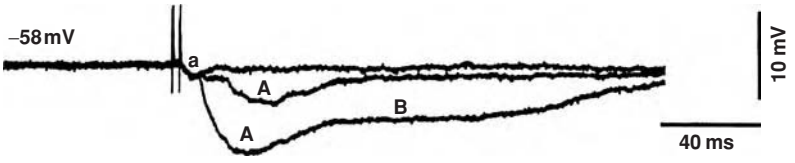

Fig. 1.9 Three types of IPSPs in TC neurons from anterior nuclei *in vivo*, induced by local-circuit neurons in the decorticated cat. An isolated $GABA_a$-IPSP could be evoked by a single stimulus, with the lowest intensity, applied to the mammillary body; two stimuli evoked both $GABA_a$- and $GABA_A$-IPSPs; and only by increasing the stimulation strength of the two stimuli was the full sequence ($GABA_{a\text{-}A\text{-}B}$) evoked. Modified from Paré *et al.* (1991).

inputs from the reticular nucleus (Steriade *et al.*, 1984). Stimulation of the afferent pathway from the mammillary nucleus to the anterior thalamic nuclei gave rise to a Cl^--dependent IPSP that had the shortest latency and very low amplitude, hence the term 'miniature' or $GABA_a$-IPSP (Paré *et al.*, 1991).[11] The reasons behind ascribing the $GABA_a$-IPSP to its generation by presynaptic dendrites are (a) the fact that it is selectively elicited by axons arising in the mammillary body, which have access to presynaptic dendrites, whereas it is not evoked by setting into action corticothalamic axons of which the overwhelming majority do not contact presynaptic dendrites; and (b) when Cl^- is injected into a neuron, the $GABA_A$-IPSP reverses before the $GABA_a$-IPSP, thus indicating that the synaptic sites responsible for the former are closer to the soma than those responsible for the latter. The failure to detect the miniature $GABA_a$-IPSP in other studies is probably due to the fact that minimal stimulation strength has to be used to reveal this 'miniature' IPSP in isolation. With slightly increased stimulation intensity, the $GABA_a$-IPSP is immersed in the following $GABA_A$-IPSP that has much greater amplitude (Paré *et al.*, 1991; Steriade, 2004a) see also (Figure 1.9).

The long-lasting inhibition exerted by RE neurons on TC neurons was demonstrated by *(a)* abolition of the prolonged, biphasic $GABA_{A\text{-}B}$ IPSPs in TC neurons and their replacement by short-lasting IPSPs produced by local-circuit neurons, after disconnection of relay nuclei from the RE nucleus (Steriade *et al.*, 1985); (b) dual extra- and intracellular recordings from these two neuronal types *in vivo* (Steriade & Contreras, 1993; Timofeev & Steriade, 1996; Contreras & Steriade, 1997a,b) and *in vitro* (Bal *et al.*, 1995b), showing that spike-bursts in RE neurons are followed by IPSPs in target TC neurons (Figure 1.10A) and by rhythmic sequences of inhibition-rebound sequences, within the frequency range of spindles, in thalamocortical neurons (Figure 1.10B); and (c) the effects of stimulating RE neurons in thalamic slices (Thomson, 1988a,b): pulse-trains to RE neurons triggered GABA-mediated IPSPs in TC cells, at frequencies similar to those displayed by sleep spindles, thus corroborating the idea of the role played by RE neurons in initiating spindle sequences in dorsal thalamus (Steriade *et al.*, 1987a). The IPSPs evoked by RE stimulation

[10] (*cont.*) (perigeniculate) sector evoked an IPSP, mediated exclusively by bicuculline-sensitive $GABA_A$ receptors (Zhu & Lo, 1999). See text, Steriade (1999) and Steriade *et al.* (1985) for functional consequences of this connection from the thalamic RE cells to local-circuit GABAergic cells.

[11] The presence of $GABA_a$-IPSP was also revealed in LG nuclei of rats investigated in rat LG slices, maintained *in vitro* (Soltesz & Crunelli, 1992; Cox *et al.*, 1998).

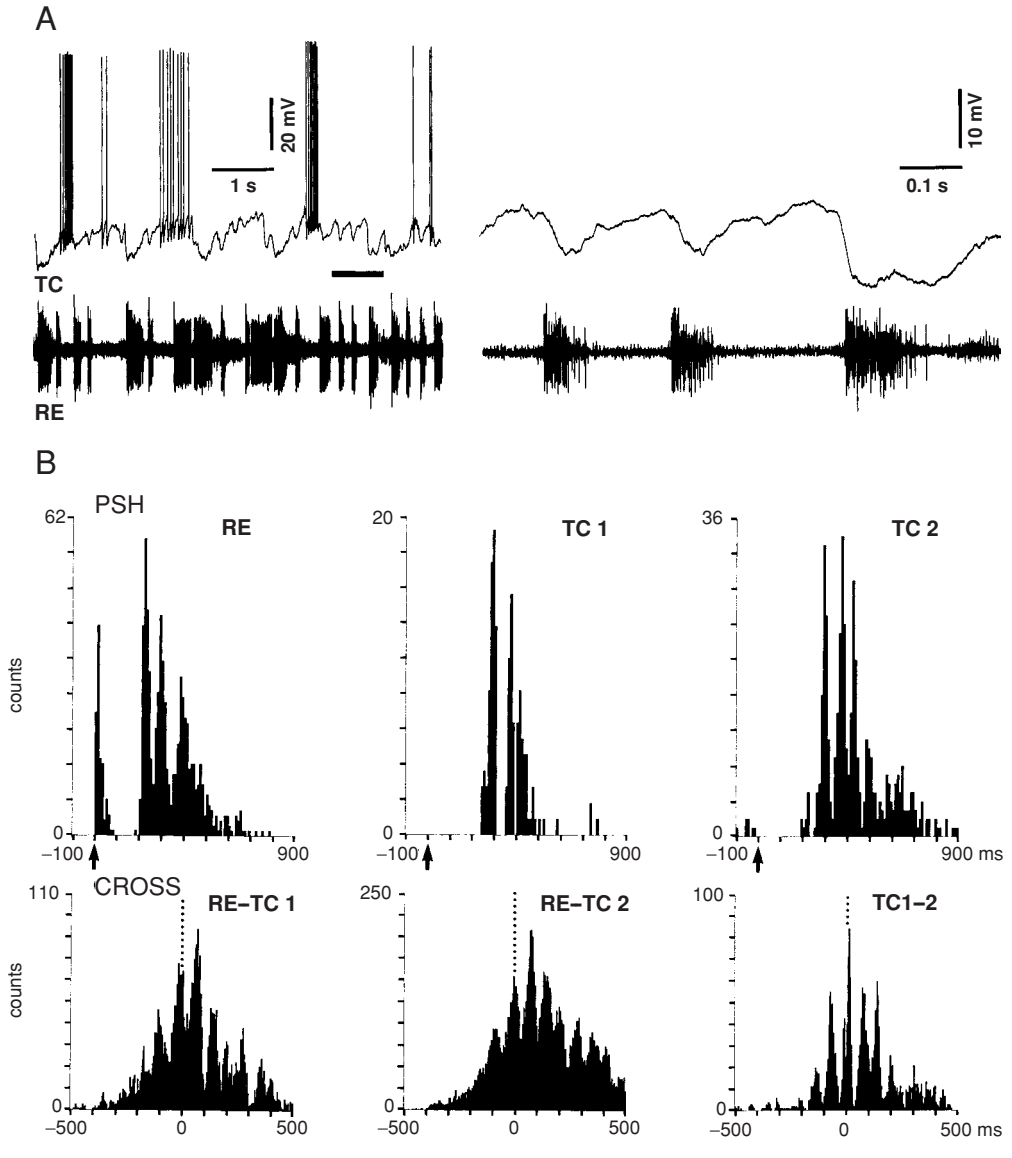

Fig. 1.10 Inhibition of TC neurons by RE neuronal activity. Cortically elicited spindles by inhibiting TC neurons via prior excitation of RE neurons. Cats under ketamine–xylazine anaesthesia. (A) Simultaneous intracellular recording of TC neurons from the VL nucleus and extracellular recording of RE neuron from rostrolateral district of the nucleus. The part marked by a horizontal bar (below the intracellular trace) is expanded on the right. Note spike-bursts in RE neuron producing IPSPs in VL neuron; also note the relation between increased duration of spike-burst in RE neuron and increased duration of IPSP in VL neuron. (B) Cortical stimulation elicited synchronized spindle oscillation in RE and TC cells 1 and 2 (TC1 and TC2). Poststimulus histograms (PSHs) show that cortical stimulus (arrow at time 0) induces early neuronal firing in the RE neuron and, simultaneously, firing suppression followed by rhythmic discharges in both TC neurons. Crosscorrelograms (CROSS) show that the RE neuron fired first to cortical stimulus, before the two TC neurons. Modified from (A) Steriade & Contreras (1993) and (B) Contreras & Steriade (1997a).

were biphasic, similar to the responses elicited by electrophoretically applied GABA (Thomson, 1988a,b).

The above data did not take into consideration the connection from RE neurons to local-circuit GABAergic neurons that are present in all relay nuclei of the dorsal thalamus of felines and primates. This connection[12] may produce significant effects on TC neurons, all the more so as, in other brain structures, GABAergic neurons are much more sensitive to GABA than other neuronal types (Grace & Bunney, 1979, 1985). Indeed, a greatly increased incidence of IPSPs in TC neurons was observed after destruction of RE neurons, reflecting the release from the inhibition of local interneurons after the excitotoxic lesion of RE perikarya (Steriade *et al.*, 1985). The connection between the two types of thalamic GABAergic cell, RE and local-circuit interneurons, may also be important for focusing attention on relevant signals. In this hypothesis (Steriade, 1999), RE neurons may contribute to enhance relevant activity by inhibiting the appropriate pool of local-circuit GABAergic neurons. Simultaneously, the activity in adjacent RE areas would be suppressed by RE-to-RE GABAergic contacts within the nucleus. The consequence would be the disinhibition of related local interneurons and the inhibition of weakly excited TC neurons in areas adjacent to the active focus (see Figure 1.7).

The arborization of RE axonal terminals in the dorsal thalamus is clustered or diffuse (Cox *et al.*, 1996)[13]; similarly, inhibitory strengths of connections from RE to VP cells, as investigated by whole-cell recordings in rat thalamic slices, are positively correlated with the density of axonal swellings of the presynaptic RE neurons (Cox *et al.*, 1997).

The intranuclear inhibition in the RE nucleus, shown by dendro-dendritic contacts among RE neurons (Deschênes *et al.*, 1985; Yen *et al.*, 1985) that produce IPSPs mainly through $GABA_A$-receptor activation (Ulrich & Huguenard, 1996), is effectively recruited by cortico-RE inputs (Zhang & Jones, 2004). This effect explains the potency of corticothalamic stimulation in eliciting spindles (Steriade *et al.*, 1972) by acting on the intranuclear inhibitory network that generates spindle oscillations in pacemaking RE neurons (Steriade *et al.*, 1987a).

1.2.2 Thalamocorticothalamic reciprocal loops

Thalamocortical axons from most dorsal thalamic nuclei distribute with a trilaminar pattern, mainly to midlayers but also to layers VI and I (Steriade *et al.*, 1997). Some nuclei, such as VM and rostral intralaminar CL, preferentially project to layer I, as demonstrated morphologically (Jones, 1985; Herkenham, 1979; Glenn *et al.*, 1982; Cunningham & Le Vay, 1986) and electrophysiologically (Foster, 1980; Glenn *et al.*, 1982). Conjoined stimulation of one specific thalamic nucleus, such as the somatosensory VP, and intralaminar CL nucleus results in supralinear summation of the two inputs at cortical output layer V, demonstrating coincidence detection along the apical dendrites of deeply lying pyramidal neurons (Llinás *et al.*, 2002).

[12] See dual intracellular recordings from RE and TC neurons in Figure 11 of Timofeev & Steriade, 1996.

[13] The clustered arborization of RE axonal terminals in the VP thalamus contains a high density of axonal swellings, whereas the diffuse arborization covers a larger VP area but contains a relatively low density of axonal swellings. For the functional counterpart of this morphological dichotomy, see main text and Cox *et al.* (1997). See also the review by Guillery & Harting (2002) on the two types of action exerted by RE neurons, one of them having global effects on the thalamus, the other modulating thalamic neurons with highly specific effects, relevant for attentive states.

In the neocortex, corticothalamic neurons are located in layers VI or V (Steriade *et al.*, 1997). The corticothalamic projection outnumbers the TC one by almost one order of magnitude. Corticothalamic axons are thin (diameter $< 1\ \mu m$) and generally slow conducting. In general, thin corticothalamic axons originate in layer VI, whereas thick axons arise from layer V. Some of these large fibres are collaterals of projections to the striatum, brainstem and spinal cord (Ojima, 1994; Lévesque *et al.*, 1996).[14] Crossed pathways from the frontal cortex terminate in contralateral anterior and mediodorsal thalamic nuclei of non-human primates (Preuss & Goldman-Rakic, 1987). All these corticofugal pathways transfer to the thalamus the integrated activity of intracortical pathways, as shown by antidromic activation of corticothalamic neurons that receive monosynaptic EPSPs from ipsilateral cortical stimulation (Figure 1.11) or direct excitation from callosal pathways (Steriade *et al.*, 1974b; Cissé *et al.*, 2003).

The corticothalamic projection to both RE and TC neurons is glutamatergic, therefore excitatory. However, synchronous volleys occurring naturally during low-frequency cortical oscillations or induced by electrical stimuli to the cortex produce an early depolarization and rhythmic spike-bursts in RE neurons, whereas they induced a prolonged hyperpolarization in TC neurons, consisting of a biphasic ($GABA_{A\text{-}B}$) IPSP followed by postinhibitory rebounds (Figure 1.12). These IPSPs are bisynaptic and are due to the prior activation of RE neurons. The role of RE neurons in the IPSP–rebound sequences of TC neurons is demonstrated by data showing that, following excitotoxic lesions of RE neurons or transections separating them from the remaining thalamus, the prolonged IPSPs and postinhibitory spike-bursts in TC neurons disappear, and that these neurons are targets of numerous, short-lasting IPSPs from local interneurons (Steriade *et al.*, 1985).

The contrasting effects (excitation and inhibition) of corticothalamic synchronized volleys on RE and TC neurons, respectively, are due to the fact that the numbers of glutamate receptor subunits GluR4 are about 3.7 times higher at corticothalamic synapses in RE neurons, compared with TC neurons. Moreover, the mean peak amplitude of corticothalamic excitatory postsynaptic currents (EPSCs) is about 2.5 times higher in RE than in TC neurons.[15] Thus, the direct excitation of TC neurons by corticothalamic glutamatergic pathways is overwhelmed by the potent inhibition mediated by prior excitation of RE neurons. The synchronous discharges of corticothalamic neurons during slow sleep oscillations excite RE neurons, eventually inducing prolonged hyperpolarizations and rebound spike-bursts in target TC neurons (Contreras & Steriade, 1995). Similar phenomena occur during cortically generated spike-wave seizures, when RE neurons faithfully follow every paroxysmal depolarizing shift in cortical neurons whereas a majority of TC neurons are steadily hyperpolarized and display phasic IPSPs (Steriade & Contreras, 1995)[16] (Figure 1.12B).

[14] Paré & Smith (1996) described thick cortical axons ending in association (lateroposterior–pulvinar) nuclei of the cat, contributing clusters of large-sized varicosities.

[15] Golshani *et al.* (2001) used both estimation of glutamate receptor subunits GluR4 and electrophysiological recordings in thalamic slices. See similar data, with more GluR4 units at cortico-RE synapses than at cortico-VP synapses, by Mineff & Weinberg (2000). See also review by Jones (2002).

[16] Reviewed in Crunelli & Leresche (2002) and Steriade (2003a).

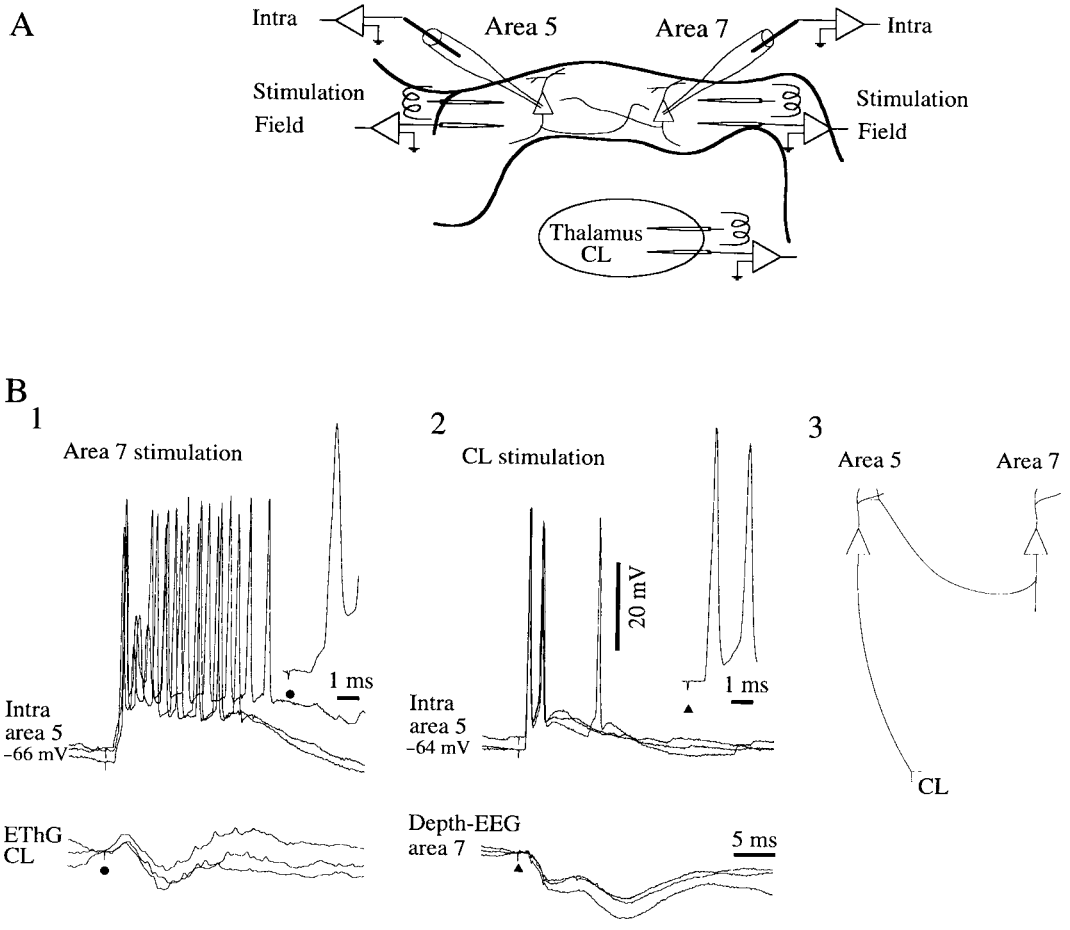

Fig. 1.11 Corticocorticothalamic pathways. (A) Schematic drawing indicating the location of recording and stimulating electrodes. Intracellular recordings from suprasylvian areas 5 and 7 were performed in conjunction with field potential recordings from the vicinity of micropipettes and from the central lateral (CL) thalamic nucleus. Stimulation was applied to areas 5 and 7. (B) Cortical and CL thalamic stimulation demonstrates interactions between area 5, area 7 and CL. (B1) Stimulus to area 7 (dot) evoked monosynaptic EPSP in area 5 neurons and short-latency excitation (focal negativity) in the CL field potential. (B2) CL stimulation (triangle) resulted in antidromic activation of area 5 neurons and short-latency excitation in field potential from area 7. Three superimposed traces in each case. (B3) Corticothalamic circuit inferred from the above data and indicating that the cortico-CL neuron in area 5 receives monosynaptic projections from area 7. Modified from Neckelmann *et al.* (1998).

Excitatory cortical actions on TC neurons can be revealed when RE neurons fire in the single-spike mode, as in wakefulness (Steriade *et al.*, 1986). In this circumstance, the inhibition they generate in TC neurons is less pronounced than when they fire long spike-bursts. During brain-active states, pools of corticothalamic neurons fire synchronously within the beta–gamma frequency band, at 20–40 Hz (Steriade *et al.*, 1996a) and may activate high-threshold Ca^{2+}

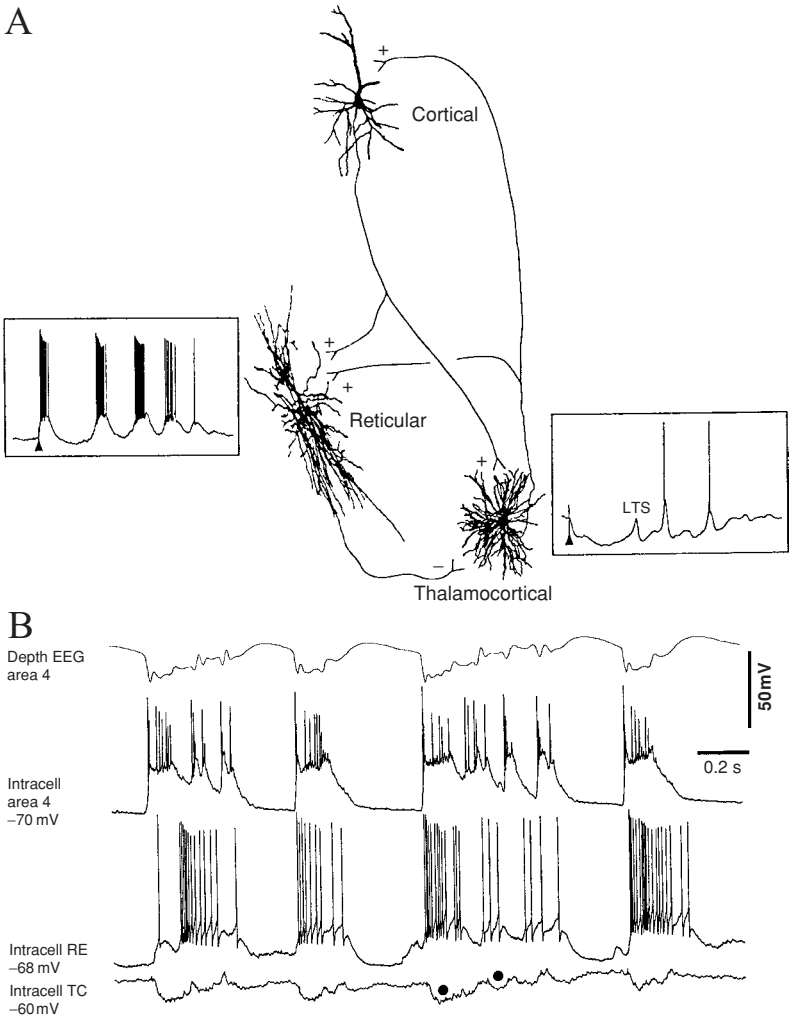

Fig. 1.12 Functional relations between corticothalamic, thalamic RE and TC neurons. (A) Three neurons (cortical, RE and TC) were intracellularly recorded and stained in cats. Signs of excitation and inhibition are indicated by plus and minus signs. For the sake of simplicity, local-circuit inhibitory neurons in the cortex and thalamus are not illustrated. Insets represent the response of RE and TC neurons to cortical stimulation (arrowheads point to stimulus artefacts). The GABAergic RE neuron responded to cortical stimulation with a high-frequency spike-burst, followed by a sequence of spindle waves on a depolarizing envelope (membrane potential −68 mV). The TC neuron responded to cortical stimulation (arrowhead) with a biphasic IPSP, leading to a low-threshold spike (LTS) and a sequence of hyperpolarizing spindle waves (membrane potential −70 mV). (B) Relations between cortical (area 4), RE and TC neurons of the cat during a spontaneously occurring, cortically generated seizure with polyspike-wave (PSW) complexes at 2 Hz. Note IPSPs in TC neuron (filled circles) in close time relation with spike-bursts fired by RE neuron, driven from cortex. Modified from Contreras & Steriade (1996), Lytton *et al.* (1997) and Steriade (2001c).

conductances of the P/Q type, which are preferentially located in the dendrites of TC neurons (Pedroarena & Llinás, 1997), thus generating fast oscillations in corticothalamocortical loops (Steriade *et al.*, 1996b).

In the auditory (MG) thalamic relay nucleus, the effects exerted by corticothalamic volleys is different in the two main sectors of the nucleus. Corticofugal depolarization and potentiation of firing as well as auditory responses are observed in the lemniscal part (ventral division) of the MG, whereas hyperpolarization, suppressed firing and auditory responses are seen in the non-lemniscal (dorsal part) of the MG (Yu *et al.*, 2004).

1.3 Intrinsic neuronal properties and their modulation by synaptic activity

We first enumerate the most important intrinsic properties of thalamic neurons and thereafter focus on the effects of synaptic activities arising in ascending and corticothalamic pathways on two major voltage-gated conductances.

1.3.1 Different voltage-gated conductances in thalamic neurons

The intrinsic electrophysiological properties of TC neurons recorded from different dorsal thalamic nuclei are similar.

The low-threshold transient Ca^{2+} current

This current (I_T) is de-inactivated by membrane hyperpolarization and underlies low-threshold spikes (LTSs) crowned by rebound spike-bursts consisting of high-frequency, fast Na^+ action potentials[17] (Figure 1.13A). The research that led to the discovery of two firing modes in thalamic neurons, tonic firing at relatively depolarized membrane potentials (−55 to −65 mV) and burst discharges at more hyperpolarized levels (−70 to −80 mV), was conducted during the early 1980s *in vitro* (Llinás & Jahnsen, 1982; Jahnsen & Llinás, 1984a,b) and *in vivo* (Deschênes *et al.*, 1982, 1984; Roy *et al.*, 1984) (Figure 1.13). Single-spike responses during states of tonic activation, such as waking, and burst responses at longer latencies during slow-wave sleep, had been previously recorded extracellularly in TC neurons (Steriade *et al.*, 1971) (Figure 1.14A). The intracellular aspects of TC cells' responses to afferent stimulation at depolarized levels (with action potentials), the resting level (with EPSPs), and under hyperpolarization (with LTS in isolation or crowned by spike-burst), are shown in Figure 1.14B. The refractory phase of the LTS is about 150–200 ms (Llinás & Jahnsen, 1982; Jahnsen & Llinás, 1984a,b; Deschênes *et al.*, 1982, 1984; Roy *et al.*, 1984). A special class of TC neurons, recorded from the large-cell part of rostral intralaminar nuclei, generate unusually high-frequency (900–1000 Hz), rhythmic (20–60 Hz) spike-bursts at relatively depolarized levels and their LTSs have a much shorter

[17] Reviewed in Llinás (1988) and Huguenard (1996).

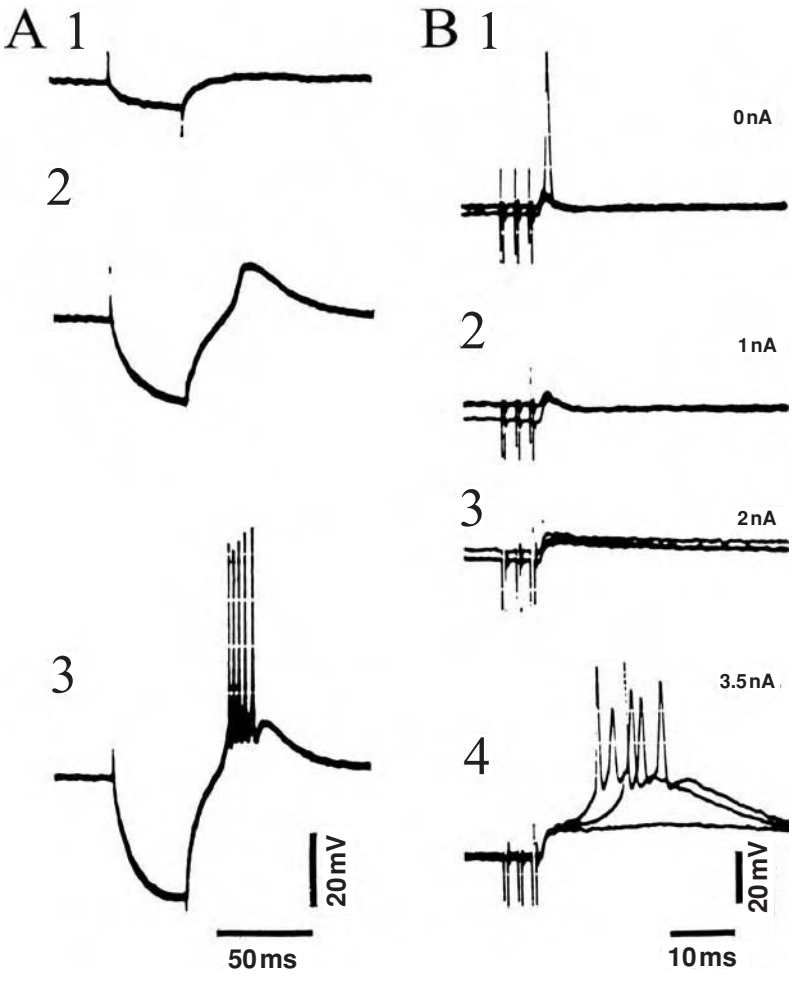

Fig. 1.13 Low-threshold spikes (LTSs) in TC neurons of cats under pentobarbital anaesthesia. (A) Direct stimulation of ventrolateral (VL) TC neuron at resting membrane potential by hyperpolarizing current pulses with increasing intensities (0.5 nA, 1 nA and 1.5 nA in 1, 2 and 3, respectively). Note LTS in isolation in 2 and LTS crowned by high-frequency burst in 3. (B) Effect of membrane hyperpolarization on VL cells' response to brachium conjunctivum (BC) stimulation (three stimuli). Note response consisting of single action potential at resting membrane potential (0 nA) and burst responses with membrane hyperpolarization (3.5 nA). Modified from Deschênes *et al.* (1982).

refractory phase (60–70 ms), which allows them to rebound following each IPSP during sleep spindles (Steriade *et al.*, 1993c).

Low-threshold spike-bursts, fulfilling the criteria of Ca^{2+}-dependent LTSs, have also been recorded from the human thalamus in patients suffering from neurogenic pain, tinnitus, abnormal movements and epilepsy (Jeanmonod *et al.*, 1996; Lenz & Dougherty, 1997). The interest in LTSs prompted a series of hypotheses that predicted their implication in scanning attention in waking and assumed that 'burst mode is a normal firing mode of thalamic neurons during waking state', a 'wake-up call' in TC systems (Sherman, 2001, p. 344). This stands in contrast to data in the literature. Indeed, waking is a behavioural state characterized by increased reactivity and is defined by activation processes in thalamocortical systems. A major feature of brain activation is the tonic depolarization of thalamic relay neurons, which prevents the occurrence of spike-bursts (Llinás & Jahnsen, 1982; Jahnsen & Llinás, 1984a,b; Deschênes *et al.*, 1982, 1984; Roy *et al.*, 1984). Intracellular studies on LG relay neurons demonstrated that hyperpolarization (during which the low-threshold Ca^{2+}

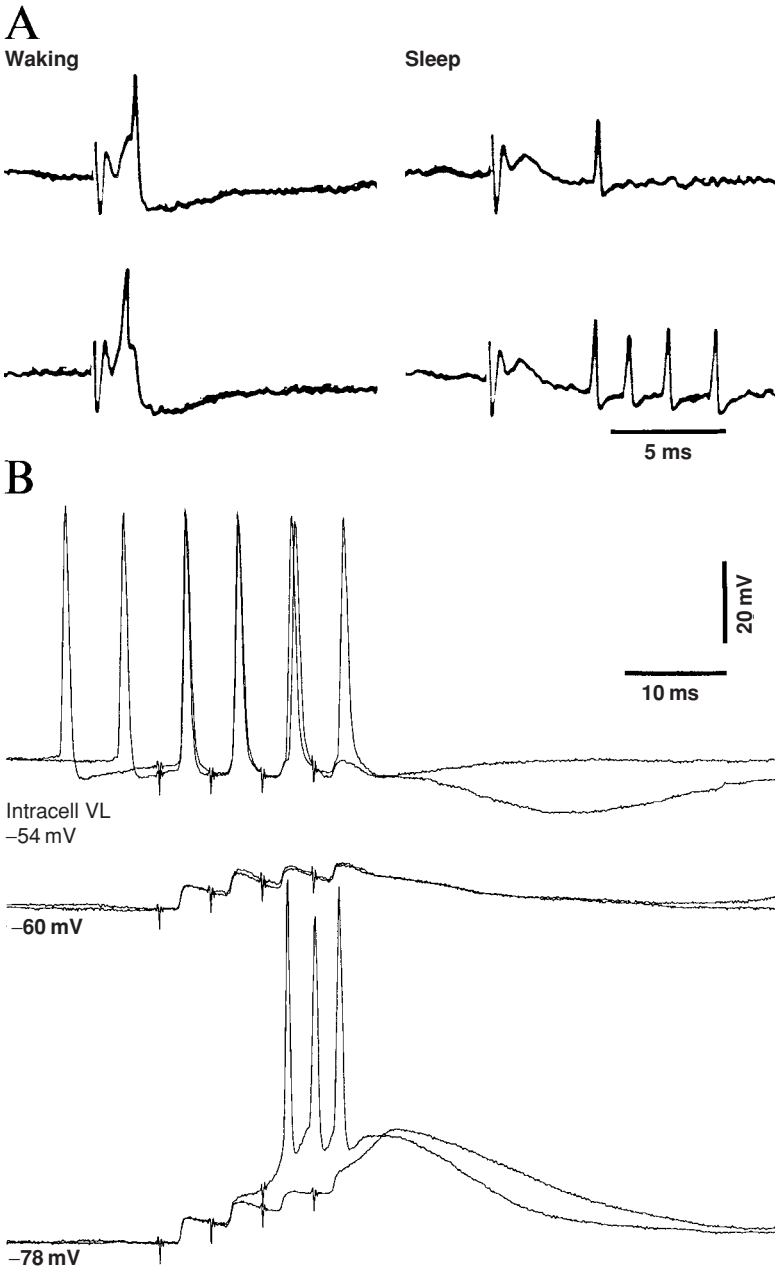

Fig. 1.14 Monosynaptic, single-spike responses of cat TC neurons during waking develop into burst responses at longer latencies during resting sleep associated with membrane hyperpolarization. (A) Stimulation of the brachium conjunctivum (BC) evokes single spike in a ventrolateral (VL) TC neuron during waking, whereas a longer-latency response, sometimes a spike-burst, is elicited during EEG patterns of sleep. (B) Intracellular recording of TC (VL) neuron under ketamine–xylazine anaesthesia. Four BC stimuli at 200 Hz evoked monosynaptic EPSPs and action potentials under slight steady depolarizing current (−54 mV) and EPSPs at rest (−60 mV). During hyperpolarizing current (−78 mV) the cell responded with EPSPs, leading to LTS in isolation (bottom trace, response to the fourth stimulus) or crowned by a high-frequency burst of action potentials. Modified from (A) Steriade *et al.* (1971) and (B) unpublished data by M. Steriade & D. Contreras.

conductance is de-inactivated) characterizes slow-wave sleep, whereas brain-active states of waking and REM sleep are associated with depolarization of LG neurons (Hirsch *et al.*, 1983). This is why LG and other TC neurons fire spike-bursts during slow-wave sleep and single spikes during waking. A study on LG thalamic neurons in chronically implanted cats, concluded that, 'during wakefulness, $< 1\%$ of action potentials are associated with bursting' and found 'negative relationships between attention and bursting' (Weyand *et al.*, 2001, pp. 1107,

[18] In LG slices, local interneurons display an oscillatory property within a frequency range of 5–15 Hz, similar to that previously reported *in vivo* at the level of other thalamic nuclei (see Steriade *et al.*, 1972).

1113). Recent intracellular recordings of TC neurons in conscious, awake animals have similarly shown that *c.*1% of neurons (three of the 272 neurons recorded from the posterolateral thalamus and the mid-thalamus) had spontaneous LTS discharges (Woody *et al.*, 2003). Then, the burst mode is *not* a normal firing mode of TC neurons during waking. Actually, why would a 'wake-up call' (Sherman, 2001) be needed if the animal were already awake? When animals are somnolent, there is a slight hyperpolarization of thalamocortical neurons during which spike-bursts may be generated, but this state does not represent the active state of wakefulness during which scanning attention operates (Steriade, 2001d).

At variance with the T-channels of TC neurons, which are located in the soma and proximal dendrites, the T-channels of RE neurons are located in dendrites, especially in distal dendrites (Huguenard & Prince, 1982; Destexhe *et al.*, 1996). The LTSs of RE neurons generate peculiar spike-bursts that are much longer (30–80 ms, but up to 1 s) and display an accelerando–decelerando pattern, compared with the shorter (5–15 ms) spike-bursts with progressively increasing interspike intervals in TC neurons (Domich *et al.*, 1986). Intracellular recordings *in vivo* revealed spike-bursts in presumed dendritic recordings from RE neurons and demonstrated the graded nature of dendritic LTSs as a function of the level of membrane hyperpolarization and the intensity of depolarizing inputs (Contreras *et al.*, 1993). The highly excitable dendritic tree and the graded bursting behavior of RE neurons support their role as generator and synchronizer of spindle rhythmicity *in vivo* (Steriade *et al.*, 1987a). It is likely that the very long dendrites of RE neurons are impaired when slices are prepared; this may explain, among other factors, the absence of spindles from thalamic slices (Von Krosigk *et al.*, 1993).

Local-circuit GABAergic thalamic cells display burst firing (but of longer duration and lower intraburst frequency than the bursts of TC neurons) when a depolarizing step is imposed at a slightly hyperpolarized membrane potential (Zhu, *et al.*, 1999a,b).[18] In earlier studies (Pape *et al.*, 1994; Pape & McCormick, 1995), the ability of local thalamic interneurons to display LTSs and spike-bursts was investigated with emphasis on the functional balance between two opposing currents (I_T and I_A) in such low-threshold bursts.

High-voltage Ca^{2+} currents

High-voltage Ca^{2+} currents have been described in thalamic neurons (Pedroarena & Llinás, 1997; Llinás & Jahnsen, 1982; Jahnsen & Llinas, 1984a,b; Hernández-Cruz & Pape, 1989; Kammermeier & Jones, 1997). These Ca^{2+} channels are clustered at the basis of dendrites in TC neurons, whereas they are more evenly distributed in the soma of local-circuit and RE neurons (Budde *et al.*, 1998). In TC neurons, augmenting responses, defined as progressively increasing their size from the second response to a pulse-train at 10 Hz, develop in two steps: the first one is the transformation of the early EPSP into an LTS as a result of the IPSP produced by the first stimulus in the train, and in the

second step the LTS is truncated by a secondary depolarizing response that develops at a membrane potential more positive than –55 mV and is ascribed to a high-voltage Ca^{2+} current.[19]

[19] See Figure 7 in Steriade & Timofeev (1997).

Persistent Na^+ current

This current ($I_{Na(p)}$), initially described in thalamic relay cells (Llinás & Jahnsen, 1982; Jahnsen & Llinás, 1984a,b), is also present in RE neurons. Extracellular recordings of RE neurons during natural states of vigilance showed that, during slow-wave sleep, some RE neurons fire spike-bursts lasting *c.* 50–100 ms, whereas other RE neurons display a prolonged (up to 1 or 2 s) tonic tail of single action potentials after the spike-bursts (Steriade *et al.*, 1986). Experiments *in vitro* showed that this prolonged depolarization is due to either a $I_{Na(p)}$ or a Ca^{2+}-activated non-selective cation current (Kim & McCormick, 1998).

The $I_{Na(p)}$ can generate plateau potentials and membrane bistability (Llinás, 1988; Crill, 1996). This has been demonstrated, among many neuronal types, in dorsal thalamic neurons (Williams *et al.*, 1997; Toth *et al.*, 1998; Hughes *et al.*, 1999). Experiments *in vivo* showed that a subgroup (20%) of RE neurons displayed membrane bistability that consisted of two alternate membrane potentials, separated by *c.*17–20 mV (Fuentealba *et al.*, 2004b). Whereas non-bistable (common) RE neurons fired rhythmic spike-bursts during spindles, bistable RE neurones fired tonically, with burst modulation, throughout spindle sequences (Figure 1.15). The transition from the silent to the active state in bistable RE neurons is a regenerative event that can be activated by brief depolarization, whereas brief hyperpolarizations may switch the membrane potential from the active to the silent state. The suggestion that $I_{Na(p)}$ is responsible for the generation of bistability in RE neurons is based on the fact that addition of QX-314 in the recording micropipette either abolished or disrupted membrane bistability (Fuentealba *et al.*, 2004b). Membrane bistability may play an important role in different patterns of spindles displayed by TC neurons. Indeed, intracellular recordings of thalamic relay cells show at least two different patterns during spontaneously occurring spindles. The two patterns displayed by cell 1 and cell 2 in Figure 1.16 may be related to the actions exerted by non-bistable and bistable RE neurons, respectively. Non-bistable RE neurons fire stronger bursts, with higher intraburst frequencies, which are assumed to generate deeper and longer IPSPs in TC neurons. By contrast, IPSPs with lower amplitudes and higher frequency, up to 20 Hz, are likely generated by single action potentials in RE neurons, as they occur during the depolarizing plateau in bistable cells. Supporting these results, computational models of thalamic networks, including bistable RE neurons, showed a significant shaping of oscillations in TC neurons by bistable RE neurons (Fuentealba *et al.*, 2004b).

Hyperpolarization-activated cation current

This current (I_H) was described in TC neurons from different dorsal thalamic nuclei and its role in the generation of rhythmic LTSs

[20] In the auditory MG nucleus, I_H is present in the ventral (lemniscal) part, but is absent from the dorsal (non-lemniscal) part (Hu, 1995).

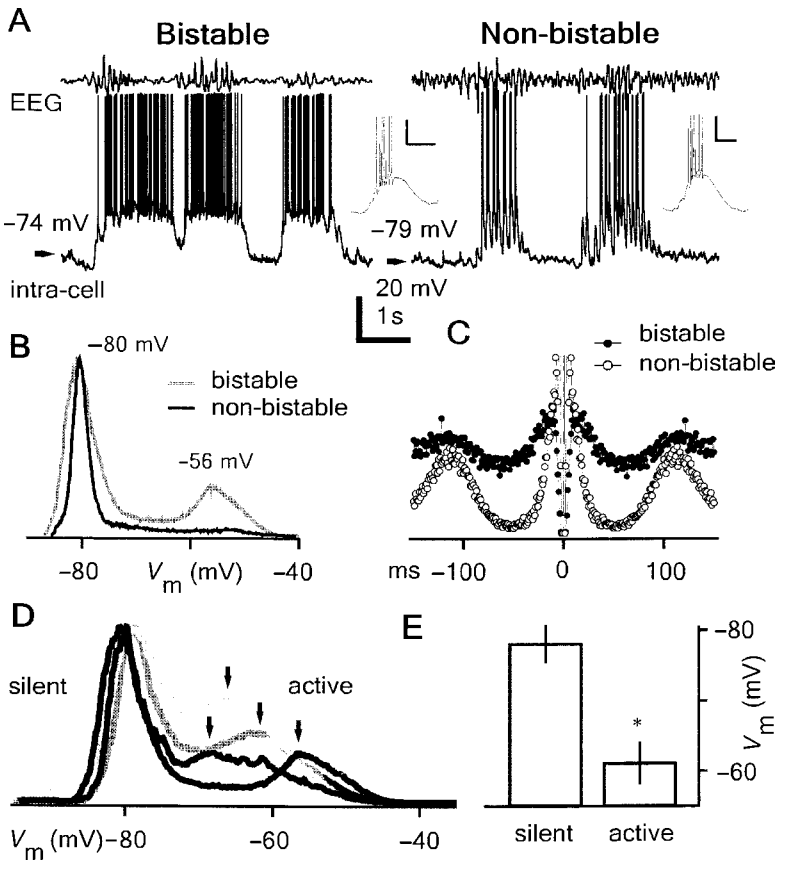

Fig. 1.15 Membrane bistability in RE neurons during spontaneously occurring spindles. Cat under barbiturate anaesthesia. (A) Cortical EEG and intracellular recordings from two RE neurons. Typical low-threshold spike-bursts of each of these RE cells are expanded in insets. The bistable neuron displayed sustained depolarizations throughout spindle waves. The non-bistable neuron fired spike-bursts, separated by phasic hyperpolarizations, during spindling. Scale bars: 50 ms, 20 mV. (B) V_m distribution from bistable and non-bistable cells in (A) taken from a 5 min period of spontaneous activity. Only bistable neurons showed bimodal V_m distributions. Bin size, 1 mV. (C) Autocorrelograms of action potentials for the same periods used in (B). Non-bistable cells discharged at the spindle frequency (*c.*9 Hz), showing clear peaks at *c.*110 ms delay, whereas bistable cells showed less marked correlation with spindle frequency. Bin size, 1 ms. (D) Bistability is a graded property. Different bistable RE neurons (represented by different grey tones) displayed diverse patterns of V_m distributions, but all showed two discrete peaks (though at different positions). Note constancy of the first peak (*silent*) and variable position of the second peak (*active*, arrows). Bin size, 1 mV. (E) Silent and active states during membrane bistability presented different membrane potentials (mean ± SD, $n = 9$), * $p < 0.001$. Modified from Fuentealba *et al.* (2004b).

within the frequency range of 1–4 Hz was assessed *in vitro*, *in vivo* and *in computo* (Leresche *et al.*, 1990, 1991; McCormick & Pape, 1990a,b; Soltesz *et al.*, 1991; Steriade *et al.*, 1991a; Curró Dossi *et al.*, 1992a; Toth & Crunelli, 1992).[20] I_H with similar features was also found in local interneurons of the LG nucleus (Zhu *et al.*, 1999c).

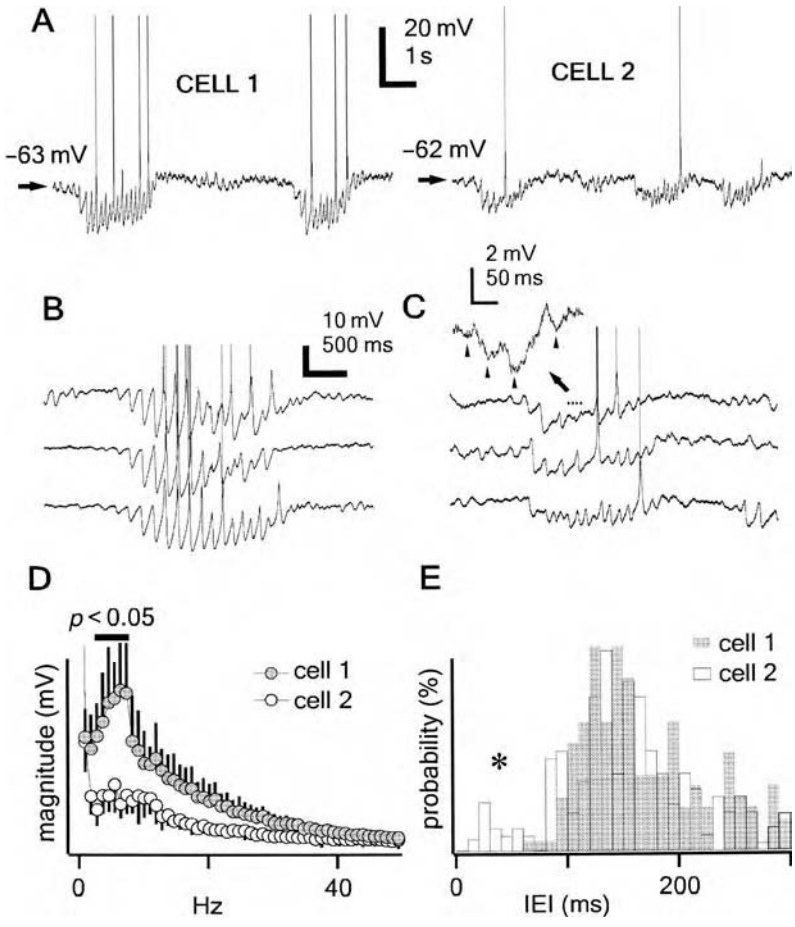

Fig. 1.16 Different spindling patterns in TC cells reflect various firing patterns in RE bistable and non-bistable neurons. (A) Intracellular recordings of two TC neurons (VL nucleus) during spindle activity. (B, C) Three different spindle sequences for each of the above cells. Note highly regular activity and early rebound bursting in cell 1. Inset in cell 2 shows three IPSPs (arrows) at much higher frequency (*c.*20 Hz) than the usual frequency range of spindles (see text). (D) Average of frequency spectra of spindle periods ($n = 10$, mean ± SD) in both cell 1 and cell 2 neurons. Bin size, 1 Hz. Note a clear peak around 7 Hz for cell 1. (E) Histograms of interevent intervals (IEI) for presumed IPSPs ($n = 400$) in both cell 1 and cell 2 during spindle waves. Bin size, 10 ms. Note the presence of a tail at short intervals (< 100 ms) for cell 2 (asterisk). Modified from Fuentealba *et al.* (2004b).

1.3.2 Synaptic activity strongly modulates intrinsic properties of thalamic cells

The LTS and rebound spike-burst of TC neurons are greatly reduced or absent when these neurons are bombarded by synaptic activity, as is the case *in vivo*. Figure 1.17A illustrates the responses of a TC neuron, recorded from the VL nucleus of a decorticated cat. These responses were elicited by hyperpolarizing current pulses, leading to Ca^{2+} spikes in isolation or crowned by fast Na^{+} action potentials, during periods without (A) and with (B) synaptic activity (Timofeev & Steriade, 1997). The apparent input resistance during periods with fast oscillations (*c.* 100 Hz) decreased by 27% compared with epochs without such fast synaptic activity. During the fast oscillations, the LTS was greatly reduced, such that the rebound spike-burst was absent.

The advantage of a new preparation in which intracellular recordings from thalamic neurons could be performed without ablation of the overlying neocortex (Nita *et al.*, 2003) is the possibility of investigating the contribution of voltage-gated conductances when the activity of corticothalamic neurons varies in intensity. Two methods were used to test the hypothesis that cortical synaptic impingement on

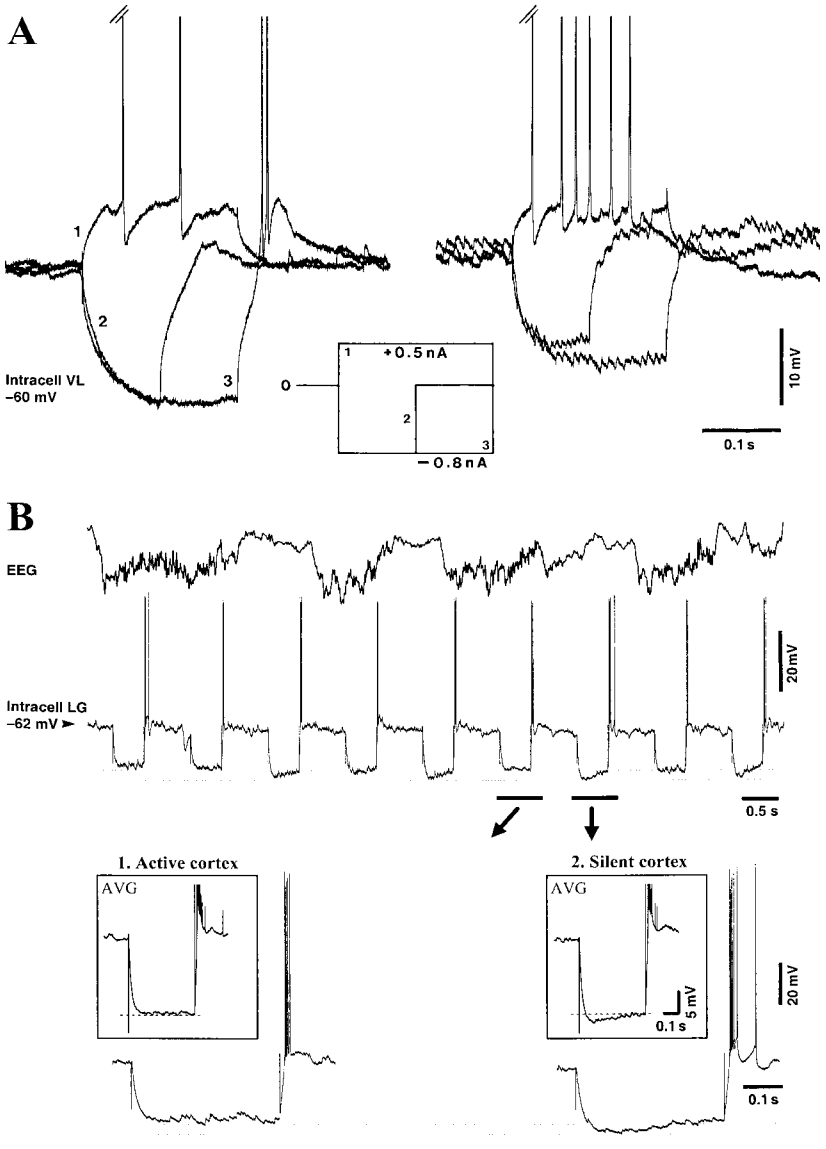

Fig. 1.17 Modulation of intrinsic neuronal properties of TC neurons by synaptic activity in ascending and corticothalamic pathways. Cats under ketamine–xylazine anaesthesia. (A) Amplitude of depolarizing (1) and hyperpolarizing (2, 3) current pulses are indicated. Left part depicts the responses of a TC neuron in the VL nucleus in the absence of fast oscillations arising in the cerebellothalamic pathway; right part shows the strong diminution of LTS and rebound spike-burst during the presence of these fast oscillations. (B) Relationship between cortical slow oscillation and the expression of I_H in an LG neuron. Cortical depth-EEG and intracellular recording of LG neuron. The I_H was elicited by hyperpolarizing current pulses only when the cortex was in a period of disfacilitation (positive waves). Below, individual sweeps of hyperpolarizing current pulses expanded from the trace above. They correspond to a pulse delivered during active EEG (1) and another one during disfacilitation (2). For each situation, the average pulse responses ($n = 20$) are depicted in inset. These pulse responses are surrounded by the inferior and superior envelopes of the standard deviation of the averages (in grey). Each of the chosen sweeps occurred entirely during either active, negative EEG (1) or silent, positive EEG (2) epochs of the slow oscillation. Modified from (A) Timofeev & Steriade (1997) and (B) Nita *et al.* (2003).

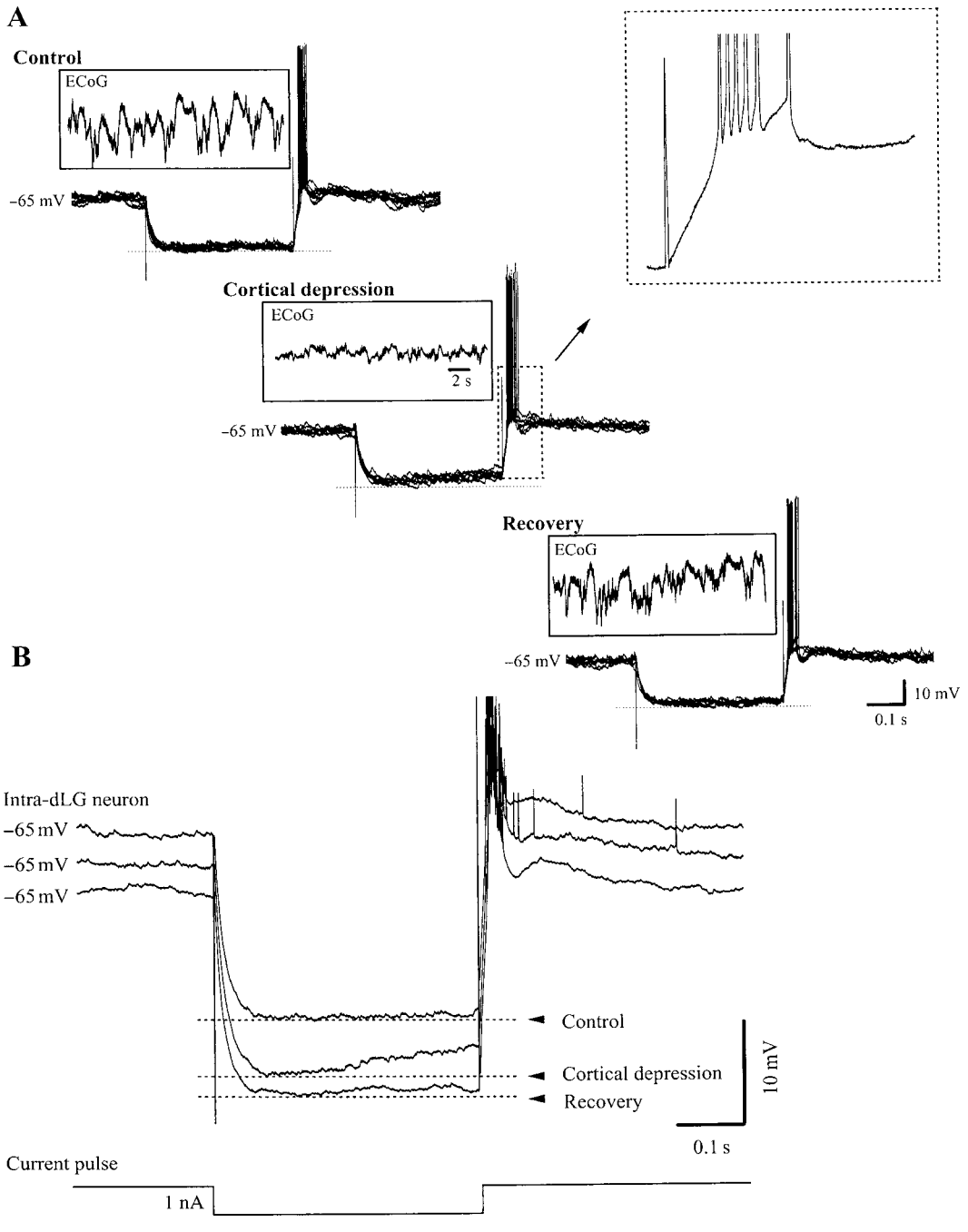

Fig. 1.18 Alterations in I_H of LG neuron before, during and after cortical depression. Cat under ketamine–xylazine anaesthesia. (A) Superimposition of individual sweeps during hyperpolarizing current pulses and depth-EEG recording before, during and after (recovery) cortical depression induced by topic application of a concentrated K^+ solution on the primary area 17 of the visual cortex. Only those sweeps occurring at comparable V_m (− 65 mV) were retained for analysis. (B) Averaged sweeps ($n = 20$) before, during and after cortical depression. The I_H was observed only during cortical depression. Modified from Nita *et al.* (2003).

thalamic neurons may preclude the expression of the hyperpolarization-activated depolarizing sag (I_H): (a) by analysing, during the slow (< 1 Hz) oscillation, the impact of periodic hyperpolarizations associated with disfacilitation in cortical networks (Figure 1.17B); and (*b*) by reversibly depressing cortical activity (Figure 1.18). In both cases, I_H appeared to be concealed by the synaptic activity arising in the cortex. The slow oscillation (Steriade *et al.*, 1993e,f) comprises two different activity levels in cortical networks: an active ('up') state during which cortical neurons are depolarized and fire action potentials, and a silent ('down') state in which cortical neurons are hyperpolarized by a disfacilitation process (Contreras *et al.*, 1996b). The results in Figures 1.17B and 1.18 indicate that the absence of an active cortical network constitutes a necessary condition for the expression of hyperpolarization-activated depolarizing sags (I_H).

It is known that a pacemaker, clock-like oscillation within the frequency range of delta waves (1–4 Hz) results from the interplay between two voltage-gated inward currents of TC neurons (Leresche *et al.*, 1990, 1991; McCormick & Pape, 1990a,b; Soltesz *et al.*, 1991; Steriade *et al.*, 1991a; Curró Dossi *et al.*, 1992a; Toth & Crunelli, 1992).[20] The reduced expression of I_H in cortically intact preparations has consequences for the incidence and generation mechanisms of clock-like delta oscillations in the visual thalamus. Beyond the interference of retinal inputs with clock-like delta oscillations in LG neurons (Nuñez *et al.*, 1992b), the periodic activation of the cortical network during the depolarizing phase of the slow oscillation would disrupt any possible sequences of clock-like delta cycles. In spite of this, I_H could still promote delta rhythmicity during conditions associated with prolonged loss of consciousness such as coma or burst suppression, during which the cortical activity is depressed. Burst suppression is accompanied by a steady hyperpolarization of about 10 mV of cortical neurons and long periods of reduced responsiveness to synaptic volleys, whereas TC neurons display clock-like delta oscillations.[21] The utility of I_H under such conditions could rely on its ability to maintain a minimal neuronal activity in the thalamus with negligible energetic impact on target structures.

[21] See Figures 9 and 10 in Steriade *et al.* (1994a).

Chapter 2

Morphology and electroresponsive properties of neocortical cells

The prerequisite for discussing changes in responsiveness and sculpting inhibitory processes of neocortical neurons during different behavioural states (see Chapters 6 and 7) is the description of various neuronal types and their functional properties, which is the subject of this chapter.

2.1 Varieties, immunoreactivity and connectivity of neocortical neuronal classes

The mammalian neocortex is a laminated structure that contains up to 28×10^9 neurons that are connected by about 10^{12} synapses. The attempt to simplify the functional complexity of the neocortex started with the description of the columnar organization into modules that have a basic similarity of internal design and operation (see Mountcastle, 1997, 1998). The neocortex consists of a large population of long-axon (output) neurons that are excitatory and reciprocally connected to each other in the same and/or opposite hemisphere as well as to thalamocortical (TC) neurons, and a smaller population of local-circuit inhibitory neurons.

Besides morphological techniques that distinguish these two neuronal classes (Figures 2.1–2.3), physiological identification of output neurons is possible using antidromic and orthodromic activations (Figures 2.4 and 2.5), which determine the sources of synaptic inputs and neuronal targets (Evarts, 1964, 1965;[1] Steriade *et al.*, 1974a[2]) thus leading to systematizations with a limited number of neuronal categories. These are rather difficult techniques in behaving animals; with some exceptions (Steriade *et al.*, 2001a,b),[3] they are rarely used nowadays. Neocortical neurons have been classified into four categories according to their intrinsic electrophysiological properties, as determined by responses to intracellular current pulses (see Section 2.3). However, it was shown that, far from being inflexible, the incidence and properties of various neocortical cell classes may vary as a result of changes in membrane potential, as occurs during natural shifts in

[1] These are the first extracellular studies in which corticospinal neurons were antidromically identified in chronically implanted, naturally awake and sleeping monkeys.

[2] See Figure 2.4 for sites of stimulating electrodes used in that study for the antidromic identification of corticothalamic and cortico-brainstem neurons in chronically implanted macaque monkey.

[3] In these first intracellular studies of neocortical neurons during natural states of vigilance in chronically implanted cats, corticofugal cells were antidromically identified from related thalamic nuclei and contralateral cortical areas.

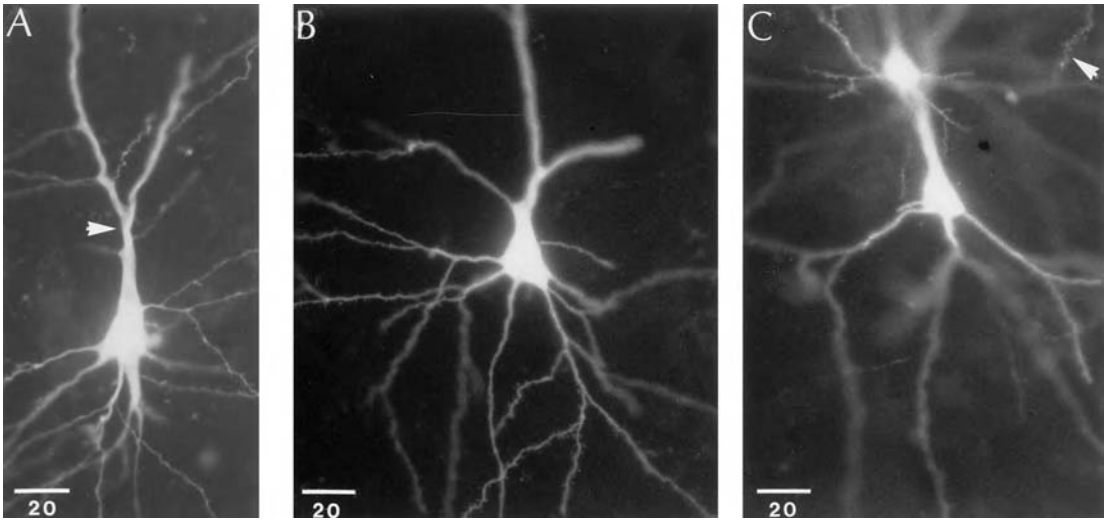

Fig. 2.1 Neocortical pyramidal neurons. Intracellular recordings and staining with Lucifer Yellow (LY) in cats under urethane anaesthesia. (A) Regular-spiking neuron, at 0.8 mm depth in area 5, antidromically activated from thalamic CL and LP nuclei, and orthodromically driven from the contralateral cortex. Arrow points to bifurcation of the apical dendrite. (B) Regular-spiking neuron, at 0.9 mm depth in area 7, synaptically driven from thalamic nuclei LP and CL. (C) Dye coupling following LY injection in a single cell at a depth of 0.5 mm in area 5; arrow points to a dendrite of larger-size, deeper-located neuron. Calibration bars, 20 μm. Modified from Steriade *et al.* (1993a).

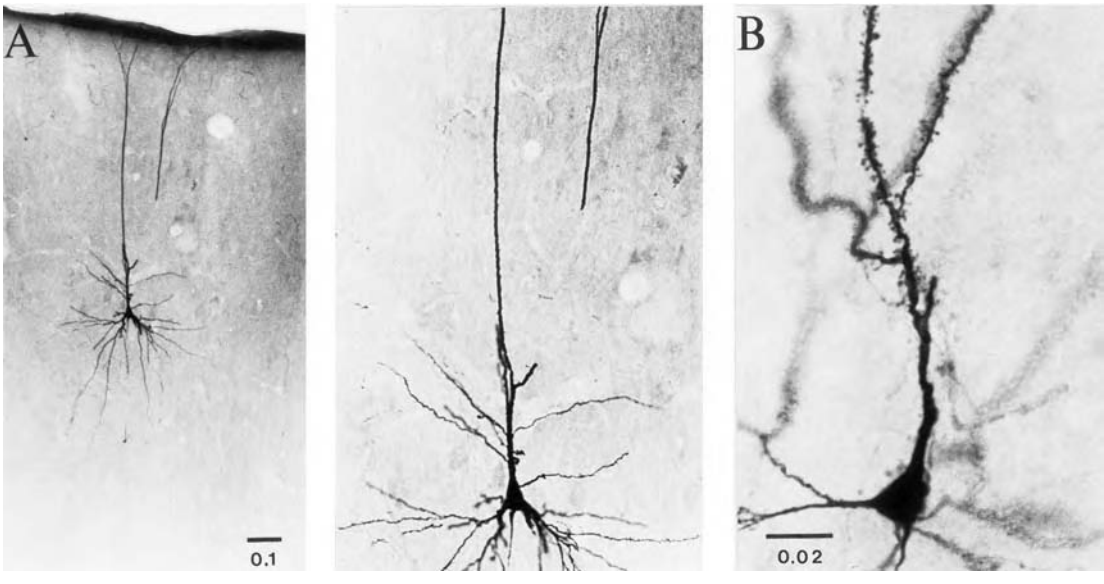

Fig. 2.2 Neocortical pyramidal neurons. Intracellular recordings and staining with neurobiotin in cats under barbiturate (A) and ketamine–xylazine (B) anaesthesia. (A) Neuron located in layer V of primary somatosensory cortex. At right, magnification of perisomatic region. (B) Superficial pyramidal cell (0.3 mm depth in the primary somatosensory cortex); note apical dendrite covered by spines. Calibration bars, mm. Modified from (A) Contreras *et al.* (1997a) and (B) Contreras & Steriade (1995).

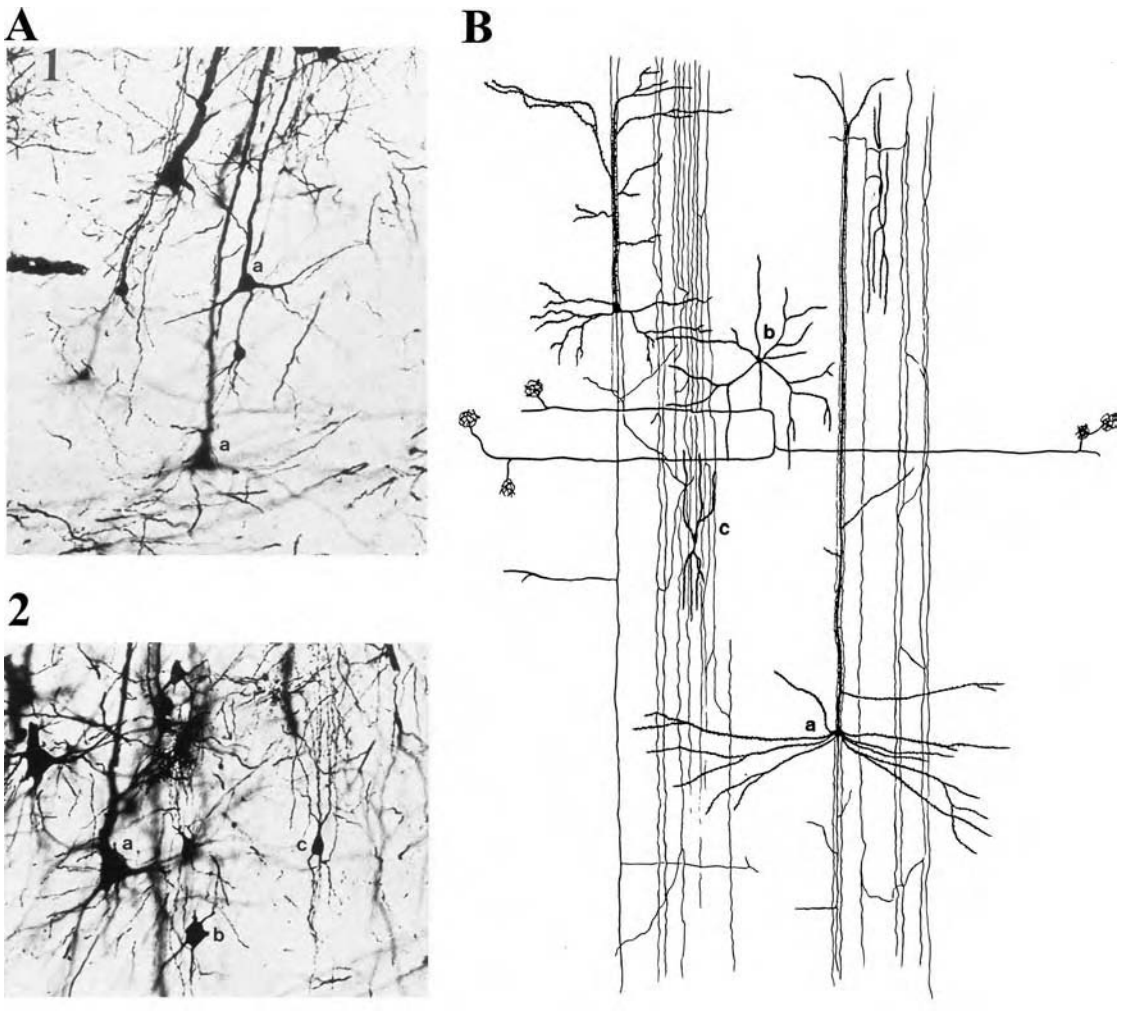

behavioural state. As a result, the same neuron may display several discharge patterns that are otherwise ascribed to different neuronal types (Steriade, 2004a).

Fig. 2.3 Neocortical pyramidal and local-circuit neurons. (A1–2) Golgi staining of macaque monkey's precentral neurons: a, pyramidal neurons; b, basket-type local interneuron; c, double-bouquet dendritic cell. (B) Free-hand drawing summarizing some pyramidal and local-circuit inhibitory neurons; a–c, same types of neurons as in (A). (A) Unpublished slide of M. Steriade (1949); (B) modified from Colonnier (1966).

2.1.1 Long-axon pyramidal neurons

Long-axon pyramidal neurons are located in cortical layers II to VI and constitute the majority (70%–80%) of the total neuronal population in the neocortex. Although intracellularly stained pyramidal neurons typically display rich basal dendrites and a prominent apical dendrite that gives off a number of oblique branches (Figure 2.1A, B) covered by spines (Figure 2.2B), they are heterogeneous with regard to soma size, spine density and pattern of axonal collaterals (DeFelipe & Fariñas, 1992). For a lively discussion on specificity and non-specificity of synaptic connections of pyramidal neurons in different species and neocortical areas, columnar organization, dendritic spine morphology, and role of functional pumps in different types of spiny pyramidal neurons, see DeFelipe *et al*. (2002).

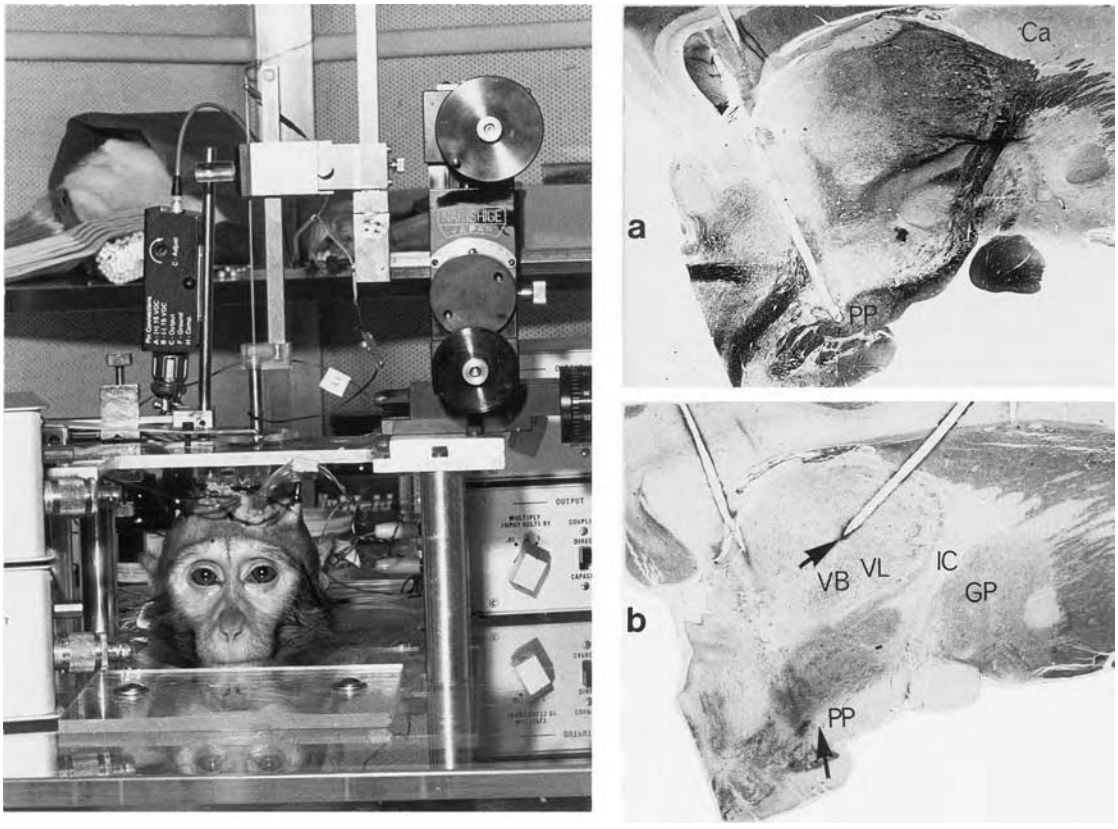

Fig. 2.4 Location of stimulating electrodes for physiological identification of precentral pyramidal neurons in chronically implanted *Macaca mulatta*. Left, awake monkey sitting in a primate chair during recordings. Right, sagittal sections stained with myelin (*a*) and Nissl (*b*) methods. (a) Electrode inserted into pes pedunculi (PP). (b) Electrode inserted at the transition zone between ventrolateral (VL) and ventrobasal (VB) thalamic nuclei (another trace of electrode terminated in PP, arrow). Other abbreviations: IC, internal capsule; GP, globus pallidus. Unpublished figure, from experiments by Steriade *et al.* (1974a).

[4] These morphological differences between corticotectal and callosal neurons were associated with different electrophysiological properties, the former being of the bursting type, whereas every cell projecting to the opposite visual cortex was a non-burster.

The morphological differences between pyramidal cells located in various cortical layers are exemplified by neurons located in deep and superficial layers. Thus, layer V pyramidal neurons of rat visual cortex projecting to the superior colliculus have thick apical dendrites with a florid terminal arborization in layer I, whereas pyramidal neurons from the same layer but projecting to the contralateral visual cortex have thinner apical dendrites that terminate below layer I (Kasper *et al.*, 1994a,b).[4] Whereas the apical dendrites of deeply lying pyramidal neurons begin to arborize between layers V and IV, those of pyramids located in layers II–III begin to divide immediately at their origin from the apex. Although attention is usually focused on the apical trunk of dendrites, the basal dendrites are much more luxuriant in both deeply lying and more superficial pyramidal neurons. The transmitter used by all pyramidal neurons is glutamate or aspartate (Baughman & Gilbert, 1980; Fonnum *et al*, 1981).

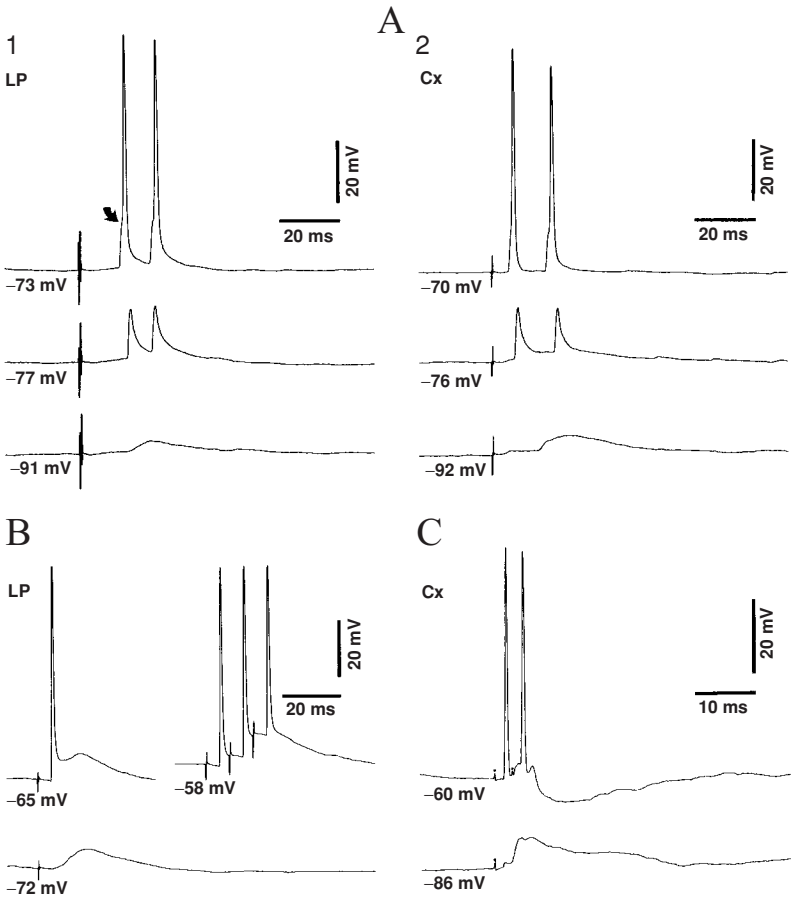

Fig. 2.5 Physiological identification of neocortical neurons from association areas 5 and 7 by antidromic and orthodromic activation. Intracellular recordings in cats under urethane anaesthesia. (A–C) Three different regular-spiking, slowly adapting neurons. (A) Neuron recorded at a depth of 1.1 mm in area 5, synaptically driven from both thalamic LP nucleus (l, latency 14 ms) and homotopic area in the contralateral suprasylvian area 5 (2, latency 5 ms). (B) Cell recorded at 1.3 mm depth in area 7, antidromically activated from thalamic LP nucleus (latency 4.3 ms). (C) Neuron recorded at 0.5 mm depth, backfired from the contralateral cortex. Modified from Steriade *et al.* (1993e).

The targets of axons from pyramidal neurons located in layer VI are thalamic specific, association (see Figure 2.5B) and RE nuclei; layer V pyramids project to thalamic intralaminar nuclei, basal ganglia, superior colliculus, other brainstem nuclear aggregates and the spinal cord; and layers II–III pyramids mainly project to ipsi- and contralateral cortical areas (Jones, 1984). The axonal recurrent collaterals of pyramidal neurons distribute over short distances (0.2–0.3 mm) to the same or supervening layers. However, some axons from layer V pyramidal neurons may run up to 4–6 mm, or even more, in horizontal or oblique directions.

The afferents to pyramidal neurons arising from other pyramidal neurons within the ipsilateral or opposite neocortex or from the thalamus are all excitatory. They have been studied by current source–density analyses and intracellular recordings. Although thalamic connections contribute about 10% of excitatory synapses to the neocortex, the overwhelming majority of excitatory synapses arises within the cortex, originating from pyramidal and spiny stellate cells (White, 1989; Braitenberg & Schüz, 1991). Axons of TC cells reach mainly mid-layers IV and lower III, but also layers VI and I; corticocortical afferents reach mainly layers II–III. The same cortical neuron

[5] Latencies of callosally evoked responses as long as 19–20 ms (see neuron recorded at 0.8 mm in Figure 7*B2* in that paper) do not necessarily reflect polysynaptic pathways because antidromic response latencies in callosal neurons could be as long as 18.5 ms, indicating that some callosal neurons have very slow conduction velocities.

[6] Spiny non-pyramidal neurons are mainly located in layer IV but their axons tend to ramify in supragranular layers where they form asymmetric synapses to dendritic spines (LeVay, 1973; Somogyi, 1978).

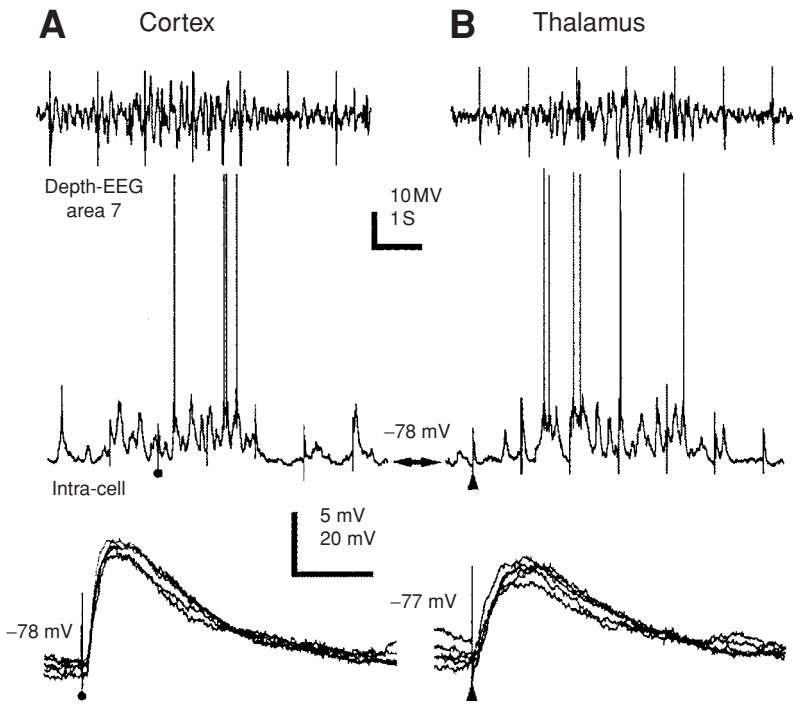

Fig. 2.6 Electrophysiological identification of ipsilateral cortex and thalamic afferents to neocortical neuron. Cat under barbiturate anaesthesia. (A, B) Two traces representing depth-EEG and intracellular recording from area 7 during the spindle oscillation (7–14 Hz). Seven stimuli to closely located site in cortical area 7 (A) or thalamic lateroposterior (LP) nucleus (B) were applied during active (spindles) and silent phases (interspindle-lulls) of the spindle oscillation. In (A) five superimposed traces illustrate *Cx*-evoked intracellular responses, consisting of short-latency, monosynaptic EPSPs. In (B) EPSPs are elicited in cortical neurons by stimulating LP thalamic nucleus (5 superimposed traces). Note that EPSPs are also short-latency and monosynaptic. Thalamic (Th) and cortical (Cx) stimuli artefacts are marked by triangles and filled circles, respectively. Modified from Fuentealba *et al.* (2004c).

may display monosynaptic EPSPs from both ipsilateral cortex and thalamus (Figure 2.6). The median latencies of callosally evoked EPSPs are 1.5–4 ms in various cortical cell classes (Figure 2.7) but fast-rhythmic-bursting neurons display EPSPs whose amplitudes are three-fold larger, and latencies two- or threefold shorter, than those found in the three other cellular classes (Figure 2.8) (Cissé *et al.*, 2003).[5] Converging callosal and thalamic inputs can be recorded in the same cortical neuron. Some cortical neurons are excited monosynaptically through the callosal pathway and identified antidromically from appropriate thalamic nuclei, thus revealing a callosal–corticothalamic pathway (Cissé *et al.*, 2003).

As to intrinsic cortical connections made by recurrent collateral axons of pyramids within cortical columns, axons arising in layers VI and IV are directed to layer III and another synaptic step occurs from layer III to layer II. In addition, descending inputs link layer IV neurons to layer V and VI neurons. Finally, spiny stellate cells[6] also

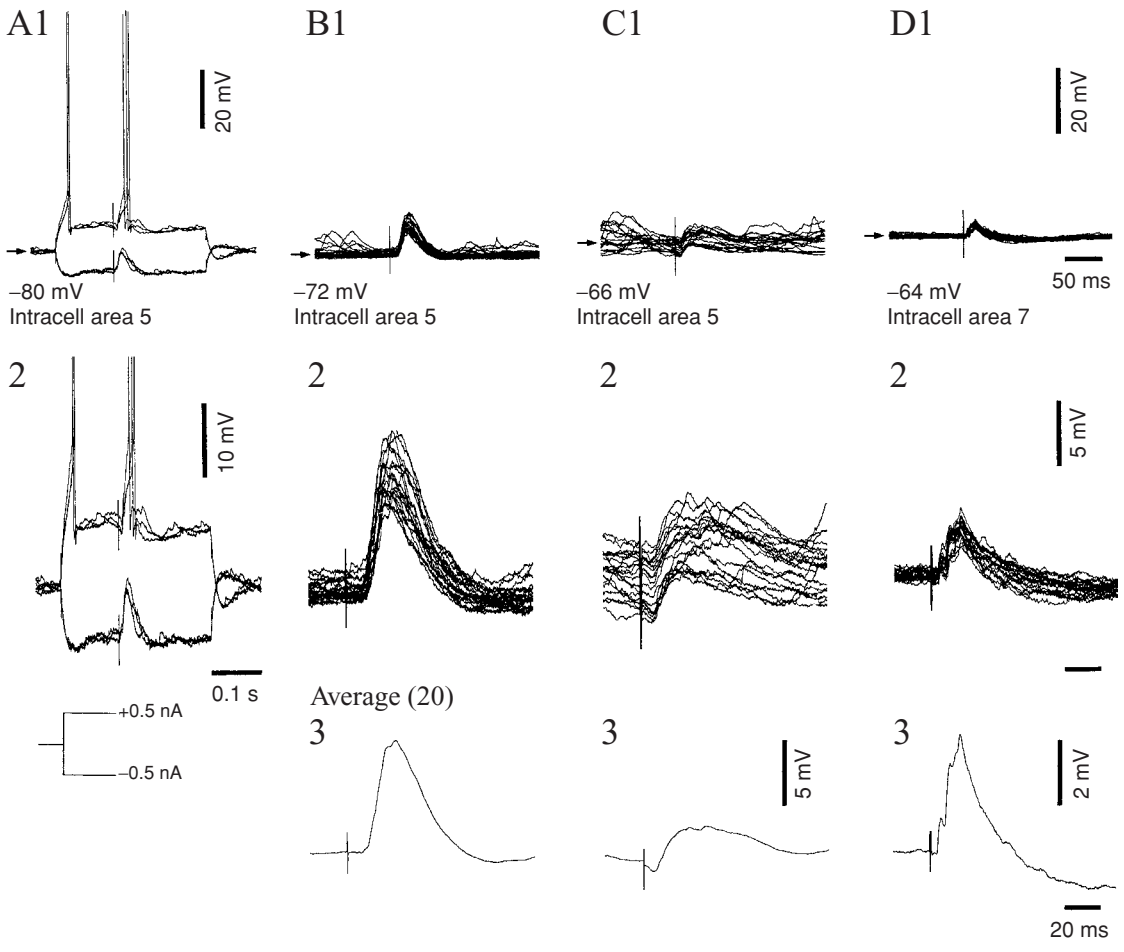

Fig. 2.7 Various types of EPSPs in neocortical neurons evoked by stimulating homotopic sites in the contralateral areas 5 and 7. Four different neurons (A–D) in cats under barbiturate anaesthesia. In (B–D) gain in panel 2 is four times higher than in panel 1. Bottom panels 3 in (B–D) are averages of 20 responses. In (A) contralateral cortical stimuli were applied during depolarizing (+0.5 nA) and hyperpolarizing (−0.5 nA) current pulses of 0.3 s duration. Resting membrane potential is marked by arrows. Modified from Cissé *et al.* (2003).

provide recurrent excitation that can amplify the initial signal in TC pathways, which may extract signals from noisy input patterns (Douglas *et al.*, 1995; Stratford *et al.*, 1996).

2.1.2 Local-circuit inhibitory neurons

There are several types of local inhibitory (GABAergic) interneurons in the neocortex. Some of them are immunoreactive for somatostatin, cholecystokinin, calbindin, vasointestinal peptide and other peptides (Jones, 1975; Somogyi *et al.*, 1983, 1985; DeFelipe & Jones, 1992; Cauli *et al.*, 1997; Kawaguchi & Kubota, 1997).[7]

There are four main classes of local-circuit inhibitory cells. Basket cells (see Figure 2.3) are located in all layers, but especially III and deep

[7] Two subtypes of electrophysiologically characterized interneuron display different immunoreactivity: low-threshold spike (LTS) cells mainly contain calbindin, whereas fast-spiking (FS) cells contain parvalbumin (Kawaguchi & Kubota, 1993). A model of spatial working memory proposed that parvalbumin-containing interneurons produce widespread inhibition by targeting the perisomatic region of pyramids, whereas localized disinhibition of pyramidal neurons would be produced by calretinin-containing interneurons targeting other interneurons (Wang *et al.*, 2004).

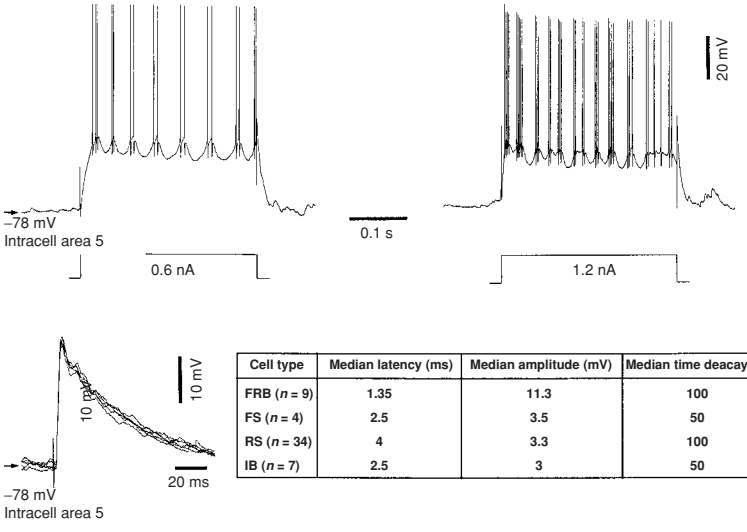

Cell type	Median latency (ms)	Median amplitude (mV)	Median time deacay (ms)
FRB (n = 9)	1.35	11.3	100
FS (n = 4)	2.5	3.5	50
RS (n = 34)	4	3.3	100
IB (n = 7)	2.5	3	50

Fig. 2.8 Fast-rhythmic-bursting (FRB) neurons display callosally evoked EPSPs with highest amplitudes and shortest latencies. Cats under barbiturate anaesthesia. Top panel, identification of FRB neuron by depolarizing current steps (0.5 and 0.7 nA). Bottom left, superimposed EPSPs in the FRB cell depicted above. Bottom right, median latency (ms), median amplitude (mV), and median time decay (ms) in a sample of 54 neurons, consisting of four neuronal types: FRB, fast-spiking, regular-spiking and intrinsically bursting, as identified by their responses to depolarizing current pulses. Modified from Cissé *et al.* (2003).

[8] Tamás *et al.* (1997) found autapses in smooth dendrite-targeting neurons from layers II to V.

layers, and have axons that contact the somata of pyramidal neurons. Chandelier cells are found in layers II–III and their main target is the initial axonal segment of pyramidal cell axons (Somogyi, 1977). Double bouquet cells (Figure 2.3) are concentrated in layers II–III, but some are also found in deep layers and their vertical axons contact both pyramidal and other local-circuit cells. Neurogliaform cells, the smallest interneurons, are located in layer I, where they display a very dense axonal arbor (Hestrin & Armstrong, 1996).

Local inhibitory interneurons self-innervate through autapses.[8] They also form networks of GABAergic cells linked by electrical synapses which are thought to play a role in promoting synchronous activity in the cerebral cortex (Galarreta & Hestrin, 1999, 2002). Chemical synapses among basket-type cells may lead to lateral disinhibition of pyramidal neurons by inhibiting large basket cells (Kisvárday *et al.*, 1993). Comparison between interconnected networks of three classes (basket-type, double bouquet dendritic, and dendrite-targeting) of GABAergic interneurons suggested, on the basis of the strength of innervation and proximal placement of synapses, that basket-type cells play a prominent role in the activity of GABAergic networks in layers II–V (Tamás *et al.*, 1998).

Distinct classes of GABAergic interneurons innervate pyramidal cells in a domain-specific manner. The basic circuit is repeated in each layer, and both tangential and columnar connections are established through specific links between local-circuit inhibitory and pyramidal excitatory neurons (Somogyi *et al.*, 1998). Besides the termination of interneuronal axons in the perisomatic domain of pyramidal neurons, some GABAergic cells (such as double bouquet, neurogliaform and bitufted cells) terminate on the distal dendrites of pyramidal neurons (Somogyi & Cowey, 1981).

With paired recordings from presynaptic interneurons and postsynaptic pyramidal cells, $GABA_A$ receptors in the perisomatic domain

of pyramidal cells were activated by three classes of interneurons (fast-spiking, burst firing and regular-spiking) (Thomson *et al.*, 1996). Simultaneous recordings from pyramidal cells and local interneurons demonstrated that the same axon of a pyramidal neuron innervating another pyramidal cell and a local inhibitory interneuron displayed synaptic depression in the former case and facilitation in the latter (Thomson & Deuchars, 1997; Markram *et al.*, 1998). These data led to a better understanding of the rules underlying frequency-dependent plasticity. Paired-cell recordings also revealed networks of electrically and chemically coupled inhibitory interneurons. Whereas chemical inhibitory synapses are found between both fast-spiking and low-threshold spike interneurons, electrical synapses are only found among the same type of local-circuit inhibitory cells (Gibson *et al.*, 1999). The connections of various types of cortical interneurons, in particular those of axoaxonic chandelier cells (Somogyi, 1977), are important for both normal and paroxysmal properties of cortical neurons.[9]

Besides their role in sculpting inhibitory processes during adaptive states of vigilance, local cortical interneurons display a spectacular, selective firing during ocular saccades in REM sleep. This was initially reported by using extracellular recordings of association cortical units that were assumed to be interneurons. These cells discharged high-frequency spike-bursts in response to thalamic stimulation (Figure 2.9A) and were not antidromically activated from all distant stimulated sites (Steriade, 1978). This was confirmed with intracellular recordings of electrophysiologically identified fast-spiking neurons during the natural sleep cycle (Figure 2.9B) (Timofeev *et al.*, 2001b). The spike-bursts of local interneurons impose IPSPs onto regular-spiking pyramidal cells during ocular saccades in REM sleep (Timofeev *et al.*, 2001b).

[9] See note [38] of Chapter 2 in Steriade (2003a).

2.2 Intracortical, corticothalamic and other long-axon projections

Local circuits link different cortical layers. Corticocortical inputs mainly reach layers II–III (but also deep layers V and VI), whereas afferents from TC neurons reach mainly midlayers IV and lower II (but also layers VI and I). Briefly, axons from neurons located in layers IV, V and VI ascend to layer III neurons and another synaptic step occurs from layer III to layer II, while descending inputs link layer IV neurons to layer V and VI neurons (Mountcastle, 1997, 1998; Jones, 1991). Data obtained from dual intracellular recordings in slices of adult neocortex specified, however, the selectivity in the interlaminar connections of different cortical cell types, namely, ascending layer V axons do not target layer III pyramidal neurons but may target some local interneurons (Thomson & Morris, 2002). Studies with dual voltage recordings in the developing rat neocortex showed that, within

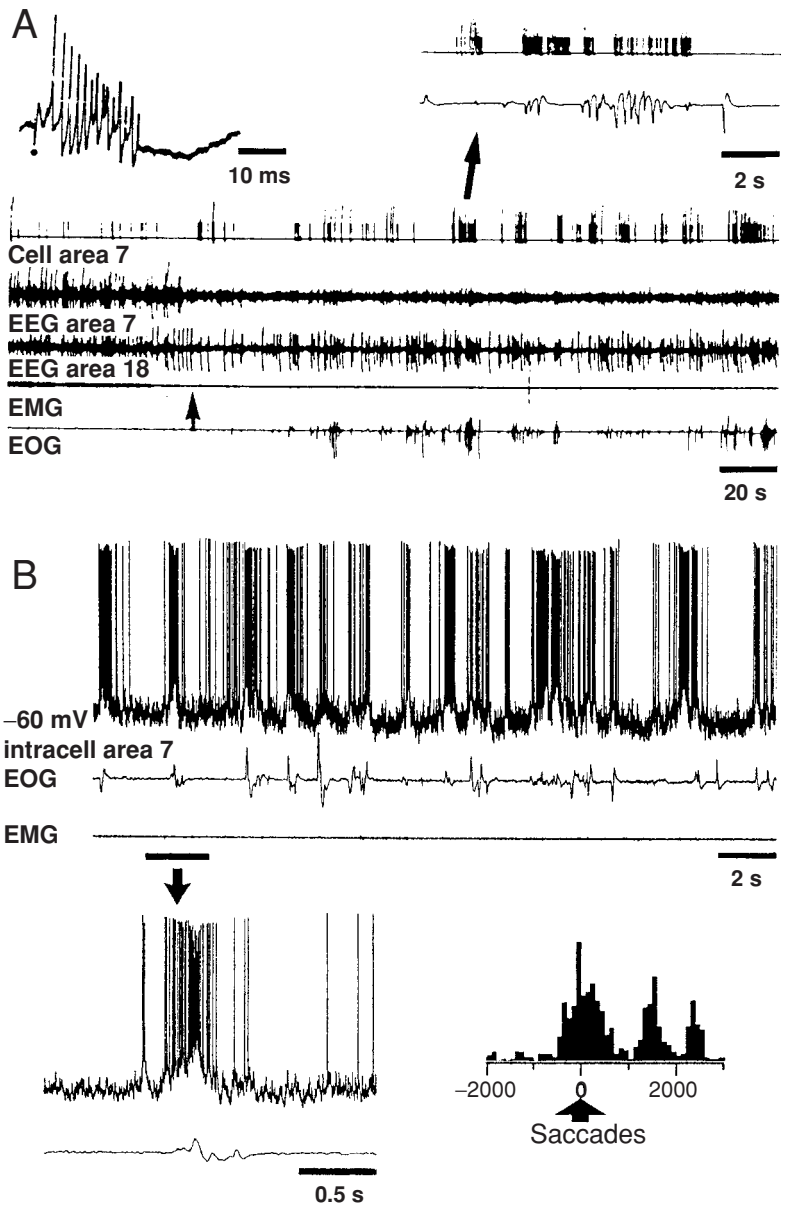

Fig. 2.9 Selectively increased firing of cortical local-circuit (fast-spiking) neurons during ocular saccades in REM sleep. Extracellular (A) and intracellular (B) recordings from association cortex in chronically implanted cats. (A) Five traces depict (from top to bottom): spontaneous firing (recorded on paper) of putative interneuron from area 7; focal slow waves from area 7, recorded through the same microelectrode that recorded action potentials; depth-EEG waves from visual cortex; electromyogram (EMG); and eye movements (EOG). Top: bursting response to stimulation of thalamic lateral posterior nucleus (stimulus artefact indicated by dot). Arrow (upward) indicates expanded epoch with unit firing and eye movements. Arrow below EMG indicates onset of REM sleep (muscular atonia). In contrast with the sustained firing of corticothalamic neurons during REM sleep (see Steriade, 1978), the presumed local-circuit neuron, tentatively identified by its bursting responses and absence of antidromic invasion from all stimulating sites,

layer V, 70% of synaptic connections between pairs of pyramidal neurons are unidirectional and 30% are birectional (Markram *et al.*, 1997). In addition to these connections among neighbouring pyramidal cells, distantly located neurons are linked by monosynaptic connections, as revealed by dual intracellular recordings *in vivo*; these connections have been implicated in the synchronization of low-frequency rhythms that occur during slow-wave sleep.[10]

As to the power of inhibitory effects exerted by local interneurons on pyramidal neurons, dissimilar results were obtained *in vitro* and *in vivo*. Experiments on cortical slices reported more prominent IPSPs in regular-spiking neurons in layers II–III compared with those in layer V (Silva *et al.*, 1991; Van Brederode & Spain, 1995). In contrast, experiments *in vivo* on visual cortex found that IPSPs are more prominent in deep layers compared with neurons recorded from layers II–III, or reported no preferential location of IPSPs between superficial and deep layers (Douglas & Martin, 1991).[11] Such differences, as well as the differences between the nature of IPSPs' components, may reflect regional variations, differences in the afferents recruited by electrical stimuli and/or the presence of rich spontaneous activity in intact brain preparations versus negligible background activity *in vitro* (Douglas & Martin, 1991).

Local intracortical connections may be coupled with corticothalamic projections. Thus, monosynaptic EPSPs could be elicited from area 7 to a neuron located in area 5 that was also antidromically activated from the intralaminar thalamus (see Figure 2.11). Cortical projections to the thalamus originate from neurons in cortical layers VI or V that return axons to the nucleus that provides inputs to that cortical area; corticothalamic neurons outnumber TC ones by about one order of magnitude.[12] Generally, layer VI cortical neurons project to thalamic specific and reticular (RE) nuclei whereas layer V cortical neurons project to intralaminar and some association nuclei as well as the tectum.[12]

Two major functional roles, which have received attention in recent studies, are fulfilled by TC and corticothalamic neurons.

(a) Thalamic inputs from specific and intralaminar nuclei may summate at cortical output neurons in layer V and demonstrate coincidence detection along their apical dendrites (Llinás *et al.*, 2002). Ca^{2+} spike firing activated by back-propagating action potential

fired spike-bursts closely related to ocular saccades in REM sleep. (B) Ocular saccades during REM sleep are associated with increased firing rate in an electrophysiologically identified fast-spiking (FS) cortical neuron. Three traces depict (from top to bottom): intracellular activity of area 7 neuron, eye movements and electromyogram. Upper panel shows that FS neuron (identified by responses to depolarizing current pulses; not shown) increased firing rate during ocular saccades in REM sleep. An ocular saccade is expanded below (horizontal bar and arrow). At right, peri-saccade histogram of neuronal firing. Modified from Steriade (1978, 2004a) and Timofeev *et al.* (2001b).

[10] Amzica & Steriade (1995a,b) described reciprocal connections, revealed by monosynaptic EPSPs, between adjacent association areas 5 and 7 in the cat cortex. The longest intracortical connection links have been described in the neocortex of macaques, by using double labelling of WGA-HRP (or [^{3}H] leucine and proline) placed in the parietal area 7a and WGA-HRP (or tritiated amino acids) in the frontal area 46; these and other experiments showed reciprocal connections between areas 7a and 46 as well as rostral frontal and temporal or cingulate areas (reviewed in Goldman-Rakic, 1987, 1988).

[11] At variance with these data collected from visual cortex, the results of experiments *in vivo* on association cortex could not find any prevalent depth for the location of neurons displaying large IPSPs (Contreras *et al.*, 1997c). In addition, the biphasic, $GABA_{A\text{-}B}$ IPSPs described *in vitro* (Connors *et al.*, 1988) are different from the prolonged, monophasic $GABA_A$, Cl^--dependent IPSPs found *in vivo* (Contreras *et al.*, 1997a,c). The tail of the hyperpolarization in the latter experiments was ascribed to disfacilitation owing to the disruption of the important background activity that is present *in vivo*.

[12] Reviewed in the monograph by Steriade *et al.* (1997). The principle of reciprocity of connections between a given cortical area and the thalamic nucleus from which it receives afferents is generally valid, but some exceptions are notable. For example, there is an apparent lack of projections from visual areas 17 and 18 to the thalamic central lateral intralaminar nucleus that projects to those areas (Cunningham & LeVay, 1986). See also a theoretical view by Deschênes *et al.* (1998), discussing reciprocity versus parity in corticothalamic projections.

(BAP) from layer V pyramidal neurons may provide a potential mechanism for binding different cortical layers, as a single BAP facilitates the initiation of these potentials when it coincides with distal dendritic input within a time window of several milliseconds (Larkum *et al.*, 1999).

(b) Corticothalamic inputs prevalently act on thalamic RE neurons, compared with TC neurons. This finding, which has important consequences for both normal and paroxysmal events, was demonstrated in quantitative electron microscopic studies[13] and dual whole-cell recordings (Golshani *et al.*, 2001). Thus, the amplitudes of cortically elicited excitatory postsynaptic currents (EPSCs) in thalamic RE neurons are 2.4 times larger than in TC neurons, a difference that is related to the fact that GluR4-receptor subunits at synapses on RE neurons outnumber those on TC cells by 3.7 times (Golshani *et al.*, 2001). These differences account for the striking contrast between the effects exerted by corticothalamic neurons on thalamic RE and TC cells. Indeed, despite the fact that all corticothalamic neurons are glutamatergic and excitatory in nature, synchronous electrical volleys or spontaneously occurring spike-bursts (as is the case during slow-wave and cortically generated seizures) produce excitation in RE neurons and, as a result, prolonged, biphasic $GABA_{A\text{-}B}$ IPSPs in TC cells.[14] This effect also explains the power of cortical inputs in eliciting spindle oscillations in TC neurons (Steriade *et al.*, 1972; Contreras & Steriade, 1996) since RE neurons are initiators and pacemakers of spindles (Steriade *et al.*, 1985, 1987a; Bazhenov *et al.*, 1999, 2000). Figure 2.10 shows the generation of spindles in a TC neuron following a single cortical stimulus and the decreased synaptic excitability of that neuron during the cortically evoked spindle sequence (Fuentealba *et al.*, 2004c).

The direct, excitatory actions of corticothalamic cells on thalamic relay cells can be observed in isolation by performing excitotoxic lesions of RE neurons or transections separating them from RE neurons (Steriade & Deschênes, 1987; Deschênes & Hu, 1990). In addition, during the single-spike, tonic firing mode of RE neurons, as in brain-active states of vigilance (Steriade *et al.*, 1986), the effect of corticothalamic inputs is not prolonged IPSPs in thalamic relay cells, but may rather activate high-threshold Ca^{2+} conductances and generate fast oscillations (Pedroarena & Llinás, 1997).

Besides the temporal summation of thalamic inputs acting on different compartments of cortical pyramidal neurons, revealed *in vitro* (Llinás *et al.*, 2002), the convergence of thalamic and cortical afferents was investigated intracellularly *in vivo* and the results showed complex interactions between these two different inputs (Fuentealba *et al.*, 2004c). In contrast to facilitation, at both short and long intervals, of responses evoked in homosynaptic, thalamocortical pathways,[15] heterosynaptic interactions between either cortical and thalamic, or thalamic and cortical, inputs generally produced decreases in the peak amplitudes and depolarization area of evoked EPSPs, with

[13] Liu & Jones (1999) examined the relative contributions of different types of synapse distributed on all portions of the dendritic tree of thalamic RE cells. The majority of excitatory afferents to these cells derived from the cerebral cortex, with a smaller number originating from collateral axons of TC cells.

[14] See Figure 1 in Steriade (2000). During cortically generated seizures, too, bursting in thalamic reticular cells, which faithfully follow each paroxysmal depolarizing event in cortical neurons, accounts for the prolonged hyperpolarization and inactivity of thalamocortical cells (Steriade & Contreras, 1995; Pinault *et al.*, 1998; reviewed in Crunelli & Leresche, 2002; Steriade, 2003a).

[15] Progressive and strong facilitation by stimulating the homosynaptic thalamocortical pathway is seen at time-intervals longer than 60 ms, which represents the mechanism of thalamocortical augmenting responses (Steriade *et al.*, 1998b). All cortical neurons stimulated from thalamic pathways display maximal amplitude of the secondary EPSP at *c.*100 ms, consistent with stimulation within the frequency (10 Hz) of spindles, which is typically used to induce augmenting potentials. Rhythmic volleys produce augmenting responses during the pulse-trains but also facilitation outlasting the stimulation period.

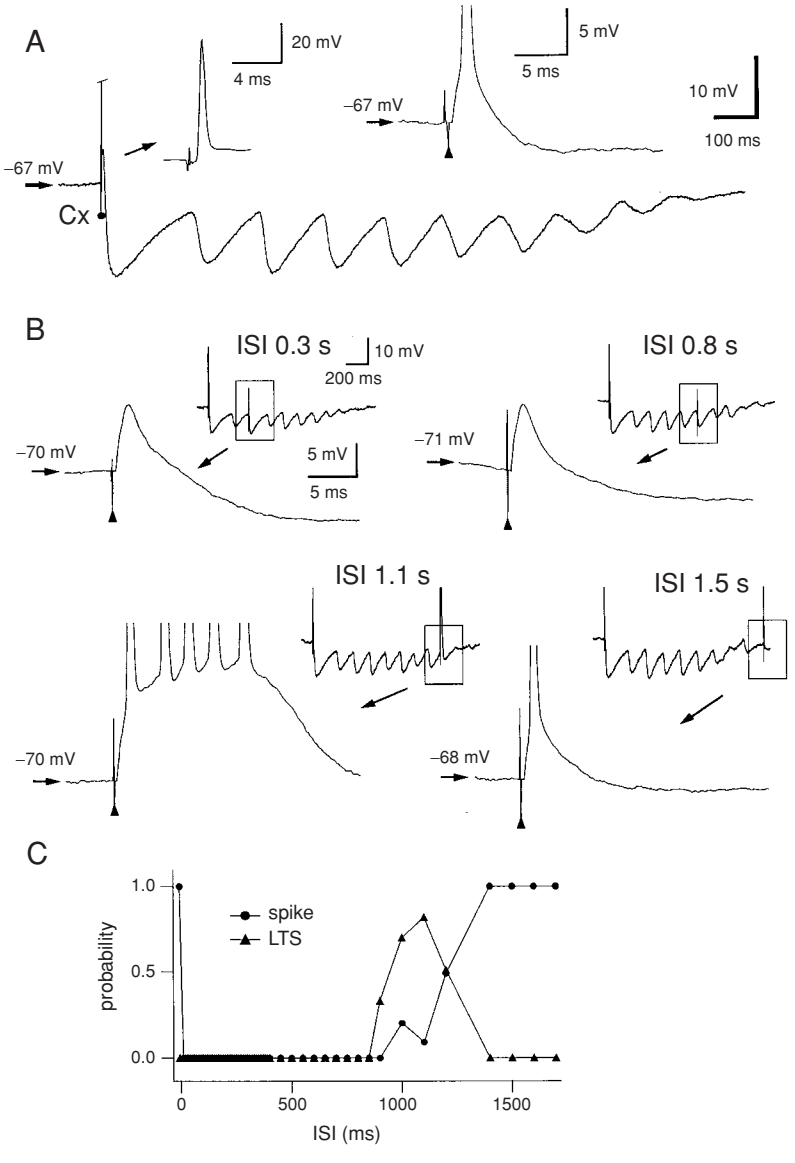

Fig. 2.10 Evolution of cortically (Cx) induced decreased excitability of antidromically identified thalamocortical neuron during spindle sequence elicited by Cx stimulus. Cat under barbiturate anaesthesia. Recording and stimulation within thalamic ventrolateral (VL) nucleus. Cx stimulus applied to area 4. (A) Spindle sequence elicited by Cx stimulus. Insets show antidromic invasion of VL neuron from area 4 (left), and thalamically (Th) induced EPSP leading to action potential in VL neuron (right). (B) Th-evoked EPSPs at different interstimulus intervals (ISIs) following the onset of spindle sequence (0.3 s, 0.8 s, 1.1 s and 1.5 s), as indicated with arrows in the above depicted (minimized) spindles). Note abolition of action potential at 0.3 s and 0.8 s (evoked in A), rebound low-threshold spike-burst at 1.1 s (the end of spindle), and recovery of the control response with single action potential at 1.5 s (after cessation of spindle sequence). (C) Plot showing the probability of a single spike (spike) and low-threshold spike (LTS) at different time intervals following a cortical stimulus. Modified from Fuentealba *et al.* (2004c).

maximal effects at *c.*10 ms and lasting from 60 ms to 100 ms. All neurons tested with thalamic followed by cortical stimuli showed a decrease in apparent input resistance, whose time-course paralleled that of decreased responses (Fuentealba *et al.*, 2004c).

Finally, corticofugal inputs do not only act on the ipsilateral thalamus, as there are modest crossed projections that originate in the frontal lobe of macaques (Goldman, 1979; Preuss & Goldman-Rakic, 1987) and the motor cortex of rats and cats (Molinari *et al.*, 1985). In monkeys, the contralateral thalamic targets are mainly the antero-medial and midline nuclei (Goldman, 1979; Preuss & Goldman-Rakic, 1987). In cat, the contralateral targets of motor cortex projections are intralaminar, ventromedial and ventrolateral nuclei (Molinari *et al.*, 1985). Finally, crossed corticostriatal projections that arise in the

medial agranular cortical field (Wilson, 1987) may ultimately affect the thalamus through a series of synaptic steps in the basal ganglia. Then, the cerebral cortex can influence the thalamus via a rich axonal network that collateralizes to both the striatum and thalamus (Paré & Smith, 1996).

2.3 Intrinsic properties of cortical cells and their changes by synaptic activity

Since the advent of the slice preparation, more than two decades ago, neocortical neurons have been classified according to their intrinsic electrophysiological properties, as determined by responses to intracellular current pulses. Previously, brain functions were only considered in the light of input–output operations and intrinsic properties of cortical neurons were generally neglected. However, work on central neurons in mammalian slices maintained *in vitro* led to the discovery of a host of voltage-gated conductances, which replaced the purely reflexologic view of neurons with the concept that intrinsic neuronal properties generate internal computational states that serve as a reference frame for incoming signals (Llinás, 1988). Although some *in vitro* investigators (Connors & Gutnick, 1990) expressed cautionary notes that emphasized the abnormal reactions of the traumatized tissue and its isolation from other brain structures, which may change neuronal properties, the investigation on slices continued to evolve because of the stability of recordings, the possibility of changing the bathing milieu, and the potential for investigating simultaneously different compartments of the neuron. The consensus was reached that global events (such as sensorimotor operations, neuronal bases of states of vigilance and abnormal developments of brain functions) have to be studied in the intact brain, whereas analytical data (such as the ionic nature of different conductances, interactions between somatic and dendritic currents, and various receptor types) should be investigated in slices. Of course, both *in vivo* and *in vitro* approaches are required for the understanding of the role played by neocortical neurons in brain functions. We will start (Section 2.3.1) by briefly exposing the characteristics of four major neuronal classes and major conductances of neocortical neurons. Next (Section 2.3.2), we will show how firing characteristics may change during silent states and epochs with intense synaptic activity as well as during natural shifts between states of vigilance so that the same neuron may display several discharge patterns (Steriade, 2001a,b, 2004a).

2.3.1 Voltage- and transmitter-gated conductances

Three classes of cortical neurons (regular-spiking, RS; intrinsically bursting, IB; and fast-spiking, FS) were described during the 1980s (Connors *et al.*, 1982; McCormick *et al.*, 1985), while the fourth class

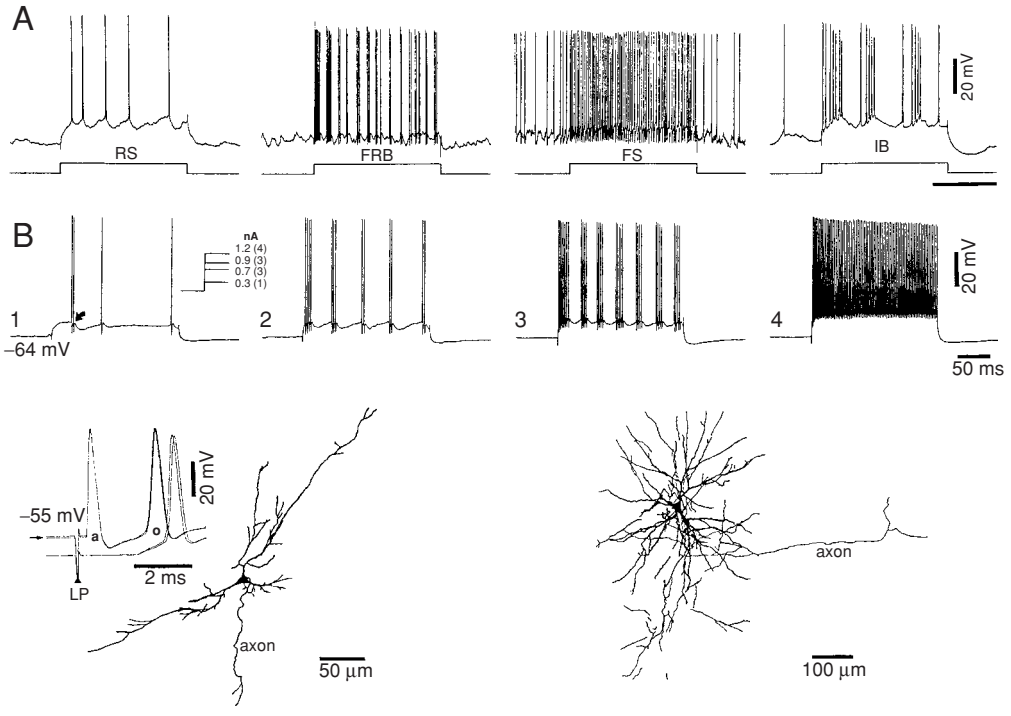

Fig. 2.11 Four neuronal types in neocortex and changes in firing patterns with shifts in membrane potential. (A) Intracellular recordings in chronically implanted, naturally awake and sleeping cats. Responses of regular-spiking (RS), intrinsically bursting (IB), fast-rhythmic-bursting (FRB) and fast-spiking (FS) neurons, recorded from motor area 4, to depolarizing current pulses (0.8 nA, 0.2 s) during quiet wakefulness. (B) Intracellular recording of cortical neuron from association area 7 projecting to, and receiving inputs from, the thalamic lateroposterior nucleus in cat under ketamine–xylazine anaesthesia. Depolarizing current pulses at different intensities (shown in 1 and 2) elicited changing patterns, from RS (1) to FRB with spike-bursts at 25–35 Hz (2–3) and, eventually, to FS patterns (4). A depolarizing afterpotential (DAP) is indicated by the arrow in 1. Below, intracellular recording and staining of two neurons. At left, antidromic identification of corticothalamic neuron projecting to thalamic lateral posterior nucleus (antidromic, a, and orthodromic, o, response at −55 mV; at slightly more hyperpolarized level, antidromic response failed). Close to it, intracellular staining of a corticothalamic neuron that was antidromically identified by stimulating the thalamic rostral intralaminar centrolateral nucleus. At right, intracellular staining of local-circuit neuron of the basket type, whose changes in firing patterns were identical to those of long-axoned pyramidal neurons. Modified from Steriade (1997a, 2004a) and Steriade *et al.* (1998a).

(fast-rhythmic-bursting, FRB) was analysed during the 1990s (Gray & McCormick, 1996; Steriade *et al.*, 1996a, 1998b). These four neuronal types are depicted in Figure 2.11A and are characterized by the following features.

(a) RS neurons generate trains of single spikes that adapt quickly or slowly in response to maintained depolarization. They constitute the majority of cortical neurons and are typically pyramidal-shaped (but some of them are spiny stellate neurons). (b) IB neurons generate clusters of action potentials, with spike inactivation followed by

hyperpolarization and neuronal silence, and are pyramidal-shaped. (c) FRB neurons give rise to high-frequency (300–600 Hz) spike-bursts recurring at fast rates (30–50 Hz) within a certain range of membrane potential. FRB neurons are either pyramidal or local-circuit neurons of the basket type (Figure 2.11B). (d) FS neurons fire thin action potentials (like FRB cells), sustain very high firing rates without frequency adaptation, and are local inhibitory neurons.

The above systematization is taken by some authors as sharply dividing the four neuronal classes and locates different cell types within distinct cortical layers (Gray & McCormick, 1996; Nowak *et al.*, 2003[16]), such as IB neurons in deep layers (Connors & Amitai, 1995) or FRB neurons as pyramidal-shaped cells in superficial layers II–III (Gray & McCormick, 1996; Nowak *et al.*, 2003). However, the only value of this sharp distinction and morphological location is didactic because of its simplicity, while not taking into consideration the complexity of the intact brain. Indeed, as shown below, one neuronal type may display different firing patterns (thus encompassing the electrophysiological features of other neuronal classes), or may be present in virtually all cortical layers from II to VI (as is the case not only with RS neurons, but also with IB and FRB neurons). Moreover, some cell types are abundant in the particular condition of cortical slices *in vitro* or cortical slabs *in vivo* under anaesthesia but their incidence is negligible in the intact cortex of an awake animal.

The changes from one firing pattern into a different one in the same neuron, as a function of changes in membrane potential that in turn depend on the behavioural state, challenges the simple categorization into four distinct neuronal classes. Such changes are due to the presence of intact connectivity and intense synaptic activity *in vivo*, especially during natural states of vigilance in the unanaesthetized animal (Steriade *et al.*, 2001a,b), as opposed to the absence of or negligible background activity *in vitro* (Paré *et al.*, 1998a). Even *in vitro*, with an increase in the thickness of cortical slices by only 0.1 mm, the average probability of each interneuron innervating neighbouring pyramidal neurons increases three to four times (Thomson *et al.*, 1996). The ability of synaptic inputs to alter the basic electrophysiological features of cortical neurons blurs the borders between the various cell types. The statement (Gupta *et al.*, 2000) that, compared with the neuronal responses observed *in vivo*, controlled conditions *in vitro* lead to distinct electrophysiological responses of various neuronal classes is valid, but the uncontrolled synaptic noise is the brain's reality. Before entering this discussion (see Section 2.3.2), we expose further details concerning the intrinsic and synaptic neuronal properties of neocortical neurons.

At variance with the initial assumption that IB neurons are located in a narrow range of depths comprising layer IV and the more superficial parts of layer V (Connors *et al.*, 1982; McCormick *et al.*, 1985; Connors & Amitai, 1995), such neurons were also found not only in layer III, both *in vivo* (Steriade *et al.*, 1993e) and *in vitro* (Nishimura *et al.*, 2001), but also in all cortical layers below layer I (Nowak *et al.*,

[16] This study further divided IB cells into three subclasses, but the authors recognized that the properties leading to this subcategorization are not totally clear.

2003; Chen *et al.*, 1996). This refutes the claim that IB cells are characterized by a 'unique anatomy' (Connors & Amitai, 1995). The spikes comprising the bursts of IB neurons are triggered by the depolarizing after-potential (DAP) of the first spike (Nishimura *et al.*, 2001; Friedman & Gutnick, 1989; Yang *et al.*, 1996).[17] DAPs are enhanced, rather than blocked, by Ca^{2+} channel blockade, which led to the conclusion that the main function of Ca^{2+} influx (at least in layer III IB neurons) is to activate Ca^{2+}-dependent K^+ conductances that prevent or limit burst firing (Nishimura *et al.*, 2001). In some IB neurons, the initial spike-bursts are followed by tonic firing of single action potentials, as in RS cells, both *in vitro* (Connors & Gutnick, 1990) and *in vivo* (Nuñez *et al.*, 1993). A comparison between IB and RS firing patterns in layer V pyramidal neurons revealed that small dendritic depolarization evoked repetitive spike-bursts, whereas after larger dendritic depolarization the initial burst firing was followed by regular firing of single action potentials (Schwindt & Crill, 1999).

In the visual cortex, FRB neurons have exclusively been identified as pyramidal-shaped cells, located in layers II–III (Gray & McCormick, 1996; Nowak *et al.*, 2003). In other studies, however, done on motor, suprasylvian (Steriade *et al.*, 1998a) and visual areas,[18] FRB neurons were also found in infragranular layers. Antidromic invasion from thalamic nuclei showed that deeply lying FRB cells are corticothalamic and intracellular staining demonstrated that, besides the population of pyramidal cells, some FRB neurons are local-circuit, sparsely spiny or aspiny, smooth multipolar or basket-type interneurons (see Figure 2.11B) (Steriade, 1997a; Steriade *et al.*, 1998a). The thalamic projections of cortical FRB neurons, and especially those directed to intralaminar nuclei (Figure 2.11B) may synchronize cortical and thalamic fast activity in the beta/gamma frequency range (Steriade *et al.*, 1991b, 1996a,b), and feed back the integrated activity to widespread cortical areas. As to the transition from RS to FRB and further to FS firing patterns, as seen in different cortical areas *in vivo* (Steriade *et al.*, 1998a) (see Figure 2.11B), a multi-compartment 11-conductance modelling study showed that increasing somatic depolarization leads to such changes (Traub *et al.*, 2003). In particular, the transition from RS to FRB patterns was ascribed to $I_{Na(p)}$ and to a reduction in fast voltage- and Ca^{2+}-dependent K^+ conductances (Traub *et al.*, 2003). The FRB-like firing pattern, with rates of spike-bursts up to 40 Hz and unusually high (900–1000 Hz) intraburst frequencies, have also been recorded intracellularly in thalamocortical cells from a restricted sector of the rostral intralaminar nuclei (Steriade *et al.*, 1993c) and, extracellularly, from the same type of thalamic neurons during natural brain-active states of wakefulness and REM sleep (Steriade *et al.*, 1993c; Glenn & Steriade, 1982). Those very fast-conducting (40–50 ms^{-1}) thalamocortical neurons also displayed rhythmic spike-bursts around 40 Hz during the depolarized states of brain-active epochs, instead of the common firing mode of thalamic neurons, with a tonic mode consisting of single action potentials during relative depolarization. Like FRB cortical neurons, the spikes of thalamic intralaminar neurons

[17] The transition to burstiness in FRB cells is also due to the DAP in the spike-bursts of those cells (see Gray & McCormick, 1996; Steriade *et al.*, 1998a).

[18] FRB neurons were found in layer VI of the visual cortex and were physiologically identified as simple cells (Cardin *et al.*, 2005). In fact, the deep location of neurons with an FRB pattern was first reported in a study of layer VI neurons *in vitro*, reporting that with prolonged depolarizing current pulses, the RS-like firing was transformed into FRB-like firing (see Figure 3, A and C, in Kang & Kayano, 1994).

[19] The spiny or sparsely spiny interneurons described in this article produced fast IPSPs (probably $GABA_A$ mediated) in postsynaptic pyramids (see Figure 9 in that paper; see also Deuchars & Thomson, 1995a).

[20] In that *in vivo* study, IB cells were only occasionally recorded (less than 7% of the total neuronal sample) and therefore were not included in the analysis.

are of very short duration. The high-frequency repetitive firing of FRB neurons is probably related to the presence of voltage-gated K^+ currents of the Kv3 subfamily, which are characterized by very fast deactivation rates, a property that underlies fast repolarization of action potentials without compromising spike initiation or height (Rudy & McBain, 2001). The very brief duration of spikes fired by FRB neurons, *c.*0.3 ms at half amplitude, may be ascribed to these K^+ currents. Actually, FRB pyramidal neurons have been described in cats (Gray & McCormick, 1996; Steriade *et al.*, 1996a, 1998a) but have not yet been described in rodents, in which Kv3 proteins have not been detected in cortical pyramidal neurons (Chow *et al.*, 1999).

Neurons firing with FS patterns are conventionally regarded as representing local-circuit GABAergic neurons, although some local inhibitory neurons fire single action potentials, like RS cells, or spike-bursts (Thomson *et al.*, 1996; Deuchars & Thomson, 1995b[19]). Similarly, some corticothalamic neurons, by definition long-axoned and excitatory in nature, discharge with FS patterns at given levels of depolarization (Steriade *et al.*, 1998a) (see Figure 2.11B). In contrast to classical FS neurons that discharge with very high firing rates, large cholecystokinin basket cells discharge very similarly to pyramidal neurons (Kawaguchi, 2001). Autaptic neurotransmission was found among some FS neurons (Bacci, *et al.*, 2003).

The density of the hyperpolarization-activated cation current (I_H) (Pape, 1996) is higher in the distal dendrite of layer V pyramidal neurons, compared with the proximal dendritic regions and soma, and it may disconnect somatic and dendritic spike initiation zones in those neurons (Berger *et al.*, 2003). I_H, coupled with the low-threshold spike (LTS) and/or the persistent Na^+ current, is implicated in the subthreshold resonance of cortical neurons that mediates normal oscillatory behaviour (Hutcheon *et al.*, 1996) as well as in rhythmic paroxysmal events, characteristic of epileptiform states (Foehring & Waters, 1991; Di Pasquale *et al.*, 1997; Timofeev *et al.*, 2002a; Timofeev & Steriade, 2004).

At variance with the appearance of LTSs in virtually all thalamic neurons, the incidence of such events in cortical neurons was differently reported by various authors. Some reported the presence of LTSs in RS pyramidal neurons from layers V–VI of the medial frontal cortex (de la Peña & Geijo-Barrientos, 1996). Others found LTS-firing neurons in only 10%–15% of explored neurons in the suprasylvian association cortex (Paré & Lang, 1998; Destexhe *et al.*, 2001). In the primary visual cortex, LTS neurons were considered a special type of cell as none of the RS, FS and FRB neurons could generate LTSs (Contreras & Palmer, 2003).[20] Finally, LTSs induced by depolarizing current pulses at hyperpolarized potentials were observed in LTS interneurons, but not in FS cells (Kawaguchi, 1993).

Besides the intrinsic properties of cortical neurons, some synaptic events are crucial in determining neuronal output. Fast prepotentials (FPPs), all-or-none events triggered by synaptic inputs, have been recorded in both anaesthetized and unanaesthetized cats

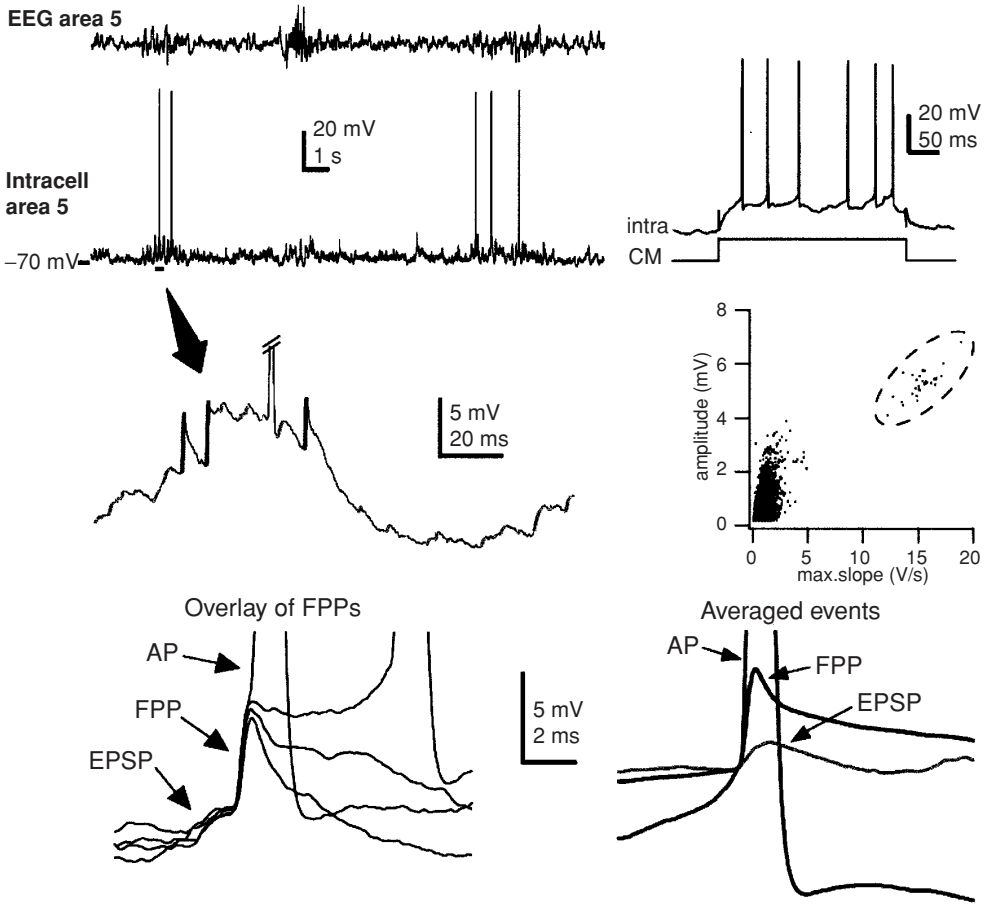

Fig. 2.12 Fast prepotentials (FPPs) in regular spiking (RS) neocortical neurons of cat *in vivo*. Barbiturate anaesthesia. Top left, electroencephalogram (EEG) and intracellular recording in area 5. The neuron was electrophysiologically identified as RS (top right). A part of the intracellular recording is expanded below (arrow). Different depolarizing events extracted are indicated in green (EPSPs) and blue (FPPs). Plotting the amplitude vs. the maximum slope for the selected events (middle panel, right) revealed an FPP population characterized by high-amplitude and fast-rising phase (dashed blue line). The bottom panel shows, on the left, an overlay of four EPSPs leading to FPPs in isolation or leading to full-blown action potential (AP). At right, the superimposition of averaged APs (red trace, truncated), FPPs (blue trace), and 'fast' (max. slope >3 V/s) EPSPs (green trace). Modified from Crochet *et al.* (2004). See Plate 1.

in *c.*20% of RS and IB neurons (Crochet *et al.*, 2004). These events (Figure 2.12), different from EPSPs,[21] were suppressed by hyperpolarization (Figure 2.13). FPPs could be selectively evoked by activation of specific cortical inputs, but not thalamic ones,[22] and allowed neurons to fire at a level of membrane potential more hyperpolarized by *c.*5 mV. Thus, FPPs represent a powerful mechanism to boost the output of neocortical neurons in response to given inputs. These data (Crochet *et al.*, 2004) suggest that FPPs represent attenuated spikes generated in hot spots of the dendritic arbor, which constitute a powerful

[21] Whereas spontaneous EPSPs were characterized by low-amplitude and slow-rising phase, FPPs were high-amplitude (average 6.2 mV) and fast-rising events (see Crochet *et al.*, 2004). The rise-time of FPPs was significantly shorter than the rise-time of the EPSPs.

[22] That FPPs could be elicited by activation of specific cortical inputs but not by thalamic ones (see Figure 6 in Crochet *et al.*, 2004) is at variance with data pointing to thalamic inputs in generating FPPs in cortical neurons (Deschênes, 1981).

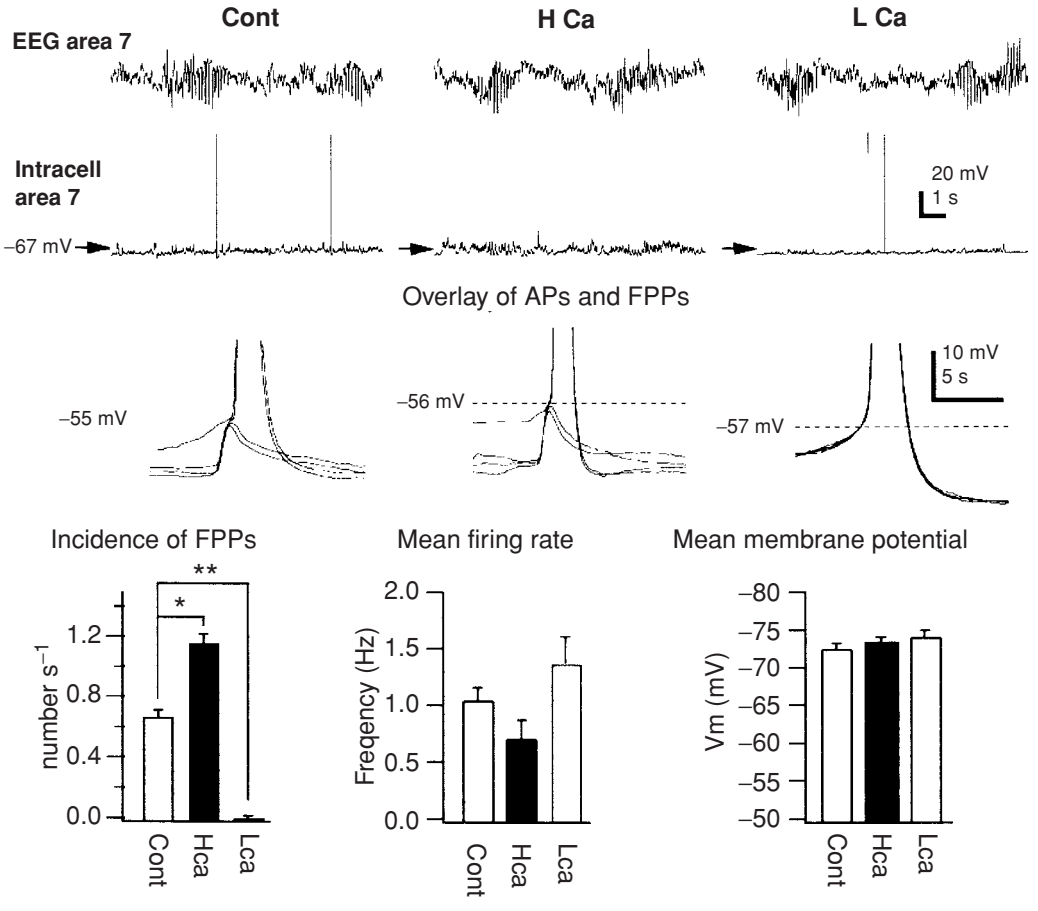

Fig. 2.13 FPPs' generation depends on synaptic transmission. Cat under barbiturate anaesthesia. The upper panel shows the EEG and intracellular recording of a cortical neuron in three conditions of extracellular Ca^{2+} ($[Ca^{2+}]_o$). The same neurons were recorded while a microdialysis probe inserted in the vicinity of the pipette was perfused with normal artificial cerebrospinal fluid (ACSF) (control, Cont), with ACSF enriched in Ca^{2+} (High Ca^{2+}, H Ca) and with Ca^{2+} free ACSF (low Ca^{2+}, L Ca). Note the increase and decrease of the background synaptic activity in H Ca and L Ca conditions, respectively. The middle panel shows the superimposition of action potentials (APs) and FPPs for the three conditions. Note the presence of FPPs in isolation, FPPs of leading to APs, and APs arising from summation of EPSPs in Cont and H Ca conditions whereas in L Ca condition all APs arose from EPSPs. Note also the change in firing threshold for axosomatic APs. The left bottom panel shows the mean incidence (±SEM) of FPPs in the three conditions of extracellular Ca^{2+} calculated for the neuron depicted in the upper panels. The middle and right bottom histograms show the mean firing rates and mean V_m s (±SEM) calculated for 10 cortical neurons in the three conditions. Asterisks represent significant difference: *, $p < 0.05$; and **, $p < 0.01$. Modified from Crochet *et al.* (2004).

mechanism to reinforce the functional connections between specific elements of the cortical networks.

2.3.2 Modulation of intrinsic properties by synaptic activity and behavioural states

The difficulty of extrapolating from experiments *in vitro* to the situation in the intact brain has been repeatedly emphasized (Steriade, 2001a,b, 2004a; Paré *et al.*, 1998a; Svoboda *et al.*, 1997; Destexhe *et al.*, 2003). It is due to differences in the membrane potential, input resistance, ionic composition, spontaneous synaptic activity and degree of channel activation/inactivation. These factors influence the variability and frequency of discharges and neuronal responsiveness as well as the incidence and firing patterns of different cellular types.

The differences between recordings *in vivo* of neocortical neurons under anaesthesia and recordings *in vitro* of the same type of neuron have been analysed; the results are as follows. The standard deviation of the intracellular signal is 10–17 times lower *in vitro* than *in vivo*; and the apparent input resistance (R_{in}) measured *in vivo* during quiescent periods was reduced by up to 70% during epochs associated with intense synaptic activity and increased by 30%–70% after tetrodotoxin (TTX) application *in vivo*, approaching the values *in vitro* (Paré *et al.*, 1998a). The negative membrane potential and higher R_{in} of cortical neurons recorded *in vitro* are similar to the values found in small cortical slabs *in vivo* (−70 mV and 49 MΩ) compared with −62 mV and 22 MΩ for the intact cortex (Timofeev *et al.*, 2000). Combined computational and intracellular studies reported that, with injection of background synaptic noise, cortical neurons were depolarized by 10–15 mV, their R_{in} decreased fivefold, and spontaneous firing had a high coefficient of variation, approaching the values observed *in vivo* (Destexhe & Paré, 1999, 2000; Fellous *et al.*, 2003; Rudolph & Destexhe, 2003).

Experimental evidence shows that the spontaneously occurring and/or stimulus-evoked firing of neurons recorded from neocortical slices *in vitro* displays much less variability than *in vivo* (Snowden *et al.*, 1992). In intact-brain animals, neocortical neurons fire spontaneously with irregular interspike intervals during all behavioural states. However, the degree of irregularity depends on the state of vigilance. This was observed during the natural waking–sleep cycle of chronically implanted primates and cats (Evarts, 1964, 1965; Steriade *et al.*, 1974a; Steriade, 1978). Despite the fact that cortical neurons are bombarded with synaptic inputs during the brain-active state of wakefulness, they display more regular spontaneous discharges during waking than in resting sleep (Evarts, 1964, 1965; Steriade, 1978; Steriade *et al.*, 2001a,b),[23] as well as an increased and stable R_{in} (Steriade *et al.*, 2001a,b). The increased and stable R_{in} during wakefulness may be explained by acetylcholine and glutamate acting at metabotropic receptors during this brain-active state. These neuromodulators are released by cholinergic nucleus basalis neurons and glutamatergic thalamocortical neurons, which fire at high rates

[23] During wakefulness, the spontaneous firing of electrophysiologically identified corticothalamic and corticospinal neurons is tonic, with single action potentials recurring without large variations in interspike intervals. In contrast, during slow-wave sleep, spike-bursts of irregularly distributed action potentials are interspersed with long periods of neuronal silence. Correlatively, during waking, the interspike interval histograms show a Gaussian-like distribution, whereas during sleep the distribution is Poisson-like, with almost 20% of intervals very long. These data, from extracellular recordings (Steriade, 1978; Steriade *et al.*, 1974a), have recently been substantiated using intracellular recordings in behaving animals (Steriade *et al.*, 2001a,b).

during wakefulness and increase the R_{in} of neocortical neurons (see Steriade, 2001a,b, 2004a). The reliability of firing patterns increases with fluctuating current waveforms applied in cortical slices, resembling high-frequency synaptic activity *in vivo*, and a role for spike timing in the processing of cortical information was postulated (Mainen & Sejnowski, 1995). Cholinergic stimulation in cortical slices increases the firing rate of neocortical neurons, but displaces by less than 3 ms the spike times in response to fluctuating inputs, thus enhancing spike timing by recruiting additional spikes, without losing the precision of information (Tang *et al.*, 1997).

Experiments *in vivo* have demonstrated that the spontaneous activity of cortical neurons during alertness, either spontaneous in naturally awake animals or elicited by stimulating brainstem cholinergic nuclei, is characterized by high-frequency (30–40 Hz) oscillations, which are not random but synchronized among closely spaced neuronal populations (Steriade *et al.*, 1996a). The physiological condition of increased alertness is associated with an increased intrinsic and synaptic responsiveness, as well as with a reduced duration of hyperpolarizations coupled to the enhancement of short inhibitory processes produced by local-circuit GABAergic neurons (Steriade & Deschênes, 1974; Livingstone & Hubel, 1981).[24]

The high background synaptic activity of cortical neurons in the intact cortex investigated *in vivo* characterizes not only the states of increased brain alertness but also slow-wave sleep and states in which sensory stimulation is absent (Steriade *et al.*, 2001a,b). The high level of spontaneous activity, occurring either spontaneously *in vivo* or mimicked by ionic manipulations and electrical stimulation *in vitro*, was implicated in the generation of spontaneously occurring brain rhythms, synchronized among distant or neighbouring pools of cortical neurons (Steriade *et al.*, 1993e, 1996a; Mao *et al.*, 2003).[25] Computational and *in vitro* studies (Hô & Destexhe, 2000; Shu *et al.*, 2003) have reproduced the intense background activity observed *in vivo* (Steriade *et al.*, 2001a,b) by injecting currents or by comparative analysis of the depolarizing ('up') and hyperpolarizing ('down') phases of the slow oscillation (Steriade *et al.*, 1993e,f; Sanchez-Vives & McCormick, 2000). In these conditions, it was found that background activity enhances the probability of supra-threshold response to otherwise undetectable inputs and decreases the latency and jitter of action potentials (Hô & Destexhe, 2000; Shu *et al.*, 2003).

The high levels of spontaneous synaptic activity seen *in vivo* also affect the likelihood that action potentials (AP) generated in the initial axonal segment will back-propagate to the dendrites. AP back-propagation was mainly described in slices maintained *in vitro* (Larkum *et al.*, 1999; Stuart & Sakmann, 1994; Stuart *et al.*, 1997). *In vivo*, however, it would be expected that high levels of background firing would severely limit back-propagation. Even *in vitro*, unitary IPSPs abolish the Ca^{2+} influx associated with back-propagating APs (Larkum *et al.*, 1999). Studies *in vivo* have investigated the dendritic Ca^{2+} dynamics in neocortical vibrissae cortex and concluded that the

[24] See Figures 4.8 and 4.14 in Steriade (2003a), with intracellular recordings in naturally awake and sleeping animals, showing enhancement of intrinsic somatic excitability tested by depolarizing current pulses, and persistence of short but large-amplitude IPSPs, during brain-active states of waking and REM sleep.

[25] See also the modelling study by Wiedermann & Lüthi (2003).

greatest number of APs in response to whisker deflections occurred in the proximal part of apical dendrites, whereas it decreased steeply with increasing distance from the soma (Svoboda *et al.*, 1997, 1999). Intracellular recordings from RS pyramidal neurons in layers II–III of the primary somatosensory cortex showed that Na^+ APs in the soma are rapidly attenuated at small distances from the soma (80 μm), becoming only one third to one quarter of the soma amplitude at a distance of 150 μm (Svoboda *et al.*, 1999). The weakening of back-propagating APs is especially seen with inhibition (Larkum *et al.*, 1999; Frégnac, 1999). The effect of synaptic inputs on soma–dendrite interactions was investigated in cat neocortex *in vivo*, using intracellular recordings and computational models. This analysis led to the conclusion that IPSPs of sufficient amplitude can reduce or prevent the back-propagation of APs into the dendrites (Paré *et al.*, 1998b).

Probably the most dramatic influences exerted by synaptic activity and shifts in natural states of vigilance are those that affect the firing patterns of different neuronal types in neocortex and, consequently, the incidence of electrophysiologically defined cellular classes. These changes are discussed below.

The firing pattern of each of the four cell types in neocortex (RS, FRB, FS and IB; see above Section 2.3.1) can be transformed by slight changes in membrane potential during application of direct current or during shifts from one state of vigilance to another. Therefore, there is no 'unique physiology' for any of these four cortical cellular classes, as was assumed to be the case in IB neurons (Connors & Amitai, 1995). Two major examples follow. (a) The spike-bursts of IB neurons may shift to the strikingly different single action potentials of RS neurons when a steady depolarizing current of merely 0.2 nA is applied (Timofeev *et al.*, 2000). This transformation occurs not only with intracellular current but also when synaptic activity increases, leading to slight depolarization of IB neurons (Steriade *et al.*, 1993a) (Figure 2.14A). Also, the transition from IB to RS firing patterns was reported in chronically implanted animals, during transition from natural slow-wave sleep to either waking or REM sleep (Steriade *et al.*, 2001a,b) (Figure 2.14B). The opposite transition, from RS to IB firing, is observed in cases where marked depolarizations (*c.*7–10 mV) activate the persistent Na^+ current, which generates depolarizing after-potentials. When such depolarizations occur, the incidence of IB-like spike-bursts is much higher during brain-active states than during slow-wave sleep (Figure 2.15). Thus, the IB firing pattern appears in a relatively discretely range of membrane potentials. (b) With slight changes in the membrane potential, the discharge pattern of FRB neurons shifts to two other forms of action potential timing characteristic of RS and FS neurons. Thus, FRB neurons can fire like RS cells when they are slightly hyperpolarized or like FS neurons when they are slightly depolarized (see above, Figure 2.11B). Similar changes occur in antidromically identified corticothalamic cells and in local-circuit inhibitory neurons (Steriade *et al.*, 1998a). Such shifts in firing patterns have also been obtained in computational studies, where the

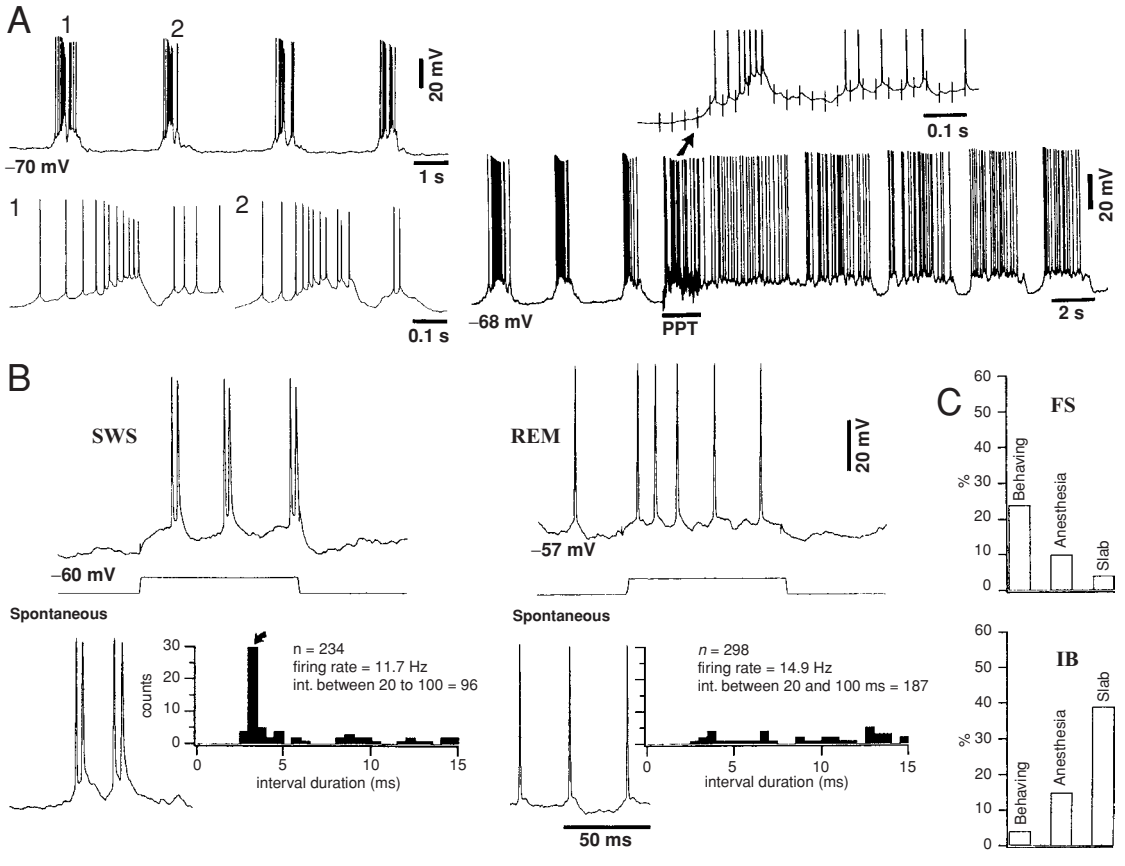

Fig. 2.14 Transformation of intrinsically bursting (IB) into regular-spiking firing pattern. (A) Intracellular recordings in cats under urethane anaesthesia. Left, slow oscillation in IB neuron from area 5. Depolarizing components 1 and 2 are expanded below. Right, changes in firing pattern of slowly oscillating IB neuron from area 7 into tonically firing, regular-spiking (RS) pattern following stimulation (30 Hz, 1.8 s) of pedunculopontine tegmental (PPT) nucleus. Onset of PPT-induced response is expanded above (arrow; action potentials truncated). (B) Intracellular recordings in chronically implanted, naturally awake and sleeping cat. IB cell from association area 7 transformed its firing patterns into that of RS cell when the animal passed from slow-wave sleep (SWS, membrane potential −60 mV) to REM sleep (−57 mV). Responses to depolarizing current pulses and, below, spontaneously occurring discharges. Note spike-doublets in SWS and single spiking in REM sleep. The interspike interval histograms of spontaneous firing in each state of vigilance show a mode at 3–3.5 ms (arrow) in SWS (reflecting bursting activity), absence of this mode in REM sleep, and many more longer intervals (20–100 ms) in REM sleep, reflecting single spike firing. (C) Percentage distribution of FS and IB cortical neurons under different experimental conditions: behaviourally awake cats with intact brain, intact cortex of cats under deep anaesthesia (ketamine–xylazine and urethane), and small isolated cortical slabs *in vivo* under ketamine–xylazine anaesthesia. Modified from Steriade *et al.* (1993a) and Steriade (2004a).

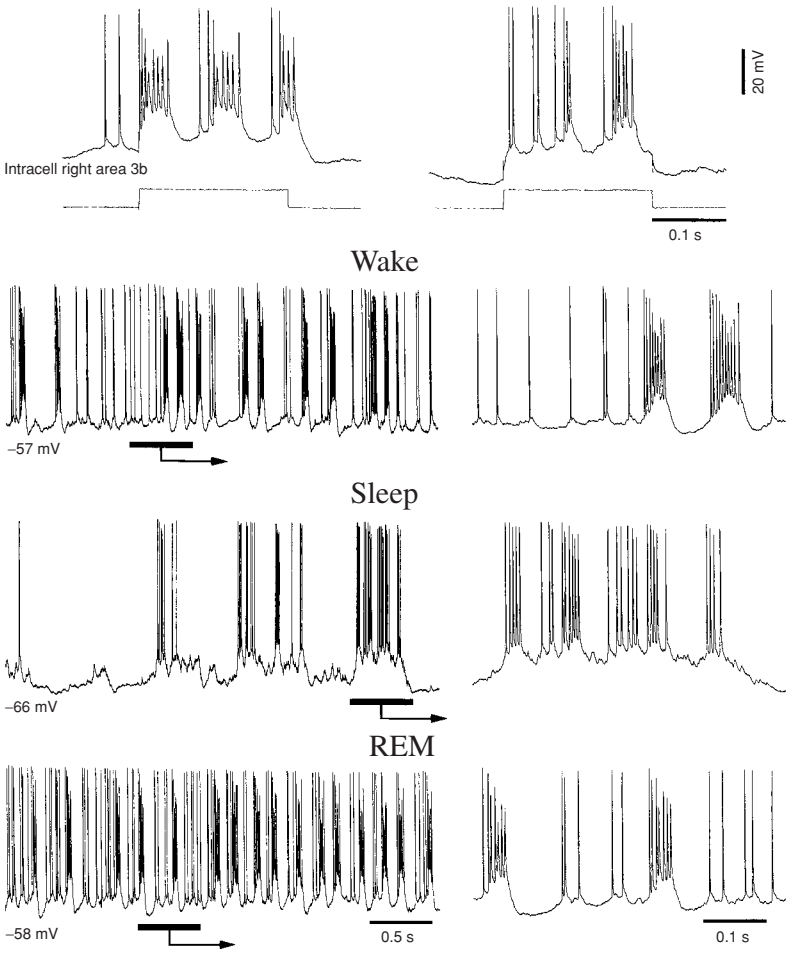

Fig. 2.15 Higher incidence of spike-bursts fired by intrinsically bursting (IB) cortical neuron during waking and REM sleep states than in slow-wave sleep, when the membrane potential during brain-active states is markedly depolarized (c.9 mV), thus contrasting with the slight depolarization that occurs usually. Intracellular recording from somatosenstory cortex in chronically implanted cat. Top, responses of IB cell to depolarizing current pulses. Below, firing patterns of IB neuron during waking, slow-wave sleep and REM sleep. Parts marked by horizontal bars and arrows are expanded at right. Unpublished data by M. Steriade, I. Timofeev and F. Grenier.

ionic conductances that underlie these changes have been identified (Traub *et al.*, 2003; Wang, 1999).

The above alterations in firing patterns during different states have important consequences for the incidence of different cell classes. Indeed, the transformation of IB-type firing patterns into RS-type under slight depolarization explains the low percentage (<7%) of such cells in acute experiments on intact cortex of anaesthetized animals (Contreras & Palmer, 2003) and even lower proportions (4%) during wakefulness in chronically implanted animals (Steriade *et al.*, 2001a,b), compared to the high percentages (40%–60%) in isolated cortical slabs (Timofeev *et al.*, 2000) or in slices maintained *in vitro* (Nishimura *et al.*, 2001; Yana *et al.*, 1996). The very low proportions of IB neurons during natural wakefulness (Steriade *et al.*, 2001a,b) and the location of such neurons in infragranular as well as supragranular layers (Nowak *et al.*, 2003; Steriade *et al.*, 1993e; Nishimura *et al.*, 2001) cast doubt on the assumption that deeply lying bursting neurons selectively generate consciousness (Koch, 1998), which preferentially occurs during waking. On the other hand, FS neurons are found in a relatively

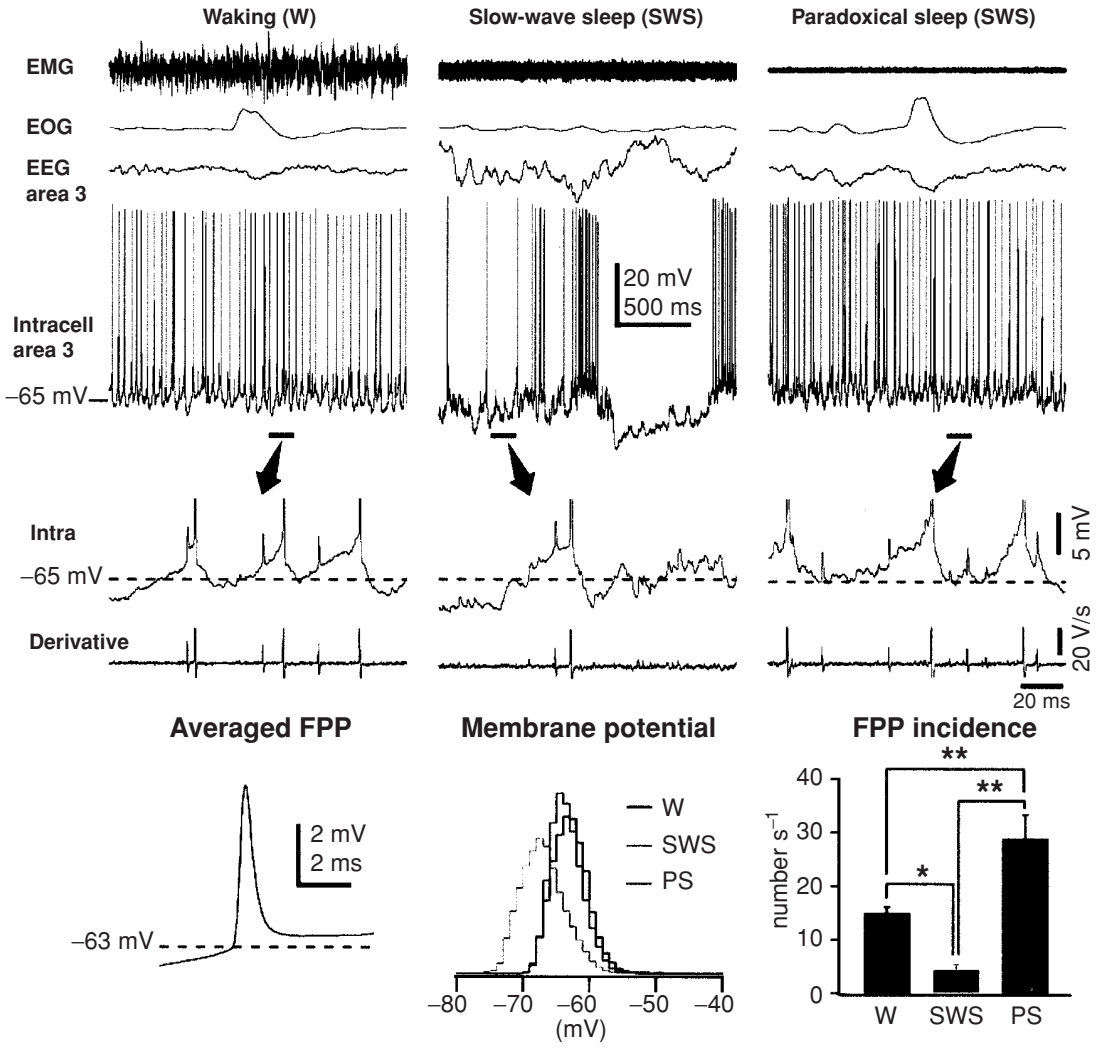

Fig. 2.16 Fast prepotential (FPP) generation is regulated across the states of vigilance. Four traces in the top panel depict electromyogram (EMG), electro-oculogram (EOG), EEG from the depth of right cortical area 3 (somatosensory), and intracellular recording from left area 3. The same neuron was recorded during waking (W), slow-wave sleep (SWS) and paradoxical (PS) sleep (REM sleep). Parts of the intracellular recording marked by horizontal bars are expanded below. The derivative of the intracellular signal revealed the presence of FPPs (action potentials are truncated in the intracellular recording and its derivative). Note the absence of FPP when the cell is more hyperpolarized than −65 mV. The left bottom panel shows averaged FPPs. The middle bottom panel shows the distribution of V_m of the neuron depicted in the three behavioural states (W, red; SWS, green and PS, blue). The right bottom panel shows the mean incidence of FPPs in the three behavioural states calculated for eight neurons. Asterisks represent significant difference: *, $p < 0.05$; **, $p < 0.01$. Modified from Crochet *et al.* (2004). See Plate 2.

high proportion (25%) during natural waking (Steriade *et al.*, 2001a,b), much higher than usually reported in the intact cortex of animals under anaesthesia (10%) or in isolated cortical slabs. This increased proportion of FS-type firing pattern during the wakeful state may be explained by the transformation of FRB-type neurons into FS-type neurons with increased levels of depolarization (see Figure 2.11B).

The incidence of some forms of synaptic activity, such as fast prepotentials (FPPs), is also modulated by natural states of vigilance (Crochet *et al.*, 2004). Thus, FPPs are present in all behavioural states but their frequency varied with the membrane potential (Figure 2.16). During slow-wave sleep, the mean membrane potential was more hyperpolarized and the incidence of FPPs was the lowest (*c.*4.5 Hz). It was significantly higher during waking (*c.*15 Hz) and REM sleep (29 Hz).

The above results cast doubts on the validity of an inflexible systematization of neocortical neurons into four cell classes. Intrinsic cellular properties, which are best studied in slices, are modulated and even overwhelmed by the high synaptic activity in the intact brain of behaving animals (Steriade, 2001a,b, 2004a).

Chapter 3

The amygdala

This chapter describes the structure and connections of the amygdala, emphasizing three of its main components: the basolateral complex, the central nucleus and the intercalated cell masses. As we shall see in detail below, the basolateral complex is a cortex-like structure that receives most sensory inputs to the amygdala and projects to the central nucleus. In turn, the central nucleus contributes most amygdala projections to brainstem nuclei generating components of fear responses. However, because it would be would be maladaptive if all sensory inputs triggered fear, impulse traffic between the basolateral complex and central nucleus must be flexibly gated as a function of the particular combination of sensory inputs and environmental signals confronting the organism. This is the function of the intercalated cell masses, clusters of GABAergic neurons that receive glutamatergic inputs from the basolateral complex and project to central nucleus. This chapter will describe the connectivity and physiological properties underlying this process. Their system-level consequences will be considered later in this book (Chapter 9).

3.1 Is the amygdala a valid anatomical concept?

The amygdala is a nucleated structure located in the depth of the temporal lobe (Figures 3.1 and 3.2). Early anatomists divided the amygdala into three groups of nuclei (Johnston, 1923; Humphrey, 1936; Fox, 1940; Crosby & Humphrey, 1941): (1) the basolateral complex, comprised of the lateral, basolateral and basomedial nuclei; (2) the corticomedial group including the central, medial and cortical nuclei; and (3) an ill-defined anterior group including the anterior amygdaloid area, the nucleus of the lateral olfactory tract and the intercalated cell masses. Subsequent anatomical investigations provided some support for this division. Indeed, a useful albeit simplified statement emerging from these studies is that most cortical projections of the amygdala arise from the basolateral complex (Krettek & Price, 1977a,b; Amaral & Price, 1984) whereas the corticomedial group is

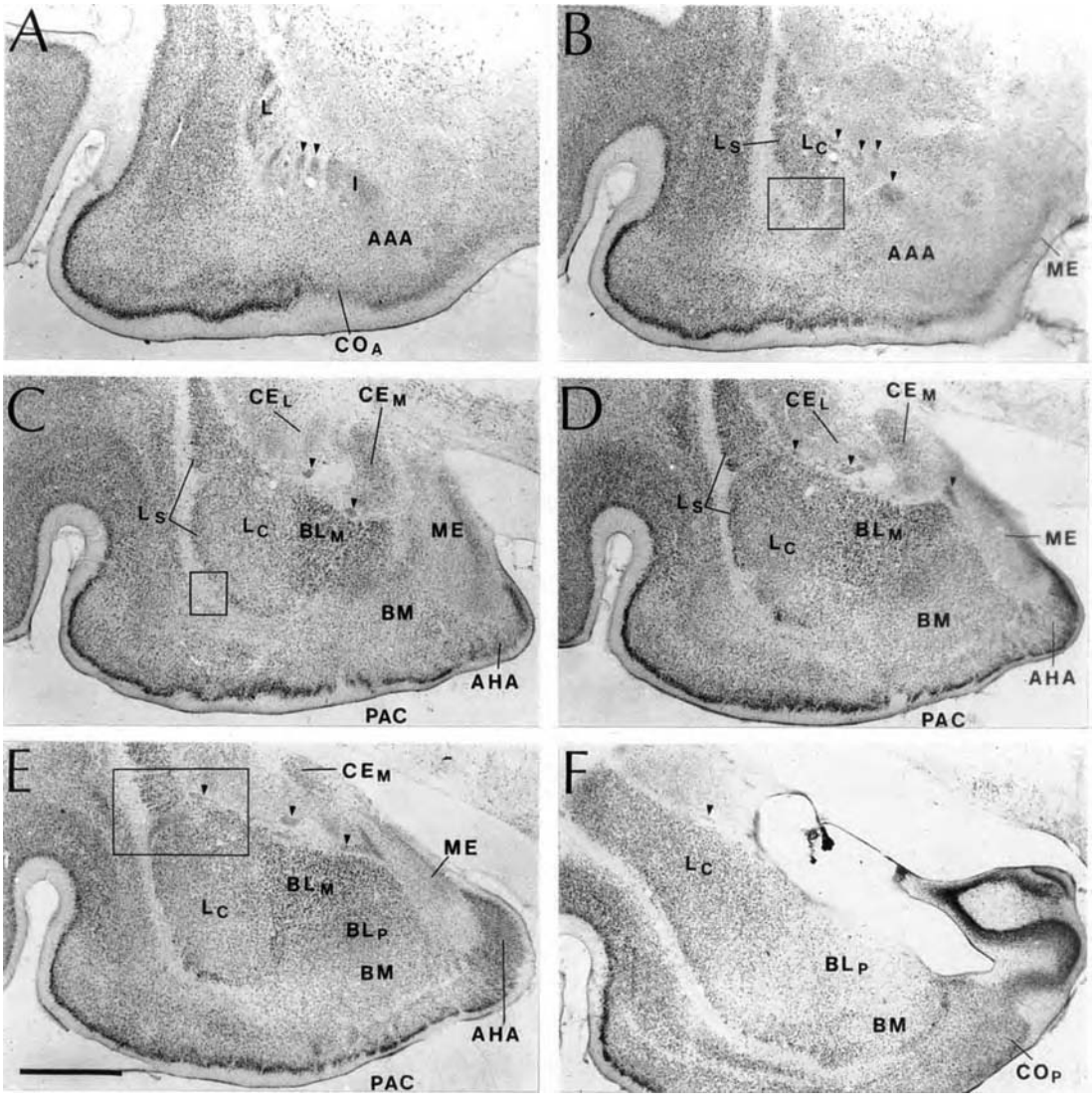

Fig. 3.1 The amygdala of the cat as shown on coronal sections arranged from rostral in (A) to caudal in (F). Thionin stain. Scale bar corresponds to 2 mm and is valid for all panels. Areas delimited by squares in (B), (C) and (E) are expanded in Figure 3.2. Arrowheads mark intercalated cell masses. Abbreviations: AAA, anterior amygdaloid area; AHA, amygdalo-hippocampal area; BL, basolateral nucleus; BM, basomedial nucleus; CEL, central lateral nucleus; CEM, central medial nucleus; COA, anterior cortical nucleus; COP, posterior cortical nucleus; I, intercalated cell mass; LC, core of the lateral nucleus; LS, shell of the lateral nucleus; ME, medial nucleus; OT, optic tract; PAC, periamygdaloid cortex; PU, putamen. Modified from Paré & Smith (1993a).

mainly related to structures involved in visceral and autonomic processes (Holstege, 1990; Hopkins & Holstege, 1978).

Nevertheless, several factors suggest that this tripartite classification is not valid. First, although the use of the term nucleus is appropriate for nuclei such as the lateral, basolateral and basomedial

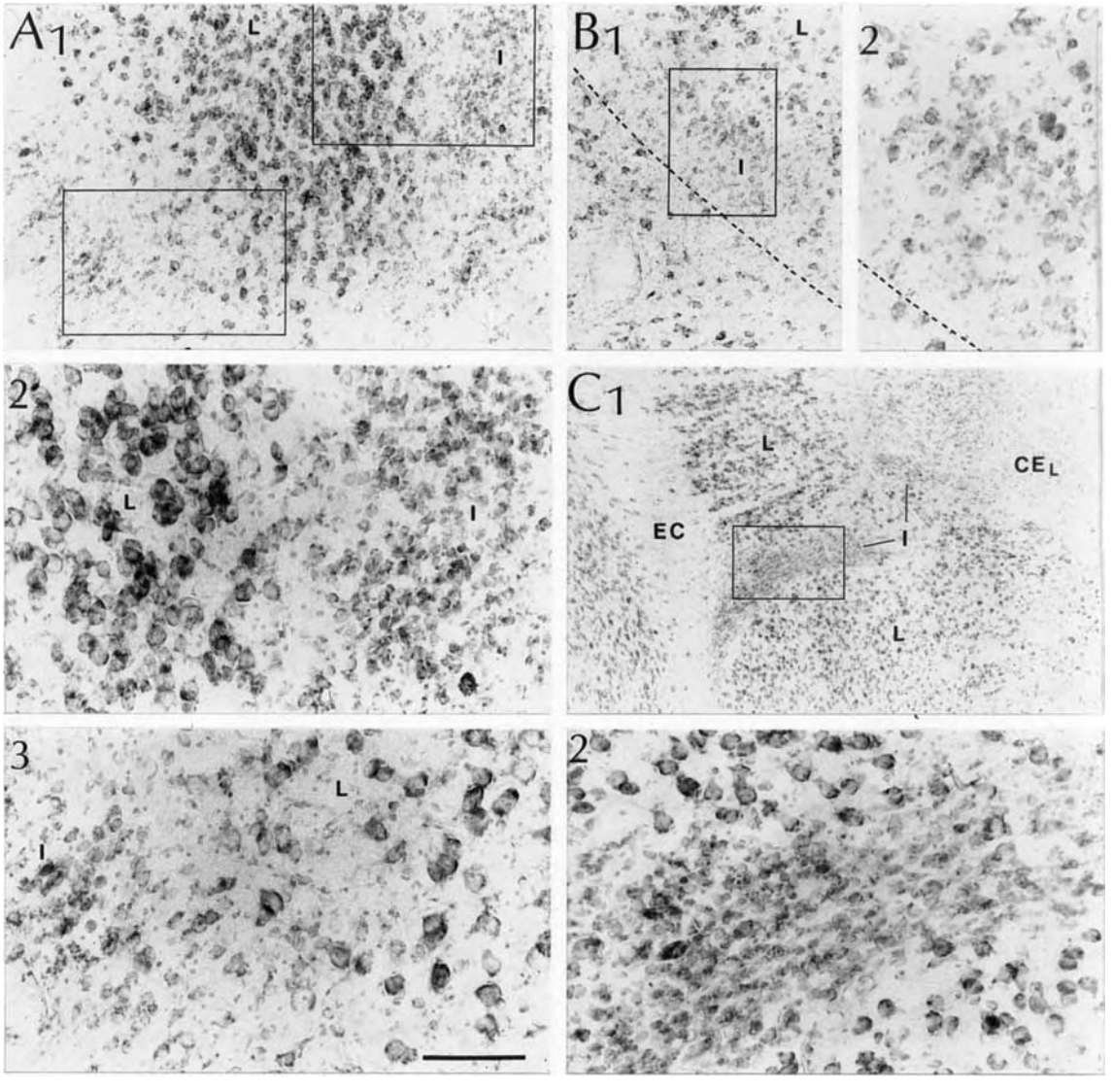

Fig. 3.2 Intercalated cell masses (I) located along the medial and lateral edges of the lateral nucleus. Dashed lines indicate external capsule. Thionin stain. Note small diameter of intercalated neurons compared with cells of the lateral nucleus. Areas delimited by squares in panels 1 are expanded in panels 2–3. Scale bar in (A3) corresponds to 0.25 mm in (A1) and (B1), to 0.5 mm in (C1), and to 0.1 mm in (A2–3) and (C2). Modified from Paré & Smith (1993a).

nuclei, it is a misnomer for the cortical nuclei. Indeed, these nuclei display a laminar organization and cellular composition typical of cortex (Figure 3.3A). This is in contrast to the central nucleus for instance where neurons are oriented randomly (Figure 3.3B) (McDonald, 1992a).

Second, the cellular composition and neurotransmitter content of the central and medial nuclei is completely distinct from that of the so-called cortical nuclei. For instance, when one examines the distribution of neurons expressing glutamic acid decarboxylase (GAD), the synthetic enzyme of GABA, in the amygdala and surrounding structures (Figure 3.4), it becomes clear that the central and medial nuclei contain a much higher number of positive neurons than the cortical nuclei and basolateral complex, for instance (Figure 3.4). In fact, the central and medial nuclei appear to form a continuous band of cells with the putamen (Esclapez *et al.*, 1993).

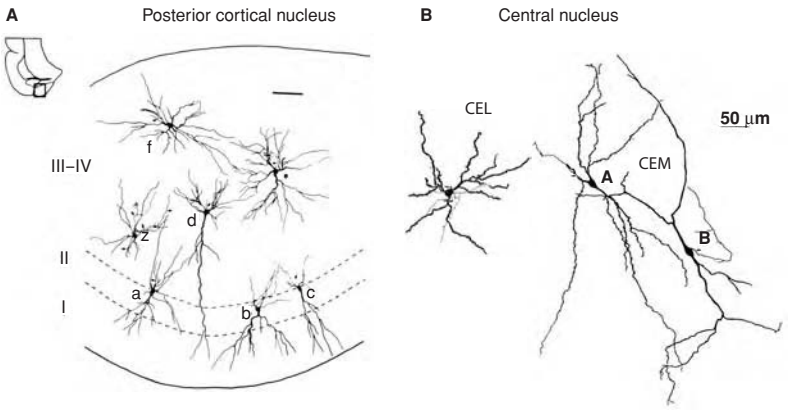

Fig. 3.3 Golgi-impregnated neurons in posterior cortical nucleus (A) and central nucleus (B). Roman numerals in (A) indicate layers. Cells a–e in (A) are spiny pyramidal neurons with a dominant apical dendrite oriented perpendicular to the cortical surface. In contrast, CE neurons (B) are oriented randomly. Scale bar in (A), 100 μm. Modified from McDonald (1992a).

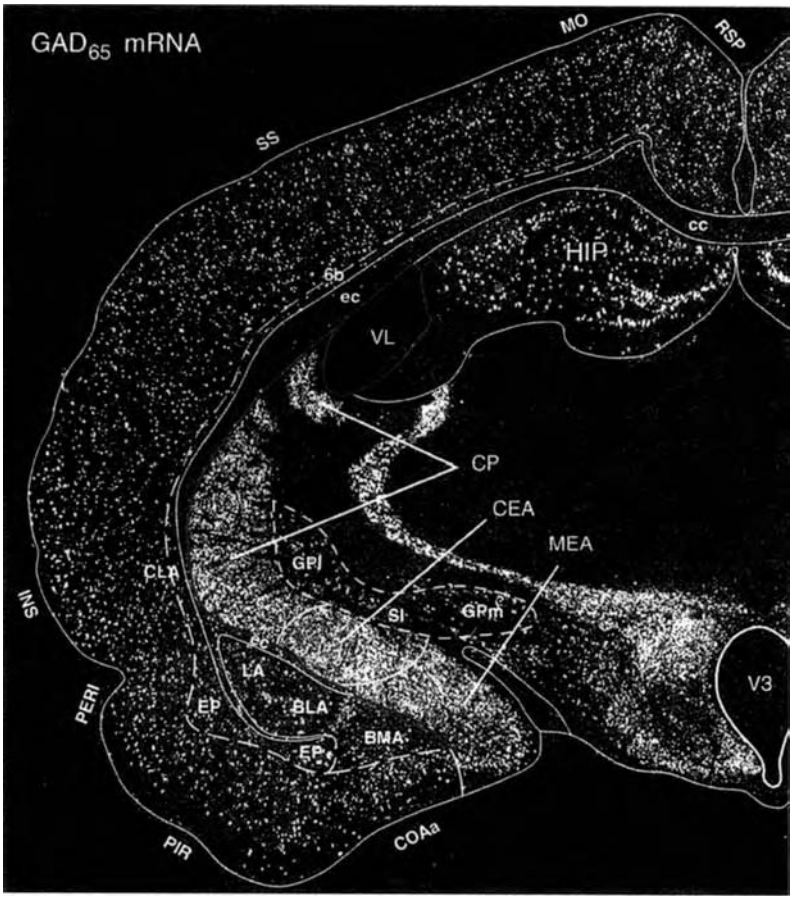

Fig. 3.4 Distribution of neurons expressing glutamic acid decarboxylase (GAD-65) in rat. *In situ* hybridization; autoradiograph in dark field. Note how the striatum (CP) and central nucleus of the amygdala (CEA) appear to form a continuous region where GAD-65-expressing neurons are especially concentrated. Abbreviations: BLA, basolateral nucleus of the amygdala; BMA, basomedial nucleus of the amygdala; cc, corpus callosum; CLA; claustrum; COAa, anterior cortical nucleus of the amygdala; ec, external capsule; EP, endopiriform nucleus; HIP; hippocampus; INS, insula; MEA, medial nucleus of the amygdala; MO, motor cortex; PERI, perirhinal cortex; PIR, piriform cortex; SS, somatosensory cortex; VL; lateral ventricle; V3; third ventricle. Modified from Swanson & Petrovich (1998).

The fact that the corticomedial group is composed of nuclei that do not belong together becomes even more obvious when one considers connectivity. For instance, the central nucleus contributes most projections of the amygdala to the brainstem, whereas the cortical and medial nuclei have sparse projections to the brainstem (De Olmos, 1990). On the input side, the cortical and medial nuclei receive inputs

from the main and/or accessory olfactory bulbs, whereas the central nucleus does not (Scalia & Winans, 1975).

Such data has led some, chief among them Swanson and Petrovich, to conclude that the amygdala is not a valid anatomical concept. They asserted that what investigators usually refer to when talking about the amygdala is in fact a disparate collection of structures that are functionally and anatomically heterogeneous (Swanson & Petrovich, 1998).

Our position on whether the term amygdala should be used is the following. True, as actually defined, the amygdala includes nuclei that have little to do with each other anatomically and functionally. The medial and cortical nuclei in particular seem unrelated to the basolateral complex and central nucleus. However, even between nuclei that have a different developmental origin and cytological organization, such as the basolateral complex and central nucleus, there are powerful glutamatergic connections (Krettek & Price, 1978b; Smith & Paré, 1994; Paré *et al.*, 1995c; Pitkänen *et al.*, 1997), indicating that they are functionally related. Thus, in our opinion, the term amygdala is still a useful one, if only because everyone knows what is meant when the term is used.

When thinking about this, one should remember that other subcortical structures include nuclei that have a different embryological origin. In the case of the thalamus, for instance, the reticular thalamic nucleus derives from the ventral thalamus whereas relay nuclei derive from the dorsal thalamus. Yet they constitute a functional unit (see Chapter 1).

Accordingly, the following account will focus on a subset of amygdala nuclei that are interconnected and appear to cooperate in specific functions: the basolateral complex, intercalated cell masses and central nucleus.

3.2 Cell types and physiological properties

3.2.1 Basolateral complex

Cell types and the transmitter they use

The cellular composition of the basolateral complex is similar, if not identical, to that of the cerebral cortex,[1] despite the fact that neurons are oriented randomly in the former and perpendicular to the *pia* in the latter. As in the cortex, two main cell types prevail in the basolateral complex: (1) multipolar, pyramidal-shaped or stellate projection cells with highly collateralized axons and spiny dendrites (Figure 3.5A,B); (2) a heterogeneous group of aspiny (or sparsely spiny) local-circuit cells using GABA as a transmitter (Figure 3.5C).[2] Projection cells account for the majority of neurons in the basolateral complex (McDonald, 1992b), they use glutamate but not GABA as a transmitter, and they contribute most, if not all, projections to other amygdala nuclei and the rest of the brain.[3]

[1] Golgi studies on the amygdala (Hall, 1972a,b; Kamal & Tömböl, 1975; reviewed in McDonald, 1992a) and cerebral cortex (reviewed in Somogyi *et al.,* 1998).

[2] Rat, McDonald (1985); cat, Paré & Smith (1993a); monkey, McDonald & Augustine (1993).

[3] That projection cells of the basolateral complex use glutamate but not GABA as a transmitter was established by using a combination of anterograde tracing with *Phaseolus vulgaris* leucoagglutinin (PHA-L) and post-embedding glutamate immunocytochemistry. PHA-L injections in the lateral nucleus of the amygdala produced anterograde labeling in other amygdala nuclei and the perirhinal cortex. In these projection fields, anterogradely labelled axon terminals formed asymmetric synapses and were enriched in glutamate (Smith & Paré, 1994). Indirect support for this idea was obtained in two other studies where retrograde tracing with horseradish peroxidase (HRP) was combined with GABA-immunhistochemistry. HRP injections in the perirhinal cortex (Paré & Smith, 1994) or striatum (Carlsen, 1988) retrogradely labelled basolateral neurons that were GABA-immunonegative. In the latter study, retrograde tracing with HRP and GABA immunohistochemistry was combined with the Golgi method, revealing that aspiny GABA-immunopositive cells did not project to the striatum whereas spiny neurons did.

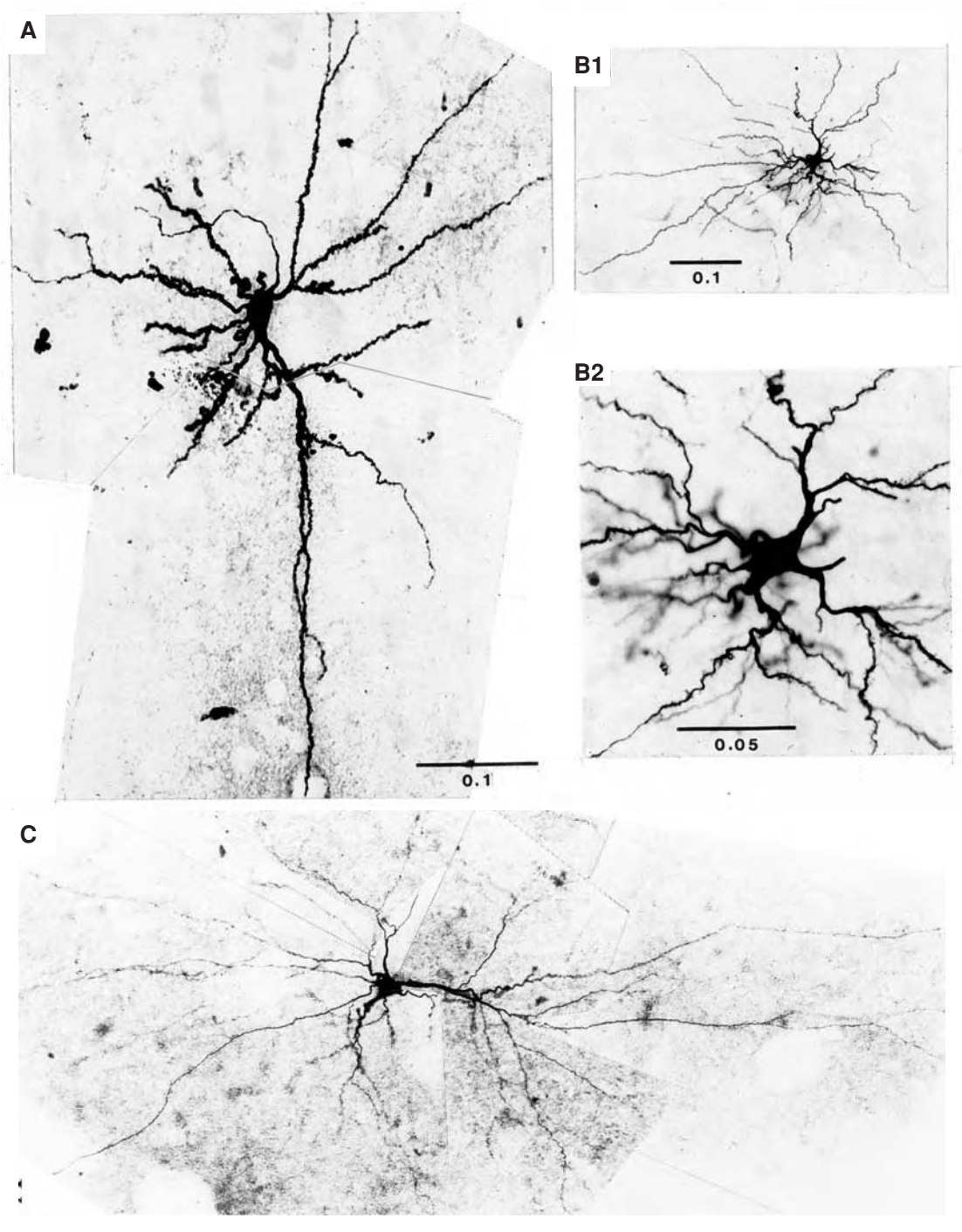

Fig. 3.5 Morphologically identified neurons of the basolateral amygdaloid complex. Neurons recorded intracellularly *in vivo* and injected with neurobiotin. (A, B) Spiny projection cells of the basolateral (A) and lateral (B) nuclei. (C) Aspiny local-circuit cell of the lateral nucleus. Scale bars in mm. (A, B) Modified from Paré *et al.* (1995b); (C) modified from Lang & Paré (1998).

As in the cortex,[4] local-circuit cells of the basolateral complex are morphologically (Hall, 1972a,b; Kamal & Tömböl, 1975; McDonald, 1992a) and neurochemically heterogeneous (Pitkänen & Amaral, 1993a,b, 1994; Kemppainen & Pitkänen, 2000; McDonald & Betette, 2001; Sorvari *et al.*, 1995; McDonald & Mascagni, 2001a,b, 2002, 2004).[5] For example, subsets of GABAergic cells express somatostatin, neuropeptide Y, cholecystokinin or vasoactive intestinal peptide (Pitkänen & Amaral, 1993a,b, 1994; Kemppainen & Pitkänen, 2000; McDonald & Betette, 2001; Sorvari *et al.*, 1995; McDonald & Mascagni, 2001a,b, 2002, 2004). In addition, calcium-binding proteins, such as parvalbumin and calbindin, colocalize with GABA, but in a higher proportion of interneurons (*c.*50%–60%) (Pitkänen & Amaral, 1993a,b, 1994; Kemppainen & Pitkänen, 2000; McDonald & Betette, 2001; Sorvari *et al.*, 1995; McDonald & Mascagni, 2001a,b, 2002, 2004; Smith *et al.*, 1998, 2000), as found in the cerebral cortex. By contrast, very few, if any, projection cells express parvalbumin.

As in the cortex, parvalbumin-immunoreactive interneurons are believed to mediate feedback inhibition. In keeping with this idea, projection-cells form asymmetric (presumably excitatory) synapses on parvalbumin-immunoreactive interneurons whereas cortical axons do not (Smith *et al.*, 1998, 2000). On the output side, parvalbumin-immunoreactive cells form numerous inhibitory synapses on the soma, initial axonal segment and proximal dendrites of projection cells (Smith *et al.*, 1998, 2000; McDonald *et al.*, 2002; Muller *et al.*, 2003). The density of these inhibitory terminals is such that they delineate the soma and proximal processes of projection cells (Pitkänen & Amaral, 1993a,b, 1994; Kemppainen & Pitkänen, 2000; McDonald & Betette, 2001; Sorvari *et al.*, 1995; McDonald & Mascagni, 2001a,b, 2002, 2004).

Physiological properties

Far less is known about the electroresponsive properties of neurons of the basolateral amygdala than in the cerebral cortex. However, the available data are consistent with what was found in cortical neurons (Connors *et al.*, 1982; McCormick *et al.*, 1985; Kawaguchi & Kubota, 1993, 1997; Kawaguchi, 2001), with a few exceptions. The following is a summary of *in vitro* (Washburn & Moises, 1992a; Rainnie *et al.*, 1993; Pape & Driesang, 1998; Pape *et al.*, 1998; Faulkner & Brown, 1999; Faber *et al.*, 2001; Martina *et al.*, 2001; Faber & Sah, 2002, 2003) and *in vivo* (Paré *et al.*, 1995b; Lang & Paré, 1997a,b, 1998; Chen & Lang, 2003) studies that correlated the physiological and morphological properties of neurons of the basolateral complex.

PROJECTION CELLS

Spiny multipolar neurons (i.e. presumed projection cells) occur in two main varieties: (1) regular spiking neurons that generate spike trains displaying frequency accommodation and (2) burst-firing cells, reminiscent of the corresponding class of cortical neurons (generating high-frequency clusters of action potentials in response to threshold

[4] Reviewed in Freund & Buzsáki (1996); Kawaguchi & Kubota (1997).

[5] Through a series of elegant immunohistochemical studies, McDonald and collaborators have concluded that GABA interneurons of the basolateral complex can be divided into four major subgroups on the basis of their peptide content: (1) PV-immunoreactive neurons (most of which are also calbindin-immunoreactive); (2) somatostatin-immunoreactive neurons (many of which are also immunoreactive for calbindin and neuropeptide Y); (3) large cholecystokinin-immunoreactive neurons (a proportion of which are calbindin-immunoreactive); and (4) small bipolar/bitufted neurons that exhibit various amounts of colocalization with cholecystokinin, vasoactive intestinal peptide and calretinin.

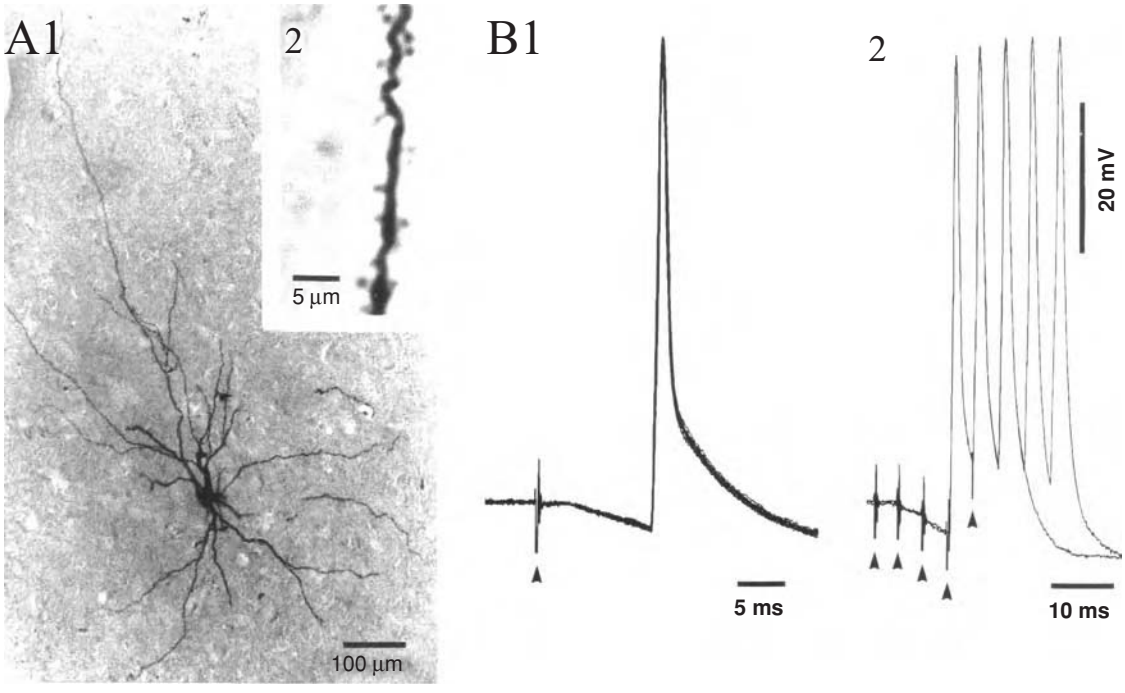

Fig. 3.6 Projection cell of the lateral nucleus of the amygdala identified (A) morphologically by intracellular injection of neurobiotin *in vivo* and (B) physiologically by antidromic invasion from the perirhinal cortex. Arrowheads in B mark perirhinal stimulus artefacts. Modified from Lang & Paré (1997a).

depolarizations). That at least some regular spiking and burst-firing cells are projection neurons was confirmed *in vivo*, by antidromically invading some of these spiny multipolar neurons from projection sites of the basolateral complex (Figure 3.6) (Paré *et al.*, 1995b; Lang & Paré, 1997a,b, 1998; Chen & Lang, 2003). Others observed a third type of spiny neuron (presumed projection cell), termed late-firing cells because they exhibit a conspicuous delay to firing following the onset of depolarizing current pulses (Washburn & Moises, 1992a; Faulkner & Brown, 1999).

Regular spiking cells are the most frequently encountered type of projection neurons (Figure 3.7A). Detailed whole-cell patch investigations of their physiological properties in slices of the rat amygdala have revealed that projection cells express a continuum of spike frequency adaptation. In response to depolarizing current injection, most cells stop firing after 2–3 spikes, but a few can fire in a sustained manner throughout the stimulus whereas others fire only once. These variations are not associated with differences in membrane potential or morphological properties. Rather, they appear to reflect variations in the density of calcium-activated potassium currents.

In vivo intracellular studies in rats yielded results similar to the *in vitro* studies, including the presence of single-firers. This is in contrast to findings in cats where projection cells rarely stopped firing during depolarizing current injection, although they did exhibit spike frequency adaptation. Given that the rat and cat *in vivo* studies were performed with the same technique, the discrepancy appears to constitute a genuine species difference.

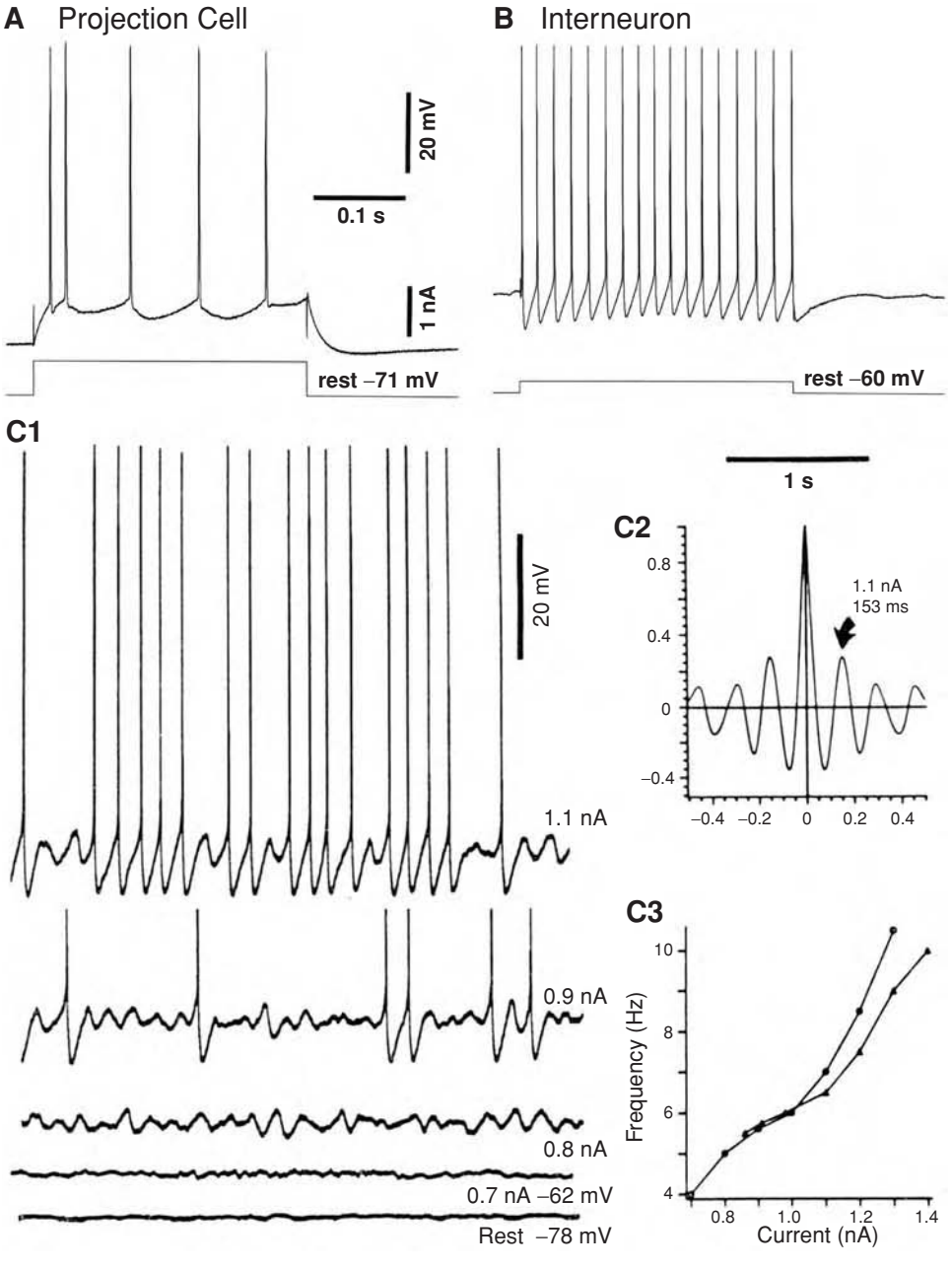

Fig. 3.7 Electroresponsive properties of a projection cell (A) and a local-circuit neuron (B) of the lateral nucleus of the amygdala. Neurons recorded intracellularly *in vivo*. Note more negative resting potential of projection cell and lack of spike frequency accommodation in the interneuron. (C) Projection cells of the lateral nucleus generates intrinsic membrane potential oscillations. (C1) Membrane potential (in *y*) as a function of time (in *x*) at different membrane potentials, as determined by intracellular current injection (numbers on the right). Note appearance of oscillation when cell is depolarized beyond −62 mV. (C2) Autocorrelation of intrinsic oscillatory activity. (C3) Dominant frequency (in *y*) as a function of injected current (in *x*) for two different cells. (A, B) Modified from Lang & Paré (1998); (C) modified from Paré *et al.* (1995b).

Finally, intracellular recordings in cats *in vivo* and in cats and guinea pigs *in vitro* have revealed that regular spiking projections of the basolateral complex can generate intrinsic subthreshold membrane potential oscillations in the theta frequency range (Figure 3.7C), similar to those described in the entorhinal cortex. These oscillations develop when neurons are depolarized just below firing threshold and they are sensitive to TTX. Such oscillations may predispose basolateral neurons to reverberate at the theta frequency during arousal.

LOCAL-CIRCUIT CELLS

Two physiological types of aspiny neurons (i.e. presumed inhibitory interneurons) have been described so far. The most frequent were termed fast-spiking cells by analogy with the corresponding class of parvalbumin-immunoreactive cortical neurons (Connors *et al.*, 1982; McCormick *et al.*, 1985; Kawaguchi & Kubota, 1993, 1997; Kawaguchi, 2001). Like their cortical counterpart, these cells generate brief action potentials and can sustain high firing rates with little or no frequency accommodation (Figure 3.7B). No such cells have been backfired from outside the amygdala (Paré *et al.*, 1995c; Lang & Paré, 1997a,b, 1998). In addition, a few aspiny neurons generating spike bursts were described (Rainnie *et al.*, 1993). To our knowledge, the peptide content of these two types of interneurons has not been investigated yet. However, considering (1) the prevalence and morphology of fast-spiking cells and (2) the great similarities existing between the physiological properties of cortical and basolateral amygdala neurons, fast-spiking cells most likely correspond to the parvalbumin-positive interneurons mediating feedback inhibition (McDonald *et al.*, 2002; Muller *et al.*, 2003).

Given the close similarities between the cortex and basolateral amygdala, future investigations will likely reveal that, as in the cortex (Connors *et al.*, 1982; McCormick *et al.*, 1985; Kawaguchi & Kubota, 1993, 1997; Kawaguchi, 2001; Thomson *et al.*, 1996; see Chapter 2), some of the regular spiking cells found in the basolateral complex are in fact local-circuit neurons.

3.2.2 Intercalated cell masses

Cell types and the transmitter they use

Despite the marked rotation imposed on the amygdala during phylogenesis, a fibre bundle known as the intermediate capsule (parallel dashed lines in Figure 3.8A) can be observed between the basolateral complex on the one hand and the central and medial nuclei on the other, in animals from insectivores to higher primates. Embedded in the intermediate capsule is a string of densely packed cell clusters commonly referred to as the intercalated cell masses (arrowheads in Figure 3.1) (Johnston, 1923; Humphrey, 1936; Fox, 1940; Crosby & Humphrey, 1941; Millhouse, 1986). Although investigators first doubted whether intercalated cells were glial or neuronal elements (Spiegel, 1919), the issue was eventually settled when their axons and dendrites were successfully impregnated in Golgi studies (Millhouse, 1986; Tömböl & Szafranska-Kosmal, 1972).

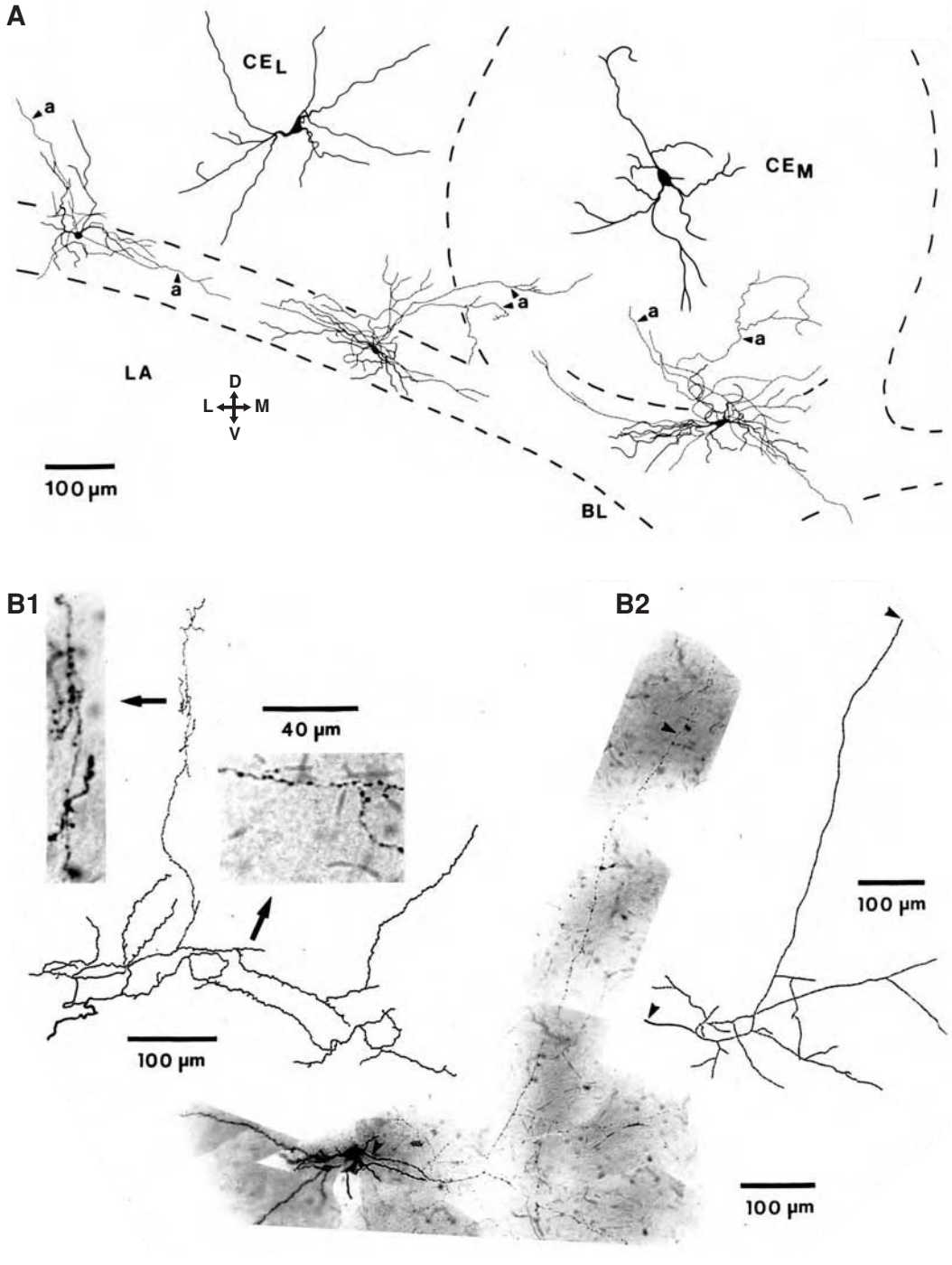

Fig. 3.8 Morphological properties of intercalated amygdala neurons. All depicted neurons were recorded with the patch method in slices of the guinea pig amygdala kept *in vitro*. (A) Intercalated neurons are sandwiched between the central nucleus (top) and basolateral amygdaloid complex (bottom), embedded in a fibre bundle termed the intermediate capsule (parallel dashed lines). (B) Intercalated cells have dorsally directed axon collaterals to the central nucleus. These axonal branches are covered with varicosities, each and every one of which presumably represents the site of GABA release. (A) Modified from Royer *et al.* (1999); (B) modified from Royer *et al.* (2000b).

The main type of cells found in the intercalated cell masses are small neurons (Figure 3.8A), around 8–19 μm in diameter, with a flattened dendritic tree that is largely confined to the intermediate capsule. These cells have spiny dendrites (Tömböl & Szafranska-Kosmal, 1972), use GABA as a transmitter,[2] and have two main axon collaterals (Figure 3.8B): one directed dorsally to the central nucleus and one directed medially to other intercalated cells.

A second, much rarer type of intercalated cells has been described (Millhouse, 1986; Tömböl & Szafranska-Kosmal, 1972). These rare intercalated cells have a very large soma (> 40 μm in diameter) with extremely long aspiny dendrites spanning much of the mediolateral extent of the amygdala. Some of these cells were reported to be immunopositive for choline acetyltransferase (Nitecka & Frotscher, 1989).

Physiological properties

Compared with the basolateral amygdala, there are very few data on the electroresponsive properties of intercalated neurons. Moreover, all available data were obtained in juvenile guinea pigs (Royer *et al.*, 1999, 2000a,b). Despite their small size and inhibitory nature, intercalated neurons do not exhibit a fast-spiking, but a regular spiking behaviour. That is, they exhibit spike frequency accommodation during prolonged depolarizations. As often seen in the rest of the amygdala, many intercalated cells display a voltage- and time-dependent inward rectification in the hyperpolarizing direction. This property presumably results from the presence of a mixed cationic conductance activated by membrane hyperpolarization and known as I_H.

Despite these common properties, intercalated cells differ from principal cells of the basolateral complex and central nucleus in two fundamental ways. First, presumably because of their small size, intercalated neurons have a much higher input resistance (usually 400–800 MΩ) than principal basolateral or central neurons (both usually well below 200 MΩ). As a result, everything else being equal, intercalated cells will tend to reach firing threshold first when receiving excitatory synaptic inputs. As will be discussed in Chapter 9, this property has important consequences for the excitability of central neurons, the main target of intercalated cells.

Second, intercalated cells express a peculiar K^+ current (termed I_{SD} for slowly de-inactivating) that activates in the sub-threshold regime, inactivates in response to depolarizations above firing threshold (Figure 3.9) in a Ca^{2+}- and Na^+-independent manner, and de-inactivates extremely slowly when the membrane potential returns to rest. As a result, following periods of intense firing, intercalated cells assume a self-sustaining state of enhanced excitability characterized by an increased input resistance and a more depolarized membrane potential (Figure 3.9A2, B2). In turn, these changes increase the probability that synaptic inputs will trigger spikes. Yet, since each of these spikes 'renews' the inactivation of I_{SD}, intercalated cells may remain in this state of enhanced excitability for a long time (Figure 3.9C2).

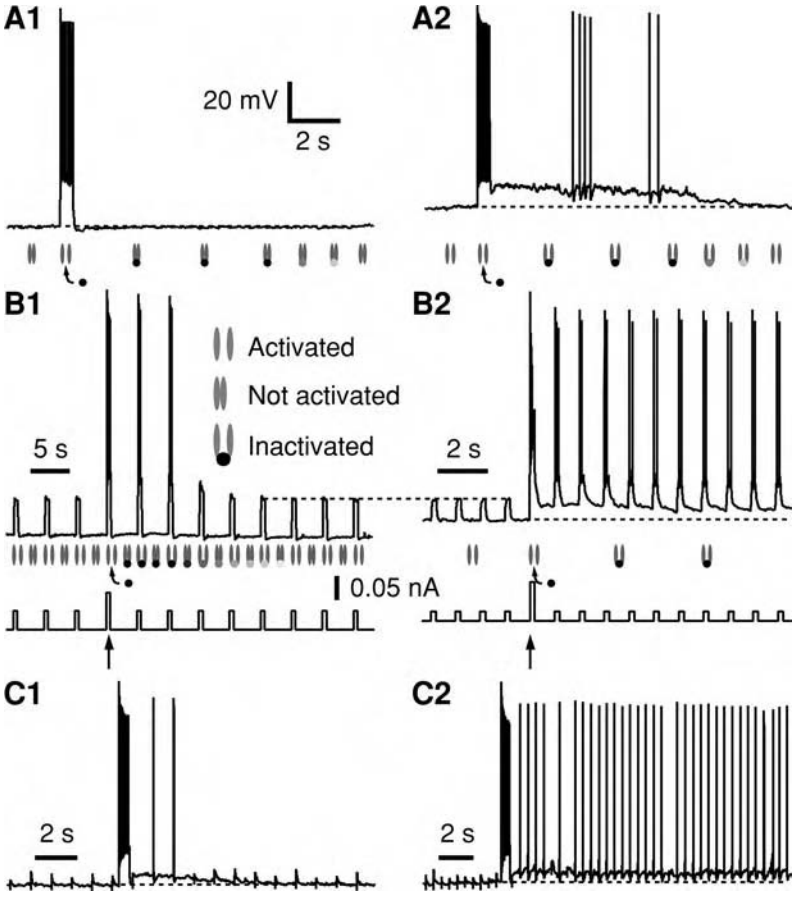

Fig. 3.9 Intercalated neurons express an unusual K^+ current, termed I_{SD}. Patch recording of an intercalated neuron in a slice of the guinea pig amygdala kept *in vitro*. Symbols indicate hypothesized state of I_{SD} channels (see legend in panel B1). In (A) and (B), the behaviour of the cell was modified by intracellular current injection. In (1) the tests were conducted from rest. In (2) the tests were conducted from −65 mV. In (C) glutamatergic afferents to the cell were activated by applying brief electrical stimuli in the basolateral nucleus and the neuron was depolarized to −65 mV by intracellular current injection. Modified from Royer *et al.* (2000a).

[6] These references propose various parcellations of the central nucleus. The lack of agreement between these various classifications is remarkable.

3.2.3 Central nucleus

Cell types and the transmitter they use

In mammals, two divisions of the central nucleus can be distinguished without special stains: a lateral and a medial one. In rats, the lateral sector of the central nucleus is currently divided in multiple compartments including, from lateral to medial, (a) the amygdalostriatal transition area, (b) the lateral sector proper, (c) the capsular portion of the central nucleus that surrounds the lateral sector ventrolaterally and, (d) wedged between the lateral and medial sectors, the intermediate subnucleus (McDonald, 1982; Cassell *et al.*, 1986; Paxinos & Watson, 1986; Jolkkonen & Pitkänen, 1998; Swanson, 1992).[6]

Yet, with some minor differences, the neuronal composition of these sub-nuclei appears to be similar (Cassell & Gray, 1989a; Hall, 1972a,b; Kamal & Tömböl, 1975; McDonald, 1982; Tömböl & Szafranska-Kosmal, 1972). Moreover, in slice studies where no special stain can be used, only two major divisions can be recognized with certainty, the medial and lateral sectors of the central nucleus. Accordingly, this simpler scheme will be used below.

In the medial sector of the central nucleus, the predominant cell type are neurons with 3–4 primary dendrites that branch sparingly and bear a moderate density of dendritic spines. The axons of these cells bear varicosities and exit the nucleus medially and dorsally. In addition, the central nucleus contains a minority of cells with very long dendrites devoid of dendritic spines.

In the lateral sector of the central nucleus, the principal cell type closely resembles the medium spiny neurons of the striatum. These cells usually have around four primary dendrites that branch multiple times and bear a high density of spines. The same cell type also predominates in the capsular portion of the central nucleus. As in the medial sector of the central nucleus, a minority of neurons are aspiny.

Although it is believed that the vast majority of neurons in the central nucleus use GABA as a transmitter,[2] the evidence is not entirely convincing, especially for projection neurons in its medial part (Figure 3.10). Indeed, studies on the distribution of GAD- or GABA-immunoreactive elements in the amygdaloid complex have reached various conclusions with some reporting very few and others numerous GABAergic cells in the central nucleus. In part, these discrepancies have resulted from whether colchicine was used or not. Nevertheless, even in studies where colchicine was used, a genuinely low concentration of GABAergic cells was found in the medial part of the central nucleus.

Moreover, other evidence suggests that projection cells of the central nucleus exert excitatory effects on their targets. First, neurons of the central nucleus projecting to the parabrachial nuclei are not GABA-immunoreactive (Sun & Cassell, 1993). Second, the axons of central medial neurons usually form asymmetric synaptic contacts with their brainstem targets (Takeuchi *et al.*, 1982, 1983), a type of synaptic specialization commonly associated with excitatory terminals. Furthermore, electrical stimulation of the central nucleus was reported to evoke short-latency orthodromic activations in most responsive neurons of the dorsal vagal and tractus solitarius nuclei (Cox *et al.*, 1986). Unfortunately, this evidence is not entirely convincing either, because electrical stimuli might have activated passing fibres.

However, other factors raise the possibility that some of the projections arising from the central nucleus are inhibitory. For instance, numerous GABA-immunoreactive cells of the central nucleus are retrogradely labelled by WGA–HRP injections in the stria terminalis nuclei and some brainstem nuclei (Sun & Cassell, 1993; Jongen-Rêlo & Amaral, 1998). Moreover, other investigators have reported that the synaptic contacts between axon terminals arising in the central nucleus and adrenergic neurons of the ventrolateral medulla are usually of the symmetric type (Cassell & Gray, 1989a; Pickel *et al.*, 1995, 1996). To our knowledge, no corroborative electrophysiological evidence exists regarding the presumed inhibitory nature of this projection. Considering the variety of brainstem and hypothalamic targets of the central nucleus and, in some cases, their opposite role

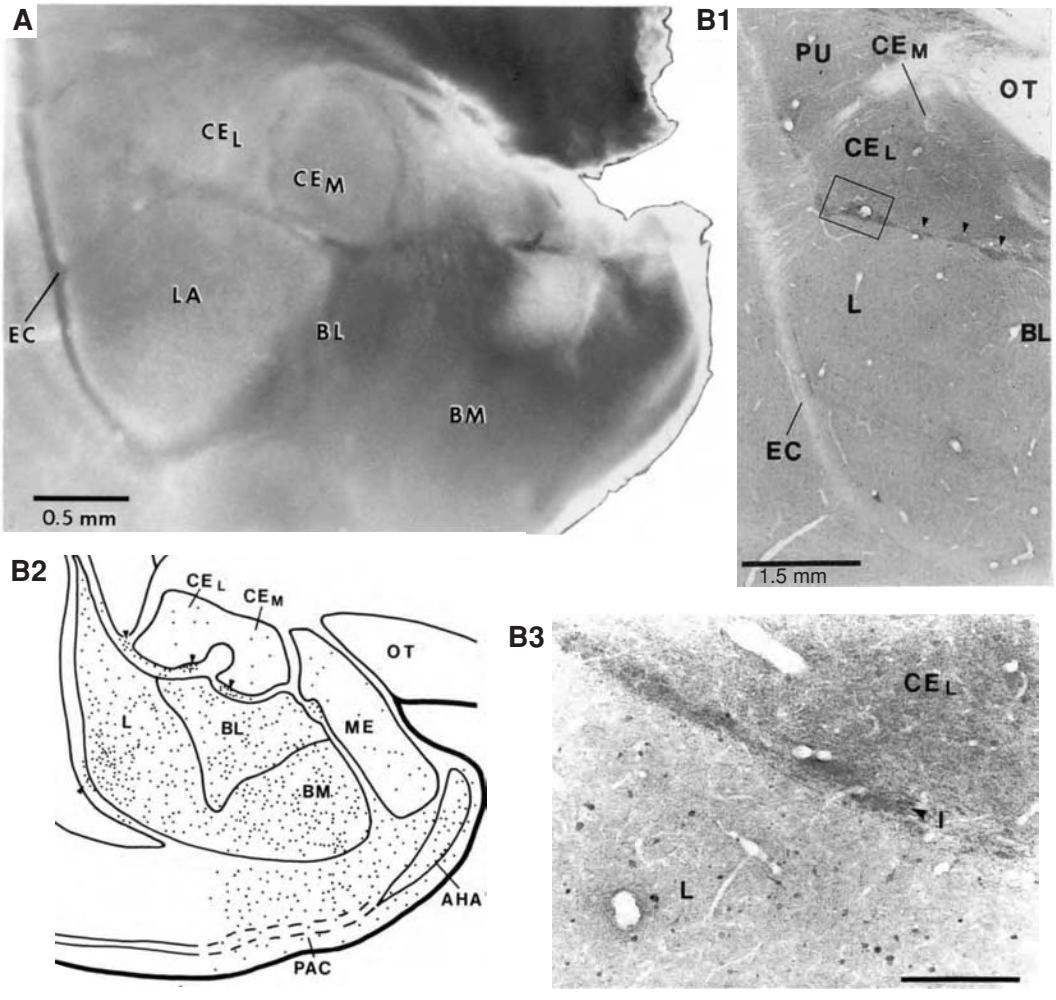

[7] Studies using the patch method: Martina *et al.* (1999); Dumont *et al.* (2002); Lopez De Armentia & Sah (2004). Studies using sharp electrodes: Schiess *et al.* (1993, 1999).

Fig. 3.10 The central nucleus contains a low number of intensely GABA-immunoreactive neurons. (A) Unstained coronal section of the guinea pig amygdala kept alive *in vitro*. Note that only two sectors of the central nucleus can be unambiguously identified in this condition. (B1) Low-power view of a coronal section of the cat amygdala processed to reveal GABA immunoreactivity. (B2) Distribution of GABA-immunoreactive neurons. Each dot stands for three immunoreactive cells. (B3) Actual GABA immunoreactivity. Scale bars in (B1) and (B3) correspond to 1.5 and 0.25 mm, respectively. (A) Modified from Royer *et al.* (1999); (B) modified from Paré & Smith (1993a).

in autonomic regulation, it is possible that central axons exert differential effects on at least some of their targets, possibly through the release of distinct transmitters.

Physiological properties

The physiological properties of central neurons have been investigated in rats, guinea pigs and cats; major species differences were reported.[7] In the guinea pig, the vast majority of cells in the lateral and medial sectors of the central nucleus exhibit a conspicuous

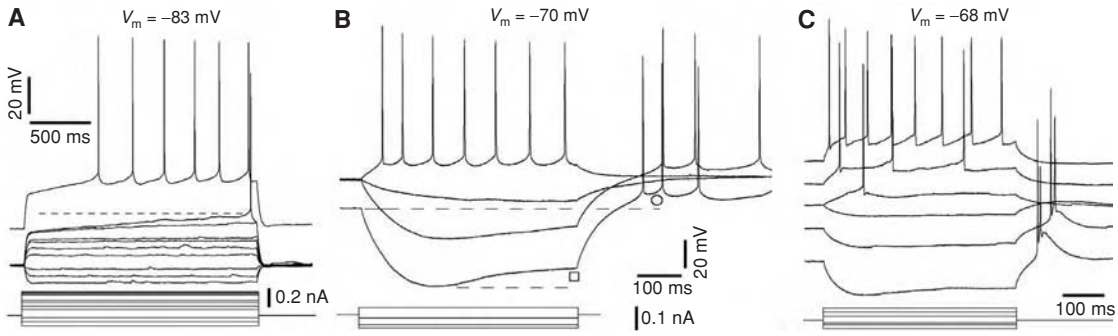

Fig. 3.11 Electroresponsive properties of central amygdala neurons. All depicted neurons were recorded with the patch method in slices of the guinea pig (A) or rat (B–C) amygdala kept *in vitro*. Modified from Dumont *et al.* (2002).

delay to firing when depolarized from hyperpolarized membrane potentials (Figure 3.11A). This delay is due to the activation of a voltage-dependent slow A-like current, sensitive to low micromolar concentrations of 4-AP. Most of these cells, termed late-firing neurons, fire single spikes but some generate high-frequency spike bursts.

In contrast, in rats and cats late-firing cells account for a minority of neurons. The prevalent cell types display a regular spiking firing pattern including varying amounts of spike frequency adaptation, the presence of a hyperpolarization-activated mixed cationic current I_H (Figure 3.11B) and, in a minority of neurons, a t-current, giving rise to low-threshold spike bursts (Figure 3.11C). Especially in rats, some investigators have relied on the shape of spike-afterhyperpolarizations (AHPs) to classify central neurons, with the majority showing medium-duration AHPs and limited spike frequency adaptation and a minority showing prolonged AHPs and marked adaptation.

In all species investigated so far, the central nucleus also contained a minority of neurons that displayed fast-spiking or burst-firing patterns. These cells had relatively depolarized membrane potentials and a higher input resistance. They may correspond to the rare intensely GABA-immunoreactive neurons described in previous studies.[2]

[8] Primate amygdala: Amaral *et al.* (1992). Rat amygdala: Pitkänen (2000).

3.3 Intrinsic and extrinsic connections

The amygdala is astonishingly promiscuous in its connectivity. Indeed, as we will now see, the amygdala has access to sensory inputs of all modalities and it projects to virtually all levels of the central nervous system, from the highest computational levels of the cerebral cortex down to brainstem nuclei involved in cardiovascular control. However, since the connectivity of the amygdala has been reviewed several times in recent years,[8] the following account will be limited to a brief overview of salient principles. Connections with neuromodulatory systems of the brainstem and basal forebrain will be discussed in a subsequent chapter.

3.3.1 Intra-amygdaloid connections

In contrast with the dorsal thalamus, where relay cells do not form synaptic contacts with each other (see Chapter 1), the amygdala is

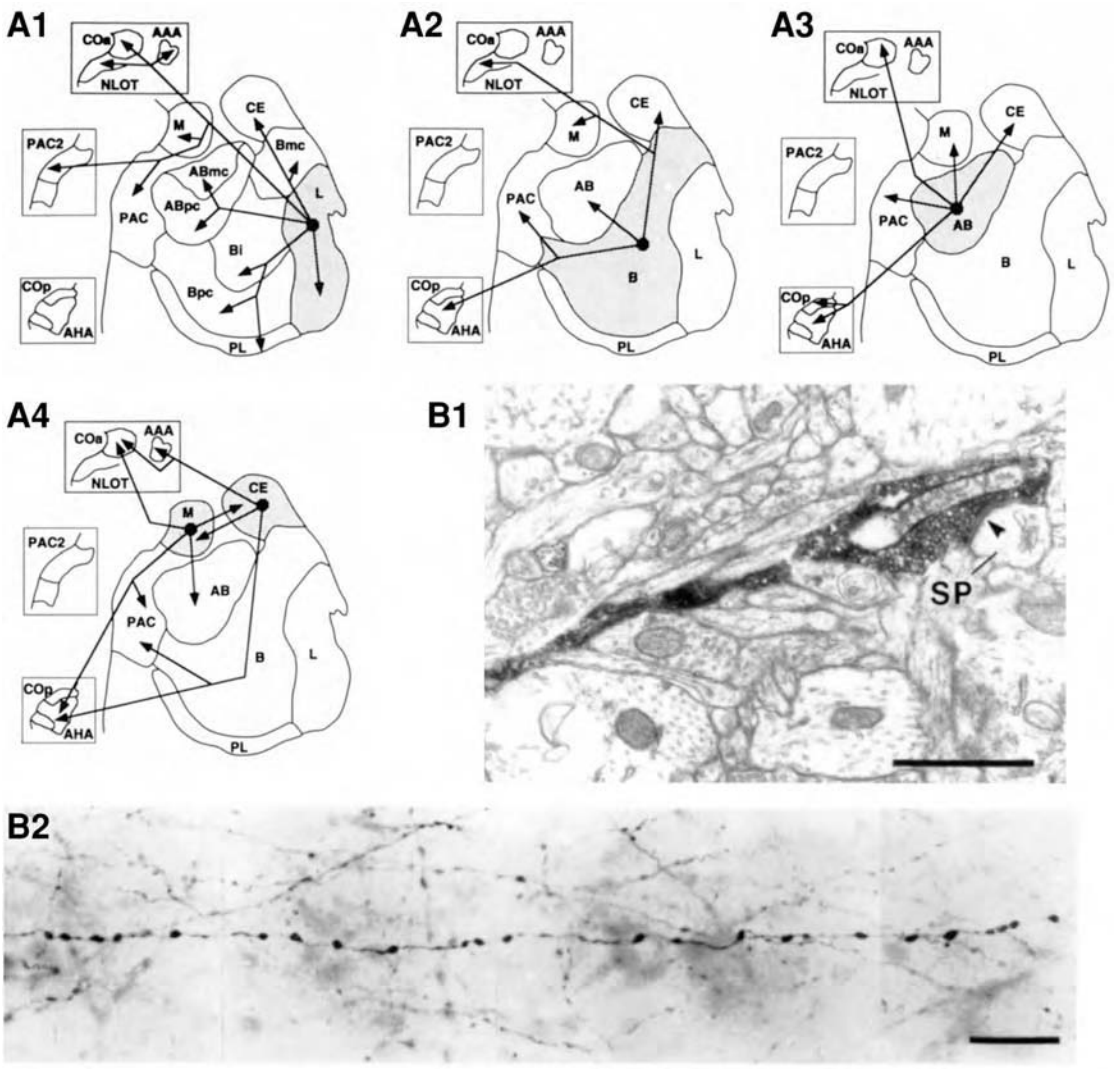

Fig. 3.12 Internuclear connections of the amygdala. (A1–4) Schemes showing the main internuclear connections of the monkey amygdala. (B1) Asymmetric synaptic contacts formed by the axon of a projection cell of the lateral nucleus onto an unlabelled spine in the basomedial nucleus. (B2) Projection cells of the lateral nucleus have highly collateralized and varicose axons. The material shown in (B1) and (B2) was obtained by performing iontophoretic injections of the anterograde tracer *Phaseolus vulgaris* leucoagglutinin in the lateral nucleus of the amygdala and observing the basomedial nucleus in the electron (B1) or light (B2) microscope. Scale bars in (B1) and (B2) correspond to 1 and 15 μm, respectively. (A) Modified from Amaral *et al.* (1992); (B1,2) modified from Smith & Paré (1994).

endowed with an extremely powerful system of intra- and internuclear glutamatergic connections,[8] with few species differences. Figure 3.12A summarizes the internuclear connections found within and between nuclei of the basolateral complex and central nucleus in primates.

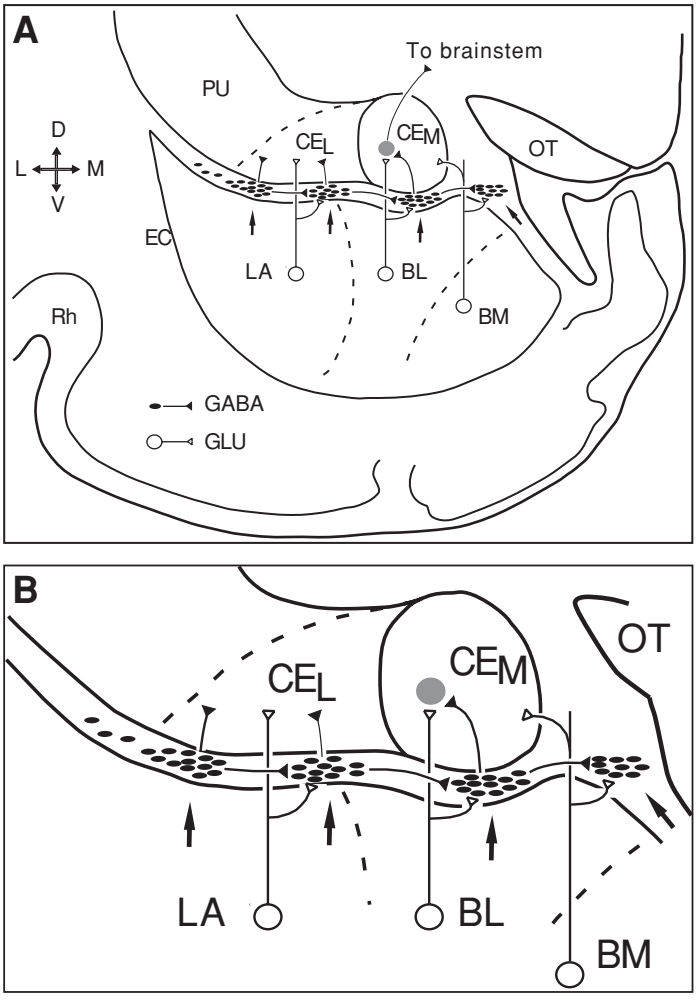

Fig. 3.13 Axons arising in the lateral and basal nuclei en route to the central nucleus excite intercalated neurons. (A) Scheme of a coronal section of the guinea pig amygdala. Cross on the left indicates orientation of the scheme (D, dorsal; V, ventral; L, lateral; M, medial). (B) Detail of A, at a higher magnification. Arrows indicate intercalated cell masses. Abbreviations: BL, basolateral nucleus; BM, basomedial nucleus; CE_L, central lateral nucleus; CE_M, central medial nucleus; LA, lateral nucleus; OT, optic tract; PU, putamen; Rh, rhinal sulcus.

Note that these connections are specific (not all nuclei project to other nuclei), that they prevalently run in a lateromedial direction, and that with few exceptions, mediodorsally located nuclei do not send return projections. Finally, most if not all these internuclear connections use glutamate as a transmitter and they form asymmetric synapses prevalently with dendritic spines (Figure 3.12B1,2).[3] As shown in Figure 3.13, basolateral axons en route to the central nucleus also form excitatory synaptic contacts with intercalated cell which in turn form inhibitory (GABAergic) synapses with central neurons (Royer *et al.*, 1999, 2000a,b).

Interestingly, the lateromedial directionality found in the links between the basolateral complex and central nucleus also characterizes the networks that link intercalated cell masses with each other. Indeed, injections of neurobiotin in intercalated cells have revealed that they are morphologically asymmetric in the lateromedial plane. In particular, their laterally directed dendrites are longer than the medial ones whereas their laterally directed axon collaterals are

shorter than the medial ones. As a result, laterally located intercalated clusters tend to inhibit more medial ones (Royer *et al.*, 1999, 2000a,b).

3.3.2 Inter-amygdaloid connections

Some amygdala nuclei have projections to the contralateral amygdala.[8] Most of these projections originate in the basal nuclei. Cortical nuclei of the amygdala contribute the rest. As is found among ipsilaterally located amygdala nuclei, the main targets of these contralateral projections are the central and medial nuclei. In addition, there are projections between the basal nuclei on both sides (Savander *et al.*, 1997).

3.3.3 Cortical connections

Basolateral complex

In lower mammals such as rodents and cats, projections of the amygdala to the cerebral cortex are much less extensive than in primates. In rats and cats, the amygdala only projects to limbic cortices and a few frontal regions, whereas in monkeys projections of the amygdala to the neocortex are profuse. Yet, in all species, the cortical projections of the amygdala mostly originate in nuclei of the basolateral complex.[8]

In rats and cats, most cortical projections of the amygdala originate in the basolateral complex and focus on limbic cortical areas of the frontal and temporal lobes. There are massive projections to the perirhinal cortex, mostly originating from the lateral nucleus (Figure 3.14) but also from the basal nuclei. There are also strong projections to the infra- and prelimbic cortex as well as to the insula, mostly originating in the basolateral nucleus, and projections to various components of the hippocampal formation, in descending order, the entorhinal cortex, subiculum, CA3, and CA1. All components of the basolateral complex contribute to these hippocampal projections. There are no amygdala projections to the dentate gyrus (Pitkänen *et al.*, 2000).

Whereas the amygdala projects to relatively restricted cortical territories in rats and cats, it receives inputs from a variety of cortical regions. There are projections from associative cortical areas of the temporal and parietal lobes that mainly target the lateral nucleus. In contrast, inputs from frontal cortical areas mainly focus on the basolateral nucleus. Components of the hippocampal formation also project to the amygdala, in descending order of importance the entorhinal cortex, subiculum and CA1 (Pitkänen *et al.*, 2000).

Central nucleus

The central nucleus contributes few, if any, projections to the cortex. Thus, in this respect it is also reminiscent of the striatum. Cortical inputs to the central nucleus are generally lighter and centred on the lateral part of the central nucleus. Usually, the same cortical regions

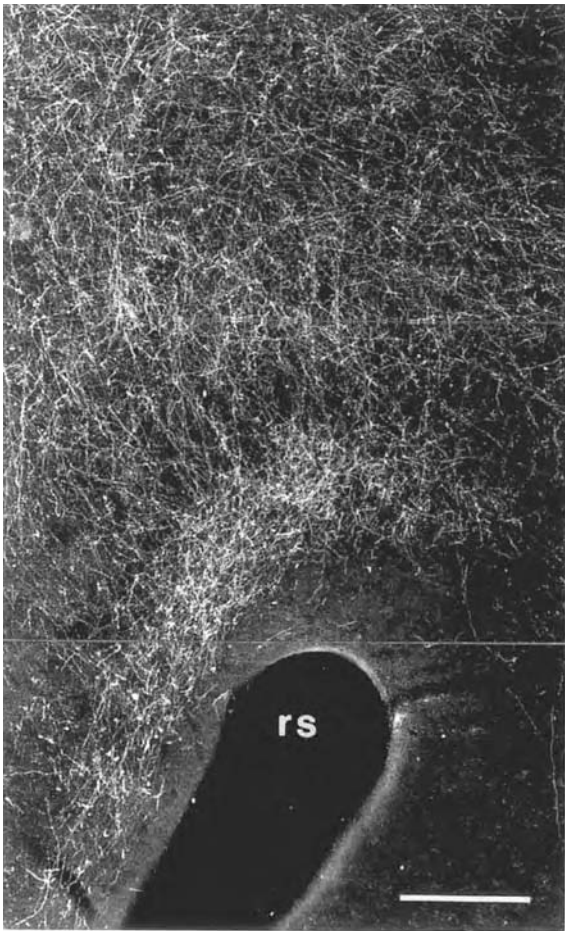

Fig. 3.14 The lateral nucleus of the amygdala projects massively to the perirhinal cortex. Dark-field photomicrograph showing the distribution of anterograde labelling following a iontophoretic injection of the anterograde tracer *Phaseolus vulgaris* leucoagglutinin in the lateral nucleus of the amygdala. Scale bar, 250 μm; rs, rhinal sulcus. Modified from Smith & Paré (1994).

that project to the basolateral complex send a projection to the lateral part of the central nucleus (McDonald, 1998).[8]

3.3.4 Subcortical connections

Striatum

There is a unidirectional projection from the amygdala to nucleus accumbens, as well as some sectors of the caudate nucleus and putamen. Amygdala fibres were reported to mainly target the striosomes. These striatal projections mostly originate from the basal nuclei; the central nucleus does not project to the striatum and the lateral nucleus does so very little.[8]

Thalamus

The amygdala projects to restricted thalamic territories. In rats and monkeys (but, strangely enough, not in cats (Krettek & Price, 1977b)), there is massive projection from the basolateral complex to the mediodorsal thalamic nucleus. In addition to this major projection, the central and medial nuclei of the amygdala project to midline thalamic nuclei, most intensely to nucleus reuniens.[8]

Most thalamic inputs to the amygdala originate in the posterior thalamic complex, including the medial division of the medial geniculate body (LeDoux *et al.*, 1990a,b; Turner & Herkenham, 1991; Linke *et al.*, 2000).

Bed nucleus of the stria terminalis

The bed nucleus of the stria terminalis (BNST) is reminiscent of the central nucleus in terms of projection sites and transmitter contents. As a result, many consider the bed nucleus of the stria terminalis to be an extension of the central and medial nuclei of the amygdala along the stria terminalis (McDonald, 2003).

Although many amygdala projections to the BNST run through the stria terminalis, some also course through the ventral amygdalofugal pathway. Projections to the BNST originate from the central, basolateral and basomedial nuclei.[8] Because the BNST and central nucleus have similar projections, the significance of these projections will be considered below, when the brainstem projections of the central nucleus are considered.

Hypothalamus

The basomedial nucleus projects to the cell-dense core of the ventromedial hypothalamic nucleus. These nuclei also project to the premammillary nucleus, in the caudal part of the hypothalamus (Krettek & Price, 1978a). In addition, there is a massive projection from the central nucleus to the lateral hypothalamus that courses mainly through the ventral amygdalofugal pathway. The basal nuclei contribute lightly to this projection.

Return projections from the hypothalamus are weak compared to amygdalohypothalamic projections. These return projections mostly originate in the ventromedial hypothalamic nucleus and caudal part of the lateral hypothalamus and target the central, medial and basal amygdaloid nuclei.[8]

Brainstem

Most brainstem projections of the amygdala originate in the central nucleus of the amygdala, particularly its medial sector (Holstege, 1990; Hopkins & Holstege, 1978). The projections of the BNST and central nucleus to the brainstem are essentially identical. From rostral to caudal, the central nucleus projects to the ventral tegmental area (VTA), substantia nigra *pars compacta* (SNc), mesencephalic reticular formation, the periaqueductal grey matter (especially ventrolaterally and dorsomedially), the pedunculopontine and parabrachial nuclei, pontine reticular formation, nucleus of the solitary tract and dorsal motor nucleus of the vagus. Some axons of the central nucleus even end in the spinal cord at cervical levels. Many of the targets of the central nucleus reciprocate the projection. This is true of the VTA and SNc, the parabrachial nucleus and nucleus of the solitary tract.[8]

Chapter 4

Rhinal and medial prefrontal cortices

This chapter describes the structure and connections of the rhinal cortices and medial prefrontal cortex. We focus on this particular subset of cortical areas because they play a key role in the formation of declarative memories. Indeed, the rhinal cortices are the gateway to and from the hippocampal formation. However, the available evidence suggests that they are not simple relays but instead filter or select inputs. Although the computational rules underlying this function still elude us, it is clear that this process is altered in emotionally arousing conditions. Indeed, memory formation for emotional charged material is generally improved and much evidence suggest that inputs from the amygdala and medial prefrontal cortex mediate this facilitation of memory by emotions. This chapter summarizes data about the structure, connectivity, and physiological properties of these cortical regions. How they interact in memory formation will be considered in Chapter 9.

4.1 Cytoarchitectural organization and cell types

4.1.1 Rhinal cortices

The rhinal cortices occupy a strategic location in the temporal lobe because they relay most sensory inputs from the neocortex to the hippocampus. Moreover, the rhinal cortices represent the main return path for hippocampal efferents to the neocortex (reviewed in Witter *et al.*, 2000). Although their precise contribution, compared with that of the hippocampus, remains debated (Brown & Aggleton, 2001), it is clear that the rhinal cortices are not simple relay stations. Indeed, rhinal neurons exhibit patterns of memory-related activity distinct from those seen in the hippocampus (reviewed in Suzuki, 1996; Eichenbaum, 2002). These include familiarity or novelty effects and stimulus-selective delay firing in delayed matching to sample tasks. Moreover, lesion studies support the idea that rhinal cortices have a unique contribution to memory (Brown & Aggleton, 2001).

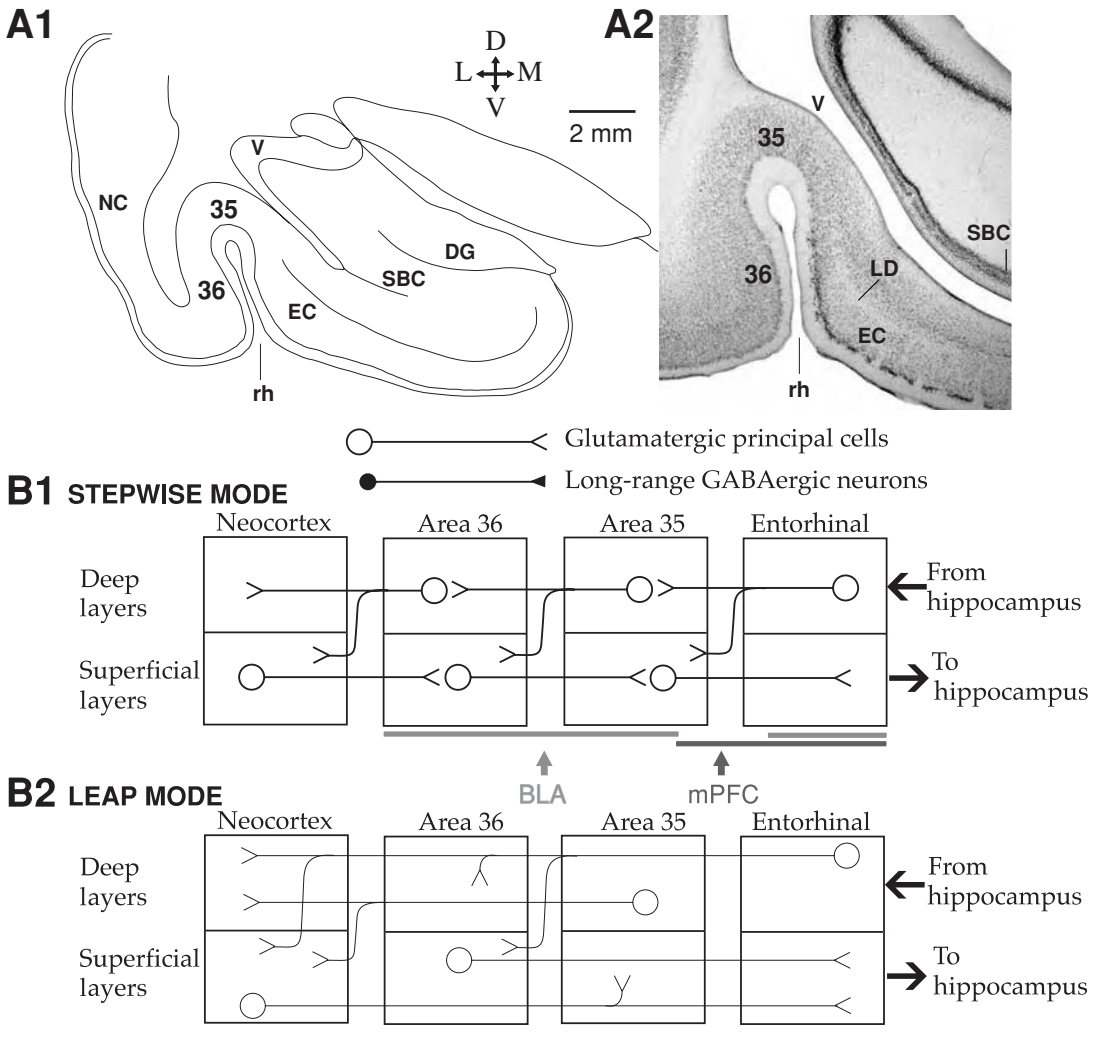

Fig. 4.1 (A1) Scheme showing relative position of perirhinal areas 36 and 35 as well as of the entorhinal cortex (EC). Cross indicates scheme orientation (D, dorsal; V, ventral; L, lateral; M, medial). (A2) Thionin-stained section. (B) Connectivity of the rhinal cortices. Layers of connectivity are artificially separated for simplicity in (B1–2). (B1) Stepwise progression of impulses through the rhinal cortices. (B2) Some neurons project beyond the adjoining area (leap mode). Coloured bars and arrows in B1 illustrate the complementary pattern of termination of afferents from the amygdala (BLA, blue) and medial prefrontal cortex (mPFC, red). Abbreviations: DG, dentate gyrus; LD, lamina desiccans; NC, neocortex; SBC, subiculum, V, ventricle. See Plate 3.

What are the rhinal cortices?

Here, we define the rhinal cortices to include the perirhinal and entorhinal cortices, located lateral and medial to the rhinal fissure, respectively (Figure 4.1A). The caudally located postrhinal cortex will not be considered, even though it is reminiscent of the perirhinal cortex in many ways (Burwell, 2001). On the basis of cytoarchitectural, immunohistochemical and hodological criteria, the perirhinal cortex

is further subdivided into two parallel cortical strips, areas 35 and 36, respectively located in the fundus and lateral bank of the rhinal sulcus (Figure 4.1A). Similarly, the entorhinal cortex has been divided into two major subfields (rostral–lateral and caudal–medial).

How can the various rhinal fields be distinguished?

As shown in Figure 4.1A, area 35 can be easily distinguished from area 36 because the former has a wider layer I. Transition from area 35 to the entorhinal cortex coincides with the thinning of layer I, the appearance of a darkly staining layer II and of a cell-poor (fibre-rich) layer, termed *lamina desiccans*, which separates deep and superficial entorhinal layers. Transition from area 35 to the entorhinal cortex also coincides with a marked increase in immunoreactivity for parvalbumin, a calcium-binding protein that is always colocalized with GABA in rhinal neurons (although the reverse is not true (Wouterlood *et al.*, 1995; Miettinen *et al.*, 1996)). Finally, the lateral and medial entorhinal fields can be distinguished by the organization of layer II and prominence of *lamina desiccans*.[1]

[1] Cat: Room & Groenewegen (1986a); guinea pig: Uva *et al.* (2004); rat and monkey: Burwell & Witter (2002).

Rhinal cell types, their transmitters and main connections

As in the neocortex and hippocampus, two main cell types can be distinguished in the rhinal cortices. (1) Most rhinal neurons are spiny glutamatergic multipolar principal cells (pyramidal-shaped or stellate). (2) The rest of the cells form a heterogeneous class of aspiny (or sparsely spiny) local-circuit neurons that use GABA as a transmitter (reviewed in Wouterlood, 2002).

ENTORHINAL NEURONS

Layer I is cell-poor, fibre-rich (Lorente de No, 1933). The main cell type in layer I is GABAergic interneurons with smooth dendrites, most of which express calretinin (Wouterlood *et al.*, 1985; Miettinen *et al.*, 1997). It has been suggested that these neurons may generate feed-forward inhibition in deeper lying principal cells, whose dendrites ramify in layer I.

Layers II and III contain spiny neurons that project to the hippocampal formation and are believed to use glutamate as a transmitter. Layer II principal cells are usually referred to as stellate neurons, whereas layer III cells are pyramidal neurons (Figure 4.2A). However, many stellate cells look like inclined pyramidal neurons. Layer II principal cells contribute a massive projection to the dentate gyrus whereas many layer III pyramidal cells project to CA1 and the subiculum (reviewed in Witter *et al.*, 1989). Physiological studies have revealed that layer II principal cells are subjected to a powerful feed-forward inhibitory control (see, for example, Finch *et al.*, 1988; Jones, 1994). In keeping with this, layers II–III also contain numerous types of aspiny GABAergic interneurons, including chandelier cells forming symmetrical synaptic contacts with the initial axonal segments of principal cells in layers II–III (Soriano *et al.*, 1993), and basket neurons (Köhler *et al.*, 1985a,b) with the typical fast-spiking firing

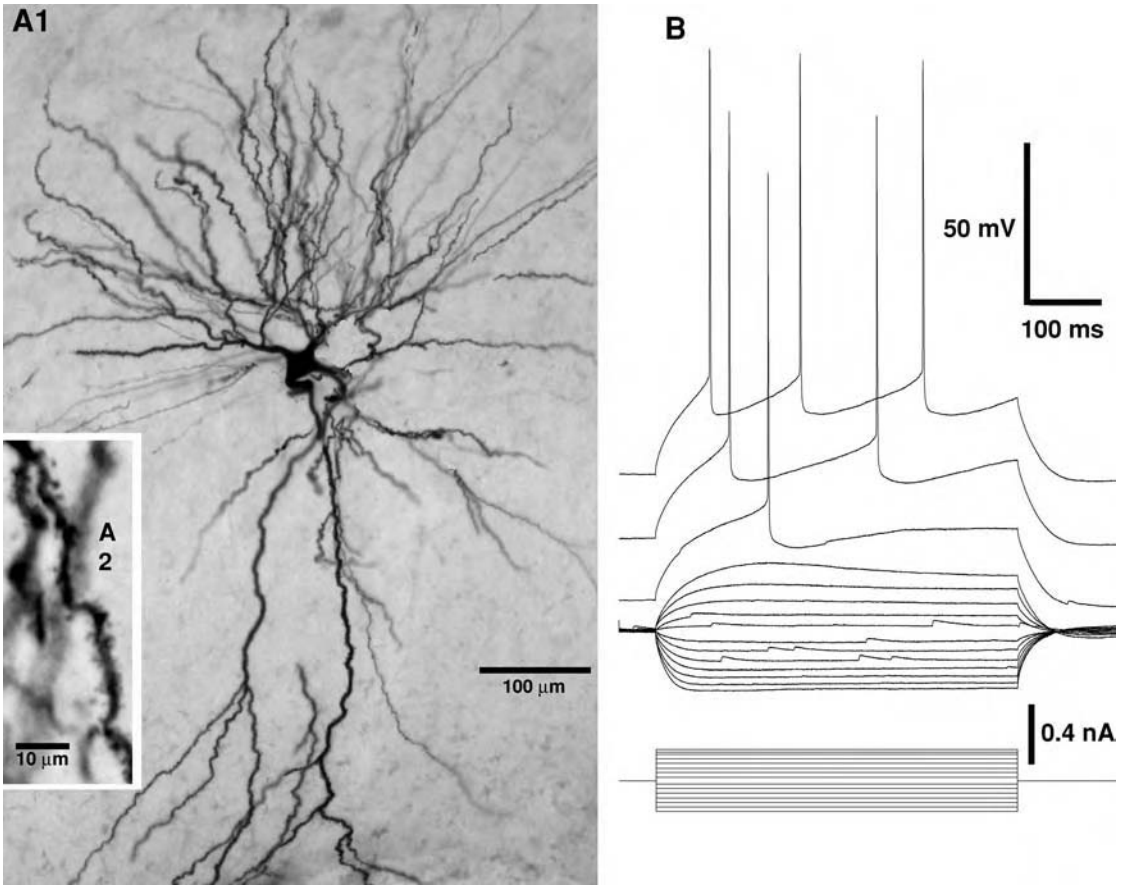

Fig. 4.2 Superficial pyramidal neuron of the entorhinal cortex. This neuron was recorded with the patch technique in a slice *in vitro*. (A) Morphological properties as identified by intracellular injection of neurobiotin at a low (A1) and high (A2) magnification. Note spiny dendrite. (B) Voltage responses to rectangular current pulses. Note regular spiking behaviour. Unpublished data of J. Apergis-Schoute & D. Paré.

pattern (Jones & Bühl, 1993). Neurons with morphological properties identical to those of basket cells stain positively for parvalbumin and form symmetrical synaptic contacts with principal cells (Wouterlood *et al.*, 1995, 2000). Aspiny neurons that express calretinin or calbindin were also reported (Miettinen *et al.*, 1997; Suzuki & Porteros, 2002).

In terms of intrinsic properties, superficial principal cells fall into the general regular-spiking category (reviewed in Alonso, 2002). Layer II stellate cells display marked spike frequency adaptation and a prominent time-dependent inward rectification in the hyperpolarizing direction. The latter property results from the presence of I_H, the hyperpolarization-activated non-selective cationic current. Some layer III pyramidal cells also exhibit inward rectification, but much less (Figure 4.2). Probably owing to this difference, layer II stellate (but not layer III) cells display subthreshold oscillatory activity in the theta range when depolarized to –60 mV and beyond. This oscillatory activity appears to result from the interaction between I_H and a persistent Na^+ current. Despite the low propensity of layer III cells to display intrinsic theta oscillations *in vitro*, they exhibit robust theta-related firing modulation *in vivo*, like layer II cells (Alonso & Garcia-Austt, 1987a,b).

Layers V–VI receive most hippocampal projections and contribute most entorhinal projections to the perirhinal cortex (reviewed in Witter *et al.*, 1989). Three main cell types have been observed in these layers. (1) There are spiny pyramidal neurons with apical dendrites extending up to the pia. (2) Also present are polymorphic cells with dendrites radiating in all directions, often reaching superficial layers. (3) Finally, there are aspiny horizontal neurons with dendritic trees of variable extent and axons with collaterals in the deep layers (see, for example, Finch *et al.*, 1988; Jones, 1994; Hamam *et al.*, 2000). These morphological differences are not systematically correlated with characteristic electroresponsive properties. Most of the cells appear to fall in the regular-spiking category (reviewed in Alonso, 2002).

PERIRHINAL NEURONS

By comparison with the entorhinal cortex, there is little information on the laminar distribution of perirhinal neurons. To our knowledge, the only available Golgi study was performed in our laboratory (C. Fuentes & D. Paré, unpublished observations). According to these results, layer I is largely free of cell bodies with the exception of a few aspiny neurons. As in the entorhinal cortex, the main cell type in layer II are spiny neurons with morphologies ranging from stellate to pyramidal. Spiny pyramidal cells predominate in all deeper layers. Tracing studies indicate that superficial perirhinal layers receive most neocortical inputs (Room & Groenewegen, 1986a). On the output side, most perirhinal projections to the entorhinal cortex originate from layer II–III neurons. Spiny cells located in deep layers project laterally to the neocortex (reviewed in Witter *et al.*, 1989).

On the basis of our own unpublished observations of brain sections prepared for amygdala studies (Paré & Smith, 1993a; Smith *et al.*, 2000), the perirhinal cortex appears to contain a variety of aspiny GABAergic neurons, similar to that found in the entorhinal cortex (Miettinen *et al.*, 1997; Suzuki & Porteros, 2002). The main type of inhibitory cells are parvalbumin-immunopositive, they are found in all layers except layer I, and they are all immunoreactive for GABA. As in the entorhinal cortex (reviewed in Wouterlood, 2002), other interneuronal markers such as calretinin and calbindin are not as useful as parvalbumin because they are expressed by both aspiny and spiny neurons (D. Paré & Y. Smith, unpublished observations). Nevertheless, aspiny calretinin interneurons are interesting because in the hippocampus they contact only other interneurons (Gulyás *et al.*, 1996). As a result, excitatory afferents to these cells would produce a disinhibition of principal cells.

Two classifications of perirhinal neurons have been proposed on the basis of their electroresponsive properties. According to some (Beggs & Kairiss, 1994; Martina *et al.*, 2001), perirhinal cells fall into the usual physiologically defined classes of cortical cells (regular-spiking, intrinsically bursting and fast-spiking). However, others have divided perirhinal cells in five categories: late-spiking, single-spiking,

fast-spiking, burst-spiking, and regular-spiking neurons (Faulkner & Brown, 1999).

In our opinion, the discrepancy between these two classifications is only apparent. First, the single-spiking cells may be considered as extreme forms of the regular-spiking variety. As to late-spiking cells, they can be transformed into regular-spiking cells by membrane depolarization. Indeed, late-spiking cells exhibit a conspicuous delay between the onset of depolarizing current pulses and spike discharges. This behaviour was observed in numerous cortical fields and subcortical structures (Bargas *et al.*, 1989; Hammond & Crépel, 1992; Martina *et al.*, 1999; Nisenbaum *et al.*, 1994; Storm, 1988). It results from a slowly inactivating K^+ conductance (I_D) that activates around −65 mV and requires a prolonged hyperpolarization for full de-inactivaton.

To the best of our knowledge, only one *in vivo* intracellular study of perirhinal neurons has been performed so far (Pelletier *et al.*, 2005a). As in other cortical fields, spiny pyramidal regular spiking neurons were the dominant cell type (Figure 4.3A,B). Intrinsically bursting cells accounted for less than 10% of the neurons (Figure 4.3C–E). Unfortunately, the stimulation protocol required to disclose the late-spiking firing pattern was not applied systematically in this study.

4.1.2 Medial prefrontal cortex

Early definitions of the prefrontal cortex were based on cytoarchitectural criteria. In primates it was noted that, in contrast to the motor and premotor cortices, prefrontal cortical areas are endowed with a well-developed layer IV. Thus, it was proposed that the prefrontal cortex consisted of those cortical areas rostral to the motor and premotor cortices that have a well developed layer IV. However, it was later noted that in other species, such as the rat, cortical areas rostral to the motor and premotor cortices are agranular. This is why connectivity became the main criterion used to delineate the prefrontal cortex.

In the late 1940s, Rose and Woolsey (1948) proposed that the prefrontal cortex is the part of the frontal lobe that derives most of its thalamic inputs from the mediodorsal thalamic nucleus. They suggested that these projections from the mediodorsal thalamic nucleus might be used to identify homologous prefrontal cortical areas in different species. By these criteria, most vertebrate species appear to have a prefrontal cortex, although its size increases tremendously in higher species. In the human brain, the prefrontal cortex is one on the most extensive cortical regions, accounting for about 30% of the cerebral cortex.

Generally, the primate prefrontal cortex is subdivided in two major areas: the dorsolateral prefrontal cortex (9, 9/46, 46, 8(FEF)) and the orbitomedial prefrontal cortex (Acg-24, prelimbic-32, infralimbic-25, orbital). These two major areas were subdivided in a multitude of ways. Because most of the connections between the amygdala and prefrontal cortex involve the prelimbic and infralimbic areas, this

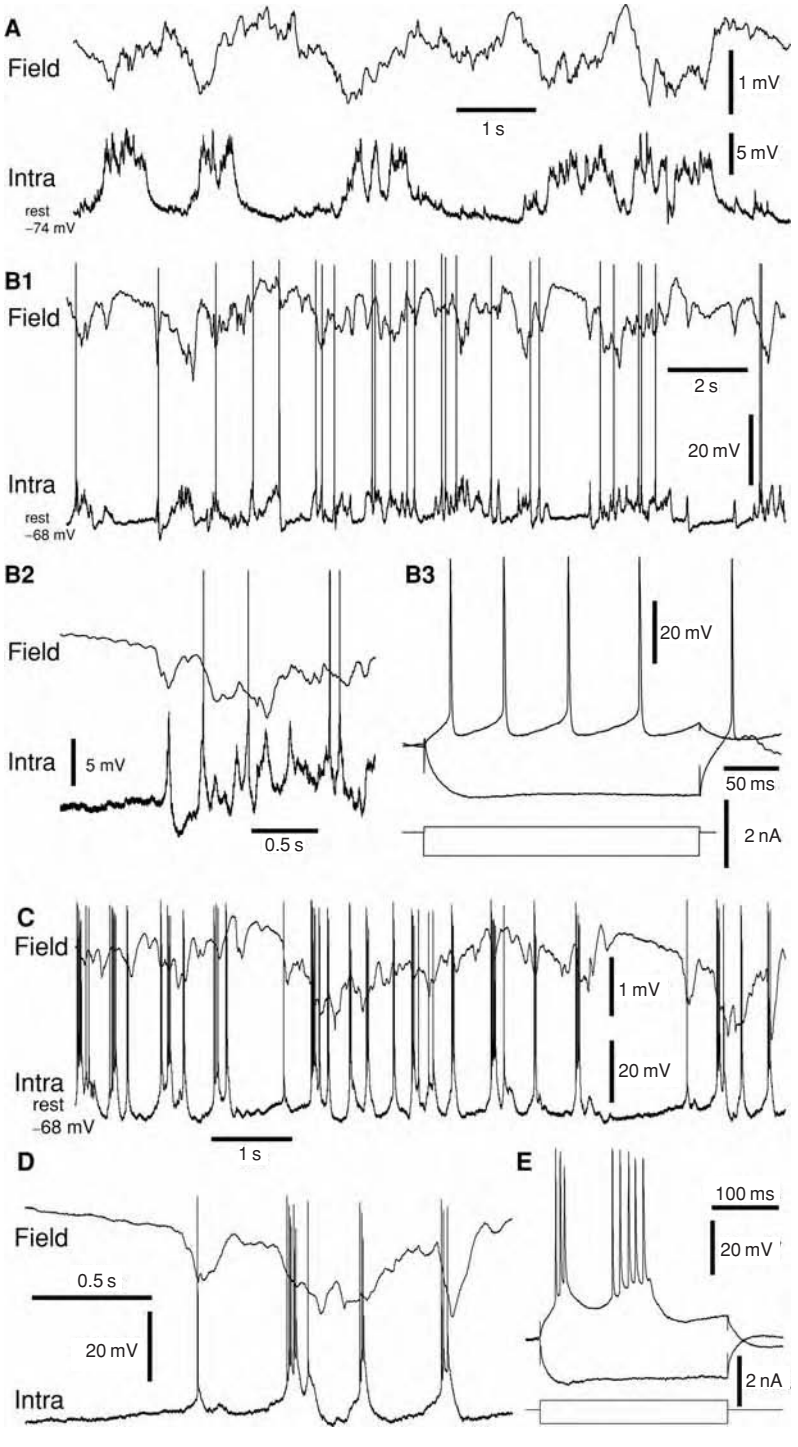

Fig. 4.3 Intracellular recordings of regular spiking (A, B) and intrinsically bursting (C–E) perirhinal neurons *in vivo*. Spontaneous (A, B1–2) and current-evoked (B3) activity. (A, B) Two different regular spiking perirhinal neurons. EEG activity (Field) recorded in the vicinity of recorded cells is depicted above the intracellular (Intra) trace in (A) and (B1–2). Spontaneous (C, D) and current-evoked (E) activity of the bursting cell is also provided. Modified from Pelletier *et al.* (2005a).

section will focus on these two areas. However, it should be noted that in primates a much larger portion of the prefrontal cortex is reciprocally linked to the amygdala.

Like Krettek and Price (1977a), we will use a combination of the criteria proposed by Brodmann (1905, 1908) and Rose and Woolsey (1948) to distinguish the infralimbic and prelimibic cortices. The prelimbic region (area 32 of Brodmann) is characterized by a homogeneous layer V where large pyramidal neurons dominate. In contrast, the ventrocaudally located infralimbic cortex (area 25 of Brodmann) has an indistinct lamination.

Little information is available regarding the electroresponsive properties of medial prefrontal neurons. In part, this reflects a cultural gap. Indeed, it appears that many electrophysiologists refer the medial prefrontal region to the anterior cingulate cortex. The available data suggest that the medial prefrontal cortex contains the usual variety of physiologically defined cell classes, including the prevalent regular spiking cells with a spiny pyramidal morphology.[2] Similarly, in one *in vivo* intracellular study of the prelimbic cortex, the vast majority of pyramidal cells were classified as regular-spiking neurons and 11% as intrinsically bursting neurons (Thierry *et al.*, 2000).

4.2 Connections

4.2.1 Rhinal cortices

The rhinal cortices are typically described as the essential relay station of sensory inputs to the hippocampus. They also constitute the main path for return hippocampal projections to the neocortex (reviewed in Witter *et al.*, 1989). With the exception of olfactory inputs that have direct access to parts of the entorhinal cortex, sensory inputs reach the hippocampus through largely parallel cascades of corticocortical connections that originate in primary sensory cortical areas, progress through a sequence of parasensory cortical areas, and ultimately end in the perirhinal cortex (Jones & Powell, 1970; Room & Groenewegen, 1986a; Turner & Zimmer, 1984; Van Hoesen & Pandya, 1975). From the primary sensory cortices to the distal unimodal parasensory areas, the representation of sensory information evolves from a topographic (somatotopic, retinotopic, etc.), feature-based representation to a complex, stimulus-centred one based on the coalescence of elementary features into larger symbolic entities (Miyashita, 1993).

Within the rhinal cortices, information would progress toward the hippocampus through the sequential, stepwise activation of longitudinal bands of cortex (neocortex to perirhinal area 36 to area 35 to entorhinal cortex to hippocampus and conversely; Figures 4.1B1 and 4.4[3]). In addition, superimposed on these transverse neocortical projections is an intrinsic system of longitudinal connections that spans the entire rostrocaudal extent of the rhinal cortices (Witter *et al.*, 1986). As a result, transversely distributed activation patterns representing sensory information about the same or different

[2] Incidentally, the first study to correlate the physiological and morphological properties of cortical neurons was performed in two cortical regions: the anterior cingulate and visual cortex (McCormick *et al.*, 1985). The authors reported that there were no significant differences in neuronal properties between these two cortical areas.

[3] This stepwise progression of impulses is not absolute, however, as some neurons project beyond the adjoining area in the lateromedial or mediolateral directions (Figure 4.1B2).

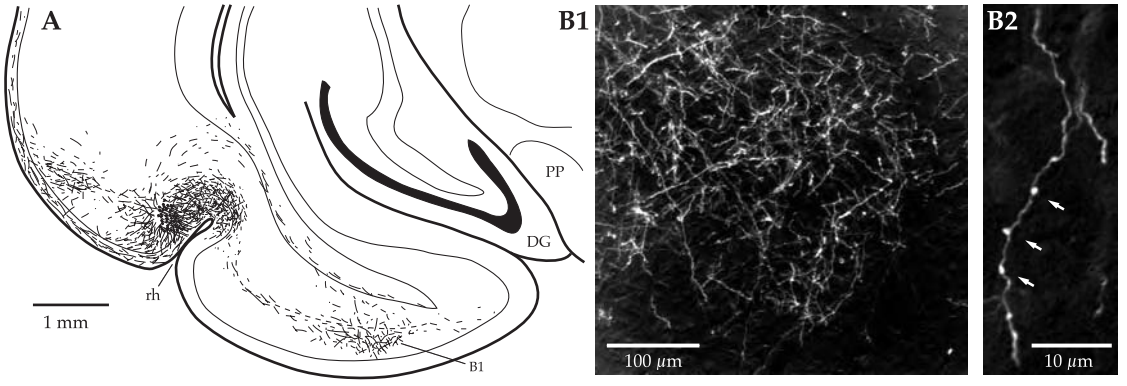

Fig. 4.4 Projections of perirhinal area 36 to other rhinal fields. Iontophoretic injection of the anterograde tracer PHA-L in area 36 produces massive labelling in area 35 and moderate labelling in the lateral entorhinal cortex of the guinea pig. (A) Mapping of the relative distribution of PHA-L immunoreactive elements. (B) PHA-L-positive axons in the lateral entorhinal cortex at a low (B1) and high (B2) magnification. Abbreviations: DG, dentate gyrus; PP, pes pedunculi; rh, rhinal sulcus. Modified from Pinto *et al.* (2006).

modalities can converge on subsets of perirhinal or entorhinal cells. This possibility is supported by the fact that, in the perirhinal cortex at least, long-range intrinsic longitudinal pathways do not engage inhibitory interneurons (Biella *et al.*, 2001, 2002; Martina *et al.*, 2001) (Figure 4.5).

In addition, the rhinal cortices have strong reciprocal connections with the medial prefrontal cortex (Hurley *et al.*, 1991; Condé *et al.*, 1995). Most rhinal projections of the medial prefrontal cortex originate from layers II–III of the infralimbic (area 25) cortex and to a lesser extent of the prelimbic (area 32) cortex (Room *et al.*, 1985; Room & Groenewegen, 1986a). Medial prefrontal projections to the perirhinal cortex target the medial-most portion of area 35 (Figures 4.1 and 4.6). The infralimbic cortex also projects to much of the lateral entorhinal cortex (superficial and deep layers). Both, the peri- and entorhinal cortices send return projections to the infra- and prelimbic cortex where rhinal axons are seen in all layers with a higher concentration in layer II. Rhinal projections are particularly strong in the infralimbic cortex and originate from deep rhinal layers (Hurley *et al.*, 1991; Condé *et al.*, 1995).

Finally, like most cortical fields, the rhinal cortices receive inputs from brainstem and basal forebrain modulatory systems (see Chapter 5), they project to the striatum (including nucleus accumbens), and they are reciprocally connected to the dorsal thalamus (principally with posterior thalamic and midline/intralaminar nuclei) (Burwell & Witter, 2002). More unusual however, are the strong reciprocal connections formed by the rhinal cortices with the basolateral complex of the amygdala (Pitkänen *et al.*, 2000). In light of recent findings implicating the medial prefrontal cortex and amygdala in the control of reward-related behaviour and emotions (Aggleton, 2000; Baxter & Murray, 2002), these results suggest that impulse traffic through the parahippocampal cortices may vary depending on the emotional significance of current environmental contingencies.

4.2.2 Medial prefrontal cortex

Tract-tracing experiments suggest that memory, viscera and emotion meet in the medial prefrontal cortex.[4] First, the medial prefrontal

[4] The following account is based on a synthesis of tract-tracing studies conducted in rats (Sesack *et al.*, 1989; Condé *et al.*, 1990, 1995; Hurley *et al.*, 1991; Terreberry & Neafsey, 1987; Takagishi & Chiba, 1991; Vertes, 2004), guinea pigs (Pritzel & Markowitsch, 1981), cats (Niimi *et al.*, 1981; Cavada & Reinoso-Suarez, 1985; Room *et al.*, 1985; Musil & Olson, 1988), rabbits (Buchanan *et al.*, 1994) and monkeys (Hardy & Leichnetz, 1981; Carmichael & Price, 1995a,b; Öngür & Price, 2000).

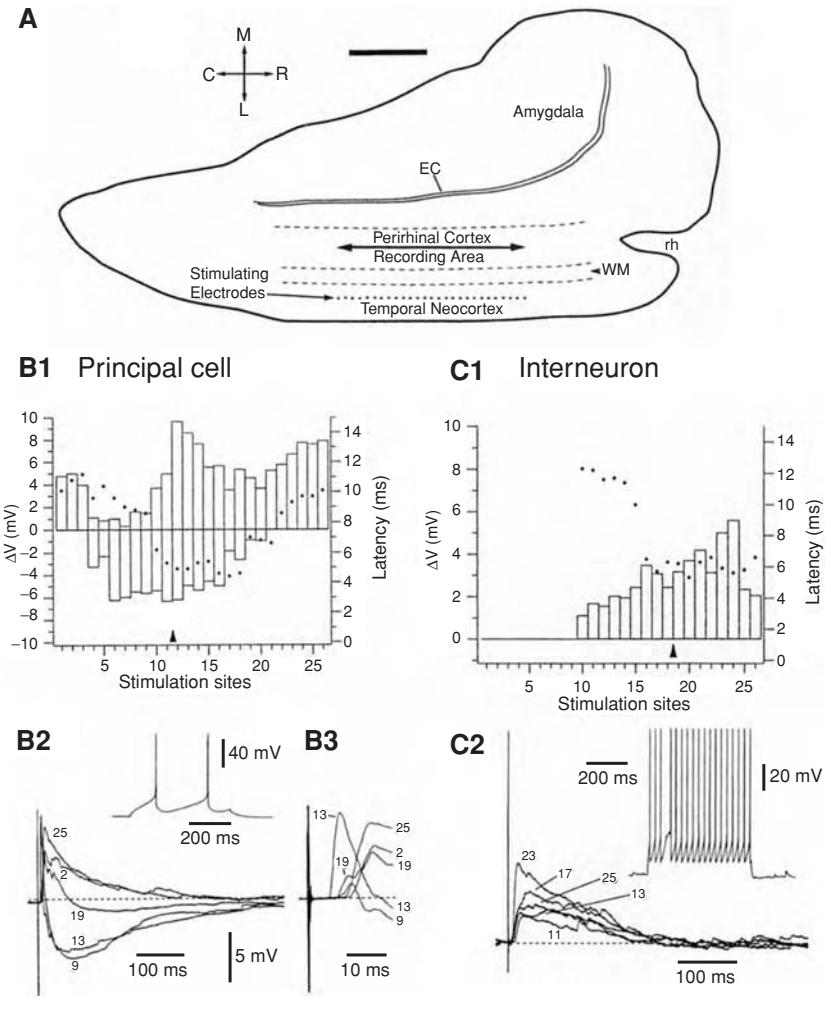

Fig. 4.5 Propagation of neocortical impulses in the perirhinal cortex. (A) Scheme showing horizontal coronal slice as it appeared in the recording chamber. Stimulation sites (dots) in the temporal cortex were separated by 160 μm. Principal cells (B) and fast-spiking interneuron (C) were depolarized to around −60 mV and their responses to neocortical stimuli were analysed. (B1, C1) Response amplitudes (left axis, bars) and latencies (right axis, dots) as a function of the neocortical stimulation sites (x-axis). The rostrocaudal position of the recorded perirhinal cells is indicated by the triangles at the bottom of each graph. (B2, C2) Examples of actual responses to neocortical stimuli (numbers indicate stimulation sites and can be related to the *x*-axes of panels B1 and C1). Neocortical stimulation sites in rostrocaudal register with principal perirhinal neurons (B1–2) elicited a sequence of excitatory and inhibitory synaptic potentials. In contrast, apparently pure excitatory responses were observed when the stimulating and recording sites were separated by 1 mm or more in the rostrocaudal axis. This result suggests that adjacent and distant neocortical stimuli influence regular spiking perirhinal neurons by pathways that respectively form and do not form synapses with inhibitory interneurons. In keeping with this, presumed interneurons (C1–2) did not respond to distant neocortical stimuli and exhibited apparently pure excitatory responses. These results suggest that neocortical inputs recruit perirhinal inhibitory interneurons located at the same transverse level, limiting the depolarization of principal perirhinal cells. In contrast, distant neocortical inputs only evoke excitation because longitudinal perirhinal pathways do not engage inhibitory interneurons. Abbreviations: EC, external capsule; WM, white matter. Modified from Martina *et al.* (2001).

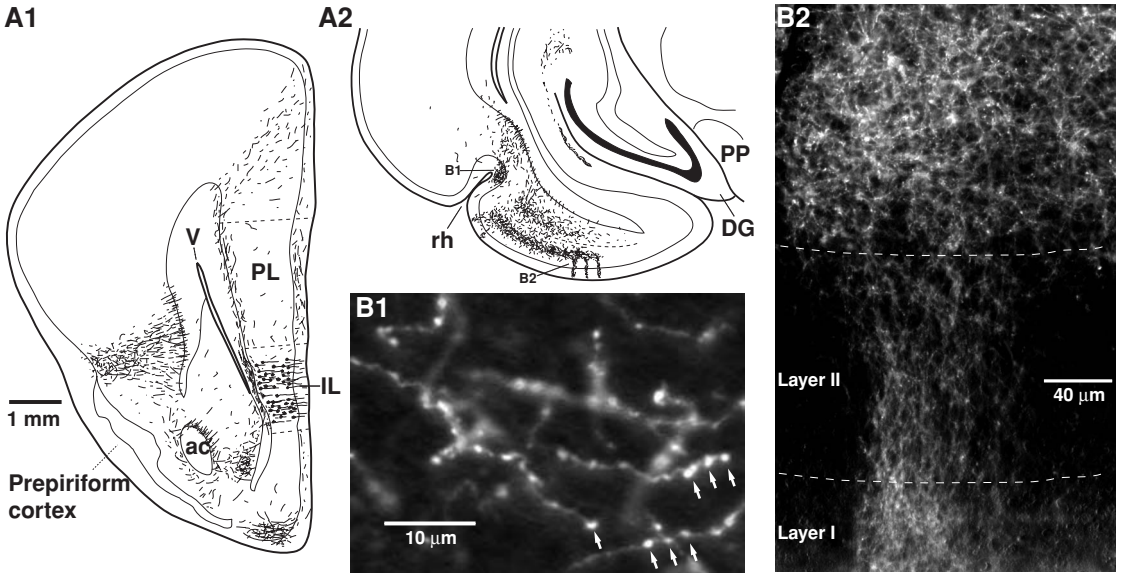

cortex has reciprocal links with several components of the declarative memory system of the temporal lobe, including the rhinal cortices (see details in Section 4.2.1) and components of the hippocampal formation (the subiculum and field CA1). Second, the insula, which is the primary viscerosensory cortex, sends a major projection to the medial prefrontal cortex. Finally, as will be reviewed in detail below (Section 4.3), the medial prefrontal cortex has robust reciprocal links with the amygdaloid complex.

In addition to links with the rhinal and insular cortices, the infra- and prelimbic regions also have ipsilateral projections to each other as well as contralateral projections to the homologous field. Links with the retrosplenial and cingulate cortex have also been reported.

Thalamic inputs to the medial prefrontal cortex originate from the medial portion of the mediodorsal thalamic nucleus and various so-called midline thalamic nuclei including the parataenial, paraventricular, rhomboid and reuniens. Most of these connections are reciprocal.

The medial prefrontal cortex projects to the ventral striatum (shell and core of nucleus accumbens) but divergent findings have been reported concerning the relative contribution of the infra- and prelimbic cortex to this projection.

Because of the infralimbic projections to the hypothalamus and brainstem, several investigators have described the medial prefrontal cortex as a primary visceromotor cortical area. This suggestion is supported by numerous reports that electrical stimulation of the medial prefrontal cortex elicits cardiovascular responses. Projections supporting this classification include those directed to the bed nucleus of the stria terminalis, lateral hypothalamus, medial preoptic area,[5] periaqueductal grey, parabrachial nucleus, nucleus of the solitary tract, dorsal motor vagal nucleus, nucleus ambiguus and the ventrolateral

Fig. 4.6 Projection of the infralimbic cortex to the rhinal cortices. Iontophoretic injection of the anterograde tracer PHA-L in the infralimbic cortex (IL) produces a focused pattern of labelling at the border between area 35 and the lateral entorhinal cortex as well as more medially in the entorhinal cortex of the guinea pig. (A) Mapping of the relative distribution of PHA-L immunoreactive elements at the level of the injection site (A1) and in the rhinal cortices (A2). (B) PHA-L-positive axons in the rhinal region (see (A2) for their location). Most labelled axons bore axon varicosities. Abbreviations: ac, anterior commissure; DG, dentate gyrus; IL, infralimbic cortex; PL, prelimbic cortex; PP, pes pedunculi; rh, rhinal sulcus; V, ventricle. A. Pinto & D. Paré, unpublished observations.

[5] Other than the medial prefrontal cortex, rather few cortical regions project to the hypothalamus; they include the olfactory cortex and subiculum.

medulla (Hurley *et al.*, 1991; Condé *et al.*, 1995). The infralimbic cortex also projects to the intermediolateral column of the spinal cord.[6]

To add to these unusual connectional properties, the infralimbic cortex projects to many modulatory cell groups, including the dorsal raphe nucleus, the ventral tegmental area and substantia nigra (pars compacta), as well as the posterior hypothalamus. These nuclei respectively constitute the main source of serotonin, dopamine and histamine inputs to the telencephalon. Finally, like many other cortical areas, the infralimbic cortex also projects to the cholinergic cells groups of the basal forebrain.

4.3 Interactions between the rhinal and medial prefrontal cortices and amygdala

4.3.1 Reciprocal links with the amygdala

Rhinal cortices

The rhinal cortices have strong reciprocal connections with the basolateral complex of the amygdala.[7] The densest perirhinal projections of the amygdala originate from the lateral nucleus, but projections from the basal nuclei are far from negligible. In rats and cats, amygdala axons mainly end in layers I–II of the perirhinal cortex but the deep layers also receive amygdala inputs. The basolateral amygdaloid complex mainly targets the ventrolateral entorhinal region. Amygdala projections focus on layer III but also extend in between the cell islands of layer II as well as in deep layers. Electron microscopic observations of amygdala axon terminals in the rhinal cortices of cats and monkeys indicate that they only form asymmetric synapses, typically with dendritic spines (Smith & Paré, 1994; Pitkänen *et al.*, 2002).[8]

Entorhinal projections to the amygdala originate in deep layers and mainly end in the basolateral nucleus. Perirhinal projections mainly originate in superficial neurons and end in the lateral nucleus, with more moderate projections to the rest of the basolateral complex. It should be noted that the lateral sector of the central nucleus also receives perirhinal and entorhinal inputs, although the relative importance of this projection varies between species. Electron microscopic observations indicate that rhinal axon terminals only form asymmetric synapses in the basolateral amygdala, typically with dendritic spines (Smith *et al.*, 2000). This appears to be typical of all cortical inputs to the basolateral complex as the same finding was reported after anterograde tracer injections in neocortical temporal (Farb & LeDoux, 1999) and medial prefrontal areas (Smith *et al.*, 2000; Brinley-Reed *et al.*, 1995).

Medial prefrontal cortex

There are strong reciprocal connections between the medial prefrontal cortex and amygdala.[9] The infralimbic cortex mainly projects to the lateral sector of the central nucleus, intercalated cell masses

[6] It is probably not a coincidence that there is an almost complete overlap between the hypothalamic, brainstem and spinal projections of the infralimbic cortex and medial sector of the central nucleus of the amygdala.

[7] The following account is based on a synthesis of the following tract-tracing studies conducted in rats (Beckstead, 1978; Krettek & Price, 1977a,b; Deacon *et al.*, 1983; Mascagni *et al.*, 1993; McDonald *et al.*, 1996; McDonald & Mascagni, 1997; Pikkarainen *et al.*, 1999; Shi & Cassell, 1999), cats (Krettek & Price, 1977a,b; Russchen, 1982a; Room & Groenewegen, 1986b; Witter & Groenewegen, 1986; Smith & Paré, 1994; Paré *et al.*, 1995c) and monkeys (Rosene & Van Hoesen, 1977; Amaral & Cowan, 1980; Amaral & Price, 1984; Amaral, 1986; Saunders & Rojene, 1988; Saunders *et al.*, 1988; Stefanacci *et al.*, 1996).

[8] This appears to apply to all cortical projections of the basolateral amygdala, as another ultrastructural study on the amygdalo-insular projection reached the same conclusion (Paré *et al.*, 1995c).

[9] The following account is based on a synthesis of the following tract-tracing studies conducted in rats (Krettek & Price, 1977a; Sarter & Markowitsch, 1983, 1984; Sesack *et al.*, 1989; Hurley *et al.*, 1991; Shinonaga *et al.*, 1994; Condé *et al.*, 1995; McDonald *et al.*, 1996; Vertes, 2004), cats (Krettek & Price, 1977a; Russchen, 1982a; Smith *et al.*, 2000), rabbits (Buchanan *et al.*, 1994) and monkeys (Amaral & Price, 1984; Barbas & De Olmos, 1990; Carmichael & Price, 1995a,b; Freedman *et al.*, 2000; Öngür & Price, 2000; Ghashghaei & Barbas, 2002).

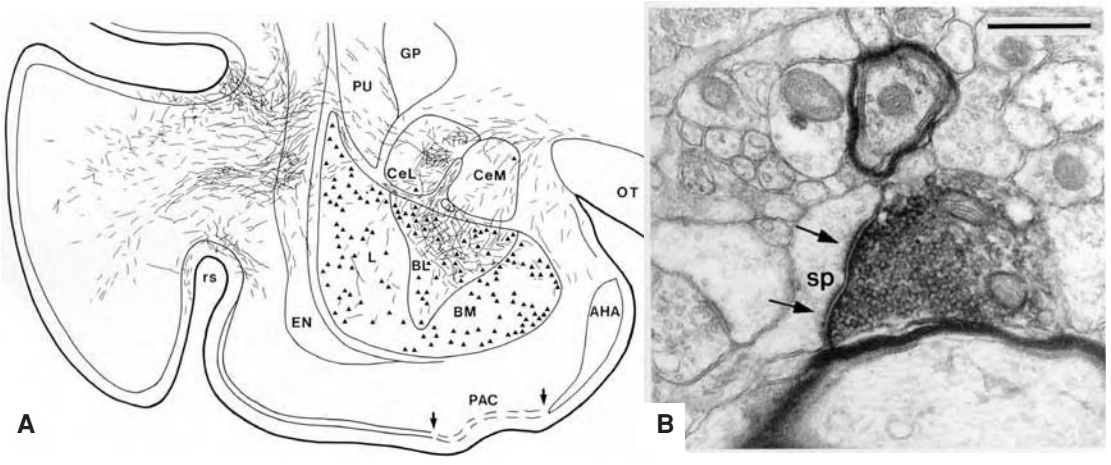

and components of the basolateral complex. There are species differences in this regard, with infralimbic projections mainly targeting the basolateral nucleus in cats (Figure 4.7A), compared with the accessory basal and lateral nucleus in rats. Similarly, the prelimbic region projects to the basolateral nucleus and ventral part of the lateral nucleus. Infra- and prelimbic projections to the central amygdala and basolateral complex originate in neurons located in layers V and II–III, respectively. Projections from the amygdala to the medial prefrontal cortex mainly originate from the basolateral and accessory basal nuclei of the amygdala.

Electron microscopic observations of medial prefrontal axon terminals in the rat and cat amygdala indicate that they only form asymmetric synaptic contacts, usually on dendritic spines (Figure 4.7B) (Smith *et al.*, 2000; Brinley-Reed *et al.*, 1995). Since principal cells of the basolateral complex are spiny whereas local-circuit neurons are aspiny or sparsely spiny, these observations imply that most medial prefrontal axons form excitatory synapses with principal cells.

Fig. 4.7 Projection of the medial prefrontal cortex to the cat amygdala. (A) Iontophoretic injection of the anterograde tracer PHA-L in the medial prefrontal cortex reveals dense projections to the basolateral nucleus, central lateral nucleus and intercalated cell masses. Projections to the lateral nucleus are modest. Each triangle represents 3 parvalbumin-immunoreactive neurons. (B) At the electron microscopic level, PHA-L-immunoreactive axon terminals were seen to form only asymmetric synapses, usually with dendritic spines. Scale bar, 0.5 μm. Abbreviations: AHA, amygdalohippocampal area; BL, basolateral nucleus of the amygdala; BM, basomedial nucleus of the amygdala; CeL, central lateral nucleus of the amygdala; CeM, central medial nucleus of the amygdala; EN, entopeduncular nucleus; GP, globus pallidus; L, lateral nucleus of the amygdala; OT, optic tract; PAC, periamygdaloid cortex; PU, putamen; rs, rhinal sulcus; sp, spine. Modified from Smith *et al.* (2000).

4.3.2 Physiological studies of amygdalorhinal relations

Conduction times between the amygdala and perirhinal cortex

Electrophysiological studies have revealed that axons from the lateral amygdaloid nucleus to the perirhinal cortex display a uniform range of conduction times despite considerable variations in the distance they must travel to reach their targets (Pelletier & Paré, 2002). This situation is reminiscent of the arrangement found in other neuronal systems where synchronized activity is critical. For instance, in the bird auditory system, where precise timing of afferent signals is key, the conduction time between the cochlear nucleus and its ipsi- and contralateral brainstem targets is kept constant by lengthening the path of axons ending ipsilaterally (Carr & Konishi, 1990). A similar situation is found in the electric organs of fish. In this case, electrocytes are activated synchronously by increasing the conduction speed of longer axons and lengthening the path of fibres terminating in more proximal portions of the electric organ (Bennett, 1970).

In the amygdaloperirhinal circuit, conduction times were studied by measuring the antidromic response latencies of lateral amygdala neurons to electrical stimuli delivered at various rostrocaudal levels of the perirhinal cortex. Although large variations in antidromic response latencies were observed, they were unrelated to the distance between the perirhinal stimulation sites and lateral amygdala neurons (Figure 4.8A). Moreover, some lateral amygdala cells with branching axons to two distant perirhinal sites (9 mm) had virtually identical conduction times to the two perirhinal sites even though the distance to target was much longer for one of the two target sites (Figure 4.8B) (Pelletier & Paré, 2002).[10]

Thus, these results indicate that the conduction speed and/or path of lateral amygdala axons are adjusted to compensate for variations in distance between the lateral amygdala and distinct rostrocaudal perirhinal sites. Whether this arrangement also characterizes amygdala projections to the entorhinal cortex has not been tested yet.

Amygdalorhinal interactions during slow-wave sleep

In contrast with thalamocortical circuits, where neuronal events often have clear correlates in the environment, the meaning of a spike train in amygdalocortical networks is not always obvious. As a result, physiologists have devoted comparatively less attention to amygdalocortical circuits. In a few studies, this problem was circumvented by examining neuronal events contributing to the generation and propagation of various EEG rhythms typical of anaesthetized or naturally sleeping brains.

In one study, field and unit recordings were performed simultaneously in the lateral amygdala and perirhinal cortex of cats anaesthetized with ketamine–xylazine (Collins *et al.*, 2001). In these conditions, the perirhinal cortex and lateral amygdala exhibited a similar pattern of spontaneous activity (Figure 4.9). Recordings at both sites were dominated by a slow oscillation at around 1 Hz onto which was superimposed a faster rhythm (*c.*30 Hz) whose amplitude fluctuated cyclically (Figure 4.9A4). Neurons of the lateral amygdala and perirhinal cortex displayed correlated modulations of firing probability in relation to both types of oscillations (Figure 4.9B). Even when the recording sites were separated by as much as 6 mm, the slow oscillation remained highly correlated (Figure 4.9C). In contrast, the correlation of fast oscillations was generally lower and decreased steeply with distance (Figure 4.9C).

In a second study, multisite extracellular recording techniques were used to track the sequence of events underlying the genesis of synchronized neuronal events, termed sharp potentials (Figure 4.10A), that occur spontaneously in the entorhinal and perirhinal cortices during EEG-synchronized states such as during slow-wave sleep or under anesthesia (Paré *et al.*, 1995a).[11] This study revealed that there are two types of entorhinal sharp potential: simple and complex. Simple sharp potentials are monophasic, depth-negative, surface-positive events (Figure 4.10B1), whereas complex sharp potentials are

[10] These results were not due to current spread because the antidromic response latency of PRH neurons to electrical stimuli applied in the PRH cortex increased linearly with the distance between the stimulating and recording sites. Second, a statistically significant correlation between conduction times and distance to target was also found in the perirhinal to LA pathway.

[11] Entorhinal sharp potentials should not be confused with sharp waves. Sharp waves are population events that result from population bursts in CA3 pyramidal neurons (Buzsáki, 1986), leading to a large negative field potential in the stratum radiatum and firing of CA1 pyramidal cells. Sharp waves occur during immobility, consummatory behaviours and slow-wave sleep. They appear to trigger, or be associated with, an increase in the amplitude of fast oscillations (*c.*200 Hz), termed ripples (Buzsáki *et al.*, 1992; Ylinen *et al.*, 1995). Although hippocampal sharp waves are known to cause an increase in the activity of deep entorhinal neurons (Chrobak & Buzsáki, 1996), they appear to be distinct from entorhinal sharp potentials. Indeed, entorhinal SPs persist under deep barbiturate anaesthesia, whereas hippocampal sharp waves are abolished in these conditions. Moreover, no systematic relation was seen between the timing of entorhinal sharp potentials and hippocampal sharp waves (Paré *et al.*, 1995a).

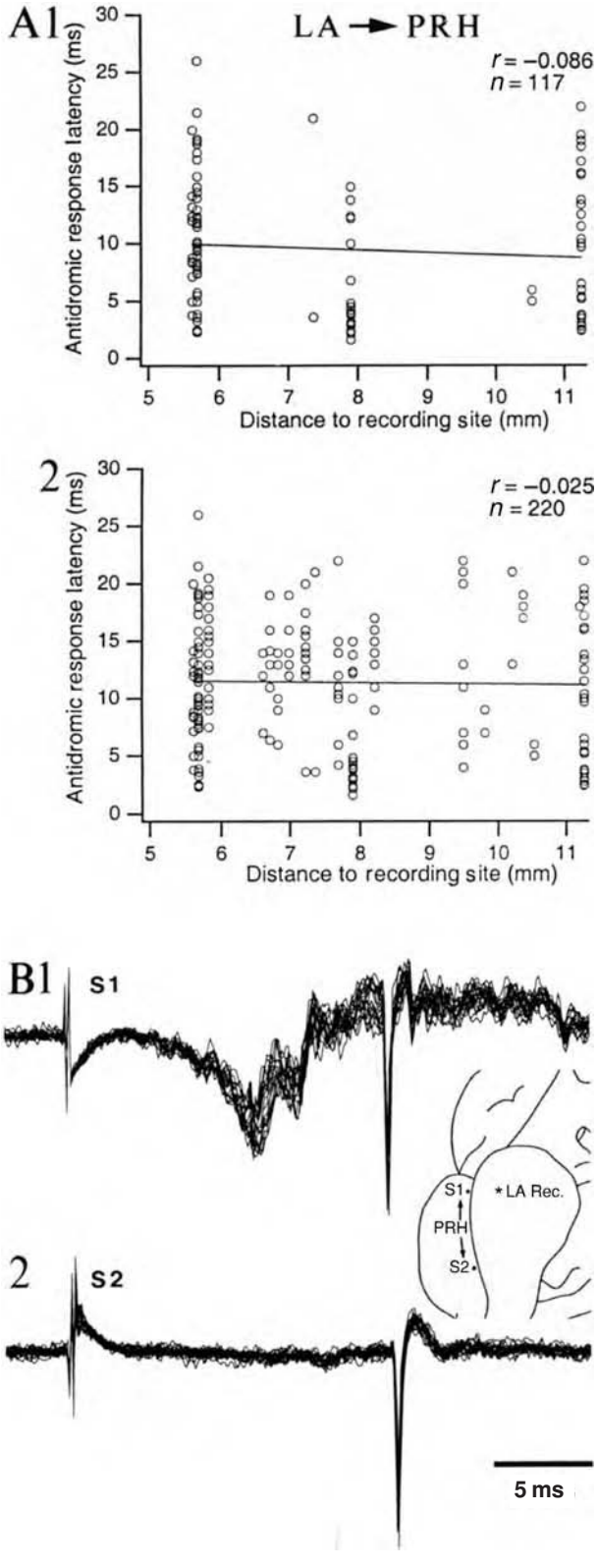

Fig. 4.8 Uniform range of conduction times from the lateral amygdala to distributed perirhinal sites. (A) Antidromic response latencies in lateral amygdala neurons (left) as a function of distance from perirhinal stimulation sites. (A1) and (A2) show data from a particular experiment and all experiments combined, respectively. (B) Example of a lateral amygdala neuron with a branching axon to distant perirhinal sites. The scheme indicates the relative position of the recorded cell (asterisk) and perirhinal stimulation sites (S1–2). Note almost identical antidromic response latencies despite strikingly different travel distances. Abbreviations: LA, lateral amygdala; PRH, perirhinal cortex. Modified from Pelletier & Paré (2002).

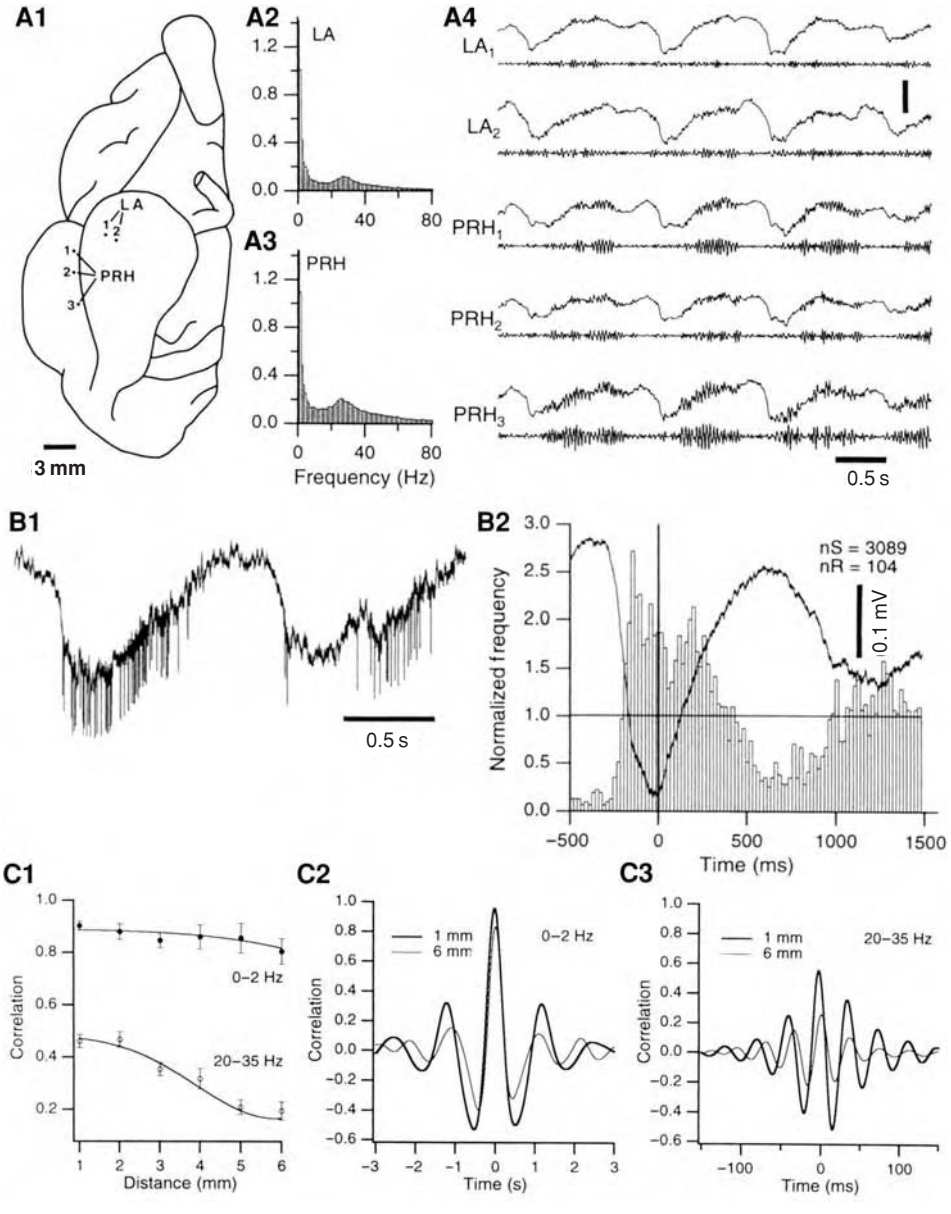

Fig. 4.9 Ketamine–xylazine induces a slow oscillation in the perirhinal cortex (PRH) and lateral amygdala (LA). (A1) Scheme indicating position of recording sites in the lateral amygdala and perirhinal cortex. (A2–3) Spectral composition of the spontaneous focal activity recorded in the LA (A2) and perirhinal cortex (A3). (A4) For each recording site, there are two traces. The top trace shows the complete signal (no filtering) whereas the lower trace was digitally filtered between 20 and 35 Hz to show the temporal relation existing between the phase of the slow oscillation and the amplitude of faster rhythms. Voltage calibration in A4 corresponds to 0.5 mV for the top traces and 0.3 mV for the bottom traces. (B) Relation between unit discharges and slow focal oscillations. (B1) Unit activity and superimposed focal activity recorded in the lateral amygdala. (B2) Peri-event histogram of neuronal discharges for the same cell. (C) Effect of distance between recording sites on the correlation between fast and slow focal waves. (C1) Correlation coefficient (*y*-axis) as a function of distance between PRH recording sites (*x*-axis) for slow (dark circles) and fast (empty circles) focal oscillations. (C2–3) Two superimposed correlograms of slow (C2) and fast (C3) oscillations with intersite distances of 1 (thick line) and 6 mm (thin line). Modified from Collins *et al.* (2001).

generally larger amplitude triphasic events (Figure 4.10B2). Whereas complex sharp potentials may occur in isolation, they are usually preceded by a simple sharp potential (50–100 ms before). The basolateral amygdaloid nucleus plays a critical role in the genesis of entorhinal sharp potentials. This statement is based on the following observations: (a) within the amygdalohippocampal circuit, neurons of the basolateral nucleus display the earliest signs of increased discharge probability in relation to simple entorhinal sharp potentials, as much as 40 ms before their peak (Figure 4.11). Second, amygdala lesions abolish entorhinal sharp potentials (Figure 4.12).

These observations in cats are consistent with findings from different laboratories and species regarding amygdalo-entorhinal relations. For instance, stimulation of the basolateral nucleus evokes depth-negative – surface-positive waves followed by a slower potential of opposite polarity in the rat entorhinal cortex (Colino & Fernández de Molina, 1986). As was the case for entorhinal sharp potentials, the depth-negative component of this field potential reversed polarity around layer II and was associated with an increased probability of neuronal discharges. During this response, most classes of entorhinal neuron displayed EPSP–IPSP sequences (Finch *et al.*, 1986).

The mechanisms allowing the basolateral nucleus to generate sharp potential-related population bursts remain unclear. Intracellular recordings of basolateral neurons obtained *in vivo* (D. Paré, unpublished observations) have revealed that sharp potential-related basolateral discharges arise from EPSPs that often give rise to spike doublets. Spike doublets or bursts with similar properties can be elicited in many basolateral neurons by depolarizing current injection. These findings suggest that basolateral neurons may, by virtue of their intrinsic membrane properties and profuse intranuclear connectivity, amplify weak extra-amygdaloid synaptic inputs into synchronized neuronal events. Because the entorhinal cortex has reciprocal connections with the basolateral nucleus, it is a good candidate for initiating and reinforcing the explosive sharp-potential-related discharge of basolateral neurons.

In naturally sleeping animals, simple entorhinal sharp potentials have no hippocampal correlate, whereas complex ones are followed by a negative potential in the dentate gyrus. The reason for this is simple: entorhinal layer II neurons only fire in relation to complex sharp potentials (Paré *et al.*, 1995a). Because the bulk of entorhinal–hippocampal projections arise in layer II stellate neurons (Ruth *et al.*, 1982; Witter & Groenewegen, 1984), their selective activation in relation to complex sharp potentials probably accounts for the observation that simple entorhinal sharp potentials have no hippocampal correlate.

At present, it is unclear why layer II entorhinal neurons are selectively activated in relation to complex sharp potentials. The fact that most complex sharp potentials are usually preceded by low-amplitude simple ones, raises the possibility that complex sharp potentials constitute a rebound phenomenon. Consistent with this idea, layer II stellate cells can generate rebound discharges at the end of

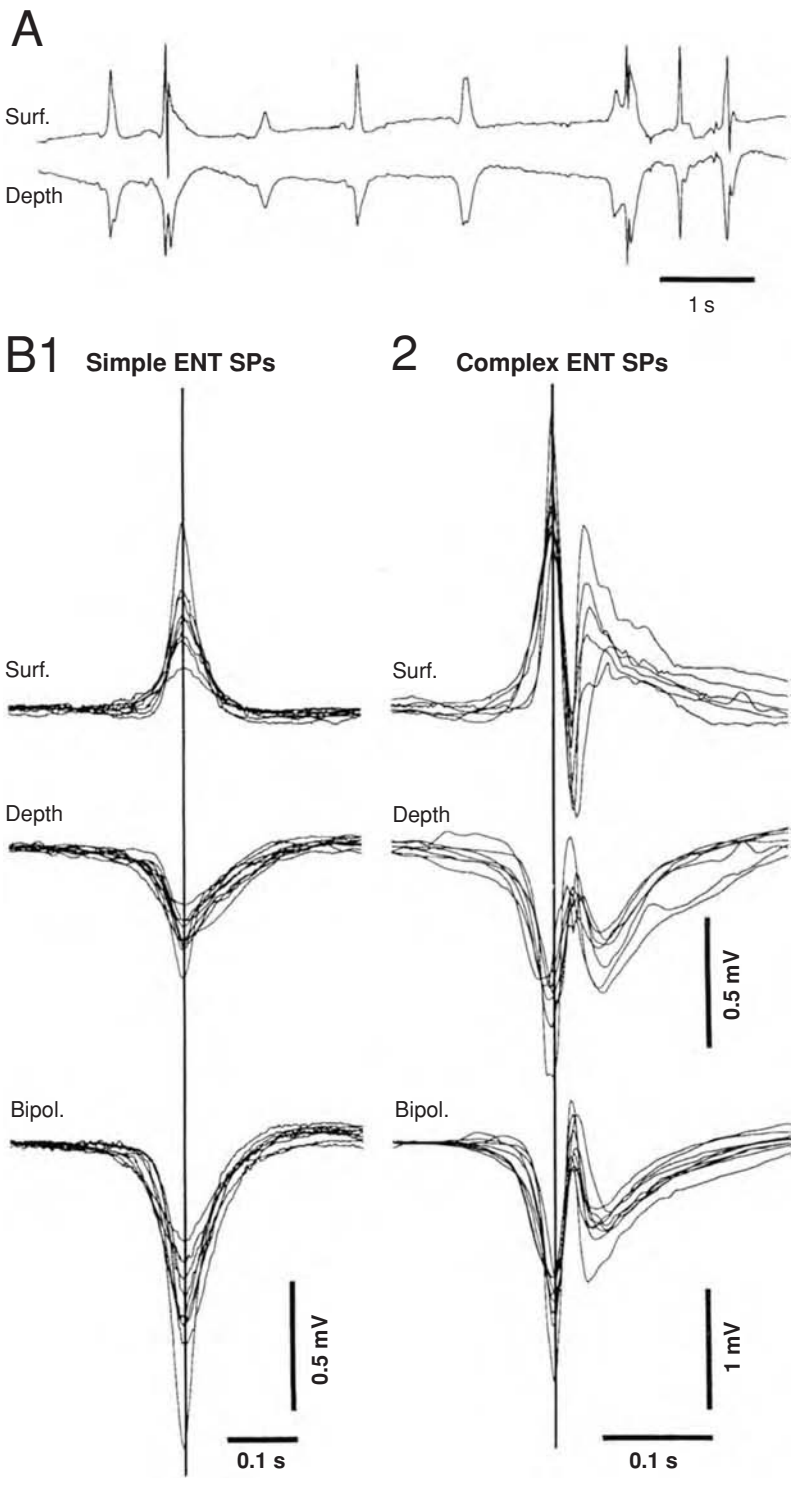

Fig. 4.10 Simple and complex sharp potentials (SPs) dominate the ENT EEG under barbiturate anaesthesia. (A) Spontaneous activity of the ENT cortex simultaneously recorded with two closely spaced electrodes, one in layer I (Surf.) and the other in the deep ENT layers (Depth). (B) Superimposed sharp potentials of the simple (B1) and complex (B2) types. Simultaneously recorded superficial (Surf.), and deep (Depth) ENT signals are displayed along with bipolarly recorded sharp potentials (Bipol.). Modified from Lang and Paré (1998).

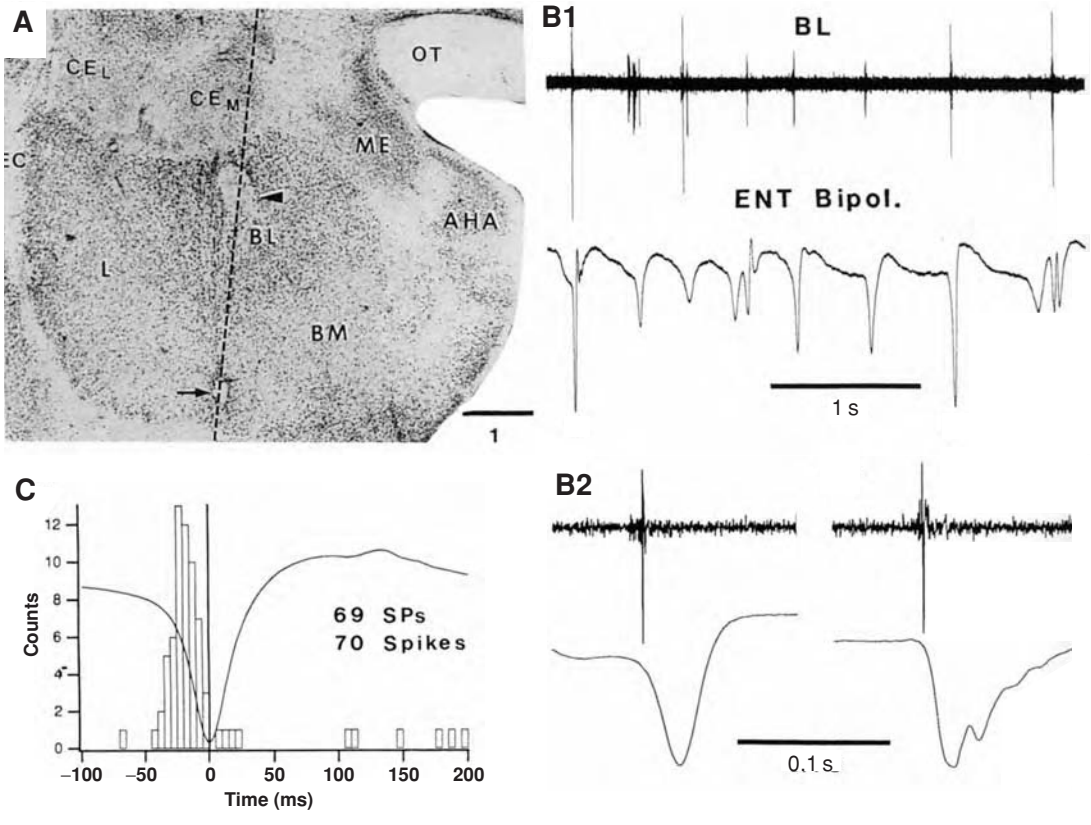

Fig. 4.11 Activity of basolateral amygdala neurons in relation to entorhinal sharp potentials. (A) Thionin-stained coronal section showing an electrode track (dashed line) across the basolateral nucleus. Two electrolytic lesions (arrowhead and arrow) mark the location of the first and last encountered neurons discharging before the negative peak of reference entorhinal sharp potentials. Calibration bar in mm. (B) SP-related activity of basolateral (BL) neurons (upper trace) recorded at the site marked by an arrowhead in (A) and simultaneously recorded entorhinal (ENT) sharp potentials (lower trace). Unit activity was highpass filtered at 300 Hz. (C) Peri-sharp potential histogram of neuronal discharges for the cell emitting the large-amplitude spikes shown in (B). Modified from Paré *et al.* (1995a).

hyperpolarizing pulses, a behaviour mediated by a hyperpolarization-activated mixed cationic current and low-threshold sodium and calcium conductances (Jones, 1990; Alonso & Klink, 1993; Klink & Alonso, 1993). Thus, the activation of layer II stellate cells in relation to complex sharp potentials may represent a rebound response mediated by intrinsic conductances but triggered by EPSPs occurring during the shallow IPSPs related to the preceding simple sharp potentials.

Surprisingly, the activation of layer II neurons in relation to complex sharp potentials gives rise to distinct hippocampal events in barbiturate-anaesthetized compared to naturally sleeping cats (Paré *et al.*, 1995a). During natural sleep, there is no trace of sharp-potential-related entorhinal inputs beyond the dentate gyrus whereas they are routinely observed under anaesthesia (Paré *et al.*, 1995a).[12]

[12] In the molecular layer of the dentate gyrus, sharp potentials appeared as negative fields with a polarity reversal close to the granule cell layer. They reached their peak 15–25 ms after complex entorhinal sharp potentials. Similar events were seen in the rat (Bragin *et al.*, 1995b). These dentate potentials, termed dentate spikes, were abolished by entorhinal lesions and were concomitant with a population burst of hilar interneurons (Bragin *et al.*, 1995b).

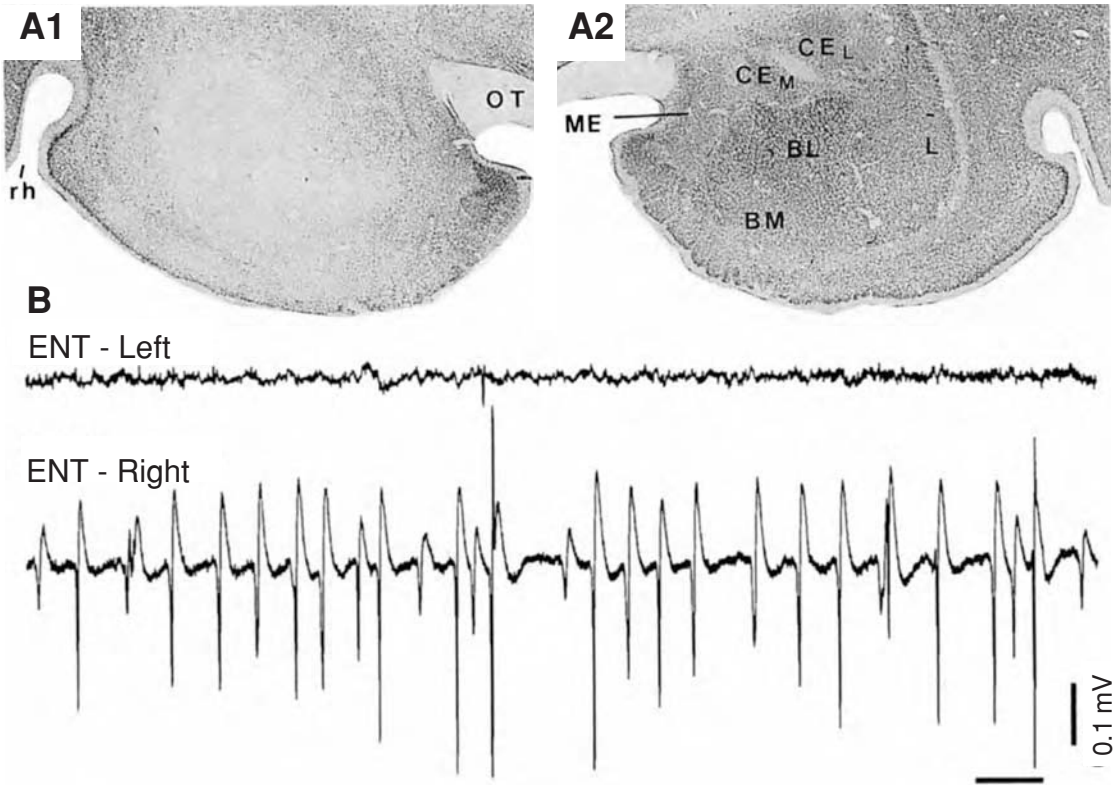

Fig. 4.12 Unilateral excitotoxic lesions of the amygdala abolish entorhinal sharp potentials ipsilaterally. (A) Thionin-stained coronal sections of the amygdala on the side ipsi- (A1) and contralateral (A2) to the lesion produced by a kainic acid injection. (B) Entorhinal field potentials on the side ipsi- (left) and contralateral (right) to the amygdala lesion. Abbreviations: BL, basolateral nucleus of the amygdala; BM, basomedial nucleus of the amygdala; CE_L, central lateral nucleus of the amygdala; CE_M, central medial nucleus of the amygdala; L, lateral nucleus of the amygdala; OT, optic tract; rh, rhinal sulcus. Modified from Paré *et al.* (1995a).

The reason why SP-related entorhinal synaptic volleys do not activate the tri-synaptic path in naturally sleeping animals may reside in the high firing threshold of granule cells. It is indeed known that the firing threshold of dentate granule cells is higher than that of hilar interneurons (Buzsáki & Eidelberg, 1982; Scharfman, 1991). According to this view, the firing of granule cells would be prevented by the activation of hilar inhibitory neurons.

Amygdalorhinal interactions during arousal and REM sleep

That the amygdalorhinal system can generate synchronized neuronal events was shown not only in anaesthetized animals and during slow-wave sleep, but also in brain-activated states such as arousal and REM sleep. The main 'limbic' EEG rhythm associated with brain activation is the theta oscillation. Several classifications of theta oscillations have been proposed (Buzsáki, 2002) depending on their

pharmacological sensitivity or behavioural correlates. From the latter standpoint, theta oscillations have been classified as type 1 theta, occurring during locomotor activity, and type 2 theta, observed in emotionally arousing conditions such as confrontations with predators or the presentation of noxious stimuli (reviewed in Robinson, 1980; Sainsbury, 1998).[13]

Theta oscillations were first observed in the hippocampus (Green & Arduini, 1954) and entorhinal cortex (Mitchell & Ranck, 1980) and then in the perirhinal cortex (Figure 4.13A) (Collins *et al.*, 1999). Given the strong reciprocal connections existing between the basolateral amygdala and rhinal cortices, it should not come as a surprise that neurons of the basolateral amygdaloid complex are also recruited by theta oscillations (Figure 4.13B). This was first shown for paradoxical sleep theta (Paré & Gaudreau, 1996), and then during the anticipation of a footshock (Paré & Collins, 2000) or the recall of a conditioned fear response (Seidenbecher *et al.*, 2003). In at least two of these studies, simultaneous recordings in the amygdala and hippocampal formation established that this oscillatory activity was correlated. The possibility that the synchronized oscillatory activity of rhinal and basolateral amygdala neurons promotes memory will be considered in Chapter 9.

4.3.3 Physiological studies of amygdaloprefrontal interactions

The influence of the medial prefontal cortex on the amygdala has attracted much attention because of recent data implicating this pathway in the extinction of classically conditioned fear responses (see Chapter 9). A first study focused on the effect of medial prefontal stimulation on the central nucleus of the amygdala, because this nucleus is believed to constitute the main output station of the amygdala for conditioned fear responses.[14] Recording extracellularly from physiologically identified brainstem-projecting central neurons in both rats and cats, this study reported that conditioning shocks to the medial prefrontal cortex dramatically reduce the responsiveness of central output neurons to inputs from the insular cortex and basolateral amygdala (Quirk *et al.*, 2003). Given that medial prefrontal axons form asymmetric (and thus presumably excitatory) synapses in the amygdala (Smith *et al.*, 2000; Brinley-Reed *et al.*, 1995), prefrontal inhibition of central neurons could occur by activating GABAergic cells with direct projections to the central nucleus, such as neurons of the intercalated cell masses or the bed nucleus of the stria terminalis. Another possibility is that prefrontal inputs cause a disfacilitation of central medial neurons via a feed-forward activation of basolateral interneurons and the consequent inhibition of basolateral projection cells.

In support of this possibility, Rosenkranz and Grace (1999, 2001) reported that electrical stimulation of the medial prefrontal cortex inhibited the responses of basolateral projection cells to inputs from cortical area Te3. However, several considerations cast doubt on the

[13] High-amplitude theta oscillations modulate the activity of essentially all types of hippocampal neurons (Buzsáki *et al.*, 1983). Despite intense scrutiny, the mechanisms underlying theta generation remain unclear (Buzsáki, 2002). However, hippocampal theta requires intact connections with the medial septum (Petsche *et al.*, 1962) and it depends on the rhythmic activity of entorhinal afferents and CA3 Schaffer collaterals (Buzsáki, 2002). Moreover, hippocampal theta is associated with cyclical amplitude modulation of gamma waves in the hilus, entorhinal cortex and CA1 (Bragin *et al.*, 1995a; Chrobak & Buzsáki, 1996, 1998).

[14] This belief is based on (1) tract-tracing data indicating that the central nucleus contributes most amygdala projections to brainstem and hypothalamic sites that mediate the behavioural and autonomic correlates of fear studies (Hopkins & Holstege, 1978; Veening *et al.*, 1984) and (2) behavioural data showing that chemical and electrical stimulation of the central nucleus elicits the correlates of fear whereas lesions of the central nucleus abolish conditioned fear responses (LeDoux *et al.*, 1988; Bellgowan & Helmstetter, 1996; De Oca *et al.*, 1998; Davis, 2000). However, this view has been challenged recently (Koo *et al.*, 2004).

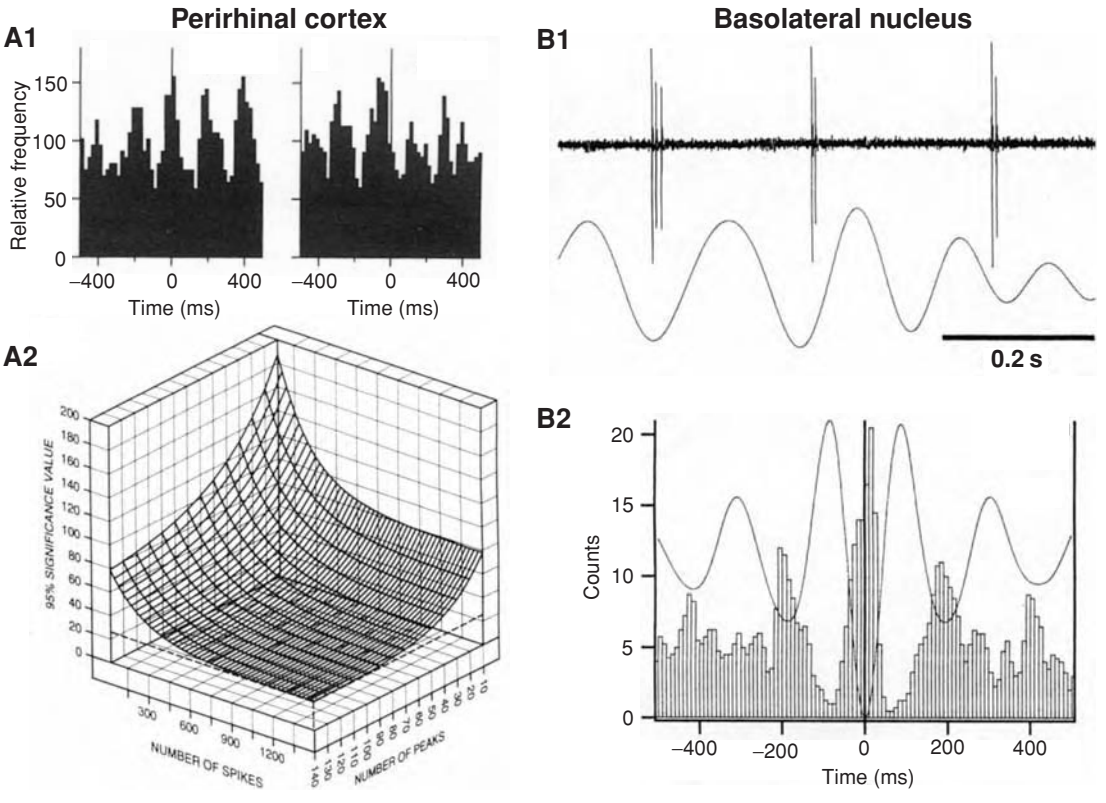

Fig. 4.13 Theta oscillations in the perirhinal cortex (A) and basolateral complex (B) of the amygdala during paradoxical sleep. (A1) Peri-event histograms (PEHs) of perirhinal firing using the positive peaks of focal theta waves (digitally filtered between 4 and 8 Hz) as reference times for two different neurons. (A2) Modulation of firing probability required to reach statistical significance in a one-tailed test ($p = 0.05$; mean + 1.64 × SD) as a function of the number of spikes and references used to generate PEHs. The 95% significance values were obtained by generating 250 shuffled spike trains from eight cells with different numbers of spikes and 10–140 reference times. Each PEH (± 500 ms) was smoothed with a moving average of 3 and the maximal difference in spike counts found between bins 80–120 ms apart (half theta wavelength) was searched within 200 ms of the reference. This difference in spike counts and that found on each side of the central peak (at 200 ms with an interbin interval of 80–120 ms) were averaged and normalized to the mean number of counts per bin in the entire PEH. For each randomly generated distribution of PEHs, 1.64 × SD was added to the average firing modulation and the data were fitted with exponential curves to generate the contour plot. (B) During paradoxical sleep, bursting neurons of the basolateral nucleus fire during the depth-negative phase of entorhinal theta. (B1) Sample of theta-related activity in a basolateral bursting cell. (B2) Superimposed spike-triggered average and peri-event histogram using the negative peak of the entorhinal EEG as zero-time. Same cell as in B1. Bins of 10 ms. Peri-event histogram was smoothed with a moving average of 3 bins. (A) Modified from Collins *et al.* (1999); (B) modified from Paré & Gaudreau (1996).

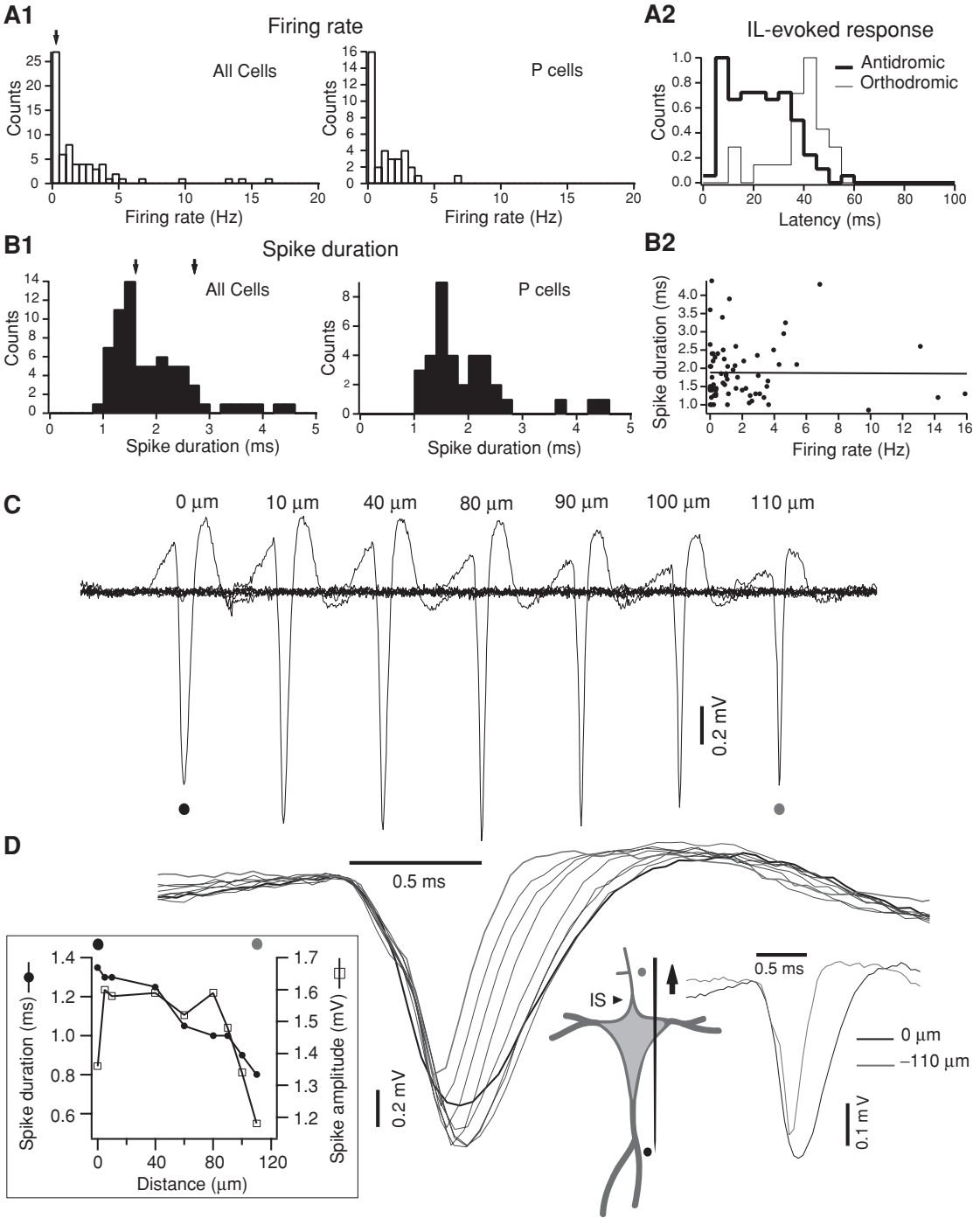

Fig. 4.14 Responses evoked by infralimbic stimulation in the basolateral amygdala. Firing rate (A) and spike duration (B) in basolateral neurons that were antidromically responsive to infralimbic stimuli (2) versus all the cells (1). (A2) Latency of infralimbic-evoked responses in the basolateral nucleus. (B2) Relation between spike duration and firing rate. (C, D) The amplitude and duration of extracellularly recorded action potentials varies with the position of the electrode tip with respect to the recorded cell. (C) Action potentials generated by the same cell as seen from different electrode positions (indicated by numbers on top). (D) Same data as in (C) but after aligning spikes to their rising phase. Scheme indicates hypothesized position of electrode relative to soma. Modified from Likhtik *et al.* (2005).

validity of this conclusion (Figure 4.14). First, the authors used firing rate and spike duration to distinguish projection cells from interneurons. In our own experiments, these criteria proved ineffective in distinguishing these two cell types (Figure 4.14A, B). Indeed, we found that some physiologically identified projection cells fired as frequently as 3 Hz (Paré & Gaudreau, 1996). This firing rate would have led Rosenkranz and Grace to classify these cells as interneurons.[15] As to the spike duration, we observed that it varied tremendously, by as much as 50%, depending on the position of the electrodes with respect to the recorded cells (Figure 4.14C,D).

Besides these methodological considerations, other lines of evidence suggest that the prefrontal-evoked inhibition of basolateral projection neurons is mediated by feedback rather than feedforward inhibition. First, prefrontal inputs to the basolateral amygdala terminate almost entirely on dendritic spines (Smith *et al.*, 2000; Brinley-Reed *et al.*, 1995) suggesting that the main targets of medial prefrontal axons are projection neurons rather than interneurons. Second, electrical stimuli delivered in the prefrontal cortex not only activate prefrontal projections to the amygdala, but also backfire amygdala axons ending in the prefrontal cortex. In fact, we have observed that prefrontal-evoked antidromic responses are more common than synaptically evoked ones in the basolateral amygdala (Likhtik *et al.*, 2005). Moreover, these orthodromic spikes occurred at a longer latency than antidromic spikes (Figure 4.14A, right). Consistent with this, we have found that the conduction time of basolateral axons to the prefrontal cortex is faster than that of prefrontal axons to the amygdala (Likhtik *et al.*, 2005). This implies that, when the medial prefrontal cortex is stimulated, antidromic impulses reach the basolateral amygdala before orthodromic ones. The significance of this observation resides in the fact that antidromic invasion of basolateral neurons likely causes the activation of their local recurrent collaterals and consequently of basolateral inhibitory interneurons. This will cause an artefactual inhibition of projection cells before the arrival of prefrontal inputs.

If this were the case, one would expect that indirect activation of the medial prefrontal cortex would be efficient in exciting basolateral projection cells. Consistent with this prediction, we have observed that physiologically identified basolateral projection cells that display no orthodromic responses to prefrontal stimulation can be synaptically activated by mediodorsal thalamic stimuli. Because there are no links between this thalamic nucleus and the amygdala in humans (Krettek & Price, 1977a), this excitation is likely indirect, via the activation of the medial prefrontal cortex (Musil & Olson, 1991). Consistent with this, lidocaine microinfusions in the medial prefrontal cortex could abolish the response evoked by stimulation of the mediodorsal thalamic nucleus (Likhtik *et al.*, 2005).

[15] Rosenkranz & Grace (1999, 2001) used a 0.5 Hz cutoff in firing rate (whereby projection cell < 0.5 Hz < interneurons). This classification of basolateral amygdala neurons on the basis of firing rate was paralleled by significant differences in spike duration.

Chapter 5

Neuromodulation and state-dependent activities in forebrain neuronal circuits

In this chapter we discuss the organization, connectivity and neuronal properties of different modulatory systems located in the brainstem core, hypothalamus and basal forebrain. These systems exert widespread effects on the thalamus, neocortex, perirhinal cortices, amygdala and related subsystems. Typically, they have an activating effect on target neurons. Activation is defined as a state of readiness in cerebral networks, a state of membrane polarization which brings neurons closer to firing threshold, thus ensuring reliable synaptic transmission and quick responses (Steriade, 1991), without, however, losing sculpting inhibitory processes of short duration that are necessary during the adaptive state of waking (Jasper, 1958; Steriade, 2003c).

One of the major points in this chapter is the demonstration that none of the ascending activating systems is *the* awakening 'centre'. In fact, no wake or sleep state can be said to have a centre and even few, if any, components of waking–sleep states have a centre. Functionally, a neural centre may be thought of as subserving only one function. A behavioural state centre would imply a group of neurons, homogeneous in their input–output organization and chemical code(s), and having the required pathways to control the activity of the final effectors of the events involved in that behavioural state (Steriade & McCarley, 2005). Among additional criteria, the centre, when deafferented from its major inputs, should continue to generate the state or to exhibit some of the defining electrographic signs of the state. Such criteria are difficult to satisfy for waking–sleep states and they even have difficulty meeting the weaker definition that a centre is an anatomically defined and localized set of homogeneous neurons serving only one function. Indeed, homogeneous cell-groups are difficult to find in the mammalian brain (see below, Section 5.1.1, on brainstem cholinergic nuclei).

With the discovery of multiple activating systems, some researchers placed exclusive emphasis on their preferred candidate structure. For example, those working on the cholinergic system linking the basal forebrain to the cerebral cortex have attempted to replace

the role of the previously demonstrated brainstem–thalamocortical system (Moruzzi & Magoun, 1949) with that of the basalocortical projection, thought to be indispensable for cortical activation. However, the reality is the presence of two parallel activating pathways, from brainstem to cortex, via synaptic relays within the thalamus or nucleus basalis. This is supported by experiments showing that brainstem-induced depolarization of cortical neurons, their enhanced excitability, and replacement of slow oscillations by fast rhythms, can be achieved after extensive ipsilateral lesions of either thalamus or nucleus basalis (Figures 6 and 7 in Steriade *et al.*, 1993a). Thus, at variance with some assumptions placing exclusive emphasis on one or another system, cholinergic neurons located in the mesopontine tegmentum or the nucleus basalis are sufficient to activate the cerebral cortex. The reciprocal connections between various neuromodulatory systems and their concerted functional operations during brain activation defy the simplistic concept of a centre.

5.1 Multiple modulatory systems in the brainstem core, hypothalamus and basal forebrain: connectivity and properties

Initially, the ascending brainstem reticular system has been regarded as having widespread energizing effects upon the forebrain. As a result, the notion of non-specificity in the activating process was introduced (Moruzzi & Magoun, 1949), similarly to the eighteenth-century concept of *sensorium commune*.[1] Although activation responses were elicited from many foci in the brainstem core, the most effective area was in the midbrain (Moruzzi & Magoun, 1949). The notion of non-specificity betrayed the primitive state of knowledge of the brainstem reticular core of that time. This was due to the fact that investigators used massive electrolytic lesions leading to axonal degeneration almost everywhere in rostral structures. However, modern tracing techniques combined with immunohistochemistry helped to define the various transmitter agents used by brainstem core neurons. This progress, coupled with electrophysiological recordings of neurons whose input–output organizations were identified by orthodromic and antidromic stimulation, challenged the notion of hypothetically ubiquitous projections of activating neurons. The notion of a monolithic brainstem reticular core, exerting global and undifferentiated energizing actions upon the forebrain, was replaced with the concept of a differentiated structure.[2]

5.1.1 Brainstem cholinergic and glutamatergic neurons

The brainstem nuclear systematization and cytoarchitecture described below derives from studies using choline acetyltransferase

[1] *Sensorium commune* was vaguely localized by the Czech physiologist Jiri Prohaska, around 1750, in a region between the medulla and the diencephalon (see the history of concepts in the central nervous system by Soury, 1899).

[2] The concept of non-specificity was challenged by Moruzzi himself (1972), after transection experiments during the late 1950s. The midpontine pretrigeminal brainstem transection, which produces a wakeful preparation, is only a few millimetres behind the low collicular transection that induces the comatose syndrome displayed by the *cerveau isolé* preparation of Bremer (1935).

(ChAT) immunoreactivity in the rat, cat and macaque monkey (Mesulam *et al.*, 1983a,b, 1984; Vincent & Reiner, 1987). However, in some species cholinergic neurons are interspersed within the same nucleus with monoamine-containing (serotoninergic and noradrenergic) and GABAergic neurons (Jones & Beaudet, 1987; Ford *et al.*, 1995; Leonard *et al.*, 1995a).

Two brainstem cholinergic cell-groups, Ch5 and Ch6, extend from the caudal part of the midbrain to the rostral pontine reticular formation (Figure 5.1). The Ch5 group corresponds to the pedunculopontine tegmental (PPT) nucleus (also termed peribrachial nucleus because its neurons surround brachium conjunctivum, the cerebellothalamic path).[3] The Ch6 group corresponds to the laterodorsal tegmental (LDT) nucleus. The PPT was first described in human material, and thereafter in other primates. It consists of medium- to large-sized, darkly stained neurons but, at least in the cat, is not a cytoarchitecturally distinct cell group. The comparative analysis of Nissl-stained and ChAT-positive neurons in the rat PPT nucleus concluded that large multipolar neurons are entirely cholinergic neurons. On average, cholinergic neurons were found to be larger than immunonegative neurons by 40% (Rye *et al.*, 1987; Honda & Semba, 1995). The average number of cholinergic cells in the PPT/LDT nuclei of humans is *c.*20 000, with 30% of cells in pars compacta of the PPT nucleus (Manaye *et al.*, 1999).

In addition to monoamine-containing neurons found in mesopontine cholinergic nuclei, especially in their caudal part (Jones & Beaudet, 1987; Ford *et al.*, 1995; Leonard *et al.*, 1995a), 15%–30% of rat PPT and LDT cholinergic neurons also display immunoreactivity for substance P and a series of other peptides (Vincent *et al.*, 1983, 1986; Saper *et al.*, 1985; Standaert *et al.*, 1986).[4] Cholinergic cells also express nicotinamide-adenine-dinucleotide- phosphate (NADPH)-diaphorase. NADPH-diaphorase is a reliable marker of brainstem cholinergic neurons in PPT/LDT nuclei.[5] The neuronal NADPH-diaphorase is the synthesizing enzyme of nitric oxide (NO), NO synthase (Dawson *et al.*, 1991; Hope *et al.*, 1991); NO exerts depolarizing actions on thalamocortical (TC) neurons (Pape & Mager, 1992).[6] Importantly, there is colocalization of acetylcholine (ACh) and glutamate in mesopontine neurons (Figure 5.2), with the greatest numbers of double-labelled cells in pars compacta of the PPT nucleus and the lowest in the dorsal part of the LDT nucleus (Lavoie & Parent, 1994; Inglis & Semba, 1996). In fact, glutamate neurons are, by far, more numerous than cholinergic neurons in the brainstem core (see Figure 5.2A). The presence of a great number of glutamatergic cells in the upper brainstem reticular formation as well as the colocalization of glutamate with ACh within the same mesopontine neurons may explain why PPT/LDT-evoked depolarizations in TC neurons may not be sensitive to scopolamine. Similarly, after scopolamine administration, the usual inhibitory action of PPT/LDT cholinergic action on thalamic reticular (RE) GABAergic neurons is replaced by

[3] The peribrachial nucleus should not be confused with the *para*brachial nucleus, which is an elongated nuclear mass located more caudally in the brainstem tegmentum and aligned lateral to the brachium conjunctivum. The parabrachial nucleus is mainly specialized in relaying taste and visceral information to the forebrain, whereas the peribrachial nucleus projects to virtually all thalamic nuclei.

[4] The colocalization of ChAT and neuropeptides may reinforce the activating effects exerted on thalamocortical systems by cholinergic neurons in Ch5-Ch6 cell-groups, since bombesine and other peptides are known to produce EEG and/or behavioural signs of arousal (Sutton *et al.*, 1982; Ehlers *et al.*, 1983; Rasler, 1984).

[5] For chronic recordings in NADPH-diaphorase-stained PPT/LDT cholinergic nuclei, see Figure 1 in Steriade *et al.* (1990a).

[6] The cholinergic axons from mesopontine cholinergic nuclei are the exclusive source of NO in the thalamic lateral geniculate nucleus (Bickford *et al.*, 1993).

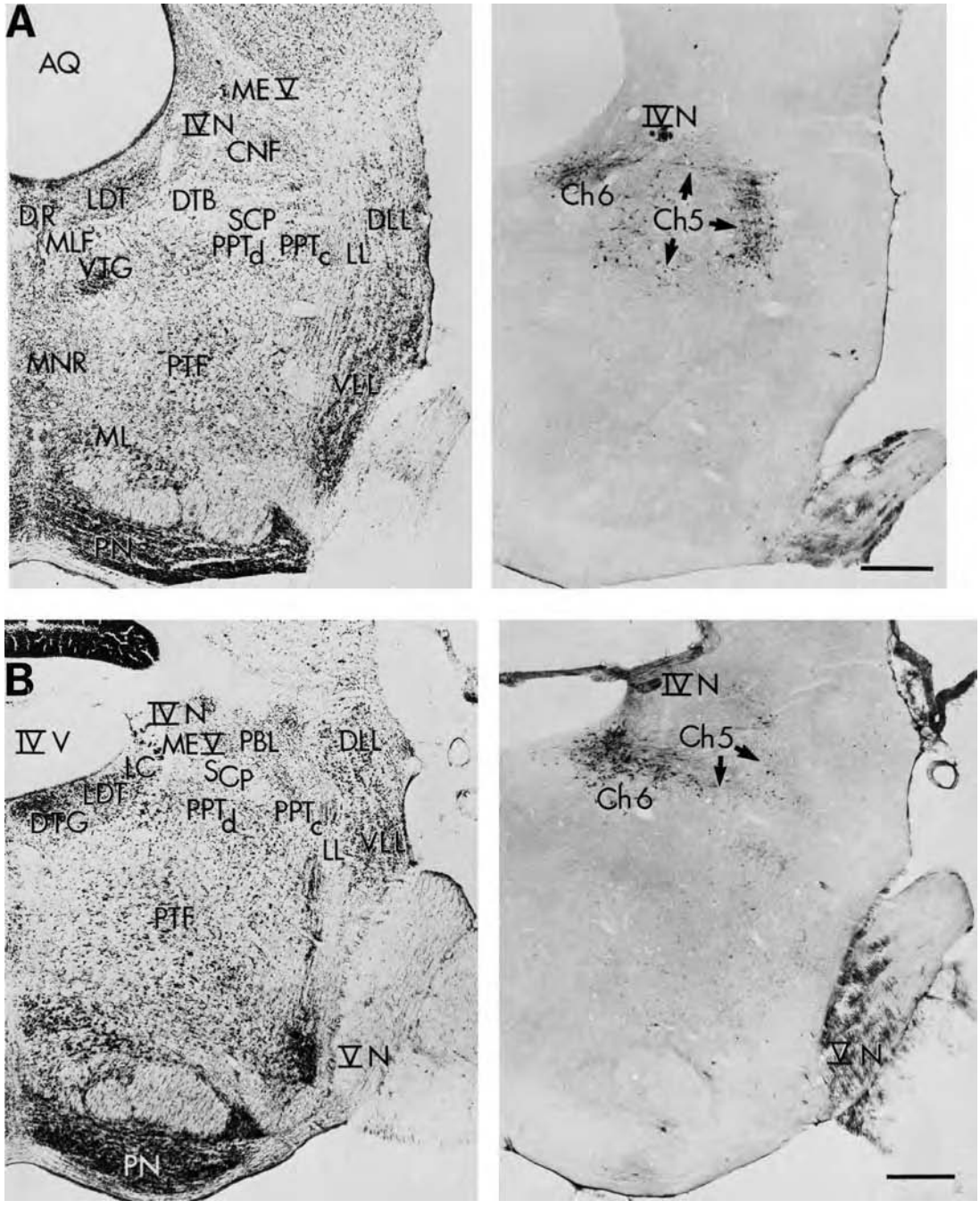

Fig. 5.1 Cholinergic cell groups at the mesopontine junction in the rat. In both (A) and (B) left sections were Nissl-stained and right (adjacent) sections were processed for immunohistochemical localization of ChAT. Ch designations identify cholinergic cell groups (see main text). Abbreviations: AQ, aqueduct; CNF, cuneiform nucleus; DLL, dorsal nucleus of the lateral lemniscus; DR, dorsal raphe; DTB, dorsal tegmental bundle; LDT, laterodorsal tegmental nucleus; LL, lateral lemniscus; ME V, mesencephalic nucleus of the trigeminal nerve; ML, medial lemniscus; LF, medial longitudinal fasciculus; MNR, medial raphe nucleus; PN, pontine nuclei; PPT_c and $_d$, pars compacta and dissipata of the pedunculopontine tegmental nucleus; PTF, pontine tegmental field; SCP, superior cerebellar peduncle; IV N, trochlear nerve; IV V, fourth ventricle; VLL, ventral nucleus of the lateral lemniscus; V N, trigeminal nerve; VTG, ventral tegmental nucleus. Scale bars, 0.5 mm. Modified from Wainer & Mesulam (1990).

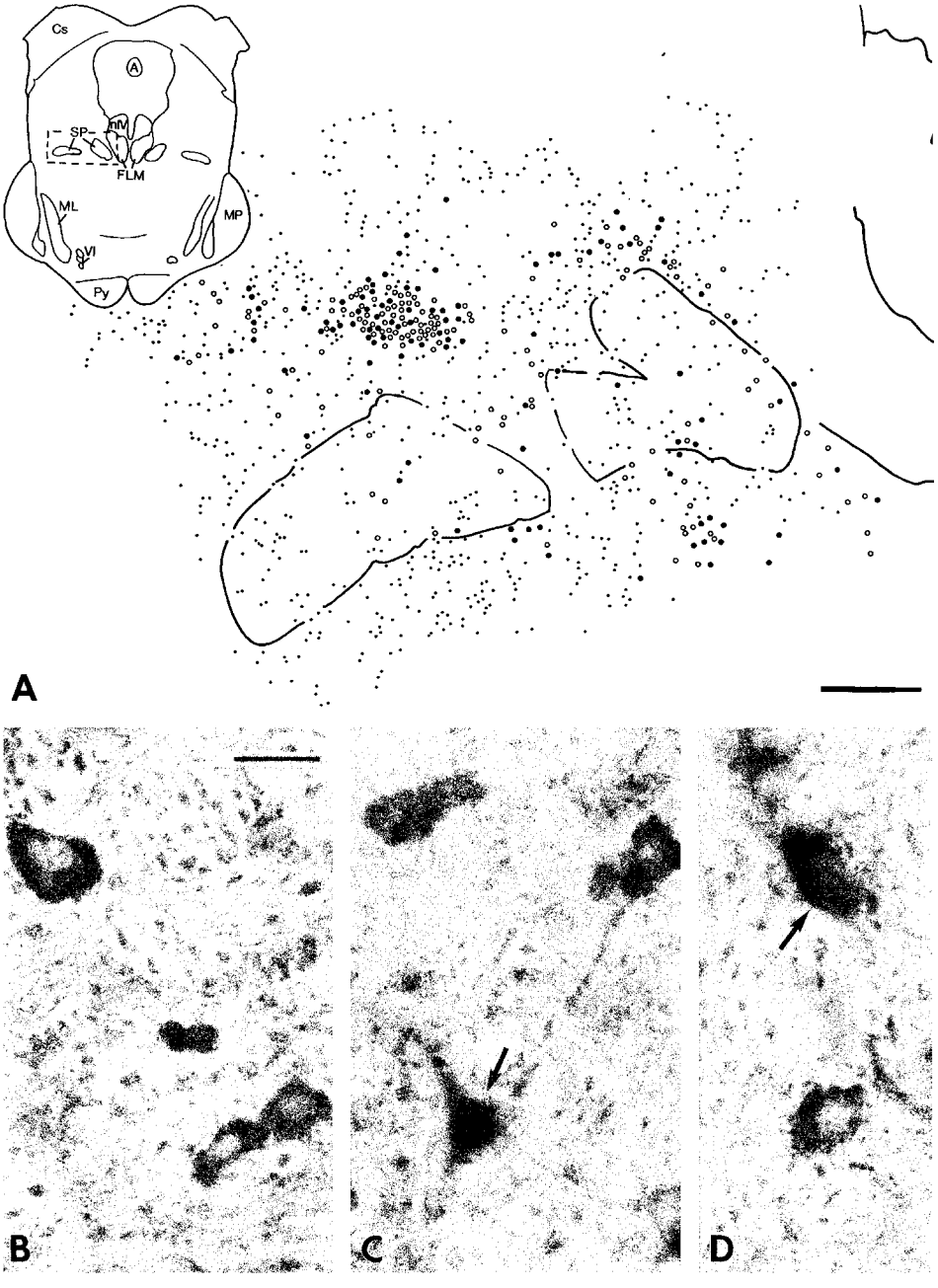

Fig. 5.2 Distribution of glutamate-immunoreactive neurons in the mesopontine tegmentum of the squirrel monkey at the level of the trochlear nucleus. (A) Schematic drawing representing neurons stained for both glutamate and NADPH-diaphorase (solid circles), whereas those labelled for NADPH-diaphorase only are illustrated by open circles. The distribution of glutamate neurons (dots) is also indicated. The section from which this drawing is derived is outlined at upper left and the rectangle delimits the section area that is illustrated. (B–D) Photomicrographs providing examples of glutamate-positive neurons. In (B) one large and two smaller glutamate-positive cells are illustrated. The arrows in (C) and (D) point to NADPH-diaphorase–glutamate double-labelled neurons that are similar in size to neighbouring neurons displaying only glutamate immunoreactivity. Scale bars: 0.3 mm (A), 30 μm (B–D). Abbreviations: A, aqueduct; Cs, superior colliculus; FLM, medial longitudinal fasciculus; ML, medial lemniscus; MP, middle cerebellar peduncle; nIV, trochlear nucleus; Py, pyramidal tract; SP, superior cerebellar peduncle; VI, sixth nerve fibres. Modified from Lavoie & Parent (1994).

depolarization (see Figure 10 in Hu *et al.*, 1989a). Also, the activation of nucleus basalis neurons by mesopontine tegmental stimulation is probably due to release of glutamate[7] because ACh is inhibitory to nucleus basalis neurons (Khateb *et al.*, 1997). Thus, the complex organization of neurons and axons in the mesopontine reticular formation challenges prior views assuming that the effects induced upon TC neurons are simply cholinergic in nature.

The inputs to mesopontine reticular formation arise in the spinal cord and sensory cranial nerves, rostrally located structures (diencephalon and telencephalon), and intrabrainstem sources. Of those, ventral thalamic, hypothalamic, neocortical and intrabrainstem projections have great functional importance. (a) The projection from zona incerta (ZI) to the rostral midbrain core, determined by retrograde transport techniques and antidromic activation of ZI neurons (Steriade *et al.*, 1982b), may be implicated in the attendance to relevant stimuli, thus preparing motor commands, since a large proportion of ZI neurons of the monkey were found to be activated when the animal reached for objects of interest (Crutcher *et al.*, 1980). (b) Descending projections also arise from posterior and anterior hypothalamic areas. The ventromedial and ventrolateral parts of the posterior hypothalamus, an area that is implicated in alertness, project to the rostral midbrain core and the mesopontine tegmentum (Paré *et al.*, 1989) (Figure 5.3). These projections may be related to the defence–aggression instinctive behaviour elicited from the hypothalamus (Chi & Flynn, 1971). The projections from the anterior hypothalamus to the midbrain reticular formation arise in the medial and lateral parts of the preoptic area (Swanson *et al.*, 1987). The ventrolateral region of the preoptic area is regarded as an active sleep-promoting structure (Szymusiak & McGinty, 1986; Sherin *et al.*, 1996; Szymusiak *et al.*, 2001) and it may exert this role by inhibiting activating structures located in the posterior hypothalamus and the rostral brainstem reticular formation (Gritti *et al.*, 1994; Sherin *et al.*, 1998; Steininger *et al.*, 2001). (c) Cortical projections to the upper brainstem reticular core mainly arise from sensorimotor areas and are all excitatory in nature. Consistent with this, cortical stimulation activates brainstem neurons at latencies lowe than 5 ms. (Ropert & Steriade, 1981). The corticoreticular feedback projections have been implicated in the maintenance of the alert condition (Bremer & Terzuolo, 1954). (d) Midbrain reticular neurons are driven from the pontine and bulbar reticular formation; inputs arising in the cerebral cortex, preoptic area, some thalamic nuclei and the bulbar reticular formation converge more often in midbrain neurons that were not backfired from distant sites than in neurons with antidromically identified projections (Steriade, 1981).[8]

The output of the upper brainstem reticular core, consisting of both cholinergic and non-cholinergic (most of them glutamatergic and possibly peptidergic) neurons, is directed both upwards and downwards. We focus here on ascending axons because these projections are heavily involved in forebrain activation processes. The rostrally directed projections distribute to the diencephalon, where

[7] This hypothesis (p. 1394 in Steriade *et al.*, 1993a) was substantiated by experimental data described in Rasmusson *et al.* (1994, 1996).

[8] Brainstem afferents synaptically activate mesopontine cholinergic neurons acting via both NMDA and non-NMDA receptors. NMDA receptors contribute to fast excitatory transmission in those cells (Sanchez & Leonard, 1996). Studies of the role played by mesopontine tegmental neurons in visually guided saccade tasks in primates led to the conclusion that the multi-modality of responses in these neurons may serve as an integrative interface between various signals required for performing purposive behaviours (Kobayashi *et al.*, 2001).

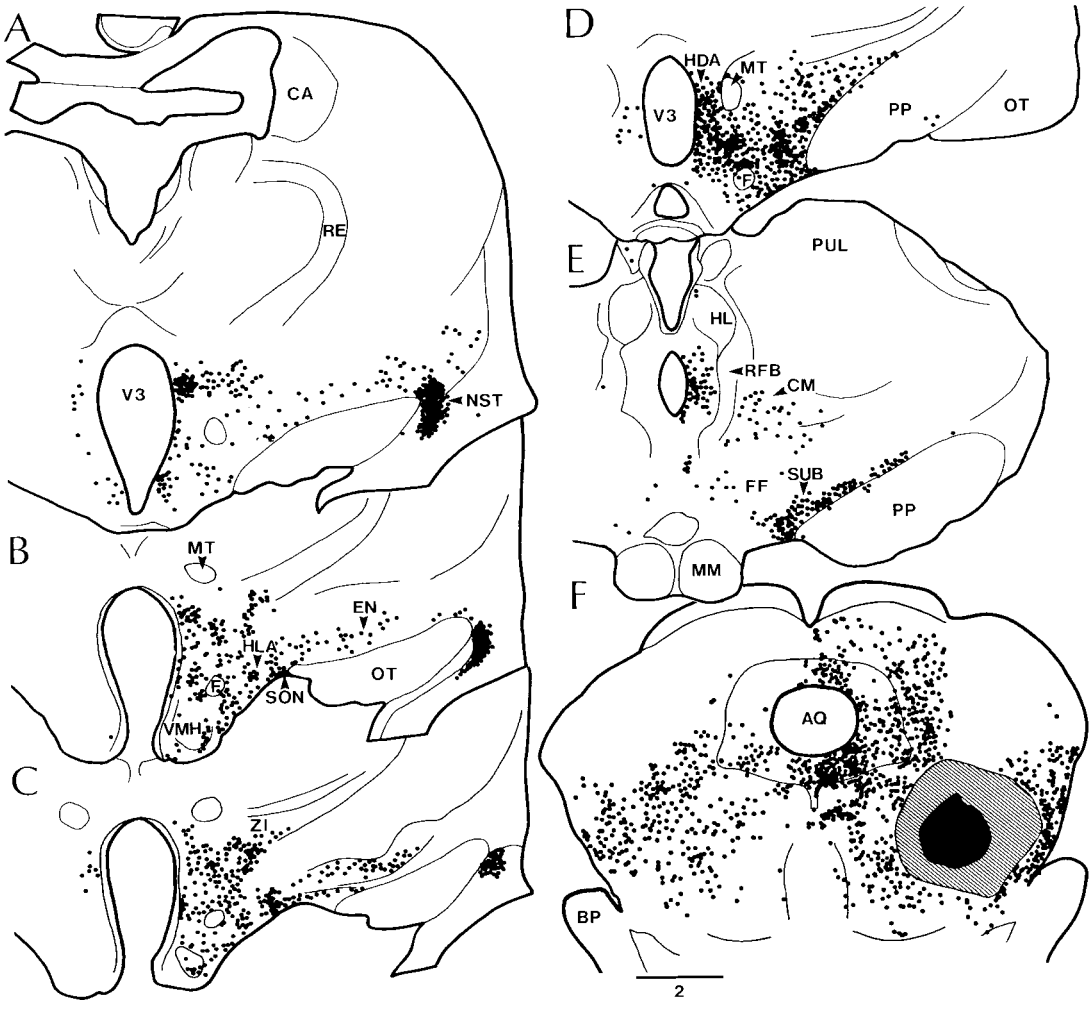

Fig. 5.3 Posterior hypothalamic and brainstem core afferents to the peribrachial (PB) area in the cat. (A–F) Six frontal sections, rostral to caudal. The site of WGA-HRP injection is shown in (F). Each dot represents one retrogradely labelled neuron. Note, in A and B, retrograde labelling in dorsomedial, ventromedial and lateral areas of the posterior hypothalamus (HDA, VMH, HLA, respectively). Note retrograde labelling in deep layers of the superior colliculus and the midbrain central grey and central tegmental field, both ipsilaterally and contralaterally to the injection site (E). Horizontal bar indicates millimetres. Other abbreviations: AQ, aqueduct; BP, brachium pontis; CA, caudate nucleus; EN, entopeduncular nucleus; F, fornix; FF, field of Forel; HL, lateral habenular nucleus; MM, mammillary bodies; MT, mammillothalamic tract; NST, nucleus of stria terminalis; OT, optic tract; PP, cerebral peduncle; PUL, thalamic pulvianr nucleus; RE, thalamic reticular nucleus; RFB, retroflex bundle; SUB, subthalamic nucleus; VM, ventromedial hypothalamic nucleus; V3, third ventricle; ZI, zona incerta. Modified from Paré *et al.* (1989).

they split into a dorsal and a ventral leaf. The dorsal system supplies thalamic nuclei, and in particular the rostral intralaminar nuclei that project to widespread cortical territories, whereas the ventral division distributes axons to the subthalamus and lateral hypothalamus, as well as to the basal forebrain. The ascending axons of

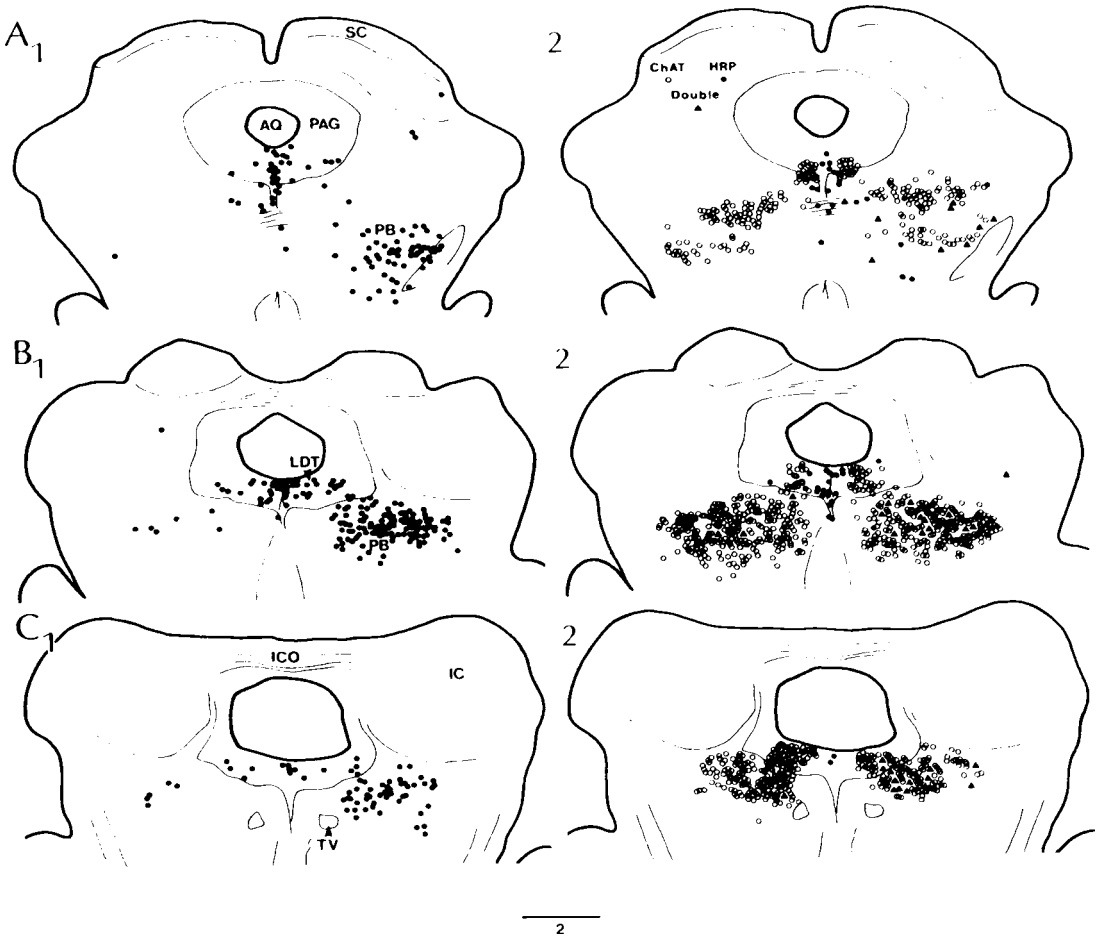

Fig. 5.4 Cholinergic and non-cholinergic brainstem neurons projecting to the right thalamic ventroanterior–ventrolateral (VA–VL) thalamic complex of cat. Staining combining the retrograde transport of wheatgerm agglutinin conjugated with horseradish peroxidase with choline acetyltransferase (ChAT) immunohistochemistry. (A–C) Three levels. At each level, the left column depicts the total number of retrogradely labelled neurons as found on five sections after the tetramethylbenzidine (TMB) procedure. The right column depicts the same levels, with three cell types (see symbols in A2), as found on two sections after TMB procedure combined with ChAT immunohistochemistry. Camera lucida localization. Horizontal bar, millimetres. Modified from Steriade *et al.* (1988).

cholinergic neurons at the midbrain–pontine junction and non-cholinergic reticular neurons of midbrain, pontine and medullary fields are overwhelmingly relayed in the thalamus; with the exception of chimpanzees (Tigges *et al.*, 1982, 1983), direct cortical projections are negligible or absent in rats, cats and monkeys (Sakai, 1985; Satoh & Fibiger, 1986). This stands in contrast to the direct cortical projections of monoaminergic brainstem nuclei (see Section 5.1.2). Brainstem cholinergic nuclei at the mesopontine junction project to virtually all (sensory, motor, association, intralaminar and reticular)

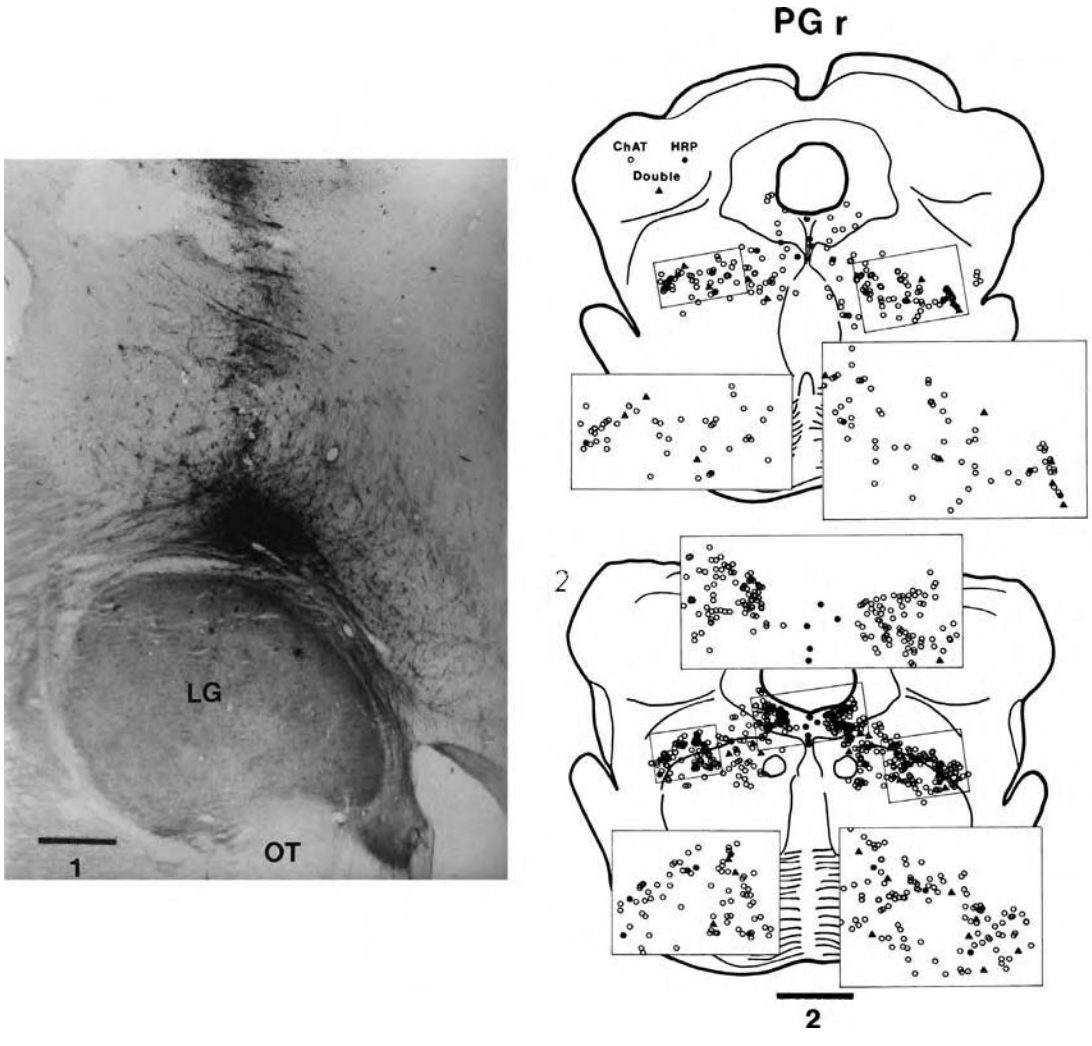

Fig. 5.5 Cholinergic and non-cholinergic brainstem reticular cells projecting to the right perigeniculate (PG) sector of the thalamic reticular nuclear complex of the cat. Localization of wheatgerm agglutinin horseradish peroxidase (HRP) injection in the PG is depicted in the left microphotograph. Bar indicates millimetres. Abbreviations: LG, lateral geniculate; OT, optic tract. Right column depicts two levels (A1 and P0.5) with the three cell types (ChAT-positive, HRP-positive, and double labelled; symbols in top drawing) as found in one section. Localization of cells by means of a computer-assisted microscope. Areas delimited by rectangles are shown at higher magnification. Modified from Smith *et al.* (1988).

thalamic nuclei (Figures 5.4 and 5.5). In addition to projections from cholinergic neurons, some associational and especially intralaminar nuclei receive a massive projection from the non-cholinergic (presumably glutamatergic) neurons located in the rostral midbrain core and rostral pontine reticular formation (Steriade *et al.*, 1988; Paré *et al.*, 1988).

The final corticopetal link of brainstem-thalamic projections was demonstrated by antidromic activation of thalamic intralaminar centrolateral-paracentral (CL-Pc) neurons from cortex and their monosynaptic excitation from the brainstem reticular core (Steriade & Glenn, 1982). This circuit exists for all cortically projecting neurons in the dorsal thalamus. However, specific relay thalamic nuclei project over relatively circumscribed cortical territories, whereas two groups of nuclei project diffusely over the neocortex: the intralaminar CL-Pc to layer I and VI, and the ventromedial (VM) nucleus to the upper third of layer I (Herkenham, 1979; Glenn *et al.*, 1982; Cunningham & LeVay, 1986). Thus, the cortical projections of CL-Pc and VM nuclei represent the substratum for the generalized activation of cortical processes set into action by the rostral reticular core. Indeed, both CL-Pc and VM thalamocortical nuclei receive massive projections from the brainstem reticular core (Steriade *et al.*, 1988; Paré *et al.*, 1988) and their neurons exert depolarizing actions in the cortex (Endo *et al.*, 1977). The axon of the same mesopontine cholinergic neuron may innervate more than one thalamic target; some neurons innervate both TC and RE neurons (Spreafico *et al.*, 1993), and some brainstem cholinergic neurons have dual projections to the thalamus and basal forebrain (Losier & Semba, 1993).

The intrinsic properties of neurons in mesopontine cholinergic nuclei have been studied in slices from newborn and adult rodents. Only few PPT/LDT cholinergic neurons display low-threshold spike-bursts in adult guinea pigs and rats (Kang & Kitai, 1990; Leonard & Llinás, 1990, 1994; Leonard *et al.*, 1995b; Takakusaki & Kitai, 1997; Takakusaki *et al.*, 1997; Homma *et al.*, 2002). This corroborates data from studies of cat cholinergic PPT/LDT neurons during natural states of vigilance showing that high-frequency spike-bursts are rarely observed during wakefulness, slow-wave sleep and REM sleep.[5] In newborn rats, however, the majority of LDT neurons that display low-threshold spike-bursts are cholinergic (Kamondi *et al.*, 1992; Luebke *et al.*, 1992), which may suggest a change in membrane properties of LDT neurons during ontogenesis. The four types of PPT/LDT neuron usually described in adult animals (Kang & Kitai, 1990; Leonard & Llinás, 1990, 1994; Leonard *et al.*, 1995b; Takakusaki & Kitai, 1997; Takakusaki *et al.*, 1997; Homma *et al.*, 2002) are as follows: (a) cells characterized by Ca^{2+}-mediated low-threshold spikes (LTSs) are a minority or virtually absent; (b) neurons characterized by a transient outward current, I_A, account for about 60% of the cells; (c) other neurons display both LTS and I_A; and (d) some cells have neither LTS nor I_A. The cell-classes LTS and LTS + I_A may be related to the burst firing of PPT/LDT neurons whose activity underlies the thalamic component of the phasic ponto-geniculo-occipital waves of REM sleep (Steriade *et al.*, 1990d). A similar bursting pattern was observed in relation to reserpine-induced ponto-geniculo-occipital waves (Paré *et al.*, 1990a). The cellular type with I_A probably corresponds to the tonically firing neurons found in the PPT/LDT nucleus during both waking and REM sleep.[5]

5.1.2 Brainstem and posterior hypothalamic monoamine-containing neurons

Three monoamine-containing cellular aggregates that exert important influences on both thalamic and cortical neurons are located in the upper brainstem (dorsal raphe (DR)), mainly consisting of neurons releasing 5-hydroxytryptamine (5-HT) or serotonin; and locus coeruleus (LC) cells that release noradrenaline (NA); and tuberomammillary area of the posterior hypothalamus (where neurons releasing histamine (HA) are located). Dopaminergic neurons in the substantia nigra and ventral tegmental area project to the striatum, basal forebrain and cerebral cortex, but their thalamic projections are quite scarce and, distinctly from other monoamine-containing neurons, there is no difference in the firing rates of dopaminergic cells during states of vigilance. We will then focus on DR, LC and HA neurons.

The serotonergic DR neurons receive afferents from other nuclei of the raphe system, LC, substantia nigra, lateral part of the posterior hypothalamus, preoptic area, lateral habenula, hippocampus, and prefrontal cortex (Aghajanian & Wang, 1977; Sakai *et al.*, 1977a). The LC is also a site of convergence of many inputs, such as from the spinal cord, fastigial nuclei of the cerebellum, various brainstem nuclei (including DR), paraventricular and lateral hypothalamic areas, medial and lateral preoptic areas, central nucleus of amygdala, and cortical areas 13 and 14 (Pickel *et al.*, 1977; Sakai *et al.*, 1977b).[9] The inputs to HA neurons in the posterior hypothalamus arise in mesopontine reticular nuclei, amygdala, septum and diagonal band nuclei, and preoptic area (Gritti *et al.*, 1994; Sherin *et al.*, 1998; Steininger *et al.*, 2001; Parent *et al.*, 1981; Sakai *et al.*, 1990).

The projections of DR neurons to the forebrain reach the hypothalamus, thalamus (mainly the ventral part of the lateral geniculate nucleus and the intralaminar nuclei), periventricular grey, striatum, globus pallidus, amygdala, diagonal band nuclei, septum, hippocampus, and glomerular layer of the olfactory bulb (Parent *et al.*, 1981; Sakai *et al.*, 1990). The 5-HT fibres that reach the cortex are concentrated in layer IV of area 17 and are homogeneously distributed in area 18 of primates (Morrison & Foote, 1986). Rostrally, LC cells project to various hypothalamic areas, thalamic nuclei, septum, amygdala, hippocampus, pyriform cortex, and neocortical areas (reviewed in Foote *et al.*, 1983). In the thalamus, the projections of both LC and DR cells to RE neurons are very dense throughout the nucleus (Figure 5.6) (Asanuma, 1992), and are of importance because of their depolarizing effect. This contrasts with the inhibition exerted on RE neurons by mesopontine and basal forebrain cholinergic neurons (McCormick & Wang, 1991; reviewed in McCormick, 1992; Steriade *et al.*, 1997).[10] The corticipetal axons of LC neurons ramify in all layers (Levitt & Moore, 1978; Lindvall *et al.*, 1978), whereas marked laminar variations are seen in striate and extrastriate cortices of primates (Morrison *et al.*, 1982). A very low proportion of NA axons engage in classical synaptic profiles and it was thus postulated that NE is mainly released in a

[9] The idea of a restricted afferent control of LC (Aston-Jones *et al.*, 1986), which stands in contrast with the multiple inputs reaching LC, was mainly based on the critique of previous results that were ascribed to diffusion of the tracer outside the LC limits, particularly in the parabrachial nucleus. However, the parabrachial nucleus was injected in control experiments and, whereas retrograde labelling was found in the preoptic area, ventromedial–dorsomedial hypothalamic areas and DR nucleus after LC injections, the same areas remained unlabelled after parabrachial injections (Cederbaum & Aghajanian, 1978).

[10] The depolarization exerted by LC neurons on thalamic RE neurons is one of the factors that may explain why spindles occur in the deafferented thalamic RE neurons *in vivo*, whereas they are absent *in vitro* (Destexhe *et al.*, 1994b; see also Chapter 6 in this volume).

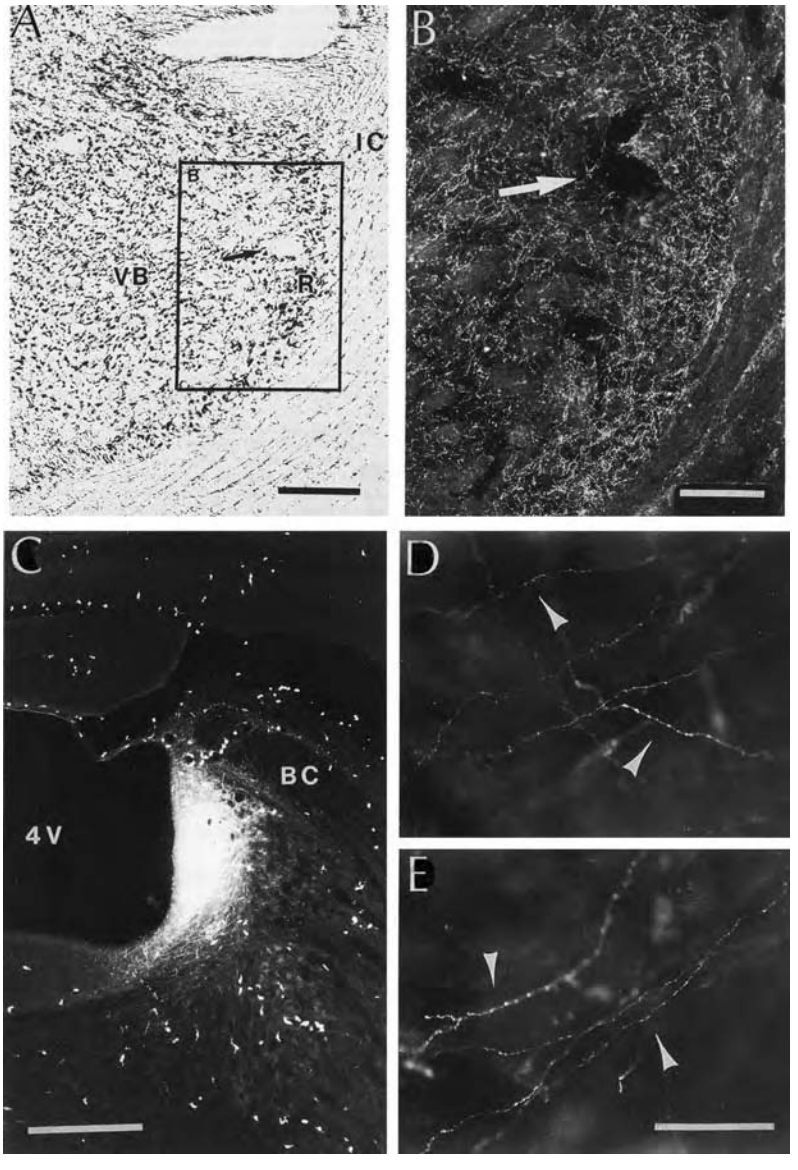

Fig. 5.6 Noradrenergic innervation of the thalamic reticular (RE) nucleus in the rat. (A) and (B) are bright- and dark-field photomicrographs of a parasagittal section through RE nucleus, illustrating dopamine-β-hydroxylase-positive axons. Area shown in the dark-field photomicrophograph is indicated by inset box in (A). Arrows in (A) and (B) indicate the same blood vessel. Scale bars, 0.5 mm (A) and 0.2 mm (B). Abbreviations: IC, internal capsule; R, reticular nucleus; VB, ventrobasal complex. (C) A Fluoro-ruby injection site in the LC, resulting in anterogradely labelled axons in the RE nucleus (D, E). Elongated axonal segments give rise to boutons *en passant* (arrowheads). Scale bars, 0.6 mm (C) and 80 μm (D, E). Abbreviations: BC, brachium conjunctivum; 4V, fourth ventricle. Modified from Asanuma (1992).

[11] Similar findings were more recently reported for the distribution of cholinergic axons in neocortex (Umbriaco *et al.* 1994; Mrzljak *et al.*, 1995; reviewed in Descarries *et al.*, 1997).

[12] Orexin (or hypocretin) neurons maintain the state of waking; they are lacking in narcoleptic animals and humans.

[13] Electrophysiological studies show that orexin neurons promote cortical activation by selectively depolarizing neurons in sublayer VIb, an action due to the inhibition of a K^+ conductance (Bayer *et al.*, 2004).

neurohumoral fashion (Descarries *et al.*, 1977; Beaudet & Descarries, 1978).[11] Finally, HA neurons of the posterior hypothalamus project to thalamic nuclei (Airaksinen & Panula, 1988; Uhlrich *et al.*, 1993) and cerebral cortex (Saper, 1987; Panula *et al.*, 1990). The descending projections from the posterior hypothalamus (Paré *et al.*, 1989) excite mesopontine cholinergic neurons and promote activation of TC neurons during wakefulness, an action mediated by HA_1 receptors (Lin *et al.*, 1996). In the peri-fornical region of the posterior hypothalamus, there are also orexinergic neurons whose axons are directed to diffusely projecting thalamic nuclei (Bayer *et al.*, 2002)[12] and cerebral cortex (Peyron *et al.*, 1998).[13]

As to the state-dependent properties of monoamine-containing cells, they all fire regularly, at relatively low rates (less than 5 Hz) during waking, progressively reduce their discharge rate during slow-wave sleep, and virtually cease firing during REM sleep (Steriade & McCarley, 2005). Their intrinsic properties have been investigated in brainstem slices. Recordings of DR neurons *in vitro* showed the presence of a spontaneous slow, regular discharge rhythm, with absence of spontaneous synaptic potentials, thus suggesting a true pacemaker organization; these neurons showed an early transient outward current with the characteristics of I_A (Aghajanian, 1985; Freedman & Aghajanian, 1987). The presence of an LTS current (I_T) was also shown in DR cells (Burlhis & Aghajanian, 1987). The rhythmic activity of DR neurons was postulated to be due to the entry of Ca^{2+} during fast Na^+ spikes, which would activate $I_{K(Ca)}$ (the current mediating after-hyperpolarizing potentials), leading to the de-inactivation of I_A and I_T. When the membrane potential depolarizes to the voltage where the LTS current is activated, a fast Na^+ spike will be generated, and the cycle repeated. In LC neurons, too, the presence of intrinsic pacemaker activity was suggested by the absence of spontaneous synaptic potentials driving repetitive discharges (Williams *et al.*, 1984).

Both 5-HT released by DR neurons and NA released by LC neurons inhibit cholinergic neurons at the mesopontine junction (Luebke *et al.*, 1992; Williams & Reiner, 1993; Leonard & Llinás, 1994; Leonard *et al.*, 2000).[14] This action is postulated to explain the shift from REM sleep, when monoamine-containing neurons are silent, to wakefulness (McCarley & Hobson, 1975).[15]

5.1.3 Basal forebrain cholinergic and GABAergic neurons

There are four cholinergic nuclei in the basal forebrain, Ch1 to Ch4 (Figure 5.7) (Mesulam *et al.*, 1983a,b, 1984; Vincent & Reiner, 1987; Wainer & Mesulam, 1990).[16] Ch1 neurons are grouped in the medial septum, which also contains a sizable proportion of non-cholinergic, GABAergic neurons. Ch2 and Ch3 neurons are located within the vertical and horizontal branches of the diagonal band nuclei and are also intermingled with GABAergic cells. The Ch4 group corresponds to nucleus basalis (NB) and cholinergic neurons are especially found within the larger region, termed substantia innominata (SI), located ventrally to the anterior commissure, extending to the internal part of the globus pallidus and caudally to the anterior part of the preoptic area.

Afferents to basal forebrain cholinergic nuclei arise in the upper brainstem core, hypothalamus, amygdala and cerebral cortex. Most inputs to Ch4 originate from non-cholinergic neurons of the brainstem reticular formation, as less than 1% of cholinergic PPT/LDT neurons project to NB (Jones & Cuello, 1989). Because ACh elicits a muscarinic-mediated hyperpolarization of cholinergic basal forebrain neurons (Khateb *et al.*, 1997), the most likely candidates for the brainstem drive to activate NB neurons are glutamatergic neurons,[7] within the limits of mesopontine cholinergic nuclei or even colocalized with

[14] In contrast to the inhibitory action of NA on brainstem cholinergic neurons, the same neurotransmitter excites non-cholinergic neurons in the LDT nucleus (Kohlmeier & Reiner, 1999).

[15] The high firing rates of PPT and LDT cholinergic neurons during waking[5] (see also El Mansari *et al.*, 1989; Kayama *et al.*, 1992) are due to the intense activity of brainstem glutamatergic neurons (Steriade *et al.*, 1982a, 1984b), which project to and excite PPT/LDT neurons (see Steriade, 1981). Another possibility, suggested by immunostaining of rat PPT/LDT neurons, is that only a group of mesopontine cholinergic neurons, bearing α_1 adrenergic receptors, are excited by NA during waking (Hou *et al.*, 2002). However, the overwhelming majority of cholinergic PPT/LDT neurons fire at high rates during waking, similarly to REM sleep (Steriade, 1981). This is confirmed by equal increases in ACh release in the thalamus during wakefulness and REM sleep (Williams *et al.*, 1994).

[16] For phylogenetic and ontogenetic (migration) aspects of basal forebrain cholinergic nuclei, see reviews by Semba (1992, 2004).

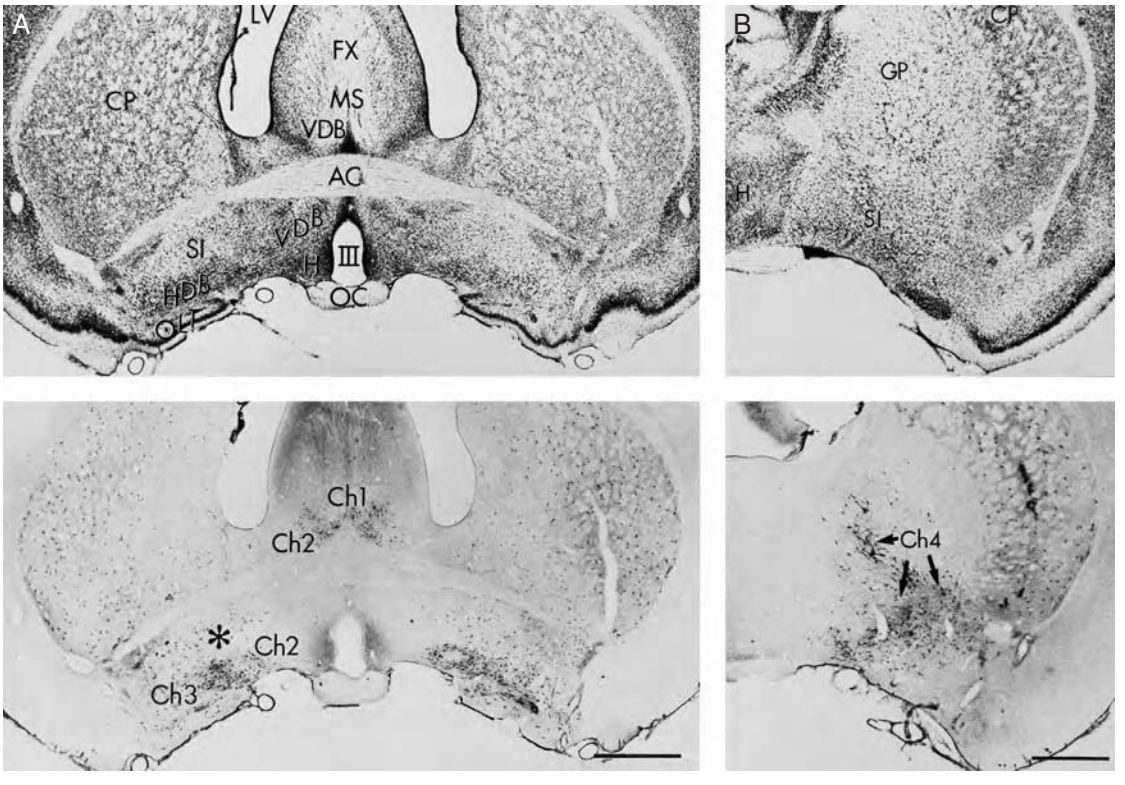

Fig. 5.7 Cholinergic cell groups of the rat basal forebrain. In each panel (A and B), there is a Nissl-stained section (top) and an adjacent section processed for ChAT immunoreactivity (bottom). Ch designations identify cell groups contained within various nuclei of the basal forebrain. Asterisk in (A) designates where neurons of the most anterior portion of Ch4 can be observed, although the main body of this group appears caudal to this level, in (B). Abbreviations: AC, anterior commissure; CP, caudate–putamen; FX, fornix; GP, globus pallidus; HDB, horizontal limb of the diagonal band nuclei; H, hypothalamus; III, third ventricle; MS, medial septum; OC, optic chiasm; OLT, olfactory tubercle; SI, substantia innominata; VDB, vertical limb of the diagonal band nuclei. Scale bars, 1 mm. Modified from Wainer & Mesulam (1990).

[17] The GABAergic projections from the ventrolateral part of the preoptic area to the posterior hypothalamus, implicated in the inhibition of the activating histaminergic system and the process of falling asleep, are referred to above (Szymusiak & McGinty, 1986; Sherin *et al.*, 1996; Szymusiak *et al.*, 2001; Gritti *et al.*, 1994; Sherin *et al.*, 1998; Steininger *et al.*, 2001).

ACh in the same PPT/LDT cells (Lavoie & Parent, 1994; Inglis & Semba, 1996). Histaminergic tuberomammillary cells also project to NB neurons and are implicated in their activation (Khateb *et al.*, 1995b). Projections from the basolateral amygdala are also excitatory; this may underlie the response of reinforcement-related neurons in the primate basal forebrain (Wilson & Rolls, 1990), whereas inhibitory projections arising in the GABAergic intercalated cell masses terminate in Ch4 and Ch2 fields (Paré & Smith, 1993a, 1994).

Basal forebrain neurons project to a limited number of thalamic nuclei, the cerebral cortex, the posterior hypothalamus and the brainstem core. Together with the brainstem–thalamocortical systems, the basal forebrain plays an important role in states of vigilance and cognitive functions (Semba, 2000; Jones, 2003, 2004).[17] Studies using retrograde tracing and immunoreactivity for ChAT have shown that the

rostral pole of the thalamic RE, mediodorsal (MD), and anteromedial (AM) nuclei of the cat and macaque monkey receive projections from cholinergic and non-cholinergic basal forebrain neurons (Figure 5.8) (Steriade *et al.*, 1987b; Parent *et al.*, 1988). The projections of basal forebrain neurons to thalamic RE nucleus have also been demonstrated using anterograde labelling of single axons from basal forebrain neurons and intracellular staining of RE neurons (Asanuma, 1992) (Figure 5.9). However, these NB projections are not exclusively cholinergic: GABAergic cells are intermingled with cholinergic ones, and a GABAergic NB projection to thalamic RE and MD nuclei was demonstrated (Asanuma & Porter, 1990; Kuroda & Price, 1991; Asanuma, 1997). As both ACh and GABA are inhibitory for RE neurons, the pacemakers of spindle oscillations, the reduction in firing rates of NB neurons plays a permissive role in spindle genesis (Buzsáki *et al.*, 1988; Steriade & Buzsáki, 1990).

The cortical projections of NB cholinergic neurons differ from area to area. In rat, the densest ACh innervation was found in the frontal cortex, followed by the occipital and parietal cortices (Mechawar *et al.*, 2000). As also mentioned above (Descarries *et al.*, 1977; Beaudet & Descarries, 1978), a low proportion of cholinergic axons form classical synaptic profiles and ACh is mainly released in the diffuse transmission type (Descarries *et al.*, 1997, 2004). Classical synaptic profiles are made by GABAergic NB neurons with cortical GABAergic neurons, also containing somatostatin, which may thus lead to disinhibition of a large proportion of pyramidal cells (Freund & Meskenaite, 1992).

The study of intrinsic properties and oscillations displayed by cholinergic NB neurons showed that, besides the tonic firing pattern shown *in vivo*, these neurons display rhythmic bursting. These bursts are mediated by a low-threshold Ca^{2+} conductance, which can be prolonged by NMDA application (Khateb *et al.*, 1992, 1995a).[18] Whereas cholinergic neurons fire rhythmic spike-bursts when hyperpolarized and tonically when depolarized, non-cholinergic NB neurons only discharge clusters of spikes interspersed with rhythmic subthreshold membrane potential oscillations when depolarized positive to –55 mV (Alonso *et al.*, 1996). Cholinergic NB neurons are excited by glutamate, NA, histamine (Khateb *et al.*, 1995b; Khateb *et al.*, 1992, 1995a; Fort *et al.*, 1995; Fournier *et al.*, 2004), but are inhibited by ACh through muscarinic receptors (Khateb *et al.*, 1997).

[18] A small proportion (<10%) of presumably cholinergic neurons recorded from the diagonal band nuclei of the basal forebrain also fire in a burst pattern (Griffith, 1988). The oscillatory bursting behaviour of basal forebrain cholinergic neurons is promoted by neurotensin (Alonso *et al.*, 1994).

5.2 The effects of different neuromodulatory systems on thalamic and cortical cells: state-dependent changes in thalamocortical systems

Data show that changes in the excitability of both thalamic and neocortical neurons are similar during waking and REM sleep, compared

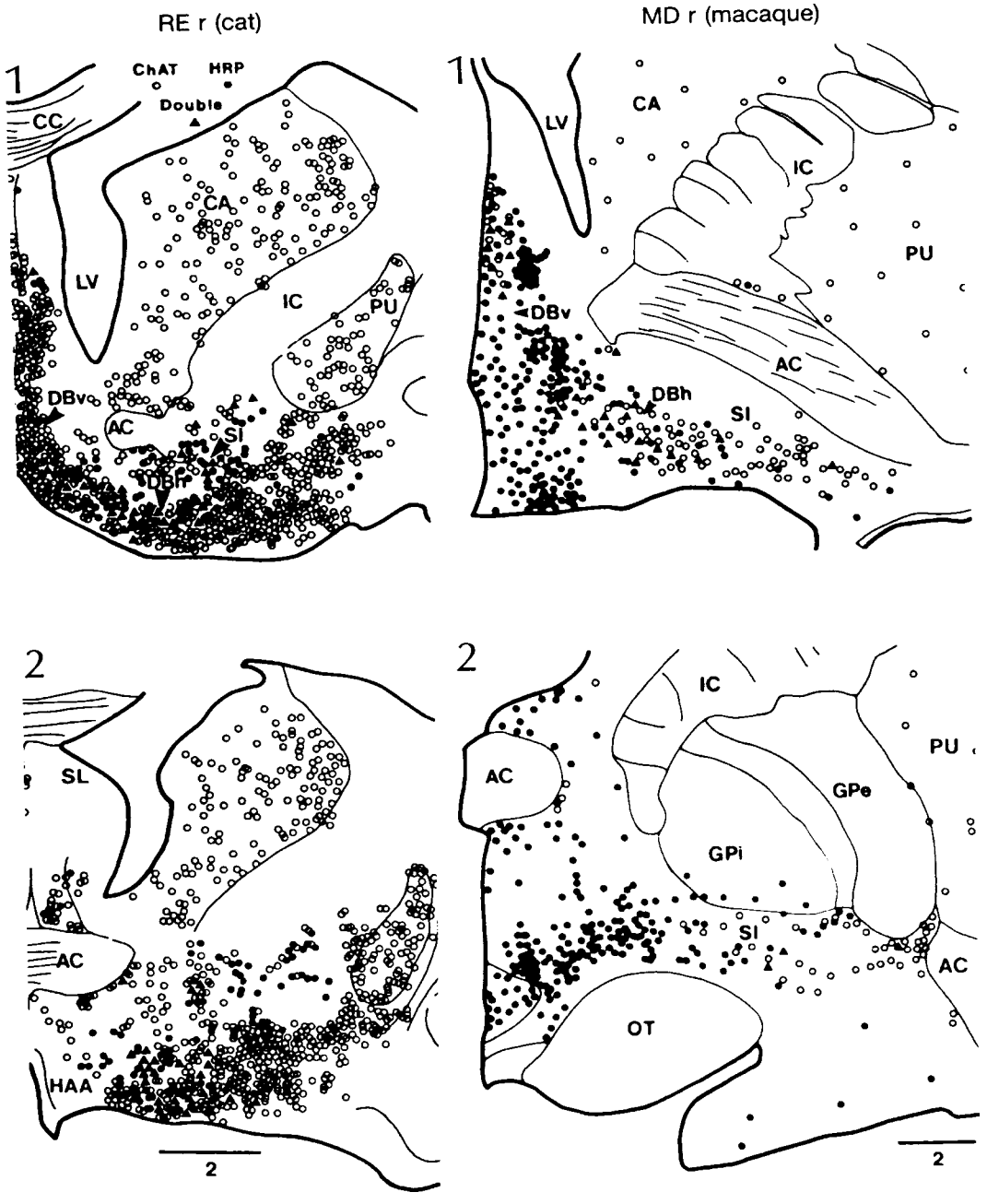

Fig. 5.8 Basal forebrain projections to the thalamic reticular (RE) and mediodorsal (MD) nuclei in cat and monkey. In each case, camera lucida drawings of two transverse sections through the right basal forebrain showing the distribution of cholinergic, HRP-positive, and double-labelled neurons (see symbols in top left section) after WGA–HRP injections in the right thalamic RE and MD nuclei. Black symbols stand for five stained neurons; each empty circle represents ten cells. Abbreviations: AC, anterior commissure; DBh and DBv, horizontal and vertical limbs of diagonal band nuclei; CA, caudate nucleus; CC, corpus callosum; GPe and GPi, external and internal parts of the globus pallidus; HAA, anterior hypothalamic area; IC, internal capsule; LV, lateral ventricle; OT, optic tract; PU, putamen; SI, substantia innominata; SL, lateral septum. Modified from Steriade *et al.* (1987b) and Parent *et al.* (1988).

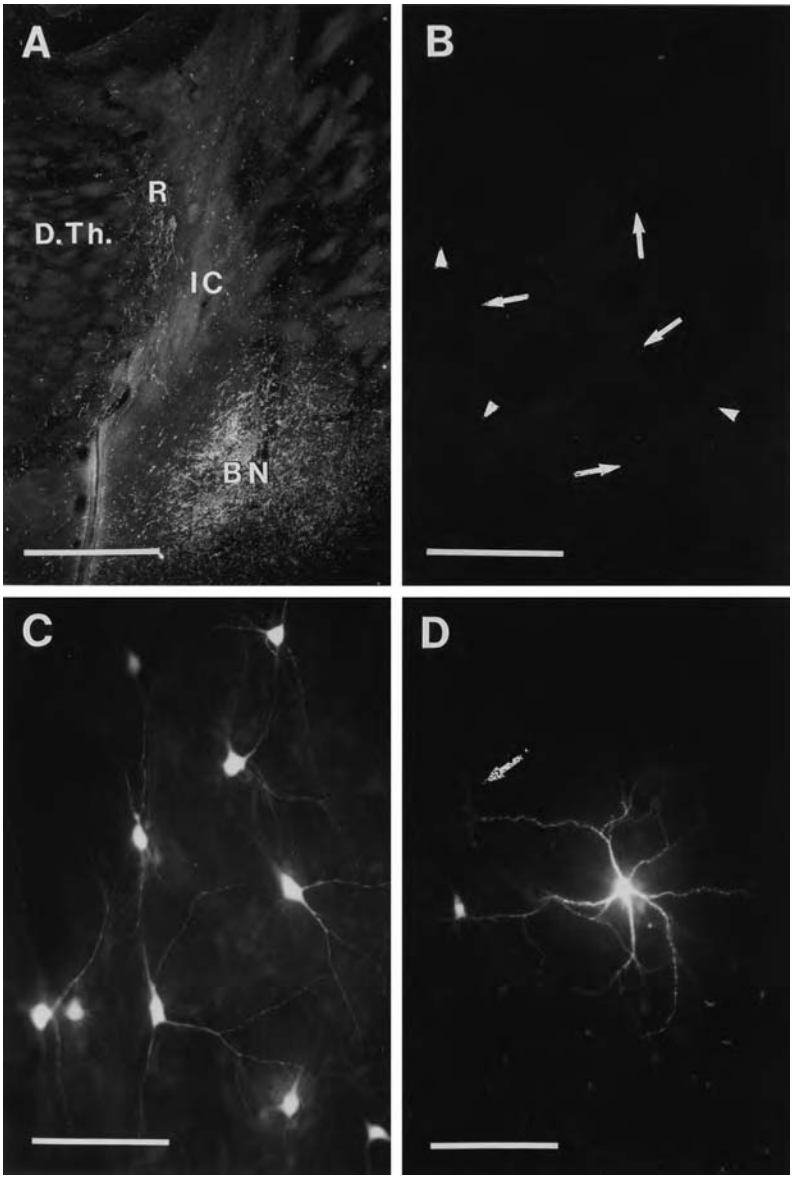

Fig. 5.9 Projections of anterogradely labelled single axons from the nucleus basalis (NB) to the rostral pole of the thalamic reticular (RE) nucleus in the rat. (A) Dark-field photomicrograph of a parasagittal section through a typical *Phaseolus vulgaris* leucoagglutinin injection site in the caudal magnocellular NB and the resulting labelling in the RE. Scale bar, 0.5 mm. (B) Arborizations of NB axons in a tangential section through the rostral RE, using rhodamine as the secondary marker for the *Phaseolus vulgaris* leucoagglutinin labelling. Bouton clusters (arrows) and boutons *en passant* (arrowheads) are apparent. Scale bar, 25 μm. (C) Lucifer yellow-injected neurons in the RE with beaded dendrite neurons. Scale bar, 0.1 mm. (D) A neuron in the adjacent thalamic ventrolateral nucleus, with smooth, radiate dendrites, which branch extensively. Scale bar, 0.1 mm. Modified from Asanuma (1992).

[19] These data result from field potential and unit recordings in animal experiments (Steriade, 1991) as well as from cortical field potential recordings in humans showing that fast-frequency (40–50 Hz) oscillations, which are present in wakefulness, disappear when the subject is in slow-wave sleep and return to waking values in REM sleep (Emerson *et al.*, 1988; Yamada *et al.*, 1988).

with slow-wave sleep.[19] Because the activity of cholinergic and glutamatergic neurons in the brainstem core, mesopontine junction, and basal forebrain is also increased during waking and REM sleep, whereas monoamine-containing neurons in the DR, LC and posterior hypothalamus virtually cease firing during REM sleep (Steriade & McCarley, 2005; Steriade, 1981; Semba, 2000; Jones, 2003, 2004; Buzsáki *et al.*, 1988; Steriade & Buzsáki, 1990),[5] we will focus on the effects of the cholinergic and glutamatergic systems on the thalamus and neocortex.

5.2.1 Thalamus

TC neurons

The thalamus is the first relay station where synaptic transmission is facilitated during natural or brainstem-elicited arousal[20] and where obliteration of afferent messages occurs from the very onset of drowsiness, without any alteration in the magnitude of the incoming signal (Steriade, 1991). This conclusion, first obtained with field potential recordings, was later confirmed with extracellular (Sakakura, 1968; Steriade *et al.*, 1977; Glenn & Steriade, 1982) or 'quasi-intracellular' (Coenen & Vendrik, 1972) recordings in specific sensorimotor or intralaminar nuclei of the thalamus. Subsequent intracellular studies demonstrated that stimulation of the upper brainstem caused a depolarization and increase in apparent input resistance of TC neurons.

Earlier studies, conducted under barbiturate anaesthesia, reported that midbrain reticular formation stimulation facilitates synaptic transmission of the afferent inflow through the lateral geniculate (LG) nucleus. This effect was hypothesized to be cholinergic and due to a global disinhibition of TC neurons through the inhibition of thalamic inhibitory neurons (Singer, 1973, 1977). However, as discussed below, subsequent intracellular studies revealed that although brainstem reticular stimulation blocks prolonged hyperpolarizing potentials, it preserves and even enhances short-lasting inhibitory processes in TC cells. This result does not support the idea of a global disinhibition.

The effect of brainstem cholinergic stimulation on intracellularly recorded thalamic LG neurons was subsequently studied in unanaesthetized cats (brainstem-transected preparations with trigeminal deafferentation) that were pretreated with reserpine for monoamine depletion (if axons from monoamine-containing nuclei are co-activated). These studies provided evidence for a direct excitation of TC neurons by cholinergic inputs (Steriade & Deschênes, 1988; Hu *et al.*, 1989b). Stimulation of brainstem cholinergic nuclei elicits two types of responses in TC neurons: an early transient (150–300 ms) depolarization, which is nicotinic in nature and is associated with a decrease in apparent input resistance; and a longer-latency (1–4 s), longer-lasting (3–5 s) depolarization that is blocked by hyperpolarization (Figure 5.10A), is accompanied by an increased input resistance (Figure 5.10B) and is muscarinic in nature (Steriade & Deschênes, 1988; Hu *et al.*, 1989b; Curró Dossi *et al.*, 1991).[21] The increased input resistance of TC neurons explains their enhanced excitability to incoming signals during brain-activated states (Sakakura, 1968; Steriade *et al.*, 1977; Glenn & Steriade, 1982; Coenen & Vendrik, 1972; Timofeev *et al.*, 1996).[20] The brainstem cholinergic effects also underlie the long-lasting potentiation of synaptic responses seen in anterior thalamic neurons (Paré & Steriade, 1990; Paré *et al.*, 1990b). This effect may be involved in mnemonic processes by controlling the flow of information along the mammillothalamic axis and by modifying the strength of connections between the hippocampus and cortical memory storage sites (Aggleton & Mishkin, 1983a,b; Squire & Alvarez, 1995; Bentivoglio *et al.*, 1997).

[20] This was first shown by recording light-evoked responses with enhanced amplitudes in the thalamic lateral geniculate nucleus during activation produced by midbrain reticular stimulation, in spite of no change in responses simultaneously recorded from optic tract fibers (Steriade & Demetrescu, 1960). These data, with brainstem reticular facilitation of rapidly recurring flash-evoked responses, were corroborated by Bremer and his colleagues (Bremer *et al.*, 1960).

[21] *In vitro* studies have reported that the muscarinic depolarization of thalamocortical neurons consists of two components: (a) the early portion is mediated by a large inward current with little change in input resistance and is mainly mediated by m3 receptors; and (b) the later portion is mediated by a small inward current associated with a large increase in input resistance and is mediated by m1 receptors (Zhu & Uhlrich 1998).

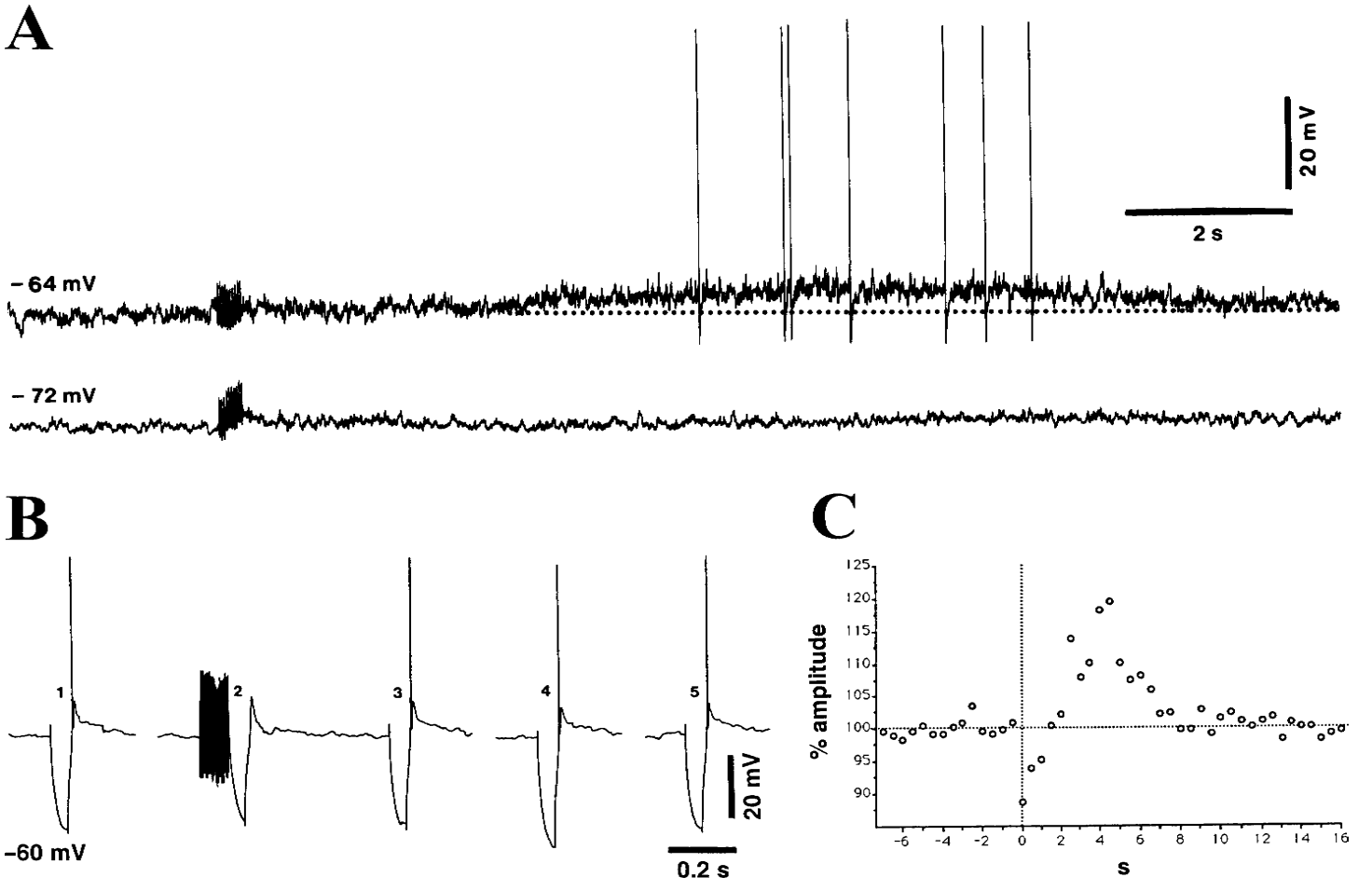

Fig. 5.10 Prolonged depolarization and increased input resistance in thalamocortical neurons following stimulation of brainstem cholinergic nuclei. Cats under urethane anaesthesia. (A) Long-lasting depolarization of thalamic centrolateral (CL) intralaminar neuron induced by a 0.3 s pulse-train at 30 Hz applied to the laterodorsal tegmental (LDT) nucleus, and its suppression under steady hyperpolarizing current. (B) Biphasic effect (increase and decrease) on membrane conductance of CL neuron by LDT stimulation (30 pulses at 300 Hz). (C) Histogram of the LDT-induced conductance changes in the same neuron as in (B). Modified from Curró Dossi *et al.* (1991).

Compared with the robust excitatory influence exerted by brainstem cholinergic neurons on TC neurons, the effects of monoamine-containing axons arising from DR and LC nuclei are weaker or diverse (Monckton & McCormick, 2002)[22] and were investigated less systemically. (a) Serotonin, released by DR neurons, hyperpolarizes TC neurons in all investigated dorsal thalamic nuclei, such as association, intralaminar, mediodorsal, ventrobasal and medial geniculate nuclei (Monckton & McCormick, 2002). (b) In the few dorsal thalamic nuclei that have been investigated, NA released by LC neurons depolarizes TC cells and enhances a hyperpolarization-activated depolarizing current, I_H, through β-adrenoceptors (McCormick & Pape, 1990b).[23] A comparison between the effects induced by LC and PPT stimulation showed that the threshold for blocking oscillatory activity characteristic for slow-wave sleep was lower, and the duration was longer, with PPT than with LC stimulation (Figures 6 and 7 in Steriade *et al.*, 1993a). (c) Histamine, released by tuberomamillary neurons, produces slow depolarizing responses in relay neurons of the dorsal lateral geniculate nucleus, associated with an increase in apparent input resistance, due to a decreased leak K^+ current (McCormick & Williamson, 1991).[24]

The obsolete view that TC neurons act as mere relays for incoming signals to the cerebral cortex was replaced by evidence that their receptive fields are different from those of their inputs. Consistent with this, their receptive fields increased in size after inactivation of $GABA_A$ receptors and their responses displayed a larger coefficient of variation than cells in prethalamic relay stations, with little variability added at the cortical level (Hubel & Wiesel, 1961; Hicks *et al.*, 1986; Salt, 1989; Alloway *et al.*, 1994; Hartveit & Heggelund, 1994). All these features demonstrate that TC cells have a higher selectivity compared with neurons recorded from brainstem afferent sources and stress the importance of intrathalamic inhibitory processes in shaping the responses of relay neurons.

RE and local-circuit GABAergic neurons

The two types of thalamic inhibitory (GABAergic) neurons are RE neurons and local-circuit neurons. RE neurons generate long-range, prolonged IPSPs in target TC cells; local-circuit neurons are involved in stimulus-specific inhibitory responses.[25] The thalamic intraglomerular circuitry, in which dendritic appendages of local inhibitory neurons contact the dendrites of TC cells, may be implicated in the discrete localization of inhibition. With GABAergic contacts confined to the region of dendritic protrusions, the depolarization caused in TC neurons by specific afferents is shunted, without however reducing electrical activity in the rest of the cell.

Setting into action brainstem ascending cholinergic systems results in the blockage of prolonged and rhythmic hyperpolarizations (of which spindles are made) in TC cells (Figure 5.11), but the preservation or even enhancement of the earliest, miniature ($GABA_a$) IPSP (Figure 5.12) that is generated by presynaptic dendrites of local-circuit inhibitory neurons (see Figure 1.9 and related

[22] In a previous study, 5-HT was found to produce a small depolarization of dorsal lateral geniculate (dLG) neurons (Lee & McCormick, 1996). Monckton & McCormick (2002) explained these opposite actions exerted by 5-HT on dLG versus many other dorsal thalamic nuclei by invoking the site of release, concentration, and postsynaptic receptor–effector mechanisms.

[23] *In vivo*, the effects of α-adrenergic drugs are dual, blocking and promoting high-voltage spindle oscillations through α-1 and α-2 receptors, respectively (Buzsáki *et al.*, 1991).

[24] *In vivo*, HA switches the burst firing of LG neurons into tonic firing and promotes sensory responses (Uhlrich *et al.*, 2002). Mice lacking brain HA are unable to remain awake and to respond to behavioural challenges (Parmentier *et al.*, 2002).

[25] Most *in vitro* studies are conducted in rodents that, with the exception of the LG nucleus, do not possess local GABAergic cells in dorsal thalamic nuclei. This is in contrast with felines and primates where there are significant numbers (*c.*25%) of local inhibitory interneurons in all dorsal thalamic nuclei (see monographs by Jones, 1985; Steriade *et al.*, 1997). This may explain some differences in results between experiments *in vivo* and *in vitro* using rodents as experimental animals, especially when the ventrobasal complex is explored (in which there are virtually no local-circuit cells).

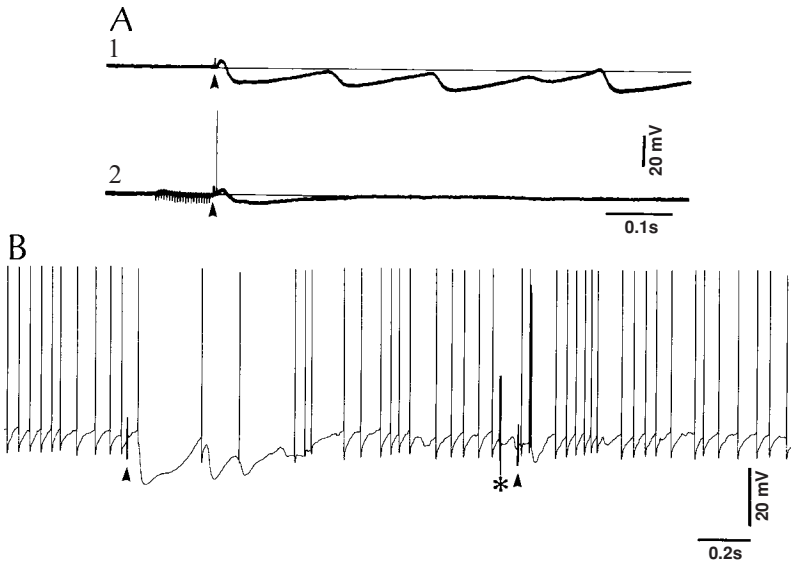

Fig. 5.11 Suppression of prolonged hyperpolarizing potentials and spindles in thalamic relay neurons by brainstem reticular formation stimulation. Cats under barbiturate (A) and urethane (B) anaesthesia. (A) Thalamocortical neuron in the ventrolateral nucleus showing cyclic hyperpolarizations in the frequency range of spindles (evoked by cortical stimulus, in 1, arrowhead) and suppression of spindles by applying a pulse-train to the midbrain reticular formation (2; also note facilitation of antidromic invasion). (B) Anterior thalamic neuron. Stimulus applied to the retrosplenial cortex (arrowhead) evokes cyclic hyperpolarizations within the frequency range of theta rhythm (4–7 Hz) and a brief pulse-train to the mesopontine cholinergic laterodorsal tegmental nucleus (asterisk) blocks long-lasting hyperpolarizations forming oscillatory responses (while preserving a short-lasting IPSP) and induces tonic firing. Unpublished data by M. Steriade & J. P. Roy (A) and modified from Curró Dossi *et al.* (1992b).

text in Chapter 1). These two different actions are explained by various effects exerted by cholinergic (and glutamatergic) neurons in the upper brainstem reticular core on RE and local-circuit inhibitory neurons.

Although in anaesthetized animals brainstem cholinergic effects on RE neurons are exclusively described as inhibitory, in unanaesthetized animals stimulation of the mesopontine PPT nucleus (after chronic bilateral lesions of locus coeruleus to allow anterograde degeneration of axons passing through the stimulated focus) induces a short-latency (5–10 ms) excitation, followed by a much longer period of suppressed firing in RE neurons (Steriade *et al.*, 1986). The two, excitatory and inhibitory, components of the RE cells' response to PPT stimulation were also found in intracellular recordings RE neurons (see Figure 10 in Hu *et al.*, 1989a). In those experiments, the early depolarization was not due to co-stimulation of noradrenergic fibres coursing through the stimulated focus as experiments were conducted on reserpine-treated animals. Also, the possibility that the early depolarization of RE (perigeniculate) neurons

[26] The suggestion that the early excitation in RE neurons is produced by nicotinic receptors (Hu *et al.*, 1989a) was subsequently confirmed in work done in thalamic slices (Lee & McCormick, 1995).

[27] The discrepancy between these and previous (McCormick & Pape, 1988) results was ascribed to different recording techniques, namely, the sharp electrodes (McCormick & Pape, 1988) could cause a Ca^{2+} influx into the cells that may occlude the muscarinic effects on I_H and I_{CAN}.

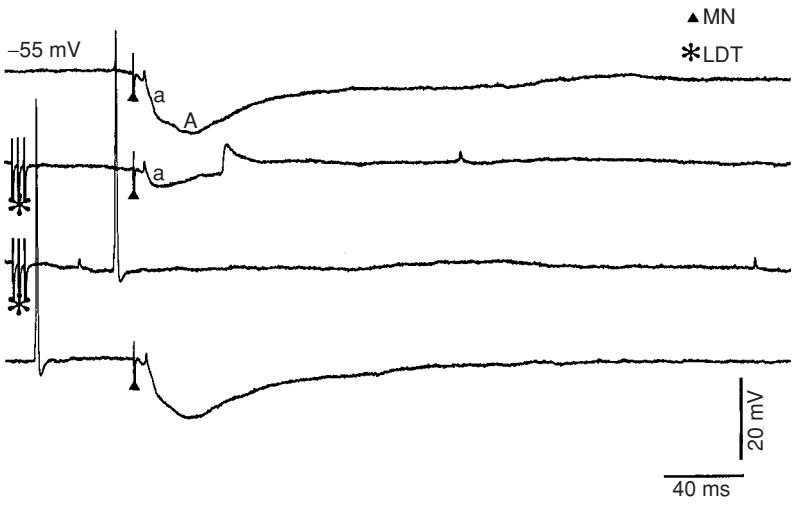

Fig. 5.12 Preservation of the earliest IPSP elicited in anterior thalamic neuron by mamillary nucleus (MN) stimulation by conditioning laterodorsal tegmental (LDT) stimulation. Cat under urethane anaesthesia. Four traces depict (from top to bottom): MN control stimulation (arrowhead) elicited an early EPSP followed by a miniature ($GABA_a$) IPSP and a $GABA_A$ IPSP; conditioning LDT pulse-train (asterisk) left intact the early EPSP and miniature $GABA_a$ IPSP but suppressed the longer-duration $GABA_A$ IPSP; LDT pulse-train alone; and control MN stimulation. Unpublished data by R. Curró Dossi, D. Paré & M. Steriade.

was due to prior excitation of LG neurons could be discarded since the latency of brainstem-RE depolarization was shorter than that of brainstem-LG excitation. The much longer hyperpolarizing response was associated with a conductance increase of the order of 40%–50% and the cholinergic nature of this component was demonstrated by its abolition after scopolamine administration. Then, brainstem reticular stimulation induces a dual response in RE neurons. While the hyperpolarization depends on muscarinic receptors the early and short-lasting excitation may be mediated by a neurotransmitter colocalized in brainstem cholinergic cells, such as glutamate (Lavoie & Parent, 1994; Inglis & Semba, 1996), or depend on nicotinic receptors.[26]

The prolonged muscarinic hyperpolarization of RE neurons, associated with increased K^+ conductance, produced brainstem cholinergic stimulation, explains the erasure of spindles in TC neurons (Figure 5.11), knowing that RE GABAergic neurons are pacemakers of this oscillation (see Chapter 6). The transition from the sleepy to the awake brain due to cholinergic modulation of the thalamus is associated with ACh-induced inhibition of GABA release from the thalamus through the activation of m2 receptors (Rowell *et al.*, 2003).

Cholinergic effects on thalamic interneurons were first described as a muscarinic-induced hyperpolarization (McCormick & Pape, 1988) but more recent studies (Zhu & Heggelund, 2001)[27] proved that they

are more complex, consisting of a muscarinic increase of a hyperpolarizing K^+ current and the enhancement of two depolarizing cation conductances, I_H and I_{CAN}. The latter results are congruent with previous experiments *in vivo* (Curró Dossi *et al.*, 1992b) showing the cholinergic-induced preservation or even enhancement of the earliest ($GABA_a$) IPSP, elicited in TC cells by the presynaptic dendrites of local interneurons. The *in vitro* study, reporting two muscarinic-induced depolarizing cation conductances (Zhu & Heggelund, 2001), concluded that activation of distal dendrites is substantially reduced by the muscarinic activity, whereas IPSPs caused by local dendrites within thalamic glomeruli are less reduced and may even be boosted by muscarinic activity, thus corroborating the results of the *in vivo* study (Curró Dossi *et al.*, 1992b).

Then, however efficiently brainstem reticular stimulation blocks long-range inhibition in TC neurons, an early inhibitory phase remains upon brainstem-evoked activation (Steriade *et al.*, 1977; Steriade, 1984). The cholinergic (muscarinic) promotion of local, fast inhibition (such as that provided by $GABA_a$-mediated IPSP) may be used to increase both the spatial and temporal resolution of sensory signals during brain activation (Zhu & Heggelund, 2001; Curró Dossi *et al.*, 1992b).

5.2.2 Neocortex

Neocortical neurons are activated by concerted actions from brainstem–thalamocortical and basalocortical systems, as well as by direct projections from histaminergic tuberomammillary neurons. None of these systems can be considered in isolation as the unique source of cortical activation, as shown by the presence of brainstem-elicited activation after extensive lesions of either ipsilateral thalamus or NB (Figures 6 and 7 in Steriade *et al.*, 1993a).[28] The most powerful inputs for setting into action NB are the glutamatergic neurons located in the upper midbrain reticular core. Some mesopontine PPT/LDT neurons use both ACh and glutamate as neurotransmitter (Lavoie & Parent, 1994; Inglis & Semba, 1996). Whereas ACh hyperpolarizes cholinergic neurons in the NB and increases their membrane conductance (Khateb *et al.*, 1997), glutamate activates cholinergic NB neurons via both AMPA and NMDA ionotropic receptors (Fournier *et al.*, 2004). This leads to EEG activation, reflected by the appearance of fast activity in the β and γ frequency range (Figures 6 and 7 in Steriade *et al.*, 1993a; Metherate *et al.*, 1992).

Cortical activation elicited by stimulation of mesopontine PPT/LDT nuclei (whose outputs are relayed by both the thalamus and basal forebrain) blocks the slow oscillation, consisting of cyclic depolarizing–hyperpolarizing sequences. This effect is strongly reduced by scopolamine, a muscarinic antagonist (Figure 5.13), but not by mecamylamine, a nicotinic antagonist (Figures 6 and 7 in Steriade *et al.*, 1993a). The same disruption of the slow oscillation is seen during short periods of spontaneously occurring cortical

[28] Dringenberg & Olmstead (2003) showed that PPT-elicited neocortical activation involves relays of brainstem ascending outputs in both central thalamus and basal forebrain. Only after concurrent inactivation of both these structures does the forebrain display, limited and short-lasting activation in response to mesopontine reticular stimulation. The temporal relation between neocortical activation and increased unit firing and neuronal excitability in central intralaminar thalamus (Glenn & Steriade, 1982) and basal forebrain (Détári *et al.*, 1997; Duque *et al.*, 2000) also indicates that both the thalamus and NB are implicated in the process of ascending activation.

[29] See also Chapter 8 of monograph by Steriade *et al.* (1997).

[30] The control of firing mode of cortical neurons by their depolarization (see also Figures 6 and 7 in Steriade *et al.*, 1993a) was also seen with slice application of noradrenaline and a glutamate metabotropic receptor agonist.

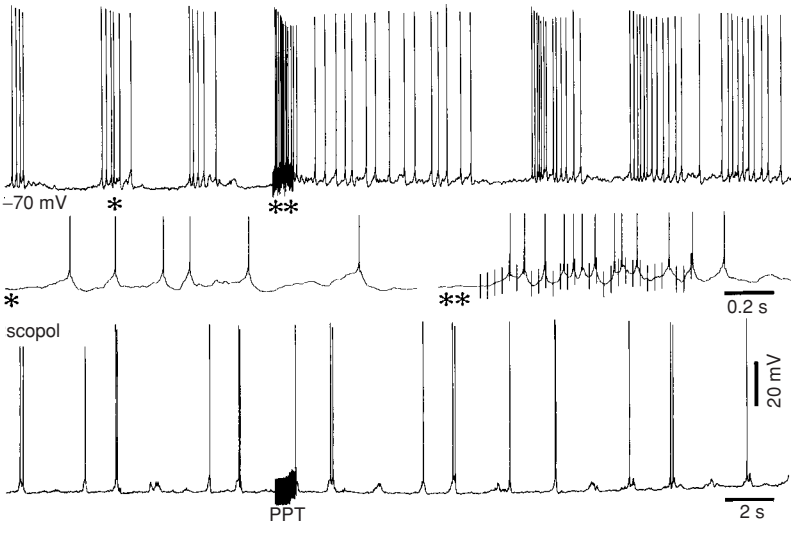

Fig. 5.13 Suppression of cortical slow oscillation by stimulation of the cholinergic pedunculopontine tegmental (PPT) nucleus is antagonized by scopolamine. Intracellular recording of a regular-spiking neuron from cortical area 5 in cat under urethane anaesthesia. Slow oscillation (0.3 Hz) was suppressed for 10 s after PPT pulse-train (30 Hz, 1s). A depolarizing phase of the slow oscillation (one asterisk) and the immediate effect of PPT stimulation (two asterisks) are expanded below at higher speed (spikes truncated). Scopolamine (scopol) administration (0.5 mg/kg, i.v.) reduced the discharges during the rhythmic depolarization as well as the duration of the silent periods (thereby increasing the frequency of the slow rhythm to 0.6 Hz) and blocked the PPT effect. Modified from Steriade *et al.* (1993a).

activation. This effect involves the blockade of hyperpolarizing phases of the rhythm (Figure 5.14). The mechanism underlying this selective suppression of hyperpolarizations is the muscarinic suppression of the voltage-dependent, Ca^{2+}-activated, or Na^{+}-activated K^{+} currents of cortical pyramidal neurons (Halliwell, 1986; Schwindt *et al.*, 1988a,b; McCormick & Williamson, 1989). The blocking of K^{+} leak and Ca^{2+}-mediated K^{+} currents in cortical neurons can also be elicited by activation of $\alpha 1$ and $\beta 1$ adrenoreceptors (Foehring *et al.*, 1989).[29]

Besides blocking the prolonged hyperpolarizations of neocortical neurons, stimulation of mesopontine PPT/LDT nuclei shifts the firing pattern of cortical cells from bursting to tonic (Figures 6 and 7 in Steriade *et al.*, 1993a; Wang & McCormick, 1993).[30] The depolarization underlying this effect may also result from cholinergically induced reduction of some forms of intralaminar inhibition in cortex, as ACh hyperpolarizes fast-spiking inhibitory interneurons in layer V, through muscarinic receptors (Xiang *et al.*, 1998).

The comparison between cortical effects induced by brief pulse-trains to PPT cholinergic nucleus and those elicited by locus coeruleus (LC) stimulation showed that both structures blocked the slow sleep oscillation though obliteration of hyperpolarizing phases of this rhythm but the threshold of this effect was lower, and its duration

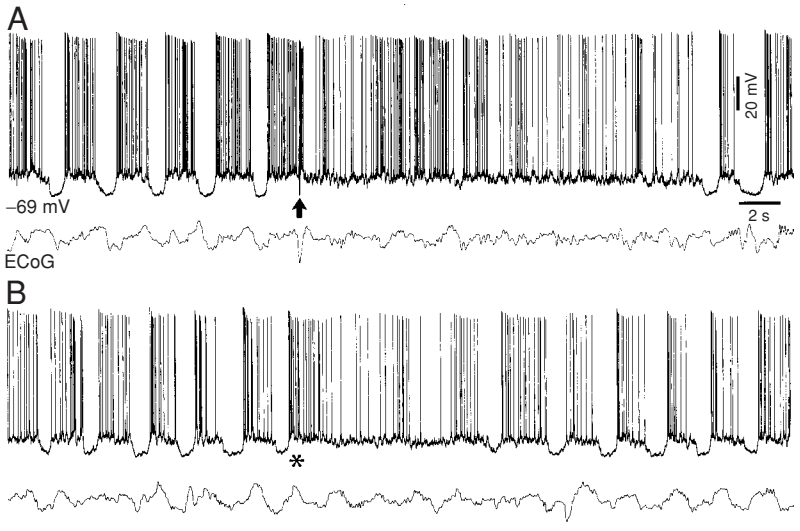

Fig. 5.14 Blockage of slow (0.4 Hz) cortical oscillation by stimulation of the brainstem pedunculopontine tegmental (PPT) nucleus (A) and by slight diminution in amplitude of EEG synchronized waves occurring spontaneously during short period of activation (B). Intracellular recording of area 5 neuron in cat under urethane anaesthesia. (A) Brief pulse-train to the PPT (5 stimuli at 100 Hz, arrow) suppressed the slow rhythm by selective blockage of hyperpolarizing phases separating the cyclic depolarizations. The cellular effect lasted for 20 s and was associated with an electrocorticogram (ECoG) response having a similar time-course. (B) Obliteration of the cellular slow oscillation occurred spontaneously during a short-lasting period of ECoG activation (starting at the asterisk). Modified from Steriade *et al.* (1993a).

longer, with PPT than with LC stimulation (Figures 6 and 7 in Steriade *et al.*, 1993a). The more powerful influence exerted by PPT, compared with LC, stimulation may be explained by reciprocal interactions between these two (cholinergic and noradrenergic) structures. LC neurons extend their long dendrites up to the PPT nucleus, where NA hyperpolarizes cholinergic neurons (Luebke *et al.*, 1992; Williams & Reiner, 1993; Leonard & Llinás, 1994; Leonard *et al.*, 2000), whereas ACh excites LC neurons via m_2 receptors (Egan & North, 1985). Thus, when PPT is stimulated, LC neurons are simultaneously activated, whereas LC stimulation may inhibit PPT neurons.

Histamine activates pyramidal neurons in neocortex through inhibition of a K^+ current, I_{AHP} (reviewed in McCormick, 1992).

5.3 Neuromodulation of amygdala, perirhinal and medial prefrontal neurons

By and large, neuromodulatory inputs to the amygdala, rhinal cortices and medial prefrontal cortex are identical to those of the neocortex, described above. Surprisingly, even though the amygdalocortical system is under the control of the same modulatory systems

as the thalamocortical network, their state-dependent fluctuations in activity are quite different (see Chapter 8).

Like the neocortex, the amygdala (Mesulam *et al.*, 1983a; Carlsen *et al.*, 1985; Rao *et al.*, 1987; Kordower *et al.*, 1989), rhinal cortices (Beckstead, 1978; Alonso & Köhler, 1984; Irle & Markowitsch, 1984; Woolf *et al.*, 1984; Luiten *et al.*, 1985; Room & Groenewegen, 1986b) and medial prefrontal cortex (McKinney *et al.*, 1983; Insausti *et al.*, 1987; Luiten *et al.*, 1987; Musil & Olson, 1988; Gaykema *et al.*, 1990) receive inputs from components of the basal forebrain, some of which use ACh as neurotransmitter (Wainer *et al.*, 1984; Woolf *et al.*, 1984, 1986; Carlsen *et al.*, 1985; Carlsen & Heimer, 1986; Manns *et al.*, 2001). The cholinergic innervation of the amygdala mostly originates in the substantia innominata and ventral limb of the diagonal band of Broca. These inputs are densest to the basolateral nucleus of the amygdala and weakest to the central nucleus of the amygdala. At the electron microscopic level, cholinergic synapses were reported to be symmetrical and to contact dendrites and spines (Carlsen & Heimer, 1986).

Like the neocortex, the amygdala, medial prefrontal cortex and rhinal cortices also receive histaminergic inputs from the tuberomammillary nucleus of the posterior hypothalamus (Ben-Ari *et al.*, 1977; Watanabe *et al.*, 1984; Köhler *et al.*, 1985a; Saper, 1985; Panula *et al.*, 1989; Rempel-Clower & Barbas, 1998; reviewed in Brown *et al.*, 2001). From the brainstem, they also receive serotonergic inputs from the raphe nuclei (mostly dorsal and median raphe nuclei) (Moore *et al.*, 1978; Kohler *et al.*, 1980, 1981; Köhler & Steinbusch, 1982; Kosofsky & Molliver, 1987; Li *et al.*, 1990; Ma *et al.*, 1991; Vertes, 1991; Vertes *et al.*, 1999) as well as noradrenergic inputs from the locus coeruleus (Swanson & Hartman, 1975; Jones & Moore, 1977; Fallon *et al.*, 1978; Russchen, 1982b; Li *et al.*, 2001, 2002). Perhaps the only difference, and even in this case only a quantitative one, is that the amygdala, and in particular its central nucleus (Loughlin & Fallon, 1983; Seroogy *et al.*, 1989; Takada, 1990; Hasue & Shammah-Lagnado, 2002), as well as the medial prefrontal cortex (Seroogy *et al.*, 1989; Williams & Goldman-Rakic, 1998; Carr & Sesack, 2000a) receive strong dopaminergic inputs originating mostly from the ventral tegmental area, substantia nigra pars compacta and retrorubral area. Some projections also arise from non-dopaminergic, possibly GABAergic neurons (Loughlin & Fallon, 1983; Carr & Sesack, 2000b). Dopaminergic inputs to the rhinal cortices exist but they are comparable in density to those reaching most of the neocortex.

An interesting property of the amygdala (Hopkins & Holstege, 1978; Wallace *et al.*, 1989, 1992; Cassell & Gray, 1989b) and medial prefrontal cortex (Carr & Sesack, 2000c; Vertes, 2004) is that they send strong projections to most of these modulatory cell groups. The majority of the return amygdala projections originate in the central nucleus (Hopkins & Holstege, 1978; Wallace *et al.*, 1989, 1992; Cassell & Gray, 1989b). This is true of projections to dopaminergic cells groups A8–9 and noradrenergic cells of the locus coeruleus, as

well as cholinergic cells of the pedunculopontine and laterodorsal tegmental nuclei. Amygdala projections to basal forebrain cholinergic cell groups also originate mostly from the central nucleus, but some also stem from components of the basolateral complex (Krettek & Price, 1978a; Jolkkonen *et al.*, 2002).

In general, most of the neuromodulatory actions documented in the neocortex are consistent with those observed in the amygdala, rhinal cortices and medial prefrontal cortex. In the following account, we will only consider examples of neuromodulatory actions in the amygdala.

ACh has complex pre- and postsynaptic actions on basolateral amygdala neurons. Muscarinic receptor activation produces a profound presynaptic inhibition of excitatory synaptic transmission (Yajeya *et al.*, 2000), the reduction of various K^+ conductances (K^+ 'leak', M-current, gK_{Ca}^{2+}) (Washburn & Moises, 1992c; Faber & Sah, 2002), the potentiation of a hyperpolarization-activated inward rectifier K^+ current and the activation of a Ca^{2+}-independent mixed cationic conductance (Yajeya *et al.*, 1999). In addition, activation of nicotinic receptors produces a rapid depolarization of GABAergic interneurons of the basolateral amygdala (Washburn & Moises, 1992b) and presynaptically enhances glutamate and GABA release (Girod *et al.*, 2000; Barazangi & Role, 2001).

Similarly, noradrenaline was reported to elicit mixed excitatory and inhibitory effects, depending on the activated receptor subtypes. The main effect of noradrenaline appears to be mediated by $\alpha 2$ receptors and involves a presynaptic inhibition of glutamate release in the basolateral amygdala. $\alpha 1$ receptors were reported to presynaptically facilitate GABA release, an effect that is reduced in stressed animals (Braga *et al.*, 2004). The effects of β-adrenoreceptor agonists are comparatively less important, but similar to those seen in the neocortex (Ferry *et al.*, 1997): a reduction of spike frequency accommodation resulting from the inhibition of some subtypes of gK_{Ca}^{2+} and a presynaptic facilitation of excitatory synaptic transmission (Huang *et al.*, 1996; Ferry *et al.*, 1997; Faber & Sah, 2002) resulting from a potentiation of some voltage-gated Ca^{2+} channel subtypes (P and/or Q) (Huang *et al.*, 1996). These studies suggest that cAMP-dependent PKA mediates both effects, but in different cellular compartments. Finally, β-receptor agonists were also reported to potentiate NMDA currents (Gean *et al.*, 1992).

As elsewhere in the brain, the effects of dopamine have been difficult to define in the amygdala.[31] First, electrophysiological studies *in vivo* reported that systemic administration of dopamine agonists could facilitate LTP induction in the lateral amygdala (Rosenkranz & Grace, 2002) in part by a D2-mediated increase in input resistance and a D1-mediated presynaptic inhibition of IPSPs (Rosenkranz & Grace, 2001). A different group also reported that dopamine facilitated LTP induction by suppressing feed-forward inhibition, but via D2 receptors (Bissière *et al.*, 2003). In their hands, this effect was mediated

[31] In part, this situation may result from the fact that most electrophysiological studies have focused on the lateral nucleus of the amygdala, where the dopaminergic innervation is lowest in density compared with other amygdala nuclei (Fallon & Ciofi, 1992).

by a presynaptic inhibition of GABA release that, paradoxically, coexists with a postsynaptic enhancement of the excitability of local interneurons (Loretan *et al.*, 2004). Finally, in another *in vitro* study, dopamine was reported to enhance the excitability of projection cells by increasing their input resistance and current-evoked firing. This effect seemed to result from the inhibition of a slowly inactivating K^+ current (Kroner *et al.*, 2005).

Chapter 6

Gating of signals in slow-wave sleep

We now discuss how external and internal signals are processed in the thalamus and cerebral cortex during the state of slow-wave sleep and during different types of anaesthesia that mimic this sleep stage. Basically, signals from the periphery are obliterated through synaptic inhibition within the thalamus and cannot be transferred to cortex, whereas corticocortical and corticothalamic circuits remain active despite disconnection from the external world. This dissociation explains why, in the absence of information from the external world, the behavioural state of slow-wave sleep is associated with processing of internally generated signals and even with synaptic plasticity. These processes may lead to consolidation of memory traces acquired during the wakeful state as well as to a form of consciousness expressed by dreaming mentation. However, prior to discussing these topics, this chapter will first describe the spontaneously occurring brain oscillations and neuronal firing patterns that characterize slow-wave sleep.

6.1 Brain oscillations during slow-wave sleep and anaesthesia in animals and humans

The three major types of brain rhythms, which appear in the state of slow-wave sleep in experimental animals and humans, are mainly generated as a consequence of the reduction in firing rates of brainstem reticular and basal forebrain activating neurons that project to the thalamus and cerebral cortex (see Chapter 5). This relation was observed by recording cellular activity in the upper reticular core and mesopontine cholinergic nuclei during the transition from wakefulness to slow-wave sleep. These experiments revealed that the firing rates of brainstem neurons, with antidromically identified ascending projections, decreased tens of seconds before the first global electrical sign that defines natural slow-wave sleep (Steriade *et al.*, 1982a, 1990c). Human studies of regional cerebral blood flow (rCBF) using positron emission tomography (PET) during states of

wakefulness and sleep have also concluded that rCBF significantly decreases during slow-wave sleep in the dorsal pons and midbrain, the thalamus and basal forebrain, and some cortical areas that receive projections from these subcortical neuromodulatory systems (Maquet *et al.*, 1997).[1] Rather than global changes in neocortex, rCBF measured with PET in humans showed major deactivation in heteromodal association areas during slow-wave sleep, whereas activity in primary and secondary sensory cortices was relatively preserved (Braun *et al.*, 1997).

The above results emphasize that a major factor in forebrain disconnection leading to slow-wave sleep is the reduced neuronal activity in the brainstem–thalamocortical axis. Thus, data favour the concept that sleep is a passive phenomenon due to the closure of cerebral gates.[2] The idea that sleep is an active phenomenon promoted by inhibitory mechanisms is based on experiments showing that some neurons in forebrain or brainstem structures preferentially fire during slow-wave sleep and/or that destruction or inactivation of those neurons prevents sleep. The ventrolateral part of the preoptic area in the basal forebrain is one of the candidates for promoting slow-wave sleep, in view of neuronal recordings and lesion experiments (Szymusiak & McGinty, 1986; Sherin *et al.*, 1996; Lu *et al.*, 2000; Szymusiak *et al.*, 2001). In addition, although the theory implicating neurons in the dorsal raphe nucleus and their major transmitter, serotonin (5-hydroxytryptamine, 5-HT), in the generation of slow-wave sleep (Jouvet, 1972) was subsequently refuted in view of decreased firing rates when the animal passes from waking to slow-wave sleep (McGinty & Harper, 1976; Trulson & Jacobs, 1979), more recent results show that some dorsal raphe neurons display the highest discharge frequencies during slow-wave sleep, with suppression of firing in waking and REM sleep (Sakai & Crochet, 2001).[3]

The two (passive and active) mechanisms of sleep onset are probably complementary rather than opposed. Indeed, the firing of some neuronal groups hypothesized to actively promote sleep, such as those of the preoptic area, may inhibit posterior hypothalamic histaminergic neurons or other neuronal aggregates with activating properties (Gritti *et al.*, 1994; Sherin *et al.*, 1998; Steininger *et al.*, 2001), thus leading to sleep through deafferentation. Therefore, the two apparently opposite concepts on mechanisms of sleep onset are probably successive steps within a chain of events, eventually leading to brain disconnection, as postulated in the passive theory of sleep. An example favouring this view may be taken from experiments with lesions or reversible inactivation of anterior hypothalamic neurons, which are hypothesized to promote slow-wave sleep. Long-lasting insomnia produced by excitotoxic lesions or functional inactivation of the medial preoptic area (Lin *et al.*, 1989; Sallanon *et al.*, 1989) was followed by sleep recovery following injection of an inhibitory substance into the activating system of the posterior hypothalamus of insomniac cats (Lin *et al.*, 1988). Thus, the integrity of preoptic areas in the anterior

[1] Marked decreases in rCBF were also found in the medial thalamus (Hofle *et al.*, 1997) and significant covariation between the midbrain and the thalamus was reported in a PET study on humans (Fiset *et al.*, 1999). This covariation is explained by direct connections demonstrated in experimental studies (see Chapter 5).

[2] The passive (deafferentation) theory of falling asleep dates back to the first century BC (see the 1988 translation of Lucretius' book, 55 BC). It was developed during the past century, mainly by Bremer, 1935) and Kleitman, 1963), and supported by cellular studies (see Steriade, 2003a,b).

[3] Other data may bring back on the scene the raphe and other 5-HT neuromodulatory actions as good candidates for inducing neuronal events related to slow-wave sleep (Steriade, 2004c). 5-HT produces a hyperpolarization of thalamocortical (TC) neurons, associated with an increased K^+ conductance (Monckton & McCormick, 2002, 2003); thus, 5-HT contributes to the thalamic blockade of signals arising in the external world and may promote the process of falling asleep. The above data might partly vindicate Jouvet's (1972) hypothesis that the action of serotoninergic dorsal raphe neurons favours the onset of sleep.

[4] Merica & Fortune (2003) presented evidence for similarity of shape and timing of various EEG frequency bands characterizing slow-wave sleep at all cortical sites of humans and advanced the hypothesis that this is due to brainstem modulation of thalamocortical systems.

hypothalamus is not a necessary condition for sleep onset, as sleep can be restored by removing the activation from posterior hypothalamic cells.

As it stands now, the idea of discrete, homogeneous neuronal groups, which would promote slow-wave sleep, is at an embryonic stage of research. What is firmly established is that reduction in neuronal activity in the upper brainstem core or transection at the collicular level in animal experiments (Steriade *et al.*, 1982a, 1990c),[2] and lesions of the midbrain–thalamic intralaminar axis (some due to thrombosis at the bifurcation of the basilary artery in humans) leads to forebrain deafferentation and various degrees of hypersomnolence or coma (Façon *et al.*, 1958; Castaigne *et al.*, 1962; Plum, 1991; Steriade, 1997b), associated with modulation of different frequency bands in brain electrical activity.[4]

6.1.1 Neuronal basis of three major sleep rhythms implicated in signal gating

The rhythms of the electroencephalogram (EEG) have been recognized since the beginnings of EEG recordings in humans and animals and some of them were thoroughly described during the 1930s and 1940s (Berger, 1929, 1937).[5] However, the neuronal mechanisms of EEG rhythms could be analysed in detail only during the past four decades and especially since 1980. We know quite well the cellular basis of three major rhythms defining slow-wave sleep (slow oscillation, spindles and delta) but we have little knowledge about the precise site(s) of production and underlying neuronal mechanism(s) of alpha waves, whose changes mark the onset of sleep[6] and which are of cortical origin, with a possible thalamic contribution.[7]

In the following, we will mainly use data from intracellular recordings, the only method to shed light on the mechanisms underlying sleep oscillations. Intracellular analyses of electrophysiologically identified neuronal types in the intact brain in naturally sleeping and awake animals (Steriade *et al.*, 2001a), demonstrate that firing patterns ascribed to intrinsic neuronal properties display dramatic alterations due to changes in membrane potential and increased synaptic activity, as it occurs *in vivo* (Paré *et al.*, 1998a; Steriade, 2001b). The major neuronal types in the neocortex and thalamus are interconnected and they operate under the control of generalized modulatory systems, a condition that cannot be explored in reduced brain preparations such as cortical or thalamic slices maintained *in vitro* (Steriade, 2001a).[8]

The three major rhythms of brain electrical activity during slow-wave sleep are the slow oscillation, spindle oscillation, and delta waves. We will describe them in this order because the slow oscillation appears from the onset of natural slow-wave sleep (Steriade & Amzica, 1998) and not only groups the other sleep rhythms, but also creates favourable conditions for the cyclic appearance of fast waves, which are conventionally regarded as exclusively characterizing waking and REM sleep.

[5] For earlier literature, see Brazier (1961).

[6] In humans, the common electrographic definition of sleep onset is the change from EEG alpha waves during relaxed wakefulness to a mixed pattern of low-voltage waves (termed stage 1 sleep). Since stage 1 sleep is not necessarily associated with perceived sleep onset in humans, the onset of sleep is considered to be the EEG correlates of stage 2 sleep (Carskadon & Dement 2000; De Gennaro *et al.*, 2001).

[7] The replacement of α waves, at sleep onset, by slower θ activity (2–7 Hz) and later on by spindles, whose frequencies (7–14 Hz) partly overlap with those of α waves, was the topic of a recent study focused on the thalamic cellular mechanisms of synchronized oscillations at α and θ frequencies (Hughes *et al.*, 2004). These authors showed that activation of metabotropic glutamate receptor (mGluR1) in slices from lateral geniculate nucleus evokes α rhythm in a subset of neurons. Since, in contrast with the thalamic origin of spindles, a series of experimental and modelling studies showed that α waves are mainly generated and spread within the cerebral cortex before reaching the thalamus (Lopes da Silva *et al.*, 1973, 1978, 1980), the results of Hughes *et al.* (2004) may indicate that corticothalamic glutamatergic projections are implicated in the production of thalamic α waves.

[8] The idea that rhythmic activities, reflecting various states of vigilance, can only be studied in intact-brain preparations was recently supported by evidence that such global brain state transitions occur simultaneously across multiple forebrain areas and important changes in neuronal synchronization predict shifts in behavioural states (Gervasoni *et al.*, 2004).

All slow-wave sleep rhythms consist of prolonged and deep hyperpolarizations in cortical and thalamic cells, bringing these neurons far from the membrane potential at which action potentials can be fired; thus, neuronal networks become unable to transfer incoming information. In the thalamus, the cyclic hyperpolarizations of TC neurons during spindles and one type of delta waves are associated with large increases in membrane conductance, so that external signals are obliterated. The thalamic gating of afferent messages arising at the periphery does not, however, prevent processing of signals generated in corticocortical and corticothalamic neuronal networks, which continue to be operational, at least partly, during slow-wave sleep. This explains why special forms of mentation (consolidation of memory traces acquired during waking) are present during this sleep stage, despite the fact that the brain is disconnected from the external world (see Sections 6.3 and 6.4).

The slow oscillation

Compared with other sleep oscillations, which were described during the 1930s, the slow rhythm (mainly 0.6–1 Hz) was described much more recently, using intracellular recordings from neocortical neurons in anaesthetized animals and EEG recordings during natural sleep in humans (Steriade *et al.*, 1993e). Subsequently, it was also described during natural slow-wave sleep of animals using intracellular (Steriade *et al.*, 2001a) and extracellular unit (Steriade *et al.*, 1996a) recordings as well as during natural sleep in humans using EEG (Achermann & Borbély, 1997; Amzica & Steriade, 1997; Mölle *et al.*, 2002; Marshall *et al.*, 2003; Massimini *et al.*, 2003)[9] and magnetoencephalographic (MEG) (Simon *et al.*, 2000) recordings. The frequency of the slow oscillation depends on the anaesthetic used and the behavioural state: it is usually between 0.3 and 0.6 Hz under urethane anaesthesia; between 0.6 and 0.9 Hz under ketamine–xylazine anaesthesia; and between 0.7 and 1 Hz (or even slightly exceeding 1 Hz) during natural sleep.[10] In acutely prepared animals, the best experimental condition for investigating the neuronal basis of the slow oscillation *in vivo* is ketamine–xylazine anaesthesia (Contreras & Steriade, 1995), which closely mimics the electrical patterns of natural slow-wave sleep.[11]

The cortical origin of the slow oscillation was demonstrated by its presence in the cerebral cortex after extensive lesions of the thalamus (Steriade *et al.*, 1993f) and its absence in the thalamus after decortication (Timofeev & Steriade, 1996). The generation of the slow oscillation in neocortex was confirmed by its presence in cortical slabs *in vivo* (Timofeev *et al.*, 2000) and in cortical slices *in vitro* (Sanchez-Vives & McCormick, 2000).[12]

Virtually all cortical neurons throughout layers II–VI, with antidromically identified thalamic or callosal projections as well as local-circuit neurons, spontaneously display the slow oscillation. This oscillation consists of prolonged depolarizing and hyperpolarizing components (Figure 6.1).

[9] The slow cortical oscillation during natural sleep in humans is reflected down to the level of spinal motoneurons, as observed by low-frequency rhythms in the EMG activity of trapezius muscle activity during slow-wave sleep (Westgaard *et al.*, 2000)

[10] Even when the frequency of slow oscillation slightly exceeds 1 Hz, this rhythm is different from delta waves that usually occur between 2 and 4 Hz. More importantly, the origin(s) and mechanisms of slow oscillation and delta potentials are dissimilar (see Section 6.1.1). As to the 'cyclic alternating pattern', it recurs at 20 s or longer intervals, is associated with enhancement of muscle tone and heart rate, and was described under the term 'arousal-related phasic events' (Terzano *et al.*, 1988), whereas the slow rhythm is blocked during arousal in acute experiments as well as during natural awakening (Steriade *et al.*, 1996a).

[11] Ketamine, a blocker of NMDA receptors, is among the most effective tools in inducing slow-wave sleep patterns over the background of a wake state (Feinberg & Campbell, 1993). Xylazine, an α2-receptor agonist, increases a K^+ conductance in a variety of central neurons (see Nicoll *et al.*, 1990). The similarity between the slow oscillation occurring in natural sleep and under ketamine–xylazine anaesthesia was shown in the same chronically implanted animal (Amzica & Steriade, 1997b)

[12] This study was conducted in ferret slices. The slow oscillation was not observed in other studies on acute brain slices from rats or other species because of absence of the required connectivity. The presence of the slow cortical oscillation in the study by Sanchez-Vives & McCormick (2000) can be ascribed to the high excitability of neurons in deep layers V/VI due to the higher concentration of K^+ in the bathing milieu used in those slices

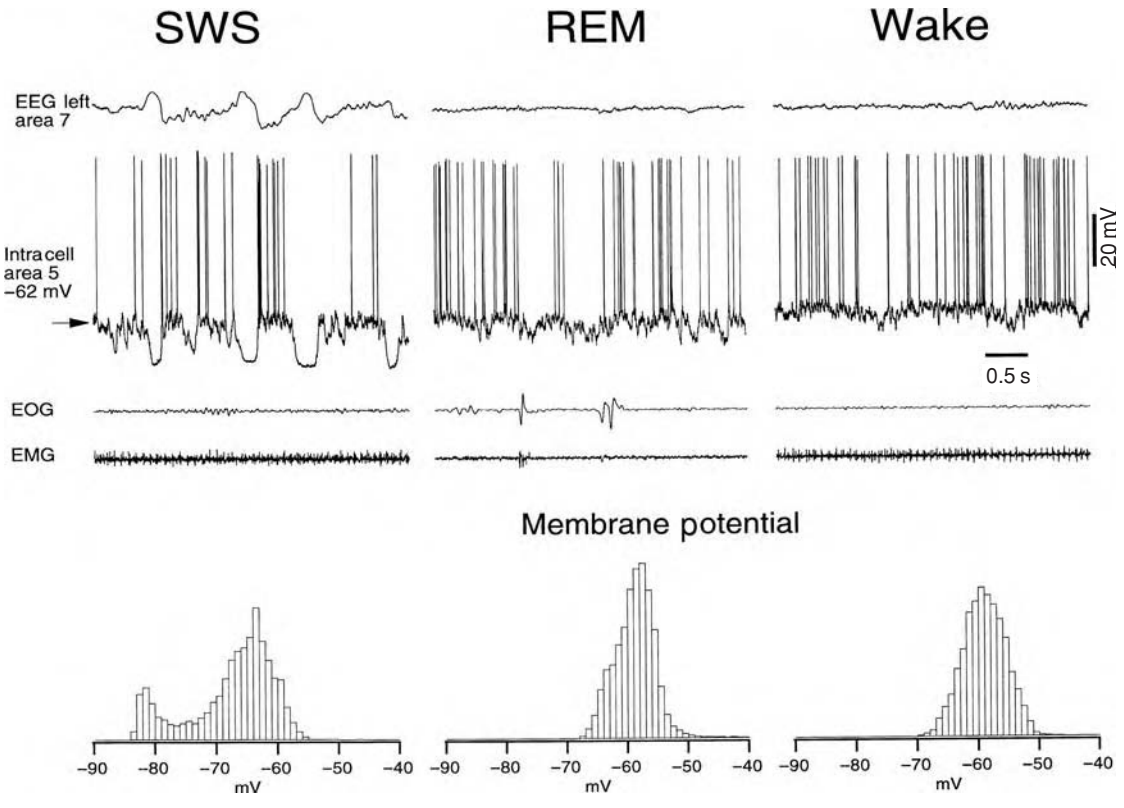

Fig. 6.1 The slow oscillation during natural slow-wave sleep (SWS) in a chronically implanted cat. The figure also shows states of REM sleep and waking. Four traces show (from top to bottom): EEG from area 7, intracellular activity of regular-spiking neuron from area 5, electrooculogram (EOG) and electromyogram (EMG). Below, histogram of membrane potential during the three states of vigilance. Note cyclic hyperpolarizations within the frequency of the slow oscillation during SWS, which are reflected in the histogram of membrane potential as a tail down to −85 mV, whereas both brain-active states (REM sleep and waking) display Gaussian-type histograms with peaks around −60 mV. Unpublished experiments by M. Steriade, I. Timofeev and F. Grenier (see also Steriade *et al.*, 2001a).

(a) The long-lasting depolarization consists of EPSPs and fast IPSPs reflecting the action of synaptically coupled local GABAergic interneurons (Steriade *et al.*, 1993e). The depolarizing component is made up of both non-NMDA- and NMDA-mediated synaptic excitatory events and a voltage-dependent persistent sodium current, $I_{Na(p)}$.[13]

(b) The long-lasting hyperpolarization, which cyclically interrupts the depolarizing phases, is a combination of an $I_{K(Ca)}$ and disfacilitation in the corticothalamic network. Indeed, recordings with intracellular pipettes filled with Cs^+, a non-selective blocker of K^+ currents, show that, although the membrane potential of cortical neurons is slightly and steadily hyperpolarized (Steriade *et al.*, 2001a) because of the diminished firing of excitatory TC

[12] (*cont.*) (3.5 mM K^+), compared with values reported *in vivo* (Lux & Neher, 1973; Gutnick *et al.*, 1979). The higher excitability of layers V/VI neurons in the *in vitro* work by Sanchez-Vives & McCormick (2000) can be seen in their Figure 2, showing that layers V/VI neurons discharged heavily during the silent phases of neurons from other layers. Intracellularly, the silent phases represent hyperpolarizing potentials. During the hyperpolarizing phases of the slow oscillation, there is virtually no spontaneously occurring action potential in any type of cortical neuron investigated *in vivo*, during natural slow-wave sleep (Steriade *et al.*, 2001a) or under anaesthesia (Steriade *et al.*, 1993e).

[13] The participation of NMDA-mediated synaptic events and $I_{Na(p)}$ was shown by the great reduction (but not abolition) of the depolarizing phase following administration of ketamine (NMDA blocker) or intracellular injection of QX-314 (a blocker of Na^+ currents), whereas

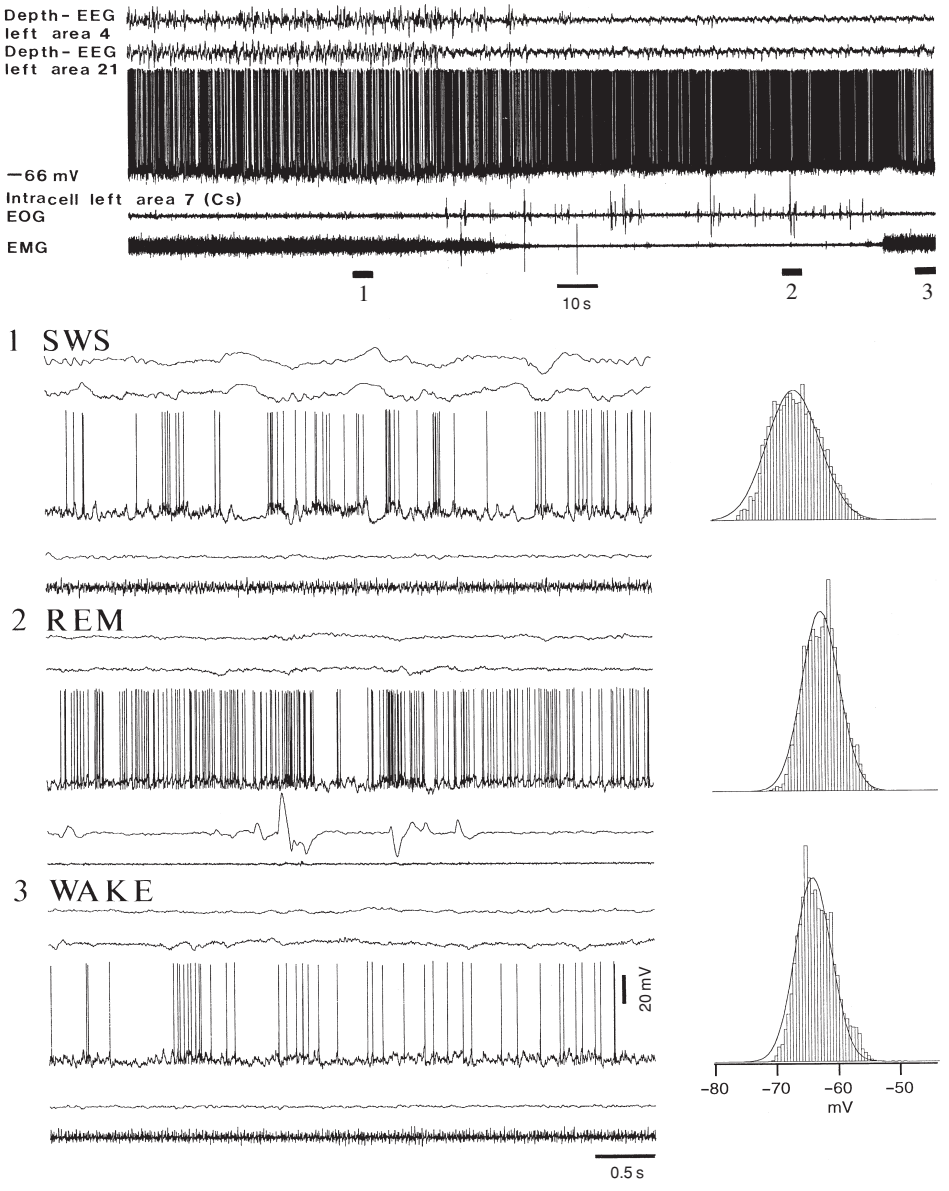

Fig. 6.2 Prolonged hyperpolarizations of the slow oscillation during natural slow-wave sleep (SWS) in chronically implanted cats are reduced by recording cortical neurons intracellularly with micropipettes filled with Cs^+. Transition from SWS to REM sleep. Top five traces: depth-EEG recordings from left areas 4 and 21, intracellular recording from cortical neurons in left area 7 (Cs^+-filled pipette), electro-oculogram (EOG) and electromyogram (EMG). Note muscular atonia and ocular saccades upon transition to REM sleep. Parts marked by horizontal bars below EMG trace and indicated by 1 (SWS), 2 (REM sleep) and 3 (waking), are expanded below. Right, histograms of membrane potential during the three states of vigilance (SWS, REM and waking). Note slightly more hyperpolarized membrane potential during SWS (compared with REM sleep and waking), but absence of the distinct hyperpolarizing tail that characterizes SWS when intracellular recordings are made with K-acetate pipettes (see Figure 6.1). Also compare prolonged and deep hyperpolarizations during SWS in the Figure 6.1 with much reduced, almost absent hyperpolarizations in this record with Cs^+-filled pipette. Data from experiments by M. Steriade, I. Timofeev and F. Grenier (see also Timofeev *et al.*, 2001b).

(Glenn & Steriade, 1982) and activating neuromodulatory systems (Steriade *et al.*, 1982a, 1990c) during slow-wave sleep, prolonged, high-amplitude and cyclic hyperpolarizing potentials (as depicted in Figure 6.1) are no longer seen (Figure 6.2) (Timofeev *et al.*, 2001b). Besides, the prolonged and cyclic hyperpolarizations are suppressed through a muscarinic-mediated effect (Steriade *et al.*, 1993a) and it is known that activation of muscarinic receptors diminishes or suppresses the voltage-, Na^+- and Ca^{2+}-dependent K^+ currents (McCormick & Williamson, 1989; Schwindt *et al.*, 1989). The disfacilitation mechanism is supported by measuring the membrane input resistance (R_{in}) and showing that R_{in} is highest during the long-lasting hyperpolarizing component of the slow oscillation (Contreras *et al.*, 1996b). One possible factor accounting for disfacilitation in neocortical networks is a progressive depletion of $[Ca^{2+}]_{out}$ during the depolarizing phase of the slow oscillation (Massimini & Amzica, 2001).

[13] (*cont.*) the initial, short-lasting excitatory event of the depolarization was left intact (Steriade *et al.*, 1993e). The presence of non-NMDA-, NMDA-mediated, and GABA-evoked synaptic events during the depolarizing phase of the slow oscillation was also shown more recently in a study on prefrontal cortex, *in vivo* as well as in organotypic cultures (Seamans *et al.*, 2003).

The slow oscillation was also investigated in simultaneous recordings from cortical neurons and glial cells (Amzica & Steriade, 1998b, 2000; Amzica & Neckelmann, 1999; Amzica *et al.*, 2002; Amzica & Massimini, 2002). The neuronal response to a cortical stimulus consists of depolarization crowned by action potentials, followed by an inhibitory potential and a rebound excitation, whereas the simultaneously recorded responses in glia is a sluggish depolarizing slope, a further depolarization and a negative wave (Amzica & Steriade, 1998b, 2000). The fact that neuronal IPSP is reflected in the glia by a depolarizing potential is explained by opening of Cl^- channels in glia by $GABA_A$ action (Kettenmann & Schachner, 1985). During the slow oscillation, the onset of the depolarizing phase in neurons is followed, after *c.*90 ms, by the depolarization of simultaneously recorded, adjacent glial cells (Amzica & Steriade, 1998b, 2000; Amzica & Neckelmann, 1999). Measurements of $[K^+]_{out}$ during the depolarizing phase of the slow oscillation indicate that glial cells phasically uptake part of the $[K^+]_{out}$ extruded by neurons (Amzica *et al.*, 2002; Amzica & Massimini, 2002). Towards the end of the depolarizing phase, the glial membrane begins to repolarize before the neurons.

All available evidence points to the slow oscillation as a characteristic sign of slow-wave sleep and brain deafferentation from sensory signals: this rhythm disappears during natural waking and REM sleep (Steriade *et al.*, 2001a; Timofeev *et al.*, 2001b) (see Figure 6.1); the cyclic hyperpolarizing phases of the oscillation are selectively obliterated and the neurons reach a steady depolarizing state by setting into action ascending activating neuromodulatory systems (Steriade *et al.*, 1993a) (see Figure 5.14); sensory stimulation selectively suppresses the state of slow-wave sleep and associated oscillations in humans (Ferrara *et al.*, 1999); synchronous sleep oscillations are relatively insensitive to incoming signals (reviewed in Steriade *et al.*, 1993d); and, during selective deprivation of slow-wave sleep in humans, large decreases in

[14] These authors claimed that a direct relationship exists between the occurrence of the slow oscillation and the periodic sensory input resulting from respiration. Figure 2C in that paper depicts two oscillation-free periods with steady depolarization associated with firing of action potentials, although the animal continued to breathe. Then, there is no obligatory relation between inhalation and slow oscillation, and the periodic behaviour of neurons in the olfactory system is *not* dependent on respiration.

[15] The slow rhythm of spindle sequences was explicitly described only two decades ago (Steriade & Deschênes, 1984) but, with the benefit of hindsight, it can be detected in earlier recordings of humans' and cats' bioelectrical activity. Although the rhythm of 7–14 Hz was intensively investigated and its cellular bases are largely known, the knowledge of intrinsic currents or synaptic actions that are implicated in the slower rhythm of 0.2–0.5 Hz is only at its beginnings.

[16] In that study, a secondary depolarization was elicited in thalamic RE neurons by cortical stimulation. Recent studies showed that this component is an all-or-none event at *c.*5 ms after the peak of the initial EPSP and is voltage-dependent, i.e. most prominent between −70 mV and −85 mV, but greatly reduced or absent at more hyperpolarized levels (Fuentealba *et al.*, 2005). The secondary component of cortically evoked EPSPs in RE neurons is due to the dendritic activation of T-currents, with a probable contribution of the persistent Na^+ current, and it affects the integrative properties of RE neurons, including their spiking output and temporal summation of incoming cortical inputs (Fuentealba *et al.*, 2005).

EEG power in the frequency range of the slow oscillation are mainly observed in frontal derivations (Ferrara *et al.*, 2002). Computational models of slow-wave sleep oscillation and its replacement by activated states in corticothalamic systems show that progressive depression of excitatory connections among cortical neurons and activation of Ca^{2+}-dependent K^+ currents lead to termination of the depolarizing phase of the oscillation, whereas summated miniature EPSPs that are present during the hyperpolarizing phase activate the $I_{Na(p)}$, depolarize the membrane potential of pyramidal cells, and trigger the depolarizing phase again (Bazhenov *et al.*, 2002). These features, namely progressive depression of excitatory inputs and depolarization with transition to activated states, are characteristic of slow-wave sleep and transition to waking or REM sleep, respectively (Steriade *et al.*, 1982a, 1990c, 2001a). The only study to report that the slow oscillation can be triggered by sensory stimulation during respiration was recorded from the rat olfactory cortex under ketamine–xylazine anaesthesia (Fontanini *et al.*, 2003).[14] However, major statements in that paper, such as the direct relation between the occurrence of slow oscillation and the periodic sensory input resulting from respiration, and strong dependence of pyramidal cell membrane potential on the respiratory cycle, are not consistent with the authors' own results (see comments in note 14). The issue is that stopping artificial respiration for short periods in acutely prepared cats does not influence the pacing of normal slow oscillation. It is possible that the rhythmic influx of air into nasal receptors may induce oscillatory behaviour in central stations implicated in olfaction. This may occur by producing summations on miniature EPSPs, which are effective in the induction of the slow oscillation in the disconnected neocortex (Timofeev *et al.*, 2000) and in computational models (Bazhenov *et al.*, 2002). The safe conclusion would be that in the olfactory system, in addition to the propensity of the piriform cortex to display the slow oscillation (possibly triggered as in other structures by descending inputs from association cortices to entorhinal cortex and, ultimately, the piriform cortex), rhythmic afferent olfactory inputs might promote a rhythmic pattern. The question to be addressed in future experiments is to what extent the slow oscillation in the piriform cortex is dependent on that recorded in the neocortex, because in most subcortical structures investigated until now, reversible inactivation of cortex or decortication abolishes the slow oscillation (reviewed in Steriade, 2001b).

The intracortical synchronization of the slow oscillation was demonstrated using dual intracellular and field potential recordings in anaesthetized (Amzica & Steriade, 1995a,b) and naturally sleeping (Destexhe *et al.*, 1999) animals and by disrupting the synchronous occurrence of the rhythm with lidocaine injections between the two recorded foci (Amzica & Steriade, 1995a,b). The shortest time-lags between the slow oscillation within adjacent fields of the association cortex are about 11–12 ms; the longest time-lags found in distant recordings (from visual and motor cortices) are 100–120 ms. Long

latencies may imply inhibition–rebound sequences in cortical networks and/or corticothalamocortical loops because, as shown below, the thalamus reflects the cortically generated oscillations. The cortical slow oscillation is also synchronized in homotopic foci of both hemispheres, as shown by coherent slow oscillations recorded intracellularly, conjointly with local field potentials, from areas linked by callosal projections (Steriade *et al.*, 1994b; Nuñez *et al.*, 1992c). The intracortical propagation and synchronization of the cortically generated slow oscillation with a similar rhythm recorded from subcortical structures are dealt with below (Section 6.1.3).

Spindles

This oscillation is a hallmark of early stages of slow-wave sleep and is defined by the association of two distinct rhythms: waxing and waning spindle waves at 7–14 Hz within sequences lasting for 1–2 seconds, and the periodic recurrence of spindle sequences with a slow rhythm, generally 0.2–0.5 Hz.[15]

Spindles are generated within the thalamus in the absence of the cerebral cortex and brainstem (Morison & Bassett, 1945), but they can be evoked by contralateral cortical stimulation through the callosal and corticothalamic paths to avoid antidromic activation of TC neurons and collateral excitation of thalamic RE neurons (Steriade *et al.*, 1972). The shape and long-range synchronization of spindles is decisively influenced by the cerebral cortex (Contreras *et al.*, 1996a, 1997b). The role of corticothalamic feedback in shaping and synchronization of spindles was demonstrated by: (a) different shape and duration of spindles as a function of cortical stimulation (Contreras & Steriade, 1996),[16] or comparing thalamic spindles in intact-cortex and decorticated animals (Timofeev & Steriade, 1996); corticothalamic volleys produce brief and waning spindle sequences that lack the initial waxing component because these volleys succeed in entraining, right from the start, a majority of the thalamic cellular population implicated in spindle genesis; (b) synchronizing RE cells, within spindle frequency, in response to cortical stimulation (Contreras & Steriade, 1996); and (c) synchronizing widespread thalamic territories to produce nearly simultaneous spindle sequences, because after decortication, the coherence of spindles is reduced (Contreras *et al.*, 1996a, 1997b).

Although the intrinsic properties of individual thalamic cells play an important role in the patterning of sleep spindles (Steriade & Llinás, 1988; Steriade *et al.*, 1990b),[17] spindling is a network phenomenon involving a recurrent inhibitory circuit that includes thalamic RE GABAergic cells, driven by TC neurons and projecting back to the latter. The RE nucleus is the pacemaker of spindles, since spindles are abolished in dorsal thalamic territories after disconnection from the RE nucleus (Steriade *et al.*, 1985)[18] and are preserved in the rostral sector of the RE nucleus deafferented from thalamic inputs (Steriade *et al.*, 1987a).

The idea that the RE nucleus is the pacemaker of spindles (Steriade *et al.*, 1987a) was subsequently confirmed in modelling studies and,

[17] Some intrinsic properties of thalamic cells are decisive in shaping spindles. For example, the Ca^{2+}-dependent low-threshold spike (LTS) crowned by Na^{+} spike-bursts is effective in the transfer of spindles to the cerebral cortex. The voltage-dependent persistent Na^{+} current, $I_{Na(p)}$, helps to generate rebound depolarizations. Indeed, after intracellular injections of quaternary derivatives of local anaesthetics, which block $I_{Na(p)}$, spindles of TC cells are transformed into a single, long-lasting period of hyperpolarization and rhythmic rebounds within the frequency range of spindles disappear (Mulle *et al.*, 1985). The Ca^{2+}-dependent K^{+} current, $I_{K(Ca)}$, or some voltage-dependent K^{+} currents may prolong the long-lasting IPSPs generated in TC cells by thalamic RE neurons (Roy *et al.*, 1984) and thus they favour the production of the LTS and induce rebound bursts in TC cells.

[18] To demonstrate that loss of spindles in cortically projecting dorsal thalamic nuclei was not due to traumatic events following the lesions of thalamic RE nucleus or transections separating it from the dorsal thalamus, another series of experiments showed that spindling is absent from the anterior thalamic nuclei of the cat (Paré *et al.*, 1987), whose neurons are naturally devoid of RE afferents (Steriade *et al.*, 1984a) but have intrinsic properties similar to those of other thalamocortical neurons (Paré *et al.*, 1987). Then, spindling is a synaptically generated oscillation in a circuit that necessarily includes the RE nucleus.

recently, in experiments performed *in vivo* (see below). The failure to find spindles in the isolated perigeniculate nucleus (posterior part of the RE nuclear complex) in slices maintained *in vitro* (Von Krosigk *et al.*, 1993) can be explained by different factors, such as a less intact and complete collection of RE cells owing to the slicing procedure (see note 13 in Steriade *et al.*, 1993d) and the absence of brainstem modulatory systems with depolarizing actions on RE neurons.[19] Modelling studies of isolated RE neurons (Wang & Rinzel, 1993; Destexhe *et al.*, 1994a; Golomb *et al.*, 1994; Bazhenov *et al.*, 1999, 2000),[20] confirmed the idea that the deafferented RE nucleus generates spindles. The computational studies reached the conclusion that densely interconnected RE cells with $GABA_A$ and/or $GABA_B$ synapses are capable of spindle oscillations and that a modest excitation from input sources is effective in fully synchronizing the isolated RE network. The excitation may come from cortex and/or from TC cells, but cortical inputs are mostly implicated because they provide a very powerful drive to RE neurons (see Contreras & Steriade, 1996).

Further evidence favouring the idea that spindles are initiated in the thalamic RE nucleus was obtained experimentally by using intracellular recordings and coupled intra- and extracellular recordings from the cat RE nucleus (Fuentealba *et al.*, 2004a). One third of intracellularly recorded RE neurons displayed prolonged hyperpolarizing potentials preceding spontaneously occurring spindle oscillations (Figure 6.3A). The late phase of the hyperpolarization led to rebound responses with different amplitudes (arrowhead in Figure 6.3A), which favoured the occurrence of bursting behaviour (Figure 6.3B). Thus, the hyperpolarization was able to switch the neuronal firing pattern from tonic to bursting so that incoming inputs, probably EPSPs of cortical origin, could elicit low-threshold spike-bursts. Indeed, cortical stimulation was able to induce hyperpolarizations preceding spindles in all tested neurons (Figure 6.3C). During the prolonged hyperpolarizations, the apparent input resistance of RE neurons could drop by 40% (Figure 6.3C), suggesting that it resulted from active inhibition rather than disfacilitation in the network. Actually, the hyperpolarization increased in amplitude as the membrane potential was depolarized, which is consistent with the activation of inhibitory conductances in RE neurons. At more negative membrane potentials, the hyperpolarization became progressively smaller until it was virtually abolished at around −100 mV to −105 mV (Figure 6.4), a value similar to the expected reversal for K^+ conductances in RE cells (Huguenard & Prince, 1994). Similar to spontaneously occurring hyperpolarizations, the voltage dependency of evoked ones proved to be consistent with the activation of K^+ conductances (Figure 6.4C). Finally, the evidence of *direct* origin of spindles within the RE nucleus was obtained by using pairs of simultaneous extracellular and intracellular recordings, to study local activities within the RE network during the hyperpolarizations preceding spindle oscillations. Figure 6.5 shows the intracellular activity of one RE neuron and extracellular activities of at least two RE units. In most cases,

[19] Destexhe *et al.* (1994b) have shown that a network of isolated RE cells does not display spindle oscillatory behaviour when no noradrenergic (NA)/serotonergic (5-HT) synapses are activated (as is the case in thalamic slices), but RE cells were brought to oscillation by activating 20% of the depolarizing NA/5-HT synapses.

[20] These experimental and computational studies demonstrated the presence of spike-bursts in thalamic RE neurons following IPSPs. Other modelling studies reported propagating activity patterns in isolated RE networks (Rinzel *et al.*, 1998). The latter authors concluded that their results apply 'to an isolated RE system (thalamic slice in which RE–RE, but not RE–TC–RE, coupling was operative) if experimental conditions were adjusted so that RE cells responded to IPSP barrages with rebound bursts' (see such postinhibitory rebound spike-bursts fired by RE neurons in Bazhenov *et al.*, 1999). These are further arguments for the notion that spindles originate in the RE nucleus.

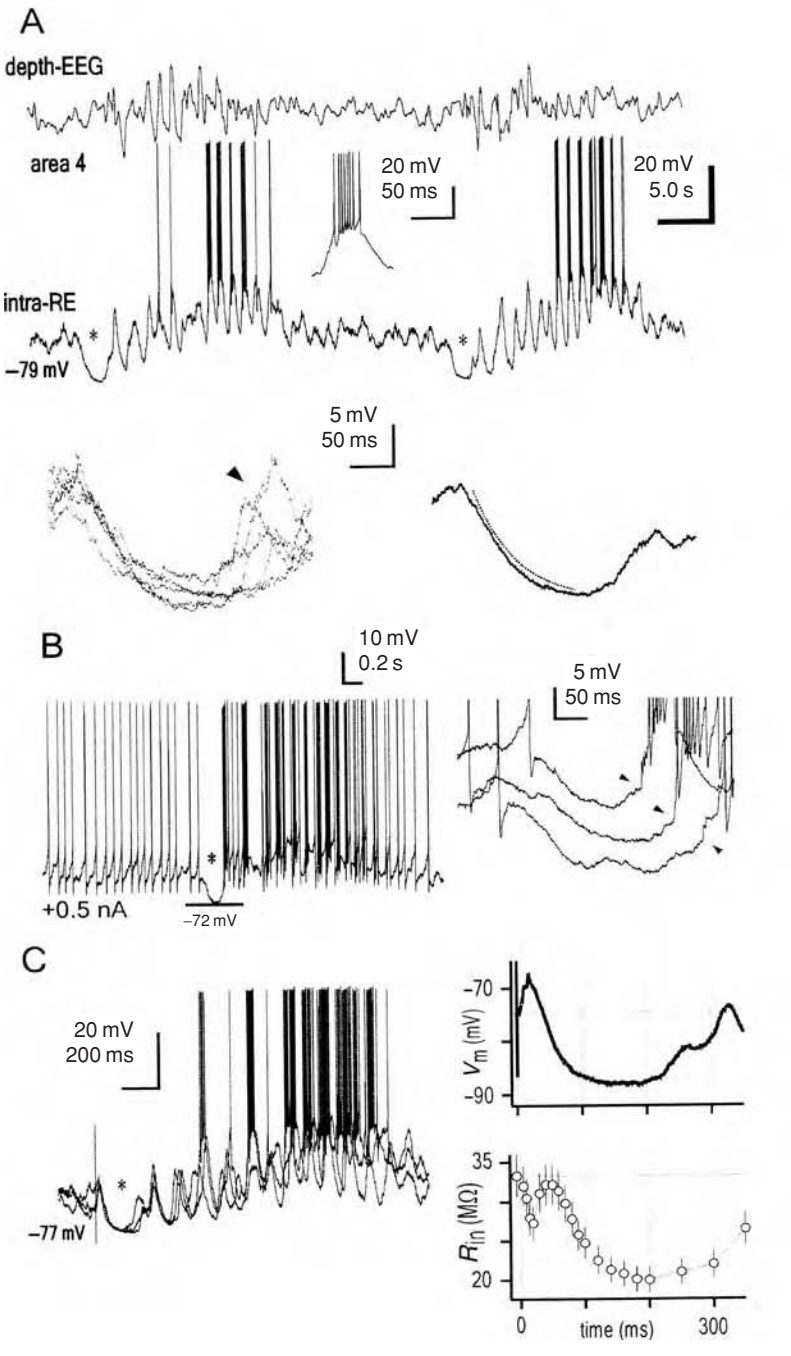

Fig. 6.3 Prolonged hyperpolarizing potentials (PHPs) precede spontaneous and evoked spindle oscillations. Cat under barbiturate anaesthesia. (A) Top: EEG from motor cortex (area 4) and intracellular recording of RE neuron from the rostral pole of the nucleus. Typical low-threshold spike-burst of RE cell expanded in inset. Below left: superimposition of PHPs ($n = 5$) shows constant activation phase followed by irregular late phase, frequently leading to rebound activities (arrowhead). Below right: averaged PHPs ($n = 20$). The activation phase (first 100 ms) was fitted with a monoexponential function ($\tau = 36$ ms). (B) Left: another RE neuron depolarized by steady current injection (+0.5 nA) and displaying spontaneous PHPs. PHPs hyperpolarized V_m to −72 mV, where low-threshold spikes (LTSs) could be generated and spindles initiated. Right: expanded epochs showing PHPs. Triangles point to the onset of LTS responses. Traces are displaced for clarity. (C) Left: superimposed traces ($n = 3$) showing responses to stimulation of cortical area 4 (same neuron as in (A). In all cases a sequence of EPSP–PHP–spindle was generated. Right top: average ($n = 10$) of early responses to cortical stimuli applied at resting V_m. Right bottom: time-evolution of R_{in} during PHP. Each point represents the slope of linear fitting to the V_m–DC relation calculated for each time point in the graph. Asterisks mark PHPs. Modified from Fuentealba *et al.* (2004d).

extracellularly recorded units fired before the onset of the intracellular spindles, the discharge being temporally related with the prolonged hyperpolarization that heralded the spindle sequence in the intracellularly recorded neuron. Therefore, the latter were correlated with action potential discharges in nearby and/or distant locations in the RE nucleus, suggesting that these potentials may be locally

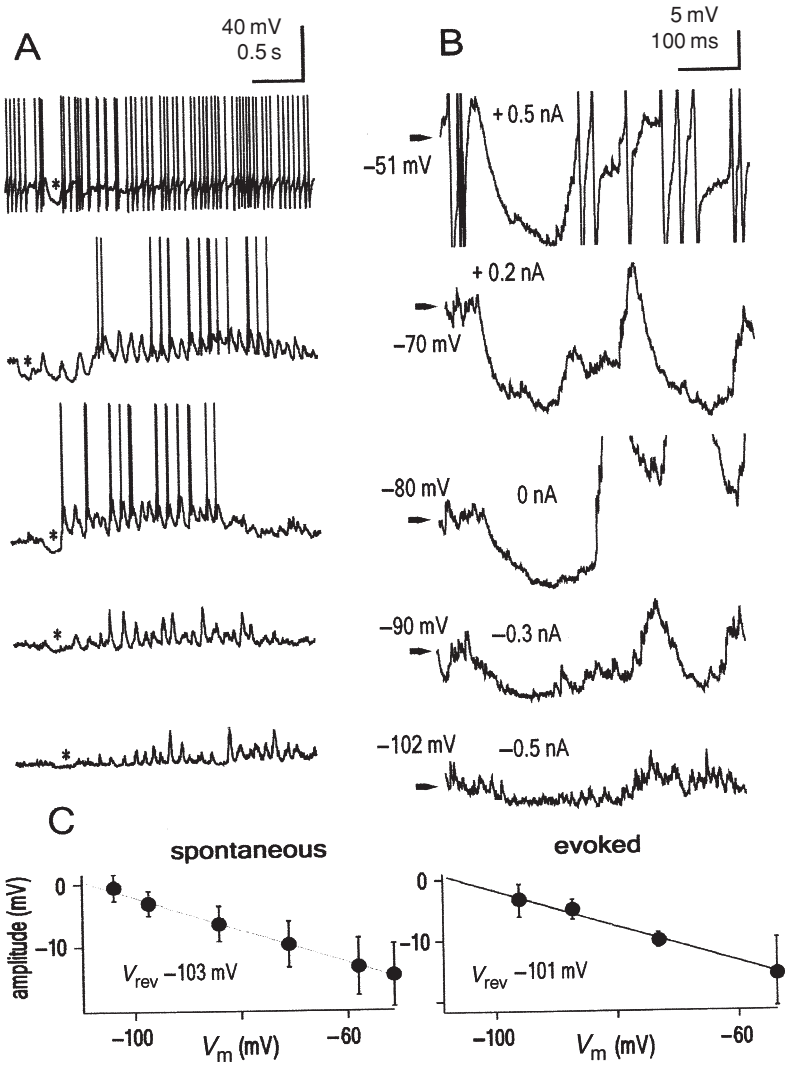

Fig. 6.4 Voltage dependency of spontaneous prolonged hyperpolarizations (PHPs) is consistent with a K^+ conductance. Cat under barbiturate anaesthesia. RE neuron displaying PHP and held at different V_m values by current injection. (A) Spindles; (B) expanded PHPs for the same periods. Values of injected current are indicated in (B). (C) Estimate of the reversal potential (V_{rev}) for spontaneous (left) and evoked (right) PHP for various neurons ($n = 5$ in each plot). Solid line represents a linear fitting, which predicts a V_{rev} of −103 mV and −101 mV for spontaneous and evoked PHPs, respectively. Modified from Fuentealba *et al.* (2004d).

generated within the RE network. In sum, the demonstration of prolonged hyperpolarizations leading to spindles, generated locally in the RE nucleus, is in keeping with the proposal that spindles are initiated in the pacemaking RE nucleus.

This idea, based on recordings of field potential and unit discharges with the frequencies of both spindle rhythms (7–14 Hz and 0.2–0.5 Hz) in the deafferented RE nucleus (Steriade *et al.*, 1987a), predicted that hyperpolarization of dendrites, due to dendrodendritic synapses of GABAergic RE neurons (Deschênes *et al.*, 1985; Yen *et al.*, 1985), would de-inactivate a low-threshold Ca^{2+} conductance, triggering a Ca^{2+} spike followed by GABA exocytosis and hyperpolarization in postsynaptic RE-cells dendrites. The hyperpolarization in synaptically coupled dendrites was thought to initiate spindle oscillation and to spread it to adjacent elements. Any idea aiming to explain the genesis of spindles in the isolated network of RE neurons implicates

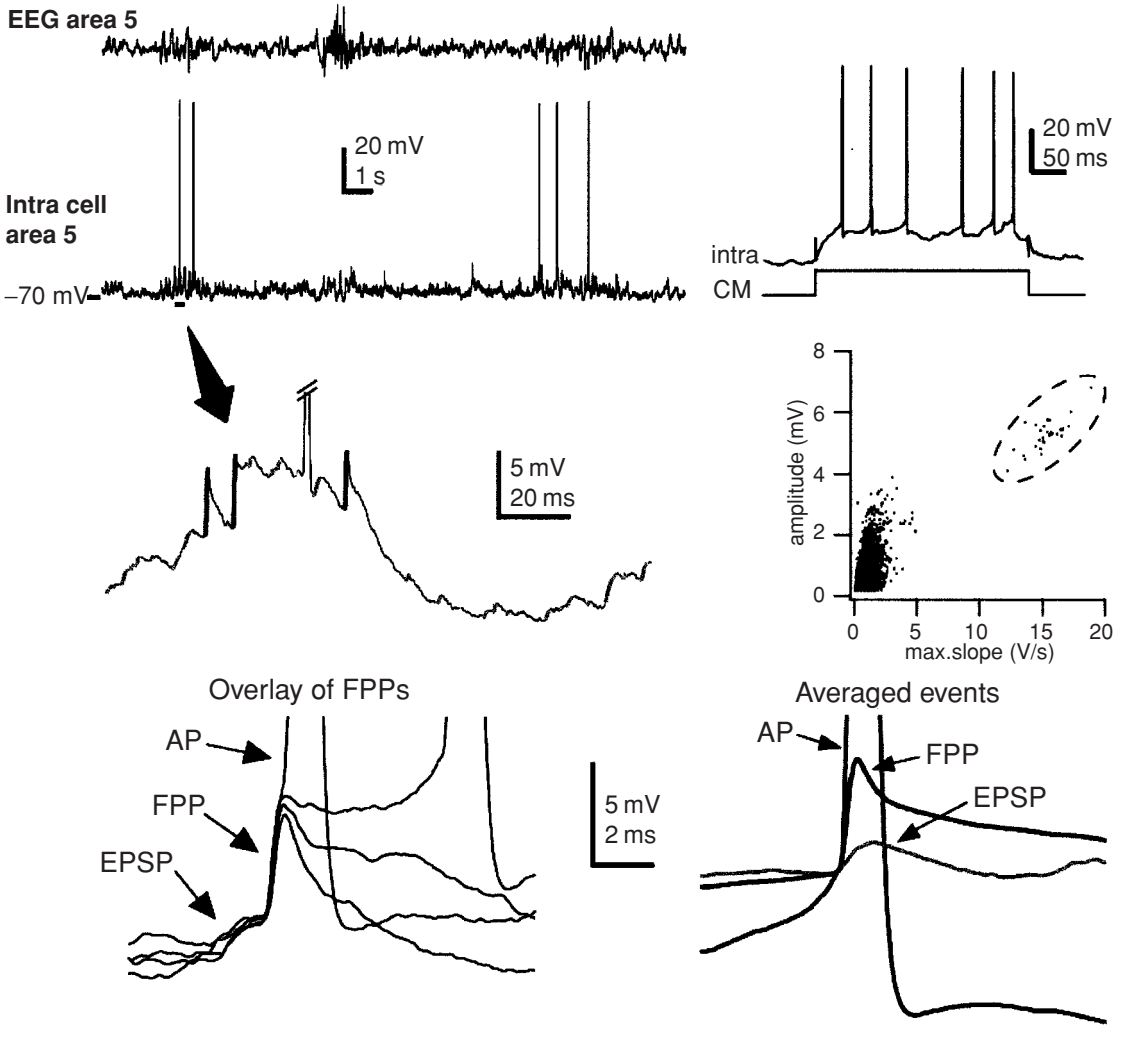

Plate 1 Fast prepotentials (FPPs) in regular spiking (RS) neocortical neurons of cat *in vivo*. Barbiturate anaesthesia. Top left, electroencephalogram (EEG) and intracellular recording in area 5. The neuron was electrophysiologically identified as RS (top right). A part of the intracellular recording is expanded below (arrow). Different depolarizing events extracted are indicated in green (EPSPs) and blue (FPPs). Plotting the amplitude vs. the maximum slope for the selected events (middle panel, right) revealed an FPP population characterized by high-amplitude and fast-rising phase (dashed blue line). The bottom panel shows, on the left, an overlay of four EPSPs leading to FPPs in isolation or leading to full-blown action potential (AP). At right, the superimposition of averaged APs (red trace, truncated), FPPs (blue trace), and 'fast' (max. slope >3 V/s) EPSPs (green trace). Modified from Crochet *et al.* (2004).

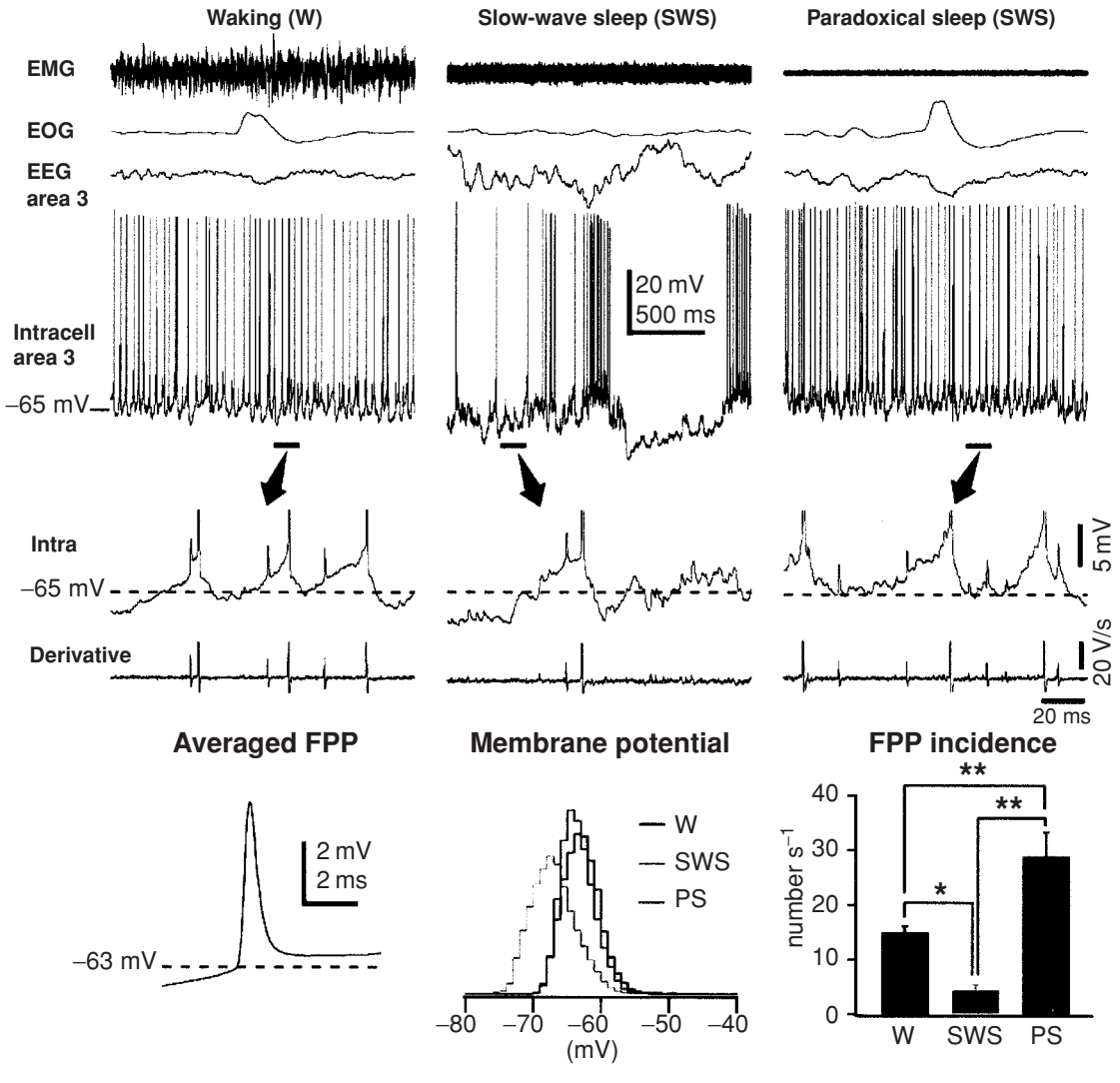

Plate 2 Fast prepotential (FPP) generation is regulated across the states of vigilance. Four traces in the top panel depict electromyogram (EMG), electro-oculogram (EOG), EEG from the depth of right cortical area 3 (somatosensory), and intracellular recording from left area 3. The same neuron was recorded during waking (W), slow-wave sleep (SWS) and paradoxical (PS) sleep (REM sleep). Parts of the intracellular recording marked by horizontal bars are expanded below. The derivative of the intracellular signal revealed the presence of FPPs (action potentials are truncated in the intracellular recording and its derivative). Note the absence of FPP when the cell is more hyperpolarized than −65 mV. The left bottom panel shows averaged FPPs. The middle bottom panel shows the distribution of V_m of the neuron depicted in the three behavioural states (W, red; SWS, green and PS, blue). The right bottom panel shows the mean incidence of FPPs in the three behavioural states calculated for eight neurons. Asterisks represent significant difference: *, $p < 0.05$; **, $p < 0.01$. Modified from Crochet *et al.* (2004).

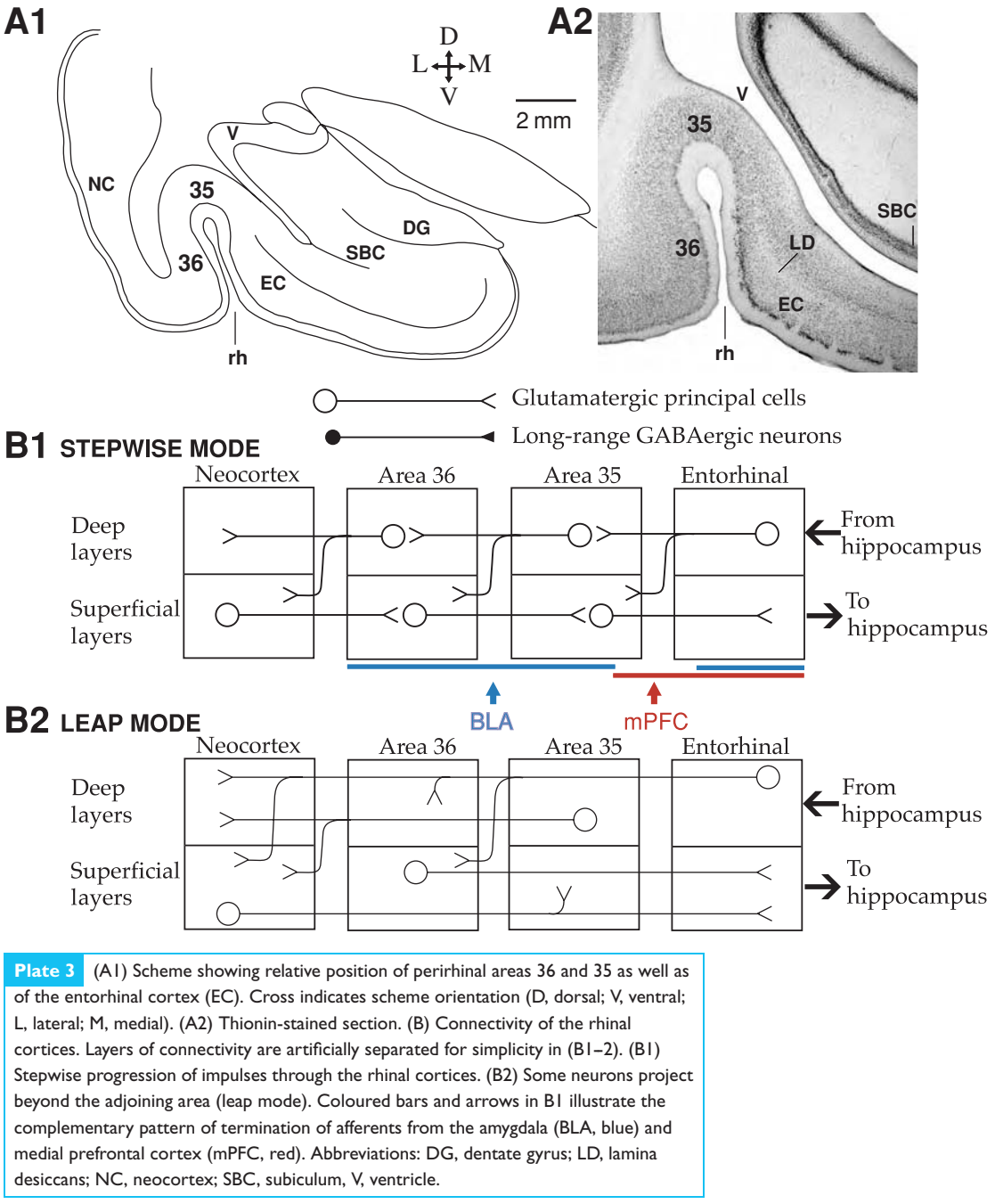

Plate 3 (A1) Scheme showing relative position of perirhinal areas 36 and 35 as well as of the entorhinal cortex (EC). Cross indicates scheme orientation (D, dorsal; V, ventral; L, lateral; M, medial). (A2) Thionin-stained section. (B) Connectivity of the rhinal cortices. Layers of connectivity are artificially separated for simplicity in (B1–2). (B1) Stepwise progression of impulses through the rhinal cortices. (B2) Some neurons project beyond the adjoining area (leap mode). Coloured bars and arrows in B1 illustrate the complementary pattern of termination of afferents from the amygdala (BLA, blue) and medial prefrontal cortex (mPFC, red). Abbreviations: DG, dentate gyrus; LD, lamina desiccans; NC, neocortex; SBC, subiculum, V, ventricle.

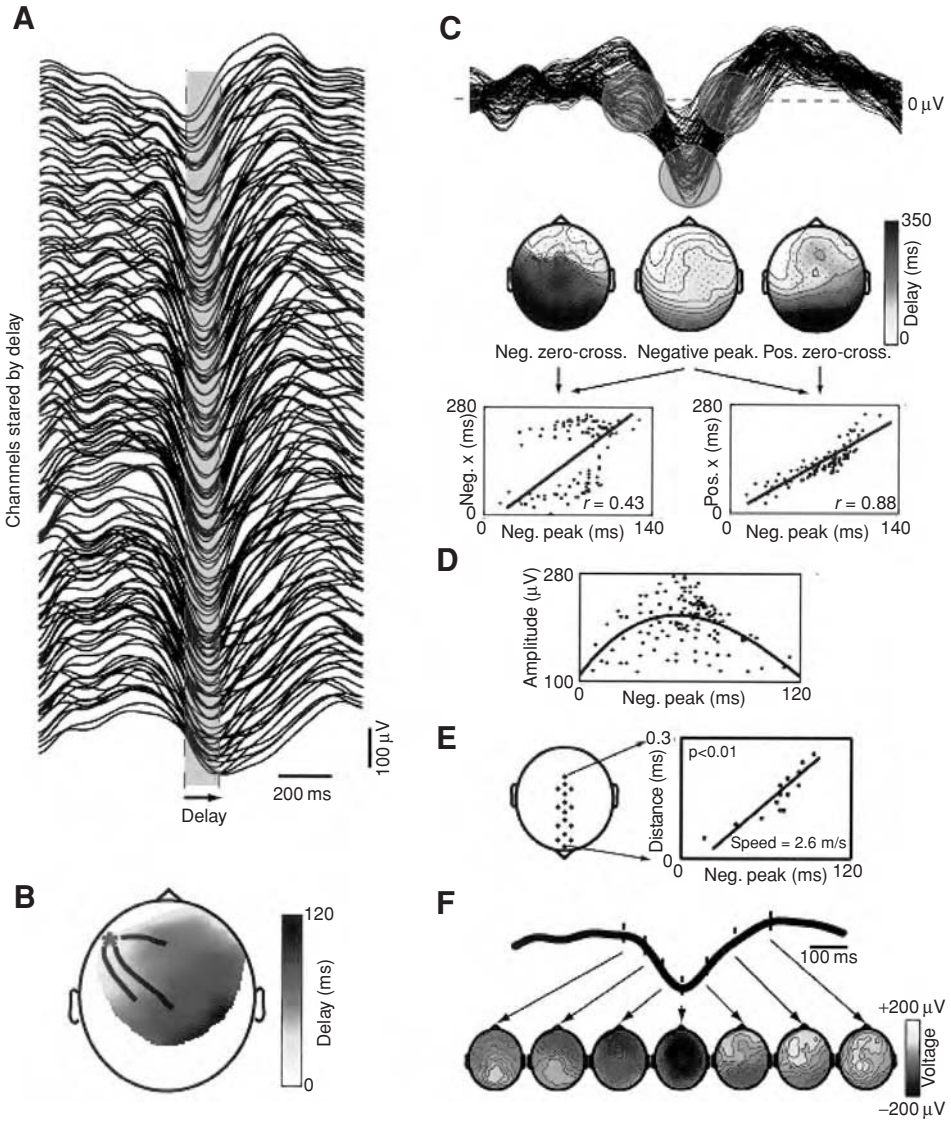

Plate 4 Propagation of the slow oscillation in human sleep. Each cycle of the slow oscillation propagates as a travelling wave. (A) Signals recorded from the channels affected by a single slow oscillation cycle, ranked from top to bottom according to the delay of the negative peak. Note that the slow oscillation is not precisely synchronous in all channels and that a continuous distribution of time lags can be measured. The width of the red area represents the maximum delay (120 ms) from the negative peak at the top trace to the negative peak at the bottom trace. (B) Spatial distribution of the delays, shown on a delay map. A red asterisk marks the location of the channel with delay = 0 (the origin). The blue lines starting around the origin represent the streamlines calculated on the vector field of delays. The slow oscillation originates locally and propagates in an orderly manner to the rest of the scalp as a travelling wave. (C) The same signals of as in (A) are superimposed; the red circles highlight the negative zero crossing, the negative peaks and the positive zero crossings on the slow oscillation recorded from all electrodes. The maps below show the topographic distribution of the delays of these three reference points. The dots represent the channels affected by the slow oscillation, and the lines are iso-delay contours. (D) Peak-to-peak amplitude of the positive wave plotted against the delay of the preceding negative wave. (E) Speed of wave propagation is measured from a row of electrodes placed on the anteroposterior axis (left). (F) Sequential voltage (average-referenced) scalp maps calculated during different phases of the same cycle analysed in the previous panels. The time of each map is indicated on the average of the slow oscillation signals recorded from all channels. Modified from Massimini *et al.* (2004).

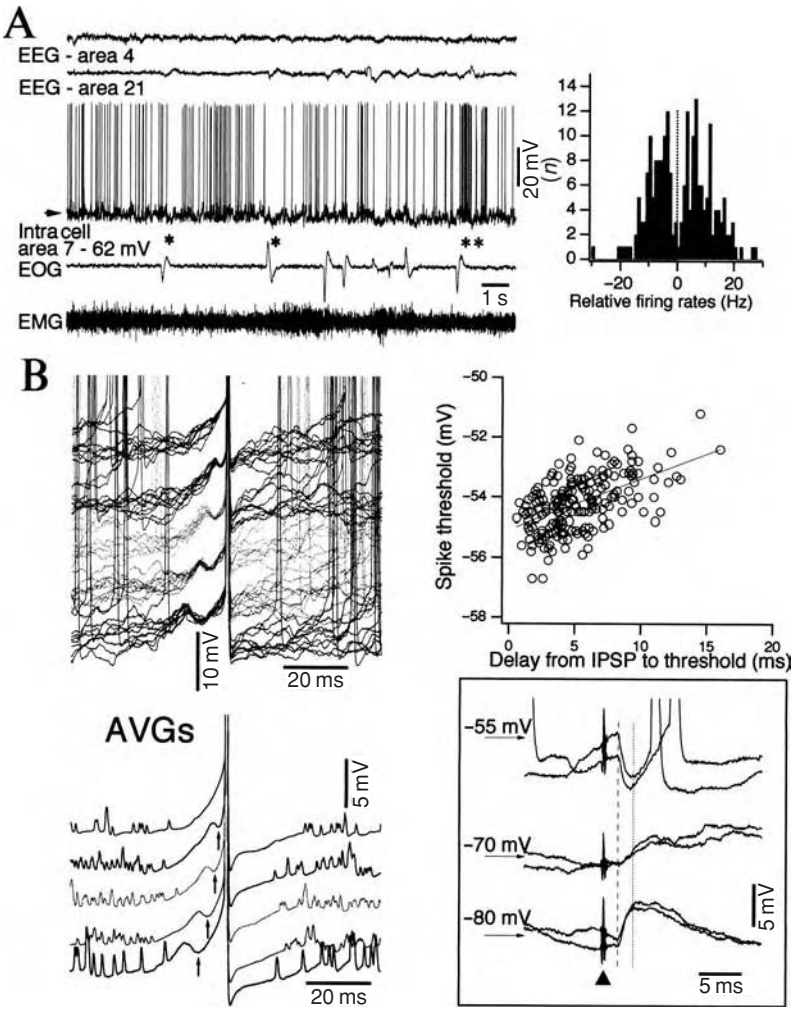

Plate 5 Spontaneous IPSPs control precise firing timing of neocortical neurons during eye movement potentials in waking. Intracellular recordings in chronically implanted cat. (A) Epoch during the waking state is characterized by activated EEG, unimodal intracellular membrane potential, eye movements and muscle tone. Single asterisks indicate decrease in firing associated with eye movements and double asterisks indicate increase in firing associated with eye movements. Histogram shows increase (blue) or decrease (red) in saccade-related firing (±500 ms around saccade) for 15 neurons (more than 200 individual saccades) in relation to mean firing rates of the same neurons. To calculate the abscissa, the firing rate during ocular saccades was subtracted from the mean firing rate. (B) More than half of spikes during waking were associated with preceding short-lasting hyperpolarizing potentials (see superimposition of individual traces and below their averages). Longer-lasting hyperpolarizations slightly decrease firing threshold (plot). In inset, another neuron from motor area 4 recorded in waking, where short-lasting IPSPs were activated by stimulation of VL thalamic nucleus. Modified from Timofeev *et al.* (2001b).

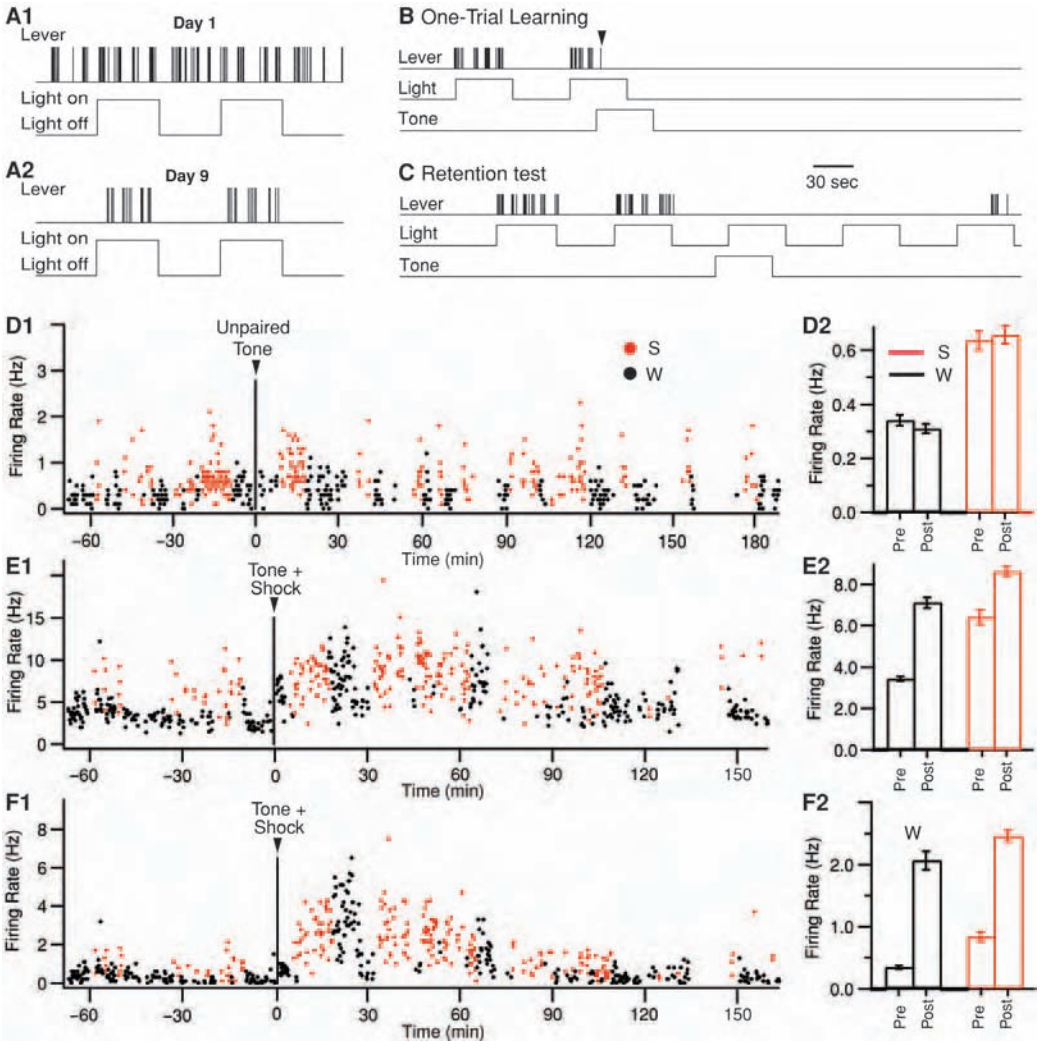

Plate 6 Firing rate of basolateral amygdala neurons during a feline analogue of the inhibitory avoidance task. (A) Cats that had been trained to press a lever repetitively for food (A1) learned that lever-pressing would only be rewarded when a light was turned on ('lights-on'), but not when it was off ('lights-off', A2). (B) The animals were presented three alternating 'lights-on and off' epochs followed by an extended 'lights-off' epoch during which the spontaneous activity of BLA neurons was recorded in both waking and slow-wave sleep. Then, the 'lights-on and -off' alternation resumed with the exception that a second stimulus (a 1 kHz tone, 50 db) was presented during the second 'lights-on' epoch. The first lever press following tone onset triggered a single brief foot-shock (0.5 s, 0.5 mA, arrowhead). Upon receiving the shock, the cat stopped pressing the lever. After the lights and tone were turned off, the spontaneous activity of BLA neurons was recorded for the next 3–4 h. (C) Two days after the introduction of the foot-shock, cats were given the opportunity to press the lever for food again. After two 'lights-on' and 'lights-off' epochs, the tone was presented 15 s before the onset of a 'lights-on' epoch and left on for 1 min. Then, the alternation between 'lights-on and -off' epochs continued normally. The cats behaved normally before the tone was turned on, but refrained from pressing the lever for several minutes after presentation of the tone. (D–F) Firing rate of BLA neurons during a control recording day (D), when only the tone was presented, and during a one-trial learning session (E–F), when the first lever press after tone onset triggered a foot-shock. Left column (1), graphs plotting firing rate (ordinate) as a function of time (abscissa, 10 s bins). Black and red symbols indicate data obtained in waking (W) and slow-wave sleep (S), respectively. The vertical line marks a 3.5 min interruption when the tone (D) or tone plus foot-shock (E–F) were presented. Right column (2), histograms showing averaged firing rates in W (black) and S (red), pre- (left) and post-tone (right). Modified from Pelletier *et al.* (2005b).

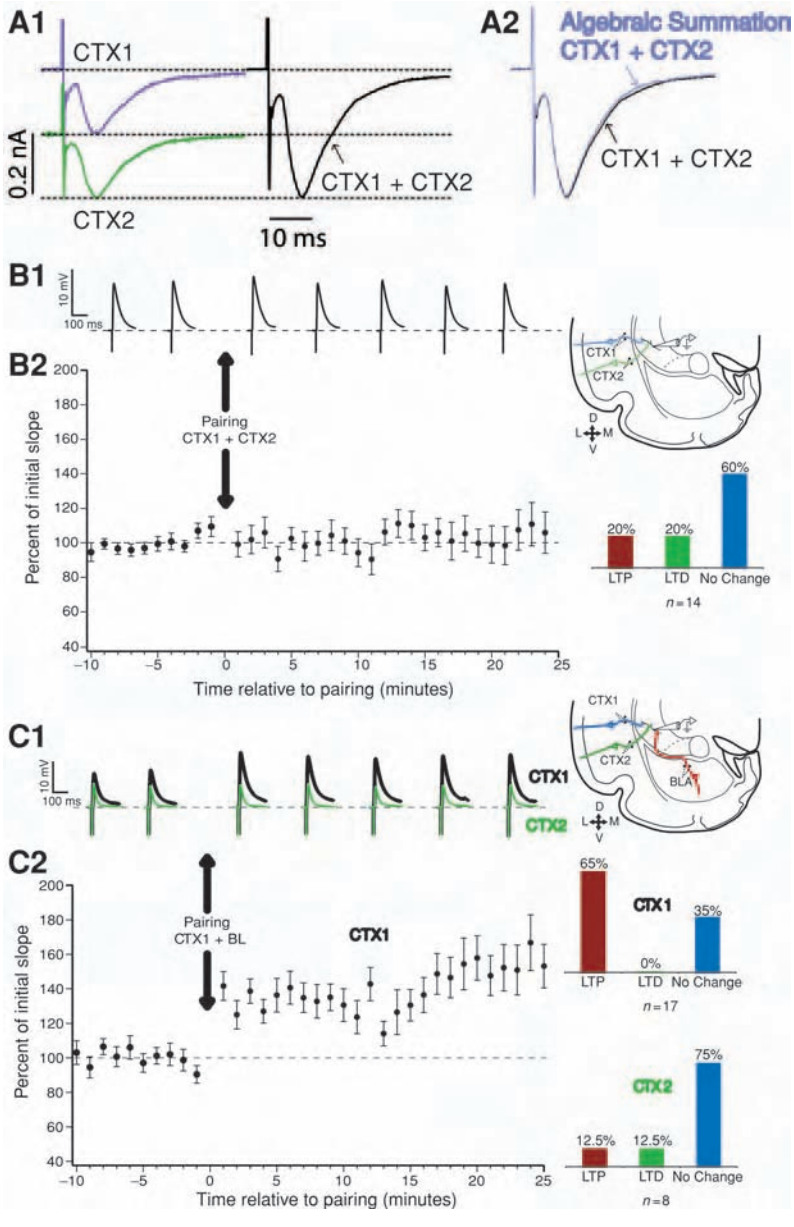

Plate 7 Amygdala activation facilitates induction of corticostriatal long-term potentiation. In coronal slices of the guinea pig amygdala, stimulating electrodes were positioned in two temporal neocortical sites and in the basolateral amygdala.
(A) Occlusion test used to determine whether the two cortical stimulation sites activated distinct sets of synapses to medium spiny striatal neurons recorded with the whole-cell patch method. In this test, the actual and predicted sum of responses evoked by two stimuli is compared. When the response evoked by paired stimuli is smaller than the algebraic sum of individual responses, this constitutes evidence that the two stimulating electrodes activate a partially overlapping set of inputs. However, the actual and predicted responses were not significantly different from each other suggesting that the two cortical stimulating electrodes activated largely non-overlapping sets of inputs converging onto medium spiny neurons. (B) Simultaneous activation of the two cortical sites paired to injection of suprathreshold current pulses in the recorded cell does not produce long-term potentiaton. (B1) Examples of responses evoked by one of the two cortical sites. The timing of these responses is indicated by the position of their peaks with respect to the abscissa of the graph just below. (B2) Amplitude of EPSPs evoked by cortical stimuli (ordinate) as a function of time (abscissa). The pairing was applied at the time indicated by the arrows. Data were normalized to baseline response amplitudes. No LTP was induced with paired cortical stimuli. (C) Simultaneous stimulation of the amygdala and cortex produces long-term potentiation of the paired cortical input whereas the responses evoked by a control (unpaired) cortical site remain unchanged. (C1) Examples of responses evoked by the paired (CTX 1, black) and unpaired (CTX 2, green) cortical stimulation sites before and after pairing of CTX1 and amygdala (arrows). (C2) Amplitude of EPSPs evoked by the paired cortical stimulation site (ordinate) as a function of time (abscissa). A.T. Popescu & D. Paré, unpublished observations.

Plate 8 Medial prefrontal firing is associated with an increased firing probability in BL neurons. The activity of simultaneously recorded mPFC (A1) and BL (A2) neurons was cross-correlated by using mPFC cells as references. (B) Examples of individual cross-correlograms obtained in different animals. (C) Cross-correlograms for all significant mPFC–BL cell cross-correlograms; bin values, expressed in z scores, are colour coded. Correlograms are ordered as a function of the position of the histogram peaks. (D) Average cross-correlograms for all available cell pairs (D1) and for those that reached significance (D2). Insets show an expanded view of the correlogram peaks. (E) Frequency distribution of the position of correlogram peaks for the data shown in (C). Modified from Likhtik *et al.* (2005).

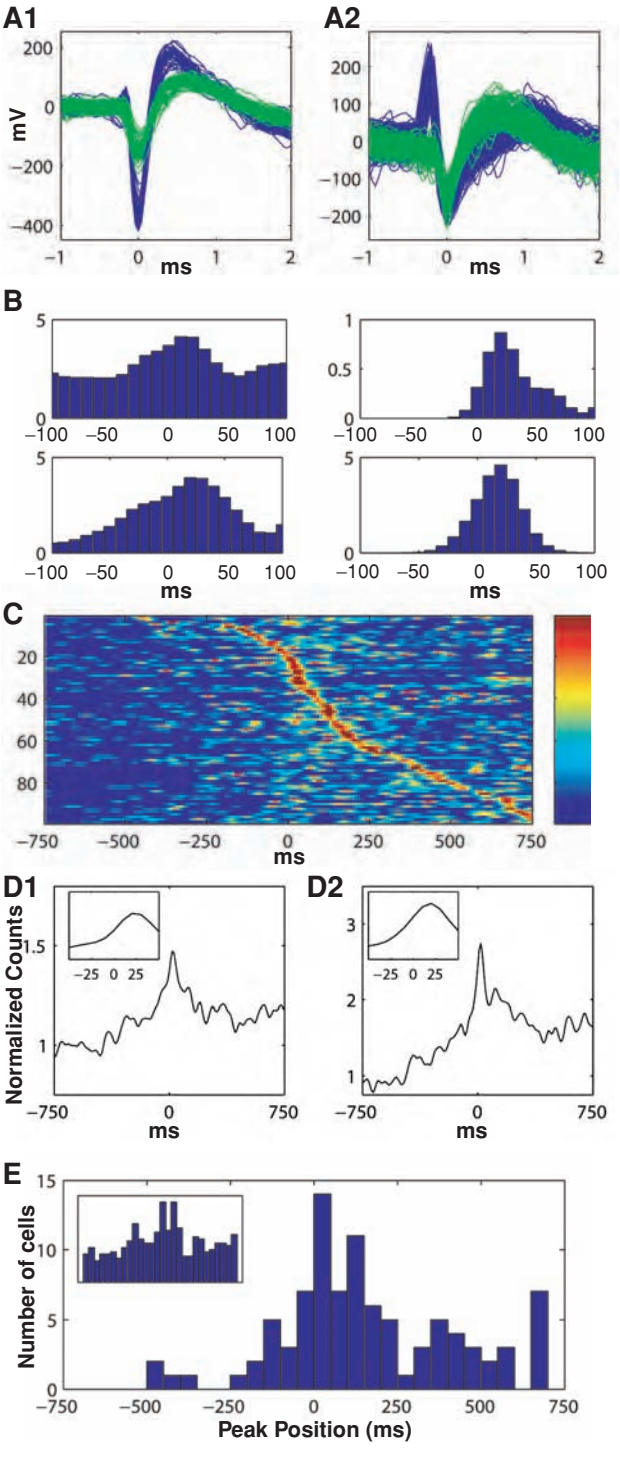

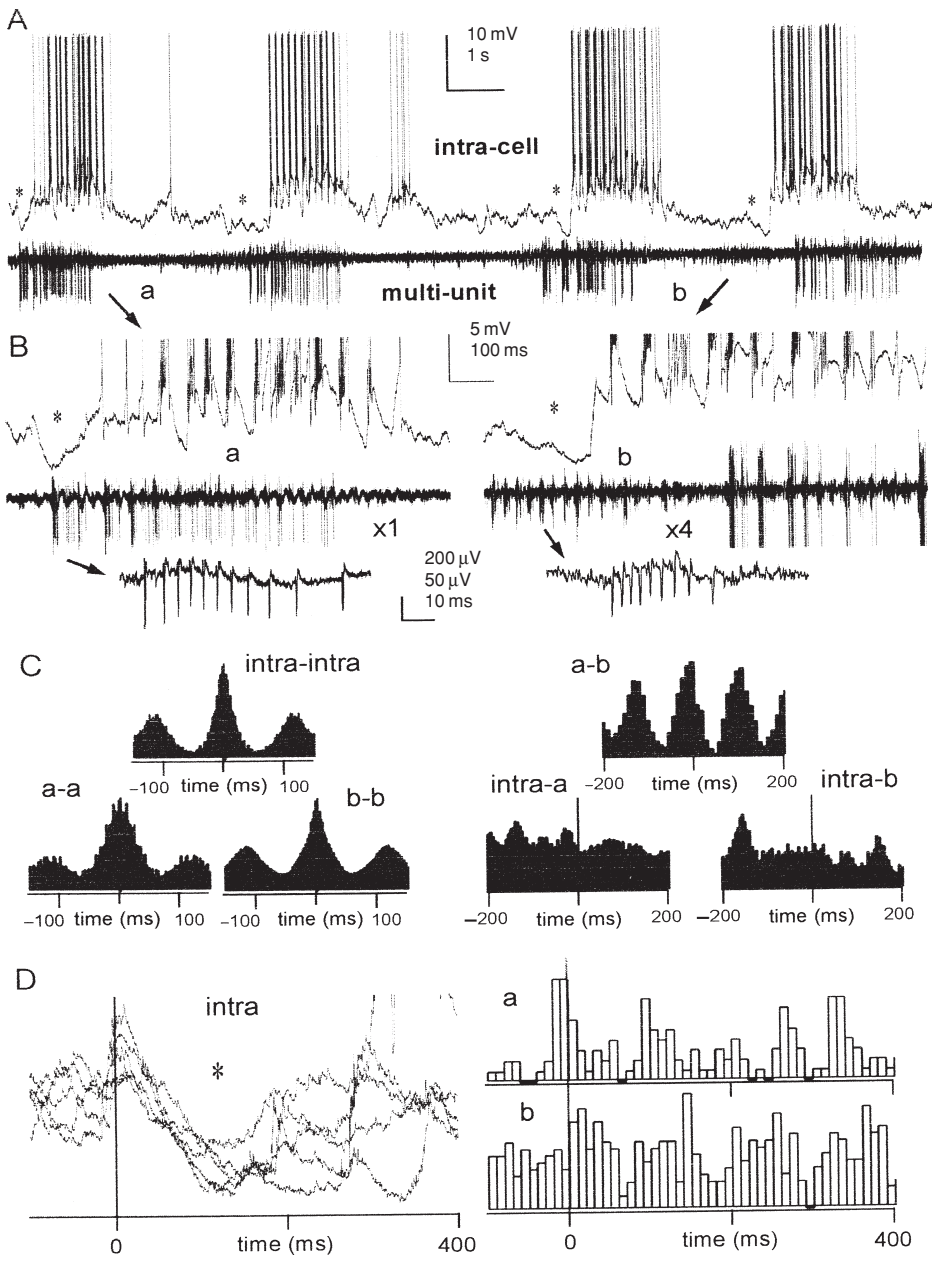

Fig. 6.5 Extracellularly recorded RE neurons fire during prolonged hyperpolarizing potentials (PHPs) of other, distantly located RE neurons. Cat under barbiturate anaesthesia. (A) Simultaneous recording of intracellular (intracell) and extracellular (multi-unit) activities in the RE nucleus. Extracellular electrode was located *c.*1 mm anterior to the intracellular electrode. Note the presence of two units in the extracellular recording (a and b). (B) Expanded traces from epochs in (A) indicated by arrows. Left panel: the first spindle sequence in (A) for both intra- and extracellular recordings. Note discharge of one unit (a) during PHP, preceding spindles. Right panel: the last spindle sequence in (A). Note the second unit (b) firing during PHP. Bottom traces depict typical accelerando–decelerando bursts for both units, which identify them as RE neurons. (C) Autocorrelograms and crosscorrelograms of action potentials for intracellular and extracellular recordings. Bin size, 1 ms and 5 ms for autocorrelograms and crosscorrelograms, respectively. (D) Five superimposed traces showing PHPs (left) and correlated discharge in both units for the same period (right). Time zero was set at the peak of depolarizing potentials preceding PHPs. Bin size, 10 ms. Modified from Fuentealba *et al.* (2004d).

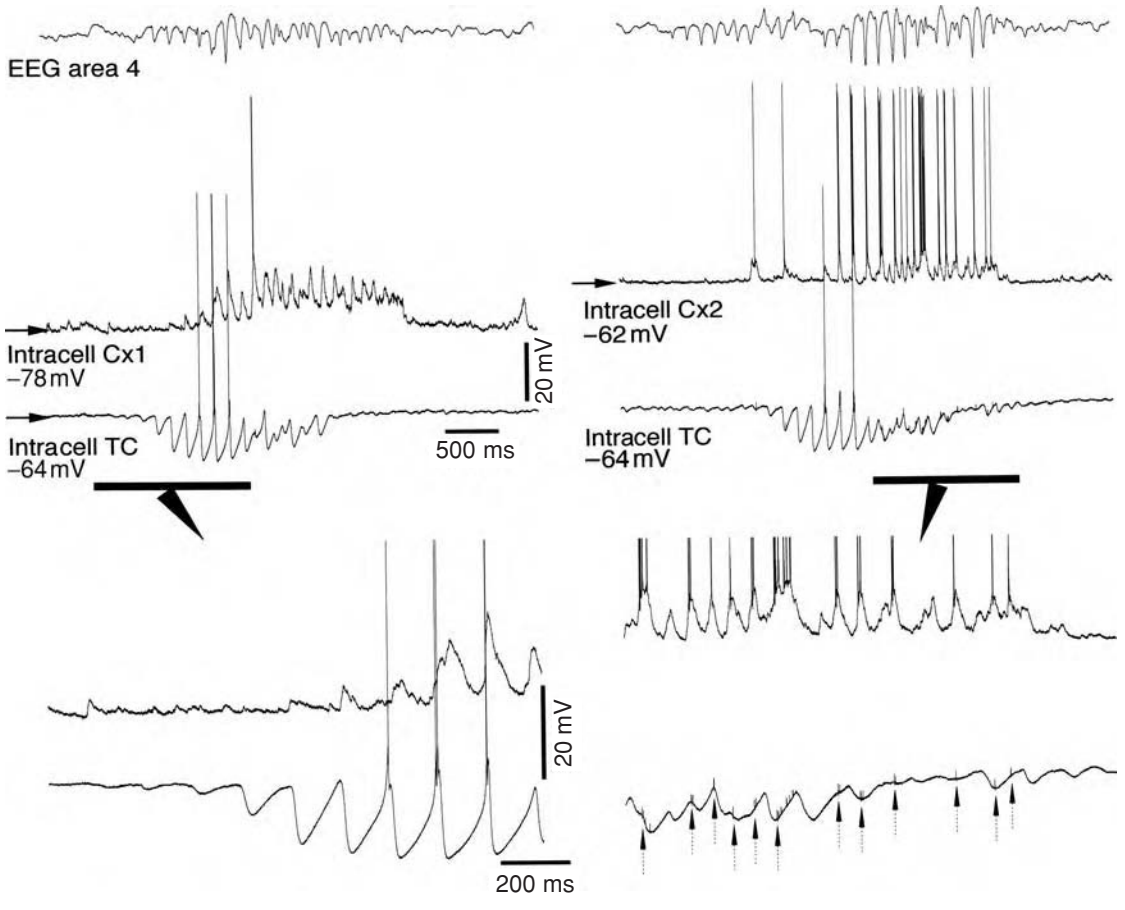

Fig. 6.6 Spindles in thalamocortical (TC) neurons and role of corticothalamic input in terminating thalamic spindle sequences. Cat under barbiturate anaesthesia. Two cortical neurons (left and right), impaled successively, were recorded simultaneously with the same thalamocortical (TC) neuron. Note depolarizing plateau in cortical neuron during late part of spindle; this depolarization, as well as the cortical EEG spindle, outlasts the termination of spindles in the TC neuron. Parts marked by horizontal bars are expanded below. Modified from Timofeev *et al.* (2001a).

the possibility that active RE neurons would hyperpolarize adjacent neurons and create an avalanche spread of the oscillation within the nucleus, with ultimate implication of target TC neurons. The source for activating a set of RE neurons that would hyperpolarize adjacent and/or more distant RE neurons may be any excitatory synaptic drive acting on these cells, most likely from the neocortex, which is known to be particularly potent in triggering (Steriade *et al.*, 1972) and synchronizing (Contreras *et al.*, 1996a, 1997b) spindles.

The idea that spindles are generated in the RE nucleus also stemmed from the patterns of spindle sequences recorded intracellularly in RE and TC neurons. Whereas spindles develop in RE cells as a slowly growing and decaying depolarization with superimposed spike barrages within the frequency of 7–14 Hz (see Figures 6.3A and 6.5A), TC cells simultaneously display 7–14 Hz IPSPs that occasionally lead to high-frequency (200–400 Hz) rebound spike-bursts (Figure 6.6)[15] (Steriade & Llinás, 1988; Steriade *et al.*, 1990b; Von Krosigk *et al.*, 1993; Andersen & Andersson, 1968; Deschênes *et al.*, 1984; Steriade & Deschênes, 1988; Bal *et al.*, 1995a; Sanchez-Vives & McCormick, 1997). These opposing patterns in RE and target TC neurons were also observed in dual simultaneous intracellular recordings

from RE and TC cells *in vivo* (Timofeev & Steriade, 1996) and *in vitro* (Bal & McCormick, 1996). The various frequencies of spindles that have been interpreted, especially by clinical EEG fellows, as reflecting different types of rhythms, do in fact depend on variations in the durations of hyperpolarizations in TC neurons. Long-duration hyperpolarizations, as they occur during barbiturate anaesthesia or deeply synchronized natural slow-wave sleep, are associated with relatively low-frequency spindles (such as those recorded from some neocortical areas in humans) whereas relatively short hyperpolarizations (70–100 ms) would result in spindles with higher frequencies.

Thus, (a) the initiation of spindles is due to activities within the GABAergic RE neurons. This is demonstrated by the fact that the first two or three IPSPs that compose spindles in TC neurons do *not* give rise to postinhibitory rebound spike-bursts that would constitute a source of excitation for RE cells (see TC activity in Figure 6.6 and other recordings in Deschênes *et al.*, 1984; Steriade & Deschênes, 1988; Bal *et al.*, 1995a; Sanchez-Vives & McCormick, 1997). (b) During the following development of spindle sequences, there is an interaction between RE and TC neurons, and the bursting of the latter transfers spindles to cortex. (c) Finally, the termination of spindles is due to both the intrinsic properties of TC cells and network operations. *In vitro* studies have proposed that spindles are terminated by a Ca^{2+}-induced upregulation of the hyperpolarization-activated depolarizing (cation) current, I_H, in TC neurons (Bal & McCormick, 1996; Lüthi & McCormick, 1998). Variations in the duration of IPSPs in TC neurons, with the consequence of different times at which postinhibitory rebound spike-bursts are fired, may be another factor for the termination of spindle sequences (Andersen & Andersson, 1968). The extreme variability of LTSs generated in the same neuron can be seen not only by applying intracellularly hyperpolarizing current pulses, but also during natural spindles (Timofeev *et al.*, 2001a). As a consequence of the asynchronous burst firing of TC neurons, the membrane potential of their targets, RE neurons, would be kept at a relatively depolarized level, thus preventing the de-inactivation of the low-threshold Ca^{2+} and reducing the firing probability of RE neurons. However, the most important source of spindle desynchronization is the corticothalamic input, since during the late phase of spindles, neocortical neurons become tonically depolarized, eventually leading to firing (Figure 6.6). Consistent with this, spike-triggered averages do not reveal a phase relationship between cortical and TC neurons. The idea that the corticothalamic input is effective in desynchronizing thalamic networks and terminate spindles was tested in a computational model (Timofeev *et al.*, 2001a) showing that the isolated RE–TC network may oscillate indefinitely and that upregulation of I_H alone (Bal & McCormick, 1996; Lüthi & McCormick, 1998) is not sufficient to terminate spindling; however, with the addition of the corticothalamic feedback, the spindles become short because most thalamic neurons are set into action from the onset of spindles and only the waning part of spindles is apparent.

Two types of delta waves

The difference between delta waves (1.5 Hz or 2–4 Hz) and the slow oscillation is emphasized by their different origin (at least one component of delta potentials is generated through intrinsic properties of TC neurons, whereas the slow oscillation is generated synaptically and intracortically), the fact that delta waves are grouped by the slow oscillation (Steriade *et al.*, 1993e; Niedermeyer, 1993), and differences in dynamics between these two oscillatory types during human sleep (Achermann & Borbély, 1997). One type of delta activity originates in the thalamus, even after decortication (Curró Dossi *et al.* 1992a),[21] via the interplay between two intrinsic currents of TC neurons (Leresche *et al.*, 1990, 1991; McCormick & Pape, 1990a,b; Soltesz *et al.*, 1991; Puil *et al.*, 1994; Pape, 1996), whereas the other type is generated in the cortex, as it survives after thalamectomy (Steriade *et al.*, 1993f; Villablanca, 1974).

In vitro (Leresche *et al.*, 1990, 1991; McCormick & Pape, 1990a,b; Soltesz *et al.*, 1991; Puil *et al.*, 1994; Pape, 1996) and *in vivo* (Curró Dossi *et al.*, 1992a) studies revealed that a clock-like oscillation within the delta frequency range is generated by the interplay of two intrinsic currents of TC cells. This intrinsic oscillation is potentiated, and multiple neurons are synchronized, by network operations involving corticothalamic projections, with an intermediate link in the RE thalamic nucleus (Steriade *et al.*, 1991a). The synchronization of TC neurons within the frequency of the clock-like delta oscillation allows this rhythm to appear in the cortical EEG.

The delta oscillation of TC neurons results from the interplay between the hyperpolarization-activated depolarizing current I_H and the transient Ca^{2+} current I_T underlying the LTS (Leresche *et al.*, 1990, 1991; McCormick & Pape, 1990a,b; Soltesz *et al.*, 1991; Puil *et al.*, 1994; Pape, 1996). *In vivo*, spontaneous delta oscillations (without injecting current pulses) can be observed following ablation of the cortical areas projecting to the recorded thalamic nucleus (Curró Dossi *et al.*, 1992a). This deafferentation sets TC cells at a more hyperpolarized membrane potential (about −70 mV or more negative values) where delta oscillations are generated. TC cells display spontaneous or cortically elicited spindle oscillations at the resting membrane potential (around −60 mV), whereas at potentials negative to −65 or −70 mV spindles progressively decrease in amplitude (owing to the partial reversal of IPSPs that compose the cyclic hyperpolarizations in TC neurons) and the oscillations are within the delta frequency range (Steriade *et al.*, 1994b; Nuñez *et al.*, 1992c). There is a progressive hyperpolarization of TC cells with the deepening of slow-wave sleep, which is attributable to the progressive decrease in firing rates of corticothalamic cells (Steriade, 1978) and thalamically projecting neurons located in the midbrain reticular formation (Steriade *et al.*, 1982a, 1990c). The transmitters of these neuronal types produce a depolarization of TC cells (reviewed in Steriade *et al.*, 1997). Human (Uchida *et al.*, 1991) and animal (Lancel *et al.*, 1992) studies also showed that spindles and delta rhythms prevail during different sleep

[21] Before this *in vivo* intracellular study, field potential and extracellular recordings showed that thalamic neurons display waves and unit discharges within delta (1–4 Hz) frequencies during EEG-synchronized sleep (Steriade *et al.*, 1971; McCarley *et al.*, 1983) and that thalamic delta waves are suppressed during EEG-activation patterns induced by midbrain reticular stimulation (Steriade *et al.*, 1971). However, those earlier observations did not elucidate the cellular mechanisms of thalamic delta waves.

stages and that these two rhythms reciprocally oscillate during EEG-synchronized sleep.

Although less systematically investigated than thalamic clock-like delta potentials, cortical delta waves, which survive thalamectomy (Steriade *et al.*, 1993f; Villablanca, 1974), are probably generated by summation of long-lasting afterhyperpolarizations (AHPs) produced by K^+ currents, mainly $I_{K(Ca)}$, in pyramidal neurons (Steriade & Buzsáki, 1990).[22] Because of the duration of EEG delta waves (more than 250 ms), only slow AHPs can be taken into consideration. The decreased excitability that accompanies the slow AHPs is consistent with the decreased synaptic and antidromic responsiveness of pyramidal tract and corticothalamic neurons during sleep epochs with delta waves (Steriade *et al.*, 1974a). In addition, slow AHPs are strongly decreased by muscarinic agonists that are unable to affect the medium-duration AHPs[22]. Obliteration of delta waves upon arousal results from the action of cortically projecting basal forebrain cholinergic neurons (Buzsáki *et al.*, 1988; Cape & Jones, 2000).

[22] *In vitro* studies by Schwindt *et al.* (1988a,b) have described three types of AHPs: fast-decaying (fAHP), medium-duration (mAHP), and slow (sAHP).

6.1.2 Grouping of spindles, delta and fast rhythms by the slow cortical oscillation

The importance of the neocortical slow oscillation, as the leading rhythm that accompanies the behavioural state of slow-wave sleep, derives from its ability to group other low-frequency rhythms generated in the thalamus (spindles and clock-like delta) by setting into action thalamic RE and TC neurons as well as fast waves (in the frequency range of beta and gamma rhythms, *c.*20–60 Hz) that appear on the depolarizing phase of the slow oscillation.

We think that this unifying concept (Steriade, 2001a; Steriade & Amzica, 1998; Steriade, 2003a), which derived from data based on simultaneous intracellular recordings from cortical and thalamic neurons *in vivo* (Contreras & Steriade, 1995) and is now supported by human EEG recordings (Mölle *et al.*, 2002; Marshall *et al.*, 2003), is more conceptually rewarding than splitting different elements of brain electrical activity into many and various frequencies. Of course, the coalescence of different oscillatory types can only be seen in intact corticothalamic systems, in contrast with simpler oscillations, within distinct frequency bands, which are seen in simplified preparations.

We will focus on the coalescence of the slow oscillation and spindles, and the coalescence of the slow oscillation and fast rhythms (Figure 6.7), because the former gives rise to a major sign of early (stage 2) slow-wave sleep and the latter may change the conventional wisdom according to which fast waves exclusively occur during brain-active states of waking and REM sleep.

The synchronous firing of cortical regular-spiking (RS) and fast-rhythmic-bursting (FRB) neurons (see Section 2.3.1) during the slow sleep oscillation impacts on thalamic circuitry by driving thalamic RE neurons, the pacemakers of sleep spindles, which induce rhythmic IPSPs – rebound burst sequences in target TC neurons (Figure 6.7).

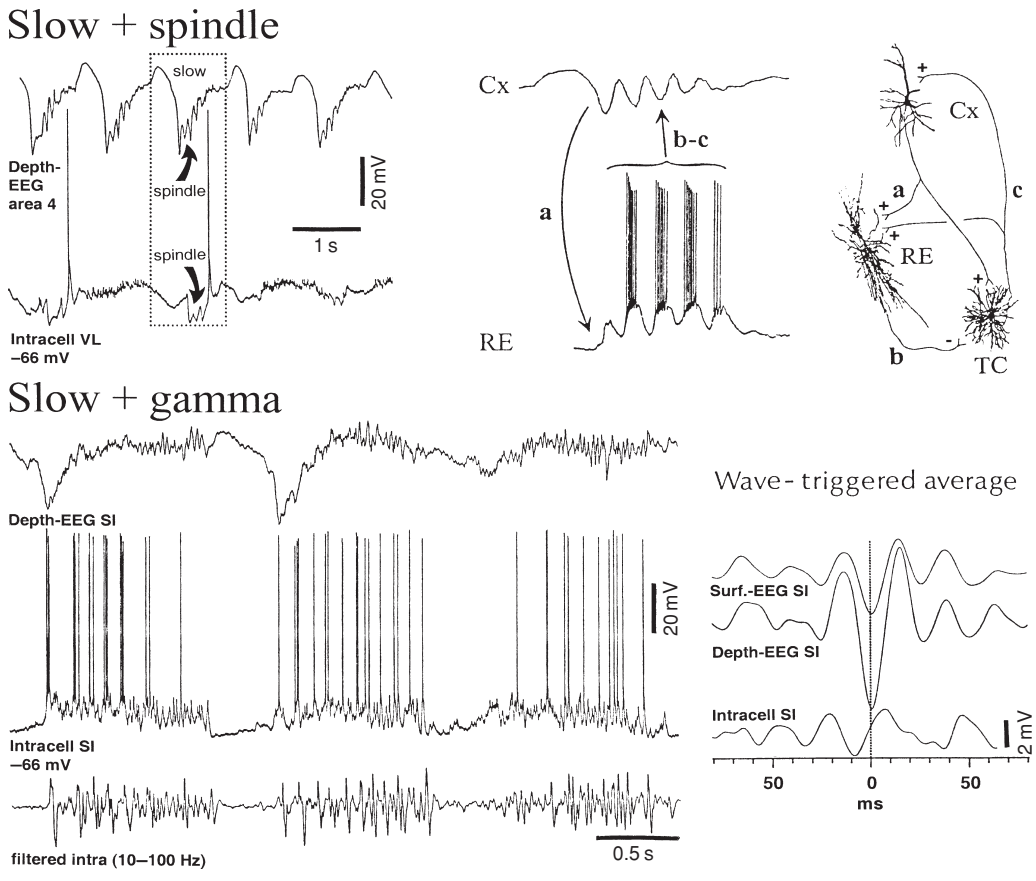

Fig. 6.7 Coalescence of low-frequency (spindle) and fast (gamma) rhythms by the slow sleep oscillation. Intracellular recordings from cortical and thalamic neurons in cats under ketamine–xylazine anaesthesia. ***Slow* + *spindle***, combined slow oscillation and spindle. Left, depth-EEG from cortical area 4 and intracellular recording of thalamocortical (TC) neuron from ventrolateral (VL) nucleus. The excitatory component (negative depth-EEG wave, downward deflection) of the slow cortical oscillation (*c.*0.9 Hz) is followed by a sequence of spindle waves at *c.*10 Hz (arrows). One typical cycle of these two combined rhythms is indicated by the dotted box; note inhibitory postsynaptic potentials (IPSPs) leading to a postinhibitory rebound. Right, top and bottom traces represent field potential from the depth of association cortical area 5 and intracellular recording from thalamic reticular (RE) neuron. In neuronal circuits (far right), synaptic projections are indicated with small letters, corresponding to the arrows at left, which indicate the time sequence of the events. The depolarizing phase of the field slow oscillation (depth-negative, downward deflection) in the cortex (Cx) travels through the corticothalamic pathway (a) and triggers in the thalamic reticular nucleus (RE) a spindle sequence that is transferred to thalamocortical cells (TC) (b) and thereafter back to the cortex (c), where it shapes the tail of the slow oscillatory cycle. ***Slow* + *gamma***, fast activity (*c.*40 Hz) crowning the depolarizing phase of the slow oscillation. Three traces depict: depth-EEG waves from primary somatosensory cortex (S1); intracellular recording from S1; and filtered intracellular trace (between 10 and 100 Hz). Note fast waves (*c.*40 Hz) during the depolarizing phase of the slow sleep-like oscillation and absence of such fast waves during hyperpolarization. Modified from Contreras & Steriade (1995), Steriade *et al.* (1996a), Timofeev & Steriade (1997) and Amzica & Steriade (2002).

The spike-bursts fired by TC cells are transferred back to cortex and they sculpt the slow oscillation (see top left and middle panels in Figure 6.7). The action of cortical RS and FRB cells on thalamic neurons depends on the behavioural state of vigilance and the related bursting or tonic firing of thalamic neurons. During slow-wave sleep, when thalamic neurons fire in the bursting mode (Steriade & Llinás, 1988; Steriade *et al.*, 1990b), corticothalamic volleys excite thalamic RE GABAergic neurons, which inhibit TC neurons. Despite the fact that corticothalamic pathways are all glutamatergic and excitatory, their prevalent action is exerted on thalamic RE neurons because the density of some subtypes of glutamate receptors is threefold higher in these neurons, compared with TC neurons (Golshani *et al.*, 2001; Jones, 2002). Then, TC neurons are inhibited and display biphasic IPSPs leading to rebound spike-bursts (see Figure 1 in Steriade, 2000), which are the neuronal basis of spindles.

Fast (beta and gamma) cortical rhythms are voltage-dependent (Steriade *et al.*, 1996a; Llinás *et al.*, 1991; Nuñez *et al.*, 1992a; Gray & McCormick, 1996; Steriade, 1997a) and are superimposed on the depolarizing phase of the slow oscillation (Figure 6.7). It was predicted that synchronization among neocortical inhibitory interneurons may generate fast oscillations (Lytton & Sejnowski, 1991). During the slow oscillation, IPSPs occur on the depolarizing phase (Steriade *et al.*, 1993e), which culminates in fast activities in the beta/gamma frequency bands (Figure 6.7). FRB neurons play a major role in the generation and synchronization of fast oscillations in corticothalamocortical loops as they project to the thalamus (Steriade *et al.*, 1998b), where they synchronize fast activities (Steriade *et al.*, 1996b), which are fed back to the cortex. Human studies during night sleep confirmed the presence of grouped beta waves in relation to the slow oscillation (Mölle *et al.*, 2002; Marshall *et al.*, 2003).

Besides the beta/gamma oscillations, ultrafast rhythms (80–200 Hz), called ripples, are superimposed over the depolarizing phase of the slow oscillation (Grenier *et al.*, 2001). The synchronous occurrence of ripples over many cortical sites is explained by their strict relation with the depolarizing phase of the slow oscillation, and the fact that the slow oscillation was found to be coherent in different (adjacent but also distant) cortical areas (Amzica & Steriade, 1995a,b). The possible involvement of inhibition in the phase-locking of neurons during ripples was corroborated by the increased activity of FS neurons in relation to ripples (Grenier *et al.*, 2001). Ripples are also found in the perirhinal cortex and hippocampus, associated with bursts of sharp potentials, during anaesthesia, behavioural immobility and natural sleep (Chrobak & Buzsáki, 1996; Collins *et al.*, 1999).

6.1.3 Intracortical and corticothalamic propagation of the slow oscillation

The coherence between slowly oscillating neurons recorded from multiple neocortical sites within the same or different hemispheres was investigated using intracellular, extracellular unit, and field potential recordings (see details above, section 6.1.1). Studies of activity during

the depolarizing phase of the cortical oscillation with two-photon Ca^{2+} imaging showed that, at peaks of synchrony, coactive cells were either distributed across the imaged field or organized in clusters (within layers II/III), layers or columns (in any layer) (Cossart *et al.*, 2003). Most cells active at peaks were pyramidal neurons, whereas the rest were local interneurons. The activity of local-circuit inhibitory neurons during the depolarizing phase of the slow oscillation was also reported using sharp micropipette recordings of formally identified basket cells (Contreras & Steriade, 1995). The idea that the principal function of the persistent activity during the recurrent activity of cortical networks is to generate mental states (Cossart *et al.*, 2003) is in line with the hypothesis that the slow and related sleep oscillations are implicated in the consolidation of memory traces acquired during wakefulness (Steriade *et al.*, 1993b; Sejnowski & Destexhe, 2000) and the presence of dreaming mentation during slow-wave sleep (see below, Sections 6.3 and 6.4). High coherence between electrode pairs was observed during slow activity in monkeys (Leopold *et al.*, 2003); long-range interactions between brain structures are currently being investigated in humans using one sort of functional magnetic resonance imaging signal, the blood oxygen level-dependent (BOLD) contrast mechanism (Logothetis, 2003).

The intracortical propagation of the slow sleep oscillation (<1 Hz) was recently studied in humans using high-density EEG recordings (Massimini *et al.*, 2004).[23] The detection of slow oscillations on the multichannel EEG is depicted in Figure 6.8. The slow oscillations originate in frontal regions and propagates in an anterior–posterior direction with a speed of 1.2–7 $m\,s^{-1}$ (Figure 6.9) (Massimini *et al.*, 2004), much faster than described in cortical slices (10–100 $mm\,s^{-1}$), where only pure neighbour-to-neighbour synaptic propagation could be observed (Sanchez-Vives & McCormick, 2000; Compte *et al.*, 2003). The anterior frontal origin of the slow sleep oscillations in the human study (Massimini *et al.*, 2004) suggested a stronger need for sleep of this cortical region, as indicated by very low cerebral blood flow values in this area (Maquet *et al.*, 1997; Braun *et al.*, 1997) and the fact that the increase in slow-wave sleep activity after sleep deprivation is highest in anterior prefrontal regions (Finelli *et al.*, 2000).

During the depolarizing phase of the slow oscillation, virtually all neocortical neurons fire and those with antidromically identified thalamic projections (Steriade *et al.*, 1993e) set into action thalamic RE neurons. This explains why these GABAergic neurons display a slow oscillation (less than 1 Hz) that is strikingly similar to that of the neocortical one (Figure 6.10) (Contreras & Steriade, 1995; Steriade *et al.*, 1993b), despite the fact that the intrinsic properties of RE neurons are quite different from those of cortical neurons. The spike-bursts of RE thalamic neurons are reflected in TC cells as rhythmic IPSPs leading to rebound spike-bursts, which are the basic mechanism for generation of sleep spindles. Then, the synchronous firing of neocortical neurons during the depolarizing component of the slow oscillation and the corticothalamic projections to RE neurons represent

[23] The authors used 256 EEG electrodes and, after rejection of noisy channels, about 180 channels per subject were retained.

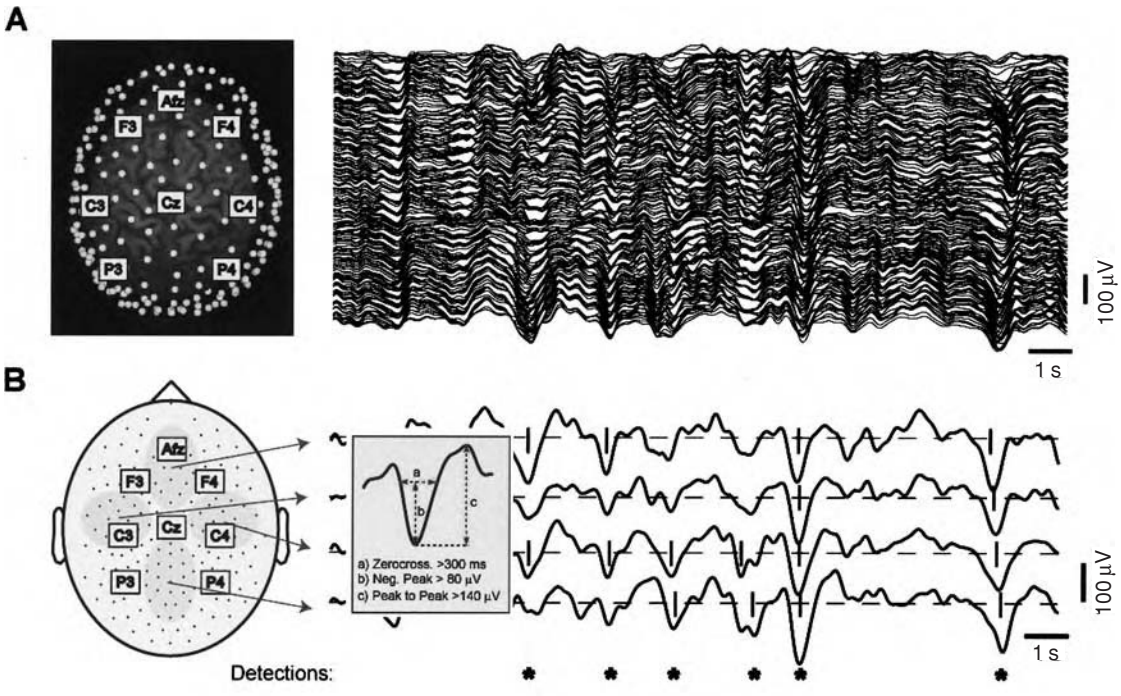

Fig. 6.8 Automatic detection of slow oscillation on the multichannel EEG during human sleep. (A) Left panel: the location of all electrodes (white dots) with respect to a subject's 3D magnetic resonance imaging (MRI) reconstructions. The labels indicate some of the equivalent electrodes in the 10–20 system. Right panel: the signals recorded from all channels during an epoch of slow-wave sleep (stage 4). Scalp positivity is upward. (B) Left, the location of all electrodes on a 2D representation of the scalp surface. Signals recorded from the electrodes included in the four grey areas were averaged to obtain the four local averages displayed on the right. Detection criteria (see Massimini *et al.*, 2004) were applied to each local average. If the criteria were met by any of the four local averages, the automatic detection algorithm stored the occurrence of a slow oscillation. Modified from Massimini *et al.* (2004).

[24] The mechanism of the slow oscillation induced in TC cells by activating the metabotropic glutamate receptors mGluR1 relies on the 'window' component of I_T and a Ca^{2+}-activated, non-selective cation current.

the mechanism that underlies the brief sequence of spindles that follows every cycle of the slow oscillation (Contreras & Steriade, 1995; Timofeev & Steriade, 1996; Contreras & Steriade, 1996). The concept of a unified corticothalamic network, implying the coalescence of various sleep oscillations by virtue of the ability of cortically generated slow oscillations to impinge on thalamic neurons and thus to group spindles within slow oscillation cycles (see Figure 6.7), is supported by recent studies of human EEGs during natural sleep (Mölle *et al.*, 2002; Marshall *et al.*, 2003). The presence of the cortically generated slow oscillation in thalamic neurons (Contreras & Steriade, 1995; Steriade *et al.*, 1993b) was also reported in a subset of TC neurons recorded in thalamic slices maintained *in vitro*, following activation of the metabotropic glutamate receptor mGluR1a (Hughes *et al.*, 2002b).[24] It is known that corticothalamic neurons use glutamate as a neurotransmitter. That the thalamic slow oscillation is dependent

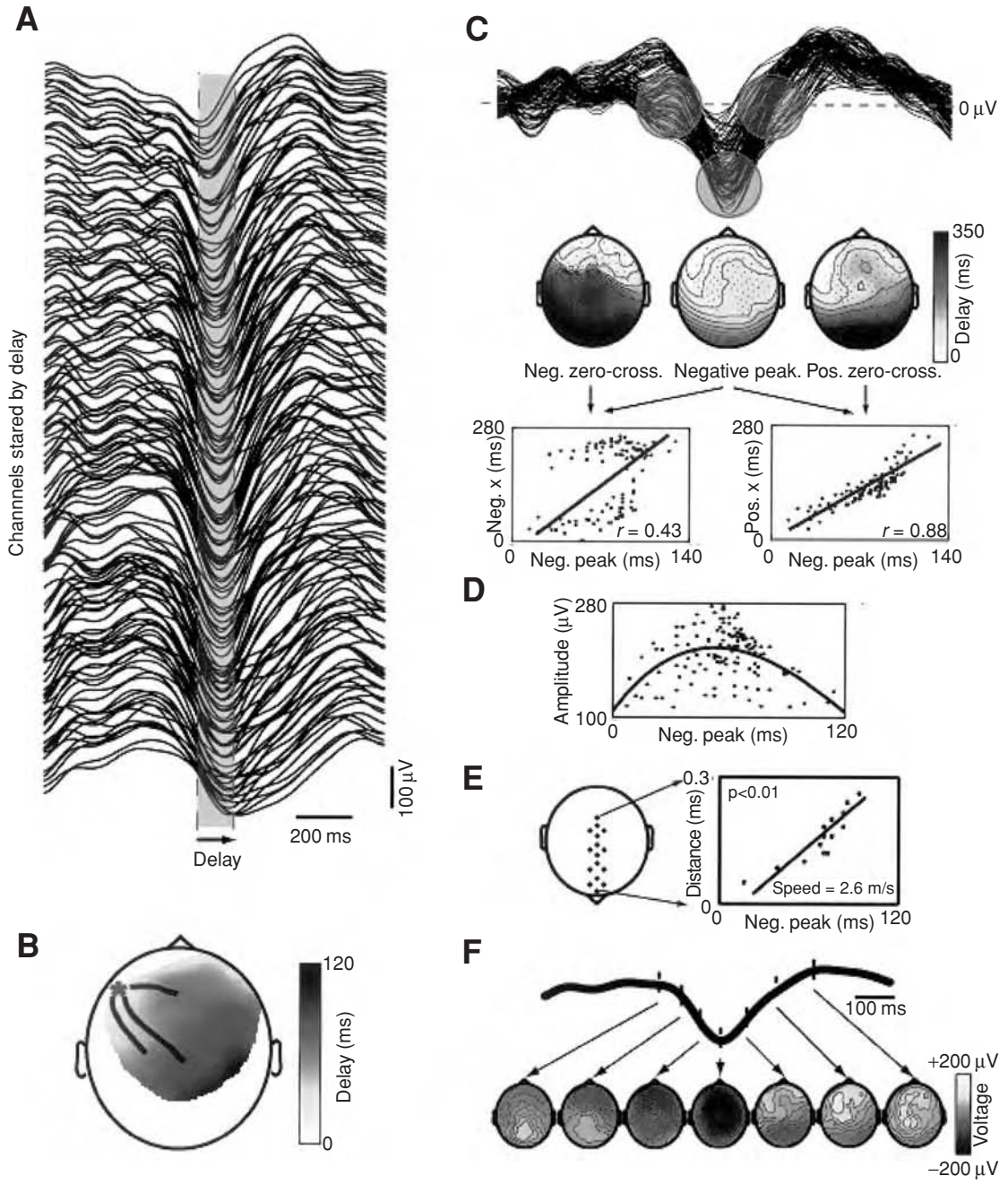

Fig. 6.9 Propagation of the slow oscillation in human sleep. Each cycle of the slow oscillation propagates as a travelling wave. (A) Signals recorded from the channels affected by a single slow oscillation cycle, ranked from top to bottom according to the delay of the negative peak. Note that the slow oscillation is not precisely synchronous in all channels and that a continuous distribution of time lags can be measured. The width of the red area represents the maximum delay (120 ms) from the negative peak at the top trace to the negative peak at the bottom trace. (B) Spatial distribution of the delays, shown on a delay map. A red asterisk marks the location of the channel with delay = 0

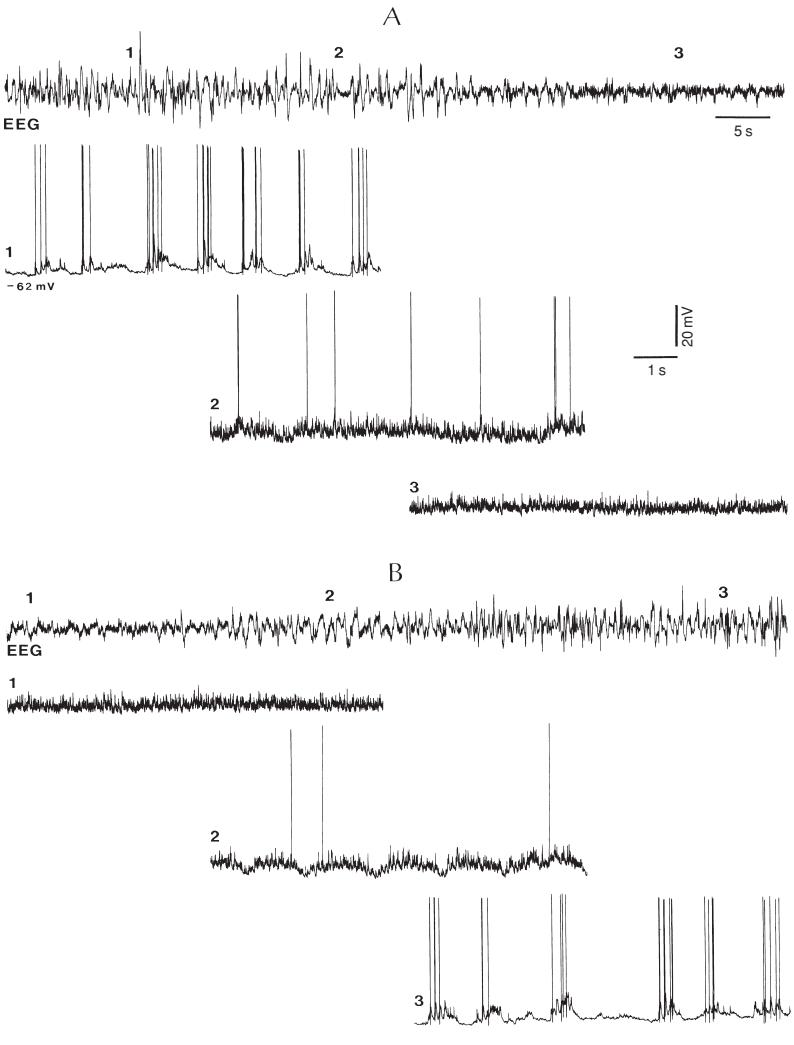

Fig. 6.10 The slow oscillation in thalamic reticular (RE) neurons. Transitions from RE intracellular activity accompanying changes in EEG-wave amplitudes. Cat under urethane anaesthesia. An RE cell from the rostrolateral sector of the nucleus was recorded together with the gross EEG from the contralateral pericruciate area. (A) During a spontaneous transition from high- to low-amplitude EEG waves, the slow oscillation in the RE neuron (1) is suppressed, with an increase in synaptic noise (2), eventually leading to absence of action potentials, with a high level of synaptic noise (3). (B) Reverse spontaneous transition (1 to 3). Modified from Contreras & Steriade (1997b).

(the origin). The blue lines starting around the origin represent the streamlines calculated on the vector field of delays. The slow oscillation originates locally and propagates in an orderly manner to the rest of the scalp as a travelling wave. (C) The same signals as in (A) are superimposed; the red circles highlight the negative zero crossing, the negative peaks and the positive zero crossings on the slow oscillation recorded from all electrodes. The maps below show the topographic distribution of the delays of these three reference points. The dots represent the channels affected by the slow oscillation, and the lines are iso-delay contours. (D) Peak-to-peak amplitude of the positive wave plotted against the delay of the preceding negative wave. (E) Speed of wave propagation is measured from a row of electrodes placed on the anteroposterior axis (left). (F) Sequential voltage (average-referenced) scalp maps calculated during different phases of the same cycle analysed in the previous panels. The time of each map is indicated on the average of the slow oscillation signals recorded from all channels. Modified from Massimini *et al.* (2004). See Plate 4.

on the neocortex was shown by the absence of slow oscillation in the thalamus of decorticated animals (Timofeev & Steriade, 1996). In addition, the slow oscillation in the non-lemniscal auditory thalamus is altered by cortical stimulation *in vivo*, leading to the termination of the oscillation or the acceleration of its rhythm (He, 2003).[25]

The relation between the cortical slow oscillation and thalamic spindles is clearly seen in the sequence of grapho-elements consisting of an ample surface-positive–negative transient (slow oscillation) followed by a few spindle waves. This sequence is termed the K-complex and is a reliable sign for stage 2 of human sleep, but survives in all stages of slow-wave sleep (Niedermeyer, 1993; Loomis *et al.*, 1938; Roth *et al.*, 1956). The K-complex, a landmark of sleep electrical patterns, was related to the slow oscillation in humans (Amzica & Steriade, 1997); its cellular substrates have been investigated in cats (Amzica & Steriade, 1997). Spectral analysis demonstrated the periodic recurrence of human K-complexes at 0.5–0.7 Hz. Analysis of the laminar profile and intracellular substrates of the K-complex during cat sleep or anaesthesia revealed that the surface-recorded, positive K-complexes reverse at a cortical depth of about 0.3 mm, and that the sharp depth-negative (surface-positive) wave of the K-complex is associated with neuronal depolarization, eventually leading to a spindle sequence. These studies indicate that the K-complexes are the expression of the spontaneously occurring, cortically generated slow oscillation. The K-complex can also be elicited by sensory stimulation.

The spindles generated by the thalamic reflection of the cortical slow oscillation are fed back to the cortex and sculpt the depolarizing component of the slow oscillation (see Figure 6.7) (Contreras & Steriade, 1995).[26] Oscillations in the frequency range of spindles (7–10 Hz) propagate in neocortical slices at *c.*30 mm s^{-1} (Wu *et al.*, 1999).

The intrathalamic and corticothalamic synchronization of spindles is quite different in the intact brain and in slices. Thus, spindles propagate along the dorsoventral axis of the lateral geniculate nucleus in slices from ferret visual thalamus (Kim *et al.*, 1995), whereas spindles are nearly simultaneous in the thalamus and cerebral cortex *in vivo*, both in acutely prepared animals and during natural sleep in cats and humans (Contreras *et al.*, 1996a, 1997b). The contrast between the simultaneity of spindle sequences *in vivo* and spindle propagation *in vitro* is due to the absence of the cortex in thalamic slices. In fact, after decortication, the simultaneity of spindle sequences throughout the thalamus is reduced without, however, showing systematic propagation as in thalamic slices (Contreras *et al.*, 1996a, 1997b). These data point to the role of corticothalamic neurons in the enhancement of synchronization and appearance of nearly simultaneous spindle sequences. The importance of corticofugal projections in governing the time-course and synchronization of rhythmic activities was also emphasized in another series of studies showing that (a) cortical

[25] The cortically generated slow oscillation was only present in non-lemniscal nuclei of the guinea pig auditory thalamus; no differences in intrinsic membrane properties were observed between lemniscal and non-lemniscal auditory neurons.

[26] Tancredi *et al.*, (2000) have shown, in thalamocortical slices, that application of the excitatory amino acid receptor antagonist kynurenic acid in the ventrobasal (VB) thalamus led to disappearance of spindles in both VB and cortex, whereas cortical application of the same substance abolished spindles at the site of application but not in the thalamus, since spindles are generated in the thalamus (Morison & Bassett, 1945).

feedback induces correlated firing in visual thalamic neurons, which increases the gain of the input for feature-linked events detected in cortex (Sillito *et al.*, 1994); and (b) in awake baby ferrets before their eyes opened, corticothalamic feedback is required to sustain correlated neuronal bursting activity in the visual thalamus as this coherent bursting decreases dramatically after cortical ablation (Weliky & Katz, 1999).

Neocortical and thalamic oscillations are also reflected in the electrical activity of the basal ganglia. The discharge properties of both subthalamic and globus pallidus neurons are related to neocortical activity, as those basal ganglia neurons fire spike-bursts with a periodicity that matches the coincident cortical slow oscillation and their oscillatory activity is lost during cortical inactivation through spreading depression (Magill *et al.*, 2000). However, the GABAergic pallidal neurons may control the discharge patterns of subthalamic neurons, which become bursting in slow-wave sleep, without any change in firing rates from waking to sleep (Urbain *et al.*, 2000, 2002). A close relation between the slow oscillation recorded from striatal neurons and neocortical activity was also observed (Wilson & Kawaguchi, 1996; Mahon *et al.*, 2001; Tseng *et al.*, 2001). Spindle frequencies are observed in globus pallidus neurons via indirect pathways involving projections from thalamic intralaminar nuclei to the striatum.

6.1.4 Reflection of the slow oscillation in amygdala and related subsystems

The basolateral complex of the amygdala and the perirhinal cortex display highly synchronous slow oscillations (Collins *et al.*, 2001), but the relation between the neocortical slow oscillation and that recorded from the perirhinal cortex is irregular, as if the rhinal cortices could generate the slow oscillation independently of neocortical areas and impose it on the amygdala (Paré *et al.*, 2002).[27] The synchronization of activities generated in the amygdala and entorhinal cortex is also observed during the sharp potentials that appear in slow-wave sleep and barbiturate anaesthesia (Paré *et al.*, 1995a).[28] Sharp potentials are generated in the amygdala, reflected in related cortical areas, and transferred from layer II of the entorhinal cortex to the hippocampus. The involvement of slow oscillatory activities of the amygdala and related subsystems in synaptic plasticity and consolidation of emotional memories (Paré *et al.*, 2002) is dealt with in Section 6.3.2.

The hippocampus also reflects slow oscillatory cortical activity: spike-bursts in deeply lying neocortical neurons trigger population events in the hippocampus associated with ripples (Sirota *et al.*, 2003),[29] which are ultrafast rhythms that preferentially occur during slow-wave sleep, superimposed on the depolarizing phase of the slow oscillation (Grenier *et al.*, 2001). Thalamocortical spindles are also reflected in the hippocampus during sleep, and spindle–ripple episodes are regarded as a mechanism of cortico-hippocampal

[27] Amygdala neurons also oscillate in the frequency range of delta waves (Paré & Gaudreau, 1996). Distinct from slow and delta oscillations, amygdala and rhinal cortices do not display spindles, probably because thalamic territories of the cat (anterior and reuniens nuclei), which send axons to the amygdala and entorhinal cortex, do not receive inputs from the spindle pacemaker (Fuentealba & Steriade, 2005), the thalamic RE nucleus (Steriade *et al.*, 1984a; Paré *et al.*, 1987; Velayos *et al.*, 1989).

[28] Events similar to sharp sleep potentials, which are generated in the amygdala–entorhinal axis of cat, have also been found in rat dentate gyrus, termed 'dentate EEG spikes', and abolished by entorhinal lesions (Bragin *et al.*, 1995b).

[29] In the hippocampus, as in neocortex, ultra-fast oscillations (ripples) are due, at least partly, to summated IPSPs in pyramidal cells, as a result of high-frequency barrages of inhibitory interneurons (Ylinen *et al.*, 1995; see also Csicsvari *et al.*, 1999).

communication that may be important for consolidation of memory (Siapas & Wilson, 1998). The coactivation of neocortex and hippocampus may provide a mechanism for recent experiences, to be selectively replayed during slow-wave sleep (Buzsáki, 1989; Wilson & McNaughton, 1994).

6.2 Neuronal firing and responses during the disconnected state of slow-wave sleep

6.2.1 Thalamus

Spike-bursts as indicators of brain deafferentation in slow-wave sleep

The spontaneous discharges of TC neurons during slow-wave sleep are characterized by high-frequency spike-bursts, which crown the low-threshold spike (LTS) that is de-inactivated by membrane hyperpolarization during this behavioural state (see Section 1.3.1). The bursting firing pattern of TC cells, which accompanies spindles, clock-like delta and slow oscillations during slow-wave sleep, stands in contrast with their tonic firing of single action potentials during waking and REM sleep (Glenn & Steriade, 1982). Thalamic RE GABAergic neurons similarly display the contrast between spike-bursts during slow-wave sleep and tonic firing during the brain-activated states of waking and REM sleep (Steriade *et al.*, 1986). Identified local-circuit inhibitory cells have not yet been investigated during natural states of waking and sleeping.

Although all studies based on intracellular recordings have emphasized that LTSs and spike-bursts require membrane hyperpolarization of TC cells, which occurs steadily during slow-wave sleep (Hirsch *et al.*, 1983), some authors have proposed that the spike-bursts fired by TC neurons are also present during waking and are beneficial for 'scanning attention' (Guido *et al.*, 1992; Reinagel *et al.*, 1999). However, those studies were conducted under anaesthesia, a condition that prevents scanning attention from being investigated. In work on naturally awake and sleeping animals, the hypothesis of scanning attention was abandoned and it was proposed that visually evoked spike-bursts in TC neurons may serve as a sort of 'wake-up' call for the cortex during inattentiveness (Guido & Weyand, 1995). However, a study on TC neurons recorded from the visual thalamus in chronically implanted cats concluded that, 'during wakefulness, less than 1% of action potentials are associated with bursting' and found 'negative relationships between attention and bursting' (Weyand *et al.*, 2001, pp. 1107 and 1113). Then, the burst mode is not a normal firing pattern for TC neurons during waking (Steriade, 2001d). The hypothesis of spike-bursts during wakeful attention is an idea that is sometimes repeated in the literature despite the fact that wakefulness is a state associated with membrane depolarization of TC neurons (Hirsch *et al.*, 1983), a

condition during which the conductance underlying spike-bursts is inactivated (Steriade & Llinás, 1988; Steriade *et al.*, 1990b).

Excitatory and inhibitory responses

The probability of antidromic responses in TC neurons decreases during slow-wave sleep, compared with waking and REM sleep (Glenn & Steriade, 1982). Complete blockage of antidromic responses and/or replacement of full responses with initial segment spikes occurs in advance of overt sleep spindles in cortical activity (Steriade *et al.*, 1971), owing to hyperpolarization of TC neurons.

The synaptic responses of TC neurons were initially studied by recording field potentials evoked by stimulating afferent pathways. This approach revealed that, at the transition from waking to drowsiness and later to slow-wave sleep, postsynaptic waves are progressively obliterated, without any change in the presynaptic deflection that monitors the magnitude of the incoming volley (Steriade, 1970). This demonstrates that *the first relay station where changes occur with transition from waking to slow-wave sleep is the thalamus* (Steriade *et al.*, 1969; Steriade, 1991).[30] More recent studies confirmed this viewpoint and showed that the responses of thalamic neurons to medial lemniscus stimulation depress at a frequency higher than 2 Hz during slow-wave sleep, thus gating the flow of sensory inputs to the cortex (Castro-Alamancos, 2002a).[31] The inhibition of synaptic transmission through the thalamus deprives the cortex of signals from the outside world and is a prerequisite for falling asleep.

Intracellular recordings of TC neurons *in vivo* showed that the magnitude of subthreshold EPSPs evoked in TC cells by afferent volleys during different epochs of the slow sleep rhythm is *not* reduced during the hyperpolarizing phase of this oscillation, but low-threshold spike-bursts are only occasionally fired (Timofeev *et al.*, 1996).[32] In contrast to the virtually unchanged monosynaptic EPSPs in TC neurons during the hyperpolarizing phase of the slow sleep oscillation, EPSPs are diminished during spindle-related IPSPs in TC neurons (Timofeev & Steriade, 1997) because of the increased membrane conductance related to the biphasic $GABA_{A\text{-}B}$ potentials that form spindles. Then, in addition to the steady hyperpolarization of TC neurons during slow-wave sleep (Hirsch *et al.*, 1983), spindle waves are most effective at blocking incoming signals en route to the cortex (Steriade *et al.*, 1969; Steriade, 1991).[30]

The changes in RE-cells' responsiveness, namely decreased probability and longer latencies of evoked discharges during slow-wave sleep compared with waking (Steriade *et al.*, 1986), are similar to those of TC neurons. This may seem unexpected because GABAergic RE neurons are conventionally thought to behave in an opposite way to their targets, TC neurons. The parallel changes in these two cellular classes can be ascribed to the fact that, during waking that is accompanied by increased responsiveness in TC neurons, directly connected RE neurons contribute to further enhance the relevant activity by

[30] It was further suggested that, by effectively reducing environmental influences on neocortical activity, spindle oscillations shift sleep into deeper stages (Buzsáki & Draguhn, 2004).

[31] In this *in vitro* study, acetylcholine and norepinephrine produced depolarization of TC neurons, brought the depressed EPSPs evoked by lemniscal stimulation (>2 Hz) close to firing threshold, and thus served to relay lemniscal inputs. Whereas during quiescent states, responses to peripheral stimulation at frequencies of more than 2 Hz are depressed, during activated states thalamic responses to high-frequency stimulation (up to 40 Hz) are relayed to the neocortex (Castro-Alamancos, 2002b).

[32] The long-lasting hyperpolarization of the slow oscillation is mainly due to disfacilitation in corticothalamic networks (see Contreras *et al.*, 1996b).

inhibiting GABAergic local-circuit neurons in dorsal thalamic nuclei (see Steriade, 2001b; Golshani *et al.*, 2001; Jones, 2002).

Inhibitory processes in TC neurons, as determined by measuring the duration of the period of suppressed firing following an afferent volley, are cyclic and prolonged during slow-wave sleep, whereas during waking the cyclic and long-lasting periods of silenced firing are suppressed but the early inhibitory phase is not eliminated (Steriade *et al.*, 1977). This contrasts with earlier views postulating a complete blockage of inhibitory processes in TC neurons upon brain activation, resulting from inhibition of inhibitory thalamic neurons (Purpura *et al.*, 1966; Singer, 1977). Such a conclusion was embarrassing, because brain operations during wakefulness require preservation of short IPSPs for the accurate analysis of rapidly recurring signals during an adaptive behavioural state. The idea that the early inhibitory phase in TC neurons is preserved during waking and brainstem reticular-induced arousal (Steriade *et al.*, 1977) was later strengthened by intracellular recordings showing that midbrain reticular stimulation blocks the long-lasting, cyclic hyperpolarizations of TC neurons, but preserves the early, short-lasting IPSP (Steriade, 1984, 2004b; Hu *et al.*, 1989b; Curró Dossi *et al.*, 1992b).[33]

Of the two GABAergic thalamic cell-classes, local-circuit neurons may assist TC neurons with discriminatory functions. The development of $GABA_A$- and $GABA_B$-mediated IPSPs in TC neurons is associated with the dendritic maturation of presynaptic interneurons (Perreault *et al.*, 2003), which explains why the inhibitory surround in the receptive field of kittens' thalamic neurons is weaker than in adult cats. The discovery of triphasic IPSPs in anterior TC neurons shed further light on the selective preservation of the earliest IPSP, with simultaneous abolition of later IPSPs. The earliest IPSP (called $GABA_a$, to distinguish it from the subsequent sequence of $GABA_{A\text{-}B}$ IPSPs) is presumably generated by GABA release from the intraglomerular presynaptic dendrites of local interneurons (Paré *et al.*, 1991; Soltesz & Crunelli, 1992; see also Section 1.2.1). The importance of this intraglomerular circuitry resides in the discrete localization of inhibition. During brain activation, $GABA_a$ IPSPs are preserved or even enhanced, whereas $GABA_B$ IPSP and occasionally $GABA_A$ IPSP are abolished (Curró Dossi *et al.*, 1992b). The preservation of the earliest, short-lasting IPSPs under condition of brain activation may assist in the enhancement of centre–surround mechanism and lateral inhibition during attentive states. Another factor that influences the receptive field of TC neurons is the action of GABAergic RE neurons as, after excitotoxic lesion of RE neurons, the average receptive field size was enlarged significantly and remained expanded for as long as one month (Lee *et al.*, 1994).[34]

6.2.2 Neocortex

Intrinsic, antidromic and synaptic responsiveness

Different types of responses by neocortical neurons (elicited by depolarizing current pulses or antidromic and orthodromic volleys) are

[33] In this *in vivo* study, the effects on the dendritic output of local inhibitory interneurons in the anterior thalamic nuclei have been investigated by stimulating mesopontine cholinergic nuclei. *In vitro* studies of lateral geniculate slices reported that activation of muscarinic receptors decreases the dendritic output of inhibitory interneurons, but activation of ionotropic and metabotropic glutamate receptors increases their dendritic output (Cox & Sherman, 2000). Stimulation of mesopontine cholinergic nuclei probably releases both ACh and glutamate, as both these neurotransmitters are co-localized in mesopontine cholinergic neurons (see Chapter 5).

[34] The enlargement of the receptive field of somatosensory neurons in the rat ventroposteromedial nucleus several hours after RE-cell lesions was nearly identical to that seen after several weeks of survival.

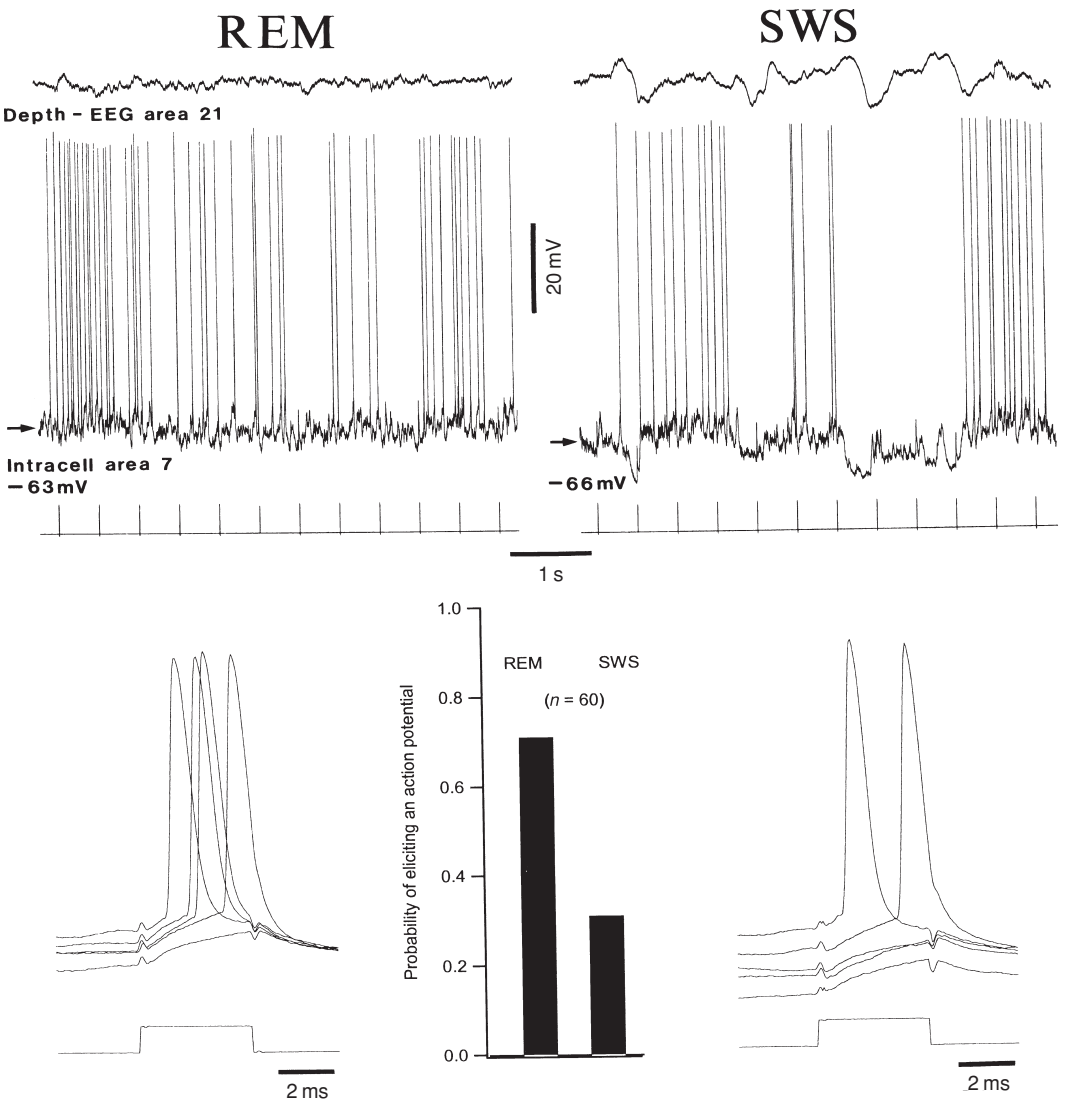

Fig. 6.11 Diminished intrinsic excitability of a cortical neuron tested by depolarizing current pulses (4 ms) during slow-wave sleep, compared with REM sleep. Intracellular recording from area 7 (together with EEG from area 21) in chronically implanted cat. Upper panel shows EEG and intracellular recordings (bottom trace, short depolarizing current pulses). Below, five superimposed traces with responses to depolarizing current pulses during REM sleep (left) and slow-wave sleep (right). Middle, histogram showing probability of action potentials evoked during REM sleep (about 70%) and slow-wave sleep (about 30%). Unpublished data by F. Grenier, I. Timofeev and M. Steriade (see Steriade *et al.*, 2001b).

diminished during slow-wave sleep, compared with waking and REM sleep. The decreased probability of responses to depolarizing pulses (Figure 6.11) and of antidromically elicited action potentials (Steriade, 1976; Steriade *et al.*, 1979) or the accentuation of the break between the initial-segment spike and the somatodendritic antidromic spike

(Steriade *et al.*, 1974a) (Figure 6.12) is probably due to the prolonged hyperpolarizations of cortical cells during the slow oscillation in naturally sleeping animals (Steriade *et al.*, 2001a). Synaptic responses elicited by stimulation of prethalamic pathways and recorded as field potentials from the cerebral cortex are also diminished in both their presynaptic and postsynaptic components. When cerebellothalamic axons are stimulated and recordings are made from cortex, the decreased amplitude of the presynaptic component, which monitors the incoming input that arises in the motor thalamus, may explain the diminished amplitude of the cortically generated postsynaptic waves (Steriade *et al.*, 1969; Steriade, 1991) (Figure 6.13A). With peripheral sensory stimuli, the surface-negative N1 component (50 ms latency) of the field response recorded from the monkey's somatosensory cortex diminishes during slow-wave sleep, compared with inactive waking, and multi-unit firings associated with this component are replaced during sleep by an inhibitory period leading to rebound spike-bursts (Cauller & Kulics, 1988) (Figure 6.13B). In such cases, the major part of the inhibition is ascribable to gating processes at the thalamic level (Steriade, 1970; Steriade *et al.*, 1969; Steriade, 1991).

Thus, cortical responses evoked by stimuli applied to prethalamic pathways are diminished or totally inhibited during slow-wave sleep, and especially during spindle episodes (Timofeev *et al.*, 1996) because they are associated with large increases in membrane conductance in TC neurons. In contrast, cortically evoked responses in cortical neurons are not diminished during slow-wave sleep (Timofeev *et al.*, 1996), and callosally evoked responses are even enhanced compared with waking (Steriade *et al.*, 1974b). The surprisingly high responsiveness of cortical neurons during slow-wave sleep is the counterpart of rather high spontaneous firing rates during this state, only slightly lower than in waking and REM sleep (Steriade *et al.*, 2001a). This is congruent with the fact that even in anaesthetized animals, primary sensory areas display an ongoing synaptic activity that is of the same order of amplitude as evoked synaptic responses (Arieli *et al.*, 1995).[35] Comparing the synaptic responsiveness of cortical neurons during the depolarizing and hyperpolarizing components of the slow sleep oscillation led to the conclusion that cortically evoked EPSPs are higher in amplitudes during the hyperpolarizations and are almost completely immersed in background activity during the depolarizing phase (see Figure 3.27 in Steriade, 2003a). The diminution or obliteration of evoked responses is also ascribable to the IPSPs that appear on the depolarizing phase of the slow oscillation (Steriade *et al.*, 1993e) and the strongly decreased input resistance of cortical neurons during this phase of the slow oscillation (Steriade *et al.*, 2001a). These results are congruent with data from rat barrel cortex showing decreased input resistance of layers II/III neurons during the depolarizing ('up') phase and more reliable whisker-evoked action potentials during the hyperpolarizing ('down') state (Petersen *et al.*, 2003).[36] Overall, these data indicate that, during slow-wave sleep, cortical neurons maintain an internal dialogue that may explain some forms of mental

[35] In another study, the same team showed that the large variability of evoked responses could be partially predicted by the preceding spontaneously occurring activity (Arieli *et al.*, 1996).

[36] These authors worked on awake rats and animals were 'never asleep' (p. 13 639). The state of 'quiet wakefulness' was associated with 'postural adjustments' and reactions to 'the visual presence of a nearby approaching object'. This is a state that is usually accompanied by blockade of the slow oscillation, with disruption of 'up' and 'down' states, and appearance of a steady depolarization in awake cats (see Figure 9 in Steriade *et al.*, 2001a). It is probable that the 'up' and 'down' states described in the article by Petersen *et al.* (2003) occurred in the drowsy state of rats or, alternatively, appeared as depolarization and short hyperpolarizing episodes in the wakeful state, without necessarily reaching the organization of a slow oscillation.

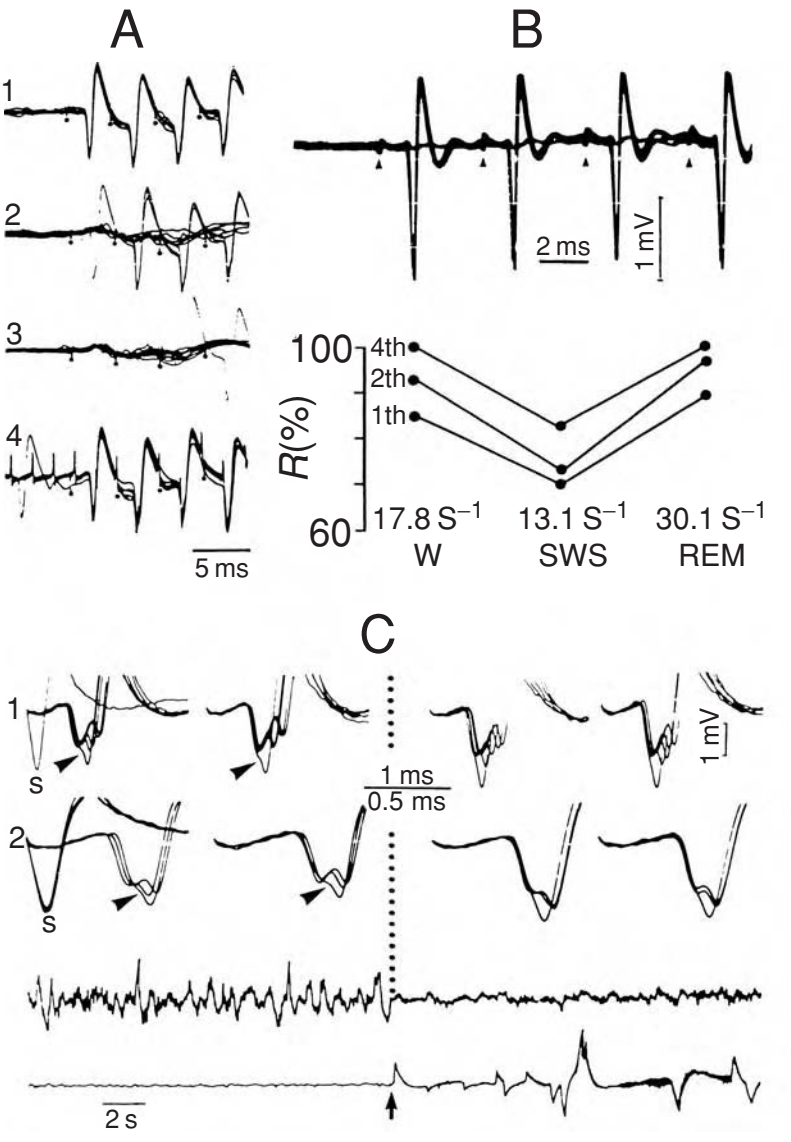

Fig. 6.12 Antidromic responses of long-axoned corticofugal neurons during waking and sleep states. (A) Facilitation of antidromic activation of cat pyramidal tract (PT) neuron during EEG activation. Full responsiveness to 4-stimulus train during control epoch of EEG activation (1), depressed responsiveness during progressively developing EEG synchronization (2, 3) and recovery of antidromic responsiveness during EEG activation elicited by a brief conditioning pulse-train (300 Hz) to the midbrain reticular formation (4). (B) Corticothalamic neuron from area 5, antidromically activated from the thalamic centre median (CM) nucleus. Chronically implanted cat. Antidromic responsiveness was investigated with 4-stimulus train (arrowheads indicate stimuli). Below, percentage responsiveness (*R*) during waking, SWS and REM sleep. Below each state is the mean firing rate (calculated during another waking–sleep cycle). (C) Patterns of antidromic invasion in precentral neuron during natural SWS (left) and awakening (right). Chronically implanted macaque monkey. Dotted line indicates arousal from SWS. Fast-conducting neuron, with 0.5 ms latency of antidromic response from pes pedunculi. 1 and 2, responses to 5-stimulus (350 Hz) and 3-stimulus (110 Hz) trains, respectively, during two passages from SWS to arousal. Third and fourth traces, EEG and eye movements. Note IS–SD fragmentation of first antidromic spike (arrowheads) during SWS and full recovery of unbroken action potentials on arousal as well as diminution of spike fragmentation of successive responses. Modified from Steriade (1976) (A), Steriade *et al.* (1979) (B) and Steriade *et al.* (1974a) (C).

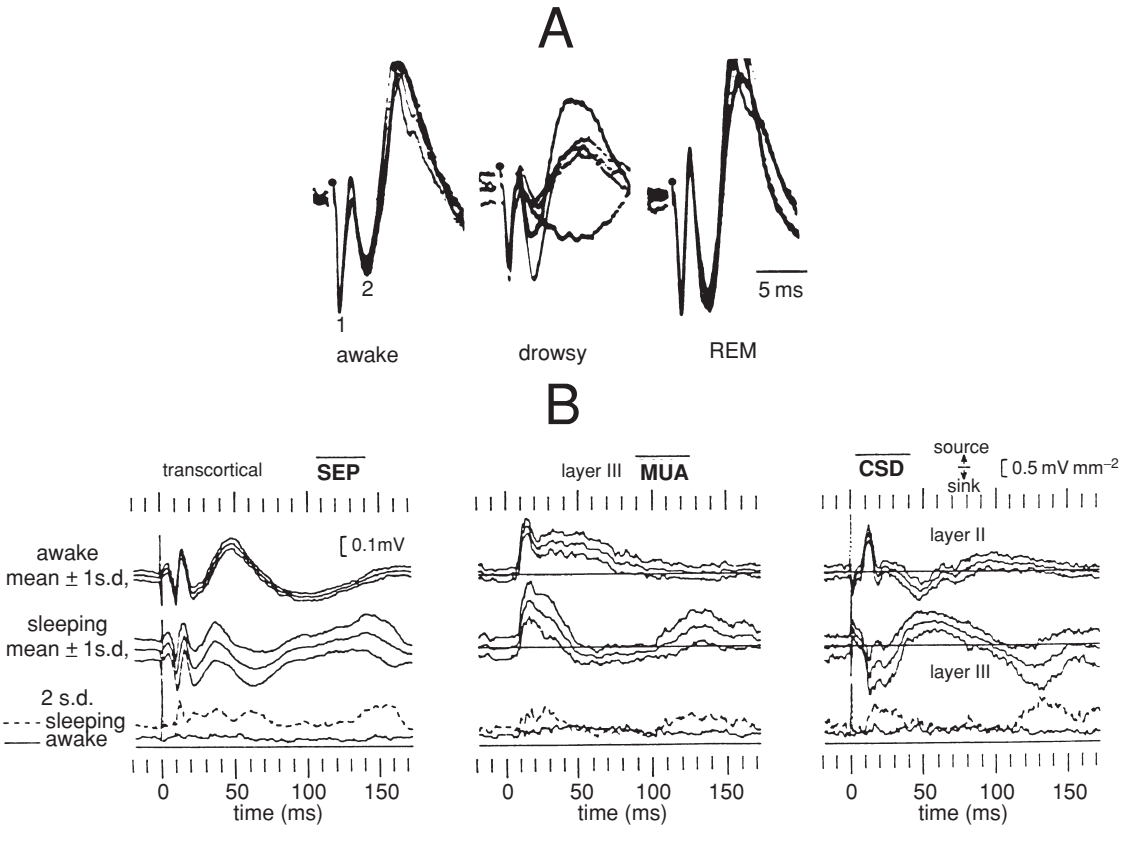

Fig. 6.13 Diminished amplitudes of cortical evoked potentials during slow-wave sleep. (A) Motor cortex field potentials evoked by stimulation of cerebellothalamic axons during waking, drowsiness (similar aspect during slow-wave sleep) and REM sleep (similar aspect in waking) in a chronically implanted cat. Component 1 corresponds to activity in the cortically projecting axons of thalamic ventrolateral neurons, whereas component 2 reflects intracortical activities. Note the decrease in both presynaptic (1) and postsynaptic (2) components during the drowsy state, and increased thalamic and cortical excitability during REM sleep. (B) Somatosensory evoked potential (SEP) during waking and slow-wave sleep in monkey. The comparisons between waking and sleep demonstrate: the reliability of the wakeful N1 component of the somatosensory evoked potential; multi-unit activity (MUA) excitability during waking in layer III and inhibition of layer III multi-unit activity during sleep; the waking N1 sink in superficial layer II and the sleep inhibitory source in layer III. Modified from Steriade *et al.* (1969) (A) and Cauller & Kulics (1988) (B).

activities, such as dreaming (see Section 6.4), despite a complete absence of information from external signals, owing to inhibition at the thalamic level.

Relatively preserved cortical functions in the absence of inputs from brainstem and thalamus were also observed in anatomoclinical studies. The dissociation between the damaged thalamus and relatively normal cerebral cortex has been reported in several studies (Kinney *et al.*, 1994; Adams *et al.*, 2000). After severe bilateral

mesencephalic and paramedian thalamic lesions, cortical circuits are preserved and the values of cortical glucose metabolism are almost normal, indicating that segregated corticothalamic neuronal networks may retain their connectivity and functional integrity. This suggests that the modular nature of individual functional neuronal circuits may underlie conscious brain function (Schiff *et al.*, 2002; Desmedt *et al.*, 1983; Allison *et al.*, 1989).

Cortical responsiveness to somatosensory stimuli was recently investigated during human sleep, taking into consideration the swing between the waking-like wave of the EEG slow oscillation ('up' state, reflecting the depolarization of neurons) and the EEG wave reflecting the silenced firing in neurons ('down' state) (Massimini *et al.*, 2003). That study assumed that the long-lasting hyperpolarization is associated with a surface-negative EEG deflection whereas the beginning of the depolarizing phase of the slow oscillation is marked by the onset of a surface-positive wave, as determined in intracellular studies on anaesthetized (Contreras & Steriade, 1995) and naturally sleeping (Steriade *et al.*, 2001a) animals. The results showed a progressive increase in the cortical postsynaptic response to somatosensory stimuli towards the transition between the surface-negative ('down') state and the surface-positive ('up') state; these changes involved both the short (N20) and long-latency (P60 and P100) components, the latter reflecting cortical processing (Massimini *et al.*, 2003). Past the point between the 'down' and 'up' states, the amplitude of the stimulus-evoked response starts to decrease and the most marked depression, especially of late, cortically generated components, is observed around the end of the positive slope. These changes corroborate the measures of apparent input resistance during the two components of the slow oscillation in natural sleep, with markedly decreased values during the depolarizing phase, compared with the hyperpolarizing phase (Steriade *et al.*, 2001a).

The peculiar feature of subgenual cingulate and orbitofrontal cortical neurons of monkeys during states of vigilance is their very low spontaneous activity in wakefulness and increased firing rates during slow-wave sleep (Rolls *et al.*, 2003). Activation of neocortical neurons during slow-wave sleep is unusual and was also found in studies on callosal neurons linking precentral motor areas in monkeys (Steriade *et al.*, 1974b). The findings on subgenual neurons may be linked to brain states in depression, predicting the possibility that reducing arousal and allowing sleep in humans would result in an increased activation of these areas (Rolls *et al.*, 2003), as found by neuroimaging studies during states of sadness (Dolan *et al.*, 1992; Drevets & Reichle, 1992).

Sculpting inhibition

During brain disconnection from the outside world, a common change in the visual cortex is a decreased response to optimally oriented moving slits of light, which may occur over a background of increased spontaneous activity, thus further decreasing the

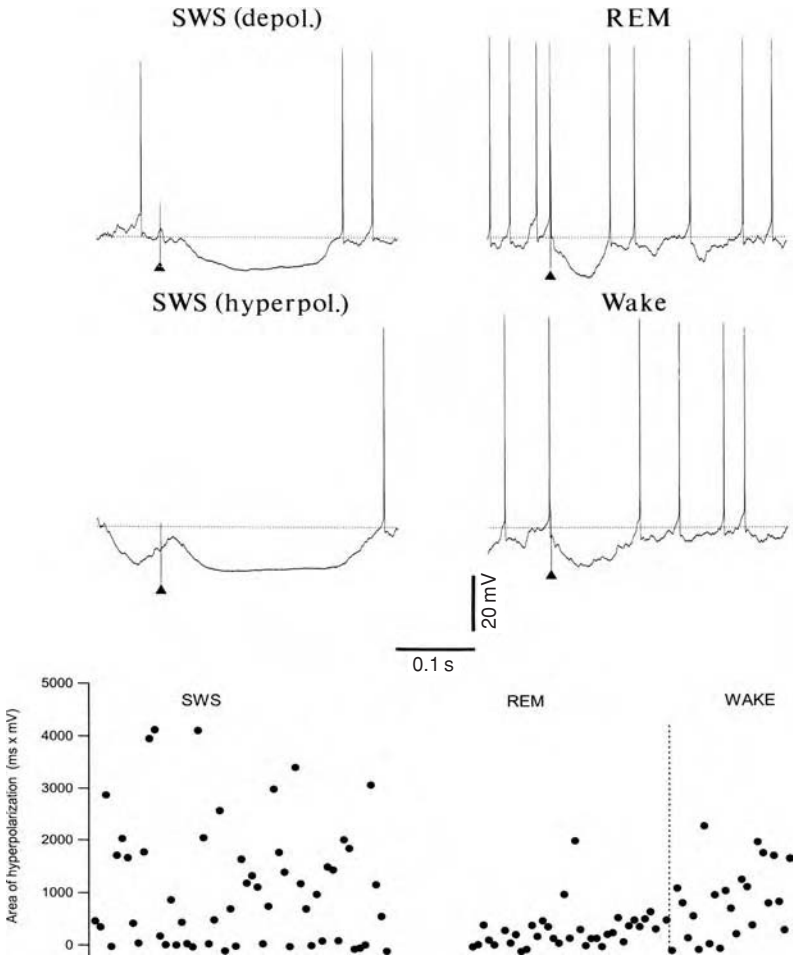

Fig. 6.14 Longer hyperpolarizations occur in cortical neurons during natural SWS, compared with REM sleep and waking. Intracellular recording of area 18 neuron (same as depicted in Figure 4.13). Stimulus to thalamic LP nucleus evoked much longer hyperpolarizations during both depolarizing and hyperpolarizing phases of slow oscillation in SWS than in REM sleep and waking. Dotted line (in all cases) is at −63 mV. Bottom panel shows the area of hyperpolarization (duration in ms × mV) measured in 1 s bins. Note shortest area of hyperpolarization in REM, followed by waking, and much more dispersed and longer hyperpolarizations in SWS. Unpublished experiments by F. Grenier, I. Timofeev & M. Steriade.

signal-to-noise ratio (Livingstone & Hubel, 1981). The decreased response selectivity to sensory stimuli during slow-wave sleep reflects less efficient inhibitory processes than during wakefulness. This was shown in feedback inhibition tests that involved antidromic stimulation of pyramidal tract neurons in the pes pedunculi, after lesion of the medial lemniscus to avoid stimulation of ascending axons. Stimulation of appropriate thalamic nuclei was also performed to test feedforward inhibition (Steriade & Deschênes, 1974). In both cases, inhibition lasted much longer during slow-wave sleep than in wakefulness. Intracellular recordings in naturally awake and sleeping animals (Steriade *et al.*, 2001b; also unpublished data by F. Grenier, I. Timofeev & M. Steriade) confirmed those earlier data and demonstrated that the evoked hyperpolarization is much longer in slow-wave sleep than in REM sleep (Figure 6.14). These recent data further showed that bisynaptic IPSPs, evoked in cortical neurons by thalamic volleys, are obvious during the depolarizing phase of the slow oscillation in slow-wave sleep (reversed IPSPs are observed during the hyperpolarizing phase of the slow sleep oscillation), but the total duration of the first period

of hyperpolarization (about 70 ms) is not different between slow-wave sleep and brain-active states. What distinguishes slow-wave sleep from either REM sleep or waking is the total duration of hyperpolarization, which may reach 0.2 s in slow-wave sleep and is much shorter during brain-active states (Figure 6.14). This is in line with earlier data from experiments on monkeys' cerebral cortex, showing cyclic, long-lasting periods of suppressed firing followed by rebound spike-bursts during slow-wave sleep, as opposed to single epochs of suppressed firing of shorter duration in waking (Steriade & Deschênes, 1974). Deep but short-lasting inhibition in waking provides a mechanism subserving accurate discrimination and faithful following of rapidly recurring inputs.

In sum, the responsiveness of neocortical neurons, as tested by antidromic and orthodromic volleys, is lower during slow-wave sleep than in the brain-active state of wakefulness. This difference may be ascribed to the higher and more stable input resistance of cortical neurons during waking (Steriade *et al.*, 2001a) (Figure 6.15). The exception of callosal (Steriade *et al.*, 1974b) and some subgenual cortical (Rolls *et al.*, 2003) neurons, which display enhanced firing rates and responsiveness in slow-wave sleep, supports the notion that an internal dialogue is maintained in some neocortical neurons during the state of slow-wave sleep, despite the absence of information from the external world owing to thalamic inhibition of synaptic transmission.

6.3 Synaptic plasticity leading to memory-like events

The rich spontaneous firing of neocortical neurons during slow-wave sleep (Steriade *et al.*, 2001a; Steriade, 1978) (see Figures 6.1 and 6.2) challenges prior assumptions that cortical neurons are inhibited and inactive in this behavioural state (Pavlov, 1923; Sherrington, 1955), which would give rise to an annihilation of mental activity and unconsciousness (Eccles, 1961). Although the thalamic gates are closed to signals from the outside world during slow-wave sleep, because of inhibition of synaptic transmission in TC neurons (Steriade *et al.*, 1969; Steriade, 1991), the intracortical dialogue and responsiveness of cortical neurons to callosal volleys are maintained (Timofeev *et al.*, 1996) and even increased (Steriade *et al.*, 1974b) during slow-wave sleep. These data suggest that this sleep state, which is commonly regarded as reflecting complete brain quiescence, may serve important cerebral functions, among them the consolidation of memory traces acquired during wakefulness (Steriade *et al.*, 1993b; Steriade & Timofeev, 2003). The fast rhythms within the beta/gamma frequency bands (generally 20–60 Hz), which are present in the background electrical activity during waking and REM sleep, also enhance the responsiveness of neocortical neurons (Steriade & Timofeev, 2003; Cissé *et al.*, 2004). Then, spontaneous brain rhythms during different states of vigilance may

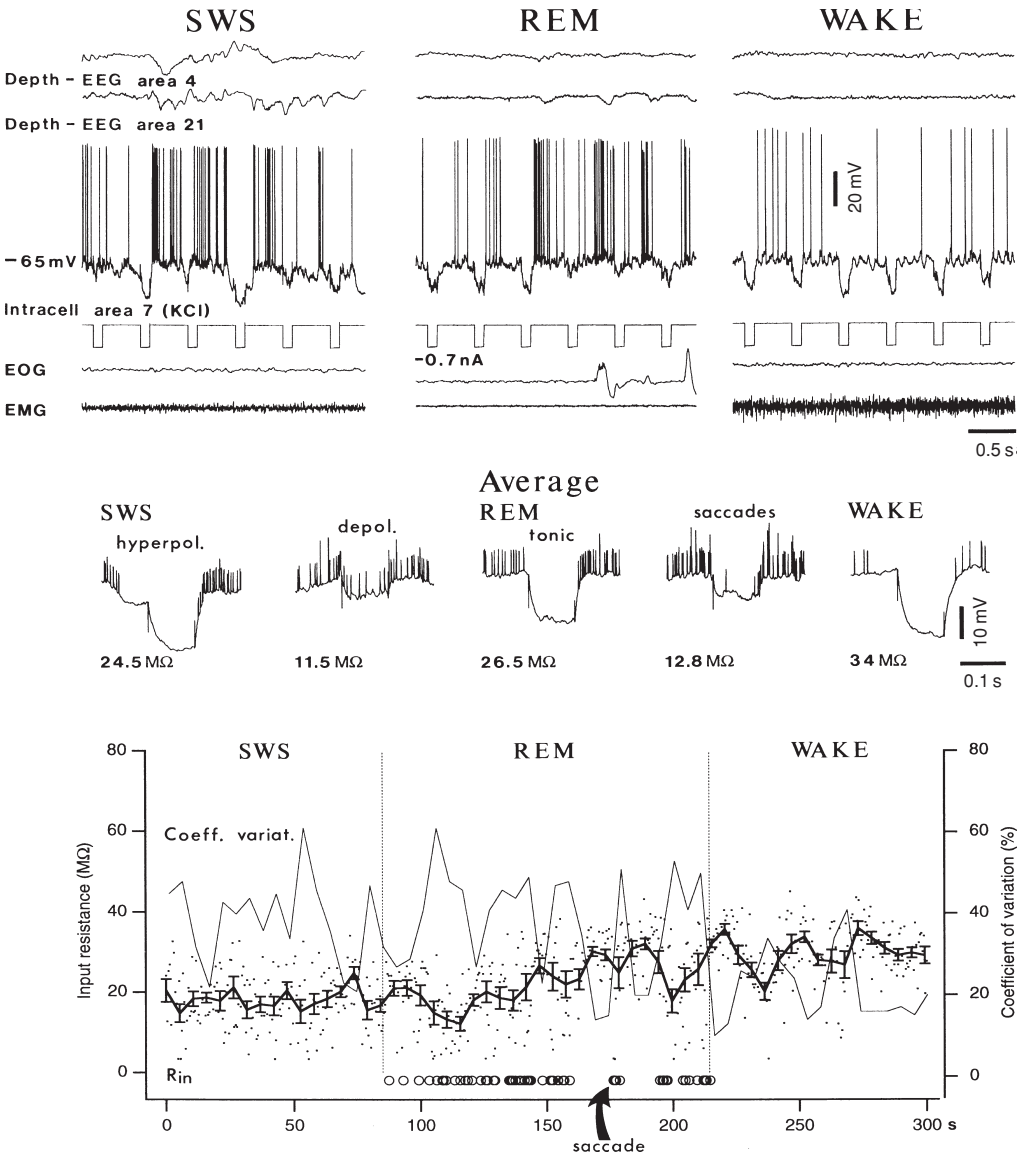

Fig. 6.15 Apparent input resistance (R_{in}) of neocortical neurons during natural states of vigilance. Chronically implanted cat. Upper panel, three periods of intracellular recording from the same regular-spiking neuron during SWS, REM sleep and waking (recording was done in this order). R_{in} was measured by applying 0.1 s hyperpolarizing current pulses every 0.5 s. Below, averages of responses of this neuron during different epochs in the three states of vigilance (note differences between the hyperpolarizing and depolarizing phases of the slow oscillation in SWS; and between epochs with and without ocular saccades in REM). The plot at bottom shows the dynamic changes in R_{in} during the three states of vigilance, obtained from continuous recording throughout the sleep–waking cycle. Dots represent individual measurements of R_{in}; thick line and SD bars, means of R_{in} from every ten consecutive measurements; thin line, the coefficient of variation from corresponding periods; circles, ocular saccades in REM sleep. Note that during quiet wakefulness R_{in} increased and this increase was associated with a decrease in the coefficient of variation. From Steriade *et al.* (2001a).

lead to increased responsiveness and plastic changes in the strength of connections among neurons, a mechanism through which information is stored.

It was Moruzzi who first elaborated the concept relating states of vigilance to plastic activity by proposing that sleep is implicated in the slow recovery of learned synapses (Moruzzi, 1966, p. 353). Although routine synapses that are concerned with transmission of signals along inborn pathways were not considered in this hypothesis, learned synapses were regarded as new contacts between neurons, extremely labile, which 'can be inferred from the study of memory and conditioned reflexes' (Moruzzi, 1966, p. 353). In recent years, the involvement of various oscillatory types occurring during slow-wave sleep and other states of vigilance in synaptic plasticity has been studied in intact-brain preparations as well as *in vitro*.

Here, we discuss the neuronal bases of synaptic plasticity occurring in the thalamus of decorticated animals, in the cortex after thalamectomy, or in intact thalamocorticothalamic systems (Section 6.3.1) and in amygdala and related subsystems (Section 6.3.2). In some instances, the progressive growing of neuronal responsiveness after rhythmic electrical stimulation within the frequency range of different brain rhythms, especially those at low frequencies (less than 15 Hz) that typically characterize slow-wave sleep, is followed by self-sustained activities that mimic responses during the prior period of stimulation. Such activities may take the form of epileptiform afterdischarges, which raises the yet unsolved issue of the close relation between synaptic plasticity underlying beneficial processes and transformation of these phenomena into paroxysmal activity under some circumstances.[37]

[37] Synaptic plasticity, such as long-term potentiation and depression, has been studied in both hippocampus and neocortex, and was most readily observed when the inhibition was minimized (reviewed in Gilbert, 1998, p. 476), an experimental condition under which different forms of paroxysmal activities may be generated (Steriade, 2003a).

6.3.1 Intrathalamic, intracortical and intact thalamocortical circuits

Probably the best elucidated neuronal substrates of thalamically generated rhythms are those underlying sleep spindles (see Section 6.1.1). The experimental model of this oscillation is the sequence of augmenting (or incremental) responses, classically defined as thalamically evoked cortical potentials that grow in size during the first stimuli at a frequency of 5–15 Hz, usually around 10 Hz, like the waxing of waves at the onset of spontaneously occurring spindle sequences (Morison & Dempsey, 1942). However, similar incremental responses can be evoked in the thalamus by stimulating the cortex within the frequency of spindle waves. Augmentation can also occur in the thalamus of decorticated animals (Steriade & Timofeev, 1997) (see Figure 6.16A,B), in the intact cortex of athalamic preparations (Steriade *et al.*, 1993f) as well as in cortical slices maintained *in vitro* (Castro-Alamancos & Connors, 1996). However, the full development of augmenting responses, leading to self-sustained activities, requires interacting thalamic and cortical networks (Steriade *et al.*, 1998c).

The long-standing idea that incremental responses are of two basically different types, augmenting and recruiting, implied

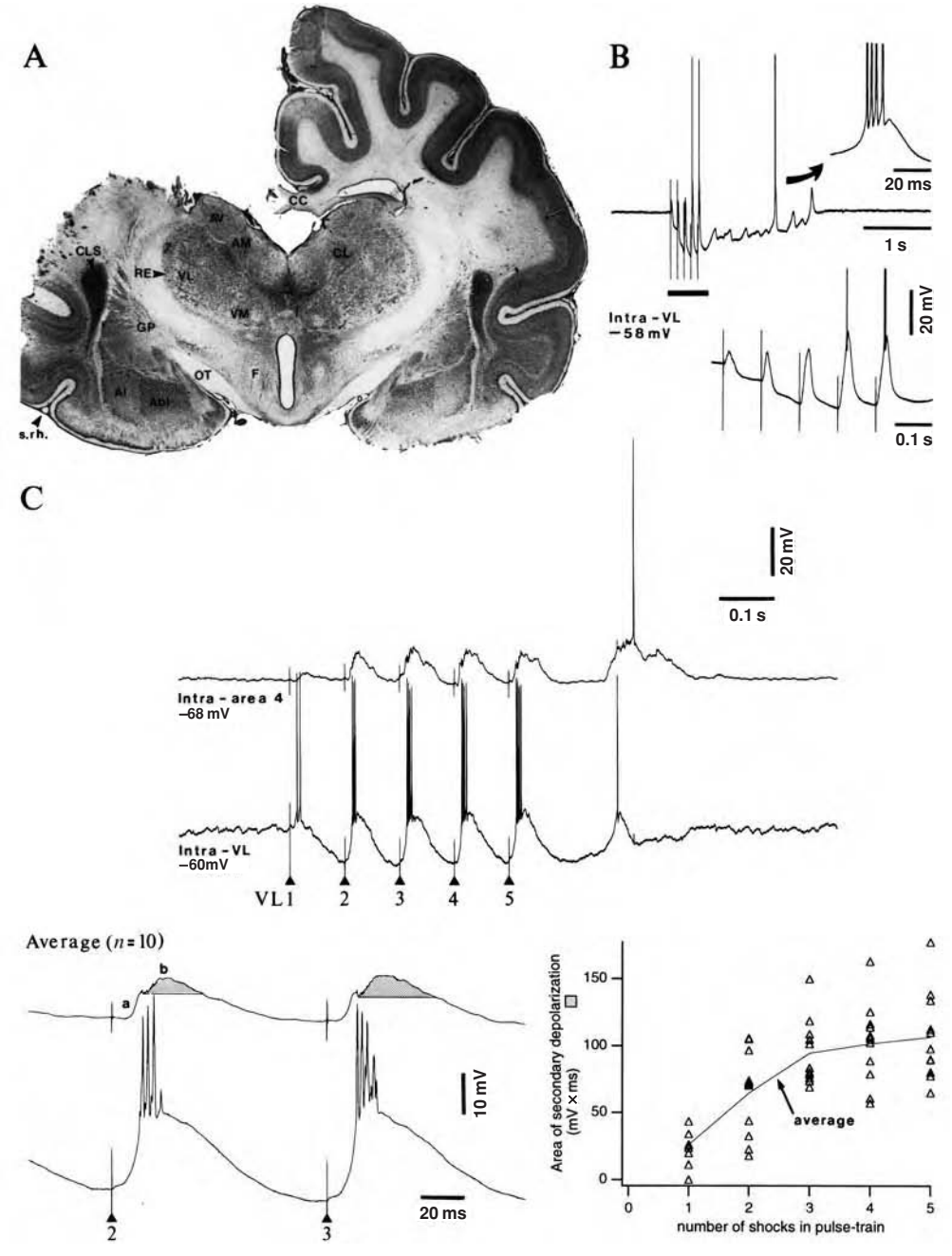

Fig. 6.16 Augmenting responses in thalamic neurons and in thalamocortical systems. (A) Hemidecortication (ipsilateral to thalamic recordings) and cut of corpus callosum. Nissl-stained section. Abbreviations: AV, AM, CL, RE, VL and VM, anteroventral, anteromedial, centrolateral, reticular, ventrolateral and ventromedial thalamic nuclei; CA, caudate nucleus; CC, corpus callosum; F, fornix; AI and Abl, lateral and basolateral nuclei of amygdala; CLS, claustrum; GP, globus pallidus; OT, optic tract; s.rh., rhinal sulcus (arrowhead). (B) Intrathalamic augmenting responses in decorticated cat (see A). Intracellular recordings from the thalamic ventrolateral (VL) nucleus under ketamine–xylazine anaesthesia show low-threshold augmenting responses of VL cells

that augmenting responses are surface-positive and elicited in localized neocortical areas by stimulation of 'specific' thalamic nuclei, whereas recruiting responses are surface-negative and elicited by stimulation of 'non-specific' thalamic nuclei. The longer latency of recruiting responses suggested a 'diffuse multineuronal system', with intralaminar nuclei serving as an intrathalamic association system (Jasper, 1949). However, there are virtually no direct pathways linking different dorsal thalamic nuclei[38] and the longer latency of cortical recruiting responses is not due to the intrathalamic spread of activity but to slower conduction velocities of axons from some thalamic nuclei projecting directly to superficial layers of the neocortex, such as the ventromedial nucleus (Glenn *et al.*, 1982). In fact, some recruiting (surface-negative, depth-positive) incremental responses may display latencies as short (4 ms) as those of augmenting responses (see Figure 4 in Steriade *et al.*, 1998b). Then, there are no pure augmenting or recruiting responses and most are mixed responses, due the multilaminar distribution of thalamic projections to cortex. For example, incremental responses evoked by rhythmic stimulation of rostral intralaminar nuclei are of the recruiting type in one cortical area and of the augmenting type in another area of the same gyrus (see again Figure 4 in Steriade *et al.*, 1998b), because intralaminar nuclei project preferentially to layer I but also to deep layers. Then, such responses mimicking spindles should all be termed incremental or augmenting.

That the cerebral cortex is not the only site of plastic operations, but also the thalamus, and that there are thalamic contributions to plasticity in various neocortical sensory and association areas, has been repeatedly shown (Steriade & Timofeev, 1997; Steriade

[38] There are no direct connections between dorsal thalamic nuclei but some thalamic nuclei may communicate through thalamocortical and corticothalamic projections or via an intermediate link in the thalamic RE nucleus (Steriade *et al.*, 1997). For example, Crabtree *et al.* (1998) showed that cells in the thalamic ventroposterior complex influence cells in the thalamic posterior complex through a disynaptic pathway involving GABAergic neurons in the RE nucleus.

←

developing from progressive increase in IPSP-rebound sequences and followed by a self-sustained spindle. Arrow indicates expanded spike-burst (action potentials truncated). The part marked by a horizontal bar and indicating augmenting responses is expanded at right. During thalamically evoked augmenting responses, the cortical augmented component (secondary depolarization, b) follows the rebound spike-burst in the thalamocortical neuron, and the depolarization area in the cortical neuron increases as a function of number of action potentials in the rebound spike-burst of the thalamocortical cell. (C) Dual intracellular recording from cortical area 4 and thalamic ventrolateral (VL) nucleus in cat under ketamine–xylazine anaesthesia. Below, average of second and third responses in cortical and VL cells. The area of secondary depolarization in the cortical neuron (b), which develops during augmentation, is marked by dots. Right, area of secondary depolarization of cortical cells as a function of the number of stimuli in the pulse-trains (the line represents the mean). In a sample of 92 cells, the maximum number of fast spikes of thalamocortical cells triggered by the LTS occurred at the third to the fifth stimulus. After having reached the maximum, the number of spikes in thalamocortical cells could decrease. The area of secondary depolarization of cortical cells also reached levels close to saturation at stimuli 3–5; however, the decrease in the depolarizing area in cortical cells was only exceptionally observed. This suggests that high levels of cortical excitability may be maintained by intracortical mechanisms. Modified from Steriade & Timofeev (1997, A, B) and Steriade *et al.* (1998c, C).

et al., 1998b; Jones & Pons, 1998; Jones, 2000). Sleep spindles and their experimental models, incremental responses, give rise to synaptic plasticity in the thalamus, even in decorticated animals (Steriade & Timofeev, 1997; Timofeev & Steriade, 1998) (Figure 6.16A, B). There are two forms of augmenting potentials. One of them is the low-threshold incremental responses that develop with progressively increased IPSPs and postinhibitory rebound excitations in TC neurons (Steriade & Timofeev, 1997) (Figure 6.16B). It is produced by incremental responses of RE neurons at a high intensity of thalamic stimulation (Timofeev & Steriade, 1998). Computational studies showed that the essential mechanisms needed for the generation of low-threshold intrathalamic augmenting responses are the transient T-current de-inactivated by membrane hyperpolarization and $GABA_B$-receptor-mediated inhibition of TC cells (Bazhenov *et al.*, 1998a). The other type of intrathalamic incrementation depends on high-threshold responses to thalamic stimuli and occurs at a depolarized level of TC neurons, due to decreasing responses in GABAergic RE neurons. Prolonged, rhythmic thalamic stimulation eliciting high-threshold potentials leads to persistent and progressive increases in depolarizing synaptic responses and decreases in inhibitory responses of TC neurons (Steriade & Timofeev, 1997). These responses depend on the activation of high-threshold Ca^{2+} channels (Hernández-Cruz & Pape, 1989; Kammermeier & Jones, 1997). The augmentation phenomenon can be observed in thalamic regions quite remote from the stimulated nucleus by recruitment of TC neurons through the lateral connectivity between GABAergic RE neurons. However, stimulation of prethalamic pathways fails to induce augmenting responses because such volleys do not directly activate RE neurons (Bazhenov *et al.*, 1998b).

In the intact brain, dual intracellular recordings of TC and cortical neurons demonstrated that augmenting responses evoked by rhythmic (10 Hz) thalamic stimulation are characterized in cortical neurons by an increase in the secondary depolarization, at the expense of the primary EPSP (Steriade *et al.*, 1998b) (Figure 6.16C). With intact cortex, only low-threshold thalamic augmenting responses are found (see also Figure 6.17a), because of the much stronger impact of corticothalamic projections on RE, compared with TC, neurons (Golshani *et al.*, 2001; Jones, 2002). In these conditions, the direct cortical excitation of TC cells is overwhelmed by their synaptic inhibition via the cortical excitation of GABAergic RE neurons (see Figure 1 in Steriade, 2000). During low-threshold augmenting responses, the secondary depolarization in neocortical neurons follows by *c.*3 ms the postinhibitory spike-burst in simultaneously recorded TC neurons (Figure 6.16C). Another factor that may account for the increased amplitude of the secondary depolarizing component during augmentation is the activation of local-circuit cortical interneurons by progressively stronger volleys from TC neurons, which would hyperpolarize pyramidal neurons and de-inactivate the Ca^{2+}-dependent low-threshold current in these neurons (Kawaguchi, 1993; de la Peña &

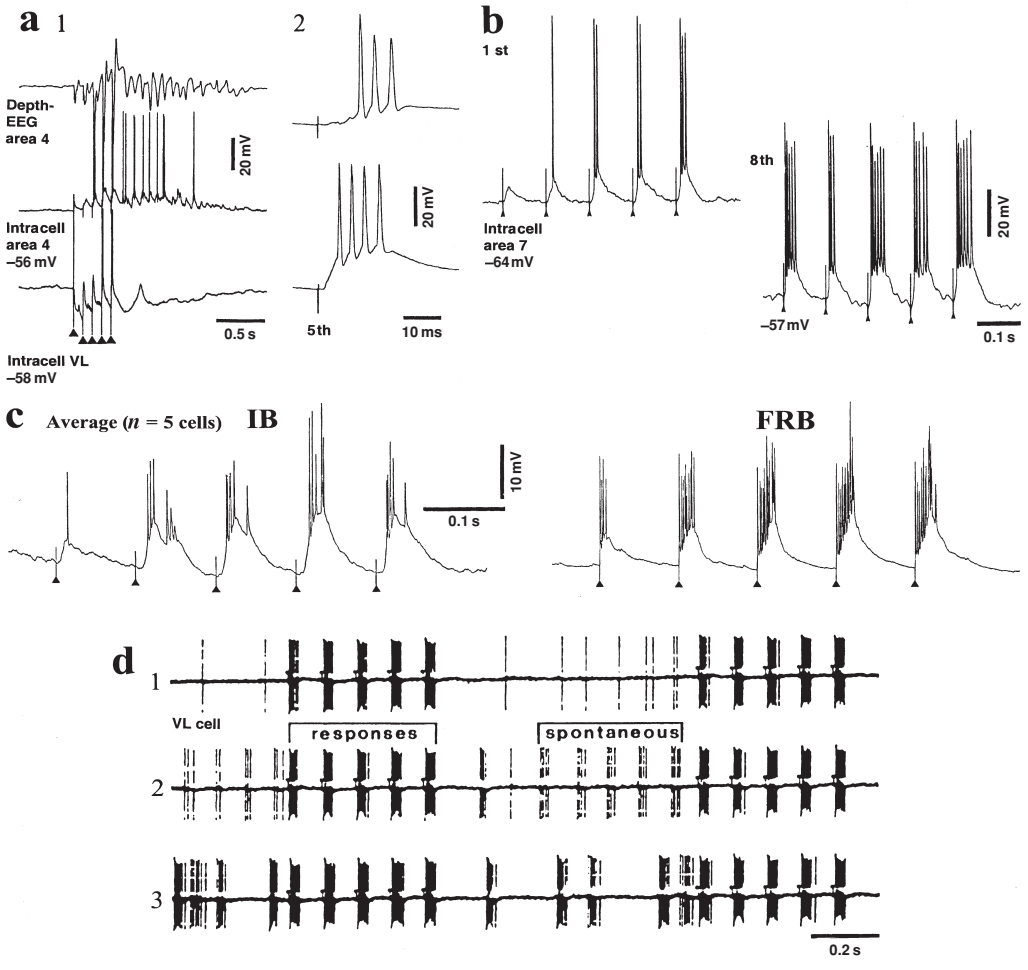

Fig. 6.17 Neuronal plasticity induced by low-frequency stimuli mimicking sleep spindles. (a) Dual simultaneous intracellular recordings from cortical and thalamocortical neurons in cat under barbiturate anaesthesia (top trace, depth-EEG from area 4). 1, Pulse-train (five stimuli at 10 Hz, arrowheads) applied to the thalamic ventrolateral (VL) nucleus produced augmenting responses in the cortical neuron, whereas the simultaneously recorded VL neuron displayed hyperpolarization. 2, Expanded fifth response; the augmented response in the cortical neuron followed the rebound spike-burst of the VL neuron. Note self-sustained oscillatory activity at 10 Hz in the cortical neuron after cessation of thalamic stimuli, despite persistent hyperpolarization in the VL neuron. (b) Cat under urethane anaesthesia. Intracellular responses of area 7 bursting cortical neuron to repetitive callosal stimulation (10 Hz). The ipsilateral thalamus was extensively lesioned by using kainic acid (see histology in Figure 10*A* of Steriade *et al.*, 1993f). The intracortical augmenting responses to the first and eighth pulse-trains are illustrated. Note depolarization by about 7 mV and increased number of action potentials within bursts after repetitive stimulation. (c) Intracellular recordings of thalamically evoked augmenting responses in IB and FRB neurons (averages of 5 neurons below 0.8 mm) of cats under barbiturate anaesthesia. (d) Extracellular recording of VL neuron in brainstem-transected cat. Motor cortex stimulation with pulse-trains at 10 Hz (stimuli are marked by dots). 1, The pattern of responses in thalamic VL neuron in early stages of rhythmic pulse-trains. 2, 3, Responses at later stages of stimulation. Note appearance of spontaneous spike-bursts resembling the evoked ones, as a form of 'memory' in the corticothalamic circuit. (a, c) Modified from Steriade & Timofeev (2001); (b) Modified from Steriade *et al.* (1993f); (d) modified from Steriade (1991).

Geijo-Barrientos, 1996), thus enhancing augmented waves. The role of cortical inhibitory interneurons in augmenting responses was also shown in a modelling study (Bazhenov *et al.*, 1998b).

Augmenting potentials leading to synaptic plasticity may take place within the neocortical circuitry in the absence of the thalamus as well as during prolonged inhibition of TC neurons. Thus, in thalamectomized animals, rhythmic stimulation of the callosal pathway within the frequency range of spindle waves eventually leads to depolarization and a significant increase in the number of action potentials in the evoked spike-bursts (Figure 6.17b). In addition, cortical augmenting responses to thalamic stimulation and self-sustained activity within the frequency range of augmenting potentials occur despite the fact that, simultaneously, TC neurons remain inhibited under the pressure of GABAergic RE neurons (Figure 6.18). Setting in action corticothalamic projections with protracted pulse-trains at 10 Hz results in evoked responses but also in 'spontaneously' occurring spike-bursts whose pattern and rhythmicity are similar to those of evoked responses, as if the repetition of volleys was imprinted in the 'memory' of the corticothalamic network (Figure 6.17d).

The preferential role played in augmentation by various cortical cell-classes, as defined electrophysiologically, was evaluated in different types of preparations. *In vitro* it was suggested that layer V intrinsically bursting (IB) neurons have the major role in the generation of augmenting responses (Castro-Alamancos & Connors, 1996). IB neurons are indeed implicated in augmenting responses generated by rhythmic stimulation of interhemispheric pathways (see Figure 6.17b), but fast-rhythmic-bursting (FRB) neurons recorded from deep cortical layers were also found to play the major role in cortical augmentation *in vivo* (Steriade & Timofeev, 2001) (Figure 6.17c). The crucial role played by FRB neurons in the widespread synchronization of augmenting responses results from thalamic projections of deeply lying cortical FRB neurons (Steriade *et al.*, 1998a) and feedback projections to the cortex, even towards areas that are remote from the site where the primary corticothalamic drive originates (Bazhenov *et al.*, 1998b; Kato, 1990). The difference between the results of *in vitro* and *in vivo* studies (namely, preferential role attributed to IB and FRB neurons, respectively) may be ascribed to the changing incidences of IB neurons in various experimental conditions: IB neurons may reach very high proportions (up to 40%–50%) in slices maintained *in vitro* (Yang *et al.*, 1996) or in cortical slabs prepared *in vivo* (Timofeev *et al.*, 2000), but the incidence of this neuronal type is lower in the intact cortex and, in naturally alert animals, IB neurons represent less than 5% of sampled neurons (Steriade *et al.*, 2001a).

The role of FRB neurons in synaptic plasticity is also emphasized by the effectiveness of callosal stimulation in eliciting short- and medium-term neuronal plasticity (Cissé *et al.*, 2004) and the fact that the amplitudes of callosally evoked EPSPs in FRB neurons are threefold larger, and their latencies two- to threefold shorter, than in all other neuronal types, including IB cells (Cissé *et al.*, 2003).

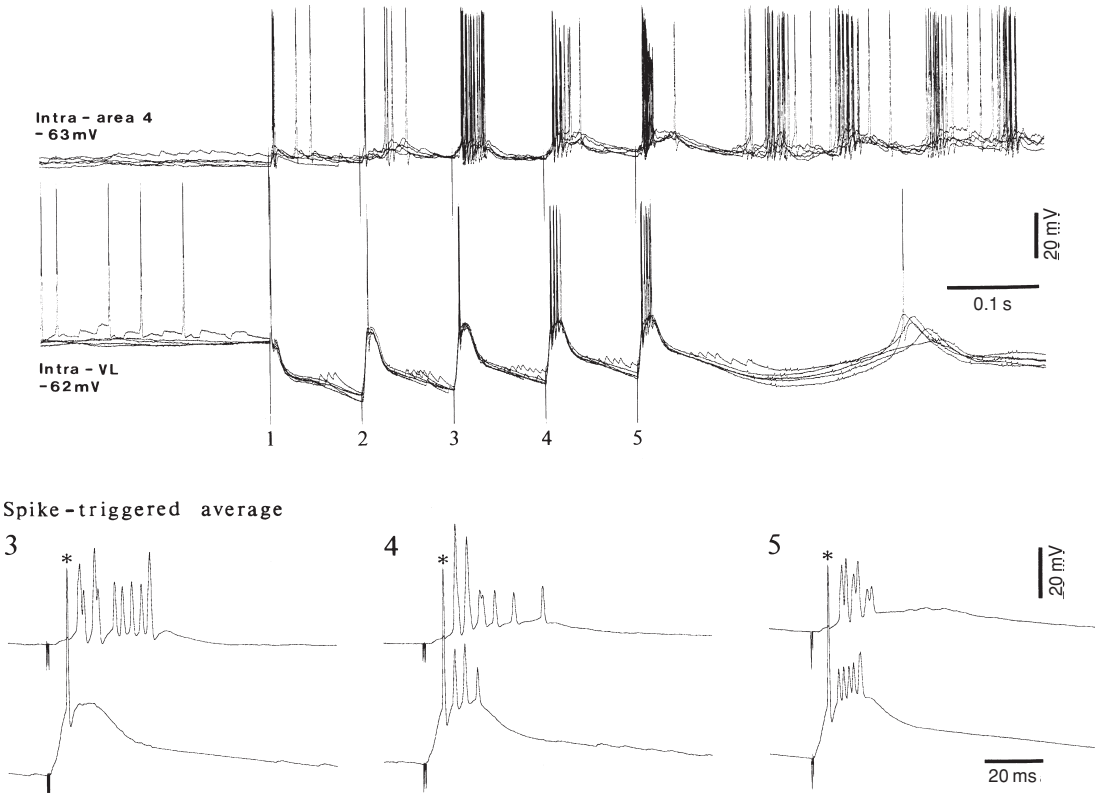

Fig. 6.18 Low-threshold augmenting responses in thalamocortical (TC) neuron precede cortical responses but cortical neuron displays self-sustained activity within the frequency range of augmenting responses whereas TC neuron remains hyperpolarized. Dual intracellular recordings from TC neuron in the VL nucleus and cortical neuron from area 4 in cat under ketamine–xylazine anaesthesia. Responses to 5-stimulus train at 10 Hz, applied to the VL nucleus. Spike-triggered averages of VL and cortical responses to third, fourth and fifth stimuli in the train (first action potentials in spike-burst of TC cell, marked by asterisks, triggered the average). Note self-sustained activity in cortical neuron, following augmentation, whereas TC neuron remained hyperpolarized because of inputs from GABAergic thalamic reticular neurons. Unpublished data by M. Steriade, I. Timofeev & F. Grenier. See also Steriade *et al.* (1998c).

Homosynaptic potentiation occurred following rhythmic pulse-trains at low-frequencies (10–20 Hz) applied to homotopic sites in the contralateral cortex, and the response potentiation lasted 5–30 min (Figure 6.19). Neurons tested with successive conditioning pulse-trains at different frequencies displayed stronger enhancement with high-frequency (40–100 Hz) than with low-frequency (10–20 Hz) rhythmic pulse-trains; above 100 Hz, the potentiation saturated. To test the possible participation of NMDA receptors in the callosally evoked potentiation of EPSPs (Kumar & Huguenard, 2001), neurons were recorded before and after microdialysis of AP-5, an NMDA receptor blocker. AP-5 suppressed the potentiation (Figure 6.20). Potentiation of callosally evoked EPSPs was not detected in neurons recorded under

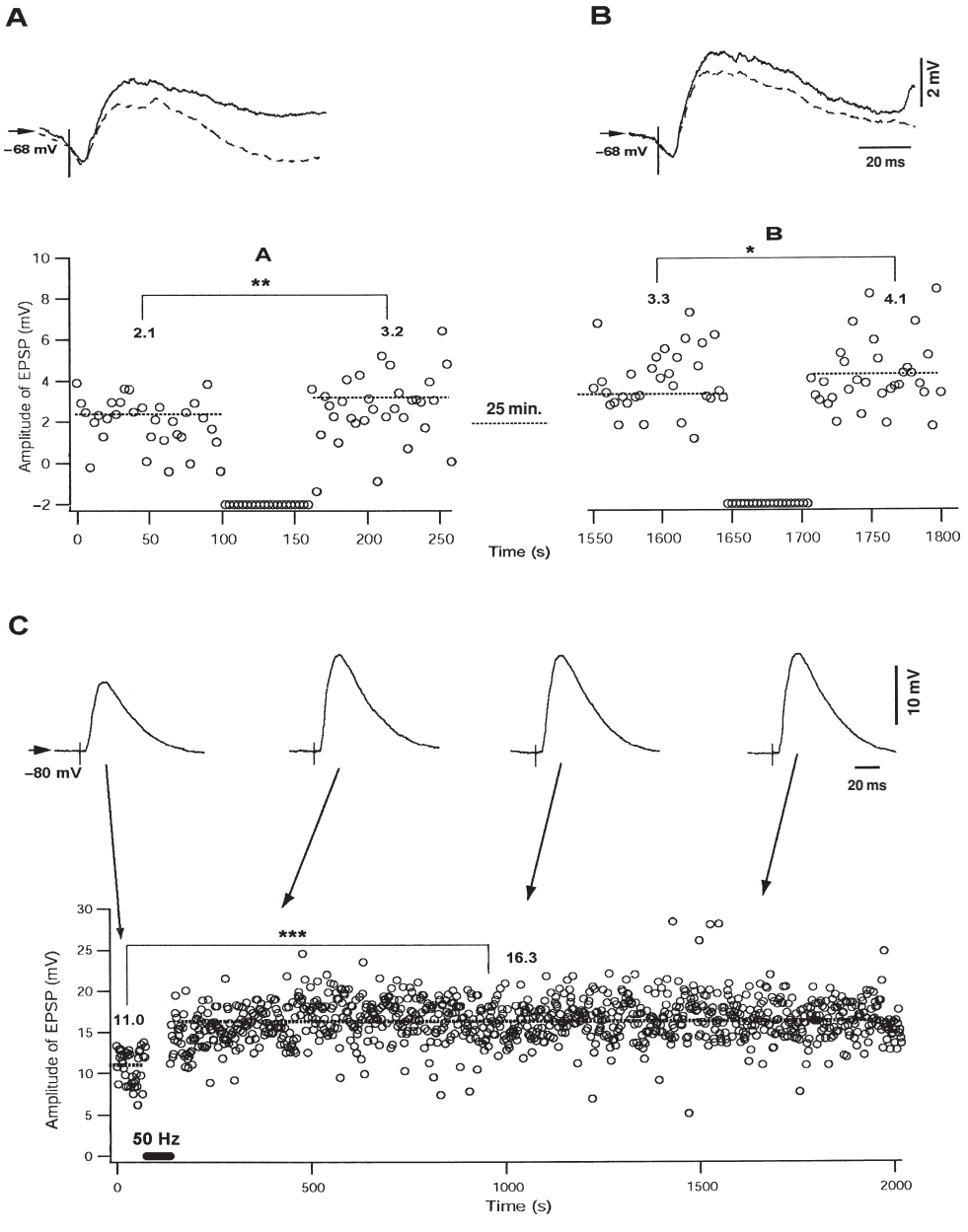

Fig. 6.19 Persistent (*c.*30 min) facilitation of tested EPSPs to callosal pathway after 10 Hz and 50 Hz. (A–B) and (C) Two regular-spiking (RS) neurons. Cat under barbiturate anaesthesia. Single and rhythmic pulse-train stimulation applied every 3 and 2 s. (A) Superimposed averaged ($n = 20$ sweeps) control responses (dotted line) and responses after conditioning stimulation at 10 Hz (continuous line). The initial negativity is interpreted as intracellular reflection of the field potential. (B) The same arrangement with conditioning pulse-train stimulation applied at 40 Hz. Bottom panel, amplitude (ordinate) of callosally evoked EPSPs in the control condition (before rhythmic pulse-trains were applied, mean 2.4 mV) and after 10 Hz stimuli (mean 3.2 mV), as well as in the control condition (*c.*25 min) after 10 Hz stimuli (mean 3.3 mV; residual facilitation after conditioning pulse-trains at 10 Hz), followed by responses to 40 Hz stimuli, and after 40 Hz stimuli (mean 4.1 mV). No stimulation was applied during the interval (*c.*25 min). (C) EPSP amplitudes before and after pulse-trains at 50 Hz. Above, averaged EPSPs ($n = 30$ sweeps) evoked by stimulating the homotopic site in the contralateral area 5; arrows indicate their corresponding level in the plot. Note the sustained potentiation after the conditioning for (*c.*30 min). The statistical tests are shown (*t*-test: *, $p < 0.5$; **, $p < 0.01$; ***, $p < 0.001$). Modified from Cissé *et al.* (2004).

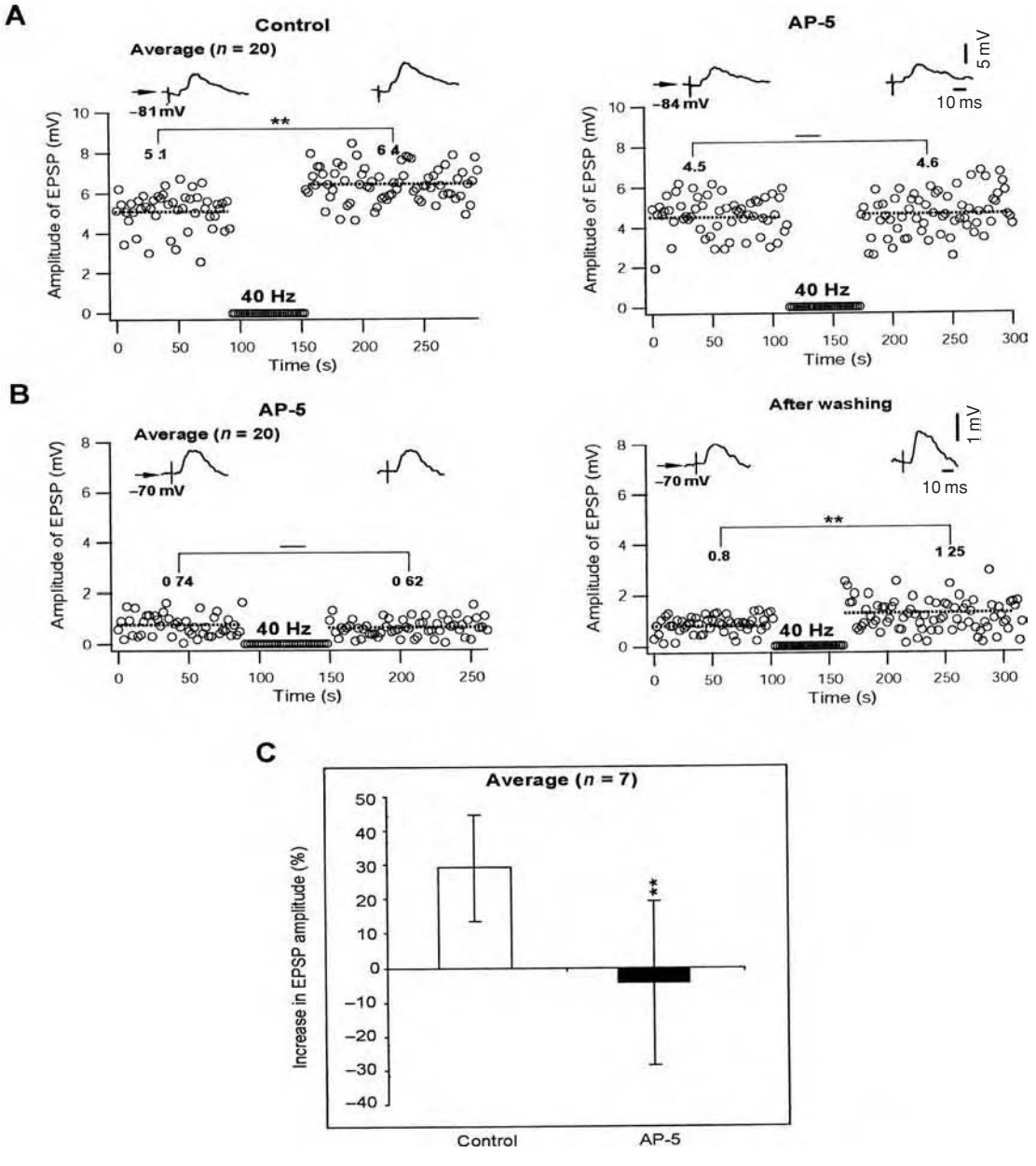

Fig. 6.20 Potentiation of callosally evoked EPSPs is dependent on NMDA receptors. Cat under barbiturate anaesthesia. (A, B) Two RS neurons. (A) Left, EPSP amplitudes before and after pulse-trains at 40 Hz during the control condition (without AP-5). Above, averaged EPSPs ($n = 20$ sweeps) evoked by stimulating the homotopic site in the contralateral area 5. Right, same arrangement during AP-5 microdialysis. (B) Left, another neuron recorded shortly within the same track, during the continuing AP-5 microdialysis. Right, after washing. (C) Callosally evoked EPSPs were measured after rhythmic pulse-trains at 40–50 Hz and compared with control EPSPs for each neuron ($n = 7$) to evaluate the facilitation in percentage during control and during AP-5 microdialysis. The statistical tests are shown (*t*-test, **, $p < 0.01$, –, not significant). Modified from Cissé *et al.* (2004).

[39] After training on a declarative learning task, the density of human sleep spindles is significantly higher, compared with the non-learning control task (Gais *et al.*, 2002).

ketamine–xylazine anaesthesia (which blocks NMDA receptors), thus indicating that the potentiation of EPSPs implicates, at least partly, NMDA receptors. The homosynaptic potentiation induced through the callosal pathway at all conditioning frequencies between 10 and *c.*200 Hz (Cissé *et al.*, 2004) stands in contrast to the depression in neocortical neurons when using heterosynaptic (cortical and thalamic) paired stimuli at intervals shorter than 50 ms (Fuentealba *et al.*, 2004c).

Most of the data discussed above were related to synaptic plasticity in thalamic, neocortical and corticothalamic systems during and following low-frequency (around 10 Hz) stimulation eliciting incremental responses within the frequency of sleep spindles. Synaptic plasticity induced by augmenting responses recorded in cortical slabs *in vivo* was compared with the plasticity that develops from natural spindles in intact-brain preparations (Timofeev *et al.*, 2002b). In isolated slabs, the greatest increase in the amplitude of depolarization and the most dramatic increase in the number of action potentials with successive stimuli at 10 Hz was found in fast-spiking (FS), presumably local inhibitory, neurons. In the intact brain, cortical stimuli applied during the depolarizing envelope of spindle sequences elicited an enhancement of the control response, which lasted from tens of seconds to several minutes (Timofeev *et al.*, 2002b). One mechanism that may explain this increased responsiveness is the high-frequency firing in response to rhythmic, repeated pulse-trains at 10 Hz, which would result in activation of high-threshold Ca^{2+} currents and enhanced $[Ca^{2+}]_I$ that, in association with synaptic volleys reaching the neuron, might activate protein kinase A (Abel *et al.*, 1997) and/or Ras/mitogen-activated protein kinase (Dolmetsch *et al.*, 2001), which are involved in memory consolidation. Thus, besides their role in cortical disconnection through inhibition of incoming messages in the thalamus (reviewed in Steriade *et al.*, 1997; Steriade, 2003a), spindles are also involved in important cerebral functions. During spindles, the rhythmic and synchronized spike-bursts of thalamic neurons depolarize the dendrites of neocortical neurons; this process is associated with massive Ca^{2+} entry (Yuste & Tank, 1996) that may provide an effective signal to efficiently activate Ca^{2+} calmodulin-dependent protein kinase II (CaMKII), which is implicated in synaptic plasticity of excitatory synapses in the cortex and other sites in the nervous system (Soderling & Derkach, 2000; see also this hypothesis in Sejnowski & Destexhe, 2000).

The experimental data and ideas that sleep spindles are associated with synaptic plasticity are supported by human studies demonstrating that the overnight improvement of discrimination tasks requires some steps, including those in early slow-wave sleep stages (Stickgold *et al.*, 2000a,b). In addition, potentiation of procedural memory formation may be associated with oscillations during early sleep stages (Gais *et al.*, 2000).[39]

Similar phenomena, with Ca^{2+} entry in dendrites and somata of cortical neurons, may occur during the rhythmic spike-trains associated with oscillations in the slow (0.5–1 Hz) or delta (1–4 Hz) frequency

bands, during later stages of slow-wave sleep. It was hypothesized that the slow oscillation is responsible for the consolidation of memory traces acquired during the state of wakefulness (Steriade *et al.*, 1993b). Sleep associated with oscillations within the frequency range of slow and delta (0.5–4 Hz) oscillations was demonstrated to be implicated in cortical plasticity evoked by monocular deprivation in the developing visual cortex (Frank *et al.*, 2001). Microelectrode recording and optical imaging showed that the effects of monocular deprivation on cortical responses are increased by a 6 h slow-wave sleep period in the dark; slow-wave sleep deprivation blocked this enhancement.

6.3.2 Amygdala, perirhinal cortex and medial prefrontal cortex

In neuroscience, probably no line of investigation has received as much attention as the cellular substrates of memory. Activity-dependent synaptic plasticity, with its best known example, NMDA-dependent long-term potentiation (LTP), has become the prevalent cellular model of memory (Bliss & Collingridge, 1993; Malenka & Nicoll, 1993). In the most studied form of LTP, as observed at hippocampal CA3 to CA1 synapses, depolarization produced by converging synaptic inputs lessens the blocking of postsynaptic NMDA receptors by Mg^{2+} ions, allowing Ca^{2+} entry into target neurons. It is commonly believed that this signal ultimately leads to the addition of new (Durand *et al.*, 1996; Shi *et al.*, 1999; W. Lu *et al.*, 2001) and/or phosphorylation of existing AMPA receptor subunits (Barria *et al.*, 1997; Lee *et al.*, 2000). Behind this well-known mechanism however, is a complex reality where numerous forms of activity-dependent LTP are observed in different classes of neuron, at different inputs to the same neurons, or depending on the way these inputs are stimulated.

This section summarizes the various forms of activity-dependent synaptic plasticity that have been observed in the amygdala, perirhinal cortex and medial prefrontal cortex. In these three instances, the impetus for studying this issue was to understand the cellular substrates of the forms of memory in which these structures participate.

Amygdala

Various lines of evidence implicate the amygdala in the acquisition of classically conditioned fear responses (Davis, 2000; LeDoux, 2000a). In this model, an innocuous sensory stimulus (conditioned stimulus, CS) is paired with a noxious unconditioned stimulus (US). As a result of the CS–US pairing, the CS acquires the ability to elicit fear responses when it is subsequently presented in isolation. As will be described in detail in Chapter 9, much data suggests that the acquisition of conditioned fear responses involves a potentiation of synapses conveying CS information (from the thalamus and/or cortex) to the amygdala.[40] Because most sensory inputs first reach the amygdala in its lateral nucleus, most studies of activity-dependent plasticity have initially focused on this structure. However, recognition that the lateral nucleus does not project to the main output structure of the

[40] There has been much debate on the nature of the amygdala's involvement in classical fear conditioning (Cahill *et al.*, 1999; Fanselow & LeDoux, 1999). Some believe that it is a critical site of plasticity; others, that it is only an essential relay of CS inputs to structures mediating fear responses. In our opinion, because the amygdala is interposed between the input and output stages of the network mediating this form of learning, it may never be possible to ascertain whether plasticity in the amygdala is necessary and sufficient. Yet it is undeniable that fear conditioning produces activity-dependent plasticity in the amygdala. Thus, it is probably safest to assume that fear conditioning produces widely distributed plasticity.

amygdala, the central nucleus, has recently led to an extension of these efforts to the central nucleus. These studies are reviewed in turn below.

It was first reported that high-frequency stimulation of cortical (Chapman *et al.*, 1990) or thalamic (Clugnet & LeDoux, 1990) inputs produces a long-term enhancement of evoked responses in the lateral nucleus of the amygdala. Although both forms of LTP required a rise in intracellular Ca^{2+} concentration in principal cells, the thalamic LTP appeared to depend on L-type Ca^{2+} channels (Weisskopf *et al.*, 1999) whereas the cortical LTP was dependent, at least in part, on NMDA receptors (Maren & Fanselow, 1995; Huang & Kandel, 1998; but see Chapman & Bellavance, 1992).

The relevance of these observations for Pavlovian fear learning was reinforced by several reports. First, it was shown that high-frequency stimulation of the thalamic medial geniculate nucleus produced a long-term potentiation of auditory-evoked responses (Rogan & LeDoux, 1995). Second, it was reported that auditory fear conditioning was accompanied by an enhancement of auditory-evoked CS responses in the lateral amygdala (Quirk *et al.*, 1995; Rogan *et al.*, 1997). Last, several studies strengthened the links between fear conditioning and slice studies of LTP. For instance, it was shown that fear conditioning produces an enhancement of responses elicited by thalamic inputs in the lateral amygdala *in vitro* (McKernan & Shinnick-Gallagher, 1997). Moreover, fear conditioning was found to occlude LTP of cortical inputs to the lateral nucleus (Tsvetkov *et al.*, 2002). Third, it was shown that fear conditioning and LTP induction in the lateral amygdala are sensitive to the same stimulus contingencies (Bauer *et al.*, 2001).

The past few years have witnessed two interesting developments: (a) insights in the regulation of LTP by inhibitory interneurons, and (b) the realization that the induction and/or expression mechanisms of LTP vary significantly depending on the induction protocol and stimulated pathways. With respect to the first point, it was shown early on that cortical inputs to fast-spiking interneurons of the lateral nucleus could undergo LTP following tetanic stimulation (Mahanty & Sah, 1998), resulting in an increase in the amplitude of $GABA_{A\text{-}B}$ IPSPs in principal cells.[41] Given the importance of depolarization for Ca^{2+} entry via NMDA receptors and voltage-gated Ca^{2+} channels, this observation raised the possibility that inhibitory interneurons were in a position to regulate activity-dependent plasticity in principal cells of the lateral nucleus.[42] In keeping with this, recent studies showed that dopamine, by suppressing feedforward inhibition, can facilitate LTP induction in principal neurons of the lateral amygdala (Bissière *et al.*, 2003).[43]

With respect to the second theme, it was first shown that LTP of thalamic or cortical inputs can be induced not only by tetanic stimulation (Huang & Kandel, 1998) but also by pairing presynaptic activation with prolonged periods of postsynaptic depolarizations (Tsvetkov *et al.*, 2002, 2004). It was reported that this form of LTP (termed LTP_{POST}) is induced by the activation of postsynaptic NMDA receptors *and*

[41] This LTP was dependent on a postsynaptic rise in Ca^{2+} concentration mediated through Ca^{2+}-permeable AMPA receptors. In a subsequent study (Bauer & LeDoux, 2004), it was reported that tetanization of thalamic inputs could produce LTP in both the tetanized thalamic and untetanized cortical pathway.

[42] The reader is reminded that principal cells of the lateral nucleus of the amygdala are subjected to powerful inhibitory pressures. Indeed, principal cells fire at extremely low rates in unanaesthetized animals (Bordi *et al.*, 1993; Gaudreau & Paré, 1996; Paré & Gaudreau, 1996). Physiological studies suggest that both synaptic ($GABA_{A\text{-}B}$) (Rainnie *et al.*, 1991; Washburn & Moises, 1992b) and synaptically activated intrinsic Ca^{2+}-dependent K^+ conductances (Lang & Paré, 1997a,b; Danober & Pape, 1998; Chen & Lang, 2003) contribute to limit their orthodromic responsiveness. Intracellular recording *in vivo* coupled to pharmacological manipulations suggest that intermediate conductance K^+ channels are particularly involved in regulating the synaptic excitability of projection cells (Chen & Lang, 2003).

[43] A previous study had shown that dopamine receptor activation could facilitate LTP induction in the lateral amygdala but the site(s) and mechanism(s) of action remained unspecified because systemic drug injections were used (Rosenkranz & Grace, 2002).

L-type voltage-gated Ca^{2+} channels, but that it is expressed presynaptically, by an increased probability of transmitter release (Tsvetkov *et al.*, 2002). Moreover, specificity of the pairing-induced LTP was found to be dependent on rapid glutamate uptake (Tsvetkov *et al.*, 2004). That is, drugs that block glutamate uptake during induction abolish the input specificity of the LTP.

Next, it was shown that *presynaptic* NMDA receptors could also lead to a form of LTP (termed LTP_{PRE}) in some conditions. Indeed, it was shown (Humeau *et al.*, 2003) that repetitive activation of thalamic and cortical inputs to principal neurons of the lateral nucleus *in vitro* produces LTP of cortical but not thalamic inputs. Activation of either pathway in isolation had no effect, indicating that this form of LTP is associative. Although this LTP is NMDA-dependent (i.e. blocked by AP-5), it was found to be independent of postsynaptic activity.[44] These results suggested that glutamate released by thalamic axons activated presynaptic NMDA receptors located on cortical axon terminals and that thalamic inputs did not express LTP_{PRE} because they lack presynaptic NMDA receptors. But if this were true, it remained unclear why cortical stimulation alone did not induce LTP_{PRE}. However, pharmacological inhibition of glutamate uptake enabled repetitive cortical stimulation to produce LTP, suggesting that the rapid clearing of glutamate from the extracellular space was responsible. Finally, evidence was provided (Humeau *et al.*, 2003) that expression of this novel form of LTP depends on an increased release probability by cortical axon terminals. Indeed, LTP_{PRE} induction was associated to decreased amounts of paired pulse facilitation, a phenomenon commonly believed to reflect synaptic release probability. Moreover, LTP_{PRE} was occluded when release probability was artificially increased by raising the extracellular Ca^{2+} concentration. To add to this complexity, a recent study by the same group (Humeau *et al.*, 2005) revealed that, for LTP_{POST}, different induction and expression mechanisms are recruited depending on the features of the pairing protocol and the identity of the stimulated afferents. For instance, whereas the study mentioned above (Humeau *et al.*, 2003) showed that cortical LTP could be induced independent of postsynaptic activity, the same group reported that activation of cortical inputs during prolonged (but not brief) postsynaptic depolarization could produce a form of LTP that occluded the induction of LTP_{PRE}, suggesting that both LTP_{PRE} and LTP_{POST} converged on a common presynaptic expression mechanism. This form of LTP was dependent on both NMDA receptor activation and activation of L-type channel for its induction. In contrast, thalamic LTP could be induced by pairing of presynaptic activity with brief *or* prolonged periods of depolarization. Interestingly, both forms of thalamic LTP required multiple sources of postsynaptic Ca^{2+} for their induction, including activation of NMDA receptors as well R- and L-type voltage-gated Ca^{2+} channels. The authors also provided evidence that the dependence of thalamic, but not cortical, LTP on R-type Ca^{2+} channels resulted from the fact that these voltage-gated Ca^{2+} channels

[44] That is, it developed even when postsynaptic cells were kept hyperpolarized, when intracellular Ca^{2+} was chelated, or when postsynaptic NMDA receptors were blocked by intracellular dialysis with MK-801, a NMDA open channel blocker.

are preferentially concentrated in spines receiving thalamic afferents. Last, the thalamic LTP produced by pairing presynaptic activation and brief depolarizations did not appear to be expressed presynaptically.

It is puzzling that there are so many forms of LTP in principal neurons of the lateral amygdala. A challenge for future studies will be to determine which form(s) of LTP is (are) used to support learning in behaving animals. In the mean time, the fact that the lateral nucleus does not send axons to brainstem projecting neurons of the central nucleus, has led some to investigate whether activity-dependent plasticity is also present in this output structure of the amygdala.

One study (Samson & Paré, 2005) tested whether thalamic inputs to central medial amygdala neurons could undergo activity-dependent plasticity. High-frequency stimulation of thalamic inputs led to a long-lasting potentiation of thalamic responses, whereas responses elicited by control basolateral stimuli remained unchanged. This thalamic LTP could be elicited after disconnection of the central medial nucleus from the rest of the amygdala, but was largely reduced when an NMDA receptor antagonist was added to the perfusate shortly before and during LTP induction. Yet, intracellular dialysis with MK-801 did not prevent induction of the thalamic LTP, suggesting that *presynaptic* NMDA receptors are required for its induction. Consistent with this, the thalamic LTP also developed when the cells were dialysed with a calcium chelator or kept hyperpolarized during induction. Last, this thalamic LTP was associated with reduced amounts of paired-pulse facilitation, suggesting that it is expressed presynaptically.

Another study (Fu & Shinnick-Gallagher, 2005) tested whether inputs from the lateral or basolateral nuclei to unspecified sectors of the central nucleus[45] could undergo activity-dependent potentiation. Although both inputs did, they required different sources of post-synaptic Ca^{2+} for their induction: L-type Ca^{2+} channels and NMDA receptors for the basolateral input, compared with only the latter for inputs from the lateral nucleus.

Rhinal cortices

Lesion and single-unit studies suggest that the perirhinal cortex plays an essential role in recognition memory (reviewed in Brown & Aggleton, 2001). Compared with hippocampal (Aggleton *et al.*, 1986; Mumby *et al.*, 1992) and entorhinal lesions (Meunier *et al.*, 1993; B. Leonard *et al.*, 1995), ablation of the perirhinal cortex produces marked impairments in tasks probing recognition memory (Zola-Morgan *et al.*, 1989; Gaffan & Murray, 1992; Meunier *et al.*, 1993, 1996; Suzuki *et al.*, 1993), particularly with long delays.[46] Consistent with this, single-unit recording studies in rats and monkeys have shown that a large proportion of perirhinal neurons display reduced responses to visual stimuli that have been presented previously, whether the animals were required to use the information to guide their behaviour or not (Brown *et al.*, 1987; Fahy *et al.*, 1993; Li *et al.*, 1993; Miller *et al.*, 1993; Sobotka & Ringo, 1993). These response decrements develop with a single-trial training, persist for a long time

[45] This is not a trivial issue, for the two following reasons. First, most brainstem projections of the central nucleus originate from its medial sector (Hopkins & Holstege, 1978). Second, the lateral nucleus has direct projections to the lateral sector of the central nucleus, but not to its medial portion. In contrast, the basolateral nucleus projects to both the medial and lateral sectors of the central nucleus (Krettek & Price, 1978b).

[46] Well-known examples of such tasks are the visual matching or non-matching to sample tasks where experimental subjects must make judgements regarding the prior occurrence of visual items that are presented infrequently across delays of various durations.

(more than 24 hours), are manifest within 90 ms of the stimulus presentation, and are much more frequently encountered in the perirhinal cortex (25% of cells) than in the hippocampus (1%) (Rolls *et al.*, 1989, 1993; Riches *et al.*, 1991; Colombo & Gross, 1994; Eichenbaum *et al.*, 1996; Xiang & Brown, 1998).

Because the latency of the response reductions is shorter in the perirhinal cortex than the changes observed in the hippocampus, prefrontal cortex, posterior visual areas and subcortical structures, it was proposed that the perirhinal cortex and adjacent inferior temporal areas generate this familiarity signal (Brown & Bashir, 2002). As a result, attention has focused on the activity-dependent plastic properties of synapses within the perirhinal cortex.

It was first reported that brief high-frequency afferent stimulation could produce an associative NMDA-dependent potentiation of evoked responses in the perirhinal cortex *in vitro* (Bilkey, 1996; Ziakopoulos *et al.*, 1999). This was not an artefact of the slice preparation, as LTP of hippocampus-evoked responses could also be induced *in vivo* following theta-burst stimuli delivered in field CA1 (Goosens & Otto, 1998). Later on, it was shown that, as had been reported in the hippocampus, local low-frequency stimulation (1 Hz) could produce a Ca^{2+}-dependent LTD or LTP of evoked responses, depending on the holding potential during induction (LTD at –70 mV; LTP at –10 mV) (Cho *et al.*, 2001).[47]

Subsequently, studies focused on LTD because of its suspected involvement in the familiarity-induced response depressions seen in studies of recognition memory. Interestingly, a close parallel was found between the effects of various drugs on recognition memory in behaving animals and how these drugs influenced LTD induction in slices. For instance, administration of the muscarinic antagonist scopolamine impaired recognition memory, reduced the familiarity-induced suppression of perirhinal firing, and blocked the induction of LTD but not LTP in perirhinal slices (Warburton *et al.*, 2003). Similarly, administration of benzodiazepines impaired both recognition memory and LTD (Wan *et al.*, 2004).

Medial prefrontal cortex

The involvement of the medial prefrontal cortex and hippocampal formation in learning and memory as well as the existence of reciprocal connections between them[48] has generated much interest in the idea of synaptic plasticity in this network. Several studies have provided evidence of activity-dependent plasticity in the hippocampal–prefrontal pathway. High-frequency stimulation of these afferents *in vivo* produces a response enhancement (Laroche *et al.*, 1990; Kim *et al.*, 2003) that can last for days in chronically implanted rats (Jay *et al.*, 1996) and depends on the activation of NMDA receptors for its induction (Kim *et al.*, 2003).[49] At odds with the neocortex and hippocampus (Bear & Abraham, 1996), however, low-frequency stimulation (1 Hz) of hippocampal afferents to the medial prefrontal cortex produces a response potentiation (Burette *et al.*, 1997), rather than a depression,

[47] The same group also provided evidence that group I and group II metabotropic glutamate receptors (mGluR) as well as NMDA receptors are required for LTD induction at –70 mV in the perirhinal cortex (Cho *et al.*, 2000). By contrast, group II mGluRs are not required when the LTD in induced from –40 mV, presumably because of the more important NMDA receptor activation at this more depolarized membrane potential. This dual requirement (mGluR plus NMDA) for LTD induction is unusual. Indeed, in most other systems, NMDA *or* mGluR receptors are required for LTD induction (Kemp & Bashir, 2001).

[48] In rats, cats and monkeys, both the subiculum and field CA1 send massive projections to the prelimbic, and to a lesser extent the infralimbic cortex (reviewed in Witter *et al.*, 1989). The return projection to the hippocampus proper is weaker and consists of a moderate projection to stratum lacunosum-moleculare. However, as discussed in detail in Chapter 4, the medial prefrontal cortex also contributes an important projection to rhinal cortices.

[49] Other cortical inputs to the prefrontal cortex can exhibit activity-dependent LTP. This is the case of inputs from the visual cortex (Kim *et al.*, 2003) and contralateral medial prefrontal cortex (Gemmell & O'Mara, 2000). In addition, it was reported that high- and low-frequency stimulation of the mediodorsal thalamic nucleus respectively produced LTP and LTD of thalamic inputs to the medial prefrontal cortex (Herry & Garcia, 2003).

unless short high-frequency trains at 1 Hz are used instead of isolated stimuli (Takita *et al.*, 1999).

Another line of research has focused on the effects of dopamine on activity-dependent plasticity of prefrontal inputs. The interest of this issue stems from data showing that dopaminergic neurons signal discrepancies between actual and anticipated rewards (reviewed in Schultz, 2002). Because the prefrontal cortex receives a strong dopaminergic input (Berger *et al.*, 1976) and is involved in working memory as well as the monitoring and planning of behavioural responses (reviewed in Fuster, 2004), it is believed that the dopaminergic signal is a key modulator of synaptic plasticity and learning.

As is typically the case with dopamine, divergent results were obtained depending on the experimental conditions (reviewed in Otani *et al.*, 2003). Studies *in vitro* seemed to indicate that dopamine facilitates LTD induction (Law-Tho *et al.*, 1995). In contrast, experiments *in vivo* have reported the opposite. Both local dopamine infusion and stimulation of the ventral tegmental area were reported to enhance LTP of hippocampal inputs to the prefrontal cortex (Jay *et al.*, 1996). Moreover, dopamine depletion resulting from lesions of the ventral tegmental area was reported to interfere with LTP expression (Gurden *et al.*, 1999).

The relevance of these observations for learning and memory was reinforced by studies that correlated synaptic efficacy in the hippocampal–prefrontal projection and learning. For instance, the acquisition of an associative learning task was reported to be associated with a delayed increase in the efficacy of hippocampal–prefrontal inputs (Doyère *et al.*, 1993). In another study, the largest changes in the efficacy of the hippocampal–prefrontal pathway were reported to coincide with maximal performance (Laroche *et al.*, 1995).

6.4 Memory consolidation and dreaming mentation during slow-wave sleep

Although some doubted that the answer to the question of sleep function would come from experiments on physiological processes (Rechtschaffen, 1998, p. 384), extra- and intracellular recordings in animals and more global (EEG, MEG) methods in humans have shown that slow-wave sleep oscillations have an important role in synaptic plasticity (see Section 6.3), supporting the idea that, sleep plays a role in the consolidation of memory traces acquired during wakefulness. However, acquisition of memory is not possible during sleep.[50]

Human data showed an overnight improvement of discrimination tasks that requires some steps, including those in early slow-wave sleep stages (Stickgold *et al.*, 2000a,b) (see also Section 6.3.1). The early part of night sleep favours retention of declarative memories (which can be brought to conscious recollection), whereas the late part of sleep favours retention of non-declarative (procedural, unconscious)

[50] Kleitman (1963) considered that learning during sleep is impossible (see other evidence supporting this view in Tononi & Cirelli, 2001) but, based on the study of Jenkins & Dallenbach (1924), he suggested that sleeping 'after memorizing suitable material favors retention'. This early idea was substantiated by many recent studies (see main text).

memories (Plihal & Born, 1997). These effects are probably due to the rhythmic bombardment of cortical neurons by high-frequency spike-bursts of thalamic neurons, as is the case in the spindle oscillations that occur mainly during the early part of nocturnal sleep, and the bursts of intracortical neurons during the slow oscillation that is pervasive throughout slow-wave sleep (Steriade, 2003a). These synchronous spike-bursts at low frequencies (0.5–15 Hz) are probably the main factors behind the synaptic consolidation of memory traces in the neocortex. The role of slow-wave sleep rhythmic activities in consolidating memories has also been investigated in the hippocampus and related subsystems: it was found that cells that increased their activities during waking also increased their discharges during subsequent epochs of slow-wave sleep (Buzsáki, 1989; Wilson & McNaughton, 1994; Pavlides & Winson, 1989).[51] One of the molecular factors that may account for memory consolidation is protein synthesis, which occurs at higher rates during slow-wave sleep than in REM sleep or wakefulness (Ramm & Smith, 1990).

The finding that neurons with increased firing rates during wakefulness also displayed enhanced firing rates during subsequent sleep epochs (Pavlides & Winson, 1989) is congruent with the hypothesis that the higher the amount of synaptic potentiation in cortical circuits during waking, the higher the increase in slow-wave activity during subsequent sleep (Tononi & Cirelli, 2003). This is also consistent with human data showing that learning increases the density of sleep spindles (Gais *et al.*, 2000). Such data are also corroborated by experiments indicating that simple sensory (auditory) stimulation during wakefulness increases the power of sleep spindles and enhances the coherence between frontal and temporal cortical regions (Cantero *et al.*, 2002).

How does acetylcholine (ACh), among the most effective activating neuromodulators of thalamocortical systems (Steriade & McCarley, 2005), influence memory consolidation during sleep? During human slow-wave sleep, memory for a declarative wordlist task was blocked after infusion of 0.75 mg physostigmine (a cholinesterase inhibitor that increases cholinergic activation) without, however, interfering with a consolidation of a non-declarative task. Because physostigmine did not modify memory consolidation during wakefulness, when cholinergic tone is maximal, it was predicted that a *low* cholinergic tone during slow-wave sleep is essential for consolidation of declarative memory (Gais & Born, 2004).[52] Since physostigmine increased spindle activity (Gais & Born, 2004) and sleep spindles are thought to enhance cortical memory integration (Steriade & Timofeev, 2003) (see experimental data in Section 6.3.1), the conclusion was drawn that physostigmine blocked declarative memory consolidation at the hippocampal level (Gais & Born, 2004).

At variance with the commonly used notion of global brain processes in slow-wave sleep, a recent study reported two major findings in humans subjects, namely: slow-wave sleep activity increases 2 hours after a motor learning task and this enhancement (about 27%)

[51] Chrobak & Buzsáki (1994) proposed that, during periods of slow-wave sleep, sharp waves (which arise in deep layers of entorhinal cortex) would favour the formation of associative links between distant cortical areas. It was suggested that this would lead to consolidation of memory traces within the neocortex independently of the hippocampus (Buzsáki, 1996).

[52] See also the commentary of Power (2004) in which the comparative role of slow-wave sleep and REM sleep in memory consolidation is discussed. Hasselmo (1999) had suggested that high levels of ACh, known to be present during both brain-activated states of waking and REM sleep (Steriade & McCarley, 2005), may set favourable conditions for encoding new information in the hippocampus, whereas lower ACh levels, present during slow-wave sleep, facilitate consolidation of memory traces by allowing spread of activity from hippocampus to entorhinal cortex, with consequent neocortical involvement (see also Buzsáki, 1996).

is expressed *locally*, in parietal association areas 40 and 7 that receive converging visual and proprioceptive inputs relevant to spatial attention and skilled actions (rotation adaptation); and a change in local slow-wave sleep activity is strongly correlated with improved task performance the next day after sleep (Huber *et al.*, 2004).

The increased cortical activity that accounts for consolidation of memory traces during slow-wave sleep also explains the presence of dreaming mentation during this state. Contrary to the assumption that dreams are exclusively confined to REM sleep, a series of studies, starting in the early 1960s and continuing to the present, have demonstrated the presence of dreaming mentation during all stages of slow-wave sleep. Basically, during slow-wave sleep, thought may be rational and repetitive, whereas during REM sleep, the internally generated perceptions are vivid, thought becomes illogical, and the intensity of emotions is higher than during slow-wave sleep (Hobson & Steriade, 1986; Hobson *et al.*, 2000). The first accounts of dreaming mentation during human slow-wave sleep were based on stage 2 awakenings (Foulkes, 1962; Rechtschaffen *et al.*, 1963; Foulkes & Schmidt, 1983), but awakenings from stages 3–4 of slow-wave sleep also reported a recall incidence of 45%–65% (Pivik & Foulkes, 1968; see also Nielsen, 2000). This recall rate is lower than that in REM sleep, when it may reach 90%–95%. In addition, dreams during slow-wave sleep are shorter than those of REM sleep (Cicogna *et al.*, 2000). Then, the brain is never 'empty': mental activity is present during all stages of normal sleep. Human studies using a sleep monitoring system that distinguishes between waking, sleep onset, slow-wave sleep, and REM sleep described the reports of subjects who awoke spontaneously or were awakened instrumentally during these different stages of the waking–sleep cycle (Hobson & Pace-Schott, 2002; Fosse *et al.*, 2004). The reports indicated reciprocal changes of thinking and hallucinations across sleep, with directed thinking (defined as continued mental effort as well as attempts to decide and plan) more frequent during slow-wave sleep and hallucinations (endogenous sensations) more frequent during REM sleep. The intensified hallucinations with transition from slow-wave sleep to REM sleep may reflect the progressive appearance of pontogeniculo-occipital waves that occur during slow-wave sleep well in advance of muscular atonia, the cardinal sign of REM sleep, and are further synchronized throughout the cortex during REM sleep (Steriade *et al.*, 1989; Amzica & Steriade, 1996).

Chapter 7

Neuronal processes and cognitive functions in brain-active states of waking and REM sleep

We now discuss the neuronal processes that account for the increased responsiveness of brainstem, thalamic and cortical neurons during wakefulness and REM sleep. The closing of thalamic gates during slow-wave sleep (see Chapter 6) is modified upon transition to both brain-active states under the influence of increased neuronal activities in ascending activating modulatory (mainly glutamatergic and cholinergic) systems. In addition, the different types of low-frequency rhythms that occur during slow-wave sleep in the disconnected brain are transformed into faster (beta and gamma) oscillations, which are thought to play a significant role in sustaining the mental activity that characterizes brain-active states.

7.1 Similarities and basic differences between waking and REM sleep

7.1.1 Global electrical signs differentiating waking from REM sleep

The global signs that characterize the two brain-active states are EEG rhythms, muscular tone, and eye movements associated with sharp waves in brainstem–thalamocortical systems. The tonic EEG activation associated with fast rhythms (usually 20–60 Hz) in waking is virtually identical to that in REM sleep, and distinguishes both of these states from the low-frequency (less than 15 Hz) oscillations that prevail during slow-wave sleep. The other tonic aspect, muscular atonia, specifically distinguishes REM sleep from the other two major states of vigilance (Jouvet & Michel, 1959) and is taken as the cardinal sign of REM sleep. Finally, phasic eye movements are voluntary during waking and occur as involuntary ocular saccades in REM sleep, when they are accompanied by spiky ponto-geniculo-occipital (PGO) potentials in brainstem and thalamocortical systems. PGO waves herald REM sleep atonia by about one minute.[1]

The above signs characterize the steady states of waking and REM sleep. As to transitional states, the shift from slow-wave sleep to

[1] See Figure 1 in Steriade *et al.* (1989).

[2] This unexpected difference between the high excitability of forebrain neurons and the inhibition of spinal cord motoneurons leading to muscular atonia led Jouvet to coin the term *sommeil paradoxal* for REM sleep.

wakefulness is usually short in duration, lasting for a few seconds and consisting of decreased amplitude and increased frequency of EEG waves that precede the abruptly increased muscular tone and eye movements that occur upon overt arousal. In contrast, the transition from slow-wave sleep to REM sleep is marked by a period of about 1 min during which the EEG is still fully synchronized, there is yet no sign of muscular atonia, but high-amplitude, single, sharp PGO waves can be recorded in the brainstem, thalamus and cortical areas. Later on, when REM sleep is fully developed, PGO waves appear as either single potentials or in clusters of smaller-amplitude potentials with a frequency of about 6 Hz.

The paradox that REM sleep, a state with a higher motor arousal threshold than slow-wave sleep, is a time when the electrical activity suggests that the cerebrum is in a highly excitable state[2] led us to define *activation* as a tonic readiness in cerebral networks that brings neuronal circuits closer to threshold, thus ensuring secure synaptic transmission and quick cellular responses, a response readiness either to messages from the outside world (as during the waking state) or to internally generated drives (as during REM-sleep), whether or not a motor reaction is generated (Steriade, 1991). This definition is based on data showing similarly enhanced excitability of thalamic and cortical neurons to synaptic and antidromic volleys during both states of wakefulness and REM sleep (see cellular data in Section 7.1.2) but does not include inhibitory processes that underlie selectivity of responses and are much less effective during REM sleep than during waking (see below, Section 7.1.3).

7.1.2 Excitation and inhibition of thalamic and cortical neurons in brain-active states

Spontaneous firing

Both thalamocortical (TC) and neocortical neurons transform their bursting pattern of spontaneous firing during slow-wave sleep into tonic, single-spike firing upon awakening or transition to REM sleep (Figure 7.1). This effect, which occurs naturally during shifts in behavioural states of vigilance, can be mimicked by stimulation of the upper brainstem reticular neurons that excite TC neurons monosynaptically (Figure 7.2).

The transformation from burst firing to tonic discharges upon entering waking or REM sleep is explained by the change in membrane potential (V_m) of TC neurons across different states of vigilance. To date, the only intracellular study of TC neurons performed in naturally waking and sleeping animals reported hyperpolarization by about 7–10 mV of these neurons during slow-wave sleep, and relative depolarization during waking and REM sleep (Hirsch *et al.*, 1983). The depolarization of TC neurons during both brain-active states leads to inactivation of the transient Ca^{2+} current (I_T) that underlies the low-threshold spike (LTS), which is crowned by high-frequency fast Na^+ action potentials during slow-wave sleep. The inactivation of I_T

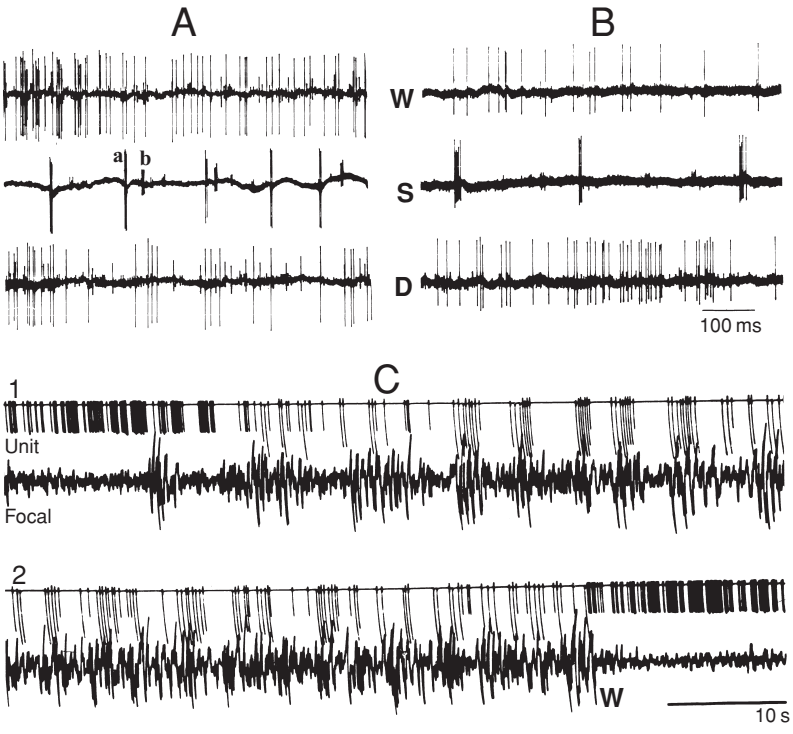

Fig. 7.1 Rhythmic spike-bursts of thalamocortical (TC) neurons during slow-wave sleep (S) is replaced by tonic, single spike discharges during brain-activated states of waking (W) and REM sleep (here abbreviated as D, for EEG-desynchronized state, although desynchronization only applies to slow waves as fast oscillations are synchronized during this state). (A, B) Two neurons in rostral intralaminar centrolateral–paracentral (CL-Pc) thalamic nuclei. Note high-frequency spike-bursts in S and their replacement by sustained discharges of single spikes in both brain-active states (W and D). (C) Neuron in the thalamic ventrolateral (VL) nucleus. Ink-written recording. The VL neuron's spikes were used to deflect a pen of the EEG machine (each deflection exceeding the common level represents a high-frequency spike-burst, >250 Hz); focal waves were recorded simultaneously through the same microelectrode. Note close time-relation between groups of spike-bursts and high-amplitude EEG spindles. EEG activation (W) was associated with tonic firing with increased discharge rates. Modified from Steriade *et al.* (1971) and Glenn & Steriade (1982).

during depolarization results in tonic, single-spike firing of TC neurons during waking and REM sleep (Steriade & Llinás, 1988).

Although I_T is expressed in a lower proportion of neocortical neurons, compared with its presence in virtually all TC neurons, similar aspects of tonic firing are seen in cortical neurons during waking and REM sleep. This is in contrast with grouped spike-trains or spike-bursts during low-frequency rhythms in slow-wave sleep. This was first reported from extracellular recordings in monkeys (Evarts, 1964) and cats (Steriade, 1978), and was more recently substantiated with intracellular recordings of different types of electrophysiologically characterized cortical neurons in natural waking and sleep states (Steriade

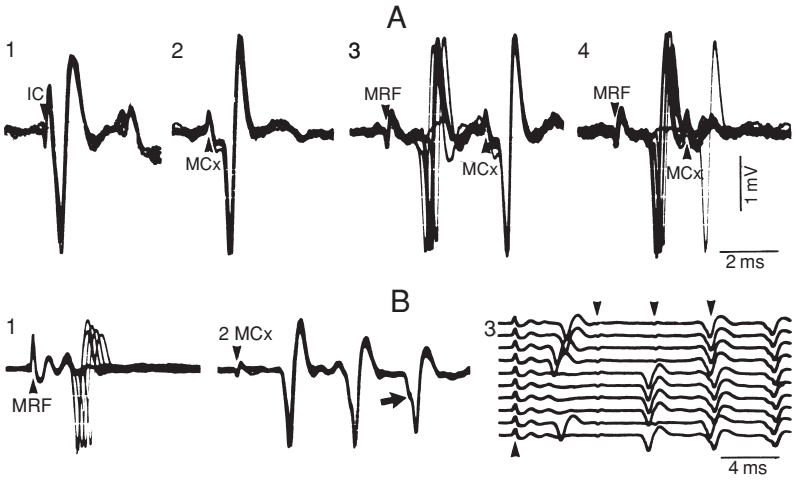

Fig. 7.2 The midbrain reticular projection to TC neurons. (A, B) Two different neurons recorded from the thalamic intralaminar centrolateral nucleus (CL) in behaving cats. There is antidromic invasion from the internal capsule (IC) and motor cortex (MCx), and monosynaptic excitation from the midbrain reticular formation (MRF). Stimulus artefacts are indicated by arrowheads (in B2 only the first stimulus of a three-shock pulse-train at 250 s^{-1} is marked). The arrow in B2 indicates fractionation of an antidromically elicited action potential to the last stimulus in the train. Collision between MRF-evoked synaptic discharge and cortical-elicited antidromic spike is seen in A4 and B3. Superimpositions of five to seven traces. Positivity downward. Modified from Glenn & Steriade (1982).

et al., 2001a). In essence, long-lasting hyperpolarizations, associated with neuronal silence, are defining features of spontaneous activities of cortical neurons during slow-wave sleep, whereas the transition from this sleep stage to wakefulness (Figure 7.3) or to REM sleep (Figure 7.4) is associated with complete obliteration of prolonged hyperpolarizations, slight depolarization and tonic, single-spike discharges. This change was observed in both regular-spiking and fast-spiking neurons (Figure 7.5), thus indicating that it is a property shared by the overwhelming majority of pyramidal and local-circuit cortical neurons. Pooled analyses of relations between the mean V_m and mean firing rates showed that, between −55 mV and −65 mV, fast-spiking (FS) neurons discharged at much higher rates than regular-spiking (RS) and fast-rhythmic-bursting (FRB) neurons during all states of vigilance but especially during waking and REM sleep (bottom panel in Figure 7.6). Thus, during the state of waking, neurons with FS and RS discharge patterns fired around 24 Hz and 9.5 Hz, respectively; at 15 Hz and 12 Hz in slow-wave sleep; and at 30 Hz and 14 Hz in REM sleep. FRB neurons fired at higher rates, compared with RS neurons, during the waking state. The increased discharge frequencies of FRB neurons during wakefulness is at least partly ascribable to the fact that they fired spontaneously with high-frequency (20–50 Hz) spike-doublets and triplets during this behavioural state. The firing rates of intrinsically bursting (IB) neurons could not be

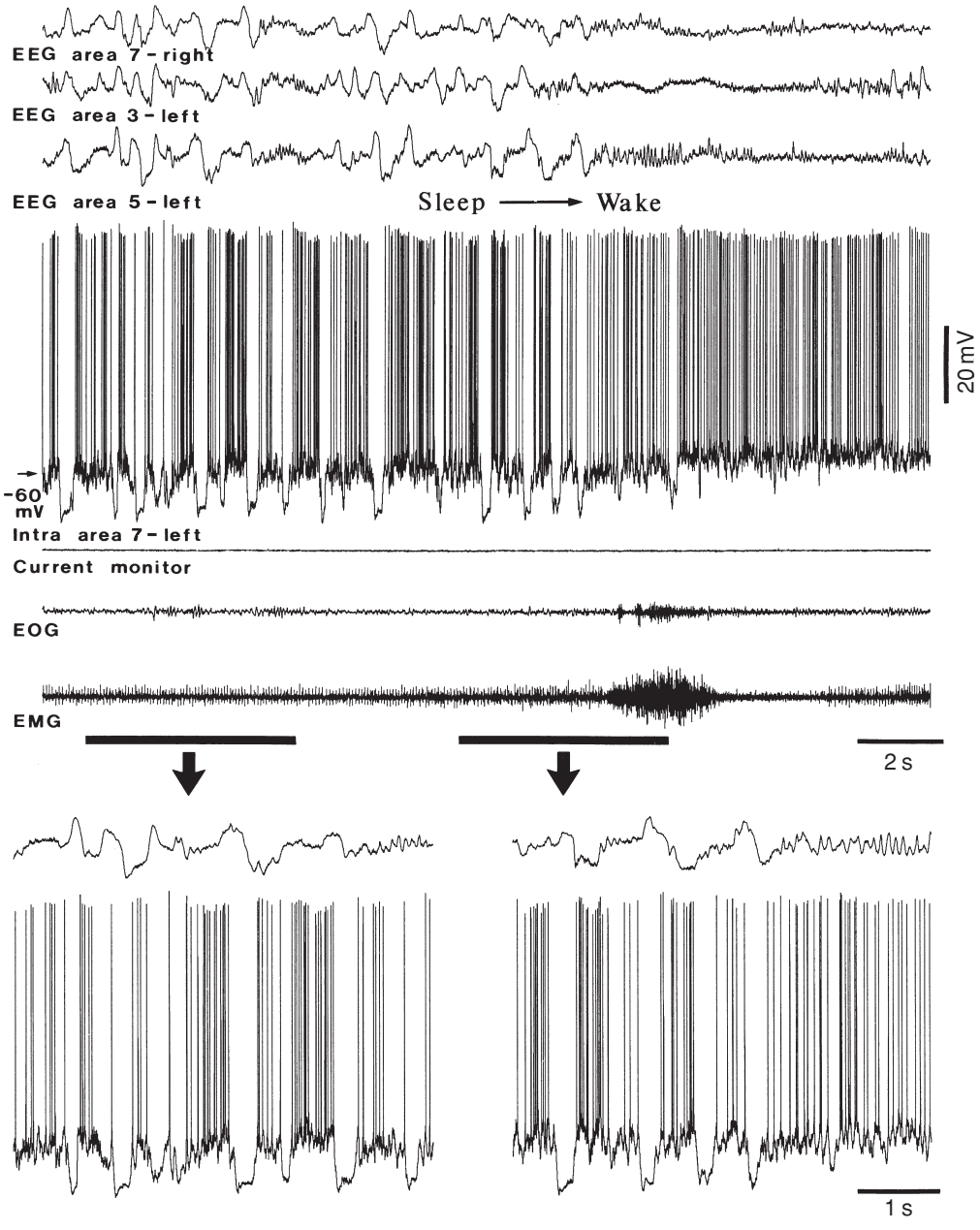

Fig. 7.3 Transformation of spontaneous firing of cortical neuron during transition from the slow oscillation during natural slow-wave sleep to wakefulness. Chronically implanted cat. Five traces depict (from top to bottom): depth-EEG from right area 7 and left areas 3 and 5; intracellular activity of regular-spiking neuron from left area 7; and electromyogram (EMG). Two epochs marked by horizontal bars are expanded below (arrows). Cyclic hyperpolarizations characterize neocortical neurons during slow-wave sleep, but their firing rate during the depolarizing phases of the slow sleep oscillation is as high as during the activated behavioural state of waking. Note phasic hyperpolarizations in area 7 neuron, related to depth-positive EEG field potentials, during sleep, tonic firing upon awakening marked by EEG activation and increased muscular tone, and slight depolarization occurring only after a few seconds after awakening and blockage of hyperpolarizations. Modified from Steriade *et al.* (2001a).

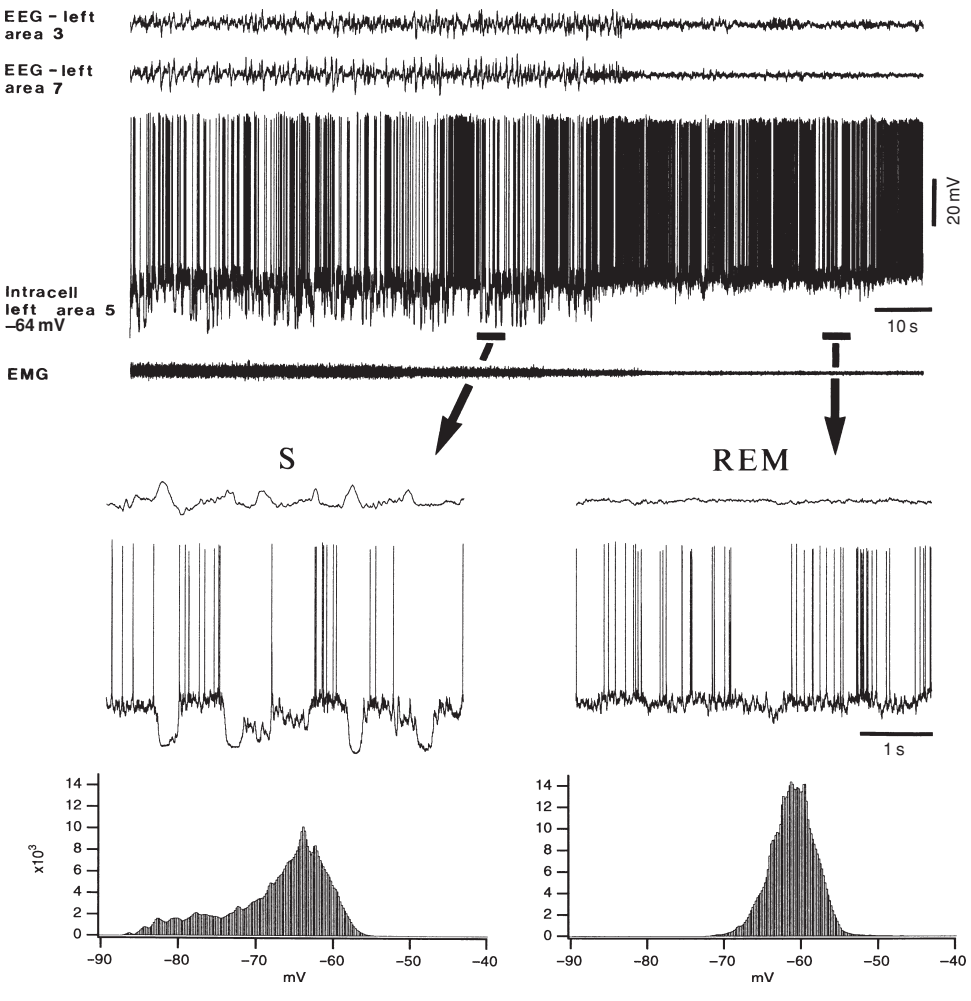

Fig. 7.4 Transition in spontaneous firing of regular-spiking cortical neuron from slow-wave sleep (S) to REM sleep. Intracellular recording from area 5, together with EEG from areas 3 and 7, and EMG. Periods marked by horizontal bars and arrows are expanded below. The bottom plots show the membrane potential during S (with a tail extending up to −85 mV) and a Gaussian-type histogram during REM sleep, around −60 mV. Note also slight depolarization upon entering REM sleep, preceding by a few seconds EEG activation and muscular atonia. From Steriade *et al.* (2001a).

evaluated in pooled analyses because IB neurons represent only a negligible proportion of neurons (5%) in non-anaesthetized, behaving preparations (Steriade *et al.*, 2001a), compared with their high incidence in anaesthetized animals or in cortical slices maintained *in vitro* (see discussion in Steriade, 2004a).

Antidromic and synaptic excitability

The probability of antidromic responses increases significantly in TC neurons during both waking and REM, compared with slow-wave sleep (Glenn & Steriade, 1982). Decreased antidromic responsiveness,

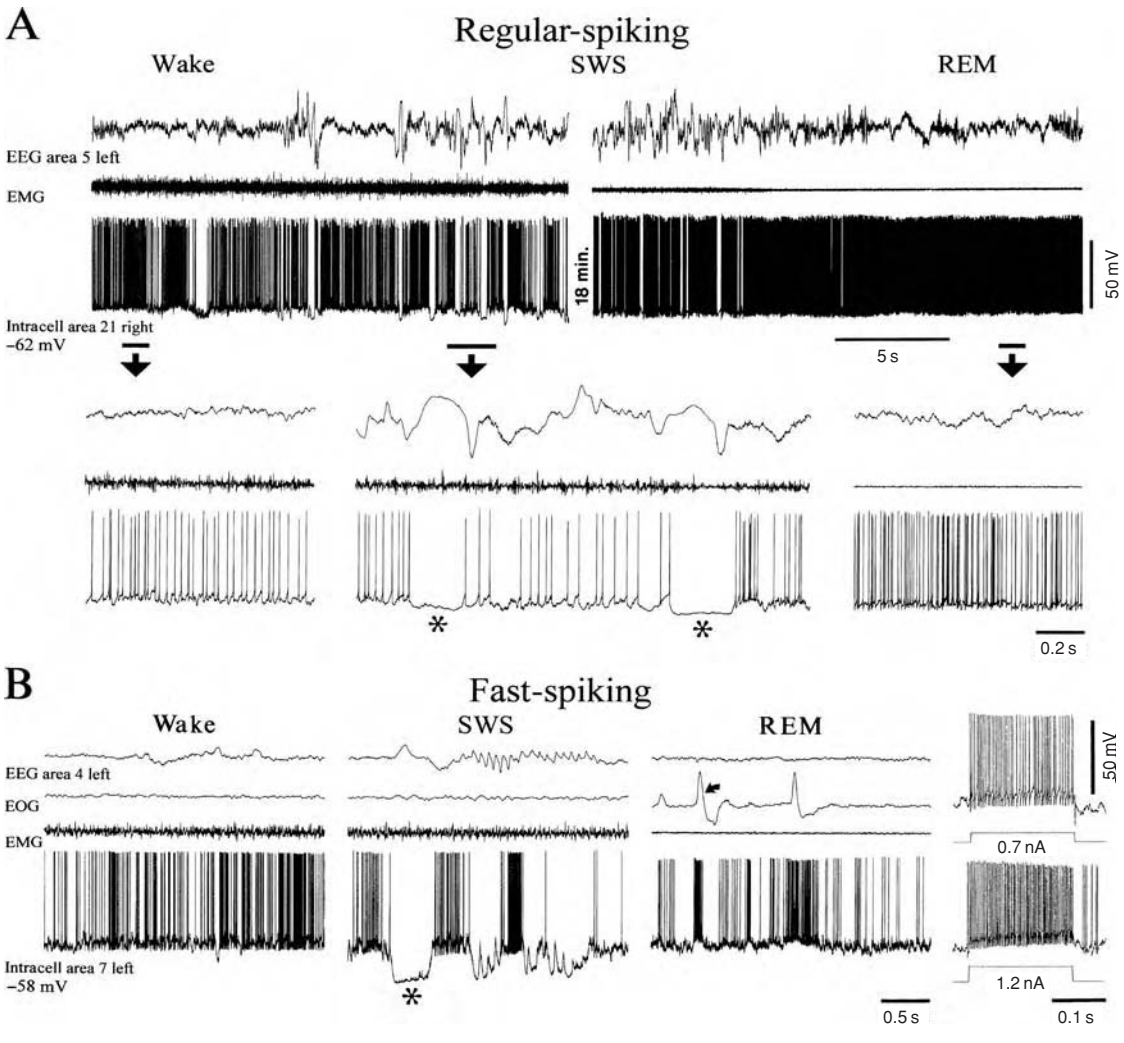

Fig. 7.5 Changes in membrane potential and firing patterns of neocortical regular-spiking (RS) and fast-spiking (FS) neurons during natural waking and sleep states in cats. (A) An RS neuron from posterior association suprasylvian area 21 was intracellularly recorded (together with EMG and EEG from area 5) during the transition from waking to slow-wave sleep (SWS) and, further, to REM sleep (there is a non-depicted period of 18 min during SWS). Periods marked by horizontal bars are expanded below (arrows). Note tonic firing during both waking and REM sleep, and cyclic hyperpolarizations associated with depth-positive EEG field potentials during SWS. (B) Activity of an FS neuron (characterized by fast and tonic firing without frequency adaptation; see at right responses to depolarizing current pulses) during waking, SWS and REM sleep. Recording with KCl-filled pipette. Tonic firing during waking and REM sleep was interrupted during SWS by long periods of hyperpolarizations and spindles, corresponding to EEG depth-positive waves and spindles. Prolonged hyperpolarization during SWS is indicated by an asterisk. Modified from Steriade *et al.* (2001a).

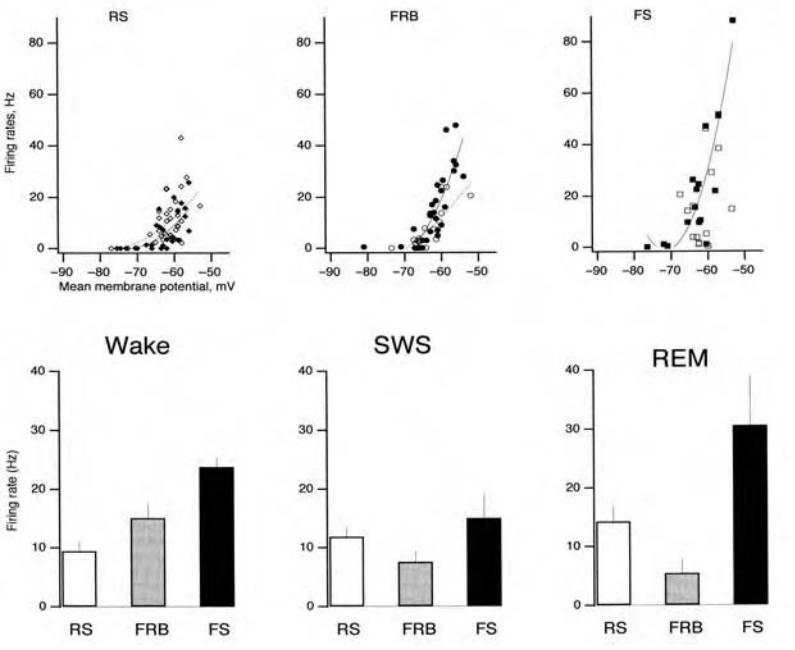

Fig. 7.6 Pooled relations between the membrane potential and firing rates in different cell types during waking and sleep states in behaving cats. Top panel: the relations between membrane potential and firing rates in a sample of 120 neurons (regular-spiking, RS; fast-rhythmic-bursting, FRB; and fast-spiking, FS), during waking (black symbols) and slow-wave sleep (SWS) (white symbols). Bottom panel: the mean firing rates of RS ($n = 47$), FRB ($n = 37$) and FS ($n = 22$) neurons during waking, SWS and REM sleep. Modified from Steriade *et al.* (2001a).

from break between initial segment (IS) and somadendritic (SD) spike to complete abolition of antidromic action potentials, was also observed as a precursor sign of sleep spindles (Steriade *et al.*, 1971). Similar enhancement of antidromic invasion was detected during waking and REM sleep, compared with slow-wave sleep, in corticothalamic (Steriade *et al.*, 1979) and corticospinal neurons in which the IS–SD break was reduced and full antidromic potentials occurred during the first seconds of awakening from slow-wave sleep, despite the fact that spontaneous firing of fast-conducting pyramidal neurons stopped during that initial period of arousal (Steriade *et al.*, 1974a).[3] More recently, the enhanced somatic excitability during brain-active states was also demonstrated by increased probability of responses to intracellularly applied depolarizing current pulses during waking and REM sleep, compared with slow-wave sleep (Steriade *et al.*, 2001b; see also Figure 6.11). The decreased incidence of antidromic responses during slow-wave sleep is ascribable to the prolonged hyperpolarizations related to the slow oscillation during this sleep stage (see Section 6.1.1).

Orthodromic responses are also enhanced in TC and, consequently, in cortical neurons, both during natural brain-active states and upon electrical stimulation of the upper brainstem reticular core (Steriade, 1970). The independence of cortical activation from TC-cell activation was demonstrated by testing cortical responses to white matter stimulation (Steriade, 1970) and recording such responses after destruction of appropriate thalamic nuclei (Steriade & Morin, 1981). The independence of arousal-induced enhancement of TC-cells' responses from events occurring in prethalamic pathways and relays was first shown by recording increased responses to light stimulation in the lateral

[3] The contrast between arrest in spontaneous discharges and enhanced antidromic excitability upon the short (*c.*10 s) period of initial arousal led us to postulate that the silenced firing was not due to inhibition but to disfacilitation. This hypothesis was supported by subsequent intracellular studies by Oshima and his team (Inubushi *et al.*, 1978a,b).

geniculate nucleus during brainstem reticular stimulation, which contrasted with unaltered responses simultaneously recorded in the optic tract (Steriade & Demetrescu, 1960).[4] The brainstem reticular-induced enhancement of TC-cells responses to afferent stimuli has been repeatedly confirmed using intracellular recordings (Timofeev *et al.*, 1996).

Here, an interesting issue has to be raised concerning the contrast between the effects of natural or brainstem reticular-elicited arousal on responses elicited by peripheral or centrally applied stimuli. Whereas responses evoked by *single* light-flashes are depressed upon arousal (Steriade & Demetrescu, 1960), responses evoked by electrically applied single stimuli to the optic tract or other afferent pathways are enhanced upon arousal in TC cells (Timofeev *et al.*, 1996) and cerebral cortex (Bremer & Stoupel, 1959; Dumont & Dell, 1960). This contrast was attributed to differences between testing stimuli, with higher synchronization induced by centrally applied volleys. In an attempt to simulate peripheral stimuli, high-frequency (200–1000 Hz) stimuli were applied to the optic tract and, indeed, the response to the first volley recorded from the lateral geniculate nucleus and visual cortex was enhanced, whereas the simulated peripheral response occurring at the end of the high-frequency pulse-train was depressed during brainstem reticular formation stimulation (Steriade & Demetrescu, 1967). These observations may be related to recent intracellular data obtained in the somatosensory system (Rosanova & Timofeev, 2005). This study reported asynchronous responses of TC neurons to tactile stimulation consisting of multiple action potentials evoked by median nerve stimulation (probably due to differences in conduction velocities of ascending prethalamic axons), and single-spike responses to medial lemniscus stimulation, all indicating increasing synchronization from peripherally evoked to centrally evoked stimuli. Studies during natural sleep and waking states in humans (Massimini *et al.*, 2003) have shown that responses to peripheral somatosensory stimuli undergo a dynamic modulation, as a function of the phases of the slow oscillation that was described at the EEG level in humans (Steriade *et al.*, 1993e; Achermann & Borbély, 1997). The N20 (primary cortical response) and P60 as well as P100 components were reduced during slow-wave sleep (mainly during the surface-negative phase of the EEG slow oscillation, which corresponds intracellularly to the prolonged hyperpolarization of this rhythm; see Section 6.1.1) and displayed increased amplitudes upon wakefulness (Massimini *et al.*, 2003).

In contrast to the enhanced excitability of TC neurons during both brainstem reticular stimulation and natural states of waking and REM sleep, thalamic reticular (RE) GABAergic neurons display a more subtle behaviour. While setting into action brainstem cholinergic neurons that hyperpolarize RE neurons, a residual excitation is observed after blocking muscarinic receptors of RE neurons, which is attributed to glutamatergic projections from the mesopontine reticular neurons (Hu *et al.*, 1989a). Indeed, during *natural* waking, RE neurons display

[4] In this article, thalamic responses to single flashes were depressed upon brainstem reticular formation stimulation, whereas responses to repetitive (above 5 s^{-1}) light stimuli were enhanced. This finding was corroborated by Bremer and his colleagues (1960) and is ascribed to the more synchronized responses evoked by central stimuli, which may also be the case with high-rate repetitive volleys applied to the sensory periphery or peripheral nerves (see main text and Steriade & Demetrescu, 1967; Rosanova & Timofeev, 2005).

higher firing rates and increased responsiveness to midbrain reticular stimuli, compared with lower probability and longer latency of action potentials elicited during slow-wave sleep (Steriade *et al.*, 1986).[5] Thus, the actions of glutamatergic projections onto RE neurons, some of them arising from mesopontine neurons in which acetylcholine (ACh) and glutamate are colocalized (Lavoie & Parent, 1994), probably prevail during waking over the inhibitory action of ACh.

The fact that RE neurons are in a state of high excitability during the natural waking state may explain the results of experiments in which unilateral lesions of the RE nucleus led to impairment of attentional orienting (Weese *et al.*, 1999) and induction of C-*Fos* protein, a marker of neuronal activity, during exploration of novel, complex environments (Montero, 1997). These data again implicate RE neurons in attentional processes. First hypothesized in the 1970s (Yingling & Skinner, 1977), this idea was also advanced in the 1980s, with the proposal that inhibitory actions exerted by RE neurons on TC cells would promote postinhibitory rebound spike-bursts in the latter and thus provide more action potentials for relevant signals en route to the cortex (Crick, 1984). However, the latter possibility is not plausible because spike-bursts in TC neurons are de-inactivated by membrane hyperpolarization, and these neurons are steadily depolarized during wakefulness when attentional orienting takes place (see Steriade, 2001d). Numerous studies have mentioned the absence or very low probability (1%) of spontaneously occurring spike-bursts during natural waking in the visual thalamus (Weyand *et al.*, 2001; Denning & Reinagel, 2005).[6] Concerning the possibility of evoked spike-bursts by visual stimuli, these should be recorded intracellularly during natural wakefulness to make the hypothesis plausible. Indeed, extracellularly recorded 'spike-bursts' may just be brisk firing of single action potentials that do not implicate postinhibitory rebound excitation.

In view of these difficulties with neuronal processes underlying attentional orienting in the thalamus, we proposed (Steriade, 1991, 1999) that the connection between the two types of thalamic GABAergic cell, RE and local-circuit interneurons (Liu *et al.*, 1995), subserves processes for focusing attention on relevant signals. Thus, while some TC neurons (say, TC1) receive prevalent excitation from afferent fibres, other TC neurons (say, TC2) receive less collaterals from these specific afferent axons. RE neurons, which are directly connected to TC1 neurons, contribute to further enhance the relevant activity by inhibiting local-circuit elements. Simultaneously, the activity in adjacent RE neurons is suppressed by axonal collateralization and dendrodendritic synapses within the RE nucleus. The consequence would be the released activity of target local-circuit inhibitory neurons and inhibition of weakly excited TC2 neurons in areas adjacent to the active focus (see Figure 4.11 in Steriade, 2001a). The functional consequences of this GABAergic-to-GABAergic projection from RE to local-circuit neurons should be investigated in major sensory dorsal thalamic relay nuclei. Suffice it to say that this connection between

[5] In those experiments, large bilateral lesions of the locus coeruleus were made to prevent excitation of passing fibres from this nucleus whose neurons exert depolarizing actions on RE neurons (see chapter 8 in Steriade *et al.*, 1997).

[6] In the study by Weyand *et al.* (2001) the conclusion was drawn of a 'negative relationship between attention and bursting' (p. 1113), contrary to the prior hypothesis that bursting may sustain scanning attention. Concerning the spike-bursts in thalamic relay nuclei other than LG, simultaneous recordings of two ventrobasal neurons in the alert state showed that one neuron fired just one burst during the entire epoch of wakefulness and the other neuron displayed no burst during that state (Swadlow & Gusev, 2001). All these results point to the absence or scarcity of spike bursts in thalamic relay neurons during the waking state.

the two inhibitory neuronal classes in the thalamus seems important: after lesions of the RE nucleus, the incidence of IPSPs in TC cells is much increased, as if local-circuit neurons were released from inhibition following removal of RE neurons (Steriade *et al.*, 1985).

Intralaminar nuclei are also involved in opening the thalamic gates to relevant signals and they participate in attentional orienting. The direct excitatory pathway from the midbrain reticular formation to thalamic intralaminar neurons (Steriade & Glenn, 1982) was explored with positron emission tomography in humans (Kinomura *et al.*, 1996). These midbrain and thalamic territories were found to be activated when subjects went from a relaxed state to an attention-demanding reaction-time task. Similarly, neurons in the centre median–parafascicular complex (caudal intralaminar nuclei) of macaque monkeys displayed task-related activity after the appearance of either the instruction cue or the target stimulus (Minamoto & Kimura, 2002). These data led to the conclusion that intralaminar nuclei play an essential role in the process of attentional orienting to external events.

To sum up, both thalamic and neocortical neurons are more excitable and more responsive to synaptic and antidromic volleys during waking and REM sleep, as compared with slow-wave sleep. The enhanced responsiveness of thalamic and cortical neurons during wakefulness is corroborated by their increased input resistance (R_{in}) during this natural state or during its experimental model, i.e. stimulation of the brainstem reticular cholinergic nuclei. Thus, after a short period of diminished R_{in} produced by stimulation of the mesopontine cholinergic nuclei and due to nicotinic excitation, TC neurons display a longer-lasting increase in R_{in}, owing to muscarinic actions (Figure 7.7) (Curró Dossi *et al.*, 1991). Cortical neurons also display increased and more stable R_{in} during the natural state of wakefulness, compared with slow-wave sleep (Steriade *et al.*, 2001a). In that study, the steady state of waking, without movements, was compared with the depolarizing phase of the slow oscillation in natural sleep, during which the membrane potential of cortical neurons is about the same as during waking (Figure 7.8). In a neuronal sample recorded intracellularly during natural states of vigilance, the R_{in} was almost double that seen during the hyperpolarizing phase of the slow sleep oscillation (30.8 $\pm$ 4.3 MΩ), compared with the depolarizing phase of this oscillation (16.8 $\pm$ 2.3), thus further indicating that the prolonged hyperpolarization is not mediated by GABAergic events (see Section 6.1.1). Moreover, the R_{in} was remarkably stable during the steady state of waking and reached higher values (31.3 $\pm$ 2.4 MΩ) than in REM sleep or the depolarizing phase of the slow oscillation (Steriade *et al.*, 2001a).

Inhibitory processes

As discussed in more detail in Chapter 1, there are two types of inhibitory (GABAergic) neurons in the thalamus: local-circuit neurons

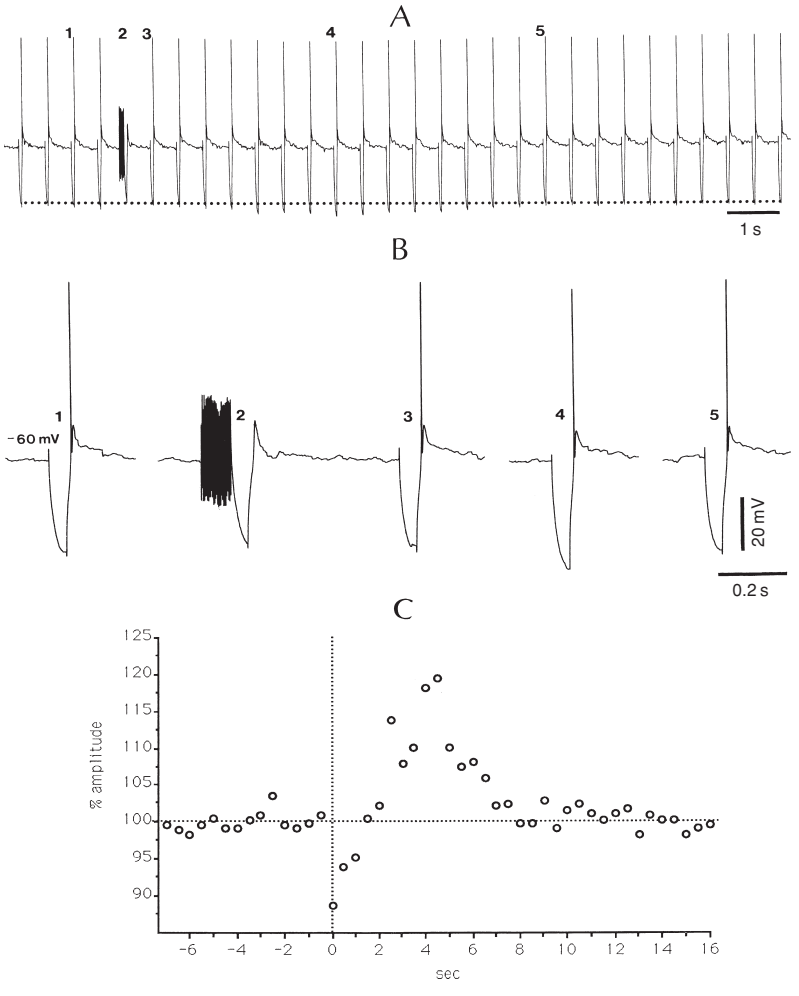

Fig. 7.7 Biphasic effect (increase and decrease) on membrane conductance evoked in thalamic centrolateral (CL) neuron by stimulation (30 stimuli) of laterodorsal tegmental (LDT) cholinergic nucleus. Cat under urethane anaesthesia. Different parts of (A) are expanded in (B). Part 1 is before the LDT pulse-train; 2 and 3 depict the increased conductance (nicotinic in nature) shortly after LDT stimulation; 4 is taken from the period with increased input resistance; and 5 is back to the control value. (C) Plot of the LDT-induced conductance changes in the same neuron. Ordinate: percentage voltage pulse amplitudes compared with the averaged values (horizontal dotted line) in the control condition, before application of LDT stimulation. Abscissa: elapsed time with respect to LDT stimulation (vertical dotted line). Modified from Curró Dossi *et al.* (1991).

[7] The $GABA_a$ or 'miniature' IPSP was also detected in the lateral geniculate nucleus (Soltesz & Crunelli, 1992).

and RE neurons. Local GABAergic neurons produce biphasic, $GABA_{A\text{-}B}$ IPSPs in TC neurons (Hirsch & Burnod, 1987; Crunelli *et al.*, 1988). As most thalamic nuclei also receive inputs from GABAergic RE neurons, the only nuclei in which the action of local-circuit neurons can be studied in isolation from RE inhibitory inputs are the anterior nuclei, which are devoid of connections from the RE nucleus in cats (Steriade *et al.*, 1984a; Velayos *et al.*, 1989). Before the $GABA_{A\text{-}B}$-mediated sequence of IPSPs, local-circuit inhibitory neurons evoke a smaller-amplitude IPSP, called 'miniature' or $GABA_a$, which is ascribed to intraglomerular processes (Paré *et al.*, 1991).[7] RE neurons receive inputs from the cerebral cortex and TC neurons, and project back to TC neurons but not to the cortex, thus forming a feedback inhibitory loop with TC neurons. Similarly to TC neurons, RE neurons operate in two functional modes: tonic discharges during brain-active states and rhythmic spike-bursts during natural slow-wave sleep (Steriade *et al.*, 1986). As yet, there is no study on state-dependent activity in formally identified local-circuit thalamic neurons.

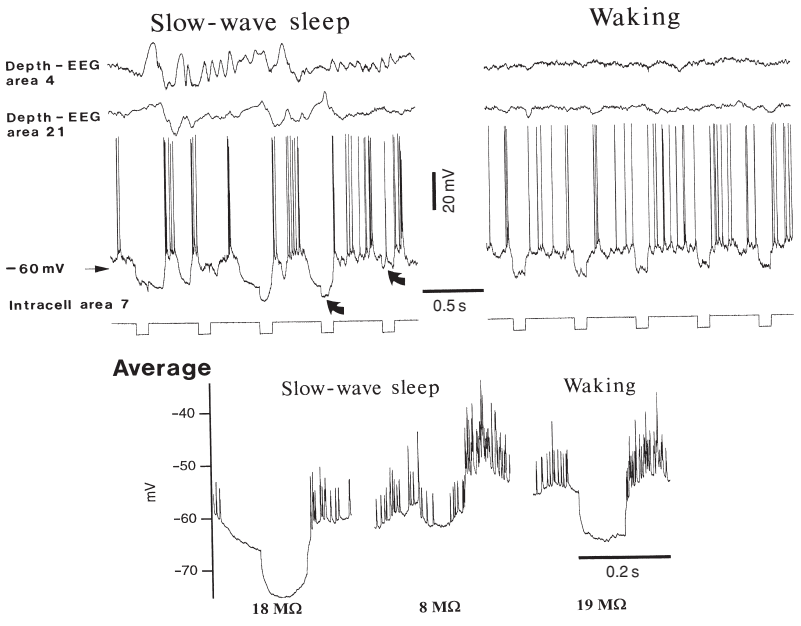

Fig. 7.8 Increased input resistance (R_{in}) of neocortical neuron during the natural state of waking. Chronically implanted cat. Recordings during slow-wave sleep (SWS) and waking. The four traces in the top panels are depth-EEG from areas 4 and 21, intracellular recording of regular-spiking neuron in area 7, and hyperpolarizing current pulses. Two oblique arrows in SWS point to hyperpolarizing pulses applied during the hyperpolarizing and depolarizing phases of the slow oscillation. Average shows decreased R_{in} during the depolarizing phase of the slow oscillation in SWS and increased R_{in} during waking (see main text for values of R_{in} in a sample of 24 neurons). Unpublished data by M. Steriade, I. Timofeev and F. Grenier (see also Figure 11 in Steriade *et al.*, 2001a).

The inhibitory processes that appear in TC cells as a consequence of actions arising in GABAergic thalamic neurons are under the influence of ascending activating neuromodulatory systems and are of two different types during the states of waking and REM sleep. On the one hand, the prolonged and rhythmic IPSPs that characterize sleep spindles in TC neurons and are due to rhythmic spike-bursts fired by RE neurons, are obliterated upon brain arousal or during stimulation of brainstem reticular cholinergic neurons (Figure 7.9) (Hu *et al.*, 1989a,b). On the other, however, the activation of thalamic neurons upon awakening is associated with processes of sculpturing inhibition that ensures finely tuned, discriminative responses. Although earlier studies considered that arousal is associated with a global disinhibition of TC neurons (Purpura, 1970; Singer, 1977), brain arousal blocks long-lasting and cyclic thalamic inhibitory processes (see Figure 7.9) but does not eliminate the early inhibitory phase (Figure 7.10) during which spontaneous firing ceases and neurons are unresponsive to antidromic or orthodromic volleys (Steriade *et al.*, 1977; Steriade, 1984). The earliest part of the prolonged IPSP, generated by the intraglomerular presynaptic dendrites of short-axon

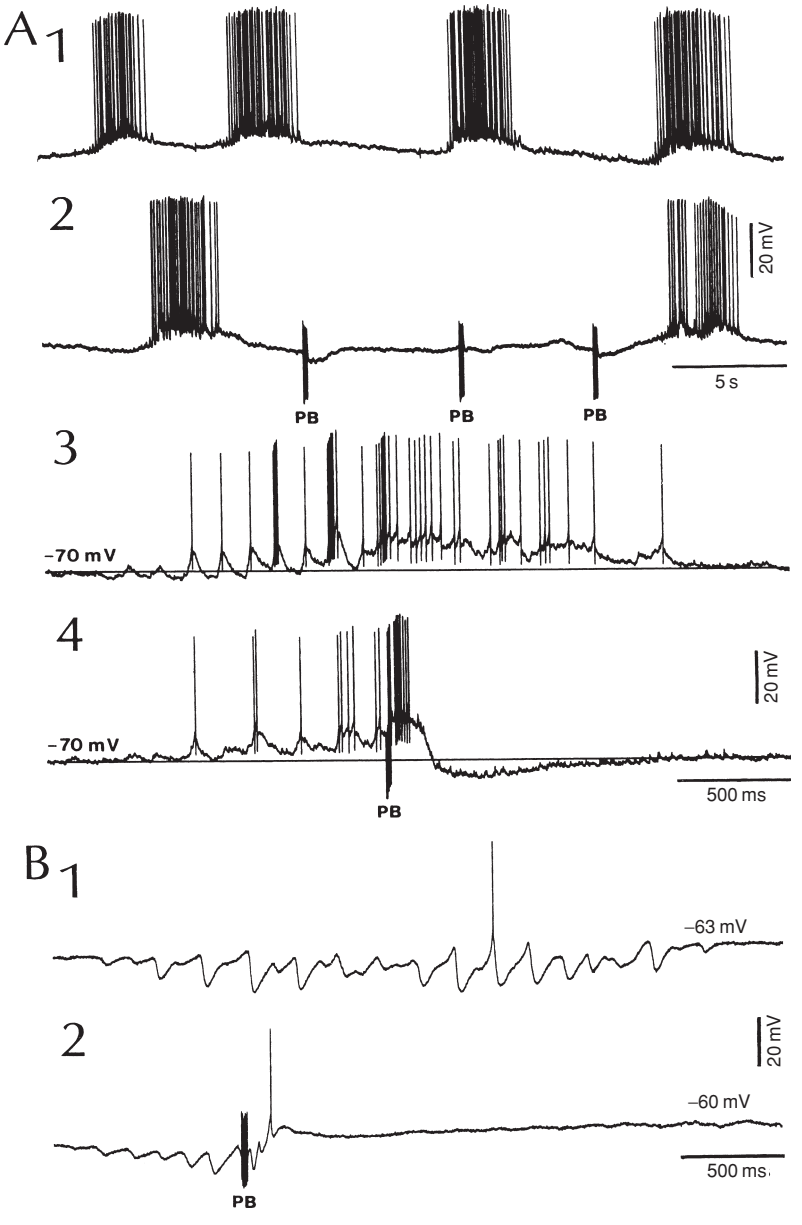

Fig. 7.9 Blockage of sleep spindle oscillations in thalamic reticular (RE) and thalamocortical (TC) neurons by stimulation of midbrain peribrachial (PB) cholinergic area. Non-anaesthetized cats, deafferented by midpontine pretrigeminal transections. (A) Intracellular recording of RE (perigeniculate) neuron during spindle oscillations (1) and blockage of spindles during three pulse-trains applied to PB area (2). Below, expanded traces of one spindle sequence (3) and its obliteration due to PB stimulation (4). (B) Intracellular recording showing a spindle sequence in a TC neuron from the lateral geniculate nucleus (1) and its suppression by a PB pulse-train (2). Modified from Hu *et al.* (1989a,b).

[8] Excitatory local circuits in neocortex use glutamate as neurotransmitter. They are found in layer IV of the visual cortex (Lund, 1973; LeVay, 1973) and relay thalamic inputs to more superficial layers (Thomson, 1997; Thomson *et al.*, 2002).

GABAergic cells, is not blocked and may even be enhanced (Curró Dossi *et al.*, 1992b) (see also Figure 5.12). This phase of the IPSP may be implicated in the high-fidelity transfer of information during the adaptive state of wakefulness.

In neocortex, there is a great diversity of short-axoned neurons: some of them are excitatory[8] but there are also many types of GABAergic inhibitory cells (Somogyi *et al.*, 1998; Gupta *et al.*, 2000; Markram *et al.*, 2004). The morphological features and connectivity of different classes of local inhibitory neurons (mainly basket cells, chandelier cells and double-bouquet dendritic cells) are discussed

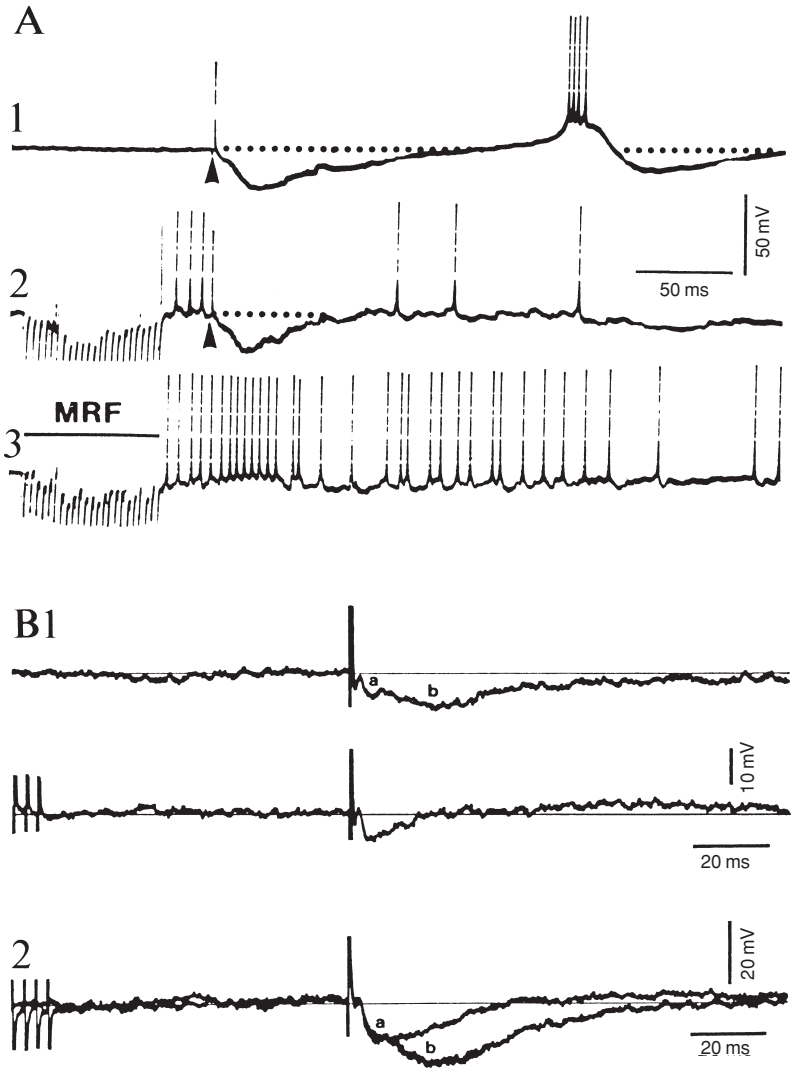

Fig. 7.10 Blockage of long-lasting inhibition but preservation of early IPSP in TC neurons during forebrain activation elicited by stimulating the midbrain reticular formation (MRF) in cats. Intracellular recordings. (A) Prolonged IPSP in TC neuron from ventrolateral nucleus elicited by motor cortex stimulation (1), suppression of the late phase but preservation of the early phase of the IPSP by conditioning pulse-train to the MRF (2), and the activating effect of MRF stimulation on spontaneous activity. (B1) Two ($GABA_A$ and $GABA_B$, a and b) components of IPSP evoked in TC neuron from lateral geniculate nucleus by optic chiasma stimulation (upper trace) and abolition of late (b) component but preservation of early (a) IPSP by conditioning pulse-train to the brainstem peribrachial cholinergic area (2). In B2, two traces are superimposed, one without and the other with peribrachial stimulation. Modified from Steriade (1984) and Steriade & Deschênes (1988).

in Section 2.1.2. These inhibitory neurons account for the increased response selectivity to sensory stimuli during waking (Livingstone & Hubel, 1981). Studies using feedback inhibition tests by stimulating antidromically pyramidal tract neurons and feedforward inhibition induced by thalamic stimulation reported that inhibition has a shorter duration during wakefulness than during slow-wave sleep. However, the brief period of inhibition seen during waking is quite efficient in providing for response selectivity, accurate discrimination and faithful following of rapidly recurring messages (Steriade & Deschênes, 1974; Steriade *et al.*, 1974b). Intracellular recordings in naturally awake and sleeping cats (unpublished data by F. Grenier, I. Timofeev and M. Steriade) confirmed these extracellular results on inhibitory processes in behaving monkeys (Steriade & Deschênes, 1974; Steriade *et al.*, 1974b). Thus, what distinguishes waking and

REM sleep from slow-wave sleep is the total duration of thalamic-evoked hyperpolarization in neocortical neurons, which is much shorter during brain-active states (see Figures 4.13 and 4.14 in Steriade, 2003a).

7.1.3 Role of ascending modulatory systems in thalamocortical activation

There are multiple neuromodulatory activating systems: brainstem reticular cholinergic and glutamatergic neurons, which may exert similar actions at the level of TC neurons (namely, the blockage of a 'leak' K^+ current), and noradrenergic neurons that also project directly to the cerebral cortex; histaminergic neurons in the posterior hypothalamus that have access to both thalamus and cortex; and cholinergic neurons in the basal forebrain that project to the cortex and to limited territories in the thalamus (mainly the reticular nucleus). In addition to their direct excitation of TC neurons (Curró Dossi *et al.*, 1991), mesopontine cholinergic neurons inhibit thalamic RE GABAergic neurons (Hu *et al.*, 1989a) and thus also exert indirect excitation, through disinhibition, of TC neurons.

The multiplicity of neuromodulatory systems, some of them apparently exerting similar activating effects on their targets, can be partly explained by the fact that they may compensate for the loss of some systems, as seen from the recovery of behavioural and/or electrographic signs of wakefulness after the comatose syndrome induced by extensive midbrain–pontine lesions in animals and humans (Batsel, 1964; Villablanca, 1965; Plum, 1991). In addition, the presence of two parallel activating pathways (from the brainstem reticular core to the cortex, via synaptic relays within the thalamus or nucleus basalis, NB) may explain the fact that brainstem-induced depolarization of cortical neurons, their enhanced excitability, and replacement of slow oscillations by fast rhythms can be achieved after extensive ipsilateral lesions of either NB or thalamus (Figure 7.11) (Steriade *et al.*, 1993a).[9] Thus, contrary to some assumptions that place exclusive emphasis on one or another system, either pedunculopontine tegmental/laterodorsal tegmental (PPT/LDT) nuclei or the NB cholinergic nucleus are sufficient to activate the cerebral cortex. The driving force for activating basal forebrain cholinergic neurons originates in the brainstem reticular non-cholinergic neurons. Indeed, less than 1% of PPT/LDT cholinergic cells were found to project towards NB and ultrastructural analyses showed that mesopontine cholinergic cells form synaptic contacts with non-cholinergic basal forebrain neurons (Jones & Cuello, 1989). Thus, the cholinergic input is not expected to activate NB cholinergic neurons. Because most brainstem reticular core neurons are glutamatergic elements that increase their firing rates during brain-active states (Steriade *et al.*, 1982a) and glutamate is colocalized with ACh in PPT/LDT neurons (Lavoie & Parent, 1994), it was hypothesized that the basic excitatory input to NB neurons originates in brainstem glutamatergic neurons (Steriade *et al.*,

[9] For extensive lesion of the nucleus basalis, see Figure 7 in that article.

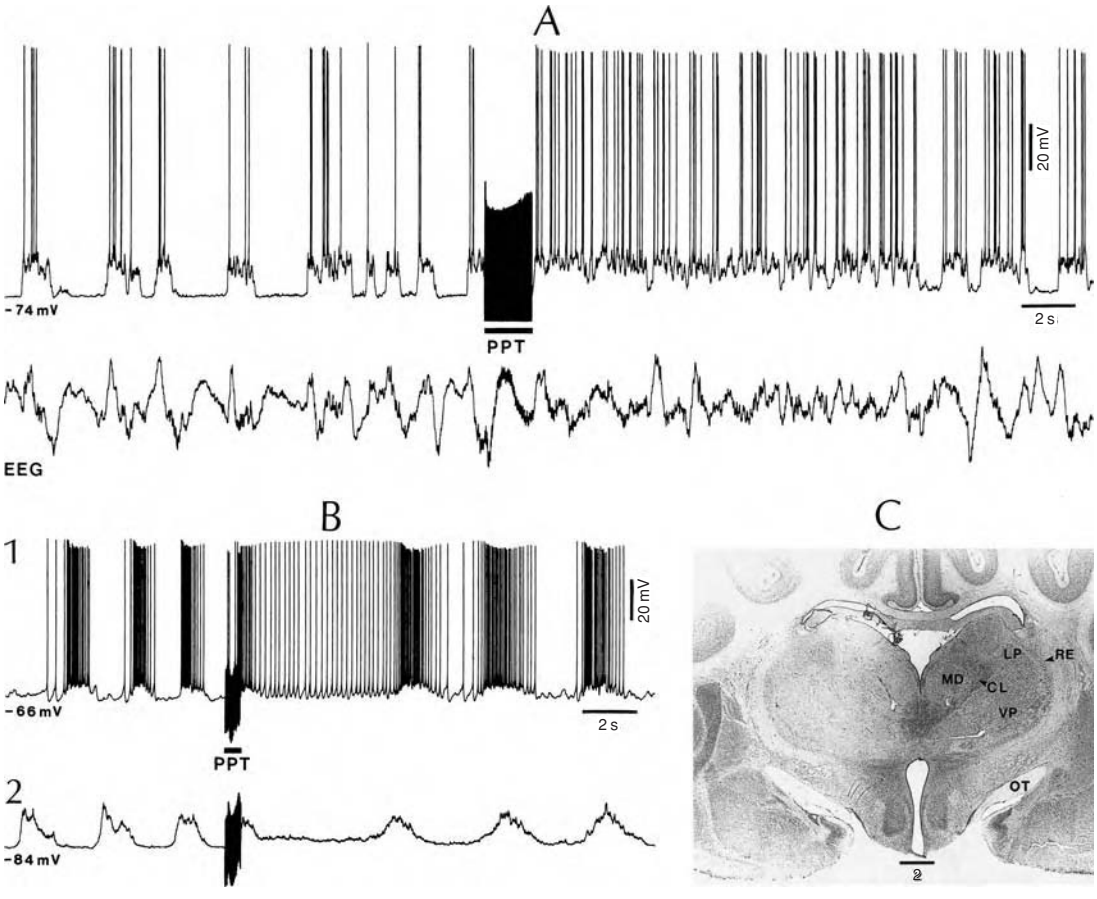

Fig. 7.11 Blockage of slow sleep oscillation by pedunculopontine tegmental (PPT) stimulation in thalamically lesioned cats. (A) Area 7 neuron, oscillating with depolarizing components separated by silent periods of of 1–3 s, in close time relation with EEG wave complexes initiated by surface-positive waves (upward deflections). PPT pulse-train (1.8 s, 30 Hz; horizontal bar) replaced the slow oscillation by tonic firing. (B) Effect of PPT pulse-train (0.6 s, 30 Hz) on slow oscillation in area 5 neuron: (B1) Under DC depolarizing current (+0.5 nA) and (B2) at the resting V_m. (C) Kainic-induced lesion of the thalamus, ipsilateral to recorded cortical neurons. CL, centrolateral nucleus; LP, lateroposterior nucleus; MD, mediodorsal nucleus; OT, optic tract; RE, reticular nucleus; VP, ventroposterior nucleus. Calibration bar is in millimetres. Modified from Steriade *et al.* (1993a).

1993a). This was confirmed experimentally (Rasmusson *et al.*, 1994, 1996).

The compensatory role that might explain the multiplicity of neuromodulatory systems is possibly just an ancillary function. The question of redundancy should be further examined (see also Berlucchi, 1997). It is likely that each neurotransmitter system plays a specific role in the concert of complex processes that occur during the shift from disconnected to activated states. In other words, how

[10] These studies concluded that the cortically projecting cholinergic system improves the accuracy of performance, the dopaminergic system improves the speed of performance, the noradrenergic system prevents interference by distracting stimuli, whereas serotonin depletion results in an increase in impulsive responses (Robbins & Everitt, 1995). See also Sarter & Bruno (2000) for differential effects of brainstem and forebrain modulatory systems in attentional processing during dreaming in REM sleep.

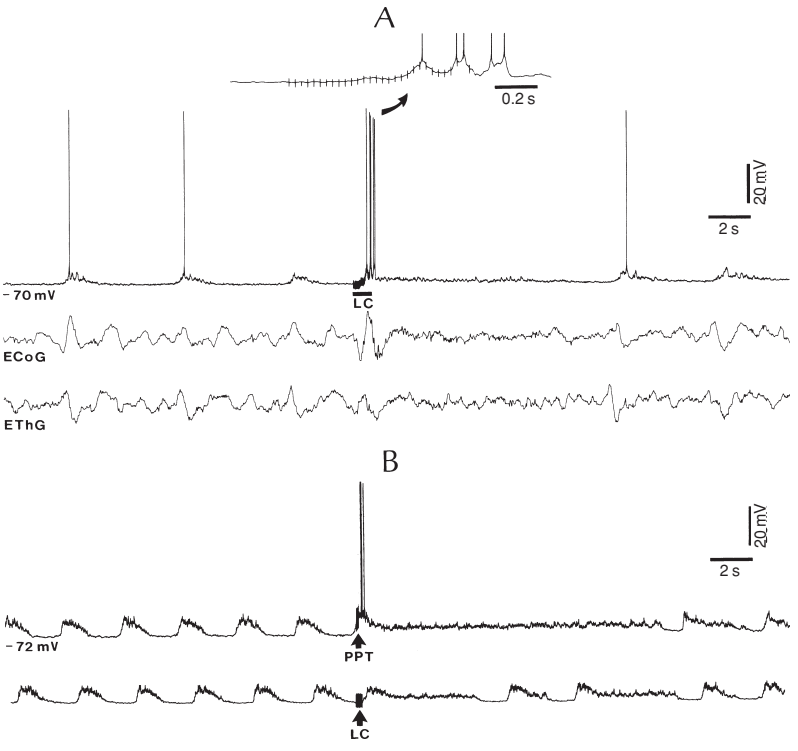

Fig. 7.12 Effects of locus coeruleus (LC) stimulation on the slow cortical oscillation. Cat under urethane anaesthesia. (A) Regular-spiking, area 5 neuron. LC pulse-train (1 s, 30 Hz; marked by horizontal bar) blocked the slow oscillation and simultaneously produced an activated electrocorticogram (ECoG) and electrothalamogram (EThG) response lasting for *c.*8 s. (B) Another area 5 neuron antidromically activated from thalamic centrolateral and lateroposterior nuclei at latencies of 5 and 4 ms, respectively. Stimulation of pedunculopontine tegmental (PPT) cholinergic nucleus (10 stimuli at 100 Hz) blocked the slow oscillation for 15 s. The same parameters of stimulation applied to LC had no effect (not shown); by increasing the duration of the LC pulse-train (30 stimuli at 100 Hz), a blocking effect appeared and lasted for 6 s. Modified from Steriade *et al.* (1993a).

are different activating systems modulating various aspects of adaptive behaviour and how are they implicated in selective attentive processes? As yet, there have been only few attempts to distinguish between the roles of cholinergic and brainstem monoaminergic systems in conditioned performances and attentional processing.[10] It is fair to state that this topic should be elucidated in further research.

The prevalent role of the brainstem cholinergic–thalamic–cortical circuit in activating cortical networks was compared with that exerted by the direct noradrenergic projections from the locus coeruleus (LC). A comparison between the effects of LC and PPT stimulation showed that, although both stimulated structures blocked the slow sleep oscillation, the threshold of this effect was lower, and its duration longer, with PPT than with LC stimulation (Figure 7.12). The more powerful effect exerted by PPT, compared with LC,

stimulation may be explained by reciprocal interactions between these two (PPT and LC) structures. LC neurons extend their long dendrites (0.4–0.5 mm) to adjacent areas, up to the PPT nucleus. Noradrenaline hyperpolarizes cholinergic neurons via α-2 receptors (Williams & Reiner, 1993; Leonard & Llinás, 1994), whereas ACh excites LC neurons via m_2 receptors (Egan & North, 1985). Thus, when PPT is stimulated, LC neurons may be simultaneously activated, whereas LC stimulation may inhibit PPT cholinergic neurons. The LC noradrenergic system is implicated in plastic changes during waking, as shown by the fact that long-term potentiation (LTP)-related genes during wakefulness can be reduced by LC lesions (Cirelli *et al.*, 1996; Cirelli & Tononi, 2000, 2004).[11] The use of combined cholinergic and noradrenergic actions showed that only low-frequency corticothalamic activity is suppressed during arousal, while the flow of high-frequency activity is preserved (Castro-Alamancos & Calcagnotto, 2001).

[11] LC controls the wake-dependent accumulation of sleep need (Cirelli *et al.*, 2005).

Low-frequency (<15 Hz) oscillatory activities, which characterize slow-wave sleep and are effective in gating (obliterating) incoming signals from the outside world, are blocked by cholinergic systems through different mechanisms implicating the mesopontine reticular core and the NB nucleus in the basal forebrain, thus shifting the state of the brain to activation processes.

(a) Sleep spindles are blocked by three non-exclusive mechanisms. Each of them may effectively suppress this oscillation by acting at the primary site of spindle genesis, the RE nucleus, or at the level of target TC neurons. Setting into action cholinergic PPT/LDT nuclei hyperpolarizes RE neurons, thus blocking the depolarizing envelope of spindle sequences in these GABAergic cells and preventing the occurrence of spindles (see Figure 7.9A). Brainstem cholinergic nuclei may also block spindles by acting directly on TC neurons, depolarizing them (see Figure 7.9B), thus preventing the occurrence of low-threshold spike-bursts, which are cardinal signs of spindles and effective in transferring thalamic spindles to the cerebral cortex. Finally, both cholinergic and GABAergic neurons in NB nucleus project to RE neurons and inhibit RE neurons.

(b) The clock-like delta oscillation, which is generated by the interplay between two intrinsic currents of TC neurons at hyperpolarized levels, is also blocked by brainstem cholinergic neurons that depolarize relay cells and thus bring them out of the voltage range at which the stereotyped delta rhythm is generated (Figure 7.13) (Steriade *et al.*, 1991a).

(c) Finally, the cortical slow oscillation is blocked by stimulating the PPT nucleus in acutely prepared animals, through selective obliteration of hyperpolarizing phases, often without significant changes in the membrane potential of neocortical cells (Steriade *et al.*, 1993a). Intracellular recordings in chronically implanted, naturally awake and sleeping cats demonstrate that the first sign of the transition from slow-wave sleep to either wakefulness or REM sleep is invariably the abolition of long-lasting hyperpolarizing potentials

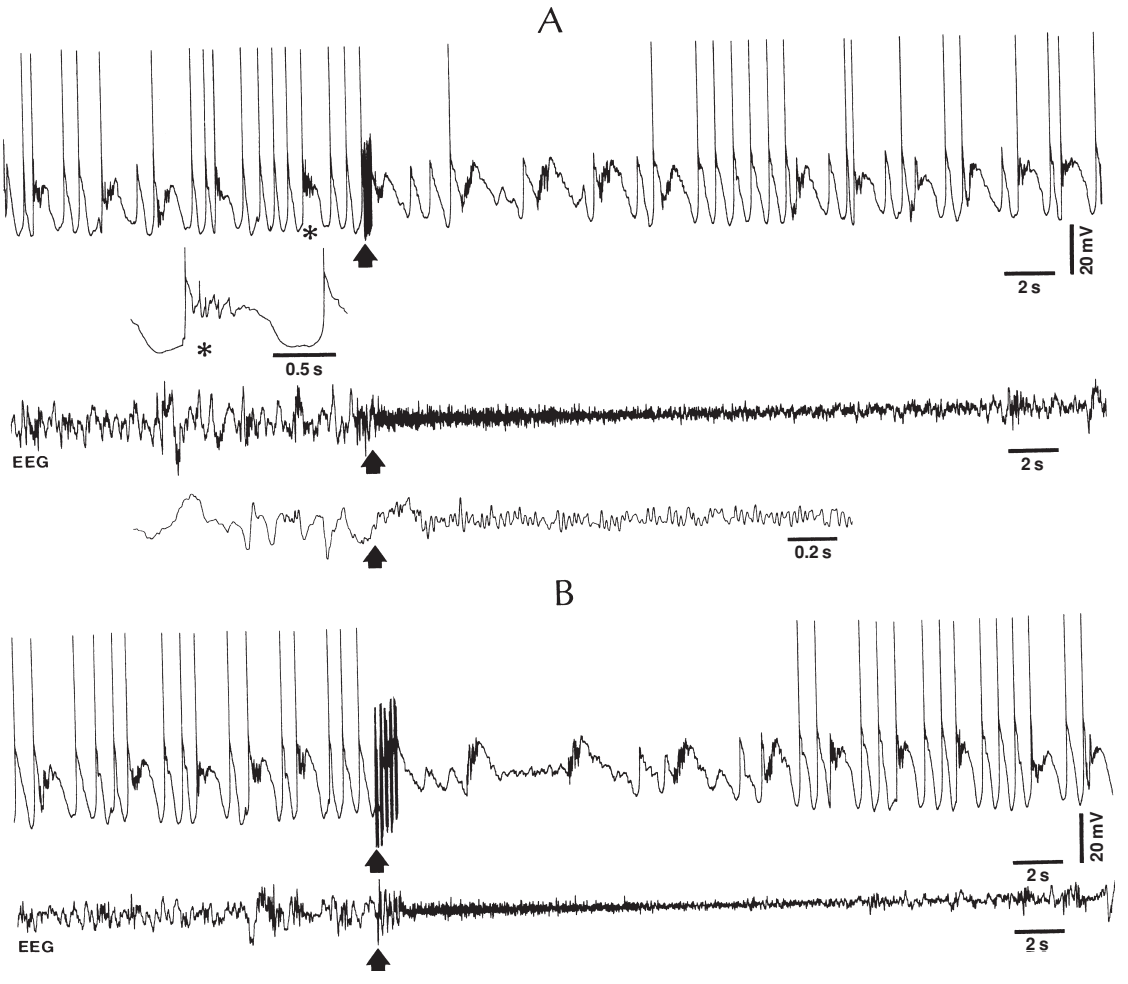

Fig. 7.13 Suppression of the clock-like delta oscillation in a thalamocortical (TC) neuron by stimulation of the pedunculopontine tegmental (PPT) nucleus, and simultaneous cortical activation with the appearance of fast (*c.*40 Hz) activity. Cat under urethane anaesthesia. Intracellular recording from TC cell in the lateroposterior (LP) nucleus, together with EEG from postcruciate gyrus. (A) A pulse-train to the PPT nucleus reduced the rhythmic (*c.*2 Hz) low-threshold spikes crowned by fast action potentials in TC cell and, simultaneously, induced fast EEG activity. The part marked by an asterisk in the intracellular trace is expanded below to show postsynaptic potentials (PSPs) whose origin is the slow cortical oscillation. The EEG before and after the PPT train is expanded below to show *c.*40 Hz activity induced by PPT stimulation. (B) Stronger effects were induced by five pulse-trains to the PPT nucleus, which completely blocked the clock like delta oscillation of the TC cell for *c.*15 seconds and simultaneously produced a long-lasting EEG activation. Modified from Steriade *et al.* (1991a).

and appearance of tonic firing (Steriade *et al.*, 2001a). Figure 7.13A shows the blockage of sleep delta waves by brainstem reticular activating systems and the appearance of fast waves within the fast (gamma) frequency range. This leads us to discuss the various types of oscillatory activities seen during waking and REM sleep.

7.2 Theta and fast rhythms during brain-active states

We will first briefly discuss the theta rhythm, which is typically seen during waking exploratory behaviour in rodents, and then focus on beta and gamma oscillations that occur during all states of vigilance but mainly during waking and REM sleep.

7.2.1 Theta rhythm

This rhythm was first described in the rabbit hippocampus during arousal elicited by sensory or brainstem reticular formation stimulation (Green & Arduini, 1954). The cellular basis of the theta rhythm (usually 5–8 Hz, sometimes up to 10 Hz) was intensively investigated in rodents, but this rhythm is less evident in other mammals and is apparently absent during normal states in humans.[12] In rodents, the theta rhythm was related to sensory processing, control of movement (Grastyan *et al.*, 1959; Buzsáki, 1996), and to the induction of long-term synaptic potentiation, a cellular model of memory.[13]

In addition to the master origin, the septohippocampal cholinergic system, theta is also believed to arise in the entorhinal cortex since atropine does not completely block this oscillation. It was proposed that NMDA receptors are critical for the atropine-resistant form of theta (Buzsáki, 2002). A dipole was found in the entorhinal cortex, one in layers I–II and the other in layer III (Alonso & Garcia-Austt, 1987a,b; Boejinga & Lopes da Silva, 1988); stellate cells in layer II display intrinsic oscillations within the theta frequency (Alonso & Llinás, 1989). The output from the enthorinal cortex activates the dentate granule cells and CA1 pyramids, regarded as the main generators of hippocampal theta waves (Bland *et al.*, 1980; Buzsáki *et al.*, 1983; Leung, 1984). Another theta dipole is set up by inhibitory currents on the somata of pyramidal neurons (Buzsáki *et al.*, 1986; Soltesz & Deschênes, 1993), generated by hippocampal local-circuit cells. Different aspects of theta generation based on intracellular recordings and modeling studies are reviewed elsewhere (Buzsáki, 2002; Traub *et al.*, 1989). As to the presence of theta activity in the neocortex, it may be due, at least partly, to bursting basal forebrain cholinergic neurons that fire in synchrony with EEG theta waves during active waking and REM sleep, but are virtually silent during slow-wave sleep (Lee *et al.*, 2005).

7.2.2 Cortical and thalamic generation and synchronization of beta/gamma rhythms

After the pioneering work of Moruzzi & Magoun (1949),[14] who elicited blockage of sleep-like low-frequency EEG rhythms and appearance of higher frequency waves by stimulating the brainstem reticular formation, Bremer *et al.* (1960)[15] were the first to report that the EEG activated response to brainstem reticular stimulation includes the

[12] In the cat, theta hippocampal activity is conspicuous during REM sleep, but occurs only exceptionally during waking (Jouvet, 1965). In humans, the presence of a theta rhythm was denied in normal states, even with deep electrodes inserted in the hippocampus (Brazier, 1968; Halgren *et al.*, 1978). Other studies indicated, however, that some waves in the theta band (4–7 Hz) may be linked to working memory (Raghavachari *et al.*, 2001; Halgren *et al.*, 2002). 'Pathological theta waves' were described as a slowing down of alpha activity, due to great reduction in cerebral blood flow (Ingvar *et al.*, 1976), to metabolic encephalopathies (Saunders & Westmoreland, 1979) or disturbances in deep midline structures (Gloor, 1976). Theta frequency (4–8 Hz) was also described in the 'thalamocortical dysrhythmia syndrome' of a series of pathological entities, such as neurogenic pain, tinnitus, Parkinson's disease, and depression (Llinás *et al.*, 1999, 2005).

[13] Induction of long-term potentiation is facilitated when the interval between stimuli corresponds to the frequency of hippocampal theta (Larson *et al.*, 1986; Larson & Lynch, 1986; Pavlides *et al.*, 1988).

[14] Moruzzi & Magoun (1949) postulated that the EEG cortical activating effect was mediated, at least in part, by the diffuse thalamic projecting system. Several decades later, neuronal recordings showed indeed that stimulation of midbrain reticular core induces monosynaptic excitation of thalamic intralaminar neurons, antidromically identified from various neocortical areas (Steriade & Glenn, 1982).

[15] Bremer *et al.* (1960) called this response *accélération synchronisatrice*, which stood in contrast with the usual designation of EEG desynchronization, generally employed by most epigones of Moruzzi and Magoun. Intracortical and corticothalamic synchronization of gamma oscillations (30–60 Hz) was later demonstrated by neuronal recordings (see main text).

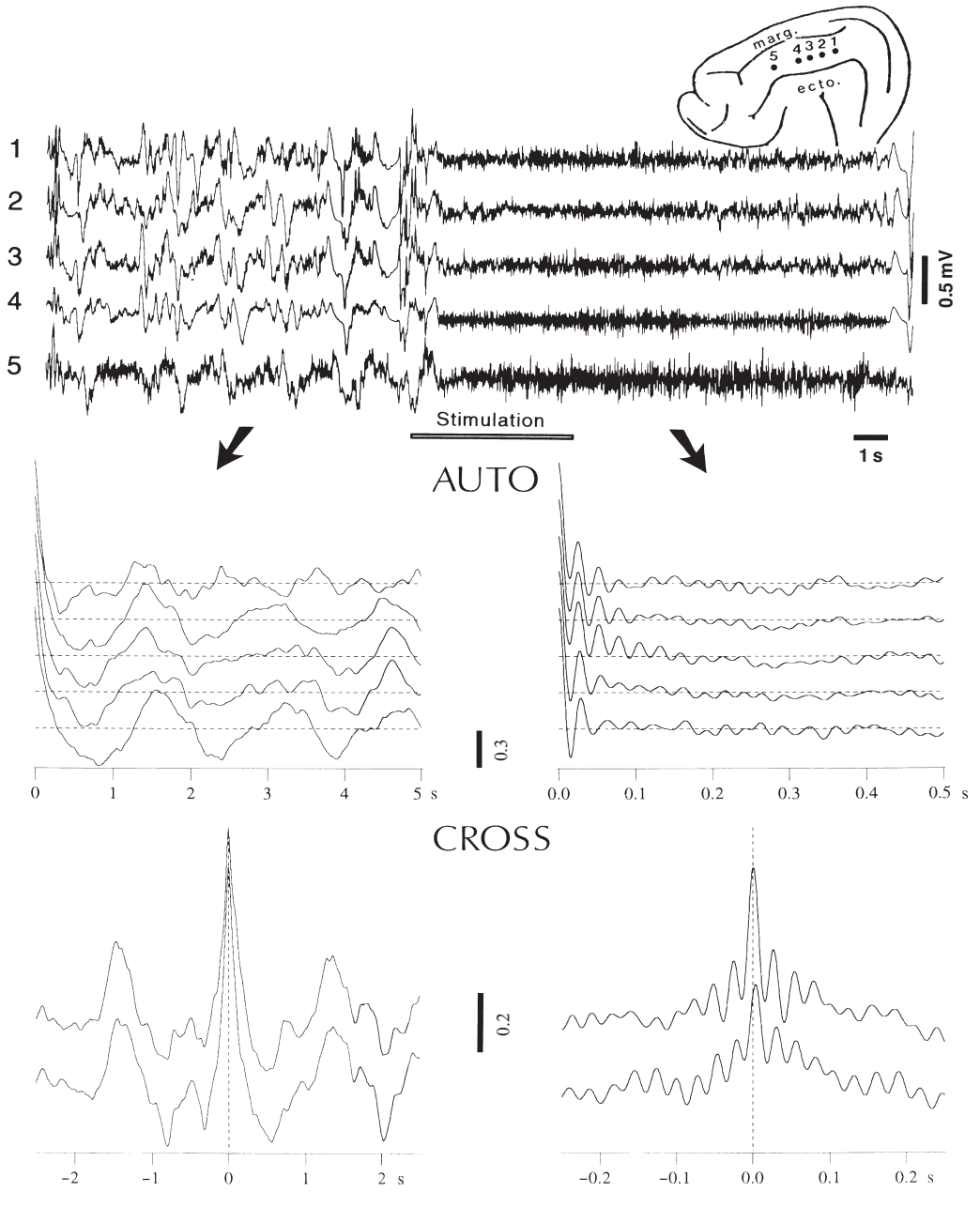

Fig. 7.14 Fast (c.40 Hz) neocortical electrical activity produced by stimulation of mesopontine cholinergic nuclei. Cat under ketamine–xylazine anaesthesia. Top, slow oscillation and its disruption by PPT pulse-train (300 Hz, horizontal bar), associated with appearance of fast activity whose amplitude exceeds that of fast waves during sleep patterns. Numbers of recorded cortical foci correspond to those indicated on the suprasylvian gyrus (areas 5 and 7) of the brain figurine. Bottom, autocorrelations (AUTO, leads 1–5) and cross-correlations (CROSS, between leads 1–2 and 1–3) from sleep and aroused epochs (arrows). Note synchronized slow oscillation (0.5 Hz) during sleep-like period and synchronization of fast rhythms (about 40 Hz) during the activated period. Modified from Steriade (1995b), Steriade *et al.* (1996a) and unpublished data by M. Steriade and F. Amzica.

appearance of peculiar fast rhythms (40–45 Hz), with regular and synchronizing acceleration (see Figure 7.14), simultaneously with the ocular syndrome of arousal. Since then, a series of studies in various cortical areas have shown the presence of 20–80 Hz (beta and gamma) waves during different conditions of increased alertness, such as intense attention, conditioned responses, tasks requiring fine movements, or responses to different sensory modalities.[16] Beta and gamma rhythms (20–50 Hz) have been conditioned and associated with their enhanced synchrony in visual and motor corticothalamic networks (Amzica *et al.*, 1997). The synchronized fast rhythmic activity led to the hypothesis that linkages between spatially distributed oscillatory elements in the visual cortex may constitute the basis for 'feature binding' and pattern recognition function (Singer, 1990) (see below, Section 7.2.3). However, beta and gamma activities (from now on, both are termed 'fast'; see the reason for that in Steriade *et al.*, 1996a)[17] are equally present in the spontaneous activity of neurons and EEG. Fast rhythms are mainly seen during brain-active states, waking and REM sleep, in animals (Steriade *et al.*, 1996a; Maloney *et al.*, 1997) and humans,[18] but are also present during the depolarizing phase of the slow oscillation during deep anaesthesia (Figure 7.15) and natural slow-wave sleep (Figure 7.16) in the cerebral cortex (Steriade *et al.*, 1996a) and thalamus (Steriade *et al.*, 1996b).

We now focus on the neuronal substrates of generation and synchronization of fast rhythms in intracortical and corticothalamic circuits. The possible significance of these activities is discussed in Section 7.3.2.

Although the role played by thalamic relay (TC) neurons in the genesis of the 40 Hz rhythm was initially denied (Gray *et al.*, 1989), subsequent studies have demonstrated that 40 Hz rhythmic activities appear in intracellularly recorded, antidromically identified TC cells (Steriade *et al.*, 1991b). The coherency between different various brain levels generating 40 Hz can be accomplished by intracortical, intrathalamic and reciprocal corticothalamic neuronal networks (see below).

The intrinsic properties of cortical and thalamic neurons have been implicated in the generation of 40 Hz activities. Thus, sparsely spinous (probably inhibitory) interneurons recorded *in vitro* from layer IV of the frontal cortex produce narrow-frequency (35–45 Hz) oscillations upon depolarization of the membrane potential; these oscillations are generated by a voltage-dependent, persistent Na^+ current, with the involvement of a delayed rectifier (Llinás *et al.*, 1991). Voltage-dependent fast rhythms have also been recorded in identified callosal neurons (Nuñez *et al.*, 1992a), and this would explain the coherence of 40 Hz rhythms in neocortical areas of both hemispheres (see also below). The dependence of fast rhythms upon neuronal depolarization explains the exclusive presence of these oscillations during the depolarizing phase of the slow oscillation in deep anaesthesia (Figure 7.15) or natural slow-wave sleep (Figure 7.16A). The best candidates for the generation and synchronization of fast cortical activities are the fast-rhythmic-bursting (FRB) neurons that are discussed and depicted in

[16] The fast (beta, 20–30 Hz; gamma, 30–60 or 80 Hz) rhythms were observed in cortex while dogs paid intense attention to a visual stimulus (Lopes da Silva *et al.*, 1970), during an enhanced level of vigilance while cats watched a visible but unseizable mouse (Rougeul-Buser *et al.*, 1983; Bouyer *et al.*, 1987), during tasks requiring fine finger movements and focused attention in the cortical neurons of monkeys (Murthy & Fetz, 1992), during performance of conditioned responses (Freeman & Van Dijk, 1988), prior to the performance of a complex task in humans (Sheer, 1984), during responses to olfactory or visual stimuli (Freeman, 1975; Eckhorn *et al.*, 1988; Gray *et al.*, 1990; Herculano-Houzel *et al.*, 1999; Siegel & König, 2003), and during the after-discharges of flash-evoked responses in the visual cortex (Steriade *et al.*, 1968). Simultaneous recordings of thalamic and scalp activities in humans, during performance of a cognitive task (semantic memory recall) showed phase-locked fast (21–34 Hz) rhythms (Slotnick *et al.*, 2002).

[17] Beta (20–30 Hz) rhythms may develop into gamma rhythms (usually 30–60 Hz) in periods as short as 0.5 s, due to slight membrane depolarization of cortical neurons. For this reason, we did not split these two oscillatory activities in distinct categories and termed both of them fast. EEG recordings during the sleep-wake cycle and cognitive activity in humans showed that there is no precise cut-off between the beta and gamma bands, as these activities may fluctuate simultaneously (Gross & Gotman, 1999). See also Slotnick *et al.* (2002),[16] reporting increased activities within both beta and gamma frequency bands (21–34 Hz) during semantic memory recall.

[18] Magnetoencephalographic recordings in awake humans (Ribary *et al.*, 1991; Llinás & Ribary, 1992, 1993) have revealed the presence of a 40 Hz oscillation over the entire cortical mantle, a phase-shift of oscillatory activity close to 12 ms between the rostral and caudal

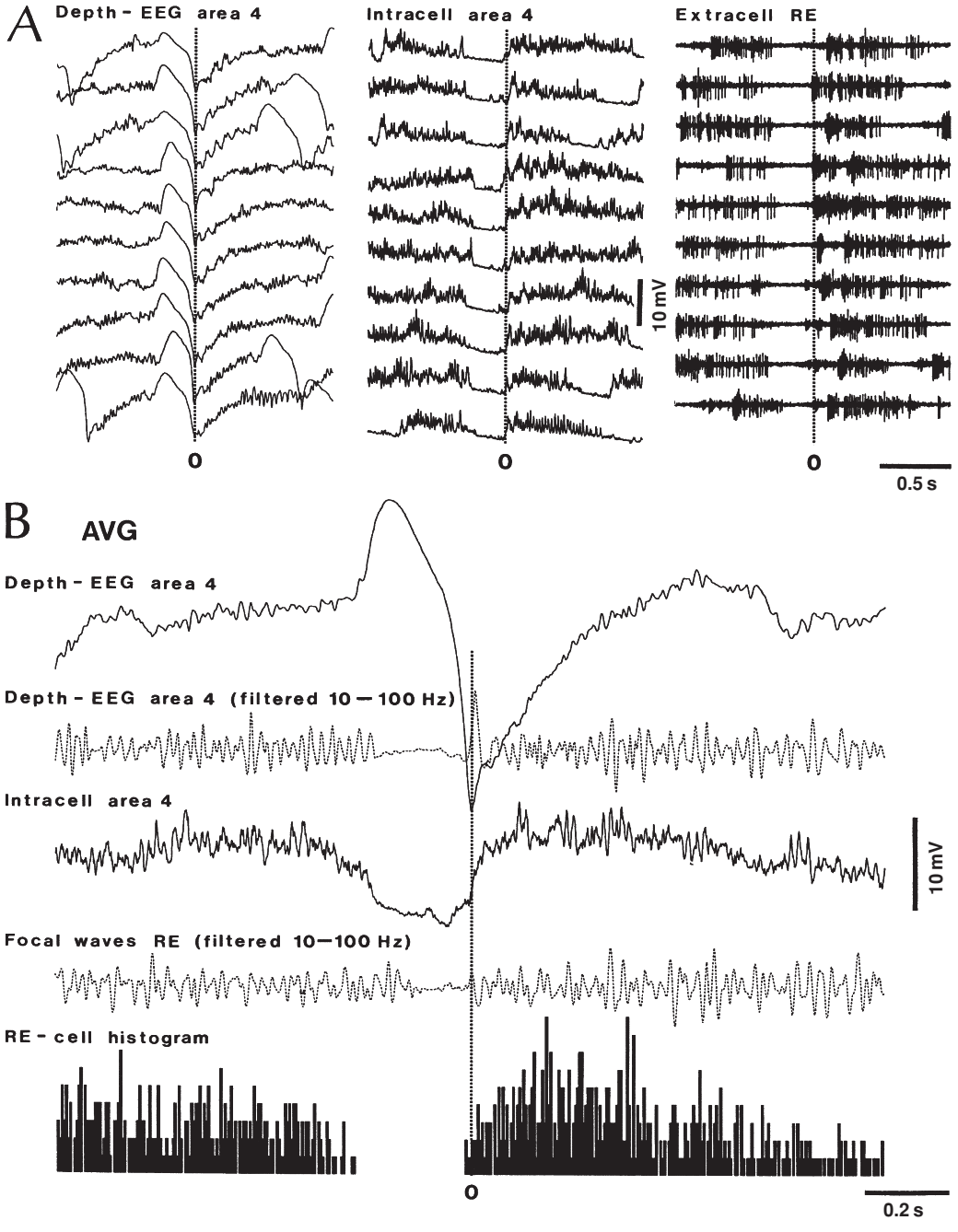

Fig. 7.15 Fast oscillations (40–45 Hz) are present in cortical neurons during the depolarizing phase of the slow oscillation and are suppressed during the depth-EEG positive phase (associated with membrane hyperpolarization) in cortical and thalamic RE neurons. Cat under ketamine–xylazine anaesthesia. (A) Simultaneous recording of depth-EEG waves from cortical area 4, intracellular activity from neuron in area 4, and extracellular activity of RE neuron from the rostral pole of the nucleus. Each column was centred on time 0 (dotted line), represented by the sharp depth-negative EEG deflection (following the prolonged depth-positive phase of the slow oscillation), which was used as a reference for aligning EEG, the intracellularly recorded area 4 neuron, and the extracellularly recorded RE neuron. (B) Average (AVG) of ten traces depicted in (A) with filtered EEG trace, filtered field potentials recorded from RE nucleus by the same microelectrode that picked up neuronal firing, and peri-event histogram of RE discharges. Modified from Steriade *et al.* (1996b).

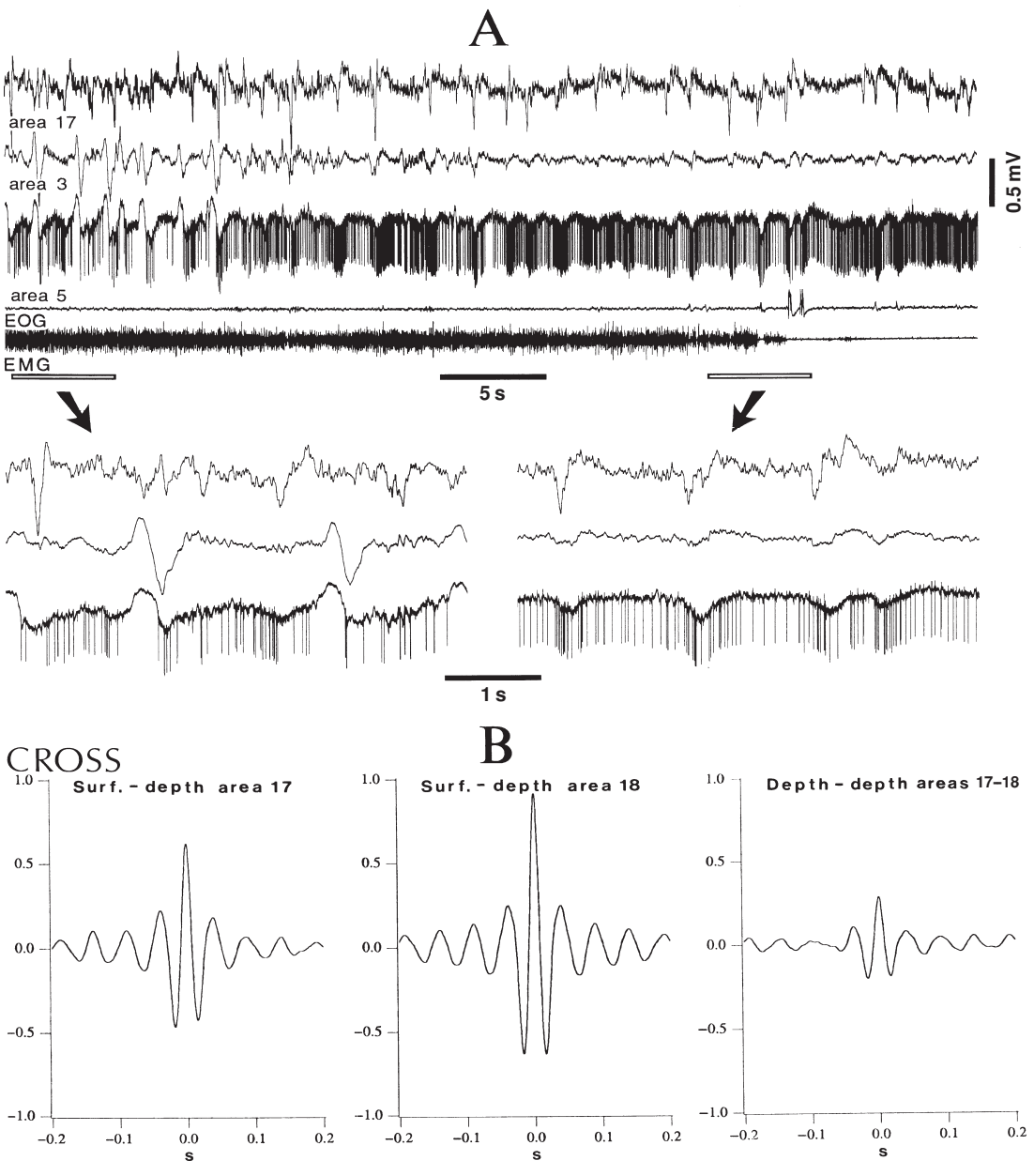

Fig. 7.16 Fast activity during transition from slow-wave sleep to REM sleep. Chronically implanted cats. (A) Simultaneous recordings of field potentials from the depth of cortical areas 17 and 3, and single unit and field potentials from area 5, electro-oculogram (EOG) and electromyogram (EMG). Two epochs from slow-wave sleep and REM sleep, indicated by horizontal bars, are expanded below (arrows) to depict changing activities in areas 17, 3 and 5. Note suppressed neuronal firing in area 5 during the depth-positive wave (reflecting neuronal hyperpolarization) in slow-wave sleep (left), and depth-positive ponto-geniculo-occipital (PGO) potentials associated with increased neuronal firing in REM sleep (right). (B) Another animal during REM sleep. Note cross-correlations (CROSS) between surface- and depth-recorded fast activity (about 20 Hz) in area 17 and rostral part of area 18, as well as between depth activities in areas 17 and 18. Modified from Steriade *et al.* (1996a).

[18] (*cont.*) poles of the hemisphere, and a synchronization of this 40 Hz activity by presentation of auditory stimuli with random frequencies.

[19] See other *in vivo* (Cardin *et al.*, 2005), *in vitro* and modelling studies of FRB neurons by Traub *et al.* (2003, 2005) and Cunningham *et al.* (2004).

[20] In the olfactory bulb, Freeman (1975) also postulated that the generation of 40–80 Hz activity depends on feedback inhibitory circuits involving local-circuit GABAergic neurons acting on output elements, the mitral cells.

[21] In that study, the short duration of oscillation suggested that a limited neuronal circuit, as in cortical slices, is inadequate to sustain oscillations for long periods.

Chapter 2 (Section 2.3.1). Importantly, FRB neurons are both long-axon excitatory (corticothalamic) and local-circuit inhibitory (basket-type) neurons (Steriade *et al.*, 1998b).[19] They may serve to synchronize fast activities within corticothalamic circuits and locally (Lytton & Sejnowski, 1991).[20]

TC cells also display depolarization-dependent fast oscillations. A class of rostral intralaminar neurons, projecting with high conduction velocities (40–50 ms^{-1}) to association cortex, fires spike-bursts at unusually high frequencies (900–1000 Hz) that recur within the frequency range of 40 Hz (Steriade *et al.*, 1993c). These intralaminar TC cells also spontaneously discharge spike-bursts during naturally activated states associated with neuronal depolarizations, waking and REM sleep.

Although the fast oscillations can be generated by the intrinsic properties of single cells, complex neuronal circuits are required for the synchronization of cellular ensembles in order for the fast rhythm to be expressed in multi-unit and EEG recordings. *In vitro* studies of rat somatosensory cortex have revealed the presence of rhythmically synchronized fast activities generated by networks of intrinsically-bursting pyramidal neurons (Chagnac-Amitai & Connors, 1989).[21] Synchronization of fast rhythms between connected neurons recorded from association (Nuñez *et al.*, 1992a) and visual (Engel *et al.*, 1991) areas of both hemispheres indicates that one of the synchronizing mechanisms of this oscillation is located at the cortical level. Cortical FRB (or 'chattering') neurons are interconnected (Steriade *et al.*, 1998a; Gray & McCormick, 1996) and this linkage also constitutes a mechanism for coherent fast activities in the visual (Gray & McCormick, 1996) and other, motor and association (Steriade *et al.*, 1998a), cortical areas. The intracortical synchronization results in fast oscillations that do not show field reversal at any depth of the cortex (Steriade *et al.*, 1996a; Steriade & Amzica, 1996) (Figure 7.17B). Volume conduction was precluded because the negative field potentials of the fast oscillations were associated at all depths with neuronal firing and were not observable in the underlying white matter. The absence of depth reversal of fast oscillations is probably due to the fact that the current flow is mainly attributable to transmembrane components and less to internal longitudinal components. Vertically distributed currents are not completely ruled out, however, as current-source–density analyses show alternatively distributed microsinks and microsources (Steriade & Amzica, 1996). In contrast with the long-range synchrony of low-frequency oscillations that occurs in slow-wave sleep, precise synchronization of fast activities is restricted to circumscribed cortical territories, usually not exceeding 5–7 mm (see cross-correlations in Figure 7.14, displaying coherent activity between leads 1–2 and 1–3, but such synchronization was not detected between leads 1 and 5). High-frequency (25–70 Hz) rhythms are also superimposed on slowly recurring potentials that last 1–3 s in the entorhinal cortex of the isolated guinea pig brain (Dickson *et al.*, 2003) and, similarly to data obtained in neocortex *in vivo* (Steriade *et al.*, 1993a), these

entorhinal fast oscillations are under cholinergic control (Dickson *et al.*, 2003).

In addition to intracortical circuits, reciprocal corticothalamic circuits generate and synchronize fast rhythms. During waking, corticothalamic projections drive thalamic GABAergic RE neurons, and their inhibitory action would sculpt the tonic firing of TC neurons, thus resulting in short IPSPs that may reinforce the fast oscillations in TC cells (Pedroarena & Llinás, 1997). At least in felines, RE cells have also access to thalamic inhibitory interneurons and this link would completely transform the simple inhibitory projection of RE cells to TC neurons; disinhibition may even prevail (Steriade *et al.*, 1985; Steriade, 1999). Figure 7.17 demonstrates the coherence of fast oscillations (35–40 Hz) between interconnected foci in association visual cortical area 21 and visual thalamic lateral geniculate (LG) nucleus (Steriade *et al.*, 1996b). The direct connection was identified by reciprocal monosynaptic responses between the two sites (Figure 7.17A). Other experiments have also shown synchronization between the visual cortex and thalamus, specifying the higher frequencies in the retina and LG (60–120 Hz) than in cortex (30–60 Hz) (Castelo-Branco *et al.*, 1998).[22] The presence of 40 Hz oscillatory neurons in the intralaminar central lateral nucleus (Steriade *et al.*, 1991b; Steriade *et al.*, 1993c), which has widespread projections to the cerebral cortex, including the visual areas (Jones, 1985; Cunningham & LeVay, 1986), is important for the idea of thalamic conjunction and synchronization of distant cortical areas.[18] Resonant fast activities in corticothalamic circuits are based on direct excitatory projections, as there is direct built-in frequency amplification in this pathway. This was demonstrated by the dramatic increase of EPSPs in target TC neurons following 30–50 Hz cortical volleys (Lindström & Wróbel, 1990). In the feedback (thalamocortical) pathway, stimulation within the frequency band of the gamma rhythm (40 Hz) results in spatially focused responses (Lindström & Wróbel, 1990), probably due to the activity of different types of local inhibitory neurons, within these fast frequencies (Llinás *et al.*, 1991; Steriade *et al.*, 1998a; Contreras & Llinás, 2001).

7.2.3 Role of fast activities in thalamocortical systems; are gamma rhythms implicated in cognition and consciousness?

In virtually all sensory systems, cortical neuronal responsiveness during the fast background electrical activity largely depends upon the enhanced synaptic transmission of incoming signals in appropriate thalamic relay nuclei. The gating role of the thalamus in cortical disconnection during slow-wave sleep and in cortical activation during waking and REM sleep was demonstrated by obliteration of postsynaptic thalamic responses to prethalamic stimuli as soon as the brain shifts its state from wakefulness to drowsiness and sleep (Steriade, 1991; Gibson *et al.*, 1999), and depolarization with increased input resistance upon awakening from sleep (Steriade *et al.*, 2001a). An

[22] See, however, Siegel & König (2003), who point to a broad frequency range of responses in the visual cortex of the awake behaving cat, from 40 Hz to well above 100 Hz.

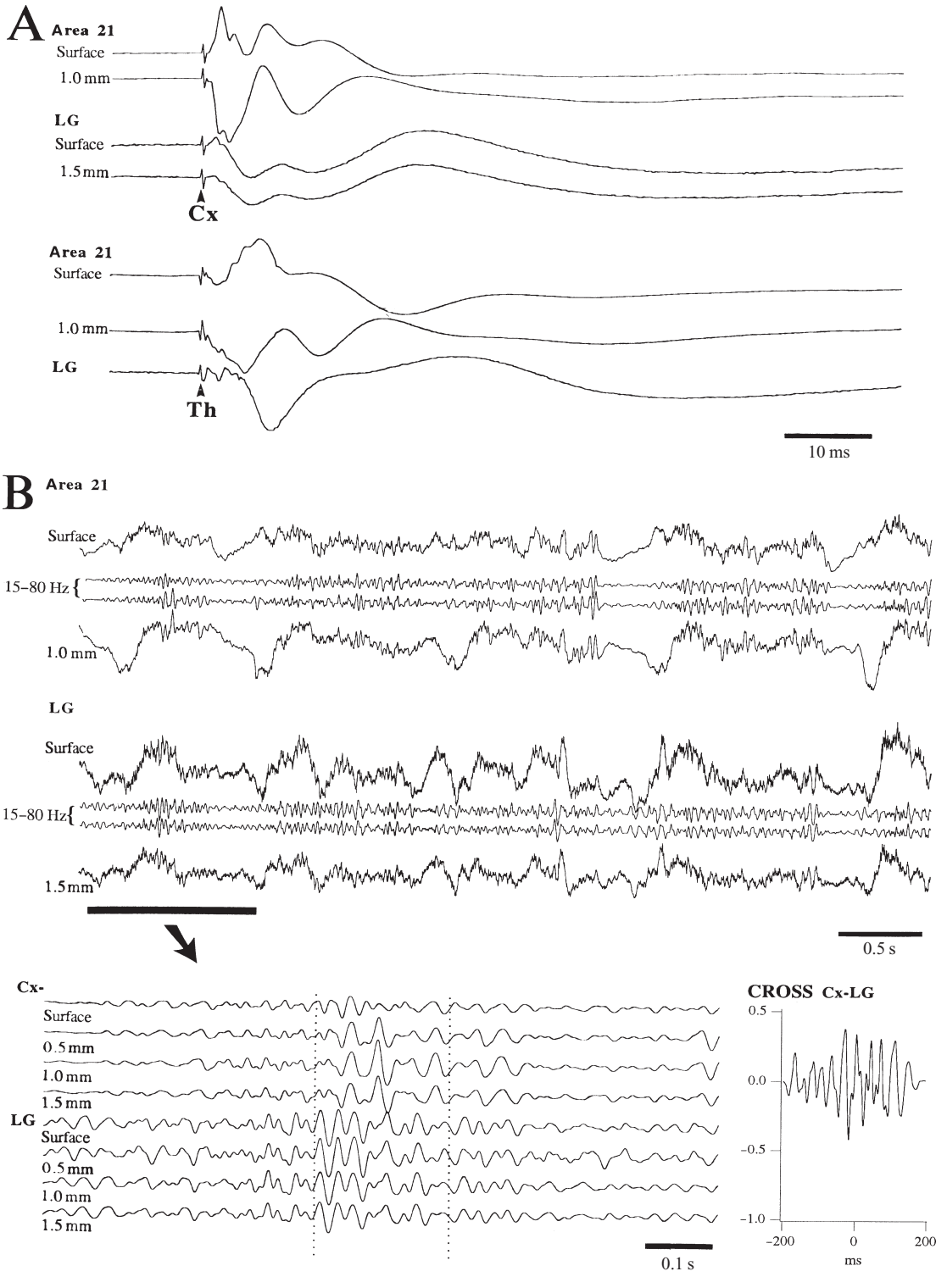

Fig. 7.17 Correlated fast oscillations (35–40 Hz) of field potentials in reciprocally related cortical and thalamic foci. Cat under ketamine–xylazine anaesthesia. (A) Physiological identification of reciprocal projections between posterior suprasylvian

extrathalamic circuit is represented by brainstem reticular activating (glutamatergic) neurons that drive cholinergic basal forebrain neurons with cortical projections, contributing to potentiation of cortical responsiveness. One exception to the rule that the thalamus is the gateway to the cortex in gating processes during states of vigilance is the olfactory system, in which the perception of smell arises in the three-layered olfactory cortex, but olfaction does not necessarily require a thalamic relay (Steriade *et al.*, 1969). Field potentials and extra- and intracellular recordings from olfactory cortex showed state-dependent changes in odorant-evoked responses, with low olfactory information during slow-wave sleep and effective signal transmission during fast wave activity,[23] in synchrony with other sensory systems (Steriade & Llinás, 1988; Steriade, 1970).

As to the role of gamma oscillations, it was proposed that, besides spatial mapping that allows a limited number of representations, a temporal component is brought about by synchronized oscillatory responses at *c.*40 Hz across spatially separate cortical columns (Singer, 1990; Murakami *et al.*, 2005).[24] The conjunction of spatial and temporal factors is the basis of functionally coherent cell assemblies. The hypothesis of 'feature binding' and pattern recognition function was based on data showing the role of synchronized 40 Hz rhythms in the mediation of responses to various sensory modalities, high-order motor functions, conditioning processes,[16] and selective visual attention (Eckhorn *et al.*, 1988; Singer, 1999). In humans, tasks probing working memory are associated with phase synchrony of beta (20 Hz) and gamma (30–40 Hz) cortical activities (Fries *et al.*, 2001). During selective somatic attention, human subjects display a transient phase-locking of gamma waves in the contralateral parietal and prefrontal cortical areas, as far as 9 cm apart (Palva *et al.*, 2005).[25] During somatosensory processing, 40 Hz oscillations become phase-locked in conjunction with the electrogenesis of the prefrontal (area 46) cognitive N140 component (Desmedt & Tomberg, 1994).[26] In sum, it was proposed that enhanced and coherent fast oscillations during depolarizing states of background neuronal activity (Steriade *et al.*, 1996a,b;

[23] Part of the pathway from the olfactory cortex to the orbitofrontal cortex passes through the thalamic mediodorsal (MD) nucleus. The question of whether conscious perception of olfaction arises in the orbitofrontal and/or olfactory cortex (Öngür & Price, 2000; Shepherd, 2005) remains open. Work by Takagi and his colleagues has shown that olfactory bulb (OB) stimulation evokes potentials in the thalamic MD nucleus and then in the orbitofrontal cortex (Tanabe *et al.*, 1975a). In addition, discrimination of odours improves from OB through olfactory cortex and further to orbitofrontal cortex (Tanabe *et al.*, 1975b).

[24] Interestingly, during slow-wave activity, the EPSPs evoked by olfactory bulb stimuli were larger during the hyperpolarizing phase of the slow oscillation, thus corroborating the idea that this component is associated with increased input resistance and is not due to an active GABAergic process, as also indicated in intracellular studies of neocortical neurons in naturally sleeping animals (see Steriade *et al.*, 2001a).

[25] These authors discussed the origin of fast activity in the cerebral cortex and suggested that FRB neurons are key elements in reciprocal corticothalamic loops that generate gamma rhythms, as demonstrated in experimental studies (Steriade *et al.*, 1998b) (see also Section 2.3.1).

[26] The parietal and prefrontal cortical areas of primates are connected through direct corticocortical areas (Petrides & Pandya, 1984).

cortical area 21 and thalamic lateral geniculate (LG) nucleus. One cortical (Cx) electrode and one thalamic (Th) electrode (each from four-electrode arrays inserted in cortex and thalamus) were used to stimulate (arrowhead) and record field potentials in both cortex (surface and 1 mm depth) and thalamus (dorsal aspect of LG nucleus and 1.5 mm deeper). Cortical and thalamic multiphasic field potentials were initiated with latency shorter than 1.5 ms, thus indicating monosynaptic responses. (B) Simultaneous recording of spontaneous activities from four cortical (surface and 0.5, 1 and 1.5 mm depth) and four thalamic (dorsal surface of LG and 0.5, 1, and 1.5 mm deeper) foci that proved to be responsive in (A). Filtered activities (15–80 Hz) are also illustrated between unfiltered traces (to simplify, only two cortical and two thalamic foci are depicted in the top panel of B). Filtered activities from the epoch marked by horizontal bar are expanded below (arrow). Note oscillations at 35 Hz in cortex and 40 Hz in thalamus. Note also in-phase oscillations at the surface and different depths of cortex. Cross-correlation (CROSS) between cortex and LG activities (Cx at time 0) shows a time-lag of 3.5–4 ms between cortex and thalamus and higher frequencies in LG. Modified from Steriade *et al.* (1996b).

Steriade & Amzica, 1996) may create a bias in favour of stimuli that appear at the attended location, thus preparing for synchronized fast activities in response to sensory inputs, associated with finely integrated motor events (Tomberg, 1999).[27]

The temporal binding hypothesis (see review by Engel *et al.*, 2001) was amply discussed and criticized. Multi-unit and field potential recordings from monkeys' visual areas showed that fast (30–50 Hz) oscillatory responses are found in less than 1% (2 of 424) recordings at 142 explored sites.[28] This very low incidence was found to be incompatible with the idea that a vivid picture of the world would depend on rhythmically synchronized neurons, which are so difficult to observe (Young *et al.*, 1992). The emphasis on binding within the gamma band (30–60 Hz) was also challenged by data showing oscillations at a much lower frequency (7–20 Hz range) in more than 90% of the cases, using also intracellular recordings that preclude the possibility that subthreshold events were not accounted for (Crick, 1994). In addition, whereas most proponents of the binding hypothesis relate fast oscillations with conscious processes of sensory perception, coherent beta/gamma oscillatory activity is also observed during deep anaesthesia and natural slow-wave sleep, superimposed on the depolarizing phase of the slow oscillation (Steriade *et al.*, 1996a,b), simply because such fast activities are voltage(depolarization)-dependent in both pyramidal and local-circuit inhibitory neurons (Steriade *et al.*, 1991b; Llinás *et al.*, 1991; Nuñez *et al.*, 1992a; Steriade *et al.*, 1998a). Other remarks concerning the temporal binding hypothesis include the fact that binding is not computed in the primary visual cortex (but in higher-order regions of the occipital cortex and posterior parietal areas) so then there is no reason to expect synchrony in that region; and the absence of any direct link between the experimental evidence and the issue of binding *per se* (Bringuier *et al.*, 1997).[29]

7.3 Phasic events in waking and REM sleep

7.3.1 Ocular movements in wakefulness

Alerting stimuli during waking have access to two distinct systems. The first one is the circuit between GABAergic neurons in the substantia nigra pars reticulata (SNr) and their target neurons in the superior colliculus (SC), pedunculopontine tegmental (PPT) nucleus, and pontine reticular formation. This circuit is responsible for the phasic shift of gaze involved in the orienting behaviour. Sensory stimuli that trigger orienting reactions produce a decrease in the discharge rate of SNr neurons, consequently releasing SC neurons from tonic inhibition. As a result, SC projections to pontine oculomotor nuclei lead to eye saccades toward the signal. The decrease in firing rates of GABAergic SNr neurons caused by sensory stimuli[30] results from direct inhibitory inputs arising in GABAergic caudate neurons, which receive projections from some fields in the upper brainstem reticular core, medial and intralaminar thalamic nuclei, and cortex

[27] The cognitive nature of the N140 component of evoked brain potentials in humans resulted from comparison with control responses to physically identical finger stimuli that were ignored by the subject and did not elicit a prefrontal N140. The first cortical response (N20) is stable across conditions and is not affected by selective attention (see Tomberg & Desmedt, 1999).

[28] Probably first proposed by Von der Malsburg (see his more recent reviews, 1995, 1999).

[29] The coherent oscillations in the monkey motor cortex and hand electromyogram during performance of tasks is also in the beta band, 20 Hz (Baker *et al.*, 1997). In humans, the rhythmic modulation was found at a frequency lower than 20 Hz (Farmer, 1998).

[30] See the evaluation of binding theory by Shadlen & Movshon (1999).

(Hikosaka & Wurtz, 1983). The hyperpolarization of premotor pontine reticular neurons during the alert state (Graybiel & Ragsdale, 1979) de-inactivates the Ca^{2+}-dependent low-threshold spike and fast Na^{+} spike-bursts, which drive oculomotor neurons.

The second system consists of the brainstem PPT and thalamic targets of SNr (such as ventromedial, VM, and rostral intralaminar neurons) that are disinhibited during the periods of silenced firing in SNr and exert depolarizing actions on neocortical neurons in superficial and deep cortical layers (Ito & McCarley, 1984). Eye-movement-related potentials in regular-spiking neocortical neurons are associated with increased or decreased firing, and short-lasting (2–5 ms) hyperpolarizations (contrasting with the longer hyperpolarizations, 10–20 ms, that accompany ocular saccades and PGO potentials in REM sleep; see below, Section 7.3.2). The eye-movement-related hyperpolarizations in waking are due to short IPSPs (2–5 ms) that delay spikes and influence firing threshold (Figure 7.18) (Glenn *et al.*, 1982). These IPSPs are Cl^{-} dependent: their reversal potential is between −65 mV and −72 mV and such hyperpolarizing potentials were not found in recordings with KCl-filled pipettes. Moreover, fast-spiking (presumably inhibitory) neurons increase their firing rates during ocular saccades in the waking state (Glenn *et al.*, 1982). Thus, the short IPSPs during waking precisely control the timing of spikes.

7.3.2 Neuronal basis and functions of ponto-geniculo-occipital (PGO) waves in REM sleep

PGO waves are cardinal signs of REM sleep when dreaming episodes occur. They are sharp field potentials, generally recorded in the thalamic lateral geniculate (LG) nucleus, where they appear in clusters of up to six waves, closely related to gaze direction in dream imagery (Timofeev *et al.*, 2001b). The term PGO refers to their presence in the visual pathway, but these potentials appear in many thalamic nuclei and cortical areas outside the visual system because the generators of PGO waves, the cholinergic neurons of brainstem PPT and laterodorsal tegmental (LDT) nuclei, have widespread thalamic projections.[31] The cholinergic nature of PGO waves is indicated by their abolition after systemic administration or iontophoretic application of nicotinic antagonists into the thalamic LG nucleus (Paré *et al.*, 1988; Steriade *et al.*, 1988). In addition, after chemical lesions of PPT cholinergic neurons, PGO waves are largely suppressed during REM sleep (Ruch-Monachon *et al.*, 1976; Hu *et al.*, 1988).

At least five types of PPT/LDT neurons with PGO-related activity have been identified. Some of these neurons have been antidromically identified from LG or rostral intralaminar nuclei. (a) One neuronal class fired groups of 3–5 spikes at relatively low frequencies (less than 150 Hz), reliably preceding by 10–25 ms the LG–PGO wave (Webster & Jones, 1988). However, this type of PGO-on bursting cell represented only about 10% of the sampled population (McCarley *et al.*, 1978; Sakai & Jouvet, 1980; Sakai, 1985). The low incidence of these PGO-on bursting cells prompted further experiments that disclosed a

[31] For example, rightward eye movements are correlated with predominantly right waves in thalamic lateral geniculate nucleus (Nelson *et al.*, 1983).

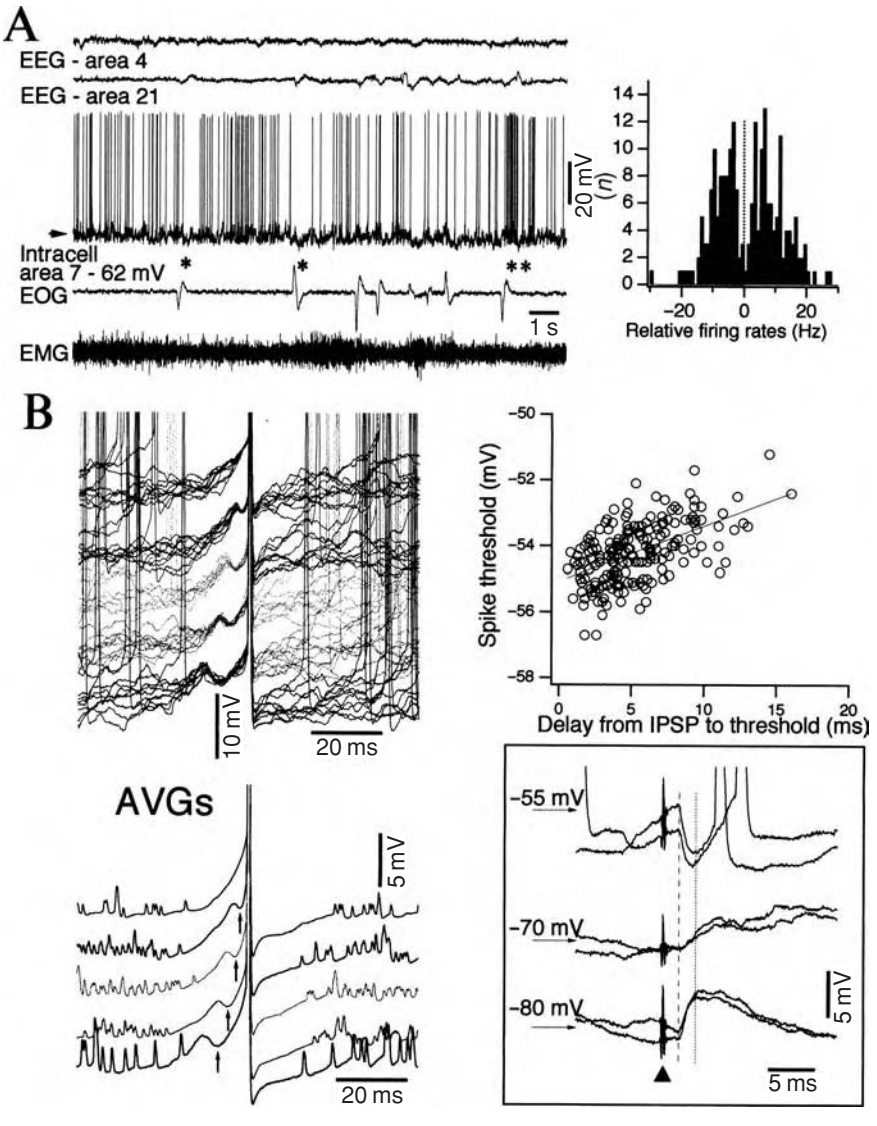

Fig. 7.18 Spontaneous IPSPs control precise firing timing of neocortical neurons during eye movement potentials in waking. Intracellular recordings in chronically implanted cat. (A) Epoch during the waking state is characterized by activated EEG, unimodal intracellular membrane potential, eye movements and muscle tone. Single asterisks indicate decrease in firing associated with eye movements and double asterisks indicate increase in firing associated with eye movements. Histogram shows increase (blue) or decrease (red) in saccade-related firing (±500 ms around saccade) for 15 neurons (more than 200 individual saccades) in relation to mean firing rates of the same neurons. To calculate the abscissa, the firing rate during ocular saccades was subtracted from the mean firing rate. (B) More than half of spikes during waking were associated with preceding short-lasting hyperpolarizing potentials (see superimposition of individual traces and below their averages). Longer-lasting hyperpolarizations slightly decrease firing threshold (plot). In inset, another neuron from motor area 4 recorded in waking, where short-lasting IPSPs were activated by stimulation of VL thalamic nucleus. Modified from Timofeev *et al.* (2001b). See Plate 5.

variety of PPT neuronal types antidromically identified from the thalamus (McCarley *et al.*, 1978; Sakai & Jouvet, 1980; Sakai, 1985). The studies revealed various cell groups, discharging single spikes, trains of single spikes, or spike-bursts with different patterns, preceding the negative peak of PGO field potential recorded from the thalamic LG nucleus. (b) Some PPT neurons fired high-frequency (500–600 Hz) spike-bursts in close temporal relation with thalamic PGO waves. However, distinctly from what was previously known (see (a)), these bursts occurred on a background of tonically increased discharge rates during REM sleep (Figure 7.19). This pattern raises the possibility that such high-frequency bursts may be generated at a depolarized level, at variance to what is expected for low-threshold Ca^{2+} spikes. As these neurons fire in relation with PGO waves on a background activity with acceleration of discharges prior to PGO waves, these bursts stood in contrast to PGO-on sluggish bursts that occurred on a silent background activity (see above (a)); the latter were interpreted as low-threshold spike-bursts (Steriade *et al.*, 1990d). (c) Other PPT/LDT neurons fired single spikes preceding by 15–25 ms the negative peak of the LG–PGO field potential. (d) Another cell class discharged trains of single spikes whose onset preceded by 100–200 ms the thalamic PGO waves. The tonic firing patterns of these PGO-on neurons was substantiated by interspike interval histograms of cellular activity taken during the period of PGO-related increased neuronal firing, indicating the presence of medium (10–25 ms) intervals and the virtual absence of short (<8 ms) intervals that would reflect spike bursts. (e) Some PPT/LDT neurons fired tonically, at high rates (>30 Hz), during epochs of REM sleep without PGO events and stopped firing prior to and during thalamic PGO waves. Such PGO-off cells are not aminergic because aminergic neurons are virtually silent during REM sleep. The presence of GABAergic neurons within PPT/LDT cholinergic nuclei[32] suggests that PGO-off neurons are GABAergic and that their silenced firing may lead to disinhibition of adjacent neurons with increased discharges during PGO waves.

Inputs to PPT/LDT neurons originate from adjacent areas in the upper brainstem reticular formation, bulbopontine reticular core, posterior and anterior hypothalamic areas, and cerebral cortex. Impulses in the PGO generators (PPT/LDT cells) can be triggered by any of these inputs through a mechanism that may be excitatory (Kosaka *et al.*, 1987) or, in the case of low-threshold spike-bursts, inhibitory (see Steriade *et al.*, 1990d). Then, PPT/LDT neurons can be regarded as the final link in the brainstem–thalamic path that generates PGO waves. As PGO potentials are thought to represent 'the stuff dreams are made of' and in view of the emotional nature of dreaming mentation in REM sleep, hypothalamic and forebrain structures that store some of the emotionally charged information might be most effective in driving the PGO–brainstem neuronal generators.

The intracellular correlates of thalamic PGO waves have been investigated in reserpine-treated animals that were deprived of retinal and visual cortex inputs to prevent synaptic bombardment

[32] If the PGO-on sluggish spike bursts (see main text) are low-threshold bursts, they would require sources of hyperpolarization. One of the likely sources of inhibition is the substantia nigra pars reticulata, which consists of GABAergic neurons that project directly to PPT (Datta *et al.*, 1991).

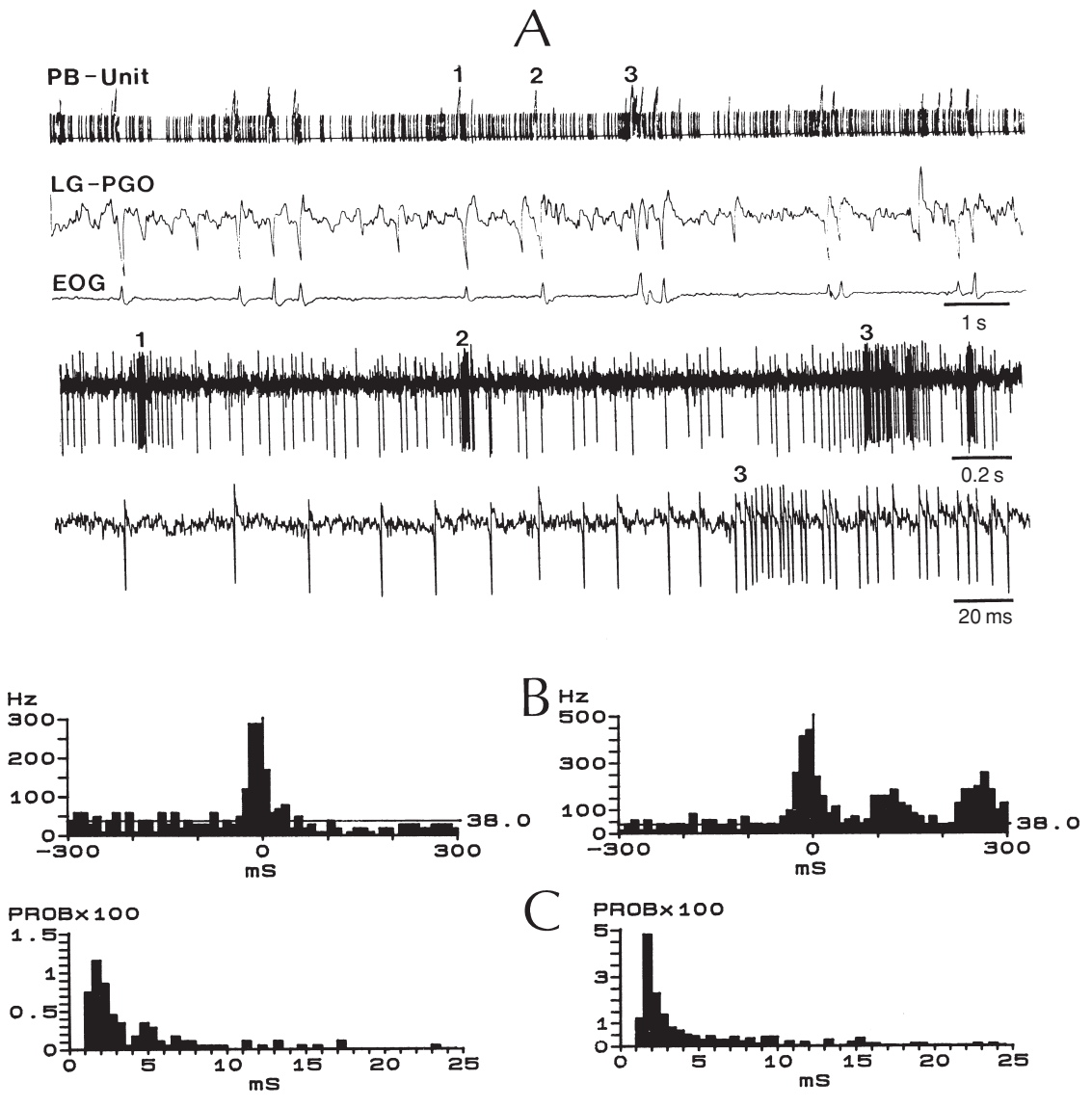

Fig. 7.19 Activity of a PGO-on burst neuron in the PPT nucleus during REM-sleep of chronically implanted cat. (A) Polygraphic ink-written record (unit discharges, deflections exceeding the common level represent high-frequency spike bursts; LG–PGO waves; and EOG) and original spikes with two different speeds, showing three (1–3) PGO-related bursts, as indicated on the first trace of the ink-written records. (B) Peri-PGO histograms (10 ms bins) of the PPT cell's discharges (time 0 is the negative peak of the LG–PGO wave) for single and clustered PGO waves (left and right panels, respectively). The level of overall spontaneous discharges in REM-sleep (38 Hz) is also indicated. (C) Interspike interval histograms (0.5 ms bins) of the PPT cell's activity during the period of increased firing rate around the PGO events for single and clustered PGO wave (left and right panels, respectively). Note very short intervals (less than 3 ms) reflecting high-frequency bursts. Modified from Steriade *et al.* (1990d).

through pathways other than brainstem–thalamic ones (Paré *et al.*, 1990b).[33] Under these conditions, the intracellular response of LG cells to PGO waves starts with a depolarizing potential (duration 0.2–0.3 s), interrupted by a short-lasting (50–60 ms) hyperpolarization whose initiation lags the onset of the depolarizing component by 40–80 ms. Upon passage of hyperpolarizing currents, the amplitude of the depolarizing potential increases, whereas the amplitude of the hyperpolarization decreases. When field potential PGO waves occur in doublets, the first wave is made of a depolarization followed by a hyperpolarization, while the second one consists of a pure depolarization. The membrane conductance increases by 25%–40% during the PGO wave, and this is observed even when the hyperpolarizing event is not detectable (Paré *et al.*, 1990b).

To sum up, the thalamic PGO wave involves a direct nicotinic excitation of LG relay cells by brainstem cholinergic neurons and the activation of intra-LG inhibitory interneurons, which display an initial depolarization during PGO field potentials, closely related to the IPSP onset in LG relay cells (Paré *et al.*, 1990b). The GABAergic RE (perigeniculate) do *not* fire in response to the brainstem peribrachial volley. Then, the only source for the PGO-related IPSPs in LG relay cells is the pool of local GABAergic interneurons.

The above data resulted from acute experiments. In chronically implanted, naturally sleeping cats, PGO precede other signs of REM sleep by about 30–90 s and appear during the preceding period of slow-wave sleep. Thus, there is a transitional period between EEG-synchronized and EEG-activated (REM) sleep, called the pre-REM period, during which PGO waves appear over the background of a fully synchronized EEG.[1] TC neurons are hyperpolarized during the pre-REM period, when the sleep EEG is still fully synchronized, whereas they are tonically depolarized by 7–10 mV during REM sleep (Hirsch *et al.*, 1983). These two states (pre-REM and fully developed REM sleep) generate different PGO-related responses in LG neurons, influencing the signal-to-noise ratio in the visual channel. Indeed, during pre-REM, the activity of LG relay cells starts with a short (7–15 ms), high-frequency (300–500 Hz) spike burst coinciding with the initial negativity of the PGO wave, and continues with a train of single spikes at 50–80 Hz, lasting for 200–400 ms (Deschênes & Steriade, 1988; Hu *et al.*, 1989c). The stereotyped features of the burst that starts the PGO-related activity of LG neurons during the pre-REM stage indicates that it is probably a low-threshold Ca^{2+} spike crowned by high-frequency Na^{+} action potentials. This is also supported by decreased probability of bursts for 300–400 ms after the PGO wave, owing to the relative refractory period of the low-threshold spike in thalamic neurons that may reach 200–300 ms (see Section 1.3.1). By contrast, during REM sleep, the spontaneous firing rate of LG cells is 1.5–3-fold higher than in pre-REM, the amplitudes of PGO waves are 2–3 times lower, and the PGO-related activity of LG neurons lacks the initial high-frequency burst that is characteristic of the pre-REM stage (Deschênes & Steriade, 1988; Hu *et al.*, 1989c). The peri-PGO histograms of neuronal activities

[33] In addition to these inputs from the upper brainstem reticular formation, neurons in the caudoventral pontine tegmentum may also trigger PGO waves (Vanni-Mercier & Debilly, 1998), probably through their projections to the final common path, PPT/LDT neurons.

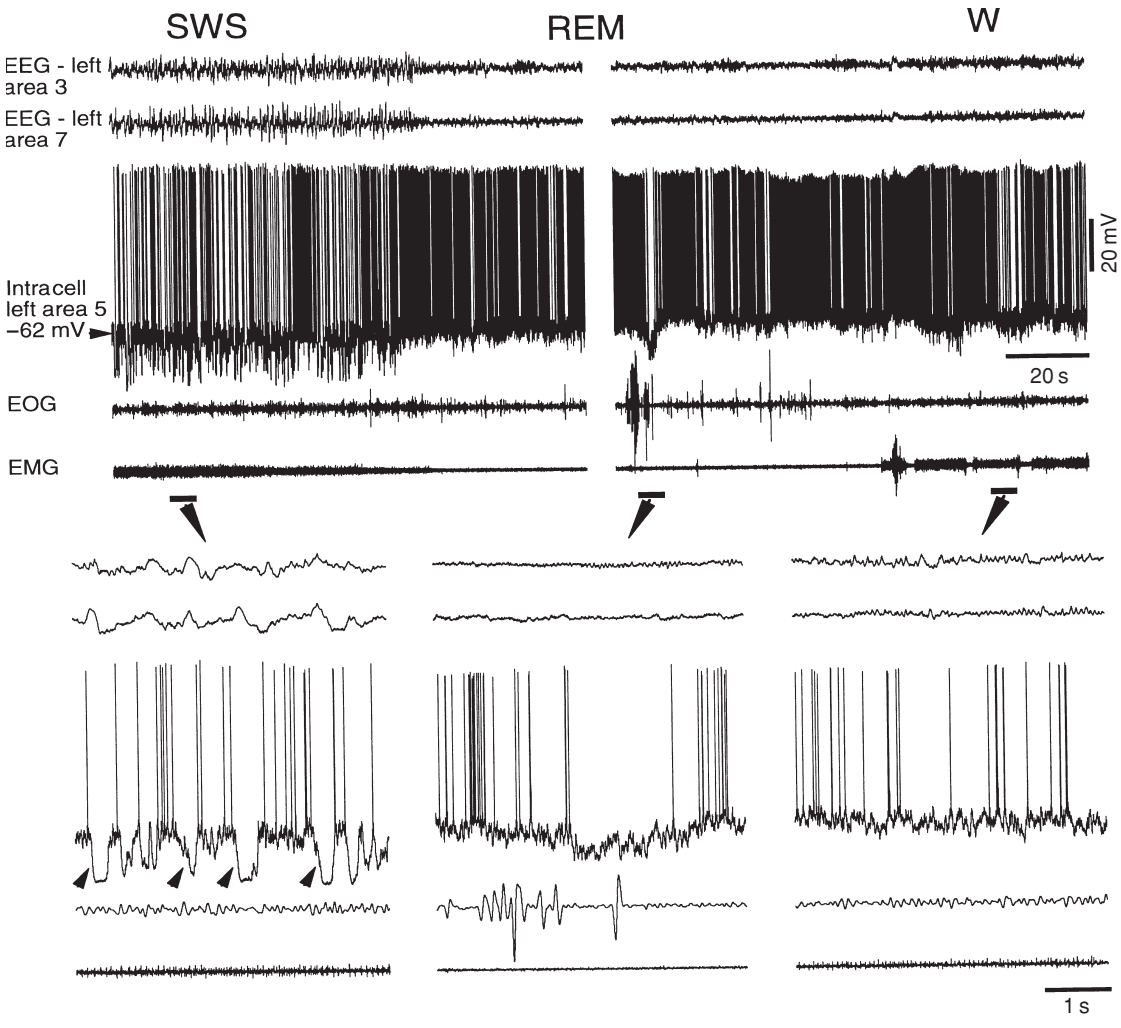

Fig. 7.20 Hyperpolarization of cortical neuron during ocular saccades in REM sleep. Chronically implanted cat. The five traces depict (from top to bottom): EEG from areas 3 and 7, intracellular activity of area 5 regular-spiking neuron (membrane potential is indicated, −62 mV), electro-oculogram (EOG) and electromyogram (EMG). Parts indicated by horizontal bars and arrows are expanded below. High-amplitude and low-frequency field potentials, intracellular cyclic hyperpolarizing potentials and stable muscle tone are distinctive features of slow-wave sleep (SWS). Low-amplitude and high-frequency field potential oscillations, tonic neuronal firing with little fluctuations in the membrane potential, rapid eye movements, and muscle atonia are cardinal features of REM sleep. Low-amplitude and high-frequency field potential oscillations, tonic firing with little fluctuations in the membrane potential, and muscle tone with periodic contractions are characteristics of the waking (W) state. Note cyclic hyperpolarizations in SWS and diminished firing rate during ocular saccade in REM sleep. Modified from Timofeev *et al.* (2001b).

in these two states show that the signal-to-noise ratio reaches values of about 6–7 during the pre-REM epoch compared to 1.5 – 2.5 during REM sleep.

As PGO waves are commonly regarded as the physiological correlate of dreaming, the greater signal-to-noise ratio in the LG-cortical channel during the pre-REM stage suggests that the vivid imagery associated with dreaming sleep may appear before REM sleep has fully developed, during a period of apparent slow-wave sleep. Discussing dreaming from experiments in cats is justified in view of the behavioural repertoire typical of dreaming mentation that was observed after preventing muscular atonia with lesions of certain brainstem reticular structures (see Figures 5 and 6 in Steriade *et al.*, 1989). The idea that PGO waves with greater amplitudes during the pre-REM stage may reflect more vivid imagery during that epoch than during REM sleep (Deschênes & Steriade, 1988; Hu *et al.*, 1989c)[1] corroborates earlier data showing that when sleep is interrupted immediately after the occurrence of the first PGO wave (in the pre-REM stage), the increased duration of the subsequent REM sleep rebound was due to phasic events (PGO waves) rather than to the loss of REM sleep *per se* (Jouvet & Delorme, 1965). This observation fits well with data on dream reports from the last epoch of EEG-synchronized sleep, which are indistinguishable from those obtained from REM sleep awakenings (Dement *et al.*, 1969).

PGO waves were thought to play a role in development and structural maturation of the brain (Hobson, 1988; see also Hobson & Pace-Schott, 2002). Indeed, in kittens with bilateral lesions of brainstem structures that contain PGO generators the somata of LG neurons have a smaller cross-sectional area than that of control animals or kittens with unilateral brainstem lesions (Roffwarg *et al.*, 1966). PGO waves also exert excitatory effects on complex neurons of the visual cortex (Davenne & Adrien, 1984) and interference with PGO waves may modify the expression of long-term potentiation in immature animals (Kasamatsu, 1976). One of the hypothesized functions of REM sleep, increasing functional connectivity and maintaining the soundness of memory traces acquired during wakefulness (Shaffery *et al.*, 2002), was previously related to the selectively increased firing of local interneurons in the association cortical areas during ocular saccades (Steriade, 1978). Intracellularly, this is reflected in inhibition of regular-spiking (pyramidal) neurons of the association cortex during saccades (Figure 7.20).

Chapter 8

Comparison of state-dependent activity patterns in the thalamocortical, hippocampal and amygdalocortical systems

8.1 The significance of neuronal oscillations in the amygdala and related cortices

Even when deprived of sensory stimulation, neurons hum continuously. That is, their membrane potential fluctuates constantly and the depolarizing phase of these oscillations sometimes gives rise to action potentials. Interestingly, this spontaneous activity is not random. Correlated neuronal events, occurring in a pulsatile or oscillatory manner, can be measured in the extracellular space as currents. These events result from non-linear interactions between the intrinsic membrane properties of neurons and the particular properties of the synaptic network of which they are a part (Llinás, 1988). Oscillations in various frequency ranges are observed in different brain regions; these rhythms vary depending on the behavioural state (Buzsáki *et al.*, 1983; Steriade, 1997a).

The relevance of oscillations to brain function stems from the fact that neuronal events underlying cognition are embedded in these endogenous rhythms. Stated otherwise, one cannot disentangle oscillations from coding in large neuronal ensembles. Moreover, during sleep, when the brain is largely disconnected from the outside world, neurons generate a variety of oscillations and synchronized population bursts that are thought to play a critical role in memory consolidation (see Section 6.3). Finally, because related parts of the brain tend to display similar oscillations, the analysis of spontaneous oscillatory activity can reveal functional kinship among brain structures.

This chapter compares the neuronal oscillations displayed by the amygdala and related cortices. The interest for this theme stems from pharmacobehavioural data suggesting that the amygdala facilitates the consolidation of emotionally arousing memories (Cahill & McGaugh, 1998). Thus, amygdala oscillations and the entrainment of related cortices might play an important role in this respect. In addition, the amygdala confronts us with an interesting question because its main afferents originate from cortical regions that have different phylogenetic origins: parasensory neocortical areas as well

as phylogenetically older temporal cortices. This raises the question as to whether the amygdala displays spontaneous rhythms typical of one or both these regions.

8.2 Overview of major thalamocortical and hippocampal electroencephalographic events

8.2.1 Neocortical rhythms

This section provides a rapid overview of the major EEG rhythms observed in the neocortex. A more in-depth description can be found in Chapter 6. During EEG-activated states, such as wakefulness and paradoxical sleep, the neocortical EEG displays activity of low amplitude and high frequency. In contrast, during slow-wave sleep, the neocortical EEG is dominated by slower waves of much higher amplitude, hence the expression 'synchronized EEG'. Although spectral analyses of the neocortical EEG reveal a continuum of frequencies during slow-wave sleep (SWS), it includes readily identifiable components.

The first EEG events to be observed when animals fall asleep are spindles. Sleep spindles are short periods (1–2 s) of waxing and waning oscillations at a frequency of 7–14 Hz that recur every 3–10 s in much of the neocortex, but are particularly obvious in areas 4–6 and areas 5–7 (Andersen & Andersson, 1968; Morison & Dempsey, 1942). Much evidence indicates that spindles are generated in the thalamus. Indeed, they vanish from cortical regions that have been isolated from the thalamus (Andersen & Andersson, 1968) and are still observed in the thalamus of decorticated animals that have received a brainstem transection (Morison & Basset, 1945). Spindles are thought to originate from reciprocal interactions between thalamic glutamatergic relay cells and GABAergic reticular neurons (Steriade, 1997a).

As sleep deepens, a second readily identifiable component is observed in the neocortical EEG: delta waves (1–4 Hz) (Ball *et al.*, 1977; Petsche *et al.*, 1984). It is believed that delta waves result from the intrinsic membrane properties of thalamocortical neurons and the synchronizing influence of cortical feedback coupled to the inhibitory influence of reticular thalamic cells (Steriade *et al.*, 1993e). In particular, the interplay between a hyperpolarization-activated mixed cationic current and a low-threshold calcium conductance allows thalamocortical cells to oscillate at the delta frequency at hyperpolarized membrane potentials (McCormick & Pape, 1990a). However, because relay cells do not communicate with each other, delta waves would not emerge in the EEG as a coherent phenomenon unless their activity was synchronized by the cortex and reticular thalamic nucleus.

Sleep spindles and delta waves do not occur randomly but appear to be grouped by a third, slower EEG oscillation (<1 Hz) termed 'slow oscillation' (Steriade *et al.*, 1993e). This oscillation has been observed in the neocortex of anaesthetized animals (Steriade *et al.*, 1993e) and

during SWS in cats (Steriade *et al.*, 1996a; Amzica & Steriade, 1998a) and humans (Achermann & Borbély, 1997). Simultaneous EEG and intracellular recordings have revealed that this oscillation comprises an EEG depth-negative phase, coinciding with an increased probability of firing in all classes of cortical cells, that alternates with an EEG depth-positive phase during which neurons are hyperpolarized (Steriade *et al.*, 1993e).

The probability of sleep spindles or delta waves increases during the depth-negative phase of the slow oscillation, suggesting that they are triggered by the synchronized discharge of cortical neurons. Moreover, faster beta and gamma rhythms tend to be more prominent during the depth-negative than the depth-positive phase of the slow oscillation (Steriade *et al.*, 1996a; Amzica & Steriade, 1998a). Nevertheless, beta and gamma oscillations appear more important in waking and paradoxical sleep, when slow EEG components disappear.

8.2.2 Hippocampus: oscillations and other population events

During locomotion and paradoxical (REM) sleep, the hippocampal EEG is dominated by a high-amplitude oscillation in the theta frequency range. During immobility, theta oscillations can also be observed when animals are aroused (as produced by the anticipation or delivery of noxious stimuli). The theta oscillation is associated with a rhythmic modulation of firing probability in virtually all types of hippocampal neurons (Buzsáki *et al.*, 1983; Bland, 1986). Inputs from the medial septum are essential for hippocampal theta (Petsche *et al.*, 1962). The rhythmic activity of entorhinal afferents also provides an essential contribution (Buzsáki, 2002). Moreover, hippocampal theta is associated with a cyclical modulation in the amplitude of gamma waves in the hilus, entorhinal cortex and field CA1 (Bragin *et al.*, 1995a; Chrobak & Buzsáki, 1996, 1998).

Although the hippocampal EEG also displays high amplitude slow waves of various frequencies during SWS, no spindles are present. Also distinct from the neocortical EEG is the occurrence of population events, termed sharp waves during SWS, immobility and consummatory behaviours. These sharp waves are thought to result from population bursts in CA3 and CA1 pyramidal neurons (Buzsáki, 1986). Sharp waves are associated with bursts of fast oscillations (*c.*200 Hz), termed ripples (Buzsáki *et al.*, 1992; Ylinen *et al.*, 1995), that are believed to reflect synchronized discharges by inhibitory interneurons.

A few studies have examined the relationship between the major EEG events observed in the neocortex and hippocampus during SWS. In particular, a significant correlation between the occurrence of spindles in the neocortex and sharp wave ripples in the hippocampus has been reported (Siapas & Wilson, 1998; Sirota *et al.*, 2003). It was similarly reported that hippocampal sharp waves were more likely to occur during the down phase of the slow oscillation (Battaglia *et al.*, 2004).[1] However, these relationships accounted only for a small

[1] The presence of correlated events in this neocortex and hippocampus was opposed (Battaglia *et al.*, 2004) to recent findings indicating that entorhinal sharp waves do not propagate to the temporal neocortex via the perirhinal cortex (Pelletier *et al.*, 2004). However, we believe that the contradiction is only apparent and reflects the erroneous assumption that the neocortex and hippocampus mostly influence each other via a cascade of corticocortical connections coursing through the perirhinal cortex. As reviewed in Chapter 4, the reciprocal connections between the medial prefrontal cortex on the one hand, and the entorhinal cortex and hippocampus on the other, constitute more direct routes of communication between these structures.

change in firing probability. This is in contrast to the dramatic augmentations in firing probability displayed by hippocampal neurons in relation to sharp wave ripples and neocortical neurons in relation to spindles.

8.3 State-dependent patterns of activity observed in the amygdala

The above indicates that distinct EEG events occur in the neocortex and hippocampus and that they fluctuate depending on the behavioural state of the subject. Because the amygdala is innervated by both these brain regions, it might display both sets of electrographic events. This section examines this issue. It will also consider the perirhinal cortex because this region is a major relay of neocortical and hippocampal inputs to the amygdala. Finally, we will focus on the basolateral amygdaloid complex because most cortical links of the amygdala originate from, and end in, this group of nuclei (see Chapter 4). We start with the main rhythms of SWS (slow oscillation, spindle waves and delta) and end with rhythms observed during EEG-activated states (hippocampal theta and fast oscillations).

8.3.1 Slow sleep oscillation

Although the hippocampal formation displays the slow oscillation under anaesthesia, its phase relation to that seen in the neocortex has not been measured yet. However, this analysis was carried out for the slow oscillation of the neocortex and rhinal cortices (Collins *et al.*, 1999). The slow neocortical and perirhinal oscillations were not synchronized (Figure 8.1), in sharp contrast with the tight synchrony observed between distant neocortical sites (Collins *et al.*, 1999) or between the basolateral amygdala and perirhinal cortex. The latter finding is especially striking because the distance between the amygdala and different rostrocaudal levels of the perirhinal cortex varies tremendously (2–12 mm). These results suggest that the slow oscillation seen in the perirhinal cortex and amygdala might be generated independently of the neocortical rhythm, but this should be tested in decorticated animals.

As was observed in the neocortex and striatum, the slow oscillation seen in the basolateral amygdala and perirhinal cortex is associated with pronounced variations in firing probability (Figure 8.2). This is an important point because it demonstrates that the oscillations are not volume-conducted from other structures. In addition, as was previously seen in the neocortex, the slow amygdala oscillation is correlated with fluctuations in the amplitude of beta and gamma activity. However, in contrast with the slow oscillation seen in the amygdala and perirhinal cortex, the coherence of gamma oscillations decreased abruptly with distance (Collins *et al.*, 2001).

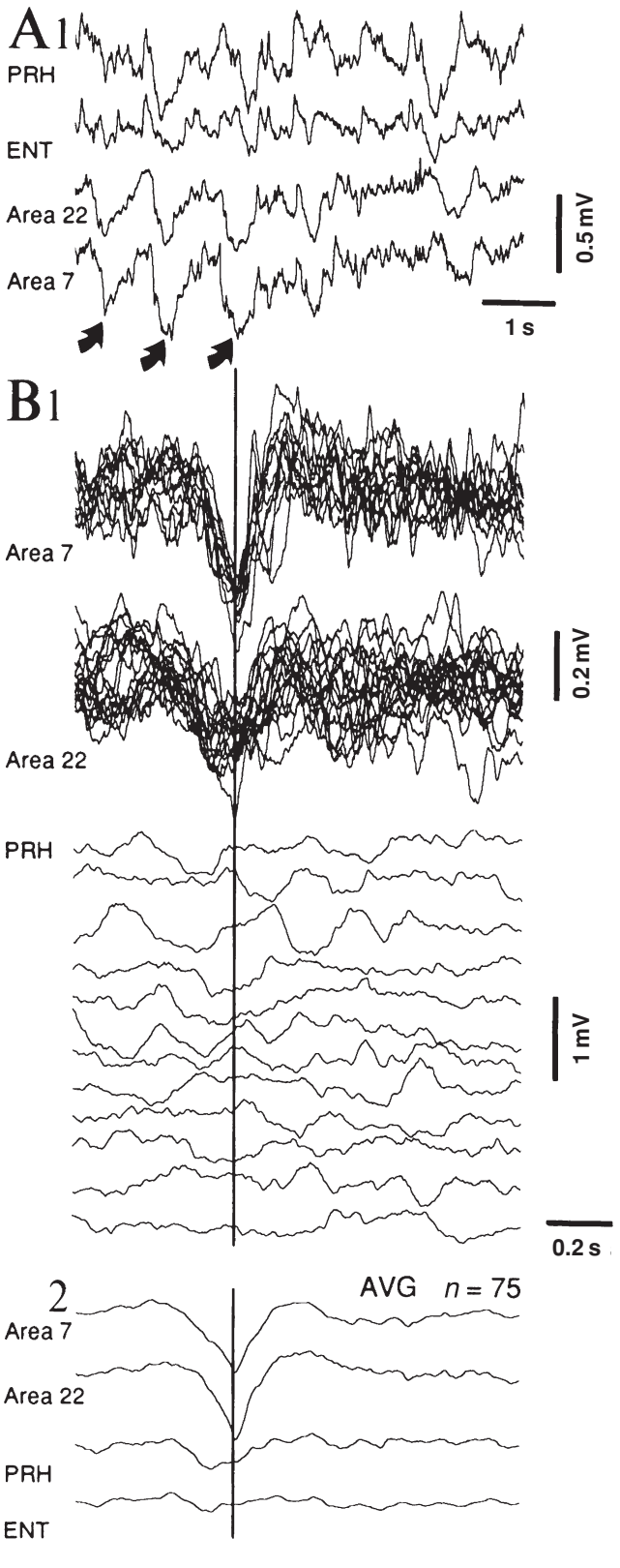

Fig. 8.1 Neocortical and rhinal slow EEG oscillation during slow-wave sleep. (A) Simultaneously recorded EEG activity of the perirhinal (PRH) and entorhinal (ENT) cortices as well as neocortical areas 22 and 7. In B, the peak of the surface-negative phase of the slow oscillation in areas 7 was used as a temporal reference to align coincident EEG activity in area 22 and the perirhinal cortex. In B1, sweeps were superimposed (areas 7 and 22) or offset (perirhinal). In B2, the data were averaged. EEG data were digitally filtered between 0 and 55 Hz. Modified from Collins *et al.* (1999).

8.3.2 Sleep spindles

Whereas sleep spindles are virtually ubiquitous in the neocortex, they seem to be absent from the basolateral amygdala (Paré & Gaudreau, 1996; Forslid *et al.*, 1986) and rhinal cortices (Collins *et al.*, 2001) (Figure 8.3). Indeed, during neocortical spindles, the amygdala exhibits delta waves (Paré & Gaudreau, 1996; Forslid *et al.*, 1986). The lack of spindles in the rhinal cortices is in keeping with the relatively meagre thalamic projections to these cortical fields (Room and Groenewegen, 1986b). The few dorsal thalamic nuclei with projections to the entorhinal cortex (reuniens and anterior thalamic nuclei (Room and Groenewegen, 1986b; Herkenham, 1978) are devoid of inputs from the thalamic pacemaker of spindle waves, the reticular thalamic nucleus (Steriade *et al.*, 1984a; Paré *et al.*, 1987; Velayos *et al.*, 1989). Similarly, most thalamic nuclei with projections to the basolateral complex, namely the paratenial and paraventricular interanteromedial nuclei (Turner & Herkenham, 1991), do not receive inputs from the reticular thalamic complex (Steriade *et al.*, 1984a; Paré *et al.*, 1987; Velayos *et al.*, 1989).

These connectional data imply that the amygdala and rhinal cortices depend on a cascade of corticocortical connections for the transfer of spindles. It is possible that the spindle-related firing degrades as it progresses through the sequence of corticocortical links that relays this activity. This effect would be compounded by the fact

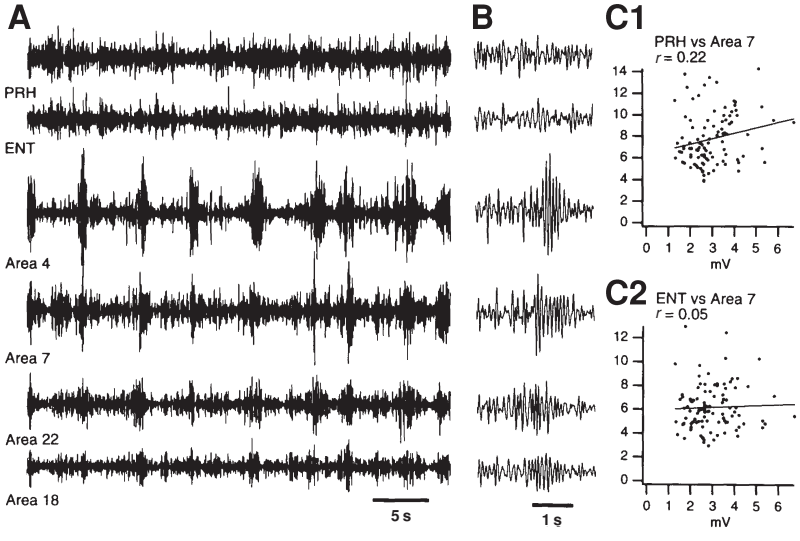

Fig. 8.3 Spindle oscillations are absent from the rhinal cortices. Surface EEG activity was recorded simultaneously from the perirhinal and entorhinal cortices as well as from neocortical areas 4, 7, 22 and 18. The data were digitally filtered between 7 and 14 Hz. This activity is depicted with a slow (A) and a fast (B) time base. Spindle waves tend to occur simultaneously in neocortical areas, independently of variations in 7–14 Hz activity occurring in the rhinal cortices. (C) Correlation between power in the 7–14 Hz bandwidth in 2 s windows for selected pairs of recording sites (indicated above each graph). Modified from Collins *et al.* (1999).

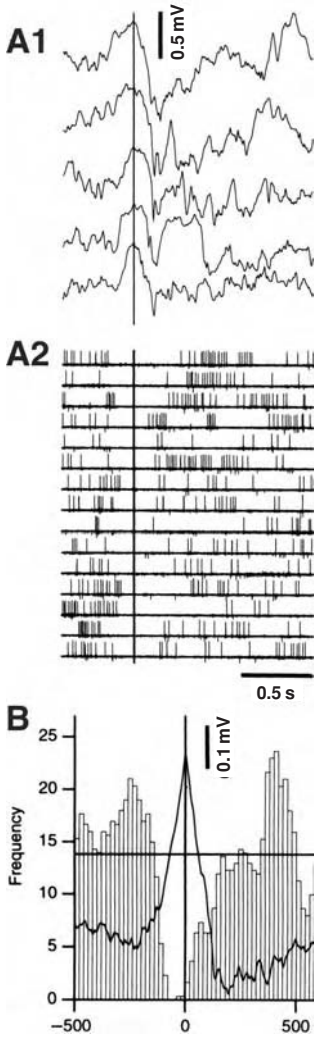

Fig. 8.2 The slow perirhinal oscillation is associated with marked fluctuations in the firing rate of perirhinal cells. Firing rates decrease during the depth-positive phase of the slow oscillation. Electrocorticogram (A1) and unit activity (A2) were recorded simultaneously by the same microelectrode. The signals were dissociated by digital filtering (A1, 0 and 55 Hz; A2, 0.3–10 kHz). The peak of the depth positive phase (A1) was used as a temporal reference to examine the related unit activity (A2) and a peri-event histogram of neuronal discharges was computed (B). Modified from Collins *et al.* (1999).

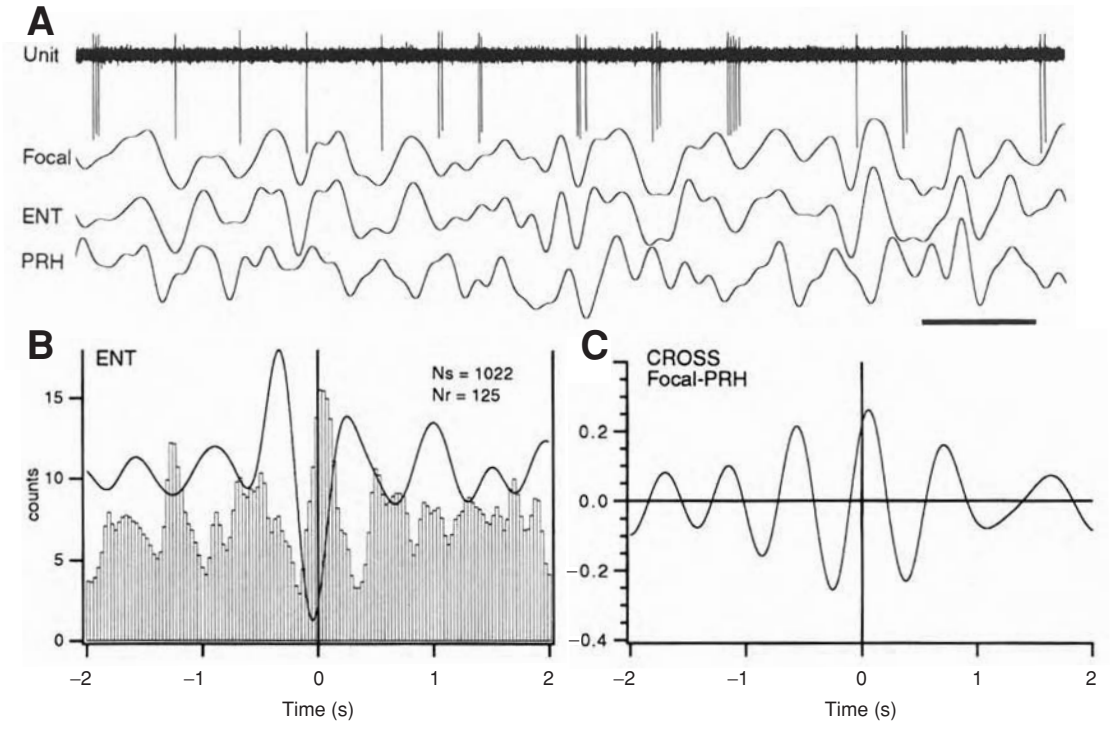

Fig. 8.4 The firing of basolateral amygdala neurons is modulated at the delta frequency during slow-wave sleep. (A) Simultaneously recorded unit activity and focal waves in the lateral amygdala as well as EEG activity in the entorhinal (ENT) and perirhinal (PRH) cortices. Note the tendency of this LA neuron to fire during the depth-negative phase of the delta oscillation present in the focal waves and rhinal EEGs (digitally filtered between 0.1 and 4 Hz). (B) Perievent histogram of neuronal discharges (same cell as in A) around the negative peak of entorhinal delta waves. (C) Cross-correlogram between the focal waves and perirhinal EEG. Modified from Paré & Gaudreau (1996).

that spindling-related inputs reaches the amygdala and rhinal cortices from multiple sources; owing to variations in conduction delays, afferent volleys would not be sufficiently synchronized for clear spindling to emerge.

8.3.3 Delta waves

Basolateral amygdala neurons do oscillate at the delta frequency during SWS (Paré & Gaudreau, 1996) and these oscillations are coherent with those seen in the rhinal cortices (Figure 8.4). The relation between neocortical and amygdala delta has not been investigated so far. However, the fact that rhinal and neocortical delta waves are not coherent lead us to assume that amygdala and neocortical delta oscillations are poorly correlated (Collins *et al.*, 1999).

8.3.4 Sharp waves

The relation between hippocampal sharp waves and amygdala activity has not been investigated so far. However, hippocampal sharp waves are likely to be reflected in the amygdala. This contention is supported by the fact that the entorhinal cortex sends a robust projection to the basolateral amygdaloid complex and that entorhinal neurons display massive increases in firing in relation to hippocampal sharp waves (Chrobak & Buzsáki, 1994, 1996).

8.3.5 Theta

Since a large proportion of entorhinal neurons display theta-related firing, the same argument would lead one to predict that basolateral

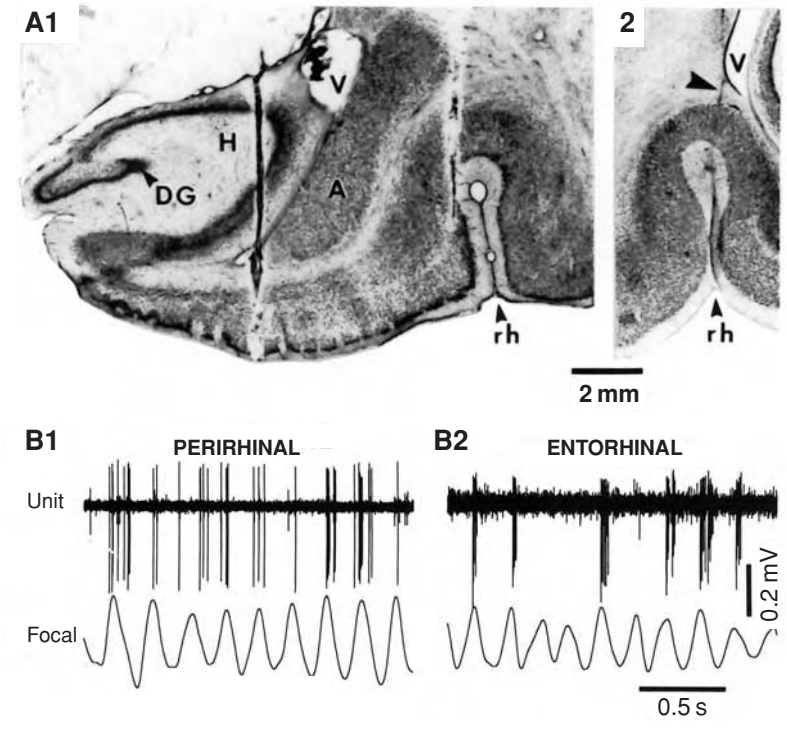

Fig. 8.5 Modulation of spontaneous firing at the theta frequency in the perirhinal and entorhinal cortices. (A) Histological control showing electrode tracks in the entorhinal (A1, left track) and perirhinal cortex (A1, right track; A2, arrowhead). (B) Spontaneous activity recorded in the perirhinal (B1) and entorhinal (B2) cortices during paradoxical sleep. The unit activity and focal waves were recorded simultaneously by the same electrodes but were isolated from each other by differential digital filtering (unit: 0.3–10 kHz; focal waves: 4–8 Hz). Abbreviations: A, amygdala; DG, dentate gyrus; H, hippocampus; rh, rhinal sulcus; V, ventricle. Modified from Collins *et al.* (1999).

neurons display theta oscillations. Consistent with this, theta activity was observed in the basolateral amygdala (Paré & Gaudreau, 1996) and perirhinal cortex (Collins *et al.*, 1999) during paradoxical sleep, albeit less prominently than in the entorhinal cortex or hippocampus. For instance, in one study (Collins *et al.*, 1999), roughly half of entorhinal neurons displayed significant theta-related firing rate modulations whereas only 16% of the cells did so in the perirhinal cortex (Figure 8.5).

Normally, theta oscillations are not seen in the amygdala or perirhinal cortex during quiet waking. They are only present during epochs of intense arousal such as during the anticipation of noxious stimuli (Paré & Collins, 2000; Seidenbecher *et al.*, 2003) or highly desirable rewards (Aleksanov, 1983). Interestingly, arousal was reported to be accompanied by an increased coherence of theta activity in the amygdala and frontal cortex (Aleksanov, 1983). In the perirhinal cortex at least, the theta oscillation is related to a cyclic modulation in the amplitude of gamma waves (Collins *et al.*, 1999), as in the hippocampus and entorhinal cortex (Bragin *et al.*, 1995a; Chrobak & Buzsáki, 1996, 1998). Consistent with this, perirhinal and amygdala theta is phase-locked to entorhinal and hippocampal theta (Collins *et al.*, 1999; Paré & Gaudreau, 1996).

8.3.6 Fast activities during arousal

Several studies have reported that arousal is associated with enhanced fast focal activities in general (Pagano *et al.*, 1964) and in 'amygdala

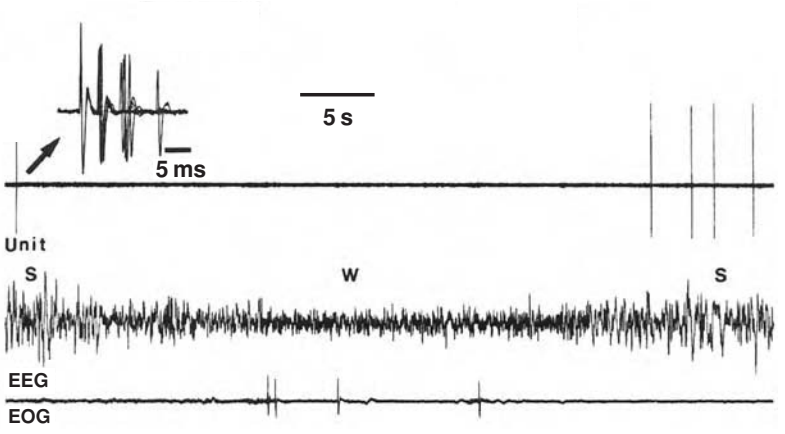

Fig. 8.6 Basolateral amygdala neurons fire at higher rates in slow-wave sleep (S) than in the waking (W) state. Simultaneously recorded basolateral unit activity, neocortical EEG and eye movements (EOG) during a transition from slow-wave sleep to waking and back to sleep. Note silencing of this cell during waking. Modified from Paré & Gaudreau (1996).

spindles' (Feshchenko & Chilingaryan, 1990). Although these 'spindles' are spindle-shaped, they should not be confused with sleep spindles because they occur during waking rather than slow-wave sleep and comprise much faster waves (beta–gamma range), as previously described in the adjacent prepyriform cortex (Freeman, 1959). Whether these so-called 'amygdala spindles' are volume-conducted from the prepyriform cortex or reflect a true amygdala rhythm remains unknown.

8.3.7 State-dependent fluctuations in the firing rates of basolateral amygdala neurons

Although the biophysical properties of projection cells in the basolateral amygdaloid complex are similar to those seen in the neocortex, they display a markedly lower level of spontaneous activity. Depending on the recording method (high-impedance microelectrodes or microwires),[2] average firing rates in quiet waking were reported to average near zero (Paré & Gaudreau, 1996; Gaudreau & Paré, 1996) or 3 Hz (Bordi *et al.*, 1993), respectively. Nevertheless, both estimates are strikingly lower than the average of 10 Hz seen in the neocortical pyramidal cells (Steriade *et al.*, 1974a; Steriade, 1978).

In a first study on this issue (Jacobs & McGinty, 1971) it was reported that the firing rates of basolateral amygdala neurons averaged 0.2 Hz in quiet waking, 0.4 Hz in paradoxical sleep and 0.6 Hz in SWS. In SWS, action potentials tended to occur in clusters as in the neocortex. However, in contrast, with neocortical cells, basolateral amygdala neurons did not seem to modify their activity in relation to the phasic events of paradoxical sleep (rapid eye movements), although they sometimes exhibited sustained 10–100-fold increase in firing rates, with no obvious correlates.

Three other studies confirmed that amygdala neurons fired at higher rates in SWS than other behavioural states (Paré & Gaudreau, 1996; Gaudreau & Paré, 1996; Bordi *et al.*, 1993) (Figure 8.6). By using hunting electrical stimuli in the perirhinal cortex to disclose the presence of silent neurons, one study revealed that most projection cells

[2] By definition, extracellular electrodes always have a sampling bias in favour of spontaneously active cells. However, the importance of this bias can be reduced by advancing the electrode slowly while delivering hunting electrical stimuli in structures connected to the recorded site. Such stimuli can disclose the presence of neurons that lack spontaneous activity but respond to the stimulus.

of the lateral nucleus had virtually no spontaneous activity throughout the sleep–waking cycle (Gaudreau & Paré, 1996). Although this approach revealed that state-dependent differences in the firing rates of projection cells of the lateral nucleus were negligible, their responsiveness to central stimuli significantly increased from waking or paradoxical sleep to slow-wave sleep. In the basolateral nucleus, projection cells had higher firing rates (0.5 Hz in waking and nearly 1 Hz in slow-wave sleep).

Thus, the state-dependent fluctuations in the activity of basolateral projection cells contrast with those observed in most neuronal populations of the prosencephalon where, compared with slow-wave sleep, waking is associated with an increased neuronal excitability (reviewed in Steriade & Hobson, 1976). One exception to this rule is the hippocampal formation where the excitability of pyramidal neurons is also higher in slow-wave sleep than waking, except for periods when the animals step in the place field of the recorded cell (Buzsáki *et al.*, 1983). These observations point to functional similarities between the hippocampal formation and the basolateral amygdala and suggest that they are subjected to modulatory influences different from the thalamocortical system.

Chapter 9

Neuronal substrates of some mental disorders

In this chapter, we discuss mental disorders that arise from alterations in brainstem–thalamic, thalamocortical and amygdalocortical neuronal circuits. Some of these abnormal activities result from diminution or pathological increase in the number of neurons, which is reflected in their functional output and leads to substantial changes at the level of their targets.

[1] See discussion on the role of prefrontal cortex in mentation and dreaming of autistic patients in Damasio (1996) and Stone *et al.* (1998).

9.1 Alterations in brainstem-thalamic and thalamocortical neuronal circuits, with emphasis on hallucinations and schizophrenia

We will first describe what is known about the role of thalamic morphological and functional modifications in the generation of autism, sleep disorders, and loss of consciousness in absence epilepsy, and will next focus on the brainstem–thalamic and basal ganglia circuits that are hypothesized to generate hallucinations in schizophrenia.

The expression of autistic disorders was ascribed by some authors to abnormal activities in some cortical areas and the thalamus. The highly attenuated dreaming in patients with autism and Asperger's syndrome (a developmental disorder regarded as equivalent to autism) was related to the ventromedial frontal cortex, which, when lesioned, gives rise to diminished dreaming.[1] The thalamus was also implicated in autism as anatomical changes and functional alterations through this anteroom to the cerebral cortex may involve disturbances of attention and sensory gating. Thus, in autism, the thalamic volume was found to be significantly different (mainly reduced) relative to normal control subjects (Herbert *et al.*, 2003; Tsatsanis *et al.*, 2003); and emotion processing results in lower regional cerebral blood flow in some cortical areas and in the thalamus (Hall *et al.*, 2003). These studies provide a possible substrate for an earlier hypothesis (Damasio & Maurer, 1978) implicating the anterior and medial nuclear groups of the thalamus, together with their cortical projection sites, in autism.

Hypersomnia associated with slowing of EEG waves and absence of activating EEG reactions was observed in humans following bilateral infarction of thalamic intralaminar nuclei, due to atheroma at the bifurcation of the basilary artery (Façon *et al.*, 1958).[2] This syndrome was ascribed to the interruption of ascending brainstem–thalamic activating systems. An opposite clinical picture was reported as 'fatal insomnia' after 'selective degeneration' of medial thalamic nuclei in humans (Lugaresi *et al.*, 1986). The 'fatal' characteristic of this prion disease can be explained by associated hypothalamic lesions leading to hypertension, pyrexia and hyperhydrosis. In fact, those thalamic lesions were not selective and the thalamic degeneration is accompanied by spongiform encephalopathy of some brainstem structures and cerebral cortex (Mizusawa *et al.*, 1988). The 'selectivity' of thalamic lesions to the anteroventral and mediodorsal thalamic nuclei (Lugaresi *et al.*, 1986) was challenged in subsequent studies showing that virtually all major thalamic nuclei as well as medial septal nuclei and a series of brainstem structures are implicated in this prion disease (Manetto *et al.*, 1992; Macchi *et al.*, 1997; Rossi *et al.*, 1998). It was then concluded that authentic cases of purely thalamic degenerations were impossible to find (Martin *et al.*, 1983).[3] The safe conclusion is that lesions in some paramedian thalamic nuclei are associated with hypersomnolence (Lugaresi *et al.*, 1986). Paramedian thalamic lesions may also produce the syndrome of akinetic mutism, with absence of incitation to action, known as *Antriebsmangel* (Lhermitte *et al.*, 1963; Segarra, 1970). One case of exception, in which a state of arousal was maintained but cognition and awareness were severely affected after bilateral thalamic atrophy was explained by extrathalamic systems implicated in cortical activation and residual neurons that were spared in thalamic intralaminar and midline nuclei (Kinney *et al.*, 1994).

The loss of consciousness that characterizes seizures with spike-wave (SW) complexes at 2–4 Hz, as in absence epilepsy, is due to the inhibition of thalamocortical (TC) neurons, thus preventing sensory signals from reaching the cerebral cortex. These seizures are cortically generated, as they survive extensive thalamectomy. The paroxysmal firing of neocortical neurons drives thalamic reticular (RE) GABAergic neurons, which impose IPSPs on TC cells. As this circuitry was amply discussed elsewhere, the reader is referred to a previous article, reviews (Steriade & Contreras, 1995; Crunelli & Leresche, 2002; Timofeev & Steriade, 2004; Steriade, 2005a,b) and a monograph (Steriade, 2003a).

Some symptoms of schizophrenia may result from a defect in the gating properties of the thalamus.[4] Other authors pointed to abnormalities in the cerebral cortex because of language (syntactic and semantic) impairments in some schizophrenic patients (Crow, 1997; see also commentary by Mackay, 1998). Still other authors hypothesized that abnormalities in extrathalamic structures would affect filtering operations in the thalamus and explain a series of

[2] This syndrome was also reported by Castaigne *et al.* (1962).

[3] These authors also reported a case with extensive lesions in many thalamic nuclei, similar to those found in 'fatal insomnia' (see Manetto *et al.*, 1992; Macchi *et al.*, 1997; Rossi *et al.*, 1998), but their patient did not present serious sleep disturbances. See also Martin (1997).

[4] Neurological abnormalities were identified by magnetic resonance imaging (MRI) as being located in some thalamic nuclei of schizophrenic patients, such as lateral and mediodorsal nuclei (Andréasen *et al.*, 1994), with the conclusion that psychotic signs in schizophrenia may be explained as a defect in gating sensory signals.

symptoms in schizophrenia. It is known that the ventral pallidum receives afferents from nucleus accumbens and prefrontal/limbic cortical areas, and projects to the thalamic mediodorsal nucleus that projects back to prefrontal cortex. It was proposed (Lavin & Grace, 1994) that the overactivation of ventral pallidum neurons leads to inhibition of thalamic RE GABAergic cells, consequently disinhibiting TC neurons that would transfer incoming signals to cortex without sculpting inhibition. This might explain the inability of schizophrenics to focus on one stimulus and/or to distinguish between relevant and irrelevant stimuli.

Hallucinatory behaviour, as occurs in schizophrenia, was ascribed to excessive driving of TC neurons by an increased number of neurons in cholinergic PPT/LDT nuclei at the mesopontine junction, or by abnormal excitation of neurons in the upper midbrain reticular core with thalamic projections (Steriade, 2005b). It was found that highly increased numbers of neurons in mesopontine cholinergic nuclei are present in schizophrenic patients, compared with control subjects (Garcia-Rill *et al.*, 1995).[5] Neurons in these cholinergic nuclei project to all thalamic nuclei of cats and primates (Steriade *et al.*, 1988; Paré *et al.*, 1988) and increase the firing rates and input resistance of TC neurons during brain arousal (Steriade *et al.*, 1991b; Curró Dossi *et al.*, 1991). The increased number of brainstem cholinergic neurons in schizophrenia (Garcia-Rill *et al.*, 1995) may lead to an increased reactivity to sensory stimuli reaching thalamic neurons, especially as this increased excitability is unrestrained by intra-thalamic inhibitory processes. Indeed, brainstem cholinergic neurons inhibit thalamic RE inhibitory neurons (Hu *et al.*, 1989a) and thus disinhibit TC neurons, further exciting them.

Despite this focus on brainstem cholinergic systems, the brainstem reticular core has many more glutamatergic than cholinergic neurons. Infusion of a powerful glutamate analogue into the upper midbrain reticular formation of cats, where there are virtually no cholinergic cells but mainly glutamatergic neurons, led to pupillary dilatation, piloerection, an EEG pattern of extreme arousal, and a hallucinatory-type behaviour that began in the first hour following the injection (Kitsikis & Steriade, 1981).[6] The animals vocalized in an attacking attitude, moved forward as if stalking prey or back as if defending themselves from an imaginary enemy. Finally, the idea that fast (gamma) oscillations are related to normal perceptions in waking or hallucinations in dreaming REM sleep and schizophrenic patients (Behrendt, 2003) should be enlarged, taking into consideration that such fast rhythms are also present during slow-wave sleep. Indeed these oscillations are voltage-dependent and they are superimposed over the depolarizing (excitatory) phase of the slow oscillation in both animals (Steriade *et al.*, 1996a,b) and humans (Mölle *et al.*, 2002). Congruently, dreaming is not exclusively occurring during REM sleep but is also present during late stages of slow-wave sleep (Hobson *et al.*, 2000; Hobson & Pace-Schott, 2002).

[5] The discrepancy between data from this and other studies (German *et al.*, 1999) may be due to the fact that Garcia-Rill used only brains from schizophrenics who died after 30 years of disease, that is, the worst of the worst cases.

[6] The hallucinatory-type behaviour described in this study appeared during the waking state and it resembled the oneiric, hallucinatory behaviour observed during REM sleep in animals with bilateral lesions of the peri-locus coeruleus region (Jouvet & Delorme, 1965).

9.2 Amygdalo-prefrontal interactions in anxiety disorders

The prevailing types of human mood disorders are anxiety disorders. They affect nearly 13% of individuals at some point in their lives and impose a heavy economic burden (an estimated $US46.6 billion in 1990 (Rice & Miller, 1995)). Congruent findings from studies of fear learning in animals and anxiety disorders in humans suggest that basic research on the circuits mediating the acquisition of fear responses constitutes our best hope of understanding and eventually treating human anxiety disorders. This section reviews data about the cerebral circuits supporting the acquisition, maintenance and extinction of conditioned fear in animals as well as human data implicating the same circuits in phobic and post-traumatic anxiety disorders.

9.2.1 Mechanisms underlying the acquisition of Pavlovian fear memories

Evidence that the lateral amygdala is a critical site of plasticity in fear conditioning

In laboratory settings, the model most frequently used to study how organisms acquire new fear responses is classical fear conditioning. In this model, a neutral environmental signal (CS; usually a tone) is paired to a noxious unconditioned stimulus (US; generally a footshock) such that the CS acquires the ability to evoke conditioned fear responses (CR). There is a remarkable similarity between the behavioural measures of conditioned fear in these animal studies and the symptoms used to diagnose anxiety disorders in humans (Davis, 1992).

Much evidence suggests that the amygdala plays a critical role in the acquisition of new fear responses. First, the lateral nucleus of the amygdala receives CS (tone) information from the auditory cortex (Romanski *et al.*, 1993) and from the posterior thalamus.[7] Second, lesioning these auditory inputs prevents the development of conditioned fear responses (LeDoux *et al.*, 1984). Third, temporary inactivation of the lateral amygdala during conditioning prevents the acquisition of conditioned fear responses (Muller *et al.*, 1997; Sacchetti *et al.*, 1999; Wilensky *et al.*, 1999). Fourth, the CS-responsiveness of lateral amygdala neurons increases as a result of CS–US pairings (reviewed in Maren & Quirk, 2004). Fifth, intra-amygdala injections of drugs blocking NMDA receptors (Fanselow *et al.*, 1994; Walker & Davis, 2002), inhibiting protein synthesis (Bailey *et al.*, 1999; Lamprecht *et al.*, 2002; Nader, 2003; Schafe *et al.*, 1999) or inhibiting protein kinases (Schafe *et al.*, 2001) prevent long-term fear memory.

These multiple lines of evidence were interpreted to mean that the lateral amygdala is the critical site of plasticity in classical fear conditioning. As a result, it is now widely believed that convergence of CS

[7] The thalamic nuclei that relay auditory inputs to the lateral amygdala are the medial geniculate nucleus (medial portion) and the posterior intralaminar nucleus (LeDoux *et al.*, 1990b; Turner & Herkenham, 1991).

and US inputs increases the efficacy of synapses conveying information about the CS to the lateral amygdala (LeDoux, 2000b; Walker & Davis, 2000). Subsequent presentations of the CS alone would evoke larger responses in the lateral amygdala (Quirk *et al.*, 1995; Collins & Paré, 2000; Repa *et al.*, 2001). Conditioned fear responses would result from projections of the lateral amygdala to the central amygdaloid nucleus (Krettek & Price, 1978b; Kapp *et al.*, 1979; LeDoux *et al.*, 1988; reviewed in Davis, 2000), which sends massive projections to the brainstem and hypothalamic sites, producing fear responses (Bellgowan & Helmstetter, 1996; Davis, 2000; De Oca *et al.*, 1998; LeDoux *et al.*, 1988). Thus, the lateral amygdala is usually conceived as the main site of plasticity, whereas the central nucleus is considered as a passive relay to downstream structures. Yet, the deficits caused by central amygdala lesions in aversive conditioning (Kapp *et al.*, 1979; Iwata *et al.*, 1986; Killcross *et al.*, 1997; Amorapanth *et al.*, 2000) are consistent with a critical role of the central amygdala in fear expression (however, see Koo *et al.*, 2004).

However, several observations suggest that the mechanisms underlying classical fear conditioning are more complex. Some of these observations suggest that the central nucleus is also an essential site of plasticity. Other lines of evidence support the view that classical fear conditioning is associated with plasticity outside the amygdala. We consider these two themes in turn below.

Fear conditioning depends on distributed plasticity within the amygdala

Central to the model described above are projections from the lateral amygdala to the central nucleus and from there to the brainstem. However, only the medial part of the central nucleus sends significant projections to the brainstem[8] and the lateral amygdala only projects to more lateral sectors of the central nucleus (Figure 9.1).[9] Thus, there are no direct links between the site of plasticity in the lateral amygdala and the site mediating expression, the central nucleus.

On the other hand, indirect routes are possible. For instance, the lateral or amygdalostriatal parts of the central nucleus were reported to project to the medial part of the central nucleus. In addition, the basal nuclei receive glutamatergic projections from the lateral nucleus (Krettek & Price, 1978b; Smith & Paré, 1994) and project to the central medial nucleus (Paré *et al.*, 1995c; Pitkänen *et al.*, 1995; Petrovich & Swanson, 1997). However, these possibilities seem unlikely because the polarity of the projection does not fit in the former case, and lesion data argues against the latter.[10]

To complicate matters further, the central nucleus also has direct access to thalamic inputs about the CS. Indeed, the posterior thalamic nucleus (PO) projects to the central medial and accessory basal nuclei (LeDoux *et al.*, 1987; Linke *et al.*, 2000; Turner & Herkenham, 1991), and parts of the inferior colliculus (external and pericentral nuclei) project to PO (Kudo & Niimi, 1980; Linke *et al.*, 2000).[11] Not only does the central amygdala have access to CS information,

[8] The lateral part of the central nucleus only projects to the parabrachial nucleus in the pons (Petrovich & Swanson, 1997) whereas the medial part of the central nucleus projects to various brainstem nuclei including the periaqueductal grey, which mediates freezing (reviewed in Davis, 2000), and the pontine reticular formation involved in fear-potentiated startle (Rosen *et al.*, 1991), as well as the pedunculopontine, dorsal motor vagal and solitary tract nuclei. Several tract-tracing studies reached this conclusion, and in a variety of species (rat, cat, rabbit) (Hopkins & Holstege, 1978; Schwaber *et al.*, 1982; Veening *et al.*, 1984; Liubashina *et al.*, 2000).

[9] Tract-tracing studies performed in rats, cats and monkeys support this statement (Krettek & Price, 1978b; Pitkänen *et al.*, 1995; Smith & Paré, 1994).

[10] The projection of the central lateral nucleus to the central medial nucleus is relatively minor (Paré & Smith, 1993b) and is GABAergic (McDonald & Augustine, 1993; Nitecka & Ben-Ari, 1987; Paré & Smith, 1993a). The latter property makes the central lateral nucleus an unlikely candidate for relaying CS information from the lateral amygdala to the central medial nucleus since chemical or electrical excitation of the latter elicits the behavioural correlates of fear (reviewed in Davis, 2000). A GABAergic projection from the central lateral nucleus would decrease rather than augment fear expression. As to the second possibility, pre-training lesions of the basal nuclei do not prevent the acquisition of conditioned fear (Amorapanth *et al.*, 2000; Holahan & White, 2002; Nader *et al.*, 2001), suggesting that this indirect pathway is not essential (but see Goosens & Maren, 2001). To settle this issue, however, post-training lesions will be needed.

[11] In addition, the PO also receives auditory inputs from the dorsal nuclei of the lateral

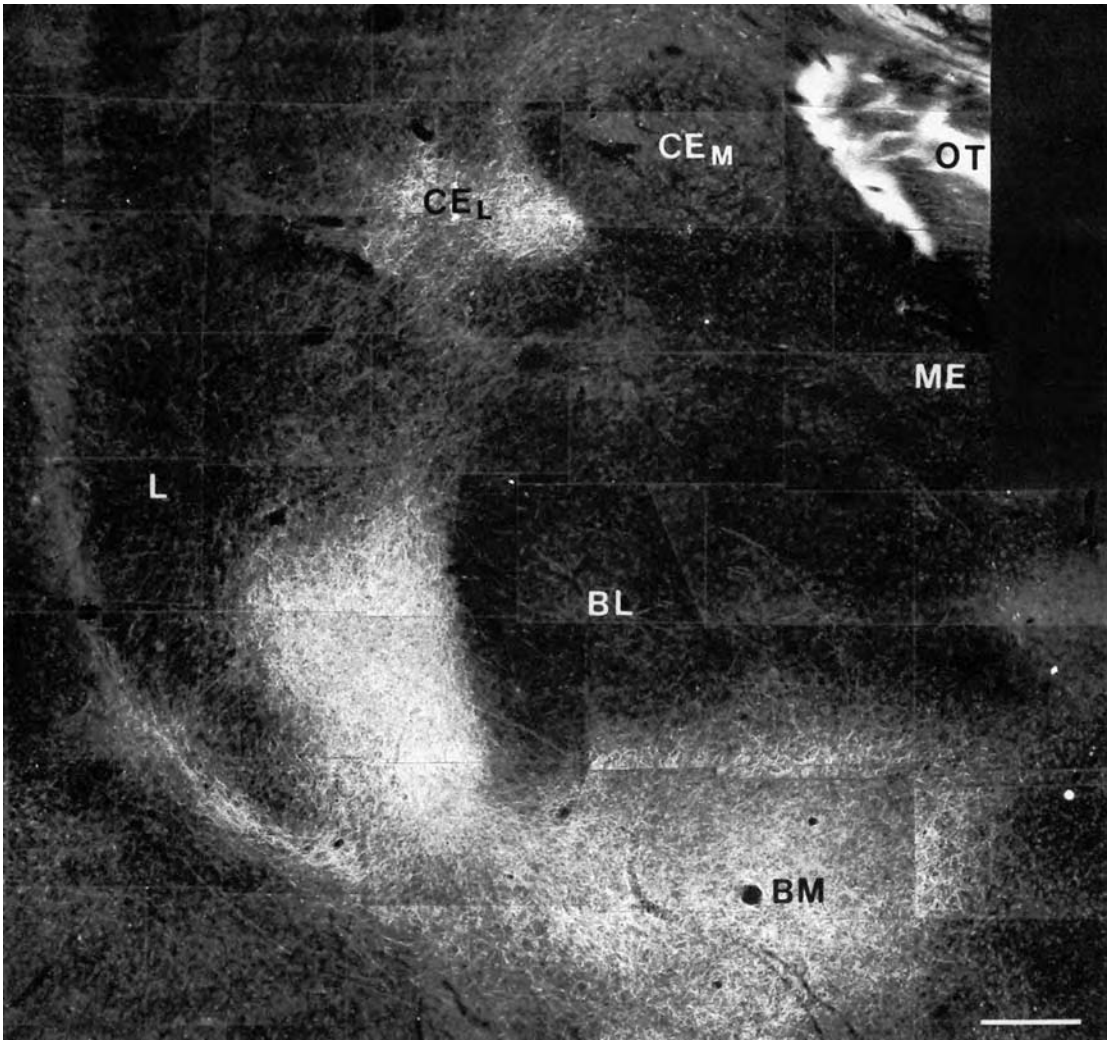

Fig. 9.1 Distribution of anterogradely labelled axons in the amygdala following a PHA-L injection in the core of the lateral nucleus. Note the presence of labelling in the basomedial nucleus and lateral part of the central nucleus. There is no anterograde labelling in the medial part of the central nucleus. Dark-field photomontage. Scale bar, 0.5 mm. Abbreviations: BL, basolateral nucleus; BM, basomedial nucleus; CE_M, medial sector of the central nucleus; CE_L, lateral sector of the central nucleus; L, lateral nucleus; ME, medial nucleus; OT, optic tract. Modified from Smith & Paré (1994).

it also receives nociceptive inputs about the US. Indeed, the central amygdala receives nociceptive information from the spinal cord and trigeminal nucleus via the parabrachial nuclear complex of the pons (Bernard *et al.*, 1990, 1992, 1993; Alden *et al.*, 1994; reviewed in Neugebauer & Li, 2003),[12] and potentially via the PO.

Given that the central amygdala receives CS and US information, it should not come as a surprise that evidence of plasticity was also seen in the central amygdala. Indeed, it was reported that local infusions

[11] (*cont.*) lemniscus (Kudo *et al.*, 1983) and of the brachium of the inferior colliculus (Kudo *et al.*, 1984). Other sensory inputs reach the PO from the superior colliculus and spinal cord (reviewed in Jones, 1985). Moreover, extracellular recordings have revealed that PO neurons respond to auditory, visual, and somatosensory stimuli (Poggio & Mountcastle, 1960; Aitkin *et al.*, 1986).

[12] Neurons of the central nucleus respond to mechanical and thermal noxious stimuli but rarely to innocuous stimuli. Some of these inputs are relayed by the parabrachial region, but the posterior thalamic complex is also a potential relay of nociceptive inputs.

of drugs that affect the central nucleus only during the acquisition phase[13] are sufficient to prevent the formation of long-term fear memory. Moreover, temporary inactivation of the central amygdala with muscimol (Wilensky *et al.*, 2000) or inhibition of protein synthesis in the central amygdala (Wilensky *et al.*, 2001) prevents the acquisition of conditioned fear responses.

Finally, thalamic inputs to the central nucleus can undergo long-term potentiation (Samson & Paré, 2005; Fu & Shinnick-Gallagher, 2005). In the first study (Samson & Paré, 2005), this thalamic LTP developed even when slices were prepared with a cut severing the connections between the lateral amygdala and central medial nucleus (Figure 9.2). The thalamic LTP was expressed presynaptically and was dependent on presynaptic NMDA receptors for its induction. At present, it is unclear whether (and how) this form of plasticity participates in fear conditioning. The fact that high-frequency activation of thalamic afferents was required for induction suggests that significant activation of presynaptic NMDA receptors only occurs during bouts of high-frequency activity. A possible explanation for this observation is that presynaptic NMDA receptors are located outside the synaptic cleft. As a result, they would only be activated when presynaptic activity is high, allowing for glutamate levels outside the synaptic cleft to rise beyond a level critical for LTP induction. Another possibility is that basal levels of presynaptic NMDA receptors on the plasma membrane are low but that high rates of presynaptic activity lead to a translocation of NMDA receptors.[14] The second possibility allows for a scenario of presynaptic coincidence detection where simultaneous activation of pathways relaying CS and US inputs would be required for induction of LTP in thalamic afferents.

Fear conditioning depends on distributed plasticity within the amygdala

That thalamic inputs to the central medial nucleus express LTP does not prove that this nucleus is a site of plasticity in fear conditioning. However, it does make this idea seem more plausible. The fact that the lateral amygdala lacks direct links to the central medial nucleus, combined with evidence that the central medial nucleus receives sensory inputs from the thalamus, indicates that it may also be a site of plasticity in fear conditioning. However, because the lateral nucleus does not project to the central medial nucleus, how do we reconcile the fact that interfering with the activity of the lateral (Muller *et al.*, 1997) *or* central amygdala (Goosens & Maren, 2003) during training prevents acquisition of conditioned fear responses? Recently, it was proposed that the key might reside in the intercalated cell masses (Paré *et al.*, 2004).

Intercalated cell masses are clusters of GABAergic neurons sandwiched between the basolateral and the central amygdala (Millhouse, 1986; Nitecka & Ben-Ari, 1987; Paré & Smith, 1993a). They receive glutamatergic inputs from the basolateral amygdala and cause feed-forward inhibition in the central nucleus (Figure 9.3A) (Paré & Smith, 1993b; Royer *et al.*, 1999). It was observed that there is a lateromedial

[13] Such as anisomycin or the NMDA receptor antagonist APV (Bahar *et al.*, 2003; Goosens & Maren, 2003).

[14] In support of this idea, an ultrastructural study reported that presynaptic NMDA receptors are concentrated in dense core vesicles in basal conditions (Paquet & Smith, 2000).

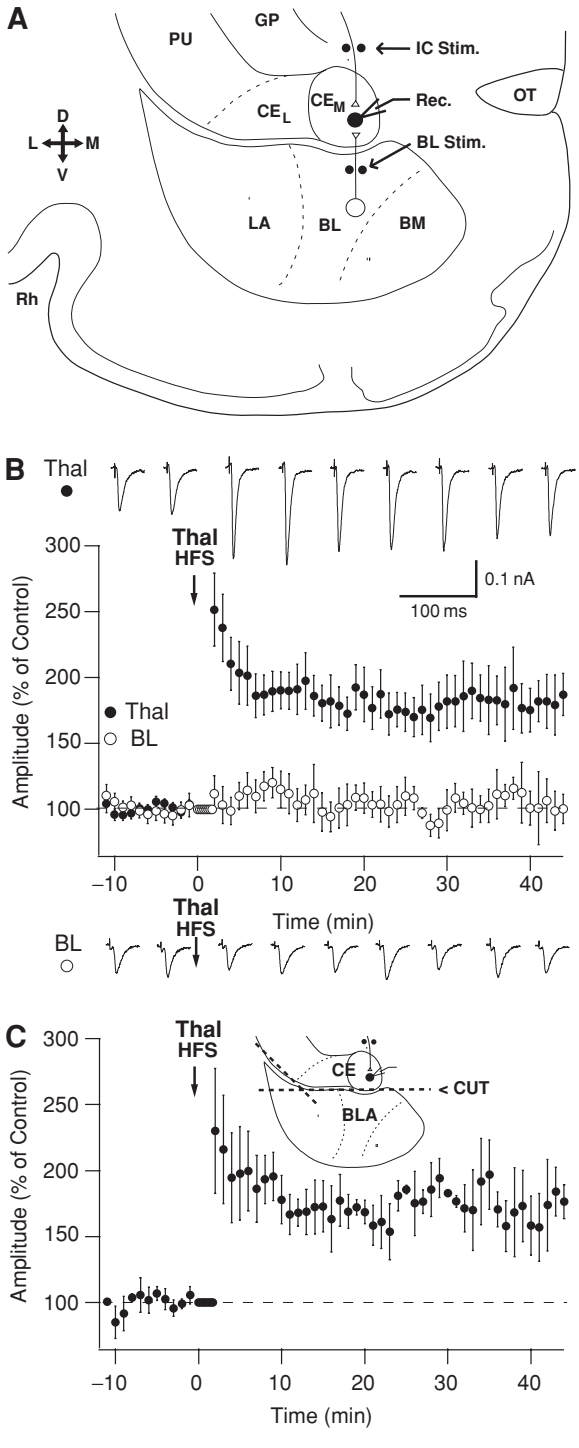

Fig. 9.2 Activity-dependent long-term potentiation of thalamic inputs to the central medial nucleus of the amygdala (CE_M). (A) Experimental set-up: scheme showing a coronal slice of the guinea pig amygdala kept *in vitro*. Black dots indicate position of stimulating electrodes (Stim.) in the internal capsule (IC) and BL nucleus. Pipette shows recording site (Rec.) in CE_M. Slice orientation is indicated by the cross on the left: D, V, L, M stand for dorsal, ventral, lateral and medial, respectively. (B) Amplitude of EPSCs evoked by activation of thalamic (filled circles) or BL (open circles) afferents (ordinate) as a function of time (abscissa). High-frequency stimulation (HFS) of thalamic afferents was applied at the time indicated by the downward arrow. Data were normalized to baseline response amplitudes. Traces above and below graph in (B) show examples of responses evoked by activation of thalamic or BL afferents, respectively. The timing of these responses is indicated by the position of their peaks with respect to the abscissa of the adjacent graph. The data plotted in (B) were obtained from intact slices, whereas those depicted in (C) were obtained from slices where the central medial nucleus was disconnected from the basolateral complex by means of cuts (inset, dashed lines). Abbreviations: BL, basolateral nucleus; BM, basomedial nucleus; CE_L, lateral sector of the central nucleus; GP, globus pallidus; LA, lateral nucleus; ME, medial nucleus; OT, optic tract; PU, putamen. Modified from Samson & Paré (2005).

correspondence between the position of intercalated neurons, where they project in the central nucleus, and where they derive their inputs from the basolateral complex (Royer *et al.*, 1999). Importantly, there are unidirectional connections between intercalated cell clusters, directed lateromedially (Royer *et al.*, 2000b). Consequently, activation

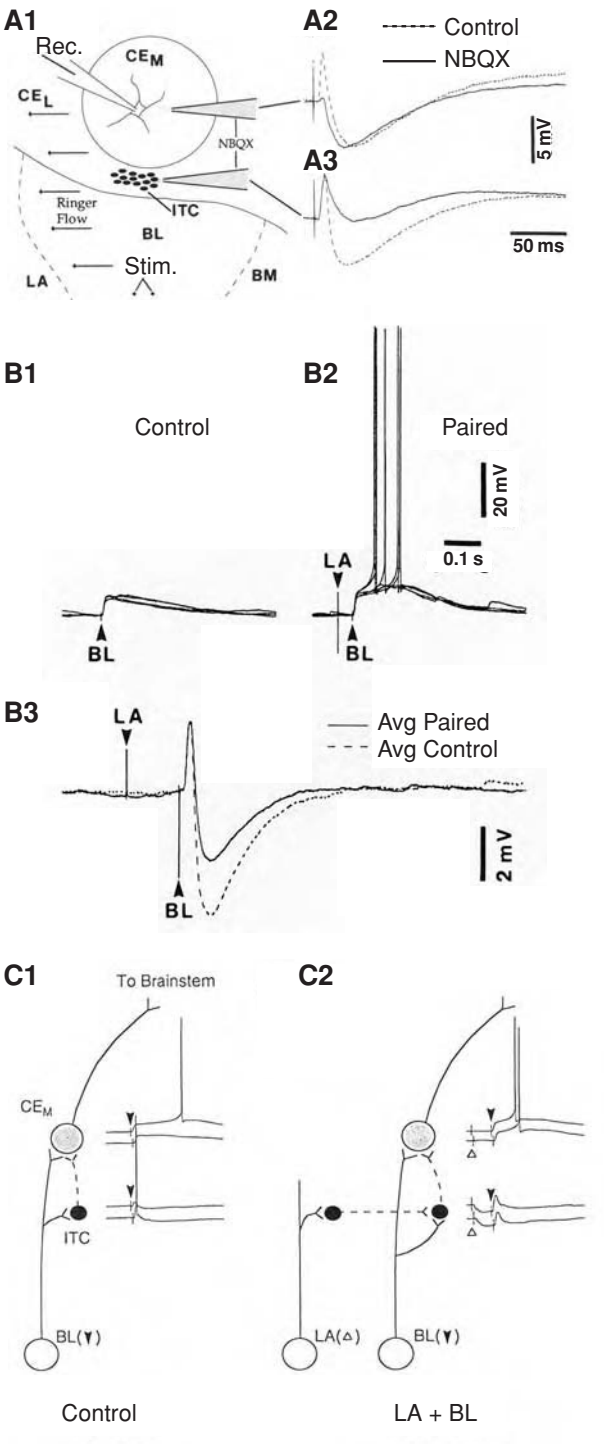

Fig. 9.3 Conditional gating of impulse traffic between the basolateral nucleus and central medial nucleus (CE_M) by intercalated neurons. (A) Scheme illustrating the approach used to test the effect of local pressure application of NBQX on CE_M responses to BL stimuli (dots). The horizontal arrows on the left indicate the direction of the Ringer flow. The ejection pipette was first positioned in the CE_M and, after a period of recovery (10 min), close to intercalated cells (ITC). The effect of NBQX pulses (1 s, 10 psi) in the CE_M and in the intercalated cell mass is shown in A2 and A3, respectively. Each trace is the average response to four BL stimuli delivered at 0.1 Hz in control conditions (dashed line) or preceded by a NBQX pulse (continuous line; pulse-shock interval of 100 ms). (B) Stimuli having no direct effects on CE_M neurons can enhance BL-evoked CE_M responses by modulating intercalated neurons. (B1) The BL-evoked responses of a CE_M neuron (Control) are enhanced when BL stimuli are preceded by a LA shock (B2, Paired). To carry out these tests, this cell was depolarized to −65 mV (with 0.01 nA) and the BL stimulation intensity gradually decreased just below firing threshold. (B3) Same protocol as in (B1, B2) but with a pipette solution containing QX-314. This CE_M cell was depolarized to −49 mV by current injection. Averages of four paired and unpaired (Control) responses. (C) Synaptic interactions postulated to explain the modulation of CE_M responses by intercalated neurons (ITC). Glutamatergic and GABAergic neurons are represented by white and black circles, respectively. Stimulation sites are indicated by symbols: BL, arrowheads; LA, empty triangle. In the two panels,

of the lateral amygdala depolarizes intercalated cells located at the same lateromedial level, causing an inhibition of more medially located intercalated neurons and the disinhibition of central medial neurons (Royer *et al*., 1999). The final consequence is a facilitation of central medial output by activation of the lateral amygdala (Figure 9.3B,C).

Thus, it is possible that potentiation of CS responsiveness in the lateral amygdala is critical to the acquisition of conditioned fear responses because it causes a disinhibition of brainstem projecting central neurons by way of intercalated neurons (Paré *et al*., 2004). In parallel, thalamic inputs to central medial neurons would undergo activity-dependent potentiation. Thus, the acquisition of conditioned fear responses may well depend on distributed storage in the amygdala.

Emotional arousal facilitates plasticity outside the amygdala

The previous section emphasized the contribution of the amygdala to the acquisition of specific fear responses as a result of paired CS–US presentations. However, even in this simple situation, animals form memories about other aspects of the conditioning context, such as the appearance of the training box. Indeed, when animals are placed in the training context, they show increased freezing in the absence of the CS (Kim & Fanselow, 1992). This form of contextual learning reflects the adaptive tendency of animals to predict danger by remembering environmental contingencies that are linked to aversive outcomes.

Post-training manipulations such as tetrodotoxin infusions in the hippocampus (Sacchetti *et al*., 1999) or hippocampal lesions (Kim & Fanselow, 1992) block contextual fear conditioning while leaving conditioned freezing to the CS intact. The effects of these manipulations are most intense when they are performed shortly after conditioning, suggesting that the hippocampus has a time-limited role in the consolidation of contextual fear memory (reviewed in Sanders *et al*., 2003). Yet, the amygdala is also involved in contextual fear memory. Indeed, infusion of NMDA receptor antagonists in the basolateral amygdala prior to conditioning prevents the acquisition of contextual and cued fear (Fanselow & Kim, 1994; Lee & Kim, 1998).

Similarly, fear conditioning studies in humans point to the complex and complementary roles played by the amygdala and hippocampal formation in learning. In one study (Bechara *et al*., 1995), intact

←

the top two traces represent the responses of CE_M neurons and the two bottom ones, those of intercalated cells. C1, in control conditions, BL inputs excite CE_M and intercalated cells. The feedforward inhibition thus generated in CE_M cells reduces their likelihood of responding to BL stimuli with orthodromic spikes. C2, inputs from the LA inhibit intercalated neurons projecting to the CE_M via the activation of other intercalated neurons located laterally. As a result, less feedforward inhibition is elicited in CE_M cells by BL inputs, resulting in a higher probability of orthodromic spiking. Modified from Royer *et al.* (1999).

subjects were compared with patients with lesions of the amygdala or hippocampal region in a classical fear conditioning task. The three groups of subjects were presented with stimuli (coloured geometrical figures), one of which predicted US delivery, while their electrodermal conductance was measured. Normal subjects developed a normal galvanic skin response to the CS and remembered which coloured stimulus predicted US delivery. Subjects with amygdala lesions did not develop a conditioned galvanic skin response but remembered which coloured stimulus predicted US. Finally, subjects with hippocampal damage developed a normal conditioned galvanic skin response but could not recollect which stimulus predicted shock delivery.[15]

This kind of double dissociation between the effects of amygdala and hippocampal damage cemented the view that distinct neuronal systems mediate different forms of memory. However, the fact that the amygdala and hippocampal system can function independently does not preclude the possibility that they can influence each other in normal conditions. In fact, much evidence suggests that the amygdala can facilitate some aspects of declarative memory formation in emotionally arousing conditions. For instance, long-term declarative memory for emotionally arousing material is generally better than for neutral events and this effect is absent in subjects with amygdala lesions (Adolphs *et al.*, 1997; Cahill *et al.*, 1995; Richardson *et al.*, 2004). Moreover, several functional imaging studies have reported a high correlation between the amount of amygdala activation at encoding and subsequent recall (Cahill *et al.*, 1996; Hamann *et al.*, 1999).

At present, it is unclear whether and how the amygdala mediates these effects. In principle, the amygdala could facilitate memory by enhancing attention at encoding or by modulating storage (reviewed in Phelps, 2004). There is evidence supporting both possibilities. With respect to the first possibility, it has been known for some time that amygdala stimulation produces an EEG activation accompanied by an orienting reaction (Ursin & Kaada, 1960; Kapp *et al.*, 1994), possibly via the substantia innominata (Dringenberg & Vanderwolf, 1996; reviewed in Davis, 2000). In humans, it was shown that attention was enhanced by emotional material and that this effect was absent in a subject with an amygdala lesion.[16]

Consistent with these results, functional imaging studies have revealed that the amygdala is activated by emotional stimuli. This activation occurs rapidly and may take place without awareness.[17] There is also evidence that the amygdala can facilitate the storage of declarative memory for emotional material. It is well known that long-term memory can be enhanced or reduced by treatments performed in the minutes to hours after learning.[18] This has led to the suggestion that memories form slowly over time, a process termed memory consolidation. What adaptive purpose could this process serve? It was proposed that it might be biologically advantageous to delay commitment of events to long-term memory until their significance could be evaluated. In other words, the process of consolidation would allow the brain to modulate the strength or extent of

[15] Similar results were obtained by LaBar *et al.* (1995).

[16] To demonstrate this, Anderson & Phelps (2001) used an experimental paradigm known as the attentional blink. In this paradigm, 15 words are presented sequentially at a rapid pace. Most words are black; one or two are green. After each sequence, the subject is required to type the green words he has seen. In normal subjects, presentation of two green words in 600 ms or less impairs perception of the second. This attentional blink is less pronounced if the interval is lengthened or if the second word is emotionally charged. The performance of a subject with a bilateral amygdala lesion did not benefit from the emotional valence of the words.

[17] In an elegant illustration (Whalen *et al.*, 1998), a backward masking procedure was used to study amygdala responses to stimuli that were not registered consciously. Subjects were presented with pictures of faces, happy or fearful. These pictures were presented for 33 ms. The offset of these pictures coincided with the onset of a second picture showing a neutral face for 167 ms. Subjects did not consciously register the first face; only the second. Yet the amount of amygdala activation was significantly higher during the presentation of the masked fearful face than happy or neutral faces.

[18] For instance, recently formed memories were reported to be susceptible to post-learning manipulations that include electroconvulsive shocks (Duncan, 1949; Gerard, 1949), protein synthesis inhibitors (Agranoff *et al.*, 1966), drug injections (McGaugh, 1966) and electrical stimulation of discrete brain regions (reviewed in McGaugh & Gold, 1976).

consolidation as a function the importance of the memory (Gold & McGaugh, 1975).

Congruently, it was shown that administration of adrenal stress hormones after learning could facilitate retention in appetitively or aversively motivated tasks (reviewed in McGaugh, 2002). As predicted by the consolidation hypothesis, the effects of stress hormones and their pharmacological analogues were time-dependent, their impact on retention decreasing as the interval between training and hormone treatment increased. These results raised the possibility that, when released during a stressful episode, these hormones could act retrogradely to affect memory of that event. In other words, the extent of consolidation would depend on the motivational or arousing consequences of an experience, as expressed by the release of stress hormones.

Subsequently, it was reported that the memory modulation produced by manipulations of stress hormone levels could be blocked by lesioning or inactivating the basolateral amygdala (BLA) or stria terminalis, but not the central amygdaloid nucleus (Liang & McGaugh, 1983; Liang *et al.*, 1990; Introini-Collison *et al.*, 1991; Roozendaal & McGaugh, 1996a,b). In keeping with these findings, post-training injections of drugs that presumably enhanced or reduced BLA activity facilitated or impaired retention, respectively.[19]

Taken together, these results suggest that stress hormones released in emotionally arousing conditions increase the activity of BLA neurons. In turn, the enhanced activity of BLA cells would facilitate memory consolidation in other brain areas via their widespread cortical and subcortical projections. Consistent with this possibility, it was reported (Pelletier *et al.*, 2005b) that emotional arousal (produced by a single foot-shock) causes a gradual increase in the firing rate of many BLA neurons (Figure 9.4) that peaked 30–50 min after the shock, was observed in waking and slow-wave sleep, and subsided within 2 h. Moreover, during this period of enhanced activity, the discharges of BLA neurons were more synchronized.

Although altering amygdala activity immediately after learning affects long-term retention, BLA lesions performed later have no effects (Parent *et al.*, 1995). This result implies that the amygdala is not the storage site of these memories. In other words, this observation suggests that the memory modulating effects of the amygdala manipulations listed above do not result from alterations of memory storage in the amygdala but in other structures that presumably constitute the storage site of particular forms of memories (reviewed in Cahill & McGaugh, 1998).[20]

How could the enhanced activity of BLA neurons facilitate memory storage in emotionally arousing conditions? In the study that examined the effect of emotional arousal on the activity of BLA neurons (Pelletier *et al.*, 2005b), firing-rate increases were observed in all nuclei of the BLA. Since these different nuclei have different projection sites,[21] this implies that the emotional arousal produced by the foot-shock caused long-lasting activity enhancements in neurons that

[19] Reduced retention was seen with local intra-amygdala injections of GABA agonists (Castellano *et al.*, 1989), beta-adrenergic antagonists (Gallagher *et al.*, 1977) and glutamate receptor antagonists (Izquierdo & Medina, 1993). Enhanced retention was seen with intra-amygdaloid injections of bicuculline (Dickinson *et al.*, 1993), and agonists of beta-adrenergic (Ferry & McGaugh, 1999; Hatfield & McGaugh, 1999) and muscarinic (Salinas *et al.*, 1997) receptors. Similarly, post-training intra-amygdaloid injections of glucococorticoids were also reported to enhance memory consolidation (reviewed in Roozendaal, 2000).

[20] The study of Packard *et al.* (1994) nicely illustrates this point. They showed that immediate post-learning injection of amphetamines in the basolateral amygdala increases hippocampal storage of spatial information (hidden platform water maze task) *and* caudate storage of response information (visible platform water maze task). Yet intra-amygdala injections of lidocaine just before testing retention had no effect on either task (Packard *et al.*, 1994). Moreover, pre-retention lidocaine injection in the hippocampus or caudate only blocked the memory potentiating effects of intra-amygdala amphetamine injection in the hidden *or* visible platform water maze task, respectively (Packard & Teather, 1998).

[21] As a group, they project to the rhinal cortices, hippocampus, insula, prefrontal cortex, striatum, etc. (reviewed in Pitkänen, 2000).

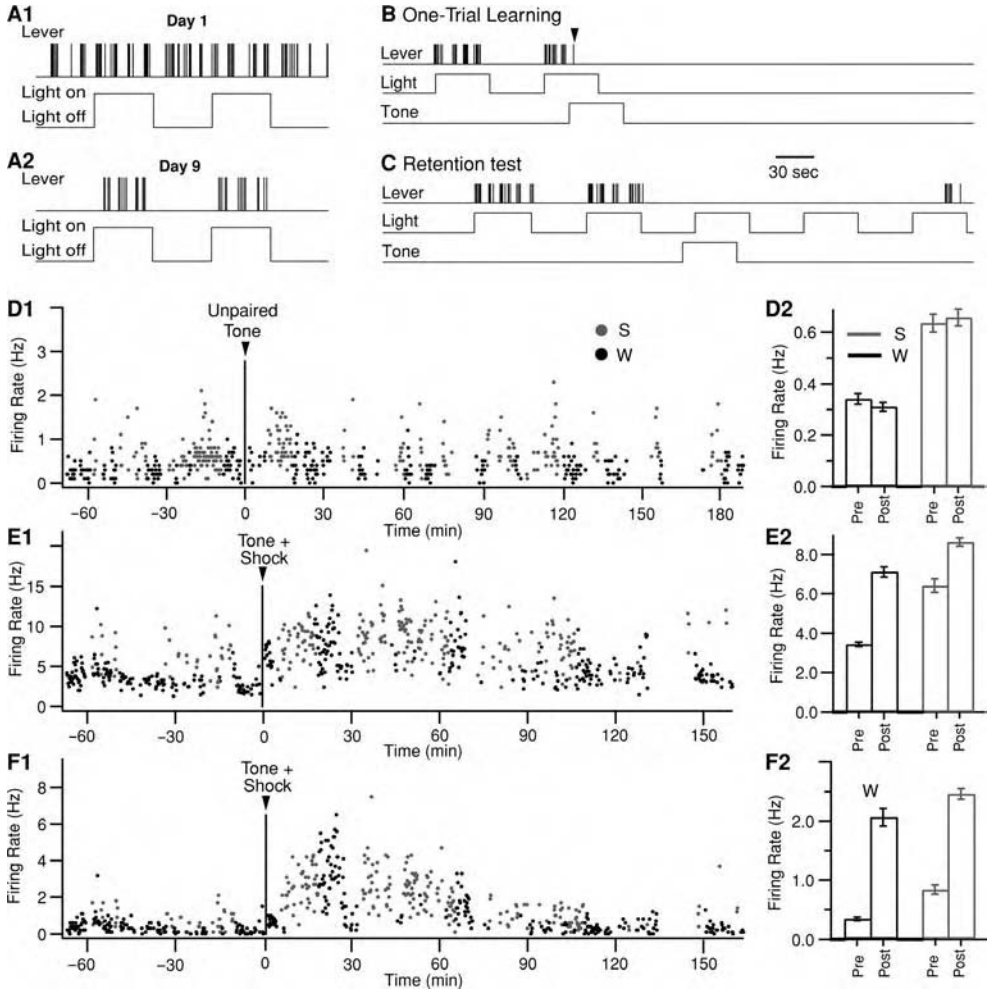

Fig. 9.4 Firing rate of basolateral amygdala neurons during a feline analogue of the inhibitory avoidance task. (A) Cats that had been trained to press a lever repetitively for food (A1) learned that lever-pressing would only be rewarded when a light was turned on ('lights-on'), but not when it was off ('lights-off', A2). (B) The animals were presented three alternating 'lights-on and -off' epochs followed by an extended 'lights-off' epoch during which the spontaneous activity of BLA neurons was recorded in both waking and slow-wave sleep. Then, the 'lights-on and -off' alternation resumed with the exception that a second stimulus (a 1 kHz tone, 50 db) was presented during the second 'lights-on' epoch. The first lever press following tone onset triggered a single brief foot-shock (0.5 s, 0.5 mA, arrowhead). Upon receiving the shock, the cat stopped pressing the lever. After the lights and tone were turned off, the spontaneous activity of BLA neurons was recorded for the next 3–4 h. (C) Two days after the introduction of the foot-shock, cats were given the opportunity to press the lever for food again. After two 'lights-on' and 'lights-off' epochs, the tone was presented 15 s before the onset of a 'lights-on' epoch and left on for 1 min. Then, the alternation between 'lights-on and -off' epochs continued normally. The cats behaved normally before the tone was turned on, but refrained from pressing the lever for several minutes after presentation of the tone. (D–F) Firing rate of BLA neurons during a control recording day (D), when only the tone was presented, and during a one-trial learning session (E–F), when the first lever press after tone onset triggered a foot-shock. Left column (1), graphs plotting firing rate (ordinate) as a function of time (abscissa, 10 s bins). Black and red symbols indicate data obtained in waking (W) and slow-wave sleep (S), respectively. The vertical line marks a 3.5 min interruption when the tone (D) or tone plus foot-shock (E–F) were presented. Right column (2), histograms showing averaged firing rates in W (black) and S (red), pre- (left) and post-tone (right). Modified from Pelletier *et al.* (2005b). See Plate 6.

project to functionally heterogeneous brain structures. Thus, these considerations suggest that the memory-modulating role of the BLA would not result from the specific activation of particular groups of neurons depending on the cause of the emotional arousal. The logical consequence of this is that the memory-modulating effect of the BLA depends on the activity patterns taking place in BLA projection sites when the emotional arousal occurred.

The fact that postshock BLA discharges are more synchronized than baseline activity also has important implications. Indeed, the conduction times of BLA axons are adjusted to compensate for variations in distance between the BLA and its targets (Pelletier & Paré, 2002). This property might allow BLA neurons to generate short time windows of depolarization that facilitate Hebbian associations between coincident, but spatially distributed, activity patterns in target structures. However, this view implies that the activity patterns that took place during the emotionally arousing event are replayed in both wake and slow-wave sleep. In support of this idea, there is now much evidence of replay in slow-wave sleep (Pennartz *et al.*, 2002, 2004) and waking (Abeles *et al.*, 1995; Seidemann *et al.*, 1996; Nadasdy *et al.*, 1999) at multiple levels of the central nervous system.

However, other data suggest that the exact timing of amygdala discharges might not be important. Indeed, a recent study reported that stimulation of the BLA could produce a NMDA-dependent potentiation of cortical inputs to medium spiny striatal neurons (Popescu *et al.*, 2005). To induce this LTP, electrical stimuli were delivered in the amygdala and/or cerebral cortex at 2 Hz, paired with suprathreshold intracellular current pulses (Figure 9.5). When amygdala and cortical stimuli were paired, an input specific LTP of cortical inputs was observed in most tested cells. In contrast, pairing two cortical sites usually had no effect.

Insights into the mechanisms underlying this phenomenon were obtained by comparing the time-dependence of NMDA receptor blocking by intracellular MK-801 at amygdala and cortical inputs. Indeed, this test revealed that NMDA receptors at amygdala inputs were blocked more rapidly by MK-801, suggesting that amygdala synapses are located at more proximal dendritic levels than cortical inputs. Moreover, the heterosynaptic facilitation of corticostriatal LTP by amygdala inputs did not occur when either the cortical or BLA stimuli were applied without coincident depolarization, or when the tests were performed in the presence of a calcium chelator or of a NMDA receptor antagonist. Yet, the LTP developed normally when the cortical and amygdala stimuli were separated by as much as 500 ms.

Although the NMDA-dependence and lax timing requirements of the LTP facilitation by amygdala inputs seem contradictory, it was proposed that propagating waves of calcium-induced calcium release bridge the spatial and temporal gap between the two inputs (Popescu *et al.*, 2005). This idea was based on previous findings indicating that Ca^{2+} entering via NMDA receptors can evoke Ca^{2+}-induced Ca^{2+} release (Emptage *et al.*, 1999) and that propagating waves of

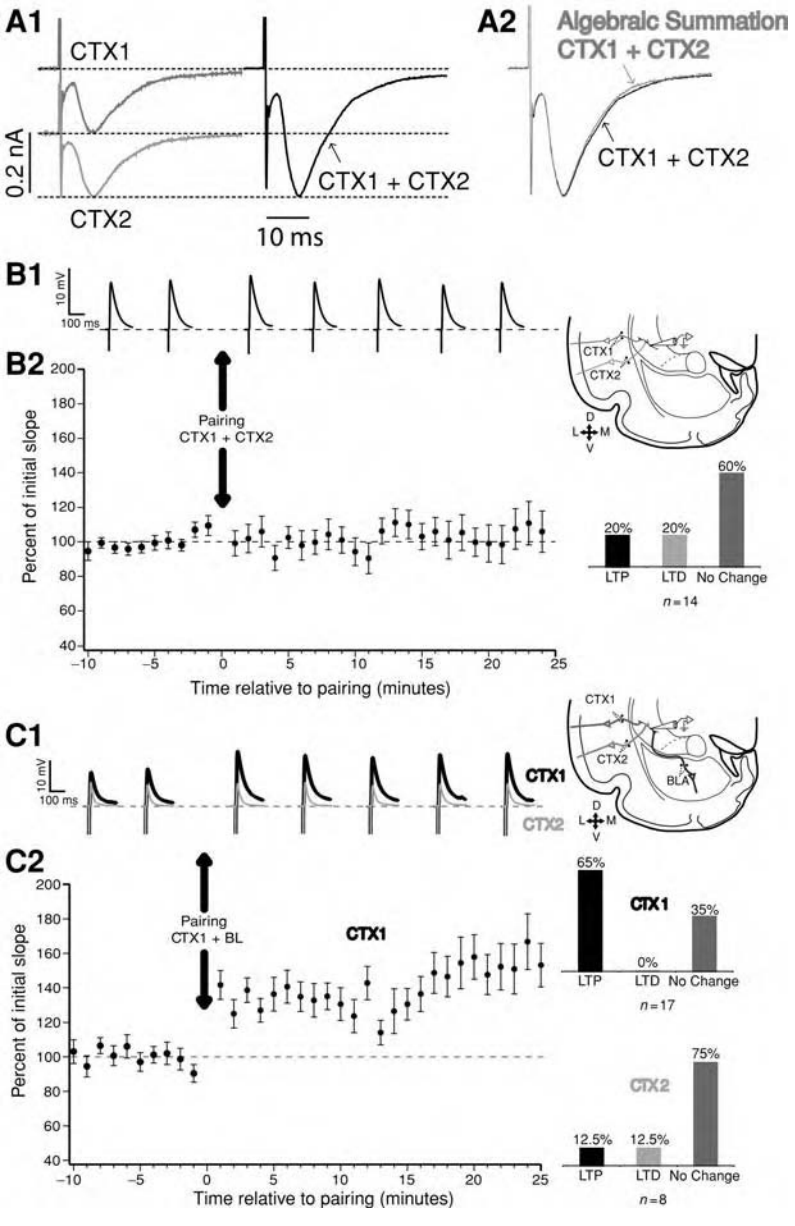

Fig. 9.5 Amygdala activation facilitates induction of corticostriatal long-term potentiation. In coronal slices of the guinea pig amygdala, stimulating electrodes were positioned in two temporal neocortical sites and in the basolateral amygdala. (A) Occlusion test used to determine whether the two cortical stimulation sites activated distinct sets of synapses to medium spiny striatal neurons recorded with the whole-cell patch method. In this test, the actual and predicted sum of responses evoked by two stimuli is compared. When the response evoked by paired stimuli is smaller than the algebraic sum of individual responses, this constitutes evidence that the two stimulating electrodes activate a partially overlapping set of inputs. However, the actual and predicted responses were not significantly different from each other suggesting that the two cortical stimulating electrodes activated largely non-overlapping sets of inputs converging onto medium spiny neurons. (B) Simultaneous activation of the two cortical

calcium-induced calcium release regulate heterosynaptic changes in other cell types (Nishiyama *et al.*, 2000). Consistent with this view, the facilitating effects of amygdala stimulation on corticostriatal LTP were not observed when the cells were dialysed with ruthenium red or cyclopiazonic acid, two drugs that block calcium-induced calcium release.[22]

[22] These two drugs interfere with calcium-induced calcium release in different ways. Cyclopiazonic acid is a Ca^{2+}-ATPase inhibitor (Demaurex *et al.*, 1992) whereas ruthenium red is an antagonist of ryanodine receptors (Xu *et al.*, 1999).

These findings suggest that, in the striatum at least, the timing requirements for LTP facilitation by the amygdala are not as stringent as typically seen for NMDA-dependent forms of LTP. This unusual property removes the requirement for a precise coordination between amygdala and cortical activity after emotional arousal. Repeated bouts of increased activity in amygdala and cortical inputs should suffice to induce a long-term enhancement in the efficacy of cortical inputs, provided they coincide in rather wide (second rather than millisecond range) time windows. Although this mechanism seems easier to implement, it also raises the risk that irrelevant inputs might be facilitated because of random coincidence. However, because projection cells of the BLA have extremely low firing rates, the risk of such random coincidence is greatly reduced.

9.2.2 Extinction of fear memories

The previous sections described how the amygdala can support the acquisition of new fear responses to stimuli that have a predictive relationship with aversive outcomes. The available data suggest that some of these associations are stored in the amygdala, but that others are stored elsewhere. However, even in these instances, amygdala activity seems to facilitate the underlying plastic events.

From a clinical perspective, however, understanding how fear memories subside is essential. Indeed, mounting evidence indicates that post-traumatic and phobic anxiety disorders reflect a failure to forget fear memories (Rothbaum & Davis, 2003). In the laboratory, this process is modelled by repetitive presentations of the CS alone. This results in the progressive decline of conditioned fear responses to preconditioning levels (Pavlov, 1927). This process, known as extinction,

←

sites paired to injection of suprathreshold current pulses in the recorded cell does not produce long-term potentiaton. (B1) Examples of responses evoked by one of the two cortical sites. The timing of these responses is indicated by the position of their peaks with respect to the abscissa of the graph just below. (B2) Amplitude of EPSPs evoked by cortical stimuli (ordinate) as a function of time (abscissa). The pairing was applied at the time indicated by the arrows. Data were normalized to baseline response amplitudes. No LTP was induced with paired cortical stimuli. (C) Simultaneous stimulation of the amygdala and cortex produces long-term potentiation of the paired cortical input whereas the responses evoked by a control (unpaired) cortical site remain unchanged. (C1) Examples of responses evoked by the paired (CTX 1, black) and unpaired (CTX 2, green) cortical stimulation sites before and after pairing of CTX1 and amygdala (arrows). (C2) Amplitude of EPSPs evoked by the paired cortical stimulation site (ordinate) as a function of time (abscissa). A.T. Popescu & D. Paré, unpublished observations. See Plate 7.

does not result from unlearning of the original association. Rather, it depends on a different, parallel learning that opposes the original association and prevents the expression of conditioned fear responses. Indeed, presentation of unsignalled shocks after extinction training can 'reinstate' conditioned fear responses (reviewed in Myers & Davis, 2002; Rescorla, 2004).

Several observations suggest that the medial prefrontal cortex (mPFC) is involved in extinction. To begin with, mPFC lesions (Morgan & LeDoux, 1995; Quirk *et al.*, 2000; but see Gewirtz *et al.*, 1997) and infusions of protein kinase (Hugues *et al.*, 2004) or protein synthesis (Santini *et al.*, 2004) inhibitors in the mPFC prevent the recall of extinction. In addition, functional imaging studies indicate that the mPFC is recruited during extinction learning (Phelps *et al.*, 2004) and that subjects afflicted with post-traumatic stress have reduced mPFC activity when they recall traumatic events (Bremner *et al.*, 1999; Shin *et al.*, 2004). Last, stimulation of the mPFC dampens conditioned fear responses (Milad & Quirk, 2002).

In parallel, other data implicate the amygdala in extinction. Intra-amygdala injections of NMDA antagonists and protein kinase inhibitors interfere with extinction (Falls *et al.*, 1992; Lu *et al.*, 2001) whereas drugs enhancing NMDA responses speed up extinction in animals (Walker *et al.*, 2002) and phobic patients (Ressler *et al.*, 2004). In addition, although CS-evoked responses decrease in BLA neurons during extinction (Quirk *et al.*, 1995; Hobin *et al.*, 2003), many BLA cells continue to respond to the CS (Repa *et al.*, 2001). These findings, combined with evidence that mPFC neurons acquire CS-evoked responses following extinction training (Milad & Quirk, 2002), support the view that interactions between the mPFC and amygdala play an essential role in extinction.

However, it is likely that several parallel processes are involved in extinction. Within a single session of extinction training, repetitive presentations of the CS probably produce an adaptation of CS-evoked responses in the amygdala. For instance, during the presentation of a long tone, the responses of lateral amygdala neurons quickly habituate (Quirk *et al.*, 1995; Hobin *et al.*, 2003). This phenomenon probably results from a mixture of feedforward and feedback inhibition and, possibly, presynaptic inhibition of transmitter release in thalamic and/or cortical afferents. However, much of the decrease in conditioned fear caused during one extinction training session recovers by the next day. In fact, several extinction training sessions are usually required to produce a complete extinction, and mPFC lesions seem to interfere with the recall of extinction training (Morgan & LeDoux, 1995; Quirk *et al.*, 2000; but see Gewirtz *et al.*, 1997).

How might the mPFC mediate extinction? In light of the fact that the projections of the amygdala to downstream structures mediating fear mainly arise from the medial part of the central amygdala (Holstege *et al.*, 1996), this nucleus may be an effective site for mPFC to control conditioned fear. Indeed, the inhibition of fear expression by

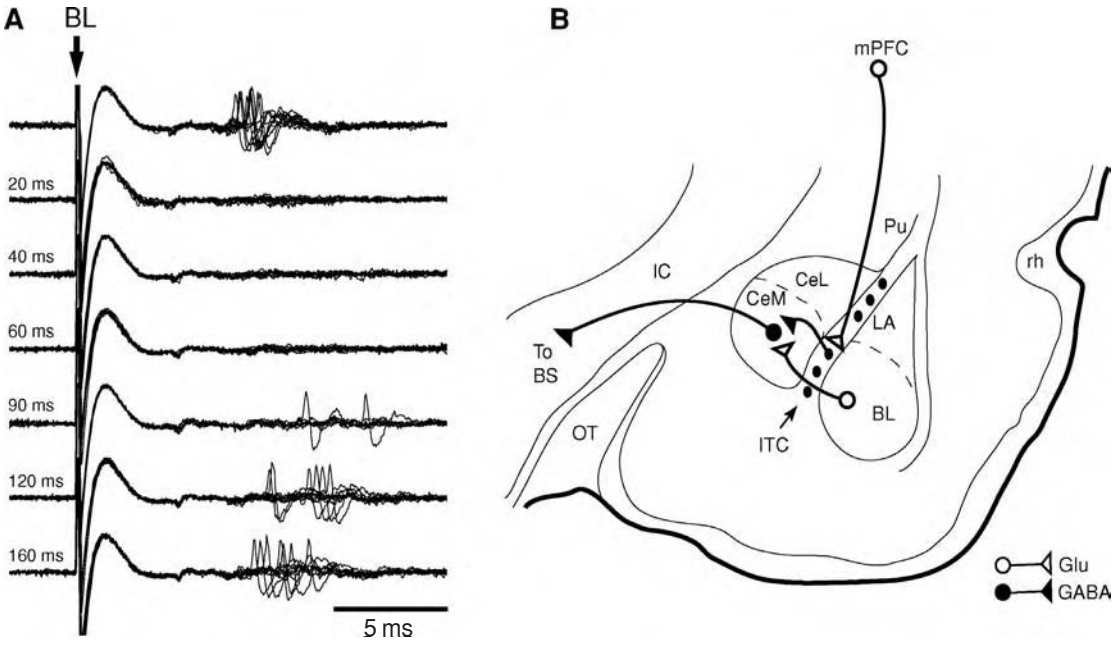

Fig. 9.6 Medial prefrontal inputs inhibit the synaptic responses of central medial neurons to basolateral stimuli. (A) Orthodromic responses of a central medial neuron to basolateral stimuli applied in isolation (top trace) or preceded by a mPFC shock using various inter-stimulus intervals (numbers on the left). (B) Scheme depicting the mPFC–amygdala interactions hypothesized to underlie the phenomenon described in (A). mPFC inhibits central medial projection neurons via GABAergic intercalated cells, thereby reducing central medial responses to inputs from BL. For clarity, several intra-amygdala projections have been omitted. Abbreviations: BL, basolateral nucleus; BS, brainstem; CeL, central lateral nucleus; CeM, central medial nucleus; ITC, intercalated cells; LA, lateral nucleus of the amygdala; rh, rhinal fissure; OT, optic tract. Modified from Quirk *et al.* (2003).

the mPFC would be most efficient if it acted before conditioned fear signals originating in the amygdala diverged to downstream effectors. In support of this proposal, it was shown (Quirk *et al.*, 2003) that mPFC stimulation reduces the synaptic excitability of central medial output neurons (Figure 9.6). However, the mechanism of the mPFC-evoked inhibition of central medial neurons remains unknown.

Axons from the mPFC ending in the amygdala are thought to use the transmitter glutamate. This view is based on the fact that they form asymmetric synapses, usually (more than 90%) with dendritic spines[23] in the amygdala. Consistent with this idea, there is a positive correlation between the activity of mPFC and BLA neurons (Figure 9.7),[24] indicating that the inhibition seen in the central medial nucleus following mPFC stimulation does not result from a disfacilitation (secondary to the inhibition of BLA neurons). In support of this contention, mPFC shocks can even prevent the orthodromic spiking evoked in central medial cells by direct electrical stimulation of the BLA (Quirk *et al.*, 2003).

[23] Rat, Brinley-Reed *et al.* (1995) cat and monkey, Smith *et al.* (2000).

[24] Although the possibility that this correlation is due to a common input cannot be ruled out, this seems unlikely because the average delay seen between mPFC and BLA firing in the cross-correlograms matches the conduction time of mPFC axons to the amygdala (mode of 24 ms), as estimated by using antidromic response latencies.

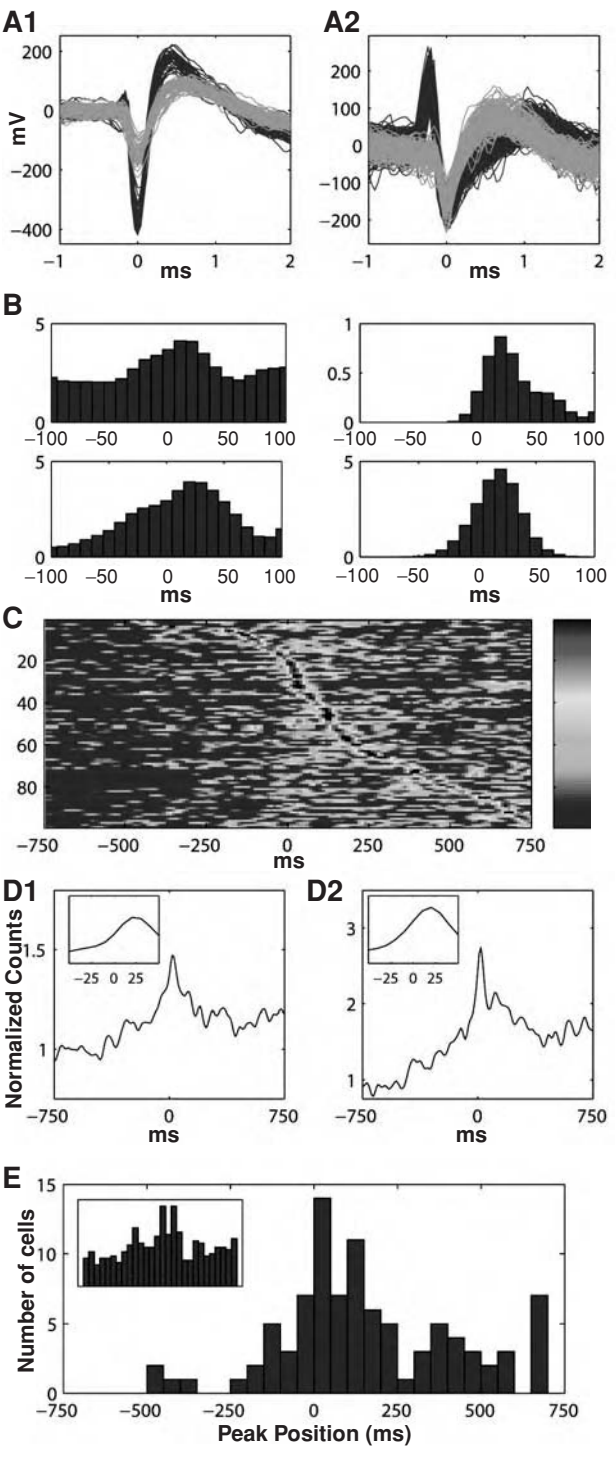

Fig. 9.7 Medial prefrontal firing is associated with an increased firing probability in BL neurons. The activity of simultaneously recorded mPFC (A1) and BL (A2) neurons was cross-correlated by using mPFC cells as references. (B) Examples of individual cross-correlograms obtained in different animals. (C) Cross-correlograms for all significant mPFC–BL cell cross-correlograms; bin values, expressed in *z* scores, are colour coded. Correlograms are ordered as a function of the position of the histogram peaks. (D) Average cross-correlograms for all available cell pairs (D1) and for those that reached significance (D2). Insets show an expanded view of the correlogram peaks. (E) Frequency distribution of the position of correlogram peaks for the data shown in (C). Modified from Likhtik *et al.* (2005). See Plate 8.

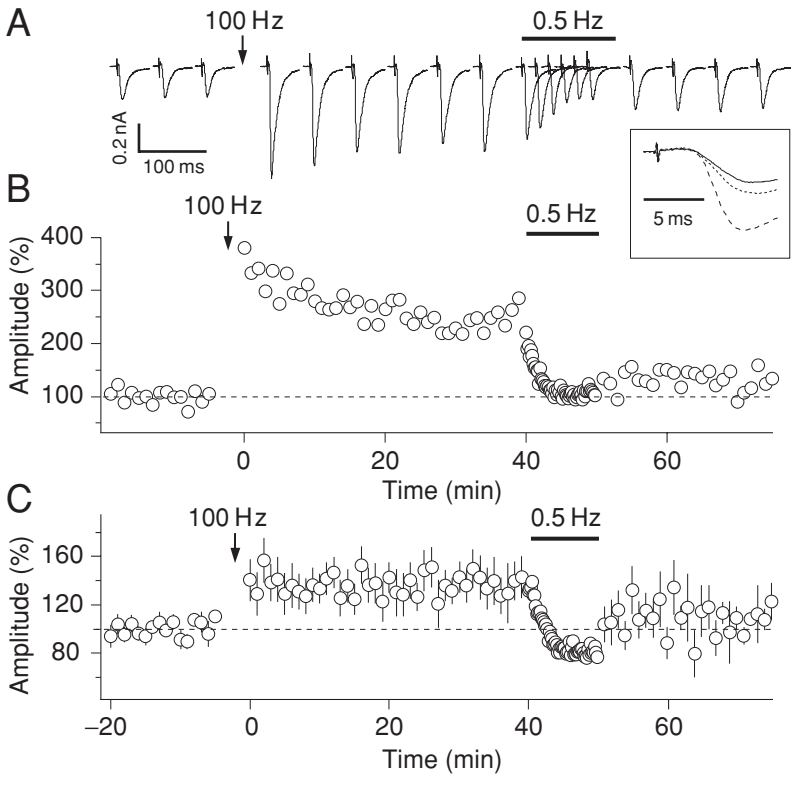

Fig. 9.8 Activity-dependent potentiation of basolateral inputs to intercalated neurons. High-frequency stimulation (HFS, 100 Hz) induces LTP of BLA-evoked responses in ITC neurons. (A) Examples of BLA-evoked EPSCs (average of 5) before/after HFS and low-frequency stimulation (LFS, 0.5 Hz). HFS produced LTP of BLA-evoked EPSPs. Then, LFS depotentiated the responses. (B) Amplitude of BLA-evoked EPSCs as a function of time for the same cell. Response amplitudes were normalized to the average in the control period. (C) Same as in (A2) but for all cells tested ($n = 24$). Modified from Royer & Paré (2002).

These findings imply that the mPFC-evoked inhibition of central medial neurons depends on an active gating mechanism located downstream of the BLA. Thus, we hypothesize that the mPFC inhibits central medial neurons by activating a population of GABAergic cells, such as found in the intercalated cell masses, that are innervated by the mPFC and send inhibitory projections to the central medial nucleus (Paré & Smith, 1993b; Royer *et al.*, 1999). Consistent with this hypothesis, it was recently reported that disinhibition of the mPFC by pricrotoxin microinfusions produces a large increase in the number of Fos immunoreactive intercalated neurons (Berretta *et al.*, 2005).

The possibility that intercalated neurons mediate the mPFC-evoked inhibition of the central medial nucleus is especially attractive because BLA inputs to intercalated cells express activity- and NMDA-dependent long-term potentiation (Figure 9.8) (Royer & Paré, 2002, 2003). This property, combined with the sensitivity of extinction to NMDA receptor antagonists (Falls *et al.*, 1992) infused in the amygdala, suggest that the function of the CS-related mPFC inputs is to cause sufficient depolarization of intercalated cells for the NMDA-dependent potentiation of BLA inputs. Consequently, during later CS presentations, cells in the BLA would evoke more inhibition than excitation in central medial output neurons, eventually leading to a suppression of conditioned fear responses.

If supported, this hypothesis would open new pharmacological avenues for the treatment of anxiety disorders. For instance, intercalated cells express extremely high levels of mu-opioid (Wilson *et al.*, 2002) and dopamine type 1 receptors (Fuxe *et al.*, 2003; Maltais *et al.*, 2000; Pinto & Sesack, 2002). Moreover, mPFC axon terminals onto intercalated cells express dopamine type 2 receptors (Fuxe *et al.*, 2003; Maltais *et al.*, 2000; Pinto & Sesack, 2002). Such data raise the prospect that extinction of pathological fear might be accelerated by targeted pharmacological interventions.

References

Abel, T., Nguyen, P. V., Barad, M. *et al*. (1997) Genetic demonstration of a role for PKA in the late phase of LTP and in hippocampus-based long-term memory. *Cell* **88**: 615–26.

Abeles, M., Bergman, H., Gat, I. *et al*. (1995) Cortical activity flips among quasi-stationary states. *Proceedings of the National Academy of Sciences USA* **92**: 8616–20.

Achermann, P. and Borbély, A. (1997) Low-frequency (<1 Hz) oscillations in the human sleep EEG. *Neuroscience* **81**: 213–22.

Adams, J. H., Graham, D. I. and Jennett, B. (2000) The neuropathology of the vegetative state after an acute brain insult. *Brain* **123**: 1327–38.

Adolphs, R., Cahill, L., Schul, R. and Babinsky, R. (1997) Impaired declarative memory for emotional stimuli following bilateral amygdala damage in humans. *Learning and Memory* **4**: 291–300.

Aggleton, J. P. (2000) *The Amygdala: A Functional Analysis*. Oxford: Oxford University Press.

Aggleton, J. P. and Mishkin, M. (1983a) Visual recognition impairment following medial thalamic lesions. *Neuropsychologia* **21**: 189–97.

Aggleton, J. P. and Mishkin, M. (1983b) Memory impairments following restricted medial thalamic lesions in monkeys. *Experimental Brain Research* **52**: 199–209.

Aggleton, J. P., Hunt, P. R. and Rawlins, J. N. (1986) The effects of hippocampal lesions upon spatial and non-spatial tests of working memory. *Behavioral Brain Research* **19**: 133–46.

Aghajanian, G. K. (1985) Modulation of a transient outward current in serotonergic neurones by alpha 1-adrenoceptors. *Nature* **315**: 501–3.

Aghajanian, G. K. and Wang, E. Y. (1977) Habenular and other midbrain raphe afferents demonstrated by a modified retrograde tracing technique. *Brain Research* **122**: 229–42.

Agranoff, B. W., Davis, R. E. and Brink, J. J. (1966) Chemical studies on memory fixation in goldfish. *Brain Research* **1**: 303–9.

Airaksinen, M. S. and Panula, P. (1988) The histaminergic system in the guinea pig central nervous system: an immunocytochemical mapping study using an antiserum against histamine. *Journal of Comparative Neurology* **273**: 163–86.

Aitkin, L. M., Irvine, D. R., Nelson, J. E., Merzenich, M. M. and Clarey, J. C. (1986) Frequency representation in the auditory midbrain and forebrain of a marsupial, the northern native cat (*Dasyurus hallucatus*). *Brain Behavior and Evolution* **29**: 17–28.

Alden, M., Besson, J. M. and Bernard, J. F. (1994) Organization of the efferent projections from the pontine parabrachial area to the bed nucleus of the stria terminalis and neighboring regions: a PHA-L study in the rat. *Journal of Comparative Neurology* **341**: 289–314.

Aleksanov, S. N. (1983) Coherent functions of the electrical activity of the hippocampus, amygdala and frontal cortex during alimentary instrumental reflexes in the dog. *Zhurnal Vysshei Nervnoi Deyatelnosti Imeni I P Pavlova* **33**: 694–9.

Allison, T., McCarthy, G., Wood, C. C., Williamson, P. D. and Spencer, D. D. (1989) Human cortical potentials evoked by stimulation of the median

nerve. II. Cytoarchitectonic areas generating long-latency activity. *Journal of Neurophysiology* **62**: 711–22.

Alloway, K. D., Wallace, M. B. and Johnson, M. J. (1994) Cross-correlation analysis of cuneothalamic interactions in the rat somatosensory system: influence of receptive field topography and comparisons with thalamocortical interactions. *Journal of Neurophysiology* **72**: 1949–72.

Alonso, A. (2002) Electrophysiology of neurones in the perirhinal and entorhinal cortices and neuromodulatory changes in firing patterns. In *The Parahippocampal Region*, ed. M. P. Witter and F. Wouterlood, pp. 89–105. Oxford: Oxford University Press.

Alonso, A. and Garcia-Austt, E. (1987a) Neuronal sources of theta rhythm in the enthorinal cortex of the rat. I. Laminar distribution of theta field potentials. *Experimental Brain Research* **67**: 493–501.

Alonso, A. and Garcia-Austt, E. (1987b) Neuronal sources of theta rhythm in the enthorinal cortex of the rat. II. Phase relations between unit discharges and theta field potentials. *Experimental Brain Research* **67**: 502–9.

Alonso, A. and Klink, R. (1993) Differential electroresponsiveness of stellate and pyramidal-like cells of medial entorhinal cortex layer II. *Journal of Neurophysiology* **70**: 128–43.

Alonso, A. and Köhler, C. (1984) A study of the reciprocal connections between the septum and the entorhinal area using anterograde and retrograde axonal transport methods in the rat brain. *Journal of Comparative Neurology* **225**: 327–43.

Alonso, A. and Llinás, R. (1989) Subthreshold theta-like rhythmicity in stellate cells of enthorinal cortex layer II. *Nature* **342**: 175–7.

Alonso, A., Faure, M. F. and Beaudet, A. (1994) Neurotensin promotes oscillatory bursting behaviour and is internalized in basal forebrain cholinergic neurons. *Journal of Neuroscience* **14**: 5778–92.

Alonso, A., Khateb, A., Fort, P., Jones, B. E. and Mühlethaler, M. (1996) Differential oscillatory properties of cholinergic and noncholinergic nucleus basalis neurons in guinea pig brain slices. *European Journal of Neuroscience* **8**: 169–82.

Amaral, D. G. (1986) Amygdalohippocampal and amygdalocortical projections in the primate brain. *Advances in Experimental Medicine and Biology* **203**: 3–17.

Amaral, D. G. and Cowan, W. M. (1980) Subcortical afferents to the hippocampal formation in the monkey. *Journal of Comparative Neurology* **189**: 573–91.

Amaral, D. G. and Price, J. L. (1984) Amygdalo-cortical projections in the monkey (*Macaca fascicularis*). *Journal of Comparative Neurology* **230**: 465–96.

Amaral, D. G., Price, J. L., Pitkänen, A. and Carmichael, S. T. (1992) Anatomical organization of the primate amygdaloid complex. In *The Amygdala: Neurobiological Aspects of Emotion, Memory, and Mental Dysfunction*, ed. J. P. Aggleton, pp. 1–66. New York: Wiley-Liss.

Amorapanth, P., LeDoux, J. E. and Nader, K. (2000) Different lateral amygdala outputs mediate reactions and actions elicited by a fear-arousing stimulus. *Nature Neuroscience* **3**: 74–9.

Amzica, F. and Massimini, M. (2002) Glial and neuronal interactions during slow waves and paroxysmal activities in the neocortex. *Cerebral Cortex* **12**: 1101–13.

Amzica, F. and Neckelmann, D. (1999) Membrane capacitance of cortical neurons and glia during sleep oscillations and spike-wave seizures. *Journal of Neurophysiology* **82**: 2731–46.

Amzica, F. and Steriade, M. (1995a) Disconnection of intracortical synaptic linkages disrupts synchronization of a slow oscillation. *Journal of Neuroscience* **15**: 4658–77.

Amzica, F. and Steriade, M. (1995b) Short- and long-range neuronal synchronization of the slow (<1 Hz) cortical oscillation. *Journal of Neurophysiology* **75**: 20–38.

Amzica, F. and Steriade, M. (1996) Progressive cortical synchronization of ponto-geniculo-occipital potentials during rapid eye movement sleep. *Neuroscience* **72**: 309–14.

Amzica, F. and Steriade, M. (1997) The K-complex: its slow (<1 Hz) rhythmicity and relation to delta waves. *Neurology* **49**: 952–9.

Amzica, F. and Steriade, M. (1998a) Cellular substrates and laminar profile of sleep K-complex. *Neuroscience* **82**: 671–86.

Amzica, F. and Steriade, M. (1998b) Electrophysiological correlates of sleep delta waves. *Electroencephalography and Clinical Neurophysiology* **107**: 69–83.

Amzica, F. and Steriade, M. (2000) Neuronal and glial membrane potentials during sleep and paroxysmal oscillations in the cortex. *Journal of Neuroscience* **20**: 6646–65.

Amzica, F. and Steriade, M. (2002) The functional significance of K-complexes. *Sleep Medicine Reviews* **6**: 139–49.

Amzica, F., Neckelmann, D. and Steriade, M. (1997) Instrumental conditioning of fast (20- to 50 Hz) oscillations in corticothalamic networks. *Proceedings of the National Academy of Sciences USA* **94**: 1985–9.

Amzica, F., Massimini, M. and Manfridi, A. (2002) Spatial buffering during slow and paroxysmal oscillations in cortical networks of glial cells *in vivo*. *Journal of Neuroscience* **22**: 1042–53.

Andersen, P. and Andersson, S. A. (1968) *Physiological Basis of Alpha Rhythm*. New York: Appleton-Century-Crofts.

Anderson, A. K. and Phelps, E. A. (2001) Lesions of the human amygdala impair enhanced perception of emotionally salient events. *Nature* **411**: 305–9.

Andreasen, N. C., Arndt, S., Swayze, V. *et al*. (1994) Thalamic abnormalities in schizophrenia visualied through magnetic resonance image averaging. *Science* **266**: 294–8.

Arieli, A., Shoham, D., Hildesheim, R. and Grinvald, A. (1995) Coherent spatiotemporal patterns of ongoing activity revealed by real-time optical imaging coupled with single-unit recording in the cat visual cortex. *Journal of Neurophysiology* **73**: 2072–93.

Arieli, A., Sterkin, A., Grinvald, A. and Aertsen, A. (1996) Dynamics of ongoing activity: explanation of the large variability in evoked cortical responses. *Science* **273**: 1868–71.

Asanuma, C. (1992) Noradrenergic innervation of the thalamic reticular nucleus: a light and electron microscopic immunohistochemical study in rats. *Journal of Comparative Neurology* **319**: 299–311.

Asanuma, C. (1997) Distribution of neuromodulatory inputs in the reticular and dorsal thalamic nuclei. In *Thalamus*, vol. 2 (*Experimental and Clinical Aspects*), ed. M. Steriade, E. G. Jones and D. A. McCormick, pp. 93–153. Oxford: Elsevier.

Asanuma, C. and Porter, L. L. (1990) Light and electron microscopic evidence for a GABAergic projection from the caudal basal forebrian to the thalamic reticular nucleus in rats. *Journal of Comparative Neurology* **302**: 159–72.

Aston-Jones, G., Ennis, M., Pieribone, V. A., Nickell, W. T. and Shipley, M. T. (1986) The brain nucleus locus coeruleus: Restricted afferent control of a broad efferent network. *Science* **234**: 734–7.

Bacci, A., Huguenard, J. R. and Prince, D. A. (2003) Functional autaptic neurotransmission in fast-spiking interneurons: a novel form of feedback inhibition in the neocortex. *Journal of Neuroscience* **23**: 859–66.

Bahar, A., Samuel, A., Hazvi, S. and Dudai, Y. (2003) The amygdalar circuit that acquires taste aversion memory differs from the circuit that extinguishes it. *European Journal of Neuroscience* **17**: 1527–30.

Bailey, D. J., Kim, J. J., Sun, W., Thompson, R. F. and Helmstetter, F. J. (1999) Acquisition of fear conditioning in rats requires the synthesis of mRNA in the amygdala. *Behavioral Neuroscience* **113**: 276–82.

Baker, S. N., Olivier, E. and Lemon, R. N. (1997) Coherent oscillations in the monkey motor cortex and hand muscle EMG show task-dependent modulation. *Journal of Physiology (London)* **501**: 225–41.

Bal, T. and McCormick, D. A. (1996) What stops synchronized thalamocortical oscillations? *Neuron* **17**: 297–308.

Bal, T., von Krosigk, M. and McCormick, D. A. (1995a) Synaptic and membrane mechanisms underlying synchronized oscillations in the ferret lateral geniculate nucleus *in vitro*. *Journal of Physiology (London)* **483**: 641–63.

Bal, T., von Krosigk, M. and McCormick, D. A. (1995b) Role of the ferret perigeniculate nucleus in the generation of synchronized oscillations *in vitro*. *Journal of Physiology (London)* **483**: 665–85.

Ball, G. J., Gloor, P. and Schaul, N. (1977) The cortical electromicrophysiology of pathological delta waves in the electroencephalogram of cats. *Electroencephalography and Clinical Neurophysiology* **43**: 346–61.

Barazangi, N. and Role, L. W. (2001) Nicotine-induced enhancement of glutamatergic and GABAergic synaptic transmission in the mouse amygdala. *Journal of Neurophysiology* **86**: 463–74.

Barbas, H. and De Olmos, J. S. (1990) Projections from the amygdala to basoventral and mediodorsal prefrontal regions in the rhesus monkey. *Journal of Comparative Neurology* **300**: 549–71.

Bargas, J., Galarraga, E. and Aceves, J. (1989) An early outward conductance modulates the firing latency and frequency of neostriatal neurons of the rat brain. *Experimental Brain Research* **75**: 146–56.

Barria, A., Muller, D., Derkach, V., Griffith, L. C. and Soderling, T. R. (1997) Regulatory phosphorylation of AMPA-type glutamate receptors by CaM-KII during long-term potentiation. *Science* **276**: 2042–5.

Batsel, H. L. (1964) Spontaneous desynchronization in the chronic cat 'cerveau isolé'. *Archives Italiennes de Biologie* **102**: 547–66.

Battaglia, F. P., Sutherland, G. R. and McNaughton, B. L. (2004) Hippocampal sharp wave bursts coincide with neocortical 'up-state' transitions. *Learning and Memory* **11**: 697–704.

Bauer, E. P. and LeDoux, J. E. (2004) Heterosynaptic long-term potentiation of inhibitory interneurons in the lateral amygdala. *Journal of Neuroscience* **24**: 9507–12.

Bauer, E. P., LeDoux, J. E. and Nader, K. (2001) Fear conditioning and LTP in the lateral amygdala are sensitive to the same stimulus contingencies. *Nature Neuroscience* **4**: 687–8.

Baughman, R. W. and Gilbert, C. D. (1980) Aspartate and glutamate as possible neurotransmitters of cells in layer 6 of the visual cortex. *Nature* **287**: 848–50.

Baxter, M. G. and Murray, E. A. (2002) The amygdala and reward. *Nature Reviews Neuroscience* **3**: 563–73.

Bayer, L., Eggermann, E., Saint-Mieux, B. *et al*. (2002) Selective action of orexin (hypocretin) on nonspecific thalamocortical projection neurons. *Journal of Neuroscience* **22**: 7835–9.

Bayer, L., Serafin, M., Eggermann, E. *et al*. (2004) Exclusive postsynaptic action of hypocretin-orexin on sublayer 6b cortical neurons. *Journal of Neuroscience* **24**: 6760–4.

Bazhenov, M., Timofeev, I., Steriade, M. and Sejnowski, T. J. (1998a) Cellular and network models for intrathalamic augmenting responses during 10-Hz stimulation. *Journal of Neurophysiology* **79**: 2730–48.

Bazhenov, M., Timofeev, I., Steriade, M. and Sejnowski, T. J. (1998b) Computational models of thalamocortical augmenting responses. *Journal of Neuroscience* **18**: 6444–65.

Bazhenov, M., Timofeev, I., Steriade, M. and Sejnowski, T. J. (1999) Self-sustained rhythmic activity in the thalamic reticular nucleus mediated by depolarizing $GABA_A$ receptor potentials. *Nature Neuroscience* **2**: 168–74.

Bazhenov, M., Timofeev, I., Steriade, M. and Sejnowski, T. (2000) Spiking-bursting activity in the thalamic reticular nucleus initiates sequences of spindle oscillations in thalamic networks. *Journal of Neurophysiology* **84**: 1076–87.

Bazhenov, M., Timofeev, I., Steriade, M. and Sejnowski, T. J. (2002) Model of thalamocortical slow-wave sleep oscillations and transitions to activated states. *Journal of Neuroscience* **22**: 8691–704.

Bear, M. F. and Abraham, W. C. (1996) Long-term depression in hippocampus. *Annual Review of Neuroscience* **19**: 437–62.

Beaudet, A., and Descarries, L. (1978) The monoamine innervation of rat cerebral cortex: synaptic and non-synaptic axon terminals. *Neuroscience* **3**: 851–60.

Bechara, A., Tranel, D., Damasio, H. *et al*. (1995) Double dissociation of conditioning and declarative knowledge relative to the amygdala and hippocampus in humans. *Science* **269**: 1115–18.

Beckstead, R. M. (1978) Afferent connections of the entorhinal area in the rat as demonstrated by retrograde cell-labeling with horse radish peroxidase. *Brain Research* **152**: 249–64.

Beggs, J. M. and Kairiss, E. W. (1994) Electrophysiology and morphology of neurons in rat perirhinal cortex. *Brain Research* **665**: 18–32.

Behrendt, R. P. (2003) Hallucinations: synchronization of thalamocortical gamma oscillations underconstrained by sensory input. *Consciousness and Cognition* **12**: 413–51.

Bellgowan, P. S. and Helmstetter, F. J. (1996) Neural systems for the expression of hypoalgesia during nonassociative fear. *Behavioral Neuroscience* **110**: 727–36.

Ben-Ari, Y., Le Gal La Salle, G., Barbin, G., Schwartz, J. C. and Garbarg, M. (1977) Histamine synthesizing afferents within the amygdaloid complex

and bed nucleus of the stria terminalis of the rat. *Brain Research* **138**: 285–94.

Bennett, M. V.L. (1970) Comparative physiology: electric organs. *Annual Review of Physiology* **32**: 471–528.

Bentivoglio, M., Aggleton, J. P. and Mishkin, M. (1997) The thalamus and memory formation. In *Thalamus*, vol. 2 (*Experimental and Clinical Aspects*), ed. M. Steriade, E. G. Jones & D. A. McCormick, pp. 689–720. Oxford: Elsevier.

Berger, B., Thierry, A. M., Tassin, J. P. and Moyne, M. A. (1976) Dopaminergic innervation of the rat prefrontal cortex: a fluorescence histochemical study. *Brain Research* **106**: 133–45.

Berger, H. (1929) Uber das Elektroencephalogramm des Menschen. *Archive für Psychiatrie und Nervenkrankheiten* **87**: 527–70.

Berger, H. (1937) Uber das Elektroencephalogramm des Menschen. Dreizehnte Mitteilung. *Archive für Psychiatrie und Nervenkrankheiten* **106**: 577–84.

Berger, T., Senn, W. and Lüscher, H. R. (2003) Hyperpolarization-activated current I_h disconnects somatic and dendritic spike initiation zones in layer V pyramidal neurons. *Journal of Neurophysiology* **90**: 2428–37.

Berlucchi, G. (1997) One or many arousal systems? Reflections on some of Giuseppe Moruzzi's foresights and insights about intrinsic regulation of brain activity. *Archives Italiennes de Biologie* **135**: 5–14.

Bernard, J. F., Huang, G. F. and Besson, J. M. (1990) Effect of noxious stimulation on the activity of neurons of the nucleus centralis of the amygdala. *Brain Research* **523**: 347–50.

Bernard, J. F., Huang, G. F. and Besson, J. M. (1992) Nucleus centralis of the amygdala and the globus pallidus ventralis: electrophysiological evidence for an involvement in pain processes. *Journal of Neurophysiology* **68**: 551–69.

Bernard, J. F., Alden, M. and Besson, J. M. (1993) The organization of the efferent projections from the pontine parabrachial area to the amygdaloid complex: A *Phaseolus vulgaris* leucoagglutinin (PHA-L) study in the rat. *Journal of Comparative Neurology* **329**: 201–29.

Berretta, S., Pantazopoulos, H., Caldera, M., Pantazopoulos, P. and Paré, D. (2005) Infralimbic cortex activation increases c-fos expression in intercalated neurons of the amygdala. *Neuroscience* **132**: 943–53.

Bickford, M. E., Günlük, A. E., Guido, W. and Sherman, S. M. (1993) Evidence that cholinergic axons from the parabrachial region of the brainstem are the exclusive source of nitric oxide in the lateral geniculate nucleus of the cat. *Journal of Comparative Neurology* **334**: 410–30.

Biella, G., Uva, L. and de Curtis, M. (2001) Network activity evoked by neocortical stimulation in area 36 of the guinea pig perirhinal cortex. *Journal of Neurophysiology* **86**: 164–72.

Biella, G., Uva, L. and De Curtis, M. (2002) Propagation of neuronal activity along the neocortical-perirhinal-entorhinal pathway in the guinea pig. *Journal of Neuroscience* **22**: 9972–9.

Bilkey, D. K. (1996) Long-term potentiation in the in vitro perirhinal cortex displays associative properties. *Brain Research* **733**: 297–300.

Bissière, S., Humeau, Y. and Lüthi, A. (2003) Dopamine gates LTP induction in lateral amygdala by suppressing feedforward inhibition. *Nature Neuroscience* **6**: 587–92.

Bland, B. H. (1986) The physiology and pharmacology of hippocampal formation theta rhythms. *Progress in Neurobiology* **26**: 1–54.

Bland, B. H., Andersen, P., Ganes, T. and Sven, O. (1980) Automated analysis of rhythmicity of physiologically identified hippocampal formation neurons. *Experimental Brain Research* **38**: 205–19.

Bliss, T. and Collingridge, G. L. (1993) A synaptic model of memory: long-term potentiation in the hippocampus. *Nature* **361**: 31–9.

Boejinga, P. H. and Lopes da Silva, F. H. (1988) Differential distribution of beta and theta EEG activity in the entorhinal cortex of the cat. *Brain Research* **448**: 272–86.

Bordi, F., LeDoux, J., Clugnet, M. C. and Pavlides, C. (1993) Single-unit activity in the lateral nucleus of the amygdala and overlying areas of the striatum in freely behaving rats: rates, discharge patterns and responses to acoustic stimuli. *Behavioral Neuroscience* **107**: 757–69.

Bouyer, J. J., Montaron, M. F., Vahnée, J. M., Albert, M. P. and Rougeul, A. (1987) Anatomical localization of cortical beta rhythm in cat. *Neuroscience* **22**: 863–9.

Braga, M. F., Aroniadou-Anderjaska, V., Manion, S. T., Hough, C. J. and Li, H. (2004) Stress impairs alpha(1A) adrenoceptor-mediated noradrenergic facilitation of GABAergic transmission in the basolateral amygdala. *Neuropsychopharmacology* **29**: 45–58.

Bragin, A., Jandó, G., Nádasdy, Z. *et al*. (1995a) Gamma (40–100 Hz) oscillation in the hippocampus of the behaving rat. *Journal of Neuroscience* **15**: 47–60.

Bragin, A., Jandó, G., Nádasdy, Z., Van, L. M. and Buzsáki, G. (1995b) Dentate EEG spikes and associated interneuronal population bursts in the hippocampal hilar region of the rat. *Journal of Neurophysiology* **73**: 1691–705.

Braitenberg, V. and Schütz, A. (1991) *Anatomy of the Cortex.* Berlin: Springer.

Braun, A. R., Balkin, T. J., Wesensten, N. J. *et al*. (1997) Regional cerebral blood flow throughout the sleep-wake cycle. *Brain* **120**: 1173–97.

Brazier, M. A.B. (1961) *A History of the Electrical Activity of the Brain.* London: Pitman.

Brazier, M. A. B. (1968) Studies of the EEG activity of limbic structures in man. *Electroencephalography and Clinical Neurophysiology* **25**: 309–18.

Bremer, F. (1935) Cerveau 'isolé' et physiologie du sommeil. *Comptes Rendus de la Société de Biologie (Paris)* **118**: 1235–41.

Bremer, F. and Stoupel, N. (1959) Facilitation et inhibition des potentiels évoqués corticaux dans l'éveil cérébral. *Archives Internationales de Physiologie* **67**: 240–75.

Bremer, F. and Terzuolo, C. (1954) Contribution à l'étude des mécanismes physiologiques du maintien de l'activité vigile du cerveau. Interaction de la formation réticulée et de l'écorce cérébrale dans le processus de l'éveil. *Archives Internationales de Physiologie* **62**: 157–78.

Bremer, F., Stoupel, N. and Van Reeth, P. C. (1960) Nouvelles recherches sur la facilitation et l'inhibition des potentiels évoqués corticaux dans l'éveil réticulaire. *Archives Italiennes de Biologie* **98**: 229–47.

Bremner, J. D., Staib, L. H., Kaloupek, D. *et al*. (1999) Neural correlates of exposure to traumatic pictures and sound in Vietnam combat veterans with and without posttraumatic stress disorder: A positron emission tomography study. *Biological Psychiatry* **45**: 806–16.

Bringuier, V., Frégnac, Y., Baranyi, A., Debanne, D. and Shulz, D. E. (1997) Synaptic origin and stimulus dependency of neuronal oscillatory activity in the primary visual cortex of the cat. *Journal of Physiology (London)* **500**: 751–74.

Brinley-Reed, M., Mascagni, F. and McDonald, A. J. (1995) Synaptology of prefrontal projections to the basolateral amygdala: an electron microscopic study in the rat. *Neuroscience Letters* **202**: 45–8.

Brodmann, K. (1905) Beitraege zur histologischen Lokalisation der Grosshirnrinde. III Mitteilung. Die Rindenfelder der niederen Affen. *Journal für Psychologie und Neurologie* **4**: 177–226.

Brodmann, K. (1908) Beitraege zur histologischen Lokalisation der Grosshirnrinde. VI Mitteilung. Die Cortexgliederung des Menschen. *Journal für Psychologie und Neurologie* **10**: 231–46.

Brown, M. W. and Aggleton, J. P. (2001) Recognition memory: what are the roles of the perirhinal cortex and hippocampus? *Nature Reviews Neuroscience* **2**: 51–61.

Brown, M. W. and Bashir, Z. I. (2002) Evidence concerning how neurons of the perirhinal cortex may affect familiarity discrimination. *Philosophical Transactions of the Royal Society of London* B**357**: 1083–95.

Brown, M. W., Wilson, F. A.W. and Riches, I. P. (1987) Neuronal evidence that inferomedial temporal cortex is more important than hippocampus in certain processes underlying recognition memory. *Brain Research* **409**: 158–67.

Brown, R. E., Stevens, D. R. and Haas, H. L. (2001) The physiology of brain histamine. *Progress in Neurobiology* **63**: 637–72.

Buchanan, S. L., Thompson, R. H., Maxwell, B. L. and Powell, D. A. (1994) Efferent connections of the medial prefrontal cortex in the rabbit. *Experimental Brain Research* **100**: 469–83.

Budde, T., Munsch T. and Pape, H. C. (1998) Distribution of L-type calcium channels in rat thalamic neurones. *European Journal of Neuroscience* **10**: 586–97.

Burette, F., Jay, T. M. and Laroche, S. (1997) Reversal of LTP in the hippocampal afferent fiber system to the prefrontal cortex in vivo with low-frequency patterns of stimulation that do not produce LTD. *Journal of Neurophysiology* **78**: 1155–60.

Burlhis, T.M and Aghajanian, G. K. (1987) Pacemaker potentials of serotonergic dorsal raphe neurons: contribution of a low-threshold Ca^{2+} conductance. *Synapse* **1**: 582–8.

Burwell, R. D. (2001) Borders and cytoarchitecture of the perirhinal and postrhinal cortices in the rat. *Journal of Comparative Neurology* **437**: 17–41.

Burwell, R. D. and Witter, M. P. (2002) Basic anatomy of the parahippocampal region in monkeys and rats. In *The Parahippocampal Region*, ed. M. P. Witter and F. Wouterlood, pp. 35–59. New York: Oxford University Press.

Buzsáki, G. (1986) Hippocampal sharp waves: their origin and significance. *Brain Research* **398**: 242–52.

Buzsáki, G. (1989) Two-stage model of memory trace formation: a role for 'noisy' brain states. *Neuroscience* **31**: 551–70.

Buzsáki, G. (1996) The hippocampo-neocortical dialogue. *Cerebral Cortex* **6**: 81–92.

Buzsáki, G. (2002) Theta oscillations in the hippocampus. *Neuron* **33**: 325–40.

Buzsáki, G. and Draguhn, A. (2004) Neuronal oscillations in cortical networks. *Science* **304**: 1926–9.

Buzsáki, G. and Eidelberg, E. (1982) Direct afferent excitation and long-term potentiation of hippocampal interneurons. *Journal of Neurophysiology* **48**: 597–607.

Buzsáki, G., Leung, L. and Vanderwolf, C. H. (1983) Cellular bases of hippocampal EEG in the behaving rat. *Brain Research* **6**: 139–71.

Buzsáki, G., Czopf, J., Kondákor, I. and Kellényi, L. (1986) Laminar distribution of hippocampal rhythmic slow activity (RSA) in the behaving rat: current-source density analysis, effects of urethane and atropine. *Brain Research* **365**: 125–37.

Buzsáki, G., Bickford, R. G., Ponomareff, G. *et al.* (1988) Nucleus basalis and thalamic control of neocortical activity in the freely moving rat. *Journal of Neuroscience* **8**: 4007–26.

Buzsáki, G., Kennedy, B., Solt, V. B. and Ziegler, M. (1991) Noradrenergic control of thalamic oscillations: the role of α-2 receptors. *European Journal of Neuroscience* **3**: 222–9.

Buzsáki, G., Horváth, Z., Urioste, R., Hetke, J. and Wise, K. (1992) High-frequency network oscillation in the hippocampus. *Science* **256**: 1025–7.

Cahill, L. and McGaugh, J. L. (1998) Mechanisms of emotional arousal and lasting declarative memory. *Trends in Neurosciences* **21**: 294–9.

Cahill, L., Babinsky, R., Markowitsch, H. J. and McGaugh, J. L. (1995) The amygdala and emotional memory. *Nature* **377**: 295–6.

Cahill, L., Haier, R. J., Fallon, J. *et al.* (1996) Amygdala activity at encoding correlated with long-term, free recall of emotional information. *Proceedings of the National Academy of Sciences USA* **93**: 8016–21.

Cahill, L., Weinberger, N. M., Roozendaal, B. and McGaugh, J. L. (1999) Is the amygdala a locus of 'conditioned fear'? Some questions and caveats. *Neuron* **23**: 227–8.

Cantero, J. L., Atienza, M., Salas, R. M. and Dominguez-Marin, E. (2002) Effects of prolonged waking-auditory stimulation on electroencephalogram synchronization and cortical coherence during subsequent slow-wave sleep. *Journal of Neuroscience* **22**: 4702–8.

Cape, E. G. and Jones, B. E. (2000) Effects of glutamate agonist versus procaine microinjections into the basal forebrain cholinergic cell area upon gamma and theta EEG activity and sleep-wake state. *European Journal of Neuroscience* **12**: 2166–84.

Cardin, J. A., Palmer, L. A. and Contreras, D. (2005) Stimulus-dependent gamma (30–50 Hz) oscillations in simple and complex fast rhythmic bursting cells in primary visual cortex. *Journal of Neuroscience* **25**: 5339–50.

Carlsen, J. (1988) Immunocytochemical localization of glutamate decarboxylase in the rat basolateral amygdaloid nucleus, with special reference to GABAergic innervation of amygdalostriatal projection neurons. *Journal of Comparative Neurology* **273**: 513–26.

Carlsen, J. and Heimer, L. (1986) A correlated light and electron microscopic immunocytochemical study of cholinergic terminals and neurons in the rat amygdaloid body with special emphasis on the basolateral amygdaloid nucleus. *Journal of Comparative Neurology* **244**: 121–36.

Carlsen, J., Zaborszky, L. and Heimer, L. (1985) Cholinergic projections from the basal forebrain to the basolateral amygdaloid complex: a combined retrograde fluorescent and immunohistochemical study. *Journal of Comparative Neurology* **234**: 155–67.

Carmichael, S. T. and Price, J. L. (1995a) Limbic connections of the orbital and medial prefrontal cortex in macaque monkeys. *Journal of Comparative Neurology* **363**: 615–41.

Carmichael, S. T. and Price, J. L. (1995b) Sensory and premotor connections of the orbital and medial prefrontal cortex of macaque monkeys. *Journal of Comparative Neurology* **363**: 642–64.

Carr, C. E. and Konishi, M. (1990) A circuit for detection of interaural time differences in the brainstem of the barn owl. *Journal of Neuroscience* **10**: 3227–46.

Carr, D. B. and Sesack, S. R. (2000a) Dopamine terminals synapse on callosal projection neurons in the rat prefrontal cortex. *Journal of Comparative Neurology* **425**: 275–83.

Carr, D. B. and Sesack, S. R. (2000b) GABA-containing neurons in the rat ventral tegmental area project to the prefrontal cortex. *Synapse* **38**: 114–23.

Carr, D. B. and Sesack, S. R. (2000c) Projections from the rat prefrontal cortex to the ventral tegmental area: target specificity in the synaptic associations with mesoaccumbens and mesocortical neurons. *Journal of Neuroscience* **20**: 3864–73.

Carskadon, M. A. and Dement, W. C. (2000) Normal human sleep: an overview. In *Principles and Practice of Sleep Medicine,* ed. M. H. Kryger, T. Roth and W. C. Dement, pp. 15–25. Philadelphia, PA: W. B. Saunders.

Cassell, M. D. and Gray, T. S. (1989a) Morphology of peptide-immunoreactive neurons in the rat central nucleus of the amygdala. *Journal of Comparative Neurology* **281**: 320–33.

Cassell, M. D. and Gray, T. S. (1989b) The amygdala directly innervates adrenergic (C1) neurons in the ventrolateral medulla in the rat. *Neuroscience Letters* **97**: 163–8.

Cassell, M. D., Gray, T. S. and Kiss, J. Z. (1986) Neuronal architecture in the rat central nucleus of the amygdala: a cytological, hodological, and immunocytochemical study. *Journal of Comparative Neurology* **246**: 478–99.

Castaigne, P., Buge, A., Escourolle, R. and Mason, M. (1962) Ramollissement pédonculaire médian, tegmentothalamique avec ophthalmoplégie et hypersomnie. *Revue Neurologique (Paris)* **106**: 357–67.

Castellano, C., Brioni, J. D., Nagahara, A. H. and McGaugh, J. L. (1989) Post-training systemic and intra-amygdala administration of the GABA-B agonist baclofen impairs retention. *Behavioral and Neural Biology* **52**: 170–9.

Castelo-Branco, M., Neuenschwander, S. and Singer, W. (1998) Synchronization of visual responses between the cortex, lateral geniculate nucleus, and retina in the anesthetized cat. *Journal of Neuroscience* **18**: 6395–410.

Castro-Alamancos, M. A. (2002a) Properties of primary sensory (lemniscal) synapses in the ventrobasal thalamus and the relay of high-frequency sensory inputs. *Journal of Neurophysiology* **87**: 946–53.

Castro-Alamancos, M. A. (2002b) Different temporal processing of sensory inputs in the rat thalamus during quiescent and information processing states *in vivo*. *Journal of Physiology (London)* **539**: 567–78.

Castro-Alamancos, M. A. and Calcagnotto, M. E. (2001) High-pass filtering of corticothalamic activity by neuromodulators released in the thalamus during arousal: in vitro and in vivo. *Journal of Neurophysiology* **85**: 1489–97.

Castro-Alamancos, M. A. and Connors, B. W. (1996) Cellular mechanisms of the augmenting response: short-term plasticity in a thalamocortical pathway. *Journal of Neuroscience* **16**: 7742–56.

Cauli, B., Audinat, E., Lambolez, B. *et al*. (1997) Molecular and physiological diversity of cortical nonpyramidal cells. *Journal of Neuroscience* **17**: 3894–906.

Cauller, L. J. and Kulics, A. T. (1988) A comparison of awake and sleeping cortical states by analysis of the somatosensory-evoked response of postcentral area 1 in rhesus monkey. *Experimental Brain Research* **72**: 584–92.

Cavada, C. and Reinoso-Suarez, F. (1985) Topographical organization of the cortical afferent connections of the prefrontal cortex in the cat. *Journal of Comparative Neurology* **242**: 293–324.

Cederbaum, J. M. and Aghajanian, G. K. (1978) Afferent projections to the rat locus coeruleus as determined by a retrograde tracing technique. *Journal of Comparative Neurology* **178**: 1–16.

Chagnac-Amitai, Y. and Connors, B. W. (1989) Synchronized excitation and inhibition driven by bursting neurons in neocortex. *Journal of Neurophysiology* **62**: 1149–62.

Chapman, P. F. and Bellavance, L. L. (1992) Induction of long-term potentiation in the basolateral amygdala does not depend on NMDA receptor activation. *Synapse* **11**: 310–18.

Chapman, P. F., Kairiss, E. W., Keenan, C. L. and Brown, T. H. (1990) Long-term synaptic potentiation in the amygdala. *Synapse* **6**: 271–8.

Chen, J. C. and Lang, E. J. (2003) Inhibitory control of rat lateral amygdaloid projection cells. *Neuroscience* **121**: 155–66.

Chen, W., Zhang, J. J., Hu, G. Y. and Wu, C. P. (1996) Electrophysiological and morphological properties of pyramidal and non-pyramidal neurons in the cat motor cortex *in vitro*. *Neuroscience* **73**: 39–55.

Chi, C. C. and Flynn, J. P. (1971) Neuroanatomic projections related to biting attack elicited from hypothalamus in cats. *Brain Research* **35**: 49–66.

Cho, K., Kemp, N., Noel, J., Aggleton, J. P., Brown, M. W. and Bashir, Z. I. (2000) A new form of long-term depression in the perirhinal cortex. *Nature Neuroscience* **3**: 150–6.

Cho, K., Aggleton, J. P., Brown, M. W. and Bashir, Z. I. (2001) An experimental test of the role of postsynaptic calcium levels in determining synaptic strength using perirhinal cortex of rat. *Journal of Physiology (London)* **532**: 459–66.

Chow, A., Farb, C., Nadal, M. S. *et al*. (1999) K^+ channel expression distinguishes subpopulations of parvalbumin- and somatostatin-containing neocortical interneurons. *Journal of Neuroscience* **19**: 9332–45.

Chrobak, J. J. and Buzsáki, G. (1994) Selective activation of deep layers (V–VI) retrohippocampal cortical neurons during hippocampal sharp waves in the behaving rat. *Journal of Neuroscience* **14**: 6160–70.

Chrobak, J. J. and Buzsáki, G. (1996) High-frequency oscillations in the output networks of the hippocampal-entorhinal axis of the freely behaving rat. *Journal of Neuroscience* **16**: 3056–66.

Chrobak, J. J. and Buzsáki, G. (1998) Gamma oscillations in the entorhinal cortex of the freely behaving rat. *Journal of Neuroscience* **18**: 388–98.

Cicogna, P, Natale, V., Occhionero, M and Bosinelli, M. (2000) Slow wave sleep and REM sleep mentation. *Sleep Research Online* **3**: 67–72.

Cirelli, C. and Tononi, G. (2000) Differential expression of plasticity-related genes in waking and sleep and their regulation by the noradrenergic system. *Journal of Neuroscience* **20**: 9184–7.

Cirelli, C. and Tononi, G. (2004) Locus coeruleus control of state-dependent gene expression. *Journal of Neuroscience* **24**: 5410–19.

Cirelli, C., Pompeiano, M. and Tononi, G. (1996) Neuronal gene expression in the waking state: a role for the locus coeruleus. *Science* **274**: 1211–15.

Cirelli, C., Gutierrez, C. M. and Tononi, G. (2004) Extensive and divergent effects of sleep and wakefulness on brain gene expression. *Neuron* **41**: 35–43.

Cirelli, C., Huber, R., Gopalakrishnan, A., Southard, T. L. and Tononi, G. (2005) Locus coeruleus control of slow-wave homeostasis. *Journal of Neuroscience* **25**: 4503–11.

Cissé, Y., Grenier, F., Timofeev, I. and Steriade, M. (2003) Electrophysiological properties and input-output organization of callosal neurons in cat association cortex. *Journal of Neurophysiology* **89**: 1402–13.

Cissé, Y., Crochet, S., Timofeev, I. and Steriade, M. (2004) Synaptic enhancement induced through callosal pathways in cat association cortex. *Journal of Neurophysiology* **92**: 3221–32.

Clugnet, M. C. and LeDoux, J. E. (1990) Synaptic plasticity in fear conditioning circuits: induction of LTP in the lateral nucleus of the amygdala by stimulation of the medial geniculate body. *Journal of Neuroscience* **10**: 2818–24.

Coenen, A. M. L. and Vendrik, A. J. H. (1972) Determination of the transfer ratio of cat's geniculate neurons through quasi-intracellular recordings and the relation with the level of alertness. *Experimental Brain Research* **14**: 227–42.

Colino, A. and Fernández de Molina, A. (1986) Electrical activity generated in the subicular complex and basolateral amygdala of the rat. *Neuroscience* **19**: 573–80.

Collins, D. R. and Paré, D. (2000) Differential fear conditioning induces reciprocal changes in the sensory responses of lateral amygdala neurons to the CS(+) and CS(−). *Learning and Memory* **7**: 97–103.

Collins, D. R., Lang, E. J. and Paré, D. (1999) Spontaneous activity of the perirhinal cortex in behaving cats. *Neuroscience* **89**: 1025–39.

Collins, D. R., Pelletier, J. G. and Paré, D. (2001) Slow and fast (gamma) neuronal oscillations in the perirhinal cortex and lateral amygdala. *Journal of Neurophysiology* **85**: 1661–72.

Colombo, M. and Gross, C. G. (1994) Responses of inferior temporal cortex and hippocampal neurons during delayed matching to sample in monkeys (*Macaca fascicularis*). *Behavioral Neuroscience* **108**: 443–55.

Colonnier, M. (1966) The structural design of the neocortex. In *Brain and Conscious Experience*, ed. J. C. Eccles, pp. 1–23. New York: Springer.

Compte, A., Sanchez-Vives, M. V., McCormick, D. A. and Wang, X. J. (2003) Cellular and network mechanisms of slow oscillatory activity (<1 Hz) and wave propagations in a cortical network model. *Journal of Neurophysiology* **89**: 2707–25.

Condé, F., Audinat, E., Maire-Lepoivre, E. and Crépel, F. (1990) Afferent connections of the medial frontal cortex of the rat. A study using retrograde transport of fluorescent dyes. I. Thalamic afferents. *Brain Research Bulletin* **24**: 341–54.

Condé, F., E., M.-L., Audinat, E. and Crépel, F. (1995) Afferent connections of the medial frontal cortex of the rat. II. Cortical and subcortical afferents. *Journal of Comparative Neurology* **352**: 567–93.

Condorelli, D. F., Belluard, N., Trovato-Salinaro, A. and Mudo, I. (2000) Expression of Cx36 in mammalian neurons. *Brain Research Reviews* **32**: 72–85.

Connors, B. W. and Amitai, Y. (1995) Functions of local circuits in neocortex: synchrony and laminae. In *The Cortical Neuron*, ed. M. J. Gutnick and I. Mody, pp. 123–40. New York: Oxford University Press.

Connors, B. W. and Gutnick, M. J. (1990) Intrinsic firing patterns of diverse neocortical neurons. *Trends in Neurosciences* **13**: 99–104.

Connors, B. W., Gutnick, M. J. and Prince, D. A. (1982) Electrophysiological properties of neocortical neurons *in vitro*. *Journal of Neurophysiology* **48**: 1302–20.

Connors, B. W., Malenka, R. and Silva, L. R. (1988) Two inhibitory postsynaptic potentials, and $GABA_A$ and $GABA_B$ receptor-mediated responses in neocortex of rat and cat. *Journal of Physiology (London)* **406**: 443–68.

Contreras, D. and Llinás, R. (2001) Voltage-sensitive dye imaging of neocortical spatio-temporal dynamics to afferent activation frequency. *Journal of Neuroscience* **21**: 9403–13.

Contreras, D. and Palmer, L. (2003) Response to contrast of electrophysiologically defined cell classes in primary visual cortex. *Journal of Neuroscience* **23**: 6936–45.

Contreras, D. and Steriade, M. (1995) Cellular basis of EEG slow rhythms: a study of dynamic corticothalamic relationships. *Journal of Neuroscience* **15**: 604–22.

Contreras, D. and Steriade, M. (1996) Spindle oscillation: the role of corticothalamic feedback in a thalamically generated rhythm. *Journal of Physiology (London)* **490**: 159–79.

Contreras, D. and Steriade, M. (1997a) Synchronization of low-frequency rhythms in corticothalamic networks. *Neuroscience* **76**: 11–24.

Contreras, D. and Steriade, M. (1997b) State-dependent fluctuations of low-frequency rhythms in corticothalamic networks. *Neuroscience* **76**: 25–38.

Contreras, D., Curró Dossi, R. and Steriade, M. (1993) Electrophysiological properties of cat reticular neurones *in vivo*. *Journal of Physiology (London)* **470**: 273–94.

Contreras, D., Destexhe, A., Sejnowski, T. J. and Steriade, M. (1996a) Control of spatiotemporal coherence of a thalamic oscillation by corticothalamic feedback. *Science* **274**: 771–4.

Contreras, D., Timofeev, I. and Steriade, M. (1996b) Mechanisms of long-lasting hyperpolarizations underlying slow sleep oscillations in cat corticothalamic networks. *Journal of Physiology (London)* **494**: 251–64.

Contreras, D., Destexhe, A. and Steriade, M. (1997a) Intracellular and computational characterization of the intracortical inhibitory control of synchronized thalamic inputs in vivo. *Journal of Neurophysiology* **78**: 335–50.

Contreras, D., Destexhe, A., Sejnowski, T. J. and Steriade, M. (1997b) Spatiotemporal patterns of spindle oscillations in cortex and thalamus. *Journal of Neuroscience* **17**: 1179–96.

Contreras, D., Dürmüller, N. and Steriade, M. (1997c) Absence of a prevalent laminar distribution of IPSPs in association cortical neurons of cat. *Journal of Neurophysiology* **78**: 2742–53.

Cossart, R., Aronov, D. and Yuste, R. (2003) Attractor dynamics of network UP states in the neocortex. *Nature* **423**: 283–8.

Cox, C. L. and Sherman, S. M. (2000) Control of dendritic outputs of inhibitory interneurons in the lateral geniculate nucleus. *Neuron* **27**: 597–610.

Cox, C. L., Huguenard, J. R. and Prince, D. A. (1996) Heterogenous axonal arborizations of rat thalamic reticular neurons in the ventrobasal nucleus. *Journal of Comparative Neurology* **366**: 416–30.

Cox, C. L., Huguenard, J. R. and Prince, D. A. (1997) Nucleus reticularis neurons mediate diverse inhibitory effects in the thalamus. *Proceedings of the National Academy of Sciences USA* **94**: 8854–9.

Cox, C. L., Zhou, Q. and Sherman, S. M. (1998) Glutamate locally activates dendritic outputs of thalamic interneurons. *Nature* **394**: 478–82.

Cox, C. L., Reichova, I. and Sherman, S. M. (2003) Functional synaptic contacts by intranuclear axon collaterals of thalamic relay neurons. *Journal of Neuroscience* **23**: 7642–6.

Cox, G. E., Jordan, D., Moruzzi, P. *et al*. (1986) Amygdaloid influences on brain-stem neurones in the rabbit. *Journal of Physiology (London)* **381**: 135–48.

Crabtree, J. W., Collingridge, G. L. and Isaac, J. T. R. (1998) A new intrathalamic pathway linking modality-related nuclei in the dorsal thalamus. *Nature Neuroscience* **1**: 389–94.

Crick, F. (1984) The function of the thalamic reticular complex: the searchlight hypothesis. *Proceedings of the National Academy of Sciences USA* **81**: 4586–90.

Crick, F. (1994) *The Astonishing Hypothesis*. New York: Charles Scribner's Sons.

Crill, W. E. (1996) Persistent sodium current in mammalian central neurones. *Annual Review of Physiology* **58**: 349–62.

Crochet, S., Fuentealba, P., Timofeev, I. and Steriade, M. (2004) Selective amplification of neocortical neuronal output by fast prepotentials *in vivo*. *Cerebral Cortex* **14**: 1110–21.

Crosby, E. C. and Humphrey, T. (1941) Studies of the vertebrate telencephalon. II. The nuclear pattern of the anterior olfactory nucleus, tuberculum olfactorum and the amygdaloid complex in adult man. *Journal of Comparative Neurology* **74**: 309–52.

Crow, T. J. (1997) Schizophrenia as failure of hemispheric dominance for language. *Trends in Neuroscience* **20**: 339–43.

Crunelli, V. and Leresche, N. (2002) Childhood absence epilepsy: genes, channels, neurons and networks. *Nature Reviews Neuroscience* **3**: 371–82.

Crunelli, V., Haby, M., Jassik-Gerschenfeld, D., Leresche, N. and Pirchio, M. (1988) Cl^- and K^+-dependent inhibitory postsynaptic potentials evoked by interneurons of the rat lateral geniculate nucleus. *Journal of Physiology (London)* **399**: 153–76.

Crutcher, M. D., Branch, M. H., DeLong, M. R. and Georgopoulos, A. P. (1980) Activity of zona incerta neurons in the behaving primate. *Society for Neuroscience Abstracts* **6**: 676.

Csicsvari, J., Hirase, H., Czurkó, A., Mamiya, A. and Buzsáki, G. (1999) Oscillatory coupling of hippocampal pyramidal cells and interneurons in the behaving cat. *Journal of Neuroscience* **19**: 274–87.

Cunningham, E. T. and LeVay, S. (1986) Laminar and synaptic organization of the projection from the thalamic nucleus centralis to primary visual cortex in the cat. *Journal of Comparative Neurology* **254**: 65–77.

Cunningham, M. O., Whittington, M. A., Bibbig, A. *et al.* (2004) A role for fast rhythmic bursting neurons in cortical gamma oscillations *in vitro*. *Proceedings of the National Academy of Sciences USA* **101**: 7152–7.

Curró Dossi, R., Paré, D. and Steriade, M. (1991) Short-lasting nicotinic and long-lasting muscarinic depolarizing responses of thalamocortical neurons to stimulation of mesopontine cholinergic nuclei. *Journal of Neurophysiology* **65**: 393–406.

Curró Dossi, R., Nuñez, A. and Steriade, M. (1992a) Electrophysiology of a slow (0.5–4 Hz) intrinsic oscillation of cat thalamocortical neurones *in vivo*. *Journal of Physiology (London)* **447**: 215–34.

Curró Dossi, R., Paré, D. and Steriade, M. (1992b) Various types of inhibitory postsynaptic potentials in anterior thalamic cells are differentially altered by stimulation of laterodorsal tegmental cholinergic nucleus. *Neuroscience* **47**: 279–89.

Damasio, A. R. (1996) The somatic marker hypothesis and the possible functions of the prefrontal cortex. *Philosophical Transactions of the Royal Society of London* B**351**: 1413–20.

Damasio, A. R. and Maurer, R. G. (1978) A neurological model for childhood autism. *Archives of Neurology* **35**: 777–86.

Danober, L. and Pape, H. C. (1998) Mechanisms and functional significance of a slow inhibitory potential in neurons of the lateral amygdala. *European Journal of Neuroscience* **10**: 853–67.

Datta, S., Curró Dossi, R., Paré, D., Oakson, G. and Steriade, M. (1991) Substantia nigra reticulata neurons during sleep-waking states: relation with ponto-geniculo-occipital waves. *Brain Research* **566**: 344–7.

Davenne, D. and Adrien, J. (1984) Suppression of PGO waves in the kitten: anatomical effects on the lateral geniculate nucleus. *Neuroscience Letters* **45**: 33–8.

Davis, M. (1992) The role of the amygdala in fear and anxiety. *Annual Review of Neuroscience* **15**: 353–75.

Davis, M. (2000) The role of the amygdala in conditioned and unconditioned fear and anxiety. In *The Amygdala: A Functional Analysis*, ed. J. P. Aggleton, pp. 213–87. Oxford: Oxford University Press.

Dawson, T., Bredt, D., Fotuhi, M., Hwang, P. and Snyder, S. (1991) Nitric oxide synthase and neuronal NADPH diaphorase are identical in brain and peripheral tissues. *Proceedings of the National Academy of Sciences USA* **88**: 7797–801.

Deacon, T. W., Eichenbaum, H., Rosenberg, P. and Eckman, K. W. (1983) Afferent connections of the perirhinal cortex in the rat. *Journal of Comparative Neurology* **220**: 168–90.

DeFelipe, J. and Fariñas, I. (1992) The pyramidal neuron of the cerebral cortex: morphological and chemical characteristics of the synaptic inputs. *Progress in Neurobiology* **39**: 563–607.

DeFelipe, J. and Jones, E. G. (1992) High-resolution light and electron microscopy immunocytochemistry of colocalized GABA and calbindin D-28k in somata and double bouquet cell axons in the monkey sensory-motor cortex. *European Journal of Neuroscience* **4**: 46–60.

DeFelipe, J., Elston, G. N., Fujita, I. *et al.* (2002) Neocortical circuits: evolutionary aspects and specificity versus non-specificity of synaptic connections. Remarks, main conclusions and general comments and discussion. *Journal of Neurocytology* **31**: 387–416.

De Gennaro, L., Ferrara, M. and Bertini, M. (2001) The boundary between wakefulness and sleep: quantitative electroencephalographic changes during the sleep onset period. *Neuroscience* **107**: 1–11.

Demaurex, N., Lew, D. P. and Krause, K.-H. (1992) Cyclopiazonic acid depletes intracellular Ca^{2+} stores and activates an influx pathway for divalent cations in HL-60 cells. *Journal of Biological Chemistry* **267**: 2318–24.

Dement, W. C., Ferguson, J., Cohen, H. and Barchas, J. (1969) Non-chemical methods and data using a biochemical model: the REM quanta. In *Psychochemical Research in Man: Methods, Strategy and Theory*, ed. A. Mandell and M. P. Mandell, pp. 275–325. New York: Academic Press.

Denning, K. S. and Reinagel, P. (2005) Visual control of burst priming in the anesthetized lateral geniculate nucleus. *Journal of Neuroscience* **25**: 3531–8.

De Oca, B. M., De Cola, J. P., Maren, S. and Fanselow, M. S. (1998) Distinct regions of the periaqueductal gray are involved in the acquisition and expression if defensive responses. *Journal of Neuroscience* **18**: 3426–32.

De Olmos, J. S. (1990) Amygdala. In *The Human Nervous System*, ed. G. Paxinos, pp. 583–708. New York: Academic Press.

Descarries, L., Watkins, K. C., and Lapierre, Y. (1977) Noradrenergic axon terminals in the cerebral cortex of rat. III. Topometric ultrastructural analysis. *Brain Research* **133**: 197–222.

Descarries, L., Gisiger, V. and Steriade, M. (1997) Diffuse transmission by acetylcholine in the CNS. *Progress in Neurobiology* **53**: 603–25.

Descarries, L., Mechawar, N., Aznavour, N. and Watkins, K. C. (2004) Structural determinants of the roles of acetylcholine in cerebral cortex. In *Acetylcholine in the Cerebral Cortex* (*Progress in Brain Research*, vol. 145), ed., L. Descarries, K. Krnjevic and M. Steriade, pp. 45–58. Amsterdam: Elsevier.

Deschênes, M. (1981) Dendritic spikes induced in fast pyramidal tract neurons by thalamic stimulation. *Experimental Brain Research* **43**: 304–8.

Deschênes, M. and Hu, B. (1990) Electrophysiology and pharmacology of the corticothalamic input to lateral thalamic nuclei: an intracellular study in the cat. *European Journal of Neuroscience* **2**: 140–52.

Deschênes, M. and Steriade, M. (1988) The neuronal mechanism of thalamic PGO waves. In *Cellular Thalamic Mechanisms*, ed. M. Bentivoglio, G. Macchi and R. Spreafico, pp. 197–206. Amsterdam: Elsevier.

Deschênes, M., Roy, J. P. and Steriade, M. (1982) Thalamic bursting mechanism: an inward slow current revealed by membrane hyperpolarization. *Brain Research* **239**: 289–93.

Deschênes, M., Paradis, M., Roy, J. P. and Steriade, M. (1984) Electrophysiology of neurons of lateral thalamic nuclei in cat: resting properties and burst discharges. *Journal of Neurophysiology* **51**: 1196–219.

Deschênes, M., Madariaga-Domich, A. and Steriade, M. (1985) Dendrodendritic synapses in cat reticularis thalami nucleus, a structural basis for thalamic spindle synchronization. *Brain Research* **334**: 169–71.

Deschênes, M., Veinante, P. and Zhang, Z. W. (1998). The organization of corticothalamic projections: reciprocity versus parity. *Brain Research Reviews* **28**: 286–308.

Desmedt, J. E. and Tomberg, C. (1994) Transient phase-locking of 40 Hz electrical oscillations in prefrontal and parietal human cortex reflects the process of conscious somatic perception. *Neuroscience Letters* **168**: 126–9.

Desmedt, J. E., Nguyen, T. H. and Bourget, M. (1983) The cognitive P40, N60 and P100 components of somatosensory evoked potentials and the earliest signs of sensory processing in man. *Electroencephalography and Clinical Neurophysiology* **56**: 272–82.

Destexhe, A. and Paré, D. (1999) Impact of network activity on the integrative properties of neocortical pyramidal neurons in vivo. *Journal of Neurophysiology* **81**: 1531–47.

Destexhe, A. and Paré, D. (2000) A combined computational and intracellular study of correlated synaptic bombardment in neocortical pyramidal neurons in vivo. *Neurocomputing* **32–3**: 113–19.

Destexhe, A., Contreras, D., Sejnowski, T. J. and Steriade, M. (1994a) A model of spindle rhythmicity in the isolated thalamic reticular nucleus. *Journal of Neurophysiology* **72**: 803–18.

Destexhe, A., Contreras, D., Sejnowski, T. J. and Steriade, M. (1994b) Modeling the control of reticular thalamic oscillations by neuromodulators. *NeuroReport* **5**: 2217–20.

Destexhe, A., Contreras, D., Steriade, M., Sejnowski, T. J. and Huguenard, J. R. (1996) *In vivo*, *in vitro* and computational analysis of dendritic calcium currents in thalamic reticular neurons. *Journal of Neuroscience* **16**: 169–85.

Destexhe, A., Contreras, D. and Steriade, M. (1999) Spatiotemporal analysis of local field potentials and unit discharges in cat cerebral cortex during natural wake and sleep states. *Journal of Neuroscience* **19**: 4595–608.

Destexhe, A., Contreras, D. and Steriade, M. (2001) LTS cells in cerebral cortex and their role in generating spike-and-wave oscillations. *Neurocomputing* **38–40**: 555–63.

Destexhe, A., Rudolph, M. and Paré, D. (2003) The high-conductance state of neocortical neurons *in vivo*. *Nature Reviews Neuroscience* **4**: 739–51.

Détári, L., Rasmusson, D. D. and Semba, K. (1997) Phasic relationship between the activity of basal forebrain neurons and cortical EEG in urethane-anesthetized rat. *Brain Research* **759**: 112–21.

Deuchars, J. and Thomson, A. M. (1995a) Single axon IPSPs elicited by a sparsely spiny interneuron in rat neocortex. *Neuroscience* **65**: 935–42.

Deuchars, J. and Thomson, A. M. (1995b) Innervation of burst firing spiny interneurons by pyramidal cells in deep layers of rat somatomotor cortex: paired intracellular recordings with biocytin filling. *Neuroscience* **69**: 739–55.

Dickinson, A. H., Meschers, M. H., Coleman, K. and McGaugh, J. L. (1993) Bicuculline administered into the amygdala blocks benzodiazepine-induced amnesia. *Behavioral and Neural Biology* **60**: 1–4.

Dickson, C. T., Biella, G. and de Curtis, M. (2003) Slow periodic events and their transition to gamma oscillations in the entorhinal cortex of the isolated guinea pig brain. *Journal of Neurophysiology* **90**: 39–46.

Di Pasquale, E., Keegan, K. D. and Noebels, J. L. (1997) Increased excitability and inward rectification in layer V cortical pyramidal neurons in the epileptic mutant mouse Stargazer. *Journal of Neurophysiology* **77**: 621–31.

Dolan, R. J., Bench, C. J., Brown, R. G. *et al.* (1992) Regional cerebral blood flow abnormalities in depressed patients with cognitive impairment. *Journal of Neurology, Neurosurgery and Psychiatry* **55**: 768–73.

Dolmetsch, R. E., Pajvani, U., Fife, K., Spotts, J. M. and Greenberg, M. E. (2001) Signaling to the nucleus by an L-type calcium channel-calmodulin complex through the MAP kinase pathway. *Science* **294**: 333–9.

Domich, L., Oakson, G. and Steriade, M. (1986) Thalamic burst patterns in the naturally sleeping cat: a comparison between cortically projecting and reticularis neurones. *Journal of Physiology (London)* **379**: 429–49.

Douglas, R. J. and Martin, K. (1991) A functional microcircuit for cat visual cortex. *Journal of Physiology (London)* **440**: 735–69.

Douglas, R. J., Koch, C., Mahowald, M., Martin, K. A.C. and Suarez, H. H. (1995) Recurrent excitation in neocortical circuits. *Science* **269**: 981–5.

Doyère, V., Burette, F., Negro, C. R. and Laroche, S. (1993) Long-term potentiation of hippocampal afferents and efferents to prefrontal cortex: implications for associative learning. *Neuropsychologia* **31**: 1031–53.

Drevets, W. C. and Reichle, M. E. (1992) Neuroanatomical circuits in depression: implication for treatment mechanisms. *Psychopharmacological Bulletin* **28**: 261–74.

Dringenberg, H. C. and Olmstead, M. C. (2003) Integrated contributions of basal forebrain and thalamus to neocortical activation elicited by pedunculopontine tegmental stimulation in urethane-anesthetized rats. *Neuroscience* **119**: 839–53.

Dringenberg, H. C. and Vanderwolf, C. H. (1996) Cholinergic activation of the electrocorticogram: an amygdaloid activating system. *Experimental Brain Research* **108**: 285–96.

Dumont, É.C., Martina, M., Samson, R. D., Drolet, G. and Paré, D. (2002) Physiological properties of central amygdala neurons: species differences. *European Journal of Neuroscience* **15**: 545–52.

Dumont, S. and Dell, P. (1960) Facilitation réticulaire des mécanismes visuels corticaux. *Electroencephalography and Clinical Neurophysiology* **12**: 769–96.

Duncan, C. P. (1949) The retroactive effect of electroshock on learning. *Journal of Comparative Physiology and Psychology* **42**: 32–44.

Duque, A., Balatoni, B., Détári, L. and Zaborsky, L. (2000) EEG correlation of the discharge properties of identified neurons in the basal forebrain. *Journal of Neurophysiology* **84**: 1627–35.

Durand, G. M., Kovalchuk, Y. and Konnerth, A. (1996) Long-term potentiation and functional synapse induction in developing hippocampus. *Nature* **381**: 71–5.

Eccles, J. C. (1961) Chairman's opening remarks. In *The Nature of Sleep*, ed. G. E. W. Wolstenholme and M. O'Connor, pp. 1–3. London: Churchill.

Eckhorn, R., Bauer, R., Jordan, W. *et al.* (1988) Coherent oscillations: a mechanism of feature linking in the visual cortex? *Biological Cybernetics* **60**: 121–30.

Egan, T. M. and North, R. A. (1985) Acetylcholine acts on m_2-muscarinic receptors to excite rat locus coeruleus neurones. *British Journal of Pharmacology* **85**: 733–5.

Ehlers, C., Hendricksen, S. J., Wang, M. *et al.* (1983) Corticotropin releasing factor produces increases in brain excitability and convulsive seizures in rats. *Brain Research* **278**: 332–6.

Eichenbaum, H. (2002) Memory representations in the parahippocampal region. In *The Parahippocampal Region*, ed. M. P. Witter and F. Wouterlood, pp. 165–84. Oxford: Oxford University Press.

Eichenbaum, H., Schoenbaum, G., Young, B. and Bunsey, M. (1996) Functional organization of the hippocampal memory system. *Proceedings of the National Academy of Sciences USA* **93**: 13500–7.

El Mansari, M., Sakai, K. and Jouvet, M. (1989) Unitary characteristics of presumptive cholinergic tegmental neurons during the sleep-waking cycle in freely moving cats. *Experimental Brain Research* **76**: 519–29.

Emerson, R. G., Sgro, J. A., Pedley, T. A. and Hauser, A. (1988) State-dependent changes in the N20 component of the median nerve somatosensory evoked potential. *Neurology* **38**: 64–7.

Emptage, N., Bliss, T. and Fine, A. (1999) Single synaptic events evoke NMDA receptor-mediated release of calcium from internal stores in hippocampal dendritic spines. *Neuron* **22**: 115–24.

Endo, K., Araki, T. and Ito, K. (1977) Short latency EPSPs and incrementing PSPs of pyramidal tract cells evoked by stimulation of the nucleus centralis lateralis of the thalamus. *Brain Research* **132**: 541–6.

Engel, A. K., König, P., Kreiter, A. K. and Singer, W. (1991). Interhemispheric synchronization of oscillatory neuronal responses in cat visual cortex. *Science* **252**: 1177–9.

Engel, A. K., Fries, P and Singer, W. (2001) Dynamic predictions: oscillations and synchrony in top-down processing. *Nature Reviews Neuroscience* **2**: 704–16.

Esclapez, M., Tillakaratne, N., Tobin, A. J. and Houser, C. R. (1993) Comparative localization of two forms of glutamic acid decarboxylase with nonradioactive in situ hybridization methods. *Journal of Comparative Neurology* **331**: 339–62.

Evarts, E. V. (1964) Temporal patterns of discharge of pyramidal tract neurons during sleep and waking. *Journal of Neurophysiology* **27**: 152–71.

Evarts, E. V. (1965) Relation of discharge frequency to conduction velocity in pyramidal tract neurons. *Journal of Neurophysiology* **28**: 216–28.

Faber, E. and Sah, P. (2002) Physiological role of calcium-activated potassium currents in the rat lateral amygdala. *Journal of Neuroscience* **22**: 1618–28.

Faber, E. S. and Sah, P. (2003) Calcium-activated K^+ (BK) channel inactivation contributes to spike broadening during repetitive firing in rat lateral amygdala neurons. *Journal of Physiology (London)* **552** (2): 482–97.

Faber, E., Callister, R. J. and Sah, P. (2001) Morphological and electrophysiological properties of principal neurons in the rat lateral amygdala in vitro. *Journal of Neurophysiology* **85**: 714–23.

Façon, E., Steriade, M. and Wertheimer, N. (1958) Hypersomnie prolongée engendrée par des lésions bilatérales du système activateur médial: le syndrome thrombotique de la bifurcation du tronc basilaire. *Revue Neurologique (Paris)* **98**: 117–33.

Fahy, F. L., Riches, I. P. and Brown, M. W. (1993) Neuronal activity related to visual recognition memory: long-term memory and the encoding of recency and familiarity information in the primate anterior and medial inferior temporal cortex and rhinal cortex. *Experimental Brain Research* **96**: 457–72.

Fallon, J. H. and Ciofi, P. (1992) Distribution of monoamines with the amygdala. In *The Amygdala*, ed. J. P. Aggleton, pp. 97–114. New York: Wiley-Liss.

Fallon, J. H., Koziell, D. A. and Moore, R. Y. (1978) Catecholamine innervation of the basal forebrain. II. Amygdala, suprarhinal cortex and entorhinal cortex. *Journal of Comparative Neurology* **180**: 509–32.

Falls, W. A., Miserendino, M. J. D. and Davis, M. (1992) Extinction of fear-potentiated startle: blockade by infusion of an NMDA antagonist into the amygdala. *Journal of Neuroscience* **12**: 854–63.

Fanselow, M. S. and Kim, J. J. (1994) Acquisition of contextual Pavlovian fear conditioning is blocked by application of an NMDA receptor antagonist D,L-2-amino-5-phosphonovaleric acid to the basolateral amygdala. *Behavioral Neuroscience* **108**: 210–12.

Fanselow, M. S. and LeDoux, J. E. (1999) Why we think plasticity underlying Pavlovian fear conditioning occurs in the basolateral amygdala. *Neuron* **23**: 229–32.

Fanselow, M. S., Kim, J. J., Yipp, J. and De Oca, B. (1994) Differential effects of the N-methyl-D-aspartate antagonist DL-2-amino-5-phosphonovalerate on acquisition of fear of auditory and contextual cues. *Behavioral Neuroscience* **108**: 235–40.

Farb, C. R. and LeDoux, J. E. (1999) Afferents from rat temporal cortex synapse on lateral amygdala neurons that express NMDA and AMPA receptors. *Synapse* **33**: 218–29.

Farmer, S. F. (1998) Rhythmicity, synchronization and binding in human primate cortex. *Journal of Physiology (London)* **509**: 3–14.

Faulkner, B. and Brown, T. H. (1999) Morphology and physiology of neurons in the rat perirhinal-lateral amygdala area. *Journal of Comparative Neurology* **411**: 613–42.

Feinberg, I. and Campbell, I. G. (1993) Ketamine administration during waking increases delta EEG intensity in rat sleep. *Neuropharmacology* **9**: 41–8.

Fellous, J. M., Rudolph, M., Destexhe, A. and Sejnowski, T. J. (2003) Synaptic background noise controls the input/output characteristics of single cells in an *in vitro* model of *in vivo* activity. *Neuroscience* **122**: 811–29.

Ferrara, M., De Gennaro, L. and Bertini, M. (1999) Selective slow-wave sleep (SWS) deprivation and SWS rebound: do we need a fixed amount per night? *Sleep Research Online* **2**: 15–19.

Ferrara, M., De Gennaro, L., Curcio, G. *et al.* (2002) Regional differences of the human sleep electroencephalogram in response to selective slow-wave sleep deprivation. *Cerebral Cortex* **12**: 737–48.

Ferry, B. and McGaugh, J. L. (1999) Clenbuterol administration into the basolateral amygdala post-training enhances retention in an inhibitory avoidance task. *Neurobiology of Learning and Memory* **72**: 8–12.

Ferry, B., Magistretti, P. J. and Pralong, E. (1997) Noradrenaline modulates glutamate-mediated neurotransmission in the rat basolateral amygdala in vitro. *European Journal of Neuroscience* **9**: 1356–64.

Feshchenko, V. A. and Chilingaryan, L. I. (1990) Dependence of electrical activity of the amygdaloid complex on level of motivation and emotional state of the dog. *Neuroscience Behavioral Physiology* **20**: 506–13.

Finch, D. M., Wong, E. E., Derian, E. L., Chen, X. H., Nowlin-Finch, N. L. and Brothers, L. A. (1986) Neurophysiology of limbic system pathways in the rat: projections from the amygdala to the entorhinal cortex. *Brain Research* **370**: 273–84.

Finch, D. M., Tan, A. M. and Isokawa-Akesson, M. (1988) Feedforward inhibition of the rat entorhinal cortex and subicular complex. *Journal of Neuroscience* **8**: 2213–26.

Finelli, L. A., Baumann, H., Borbély, A. and Achermann, P. (2000) Dual electroencephalogram markers of human sleep homeostasis: correlation between theta activity in waking and slow-wave activity in sleep. *Neuroscience* **101**: 523–9.

Fiset, P., Paus, T., Daloze, T. *et al.* (1999) Brain mechanisms of propofol-induced loss of consciousness in humans: a positron emission tomography study. *Journal of Neuroscience* **19**: 5506–13.

Foehring, R. C. and Waters, R. S. (1991) Contributions of low-threshold calcium current and anomalous rectifier (I_h) to slow depolarizations underlying burst firing in human neocortical neurons in vitro. *Neuroscience Letters* **124**: 17–21.

Foehring, R. C., Schwindt, P. C. and Crill, W. E. (1989) Norepinephrine selectively reduces slow Ca^{2+}- and Na^{+} -mediated K^{+} currents in cat neocortical neurons. *Journal of Neurophysiology* **61**: 245–256.

Fonnum, S., Strom-Mathisen, J. and Divac, I. (1981) Biochemical evidence for glutamate as neurotransmitter in corticostriatal and corticothalamic fibres in rat brain. *Neuroscience* **6**: 863–73.

Fontanini, A., Spano, P and Bower, J. M. (2003) Ketamine-xylazine-induced slow (<1.5 Hz) oscillations in the rat piriform (olfactory) cortex are functionally correlated with respiration. *Journal of Neuroscience* **23**: 7993–8001.

Foote, S. L., Bloom, F. E., and Aston-Jones, G. (1983) Nucleus locus ceruleus: new evidence of anatomical and physiological specificity. *Physiological Reviews* **63**: 844–914.

Ford, B., Holmes, C. J., Mainville, L. and Jones, B. E. (1995) GABAergic neurons in the rat pontomesencephalic tegmentum: codistribution with cholinergic and other tegmental neurons projecting to the posterior lateral hypothalamus. *Journal of Comparative Neurology* **363**: 177–96.

Forslid, A., Andersson, B. and Johansson, S. (1986) Observations on normal EEG activity in different brain regions of the unrestrained swine. *Acta Physiologica Scandinavica* **128**: 389–96.

Fort, P., Khateb, A., Pegna, A., Jones, B. E. and Mühlethaler, M. (1995) Noradrenergic modulation of cholinergic nucleus basalis neurons demonstrated by *in vitro* pharmacological and immunohistochemical evidence in the guinea pig brain. *European Journal of Neuroscience* **7**: 1502–11.

Fortin, M., Asselin, M. C., Gould, P. V. and Parent, A. (1998) Calretinin-immunoreactive neurons in the human thalamus. *Neuroscience* **84**: 537–48.

Fosse, R., Stickgold, R. and Hobson, J. A. (2004) Thinking and hallucinating: reciprocal changes in sleep. *Psychophysiology* **41**: 298–305.

Foster, J. A. (1980) Intracortical origin of recruiting responses in the cat neocortex. *Electroencephalography and Clinical Neurophysiology* **48**: 639–53.

Foulkes, D. (1962) Dream reports from different stages of sleep. *Journal of Abnormal and Social Psychology* **65**: 14–25.

Foulkes, D. and Schmidt, M. (1983) Temporal sequence and unit composition in dream reports from different stages of sleep. *Sleep* **6**: 265–80.

Fournier, G. N., Materi, L. M., Semba, K. and Rasmusson, D. D. (2004) Cortical acetylcholine release and electroencephalogram activation evoked by ionotropic glutamate receptor agonists in the rat basal forebrain. *Neuroscience* **123**: 785–92.

Fox, C. A. (1940) Certain basal telencephalic centers in the cat. *Journal of Comparative Neurology* **72**: 1–62.

Frank, M. G., Issa, N. P. and Stryker, M. P. (2001) Sleep enhances plasticity in the developing visual cortex. *Neuron* **30**: 275–87.

Freedman, J. E. and Aghajanian, G. K. (1987) Role of phosphoinositide metabolites in the prolongation of afterhyperpolarizations by alpha 1-adrenoceptors in rat dorsal raphe neurons. *Journal of Neuroscience* **7**: 3897–906.

Freedman, L. J., Insel, T. R. and Smith, Y. (2000) Subcortical projections of area 25 (subgenual cortex) of the macaque monkey. *Journal of Comparative Neurology* **29**: 172–88.

Freeman, W. J. (1959) Distribution in time and space of prepyriform electrical activity. *Journal of Neurophysiology* **22**: 644–65.

Freeman, W. J. (1975) *Mass Action in the Nervous System.* New York: Academic Press.

Freeman, W. J. and Van Dijk, B. W. (1988) Spatial patterns of visual cortical fast EEG during conditioned reflex in a rhesus monkey. *Brain Research* **422**: 267–76.

Frégnac, Y. (1999) A tale of two spikes. *Nature Neuroscience* **2**: 299–301.

Freund, T. F. and Buzsáki, G. (1996) Interneurons of the hippocampus. *Hippocampus* **6**: 347–470.

Freund, T. F. and Meskenaite, V. (1992) γ-Aminobutyric acid-containing basal forebrain neurons innervate inhibitory interneurons in the neocortex. *Proceedings of the National Academy of Sciences USA* **89**: 738–42.

Friedman, A. and Gutnick, M. J. (1989) Intracellular calcium and control of burst generation in neurons of guinea-pig neocortex *in vitro*. *European Journal of Neuroscience* **1**: 374–81.

Fries, P., Reynolds, J. H., Rorie, A. E. and Desimone, R. (2001) Modulation of oscillatory neuronal synchronization by selective visual attention. *Science* **291**: 1560–3.

Fu, Y. and Shinnick-Gallagher, P. (2005) Two intra-amygdaloid pathways to the central amygdala exhibit different mechanisms of long-term potentiation. *Journal of Neurophysiology* **93**: 3012–15.

Fuentealba, P. and Steriade, M. (2005) The reticular nucleus revisited: intrinsic and network properties of a thalamic pacemaker. *Progress in Neurobiology* **75**: 125–41.

Fuentealba, P., Crochet, S., Timofeev, I. and Steriade, M. (2002) 'Spikelets' in cat thalamic reticular nucleus in vivo. *Society for Neuroscience Abstracts* **28**: 144.19.

Fuentealba, P., Crochet, S. and Steriade, M. (2004a) The cortically evoked secondary depolarization affects the integrative properties of thalamic reticular neurons. *European Journal of Neuroscience* **20**: 2691–6.

Fuentealba, P., Crochet, S., Timofeev, I. *et al.* (2004b) Experimental evidence and modeling studies support a synchronizing role for electrical coupling in the cat thalamic reticular neurons *in vivo*. *European Journal of Neuroscience* **20**: 111–19.

Fuentealba, P., Crochet, S., Timofeev, I. and Steriade, M. (2004c) Synaptic interactions between thalamic and cortical inputs onto cortical neurons in vivo. *Journal of Neurophysiology* **91**: 1990–8.

Fuentealba, P., Timofeev, I. and Steriade, M. (2004d) Prolonged hyperpolarizing potentials precede spindle oscillations in the thalamic reticular nucleus. *Proceedings of the National Academy of Sciences USA* **101**: 9816–21.

Fuentealba, P., Timofeev, I., Bazhenov, M., Sejnowski, T. J. and Steriade, M. (2005) Membrane bistability in cat thalamic reticular neurons during spindle oscillations. *Journal of Neurophysiology* **93**: 294–304.

Fuster, J. M. (2004) Upper processing stages of the perception-action cycle. *Trends in Cognitive Sciences* **8**: 143–5.

Fuxe, K., Jacobsen, K. X., Hoistad, M. *et al.* (2003) The dopamine D1 receptor-rich main and paracapsular intercalated nerve cell groups of the rat amygdala: relationship to the dopamine innervation. *Neuroscience* **119**: 733–46.

Gaffan, D. and Murray, E. A. (1992) Monkeys (*Macaca fascicularis*) with rhinal cortex ablations succeed in object discrimination learning despite 24-hr intertrial intervals and fail at matching to sample despite double sample presentations. *Behavioral Neuroscience* **106**: 30–8.

Gais, S. and Born, J. (2004) Low acetylcholine during slow-wave sleep is critical for declarative memory consolidation. *Proceedings of the National Academy of Sciences USA* **101**: 2140–4.

Gais, S., Plihal, W., Wagner, U. and Born, J. (2000) Early sleep triggers memory for early visual discrimination skills. *Nature Neuroscience* **3**: 1335–9.

Gais, S., Mölle, M., Helms, K. and Born, J. (2002) Learning-dependent increases in sleep density. *Journal of Neuroscience* **22**: 6830–4.

Galarreta, M. and Hestrin, S. (1999) A network of fast-spiking cells in the neocortex connected by electrical synapses. *Nature* **402**: 72–5.

Galarreta, M. and Hestrin, S. (2002) Electrical and chemical synapses among parvalbumin fast-spiking GABAergic interneurons in adult mouse neocortex. *Proceedings of the National Academy of Sciences USA* **99**: 12438–43.

Gallagher, M., Kapp, B. S., Musty, R. E. and Driscoll, P. A. (1977) Memory formation: evidence for a specific neurochemical system in the amygdala. *Science* **198**: 423–5.

Garcia-Rill, E., Biedermann, J. A., Chambers, T. *et al.* (1995) Mesopontine neurons in schizophrenia. *Neuroscience* **66**: 321–35.

Gaudreau, H. and Paré, D. (1996) Projection cells of the lateral nucleus are virtually silent throughout the sleep-waking cycle. *Journal of Neurophysiology* **75**: 1301–5.

Gaykema, R. P., Luiten, P. G., Nyakas, C. and Traber, J. (1990) Cortical projection patterns of the medial septum-diagonal band complex. *Journal of Comparative Neurology* **293**: 103–24.

Gean, P. W., Huang, C. C., Lin, J. H. and Tsai, J. J. (1992) Sustained enhancement of NMDA receptor-mediated synaptic potential by isoproterenol in rat amygdalar slices. *Brain Research* **594**: 331–4.

Gemmell, C. and O'Mara, S. M. (2000) Long-term potentiation and paired-pulse facilitation in the prelimbic cortex of the rat following stimulation in the contralateral hemisphere in vivo. *Experimental Brain Research* **132**: 223–9.

Gerard, R. W. (1949) Physiology and psychiatry. *American Journal of Psychiatry* **106**: 161–73.

German, D. C., Manaye, K. F., Wu, D., Hersh, L. B. and Zweig, R. M. (1999) Mesopontine cholinergic and non-cholinergic neurons in schizophrenia. *Neuroscience* **94**: 33–8.

Gervasoni, D., Lin, S. C., Ribeiro, S. *et al.* (2004) Global forebrain dynamics predict rat behavioral states and their transitions. *Journal of Neuroscience* **24**: 11137–47.

Gewirtz, J. C., Falls, W. A. and Davis, M. (1997) Normal conditioned inhibition and extinction of freezing and fear-potentiated startle following electrolytic lesions of medical prefrontal cortex in rats. *Behavioral Neuroscience* **111**: 712–26.

Ghashghaei, H. T. and Barbas, H. (2002) Pathways for emotion: Interactions of prefrontal and anterior. *Neuroscience* **115**: 1261–79.

Gibson, J. R., Beierlein, M. and Connors, B. W. (1999) Two networks of electrically coupled inhibitory neurons in neocortex. *Nature* **402**: 75–9.

Gilbert, C. D. (1998) Adult cortical dynamics. *Physiological Reviews* **78**: 467–85.

Girod, R., Barazangi, N., McGehee, D. and Role, L. W. (2000) Facilitation of glutamatergic neurotransmission by presynaptic nicotinic acetylcholine receptors. *Neuropharmacology* **39**: 2715–25.

Glenn, L. L. and Steriade, M. (1982) Discharge rate and excitability of cortically projecting intralaminar thalamic neurons during waking and sleep states. *Journal of Neuroscience* **2**: 1287–404.

Glenn, L. L., Hada, J., Roy, J. P., Deschênes, M. and Steriade, M. (1982) Anterograde tracer and field potential analysis of the neocortical layer I projection from nucleus ventralis medialis of the thalamus in cat. *Neuroscience* **7**: 1861–77.

Gloor, P. (1976) Generalized and widespread bilateral paroxysmal abnormalities. In *Handbook of Electroencephalography and Clinical Neurophysiology*, vol. 11, Part B, ed. A. Remond, pp. 52–87. Amsterdam: Elsevier.

Gold, P. E. and McGaugh, J. L. (1975) A single-trace, two process view of memory storage processes. In *Short-term Memory*, ed. D. Deutsch and J. A. Deutsch, pp. 355–78. New York: Academic Press.

Goldman, P. S. (1979) Contralateral projections to the dorsal thalamus from frontal association cortex in rhesus monkey. *Brain Research* **166**: 166–71.

Goldman-Rakic, P. S. (1987) Circuitry of the prefrontal cortex and the regulation of behavior by representational memory. In *Handbook of Physiology*, vol. 5 (*The Nervous System*), ed. F. Plum and V. B. Mountcastle, pp. 373–417. Bethesda, MD: American Physiological Society.

Goldman-Rakic, P. S. (1988) Changing concepts of cortical connectivity: parallel distributed cortical networks. In *Neurobiology of Neocortex*, ed. P. Kakic and W. Singer, pp. 177–202. New York: Wiley.

Golomb, D., Wang, X. J. and Rinzel, J. (1994) Synchronization properties of spindle oscillations in a thalamic reticular nucleus model. *Journal of Neurophysiology* **72**: 1109–26.

Golshani, P., Liu, X. B. and Jones, E. G. (2001) Differences in quantal amplitude reflect GluR4-subunit number at corticothalamic synapses on two populations of thalamic neurons. *Proceedings of the National Academy of Sciences USA* **98**: 4172–7.

Goosens, G. and Otto, T. A. (1998) Induction and transient suppression of long-term potentiation in the peri- and postrhinal cortices following theta-related stimulation of hippocampal field CA1. *Brain Research* **780**: 95–101.

Goosens, K. A. and Maren, S. (2001) Contextual and auditory fear conditioning are mediated by the lateral, basal, and central amygdaloid nuclei in rats. *Learning and Memory* **8**: 148–55.

Goosens, K. A., and Maren, S. (2003) Pretraining NMDA receptor blockade in the basolateral complex. *Behavioral Neuroscience* **117**: 738–50.

Govindaiah and Cox, C. L. (2004) Synaptic activation of metabotropic glutamate receptors regulates dendritic outputs of thalamic interneurons. *Neuron* **41**: 611–23.

Grace, A. A. and Bunney, B. S. (1979) Paradoxical GABA excitation of nigral dopaminergic cells: indirect mediation through reticulata inhibitory neurons. *European Journal of Pharmacology* **59**: 211–18.

Grace, A. A. and Bunney, B. S. (1985) Opposing effects of striatonigral feed-back pathways on midbrain dopamine cell activity. *Brain Research* **333**: 271–84.

Grastyan, E., Lissak, K., Madarasz, I. and Donhoffer, H. (1959) The hippocampal electrical activity during the development of conditioned reflexes. *Electroencephalography and Clinical Neurophysiology* **11**: 409–30.

Gray, C. M. and McCormick, D. A. (1996) Chattering cells: superficial pyramidal neurons contributing to the generation of synchronous oscillations in the visual cortex. *Science* **274**: 109–13.

Gray, C. M., König, P., Engel, A. K. and Singer, W. (1989) Stimulus-specific neuronal oscillations in cat visual cortex exhibit inter-columnar synchronization which reflects global stimulus properties. *Nature* **338**: 334–7.

Gray, C. M., Engel, A. K., König, P. and Singer, W. (1990) Stimulus-dependent neuronal oscillations in cat visual cortex: receptive field properties and feature dependence. *European Journal of Neuroscience* **2**: 607–19.

Graybiel, A. M. and Ragsdale, C. W. (1979) Fiber connections of the basal ganglia. In *Development and Chemical Specificity of Neurons*, ed. M. Cuénod, G. W. Kreutzberg, and F. R. Bloom, pp. 239–83. Amsterdam: Elsevier.

Green, J. D. and Arduini, A. (1954) Hippocampal electrical activity in arousal. *Journal of Neurophysiology* **17**: 533–57.

Grenier, F., Timofeev, I. and Steriade, M. (2001) Focal synchronization of ripples (80–200 Hz) in neocortex and their neuronal correlates. *Journal of Neurophysiology* **86**: 1884–98.

Griffith, W. H. (1988) Membrane properties of cell types within guinea pig basal forebrain nuclei in vitro. *Journal of Neurophysiology* **59**: 1590–612.

Gritti, I., Mainville, L. and Jones, B. E. (1994) Projections of GABAergic and cholinergic basal forebrain and GABAergic preoptic-anterior hypothalamic neurons to the posterior lateral hypothalamus of the rat. *Journal of Comparative Neurology* **339**: 251–68.

Gross, D. W. and Gotman, J. (1999) Correlation of high-frequency oscillations with the sleep-wake cycle and cognitive activity in humans. *Neuroscience* **94**: 1005–18.

Guido, W. and Weyand, T. (1995) Burst responses in thalamic relay cells of the awake, behaving cat. *Journal of Neurophysiology* **74**: 1782–6.

Guido, W., Lu, S. M. and Sherman, S. M. (1992) Relative contributions of burst and tonic responses to the receptive field properties of lateral geniculate neurons in the cat. *Journal of Neurophysiology* **68**: 2199–211.

Guillery, R. W. (1969) The organization of synaptic interconnections in the laminae of the dorsal lateral geniculate nucleus of the cat. *Zeitschrift für Zellforschung und Mikroskopische Anatomie* **96**: 1–38.

Guillery, R. W. and Harting, J. K. (2002) Structure and connections of the thalamic reticular nucleus: advancing views over half of century. *Journal of Comparative Neurology* **463**: 360–71.

Gulyás, A. I., Hájos, N. and Freund, T. F. (1996) Interneurons containing calretinin are specialized to control other interneurons in the rat hippocampus. *Journal of Neuroscience* **16**: 3397–411.

Gupta, A., Wang, Y. and Markram, H. (2000) Organizing principles for a diversity of GABAergic interneurons and synapses in the neocortex. *Science* **287**: 273–8.

Gurden, H., Tassin, J. P. and Jay, T. M. (1999) Integrity of the mesocortical dopaminergic system is necessary for complete expression of in vivo hippocampal-prefrontal cortex long-term potentiation. *Neuroscience* **94**: 1019–27.

Gutnick, M. J., Heinemann, U. and Prince, D. A. (1979) Stimulus induced and seizure related changes in extracellular potassium concentration in cat thalamus (VPL). *Electroencephalography and Clinical Neurophysiology* **47**: 329–44.

Halgren, E., Bab, T. L. and Crandall, P. H. (1978) Human hippocampal formation EEG desynchronizes during attentiveness and movement. *Electroencephalography and Clinical Neurophysiology* **44**: 778–81.

Halgren, E., Boujon, C., Clarke, J., Wang, C. and Chauvel, P. (2002) Rapid distributed fronto-parieto-occipital processing stages during working memory in humans. *Cerebral Cortex* **12**: 710–28.

Hall, E. (1972a) The amygdala of the cat: A Golgi study. *Zeitschrift für Zellforschung* **134**: 439–58.

Hall, E. (1972b) Some aspects of the structural organization of the amygdala. In *The Neurobiology of the Amygdala*, ed. B. E. Eleftheriou, pp. 95–121. New York: Plenum Press.

Hall, G. B. C., Szechtman, H. and Nahmias, C. (2003) Enhanced salience and emotion recognition in autism: a PET study. *American Journal of Psychiatry* **160**: 1439–41.

Halliwell, J. V. (1986) M-current in human neocortical neurones. *Neuroscience Letters* **67**: 1–6.

Hamam, B. N., Kennedy, T. E., Alonso, A. and Amaral, D. G. (2000) Morphological and electrophysiological characteristics of layer V neurons of the rat medial entorhinal cortex. *Journal of Comparative Neurology* **418**: 457–72.

Hamann, S. B., Ely, T. D., Grafton, S. T. and Kilts, C. D. (1999) Amygdala activity related to enhanced memory for pleasant and aversive stimuli. *Nature Neuroscience* **2**: 289–93.

Hammond, C. and Crépel, F. (1992) Evidence for a slowly inactivating K^+ current in prefrontal cortical cells. *European Journal of Neuroscience* **4**: 1087–92.

Hardy, S. G. and Leichnetz, G. R. (1981) Frontal cortical projections to the periaqueductal gray in the rat: a retrograde and orthograde horseradish peroxidase study. *Neuroscience Letters* **23**: 13–17.

Hartveit, E. and Heggelund, P. (1994) Response variability of single cells in the dorsal lateral geniculate nucleus of the cat. Comparison with retinal input and effect of brain stem stimulation. *Journal of Neurophysiology* **72**: 1278–89.

Hashikawa, T., Rauseell, E., Molinari, M. and Jones, E. G. (1991) Parvalbumin- and calbindin-containing neurons in the monkey medial geniculate complex: differential distribution and cortical layer specific projections. *Brain Research* **544**: 335–41.

Hasselmo, M. E. (1999) Neuromodulation: acetylcholine and memory consolidation. *Trends in Cognitive Sciences* **3**: 351–9.

Hasue, R. H. and Shammah-Lagnado, S. J. (2002) Origin of the dopaminergic innervation of the central extended amygdala and accumbens shell: a combined retrograde tracing and immunohistochemical study in the rat. *Journal of Comparative Neurology* **454**: 15–33.

Hatfield, T. and McGaugh, J. L. (1999) Norepinephrine infused into the basolateral amygdala posttraining enhances retention in a spatial water maze task. *Neurobiology of Learning and Memory* **71**: 232–9.

He, J. (2003) Slow oscillation in non-lemniscal auditory thalamus. *Journal of Neuroscience* **23**: 8281–90.

Herbert, M. R., Ziegler, D. A., Deutsch, C. K. *et al.* (2003) Dissociations of cerebral cortex, subcortical and cerebral white matter volumes in autistic boys. *Brain* **126**: 1182–92.

Herculano-Houzel, S., Munk, M. H. J., Neuenschwander, S. and Singer, W. (1999) Precisely synchronized oscillatory firing patterns require electroencephalographic activation. *Journal of Neuroscience* **19**: 3992–4010.

Herkenham, M. (1978) The connections of the nucleus reuniens thalami: evidence for a direct thalamo-hippocampal pathway in the rat. *Journal of Comparative Neurology* **177**: 589–610.

Herkenham, M. (1979) The afferent and efferent connections of the ventromedial thalamic nucleus in the rat. *Journal of Comparative Neurology* **183**: 487–518.

Hernández-Cruz, A. and Pape, H. C. (1989) Identification of two calcium currents in acutely dissociated neurons from the rat lateral geniculate nucleus. *Journal of Neurophysiology* **61**: 1270–83.

Herry, C. and Garcia, R. (2003) Behavioral and paired-pulse facilitation analyses of long-lasting depression at excitatory synapses in the medial prefrontal cortex in mice. *Behavioral Brain Research* **146**: 89–96.

Hestrin, S. and Armstrong, W. E. (1996) Morphology and physiology of cortical neurons in layer I. *Journal of Neuroscience* **16**: 5290–300.

Hicks, T. P., Metherate, R., Landry, P. and Dykes, R. W. (1986) Bicuculline-induced alterations of response properties in functionally identified ventroposteiror thalamic neurones. *Experimental Brain Research* **63**: 248–64.

Hikosaka, O. and Wurtz, R. H. (1983) Visual and oculomotor function of monkey substantia nigra pars reticulata, IV: relation of substantia nigra to superior colliculus. *Journal of Neurophysiology* **49**: 1285–301.

Hirsch, J. C. and Burnod, Y. (1987) A synaptically evoked late hyperpolarization in the rat dorsolateral geniculate neurons *in vitro*. *Neuroscience* **23**: 457–68.

Hirsch, J. C., Fourment, A. and Marc, M. E. (1983) Sleep-related variations of membrane potential in the lateral geniculate body relay neurons of the cat. *Brain Research* **259**: 308–12.

Hô, N. and Destexhe, A. (2000) Synaptic background activity enhances the responsiveness of neocortical pyramidal neurons. *Journal of Neurophysiology* **84**: 1488–96.

Hobin, J. A., Goosens, K. A. and Maren, S. (2003) Context-dependent neuronal activity in the lateral amygdala represents fear memories after extinction. *Journal of Neuroscience* **23**: 8410–16.

Hobson, J. A. (1988) *The Dreaming Brain*. New York: Basic Books.

Hobson, J. A. and Pace-Schott, E. F. (2002) The cognitive neuroscience of sleep: neuronal systems, consciousness and learning. *Nature Reviews Neuroscience* **3**: 679–93.

Hobson, J. A. and Steriade, M. (1986) Neuronal basis of behavioral state control. In *Handbook of Physiology*, ed. V. B. Mountcastle and F. E. Bloom, section 1, vol. IV, pp. 701–823. Bethesda, MD: American Physiological Society.

Hobson, J. A., Pace-Schott, E. and Stickgold, R. (2000) Dreaming and the brain: toward a cognitive neuroscience of conscious states. *Brain and Behavioral Sciences* **23**: 793–842.

Hofle, N., Paus, T., Reutens, D. *et al.* (1997) Regional cerebral blood flow changes as a function of delta and spindle activity during slow wave sleep in humans. *Journal of Neuroscience* **17**: 4800–8.

Holahan, M. R. and White, N. M. (2002) Conditioned memory modulation, freezing, and avoidance as measures of amygdala-mediated conditioned fear. *Neurobiology of Learning and Memory* **77**: 250–75.

Holstege, G. (1990) Subcortical limbic system projections to caudal brainstem and spinal cord. In *The Human Nervous System*, ed. G. Paxinos, pp. 261–86. New York: Academic Press.

Holstege, G., Bandler, R. and Saper, C. B. (1996) The emotional motor system. *Progress in Brain Research* **107**: 3–6.

Homma, Y., Skinner, R. D. and Garcia-Rill, E. (2002) Effects of pedunculopontine nucleus (PPN) stimulation on caudal pontine reticular formation (PnC) neurons in vitro. *Journal of Neurophysiology* **87**: 3033–47.

Honda, T. and Semba, K. (1995) An ultrastructural study of cholinergic and non-cholinergic neurons in the laterodorsal and pedunculopontine tegmental nuclei in the rat. *Neuroscience* **68**: 837–53.

Hope, B., Michael, G., Knigge, K. and Vincent, S. (1991) Neuronal NADPH diaphorase is a nitric oxide synthase. *Proceedings of the National Academy of Sciences USA* **88**: 2811–14.

Hopkins, D. A. and Holstege, G. (1978) Amygdaloid projections to the mesencephalon, pons and medulla oblongata in the cat. *Experimental Brain Research* **32**: 529–47.

Hou, Y. P., Manns, I. D. and Jones, B. E. (2002) Immunostaining of cholinergic pontomesencephalic neurons for α_1 versus α_2 adrenergic receptors suggests different sleep-wake state activities and roles. *Neuroscience* **114**: 517–21.

Hu, B. (1995) Cellular basis of temporal synaptic signaling: an *in vitro* electrophysiological study in rat auditory thalamus. *Journal of Physiology (London)* **483**: 167–82.

Hu, B., Bouhassira, D., Steriade, M. and Deschênes, M. (1988) The blockage of ponto-geniculo-occipital waves in the cat lateral geniculate nucleus by nicotinic antagonists. *Brain Research* **473**: 394–7.

Hu, B., Steriade, M. and Deschênes, M. (1989a) The effects of peribrachial stimulation on reticular thalamic neurons: the blockage of spindle waves. *Neuroscience* **31**: 1–12.

Hu, B., Steriade, M. and Deschênes, M. (1989b) The effects of brainstem peribrachial stimulation on neurons of the lateral geniculate nucleus. *Neuroscience* **31**: 13–24.

Hu, B., Steriade, M. and Deschênes, M. (1989c) The cellular mechanism of thalamic ponto-geniculo-occipital waves. *Neuroscience* **31**: 25–35.

Huang, C. C., Hsu, K. S. and Gean, P. W. (1996) Isoproterenol potentiates synaptic transmission primarily by enhancing presynaptic calcium influx via P- and/or Q-type calcium channels in the rat amygdala. *Journal of Neuroscience* **16**: 1026–33.

Huang, Y. Y. and Kandel, E. R. (1998) Postsynaptic induction and PKA-dependent expression of LTP in the lateral amygdala. *Neuron* **21**: 169–78.

Hubel, D. H. and Wiesel, T. N. (1961) Integrative action in the cat's lateral geniculate body. *Journal of Physiology (London)* **155**: 385–98.

Huber, R., Ghilardi, M. F., Massimini, M. and Tononi, G. (2004) Local sleep and learning. *Nature* **430**: 78–81.

Hugues, S., Deschaux, O. and Garcia, R. (2004) Postextinction infusion of a mitogen-activated protein kinase inhibitor into the medial prefrontal cortex impairs memory of the extinction of conditioned fear. *Learning and Memory* **11**: 540–3.

Hughes, S. W., Cope, D. W., Toth, T. I., Williams, S. R. and Crunelli, V. (1999) All thalamocortical neurones possess a T-type Ca^{2+} 'window' current that enables the expression of bistability-mediated activities. *Journal of Physiology (London)* **517**: 805–15.

Hughes, S. W., Blethyn, K. L., Cope, D. W. and Crunelli, V. (2002a) Properties and origin of spikelets in thalamocortical neurones in vitro. *Neuroscience* **110**: 395–401.

Hughes, S. W., Cope, D. W., Blethyn, K. L. and Crunelli, V. (2002b) Cellular mechanisms of the slow (<1 Hz) oscillation in thalamocortical neurons in vitro. *Neuron* **33**: 947–58.

Hughes, S. W., Lörincz, M., Cope, D. W. *et al.* (2004) Synchronized oscillations at alpha and theta frequencies in the lateral geniculate nucleus. *Neuron* **42**: 253–68.

Huguenard, J. R. (1996) Low-threshold calcium currents in central nervous system neurons. *Annual Review of Physiology* **58**: 329–48.

Huguenard, J. R. and Prince, D. A. (1992) A novel T-type current underlies prolonged Ca^{2+}-dependent burst firing in GABAergic neurons of rat thalamic reticular nucleus. *Journal of Neuroscience* **12**: 3804–17.

Huguenard, J. R. and Prince, D. A. (1994) Intrathalamic rhythmicity studied in vitro: nominal T current modulation causes robust anti-oscillatory effects. *Journal of Neuroscience* **14**: 5485–502.

Hugues, S., Deschaux, O. and Garcia, R. (2004) Postextinction infusion of a mitogen-activated protein kinase inhibitor into the medial prefrontal cortex impairs memory of the extinction of conditioned fear. *Learning and Memory* **11**: 540–3.

Humeau, Y., Shaban, H., Bissière, S. and Lüthi, A. (2003) Presynaptic induction of heterosynaptic associative plasticity in the mammalian brain. *Nature* **426**: 841–5.

Humeau, Y., Herry, C., Kemp, N. *et al.* (2005) Dendritic spine heterogeneity determines afferent-specific Hebbian plasticity in the amygdala. *Neuron* **45**: 119–31.

Humphrey, T. (1936) The telencephalon of the bat. I. The noncortical nuclear masses and certain pertinent fiber connections. *Journal of Comparative Neurology* **65**: 603–711.

Hunt, C. A., Pang, D. Z. and Jones, E. G. (1991) Distribution and density of GABA cells in intralaminar and adjacent nuclei of monkey thalamus. *Neuroscience* **43**: 185–96.

Hurley, K. M., Herbert, H., Moga, M. M. and Saper, C. B. (1991) Efferent projections of the infralimbic cortex of the rat. *Journal of Comparative Neurology* **308**: 249–76.

Hutcheon, B., Miura, R. M. and Puil, E. (1996) Subthreshold membrane resonance in neocortical neurons. *Journal of Neurophysiology* **76**: 683–97.

Inglis, W. L. and Semba, K. (1996) Colocalization of ionotropic glutamate receptor subunits with NADPH-diaphorase-containing neurons in the rat mesopontine tegmentum. *Journal of Comparative Neurology* **368**: 17–32.

Ingvar, D. H., Sjölund, B. and Ardo, A. (1976) Correlation between ECG frequency, cerebral oxygen uptake and blood flow. *Electroencephalography and Clinical Neurophysiology* **41**: 268–76.

Insausti, R., Amaral, D. G. and Cowan, W. M. (1987) The entorhinal cortex of the monkey: III. Subcortical afferents. *Journal of Comparative Neurology* **264**: 396–408.

Introini-Collison, I. B., Miyazaki, B. and McGaugh, J. L. (1991) Involvement of the amygdala in the memory-enhancing effects of clenbuterol. *Psychopharmacology* **104**: 541–4.

Inubushi, S., Kobayashi, T., Oshima, T. and Torii, S. (1978a) Intracellular recordings from motor cortex during EEG arousal in unanesthetized brain preparations of the cat. *Japanese Journal of Physiology* **28**: 669–88.

Inubushi, S., Kobayashi, T., Oshima, T. and Torii, S. (1978b) An intracellular analysis of EEG arousal in cat motor cortex. *Japanese Journal of Physiology* **28**: 689–708.

Irle, E. and Markowitsch, H. J. (1984) Basal forebrain efferents reach the whole cerebral cortex of the cat. *Brain Research Bulletin* **12**: 493–512.

Ito, K. and McCarley, R. W. (1984) Alterations in membrane potential and excitability of cat medial pontine reticular formation neurons during changes in naturally occurring sleep-wake states. *Brain Research* **292**: 169–75.

Iwata, J., LeDoux, J. E., Meeley, M. P., Arneric, S. and Reis, D. J. (1986) Intrinsic neurons in the amygdaloid field projected to by the medial geniculate body mediate emotional responses conditioned to acoustic stimuli. *Brain Research* **383**: 195–214.

Izquierdo, I. and Medina, J. H. (1993) Role of the amygdala, hippocampus and entorhinal cortex in memory consolidation and expression. *Brazilian Journal of Medical and Biological Research* **26**: 573–89.

Jacobs, B. L. and McGinty, D. J. (1971) Amygdala unit activity during sleep and waking. *Experimental Neurology* **33**: 1–15.

Jahnsen, H. and Llinás, R. (1984a) Electrophysiological properties of guinea-pig thalamic neurones: an *in vitro* study. *Journal of Physiology (London)* **349**: 205–26.

Jahnsen, H. and Llinás, R. (1984b) Ionic basis for electroresponsiveness and oscillatory properties of guinea-pig thalamic neurones *in vitro*. *Journal of Physiology (London)* **349**: 227–47.

Jasper, H. H. (1949) Diffuse projection systems: the integrative action of the thalamic reticular system. *Electroencephalography and Clinical Neurophysiology* **1**: 405–20.

Jasper, H. H. (1958) Recent advances in our understanding of ascending activities of the reticular system. In *Reticular Formation of the Brain*, ed. H. H. Jasper, L. D. Proctor, R. S. Knighton, W. C. Noshay and R. T. Costello, pp. 319–31. Boston, Toronto: Little-Brown.

Jay, T. M., Burette, F. and Laroche, S. (1996) Plasticity of the hippocampal-prefrontal cortex synapses. *Journal of Physiology (Paris)* **90**: 361–6.

Jeanmonod, D., Magnin, M. and Morel, A. (1996) Low-threshold calcium spike-bursts in the human thalamus: common physiopathology for sensory, motor and limbic positive symptoms. *Brain* **119**: 363–75.

Jenkins, J. and Dallenback, K. (1924) Oblivescence during sleep and waking. *American Journal of Psychology* **35**: 605–12.

Johnston, J. B. (1923) Further contributions to the study of the evolution of the forebrain. *Journal of Comparative Neurology* **35**: 337–481.

Jolkkonen, E. and Pitkänen, A. (1998) Intrinsic connections of the rat amygdaloid complex: projections originating in the central nucleus. *Journal of Comparative Neurology* **395**: 53–72.

Jolkkonen, E., Miettinen, R., Pikkarainen, M. and Pitkänen, A. (2002) Projections from the amygdaloid complex to the magnocellular cholinergic basal forebrain in rat. *Neuroscience* **111**: 133–49.

Jones, B. E. (2003) Arousal systems. *Frontiers in Bioscience* **8**: s438–51.

Jones, B. E. (2004) Activity, modulation and role of basal forebrain cholinergic neurons innervating the cerebral cortex. In *Acetylcholine in the Cerebral Cortex* (*Progress in Brain Research*, vol. 145), ed. L. Descarries, K. Krnjević and M. Steriade, pp. 157–69. Amsterdam: Elsevier.

Jones, B. E. and Beaudet, A. (1987) Distribution of acetylcholine and catecholamine neurons in the cat brain stem studied by choline acetyltransferase and tyrosine hydroxylase immunohistochemistry. *Journal of Comparative Neurology* **261**: 15–32.

Jones, B. E., and Cuello, A. C. (1989) Afferents to the basal forebrain cholinergic cell area from pontomesencephalic — catecholamine, serotonin, and acetylcholine — neurons. *Neuroscience* **31**: 37–61.

Jones, B. E. and Moore, R. Y. (1977) Ascending projections of the locus coeruleus in the rat. II. Autoradiographic study. *Brain Research* **127**: 25–53.

Jones, E. G. (1975) Varieties and distribution of non-pyramidal cells in the somatic sensory cortex of the squirrel monkey. *Journal of Comparative Neurology* **160**: 205–68.

Jones, E. G. (1984) Laminar distribution of cortical efferent cells. In *Cerebral Cortex*, vol. 1 (*Cellular Components of the Cerebral Cortex*), ed. A. Peters and E. G. Jones, pp. 521–33. New York: Plenum.

Jones, E. G. (1985) *The Thalamus*. New York: Plenum.

Jones, E. G. (1991) Cellular organization in the primate postcentral gyrus. In *Information Processing in the Somatosensory System*, ed. O. Franzen and J. Westman, pp. 95–107. New York: Macmillan.

Jones, E. G. (1997). A description of the human thalamus. In *Thalamus*, vol. 2 (*Experimental and Clinical Aspects*), ed. M. Steriade, E. G. Jones and D. A. McCormick, pp. 425–99. Amsterdam: Elsevier.

Jones, E. G. (2000) Cortical and subcortical contributions to activity-dependent plasticity in primate somatosensory cortex. *Annual Reviews of Neuroscience* **23**: 1–37.

Jones, E. G. (2002) Thalamic circuitry and thalamocortical synchrony. *Philosophical Transactions of the Royal Society of London* B**357**: 1659–73.

Jones, E. G. and Pons, T. P. (1998) Thalamic and brainstem contributions to large-scale plasticity of primate somatosensory cortex. *Science* **282**: 1121–25.

Jones, E. G. and Powell, T. P.S. (1970) An anatomical study of converging sensory pathways within the cerebral cortex of the monkey. *Brain* **93**: 793–820.

Jones, R. S. G. (1990) Intrinsic properties of neurones in layer II of the rat entorhinal cortex in vitro. *Journal of Physiology (London)* **425**: 86P.

Jones, R. S. G. (1994) Synaptic and intrinsic properties of neurons of origin of the perforant path in layer II of the rat entorhinal cortex in vitro. *Hippocampus* **4**: 335–53.

Jones, R. S. G. and Bühl, E. H. (1993) Basket-like interneurones in layer II of the entorhinal cortex exhibit a powerful NMDA-mediated synaptic excitation. *Neuroscience Letters* **149**: 35–9.

Jongen-Rêlo, A. L. and Amaral, D. G. (1998) Evidence for a GABAergic projection from the central nucleus of the amygdala to the brainstem of the macaque monkey: a combined retrograde tracing and in situ hybridization study. *European Journal of Neuroscience* **10**: 2924–33.

Jouvet, M. (1965) Paradoxical sleep – a study of its nature and mechanisms. *Progress in Brain Research* **18**: 20–57.

Jouvet, M. (1972) The role of monoamines and acetylcholine-containing neurons in the regulation of the sleep-waking cycle. *Ergebnisse der Physiologie* **64**: 166–307.

Jouvet, M. and Delorme, J. F. (1965) Locus coeruleus et sommeil paradoxal. *Comptes Rendus de la Société de Biologie de Paris* **159**: 895–9.

Jouvet, M. and Michel, F. (1959) Corrélations electromyographiques du sommeil chez le chat décortiqué et mésencephalique chronique. *Comptes Rendus de la Société de Biologie de Paris* **153**: 422–5.

Kamal, A. M. and Tömböl, T. (1975) Golgi studies on the amygdaloid nuclei of the cat. *Journal für Hirnforschung* **16**: 175–201.

Kammermeier, P. J. and Jones, S. W. (1997) High-voltage-activated calcium currents in neurons acutely isolated from the ventrobasal nucleus of the rat thalamus. *Journal of Neurophysiology* **77**: 465–75.

Kamondi, A., Williams, J. A., Hutcheon, B. and Reiner, P. B. (1992) Membrane properties of mesopontine cholinergic neurons studied with the

whole-cell patch-clamp technique: implications for behavioral state control. *Journal of Neurophysiology* **68**: 1359–72.

Kang, Y. and Kayano, F. (1994) Electrophysiological and morphological characteristics of layer VI pyramidal cells in the cat motor cortex. *Journal of Neurophysiology* **72**: 578–91.

Kang, Y. and Kitai, S. T. (1990) Electrophysiological properties of pedunculopontine neurons and their postsynaptic responses following stimulation of substantia nigra reticulata. *Brain Research* **535**: 79–95.

Kapp, B. S., Frysinger, R. C., Gallagher, M. and Haselton, J. R. (1979) Amygdala central nucleus lesions: Effects on heart rate conditioning in the rabbit. *Physiology and Behavior* **23**: 1109–17.

Kapp, B. S., Supple, W. J. and Whalen, P. J. (1994) Effects of electrical stimulation of the amygdaloid central nucleus on neocortical arousal in the rabbit. *Behavioral Neuroscience* **108**: 81–93.

Kasamatsu, T. (1976) Visual cortical neurons influenced by the oculomotor input: characterization of their receptive field properties. *Brain Research* **113**: 271–92.

Kasper, E. M., Larkman, A. U., Lübke, J. and Blakemore, C. (1994a) Pyramidal neurons in layer 5 of the rat visual cortex. I. Correlation among cell morphology, intrinsic electrophysiological properties, and axon targets. *Journal of Comparative Neurology* **339**: 459–74.

Kasper, E. M., Lübke, J., Larkman, A. U. and Blakemore, C. (1994b) Pyramidal neurons in layer 5 of the rat visual cortex. III. Differential maturation of axon targeting, dendritic morphology, and electrophysiological properties. *Journal of Comparative Neurology* **339**: 495–518.

Kato, N. (1990) Cortico-thalamo-cortical projection between visual cortices. *Brain Research* **509**: 150–2.

Kawaguchi, Y. (1993) Groupings of nonpyramidal and pyramidal cells with specific physiological and morphological characteristics in rat frontal cortex. *Journal of Neurophysiology* **69**: 416–31.

Kawaguchi, Y. (2001) Distinct firing patterns of neuronal subtypes in cortical synchronized activities. *Journal of Neuroscience* **21**: 7261–72.

Kawaguchi, Y. and Kubota, Y. (1993) Correlation of physiological subgroupings of nonpyramidal cells with parvalbumine- and calbindinD28k-immunoreactive neurons in layer V of rat frontal cortex. *Journal of Neurophysiology* **70**: 387–96.

Kawaguchi, Y. and Kubota, Y. (1997) GABAergic cell subtypes and their synaptic connections in rat frontal cortex. *Cerebral Cortex* **7**: 476–86.

Kayama, Y., Ohta, M. and Jodo, E. (1992) Firing of 'possibly' cholinergic neurons in the rat laterodorsal tegmental nucleus during sleep and wakefulness. *Brain Research* **569**: 210–20.

Kemp, N. and Bashir, Z. I. (2001) Long-term depression: a cascade of induction and expression mechanisms. *Progress in Neurobiology* **65**: 339–65.

Kemppainen, S. and Pitkänen, A. (2000) Distribution of parvalbumin, calretinin, and calbindin-D28k immunoreactivity in the rat amygdaloid complex and colocalization with gamma-aminobutyric acid. *Journal of Comparative Neurology* **426**: 441–67.

Kettenmann, H. and Schachner, M. (1985) Pharmacological properties of γ-aminobutyric acid-, glutamate-, and aspartate-induced depolarizations in cultured astrocytes, *Journal of Neuroscience* **5**: 3295–301.

Khateb, A., Mühlethaler, M., Alonso, A. *et al.* (1992) Cholinergic nucleus basalis neurons display the capacity for rhythmic bursting activity mediated by low-threshold calcium spikes. *Neuroscience* **51**: 489–94.

Khateb, A., Fort, P., Serafin, M., Jones, B. E. and Mühlethaler, M. (1995a) Rhythmical bursts induced by NMDA in guinea-pig cholinergic nucleus basalis neurones in vitro. *Journal of Physiology (London)* **487**: 623–38.

Khateb, A., Fort, P., Pegna, A., Jones, B. E. and Mühlethaler, M. (1995b) Cholinergic nucleus basalis neurons are excited by histamine *in vitro*. *Neuroscience* **69**: 495–506.

Khateb, A., Fort, P., Williams, S. *et al.* (1997) Modulation of cholinergic nucleus basalis neurons by acetylcholine and *N*-methyl-*D*-aspartate. *Neuroscience* **81**: 47–55.

Killcross, S., Robbins, T. W. and Everitt, B. J. (1997) Different types of fear-conditioned behaviour mediated by separate nuclei within amygdala. *Nature* **388**: 377–80.

Kim, J. J. and Fanselow, M. S. (1992) Modality-specific retrograde amnesia of fear. *Science* **256**: 675–7.

Kim, M. J., Chun, S. K., Kim, Y. B., Mook-Jung, I. and Jung, M. W. (2003) Long-term potentiation in visual cortical projections to the medial prefrontal cortex of the rat. *Neuroscience* **120**: 283–9.

Kim, U. and McCormick, D. A. (1998) Functional and ionic properties of a slow afterhyperpolarization in ferret perigeniculate neurones in vitro. *Journal of Neurophysiology* **80**: 1222–35.

Kim, U., Bal, T. and McCormick, D. A. (1995) Spindle waves are propagating synchronized oscillations in the ferret LGNd in vitro. *Journal of Neurophysiology* **74**: 1301–23.

Kinney, H. C., Korein, J., Panigrahy, A., Dikkes, P. and Goode, R. (1994) Neuropathological findings in the brain of Karen Ann Quinlan. *New England Journal of Medicine* **330**: 1469–75.

Kinomura, S., Larsson, J., Gulyás, B. and Roland, P. (1996) Activation by attention of the human reticular formation and thalamic intralaminar nuclei. *Science* **271**: 512–15.

Kisvárday, Z. F., Beaulieu, C. and Eysel, U. T. (1993) Network of GABAergic large basket cells in cat visual cortex (area 18): implication for lateral disinhibition. *Journal of Comparative Neurology* **327**: 398–415.

Kitsikis, A. and Steriade, M. (1981) Immediate behavioral effects of kainic acid injections into the midbrain reticular core. *Behavioral Brain Research* **3**: 361–80.

Kleitman, N. (1963) *Sleep and Wakefulness.* Chicago: University of Chicago Press.

Klink, R. and Alonso, A. (1993) Ionic mechanisms for the subthreshold oscillations and differential electroresponsiveness of medial entorhinal cortex layer II neurons. *Journal of Neurophysiology* **70**: 149–57.

Kobayashi, Y., Inoue, Y., Yamamoto, M., Isa, T. and Aizawa, H. (2001) Contribution of pedunculopontine tegmental nucleus neurons to performance of visually guided saccade tasks in monkeys. *Journal of Neurophysiology* **88**: 715–31.

Koch, C. (1998) The neuroanatomy of visual consciousness. In *Consciousness: At the Frontiers of Neuroscience* (*Advances in Neurology*, vol. 77), ed. H. H. Jasper, L. Descarries, V. F. Castelucci and S. Rossignol, pp. 229–41. Philadelphia, PA: Lippincott-Raven.

Köhler, C. and Steinbusch, H. (1982) Identification of serotonin and non-serotonin-containing neurons of the mid-brain raphe projecting to the entorhinal area and the hippocampal formation. A combined immunohistochemical and fluorescent retrograde tracing study in the rat brain. *Neuroscience* **7**: 951–75.

Köhler, C., Chan-Palay, V., Haglund, L. and Steinbusch, H. (1980) Immunohistochemical localization of serotonin nerve terminals in the lateral entorhinal cortex of the rat: demonstration of two separate patterns of innervation from the midbrain raphe. *Anatomy and Embryology* **160**: 121–9.

Köhler, C., Chan-Palay, V. and Steinbusch, H. (1981) The distribution and orientation of serotonin fibers in the entorhinal and other retrohippocampal areas. An immunohistochemical study with anti-serotonin antibodies in the rat brain. *Anatomy and Embryology* **161**: 237–64.

Köhler, C., Swanson, L. W., Haglund, L. and Wu, J. Y. (1985a) The cytoarchitecture, histochemistry and projections of the tuberomammillary nucleus in the rat. *Neuroscience* **16**: 85–110.

Köhler, C., Wu, J. Y. and Chan-Palay, V. (1985b) Neurons and terminals in the retrohippocampal region in he rat's brain identified by anti-gamma-aminobutyric acid and anti-glutamic acid decarboxylase immunocytochemistry. *Anatomy and Embryology (Berlin)* **173:** 35–44.

Kohlmeier, K. A. and Reiner, P. B. (1999) Noradrenaline excites non-cholinergic laterodorsal tegmental neurons via two distinct mechanisms. *Neuroscience* **93**: 619–30.

Koo, J. W., Han, J. S. and Kim, J. J. (2004) Selective neurotoxic lesions of basolateral and central nuclei of the amygdala produce differential effects on fear conditioning. *Journal of Neuroscience* **24**: 7654–62.

Kordower, J. H., Bartus, R. T., Marciano, F. F. and Gash, D. M. (1989) Telencephalic cholinergic system of the new world monkey (*Cebus apella*): Morphological and cytoarchitectonic assessment and analysis of the projection to the amygdala. *Journal of Comparative Neurology* **279**: 528–45.

Kosaka, T., Kosaka, K., Hataguchi, Y. *et al.* (1987) Catecholaminergic neurons containing GABA-like and/or glutamic acid decarboxylase-like immunoreactivities in various brain regions of the rat. *Experimental Brain Research* **66**: 191–210.

Kosofsky, B. E. and Molliver, M. E. (1987) The serotoninergic innervation of cerebral cortex: different classes of axon terminals arise from dorsal and median raphe nuclei. *Synapse* **1**: 153–68.

Krettek, J. E. and Price, J. L. (1977a) Projections from the amygdaloid complex to the cerebral cortex and thalamus in the rat and cat. *Journal of Comparative Neurology* **172**: 687–722.

Krettek, J. E. and Price, J. L. (1977b) Projections from the amygdaloid complex and adjacent olfactory structures to the entorhinal cortex and to the subiculum in the rat and cat. *Journal of Comparative Neurology* **172**: 723–52.

Krettek, J. E. and Price, J. L. (1978a) Amygdaloid projections to subcortical structures within the basal forebrain and brainstem in the rat and cat. *Journal of Comparative Neurology* **178**: 225–54.

Krettek, J. E. and Price, J. L. (1978b) A description of the amygdaloid complex in the rat and cat with observations on intra-amygdaloid axonal connections. *Journal of Comparative Neurology* **178**: 255–80.

Kroner, S., Rosenkranz, J. A., Grace, A. A. and Barrionuevo, G. (2005) Dopamine modulates excitability of basolateral amygdala neurons in vitro. *Journal of Neurophysiology* **93**: 1598–610.

Kudo, M. and Niimi, K. (1980) Ascending projections of the inferior colliculus in the cat: an autoradiographic study. *Journal of Comparative Neurology* **191**: 545–56.

Kudo, M., Itoh, K., Kawamura, S. and Mizuno, N. (1983) Direct projections to the pretectum and the midbrain reticular formation from auditory relay nuclei in the lower brainstem of the cat. *Brain Research* **288**: 13–19.

Kudo, M., Tashiro, T., Higo, S., Matsuyama, T. and Kawamura, S. (1984) Ascending projections from the nucleus of the brachium of the inferior colliculus in the cat. *Experimental Brain Research* **54**: 203–11.

Kumar, S. S. and Huguenard, J. R. (2001) Properties of excitatory synaptic connections mediated by the corpus callosum in the developing neocortex. *Journal of Neurophysiology* **86**: 2973–85.

Kuroda, M. and Price, J. L. (1991) Synaptic organization of projections from basal forebrain structures to the mediodorsal thalamic nucleus of the rat. *Journal of Comparative Neurology* **303**: 513–33.

LaBar, K. S., LeDoux, J. E., Spencer, D. D. and Phelps, E. A. (1995) Impaired fear conditioning following unilateral temporal lobectomy in humans. *Journal of Neuroscience* **15**: 6846–55.

Lamprecht, R., Farb, C. R. and LeDoux, J. E. (2002) Fear memory formation involves p190 RhoGAP and ROCK proteins through a GRB2-mediated complex. *Neuron* **36**: 727–38.

Lancel, M., van Riezen, H., and Glatt, A. (1992) The time course of sigma activity and slow-wave activity during NREMS in cortical and thalamic EEG of the cat during baseline and after 12 hours of wakefulness. *Brain Research* **596**: 285–95.

Landisman, C. E., Long, M. A., Beierlein, M. *et al.* (2002) Electrical synapses in the thalamic reticular nucleus. *Journal of Neuroscience* **22**: 1002–9.

Lang, E. J. and Paré, D. (1997a) Similar inhibitory processes dominate the responses of cat lateral amygdaloid projection neurons to their various afferents. *Journal of Neurophysiology* **77**: 341–52.

Lang, E. J. and Paré, D. (1997b) Synaptic and synaptically activated intrinsic conductances underlie inhibitory potentials in cat lateral amygdaloid projection neurons in vivo. *Journal of Neurophysiology* **77**: 353–63.

Lang, E. J. and Paré, D. (1998) Synaptic responsiveness of interneurons of the cat lateral amygdaloid nucleus. *Neuroscience* **83**: 877–89.

Larkum, M. E., Zhu, J. J. and Sakman, B. (1999) A new cellular mechanism for coupling inputs arriving at different cortical layers. *Nature* **398**: 338–41.

Laroche, S., Jay, T. M. and Thierry, A. M. (1990) Long-term potentiation in the prefrontal cortex following stimulation of the hippocampal CA1/subicular region. *Neuroscience Letters* **114**: 184–90.

Laroche, S., Doyère, V., Redini-Del Negro, C. and Burette, F. (1995) Neural mechanisms of associative memory: role of long-term potentiation. In *Brain and Memory: Modulation and Mediation of Neuroplasticity*, ed. J. L. McGaugh, N. M. Weinberger and G. Lynch, pp. 277–302. New York: Oxford University Press.

Larson, J. and Lynch, G. (1986) Role of *N*-methyl-D aspartate receptors in the induction of synaptic potentiation by burst stimulation patterned after the hippocampal theta rhythm. *Brain Research* **441**: 111–18.

Larson, J., Wong, D. and Lynch, G. (1986) Patterned stimulation at the theta frequency is optimal for the induction of hippocampal long-term potentiation. *Brain Research* **368**: 347–50.

Lavin, A. and Grace, A. A. (1994) Modulation of dorsal thalamic cell activity by the ventral pallidum: its role in the regulation of thalamocortical activity by the basal ganglia. *Synapse* **18**: 104–27.

Lavoie, B. and Parent, A. (1994) Pedunculopontine nucleus in the squirrel monkey: distribution of cholinergic and monoaminergic neurons in the mesopontine tegmentum with evidence for the presence of glutamate in cholinergic neurons. *Journal of Comparative Neurology* **344**: 190–209.

Law-Tho, D., Desce, J. M. and Crépel, F. (1995) Dopamine favours the emergence of long-term depression versus long-term potentiation in slices of rat prefrontal cortex. *Neuroscience Letters* **188**: 125–8.

LeDoux, J. E. (2000a) The amygdala and emotion: a view through fear. In *The Amygdala: A Functional Analysis*, ed. J. P. Aggleton, pp. 289–310. Oxford: Oxford University Press.

LeDoux, J. E. (2000b) Emotion circuits in the brain. *Annual Review of Neuroscience* **23**: 155–84.

LeDoux, J. E., Sakaguchi, A. and Reis, D. J. (1984) Subcortical efferent projections of the medial geniculate nucleus mediate emotional responses conditioned to acoustic stimuli. *Journal of Neuroscience* **4**: 683–98.

LeDoux, J. E., Ruggiero, D. A., Forest, R., Stornetta, R. and Reis, D. J. (1987) Topographic organization of convergent projections to the thalamus from the inferior colliculus and spinal cord in the rat. *Journal of Comparative Neurology* **264**: 123–46.

LeDoux, J. E., Iwata, J., Cicchetti, P. and Reis, D. J. (1988) Different projections of the central amygdaloid nucleus mediate autonomic and behavioral correlates of conditioned fear. *Journal of Neuroscience* **8**: 2517–29.

LeDoux, J. E., Cicchetti, P., Xagoraris, A. and Romanski, L. M. (1990a) The lateral amygdaloid nucleus: sensory interface of the amygdala in fear conditioning. *Journal of Neuroscience* **10**: 1062–9.

LeDoux, J. E., Farb, C. and Ruggiero, D. A. (1990b) Topographic organization of neurons in the acoustic thalamus that project to the amygdala. *Journal of Neuroscience* **10**: 1043–54.

Lee, H. and Kim, J. J. (1998) Amygdalar NMDA receptors are critical for new fear learning in previously fear-conditioned rats. *Journal of Neuroscience* **18**: 8444–54.

Lee, H. K., Barbarosie, M., Kameyama, K., Bear, M. F. and Huganir, R. L. (2000) Regulation of distinct AMPA receptor phosphorylation sites during bidirectional synaptic plasticity. *Nature* **405**: 955–9.

Lee, K. H. and McCormick, D. A. (1995) Acetylcholine excites GABAergic neurons of the ferret perigeniculate nucleus through nicotinic receptors. *Journal of Neurophysiology* **73**: 2123–8.

Lee, K. and McCormick, D. A. (1996) Abolition of spindle oscillations by serotonin and norepinephrine in the ferret lateral geniculate and perigeniculate nuclei in vitro. *Neuron* **17**: 309–21.

Lee, M. G., Hassani, O. K., Alonso, A. and Jones, B. E. (2005) Cholinergic basal forebrain neurons burst with theta during waking and paradoxical sleep. *Journal of Neuroscience* **25**: 4365–9.

Lee, M. S., Friedberg, M. H. and Ebner, F. F. (1994) The role of GABA-mediated inhibition in the rat ventral posterior medial thalamus. I. Assessment of

receptive field changes following thalamic reticular nucleus lesions. *Journal of Neurophysiology* **71**: 1702–15.
Lenz, F. A. and Dougherty, P. M. (1997) Pain processing in the human thalamus. In *Thalamus*, vol. 2 (*Experimental and Clinical Aspects*), ed. M. Steriade, E. G. Jones and D. A. McCormick, pp. 617–51. Amsterdam: Elsevier.
Leonard, B. W., Amaral, D. G., Squire, L. R. and Zola-Morgan, S. (1995) Transient memory impairment in monkeys with bilateral lesions of the entorhinal cortex. *Journal of Neuroscience* **15**: 5367–659.
Leonard, C. S. and Llinás, R. R. (1990) Electrophysiology of mammalian pedunculopontine and laterodorsal tegmental neurons *in vitro*: implications for the control of REM sleep. In *Brain Cholinergic Systems*, ed. M. Steriade and D. Biesold, pp. 205–23. Oxford: Oxford University Press.
Leonard, C. S. and Llinás, R. R. (1994) Serotonergic and cholinergic inhibition of mesopontine cholinergic neurons controlling REM sleep: an *in vitro* electrophysiological study. *Neuroscience* **59**: 309–30.
Leonard, C. S., Kerman, I., Blaha, G., Taveras, E., and Taylor, B. (1995a) Interdigitation of nitric oxyde synthase-, tyrosine hydroxylase- and serotonin-containing neurons in and around the laterodorsal and pedunculopontine tegmental nuclei of the guinea pig. *Journal of Comparative Neurology* **362**: 411–32.
Leonard, C. S., Rao, S. and Sanchez, R. M. (1995b) Patterns of neuromodulation and the nitric oxide signaling pathway in mesopontine cholinergic neurons. *Seminars in the Neurosciences* **7**: 319–28.
Leonard, C. S., Rao, S. R. and Inoue, T. (2000) Serotonergic inhibition of action potential evoked calcium transients in NOS-containing mesopontine cholinergic neurons. *Journal of Neurophysiology* **84**: 1558–72.
Leopold, D. A., Murayama, Y. and Logothetis, N. K. (2003) Very slow activity fluctuations in monkey visual cortex: implications for functional brain imaging. *Cerebral Cortex* **13**: 422–33.
Leresche, N., Jassik-Gerschenfeld, D., Haby, M., Soltesz, I. and Crunelli, V. (1990) Pacemaker-like and other types of spontaneous membrane potential oscillations of thalamocortical cells. *Neuroscience Letters* **113**: 72–7.
Leresche, N., Lightowler, S., Soltesz, I., Jassik-Gerschenfeld, D. and Crunelli, V. (1991) Low-frequency oscillatory activities intrinsic to rat and cat thalamocortical cells. *Journal of Physiology (London)* **441**: 155–74.
Leung, L. S. (1984) Model of gradual phase shift of theta rhythm in the rat. *Journal of Neurophysiology* **52**: 1051–65.
LeVay, S. (1973) Synaptic patterns in the visual cortex of the cat and monkey. Electron microscopy of Golgi preparations. *Journal of Comparative Neurology* **150**: 53–86.
Lévesque, M., Charara, A., Gagnon, S., Parent, A. and Deschênes, M. (1996) Corticostriatal projections from layer V cells in rat are collaterals of long-range corticofugal axons. *Brain Research* **709**: 311–15.
Levitt, P. and Moore, R. Y. (1978) Noradrenaline neuron innervation of the neocortex in the rat. *Brain Research* **139**: 219–31.
Lhermitte, F., Gautier, J. C., Marteau, R. and Chain, F. (1963) Consciousness disorders and akinetic mutism. Anatomo-clinical study of a bilateral paramedian softening of the cerebral peduncle and thalamus. *Revue Neurologique (Paris)* **109**: 115–31.
Li, L., Miller, E. K. and Desimone, R. (1993) The representation of stimulus familiarity in anterior inferior temporal cortex. *Journal of Neurophysiology* **69**: 1918–29.

Li, R., Nishijo, H., Wang, Q. X. *et al.* (2001) Light and electron microscopic study of cholinergic and noradrenergic elements in the basolateral nucleus of the rat amygdala: Evidence for interactions between the two systems. *Journal of Comparative Neurology* **439**: 411–25.

Li, R., Nishijo, H., Ono, T., Ohtani, Y. and Ohtani, O. (2002) Synapses on GABAergic neurons in the basolateral nucleus of the rat amygdala: double-labeling immunoelectron microscopy. *Synapse* **43**: 42–50.

Li, Y. Q., Jia, H. G., Rao, Z. R. and Shi, J. W. (1990) Serotonin-, substance P- or leucine-enkephalin-containing neurons in the midbrain periaqueductal gray and nucleus raphe dorsalis send projection fibers to the central amygdaloid nucleus in the rat. *Neuroscience Letters* **120**: 124–7.

Liang, K. C. and McGaugh, J. L. (1983) Lesions of the stria terminals attenuate the enhancing effect of post-training epinephrine on retention of an inhibitory avoidance response. *Behavioral Brain Research* **9**: 49–58.

Liang, K. C., McGaugh, J. L. and Yao, H. Y. (1990) Involvement of amygdala pathways in the influence of post-training intra-amygdala norepinephrine and peripheral epinephrine on memory storage. *Brain Research* **508**: 225–33.

Likhtik, E., Pelletier, J. G., Paz, R. and Paré, D. (2005) Prefrontal control of the amygdala. *Journal of Neuroscience* **25**: 7429–37.

Lin, J. S., Sakai, K. and Jouvet, M. (1988) Evidence for histaminergic arousal mechanisms in the hypothalamus of cats. *Neuropharmacology* **27**: 111–22.

Lin, J. S., Sakai, K., Vanni-Mercier, G. and Jouvet, M. (1989) A critical role of the posterior hypothalamus in the mechanisms of wakefulness determined by microinjections of muscimol in freely moving cats. *Brain Research* **479**: 225–40.

Lin, J. S., Hou, Y., Sakai, K. and Jouvet, M. (1996) Histaminergic descending inputs to the mesopontine tegmentum and their role in the control of cortical activation and wakefulness in the cat. *Journal of Neuroscience* **16**: 1523–37.

Lindström, S. and Wróbel, A. (1990) Frequency dependent corticofugal excitation of principal cells in the cat's dorsal lateral geniculate nucleus. *Experimental Brain Research* **79**: 313–8.

Lindvall, O., Bjorklund, A. and Divac, I. (1978) Organization of catecholamine neurons projecting to the frontal cortex in the rat. *Brain Research* **142**: 1–24.

Linke, R., Braune, G. and Schwegler, H. (2000) Differential projection of the posterior paralaminar thalamic nuclei to the amygdaloid complex in the rat. *Experimental Brain Research* **134**: 520–32.

Liu, X. B. and Jones, E. G. (1999) Predominance of corticothalamic synaptic inputs to thalamic reticular nucleus neurons in the rat. *Journal of Comparative Neurology* **414**: 67–79.

Liu, X. B., Warren, R. A. and Jones, E. G. (1995) Synaptic distribution of afferents from reticular nucleus in ventroposterior nucleus of cat thalamus. *Journal of Comparative Neurology* **352**: 187–202.

Liubashina, O., Jolkkonen, E. and Pitkänen, A. (2000) Projections from the central nucleus of the amygdala to the gastric related area of the dorsal vagal complex: a *Phaseolus vulgaris*-leucoagglutinin study in rat. *Neuroscience Letters* **291**: 85–8.

Livingstone, M. S. and Hubel, D. H. (1981) Effects of sleep and arousal on the processing of visual information in the cat. *Nature* **291**: 554–61.

Llinás, R. R. (1988) The intrinsic electrophysiological properties of mammalian neurons: insights into central nervous system function. *Science* **242**: 1654–64.

Llinás, R. R. and Jahnsen, H. (1982) Electrophysiology of mammalian thalamic neurones *in vitro*. *Nature* **297**: 406–8.

Llinás, R., and Ribary, U. 1992. Rostrocaudal scan in human brain: a global characteristic for the 40 Hz response during sensory input. In *Induced Rhythms in the Brain*, ed. E. Basar and T. Bullock, pp. 147–54. Boston, MA: Birkhaüser.

Llinás, R. R. and Ribary, U. (1993) Coherent 40-Hz oscillation characterizes dream state in humans. *Proceedings of the National Academy of Sciences USA* **90**: 2078–81.

Llinás, R., Grace, A. A. and Yarom, Y. (1991) In vitro neurons in mammalian cortical layer 4 exhibit intrinsic oscillatory activity in the 10- to 50-Hz frequency range. *Proceedings of the National Academy of Sciences USA* **88**: 897–901.

Llinás, R. R., Ribary, U., Jeanmonod, D., Kronberg, E. and Mitra, P. P. (1999) Thalamocortical dysrhythmia: a neurological and neuropsychiatric syndrome characterized by magnetoencephalography. *Proceedings of the National Academy of Sciences USA* **96**: 15222–7.

Llinás, R. R., Leznik, E. and Urbano, F. J. (2002) Temporal binding via cortical coincidence detection of specific and nonspecific thalamocortical inputs: a voltage-dependent dye-imaging study in mouse brain slices. *Proceedings of the National Academy of Sciences USA* **99**: 449–54.

Llinás, R. R., Urbano, F. J., Leznik, E., Ramirez, R. R. and van Marle, H. H. F. (2005) Rhythmic and dysrhythmic thalamocortical dynamics: GABA systems and the edge effect. *Trends in Neurosciences* **28**(6): 325–33.

Logothetis, N. K. (2003) The underpinnings of the BOLD functional magnetic resonance imaging signal. *Journal of Neuroscience* **23**: 3963–71.

Long, M. A., Landisman, C. E. and Connors, B. W. (2004) Small clusters of electrically coupled neurons generate synchronous rhythms in the thalamic reticular nucleus. *Journal of Neuroscience* **24**: 341–9.

Loomis, A. L., Harvey, N. and Hobart, G. A. (1938) Distribution of disturbance patterns in the human electroencephalogram, with special reference to sleep. *Journal of Neurophysiology* **1**: 413–30.

Lopes da Silva, F. H., van Rotterdam, A., Storm van Leeuwen, W. and Tielen, A. M. (1970) Dynamic characteristics of visual evoked potentials in the dog. II. Beta frequency selectivity in evoked potentials and background activity. *Electroencephalography and Clinical Neurophysiology* **29**: 260–8.

Lopes da Silva, F. H. and Storm van Leeuwen, W. (1978) The cortical alpha rhythm in dog: depth and surface profile of phase. In *Architecture of the Cerebral Cortex* (IBRO monograph series, vol. 3), ed. M. A. B. Brazier and H. Petsche, pp. 319–33. New York: Raven Press.

Lopes da Silva, F. H., Van Lierop, T. H. M. T., Schrijer, C. F. M. and Storm Van Leeuwen, W. (1973) Organization of thalamic and cortical alpha rhythm: spectra and coherences. *Electroencephalography and Clinical Neurophysiology* **35**: 627–39.

Lopes da Silva, F. H., Vos, J. E., Mooibroeck, J. and Van Rotterdam, A. (1980) Relative contribution of intracortical and thalamo-cortical processes in the generation of alpha rhythms, revealed by partial coherence analysis. *Electroencephalography and Clinical Neurophysiology* **50**: 449–56.

Lopez De Armentia, M. and Sah, P. (2004) Firing properties and connectivity of neurons in the rat lateral central nucleus of the amygdala. *Journal of Neurophysiology* **92**: 1285–94.

Lorente de No, R. (1933) Studies on the structure of the cerebral cortex. I. The area entorhinalis. *Journal für Psychologie und Neurologie* **45**: 381–438.

Loretan, K., Bissière, S. and Lüthi, A. (2004) Dopaminergic modulation of spontaneous inhibitory network activity in the lateral amygdala. *Neuropharmacology* **47**: 631–9.

Losier, B. J. and Semba, K. (1993) Dual projections of single cholinergic and aminergic brainstem neurons to the thalamus and basal forebrain in the rat. *Brain Research* **604**: 41–52.

Loughlin, S. E. and Fallon, J. H. (1983) Dopaminergic and non-dopaminergic projections to amygdala from substantia nigra and ventral tegmental area. *Brain Research* **262**: 334–8.

Lu, J., Greco, M. A., Shiromani, P. and Saper, C. B. (2000) Effect of lesions of the ventrolateral preoptic nucleus on NREM and REM sleep. *Journal of Neuroscience* **20**: 3830–42.

Lu, K. T., Walker, D. L. and Davis, M. (2001) Mitogen-activated protein kinase cascade in the basolateral nucleus of amygdala is involved in extinction of fear-potentiated startle. *Journal of Neuroscience* **21**: NIL17–21.

Lu, W. Y., Man, H. Y., Ju, W. *et al.* (2001) Activation of synaptic NMDA receptors induces membrane insertion of new AMPA receptors and LTP in cultured hippocampal neurons. *Neuron* **29**: 243–54.

Lucretius, T. C. (1988) *On the Nature of the Universe* (translated by R. E. Latham). London: Penguin Books.

Luebke, J. I., Greene, R. W., Semba, K. *et al.* (1992) Serotonin hyperpolarizes cholinergic low-threshold burst neurons in the rat laterodorsal tegmental nucleus *in vitro*. *Proceedings of the National Academy of Sciences USA* **89**: 743–7.

Lugaresi, E., Medori, R. Montagna, P. *et al.* (1986) Fatal familial insomnia and dysautonomia with selective degeneration of thalamic nuclei. *New England Journal of Medicine* **315**: 997–1003.

Luiten, P. G., Spencer, D. G., Traber, J. and Gaykema, R. P. (1985) The pattern of cortical projections from the intermediate parts of the magnocellular nucleus basalis in the rat demonstrated by tracing with *Phaseolus vulgaris*-leucoagglutinin. *Neuroscience Letters* **57**: 137–42.

Luiten, P. G., Gaykema, R. P., Traber, J. and Spencer, D. G. (1987) Cortical projection patterns of magnocellular basal nucleus subdivisions as revealed by anterogradely transported *Phaseolus vulgaris* leucoagglutinin. *Brain Research* **413**: 229–50.

Lund, J. S. (1973) Organization of neurons in the visual cortex, area 17, of the monkey (*Macaca mulatta*). *Journal of Comparative Neurology* **147**: 455–96.

Lüthi, A. and McCormick, D. A. (1998) Periodicity of thalamic synchronized oscillations: the role of Ca^{2+}-mediated upregulation of Ih. *Neuron* **20**: 553–63.

Lux, H. D. and Neher, E. (1973) The equilibrium time course of $[K^+]_o$ in cat cortex. *Experimental Brain Research* **17**: 190–205.

Lytton, W. W. and Sejnowski, T. J. (1991) Simulation of cortical pyramidal neurons synchronized by inhibitory interneurons. *Journal of Neurophysiology* **66**: 1059–79.

Lytton, W. W., Contreras, D., Destexhe, A. and Steriade, M. (1997) Dynamic interactions determine partial thalamic quiescence in a computer network model of spike-and-wave seizures. *Journal of Neurophysiology* **77**: 1679–96.

Ma, Q. P., Yin, G. F., Ai, M. K. and Han, J. S. (1991) Serotonergic projections from the nucleus raphe dorsalis to the amygdala in the rat. *Neuroscience Letters* **134**: 21–4.

Macchi, G., Rossi, G., Abbamondi, A. L. *et al.* (1997) Diffuse thalamic degeneration in fatal familial insomnia. A morphometric study. *Brain Research* **771**: 154–8.

Mackay, A. V. P. (1998) Letter to the Editor. *Trends in Neurosciences* **21**: 146.

Magill, P. J., Bolam, P. and Bevan, M. D. (2000) Relationship of activity in the subthalamic nucleus – globus pallidus network to cortical EEG. *Journal of Neuroscience* **20**: 820–33.

Mahanty, N. K. and Sah, P. (1998) Calcium-permeable AMPA receptors mediate long-term potentiation in interneurons in the amygdala. *Nature* **394**: 683–7.

Mahon, S., Deniau, J. M. and Charpier, S. (2001) Relationship between EEG potentials and intracellular activity of striatal and cortico-striatal neurons: an *in vivo* study under different anesthetics. *Cerebral Cortex* **11**: 360–73.

Mainen, Z. F. and Sejnowski, T. J. (1995) Reliability of spike timing in neocortical neurons. *Science* **268**: 1503–6.

Malenka, R. C. and Nicoll, R. A. (1993) NMDA-receptor-dependent synaptic plasticity: multiple forms and mechanisms. *Trends in Neurosciences* **16**: 521–7.

Maloney, K. J., Cape, E. G., Gotman, J. and Jones, B. E. (1997) High-frequency gamma electroencephalogram activity in association with sleep-wake states and spontaneous behaviors in the rat. *Neuroscience* **76**: 541–55.

Maltais, S., Coté, S., Drolet, G. and Falardeau, P. (2000) Cellular colocalization of dopamine D1 mRNA and D2 receptor in rat brain using a dopamine receptor specific polyclonal antibody. *Progress in Neuro-Psychopharmacology and Biological Psychiatry* **24**: 1127–49.

Manaye, K. F., Zweig, R., Wu, D. *et al.* (1999) Quantification of cholinergic and select non-cholinergic mesopontine neuronal populations in the human brain. *Neuroscience* **89**: 759–70.

Manetto, V., Medori, R., Cortelli, P. *et al.* (1992) Fatal familial insomnia: clinical and pathological study of five new cases. *Neurology* **42**: 312–19.

Manns, I. D., Mainville, L. and Jones, B. E. (2001) Evidence for glutamate, in addition to acetylcholine and GABA, neurotransmitter synthesis in basal forebrain neurons projecting to the entorhinal cortex. *Neuroscience* **107**: 249–63.

Mao, B. Q., Hamzei-Sichani, F., Aronov, D., Froemke, R. C. and Yuste, R. (2003) Dynamics of spontaneous activity in neocortical slices. *Neuron* **32**: 883–98.

Maquet, P., Péters, J. M., Aerts, J. *et al.* (1996) Functional neuroanatomy of human rapid-eye-movement sleep and dreaming. *Nature* **383**: 163–6.

Maquet, P., Degueldre, C., Delfiore, G. *et al.* (1997) Functional neuroanatomy of human slow wave sleep. *Journal of Neuroscience* **17**: 2807–12.

Maquet, P., Laureys, S., Peigneux, P. *et al.* (2000) Experience-dependent changes in cerebral activation during human REM sleep. *Nature Neuroscience* **3**: 831–6.

Maren, S. and Fanselow, M. S. (1995) Synaptic plasticity in the basolateral amygdala induced by hippocampal formation stimulation in vivo. *Journal of Neuroscience* **15**: 7548–64.

Maren, S. and Quirk, G. J. (2004) Neuronal signaling of fear memory. *Nature Reviews Neuroscience* **5**: 844–52.

Markram, H., Lübke, J., Frotscher, M., Roth, A. and Sakmann, B. (1997) Physiology and anatomy of tufted pyramidal neurons in the developing rat neocortex. *Journal of Physiology (London)* **500**: 409–40.

Markram, H., Wang, M. and Tsodycs, M. (1998) Differential signaling via the same axon of neocortical pyramidal neurons. *Proceedings of the National Academy of Sciences USA* **95**: 5323–8.

Markram, H., Toledo-Rodriguez, M., Wang, Y. *et al.* (2004) Interneurons of the neocortical inhibitory system. *Nature Reviews Neuroscience* **5**: 793–807.

Marshall, L., Mölle, M. and Born, J. (2003) Spindle and slow wave rhythms at slow wave sleep transitions are linked to strong shifts in the cortical direct current potential. *Neuroscience* **121**: 1047–53.

Martin, J. J. (1997) Degenerative diseases of the human thalamus. In *Thalamus*, vol. 2 (*Experimental and Clinical Aspects*), ed. M. Steriade, E. G. Jones and D. A. McCormick, pp. 653–79. Oxford: Elsevier.

Martin, J. J., Yap, M., Nei, I. P. and Tan, T. E. (1983) Selective thalamic degeneration – report of a case with memory and mental disturbances. *Clinical Neuropathology* **2**: 156–62.

Martina, M., Royer, S. and Paré, D. (1999) Physiological properties of central medial and central lateral amygdala neurons. *Journal of Neurophysiology* **82**: 1843–54.

Martina, M., Royer, S. and Paré, D. (2001) Propagation of neocortical inputs in the perirhinal cortex. *Journal of Neuroscience* **21**: 2878–88.

Mascagni, F., McDonald, A. J. and Coleman J. R. (1993) Corticoamygdaloid and corticocortical projections of the rat temporal cortex: A *Phaseolus vulgaris* leucoagglutinin study. *Neuroscience* **57**: 697–715.

Massimini M. and Amzica F. (2001) Extracellular calcium fluctuations and intracellular potentials in the cortex during the slow sleep oscillation. *Journal of Neurophysiology* **85**: 1346–50.

Massimini, M., Rosanova, M. and Mariotti, M. (2003) EEG slow (~1 Hz) waves are associated with nonstationarity of thalamo-cortical sensory processing in the sleeping human. *Journal of Neurophysiology* **89**: 1205–13.

Massimini, M., Huber, R., Ferrarelli, F. and Tononi, G. (2004) The sleep slow oscillation as a traveling wave. *Journal of Neuroscience* **24**: 6862–70.

McCarley, R. W. and Hobson, J. A. (1975) Neuronal excitability modulation over the sleep cycle: a structural and mathematical model. *Science* **189**: 58–60.

McCarley, R. W., Nelson, J. P. and Hobson, J. A. (1978) Ponto-geniculo-occipital (PGO) burst neurons: correlative evidence for neuronal generators of PGO waves. *Science* **201**: 269–72.

McCarley, R. W., Benoit, O. and Barrionuevo, G. (1983) Lateral geniculate nucleus unitary discharge in sleep and waking: state- and rate-specific aspects. *Journal of Neurophysiology* **50**: 798–818.

McCormick, D. A. (1992) Neurotransmitter actions in the thalamus and cerebral cortex and their role in neuromodulation of thalamocortical activity. *Progress in Neurobiology* **39**: 337–88.

McCormick, D. A. and Pape, H. C. (1988) Acetylcholine inhibits identified interneurons in the cat lateral geniculate nucleus. *Nature* **334**: 246–8.

McCormick, D. A. and Pape, H. C. (1990a) Properties of a hyperpolarization-activated cation current and its role in rhythmic oscillation in thalamic relay neurones. *Journal of Physiology (London)* **431**: 291–318.

McCormick, D. A. and Pape, H. C. (1990b) Noradrenergic and serotonergic modulation of a hyperpolarization-activated cation current in thalamic relay cells. *Journal of Physiology (London)* **431**: 319–42.

McCormick, D. A. and Wang, Z. (1991) Serotonin and noradrenaline excite GABAergic neurones of the guinea-pig and cat nucleus reticularis thalami. *Journal of Physiology (London)* **442**: 235–55.

McCormick, D. A. and Williamson, A. (1989) Convergence and divergence of neurotransmitter action in human cerebral cortex. *Proceedings of the National Academy of Sciences USA* **86**: 8098–102.

McCormick, D. A. and Williamson, A. (1991) Modulation of neuronal firing mode in cat and guinea-pig LGNd by histamine: possible cellular mechanisms of histaminergic control of arousal. *Journal of Neuroscience* **11**: 3188–99.

McCormick, D. A., Connors, B. W., Lighthall, J. W. and Prince, D. A. (1985) Comparative electrophysiology of pyramidal and sparsely spiny stellate neurons of the neocortex. *Journal of Neurophysiology* **54**: 782–806.

McDonald, A. J. (1982) Cytoarchitecture of the central amygdaloid nucleus of the rat. *Journal of Comparative Neurology* **208**: 401–18.

McDonald, A. J. (1985) Immunohistochemical identification of gamma-aminobutyric acid-containing neurons in the rat basolateral amygdala. *Neuroscience Letters* **53**: 203–7.

McDonald, A. J. (1992a) Cell types and intrinsic connections of the amygdala. In *The Amygdala: Neurobiological Aspects of Emotion, Memory, and Mental Dysfunction*, ed. J. P. Aggleton, pp. 67–96. New York: Wiley-Liss.

McDonald, A. J. (1992b) Projection neurons of the basolateral amygdala: A correlative Golgi and retrograde tract tracing study. *Brain Research Bulletin* **28**: 179–85.

McDonald, A. J. (1998) Cortical pathways to the mammalian amygdala. *Progress in Neurobiology* **55**: 257–332.

McDonald, A. J. (2003) Is there an amygdala and how far does it extend? An anatomical perspective. *Annals of the New York Academy of Sciences* **985**: 1–21.

McDonald, A. J. and Augustine, J. R. (1993) Localization of GABA-like immunoreactivity in the monkey amygdala. *Neuroscience* **52**: 281–94.

McDonald, A. J. and Betette, R. L. (2001) Parvalbumin-containing neurons in the rat basolateral amygdala: morphology and co-localization of Calbindin-D(28k). *Neuroscience* **102**: 413–25.

McDonald, A. J. and Mascagni, F. (1997) Projections of the lateral entorhinal cortex to the amygdala. *Neuroscience* **77**: 445–59.

McDonald, A. J. and Mascagni, F. (2001a) Colocalization of calcium-binding proteins and GABA in neurons of the rat basolateral amygdala. *Neuroscience* **105**: 681–93.

McDonald, A. J. and Mascagni, F. (2001b) Localization of the CB1 type cannabinoid receptor in the rat basolateral amygdala: high concentrations in a subpopulation of cholecystokinin-containing interneurons. *Neuroscience* **107**: 641–52.

McDonald, A. J. and Mascagni, F. (2002). Immunohistochemical characterization of somatostatin containing interneurons in the rat basolateral amygdala. *Brain Research* **943**: 237–44.

McDonald, A. J. and Mascagni, F. (2004) Parvalbumin-containing interneurons in the basolateral amygdala express high levels of the alpha1 subunit of the GABA A receptor. *Journal of Comparative Neurology* **473**: 137–46.

McDonald, A. J., Mascagni, F. and Guo, L. (1996) Projections of the medial and lateral prefrontal cortices to the amygdala: A *Phaseolus vulgaris* leucoagglutinin study in the rat. *Neuroscience* **71**: 55–75.

McDonald, A. J., Muller, J. F. and Mascagni, F. (2002) GABAergic innervation of alpha type II calcium/calmodulin-dependent protein kinase immunoreactive pyramidal neurons in the rat basolateral amygdala. *Journal of Comparative Neurology* **446**: 199–218.

McGaugh, J. L. (1966) Time-dependent processes in memory storage. *Science* **153**: 1351–8.

McGaugh, J. L. (2002) Memory consolidation and the amygdala: a systems perspective. *Trends in Neurosciences* **25**: 456–61.

McGaugh, J. L. and Gold, P. E. (1976) Modulation of memory by electrical stimulation of the brain. In *Neural Mechanisms of Learning and Memory*, ed. M. R. Rosenzweig and E. L. Bennett, pp. 549–60. Cambridge, MA: MIT Press.

McGinty, D. J. and Harper, R. M. (1976) Dorsal raphe neurons: depression of firing during sleep in cats. *Brain Research* **101**: 569–75.

McKernan, M. G. and Shinnick-Gallagher, P. (1997) Fear conditioning induces a lasting potentiation of synaptic currents in vitro. *Nature* **390**: 607–11.

McKinney, M., Coyle, J. T. and Hedreen, J. C. (1983) Topographic analysis of the innervation of the rat neocortex and hippocampus by the basal forebrain cholinergic system. *Journal of Comparative Neurology* **217**: 103–21.

Mechawar, N., Cozzari, C. and Descarries, L. (2000) Cholinergic innervation in adult rat cerebral cortex: a quantitative immunocytochemical description. *Journal of Comparative Neurology* **428**: 305–18.

Merica, H. and Fortune, R. D. (2003) A unique pattern of sleep structure is found to be identical at all cortical sites: a neurobiological interpretation. *Cerebral Cortex* **13**: 1044–50.

Mesulam, M. M., Mufson, E. J., Wainer, B. H. and Levey, A. I. (1983a) Central cholinergic pathways in the rat: an overview based on an alternative nomenclature (Ch1–Ch6). *Neuroscience* **10**: 1185–201.

Mesulam, M.-M., Mufson, E. J., Levey, A. I. and Wainer, B. H. (1983b) Cholinergic innervation of cortex by the basal forebrain: cytochemistry and cortical connections of the septal area, diagonal band nuclei, nucleus basalis (substantia innominata), and hypothalamus in the rhesus monkey. *Journal of Comparative Neurology* **214**: 170–97.

Mesulam, M. M., Mufson, E. J., Levey, A. I. and Wainer, B. H. (1984) Atlas of cholinergic neurons in the forebrain and upper brainstem of the macaque based on monoclonal choline acetyltransferase immunohistochemistry and acetylcholinesterase histochemistry. *Neuroscience* **12**: 669–86.

Metherate, R., Cox, C. L. and Ashe, J. H. (1992) Cellular bases of neocortical activation: modulation of neural oscillations by the nucleus basalis and endogenous acetylcholine. *Journal of Neuroscience* **12**: 4701–11.

Meunier, M., Bachevalier, J., Mishkin, M. and Murray, E. A. (1993) Effects on visual recognition of combined and separate ablations of the entorhinal and perirhinal cortex in rhesus monkeys. *Journal of Neuroscience* **13**: 5418–32.

Meunier, M., Hadfield, W., Bachevalier, J. and Murray, E. A. (1996) Effects of rhinal cortex lesions combined with hippocampectomy on visual recognition memory in rhesus monkeys. *Journal of Neurophysiology* **75**: 1190–205.

Miettinen, N., Koivisto, E., Riekkinen, P. and Miettinen, R. (1996) Co-existence of parvalbumin and GABA in non-pyramidal neurons of the rat entorhinal cortex. *Brain Research* **706**: 113–22.

Miettinen, M., Pitkänen, A. and Miettinen, R. (1997) Distribution of calretinin-immunoreactivity in the rat entorhinal cortex: coexistence with GABA. *Journal of Comparative Neurology* **378**: 363–78.

Milad, M. R. and Quirk, G. J. (2002) Neurons in medial prefrontal cortex signal memory for fear extinction. *Nature* **420**: 70–4.

Miller, E. K., Li, L. and Desimone, R. (1993) Activity of neurons in anterior inferior temporal cortex during a short-term memory task. *Journal of Neuroscience* **13**: 1460–78.

Millhouse, O. E. (1986) The intercalated cells of the amygdala. *Journal of Comparative Neurology* **247**: 246–71.

Minamoto, T. and Kimura, M. (2002) Participation of the thalamic CM-Pf complex in attentional orienting. *Journal of Neurophysiology* **87**: 3090–101.

Mineff, E. M. and Weinberg, R. J. (2000) Differential synaptic distribution of AMPA receptor subunits in the ventral posterior and reticular thalamic nuclei of the rat. *Neuroscience* **101**: 969–82.

Mitchell, S. and Ranck, J. B. (1980) Generation of theta rhythm in medial entorhinal cortex of freely moving rats. *Brain Research* **189**: 49–66.

Miyashita, Y. (1993) Inferior temporal cortex: Where visual perception meets memory. *Annual Review of Neuroscience* **16**: 245–63.

Mizusawa, K., Ohkoshi, N. and Sasaki, H. (1988) Degeneration of the thalamus and inferior olives associated with spongiform encephalopathy of the cerebral cortex. *Clinical Neuropathology* **7**: 81–6.

Molinari, M., Minciacchi, D., Bentivoglio, M. and Macchi, G. (1985) Efferent fibers from the motor cortex terminate bilaterally in the thalamus of rats and cats. *Experimental Brain Research* **57**: 305–12.

Mölle, M., Marshall, L., Gais, S. and Born, J. (2002) Grouping of spindle activity during slow oscillations in human non-REM sleep. *Journal of Neuroscience* **22**: 10941–7.

Monckton, J. E. and McCormick, D. A. (2002) Neuromodulatory role of serotonin in the ferret thalamus. *Journal of Neurophysiology* **87**: 2124–36.

Monckton, J. E. and McCormick, D. A. (2003) Comparative physiological and serotoninergic properties of pulvinar neurons in the monkey, cat and ferret. *Thalamus and Related Systems* **2**: 239–52.

Montero, V. (1986) Localization of gamma-aminobutyric acid (GABA) in type 3 cells and demonstration of their source to F2 terminals in the cat lateral geniculate nucleus. *Journal of Comparative Neurology* **254**: 228–45.

Montero, V. (1997) C-*FOS* induction in sensory pathways of rats exploring a novel complex environment: shifts of active thalamic reticular sectors by predominant sensory cues. *Neuroscience* **76**: 1069–81.

Moore, R. Y., Halaris, A. E. and Jones, B. E. (1978) Serotonin neurons of the midbrain raphe: ascending projections. *Journal of Comparative Neurology* **180**: 417–38.

Morgan, M. A. and LeDoux, J. E. (1995) Differential contribution of dorsal and ventral medial prefrontal cortex to the acquisition and extinction of conditioned fear in rats. *Behavioral Neuroscience* **109**: 681–8.

Morison, R. S. and Bassett, D. L. (1945) Electrical activity of the thalamus and basal ganglia in decorticated cats. *Journal of Neurophysiology* **8**: 309–14.

Morison, R. S. and Dempsey, E. W. (1942) Mechanism of thalamocortical augmentation and repetition. *American Journal of Physiology* **138**: 297–308.

Morrison, J. H., and Foote, S. L. (1986) Noradrenergic and serotonergic innervation of cortical, thalamic, and tectal visual structures in old and new world monkeys. *Journal of Comparative Neurology* **243**: 117–38.

Morrison, J. H., Foote, S. L., O'Connor, D. and Bloom, F. E. (1982) Laminar, tangential and regional organization of the noradrenergic innervation of monkey cortex: dopamine-β-hydroxylase immunohistochemistry. *Brain Research Bulletin* **9**: 309–19.

Moruzzi, G. (1966) The functional significance of sleep with particular regard to the brain mechanisms underlying consciousness. In *Brain and Conscious Experience*, ed. J. C. Eccles, pp. 345–79. New York: Springer.

Moruzzi, G. (1972) The sleep-waking cycle. *Ergebnisse der Physiologie* **64**: 1–165.

Moruzzi, G. and Magoun, H. W. (1949) Brain stem reticular formation and activation of the EEG. *Electroencephalography and Clinical Neurophysiology* **1**: 455–73.

Mountcastle, V. B. (1997) The columnar organization of the neocortex. *Brain* **120**: 701–22.

Mountcastle, V. B. (1998) *Perceptual Neuroscience: The Cerebral Cortex*. Cambridge, MA: Harvard University Press.

Mrzljak, L., Pappy, M., Leranth, C. and Goldman-Rakic, P. (1995) Cholinergic synaptic circuitry in the macaque prefrontal cortex. *Journal of Comparative Neurology* **357**: 603–17.

Mulle, C., Steriade, M. and Deschênes, M. (1985) The effects of QX-314 on thalamic neurons. *Brain Research* **333**: 350–4.

Muller, J., Corodimas, K. P., Fridel, Z. and LeDoux, J. E. (1997) Functional inactivation of the lateral and basal nuclei of the amygdala by muscimol infusion prevents fear conditioning to an explicit conditioned stimulus and to contextual stimuli. *Behavioral Neuroscience* **111**: 683–91.

Muller, J. F., Mascagni, F. and McDonald, A. J. (2003) Synaptic connections of distinct interneuronal subpopulations in the rat basolateral amygdalar nucleus. *Journal of Comparative Neurology* **456**: 217–36.

Mumby, D. G., Wood, E. R. and Pinel, J. (1992) Object-recognition memory is only mildly impaired in rats by lesions of the hippocampus and amygdala. *Psychobiology* **20**: 18–27.

Muñoz, A., Huntsman, M. M. and Jones, E. G. (1998) $GABA_B$ receptor gene expression in monkey thalamus. *Journal of Comparative Neurology* **394**: 118–26.

Murakami, M., Kashiwadani, H., Kirino, Y. and Mori, K. (2005) State-dependent sensory gating in olfactory cortex. *Neuron* **46**: 285–96.

Murthy, V. N. and Fetz, E. E. (1992) Coherent 25- to 35-Hz oscillations in the sensorimotor cortex of awake behaving monkeys. *Proceedings of the National Academy of Sciences USA* **89**: 5670–4.

Musil, S. Y. and Olson, C. R. (1988) Organization of cortical and subcortical projections to medial prefrontal cortex in the cat. *Journal of Comparative Neurology* **272**: 219–41.

Musil, S. Y. and Olson, C. R. (1991) Cortical areas in the medial frontal lobe of the cat delineated by quantitative analysis of thalamic afferents. *Journal of Comparative Neurology* **308**: 457–66.

Myers, K. M. and Davis, M. (2002) Behavioral and neural analysis of extinction. *Neuron* **36**: 567–84.

Nadasdy, Z., Hirase, H., Czurko, A., Csicsvari, J. and Buzsáki, G. (1999) Replay and time compression of recurring spike sequences in the hippocampus. *Journal of Neuroscience* **19**: 9497–507.

Nader, K. (2003) Memory traces unbound. *Trends in Neurosciences* **26**: 65–72.

Nader, K., Majidishad, P., Amorapanth, P. and LeDoux, J. E. (2001) Damage to the lateral and central, but not other, amygdaloid nuclei prevents the acquisition of auditory fear conditioning. *Learning and Memory* **8**: 156–63.

Neckelmann, D., Amzica, F. and Steriade, M. (1998) Spike-wave complexes and fast components of cortically generated seizures. III. Synchronizing mechanisms. *Journal of Neurophysiology* **80**: 1480–94.

Nelson, J. P., McCarley, R. W. and Hobson, J. A. (1983) REM sleep burst neurons, PGO waves, and eye movement information. *Journal of Neurophysiology* **50**: 784–97.

Neugebauer, V. and Li, W. D. (2003) Differential sensitization of amygdala neurons to afferent inputs. *Journal of Neurophysiology* **89**: 716–27.

Nicoll, R. A., Malenka R. C. and Kauer, J. A. (1990) Functional comparison of neurotransmitter receptor subtypes in mammalian central nervous system. *Physiological Reviews* **70**: 513–65.

Niedermeyer, E. (1993) Sleep and EEG. In *Electroencephalography: Basic Principles, Clinical Applications and Related Fields* (4th edition), ed. E. Niedermeyer and F. Lopes da Silva, pp. 153–66. Baltimore, MD: Williams & Wilkins.

Nielsen, T. (2000) Cognition in REM and NREM sleep. *Brain and Behavioral Sciences* **23**: 851–66.

Niimi, K., Matsuoka, H., Aisaka, T. and Okada, Y. (1981) Thalamic afferents to the prefrontal cortex in the cat traced with horseradish peroxidase. *Journal für Hirnforschung* **22**: 221–41.

Nisenbaum, E. S., Xu, Z. C. and Wilson, C. J. (1994) Contribution of a slowly inactivating potassium current to the transition to firing of neostriatal spiny projection neurons. *Journal of Neurophysiology* **71**: 1174–89.

Nishimura, Y., Asahi, M., Saitoh, K. *et al.* (2001) Ionic mechanisms underlying burst firing of layer III sensorimotor cortical neurons of the cat: an in vitro slice study. *Journal of Neurophysiology* **86**: 771–81.

Nishiyama, M., Hong, K., Mikoshiba, K., Poo, M. M. and Kato, K. (2000) Calcium stores regulate the polarity and input specificity of synaptic modifications. *Nature* **408**: 554–88.

Nita, D., Steriade, M. and Amzica, F. (2003) Hyperpolarisation rectification in cat lateral geniculate neurons modulated by intact corticothalamic projections. *Journal of Physiology (London)* **552**: 325–32.

Nitecka, L. and Ben-Ari, Y. (1987) Distribution of GABA-like immunoreactivity in the rat amygdaloid complex. *Journal of Comparative Neurology* **266**: 45–55.

Nitecka, L. and Frotscher, M. (1989) Organization and synaptic interconnections of GABAergic and cholinergic elements in the rat amygdaloid nuclei: single- and double-immunolabeling studies. *Journal of Comparative Neurology* **279**: 470–88.

Nowak, L. G., Azouz, R., Sanchez-Vives, M. V., Gray, C. M. and McCormick, D. A. (2003) Electrophysiological classes of cat primary visual cortical neurons in vivo as revealed by quantitative analyses. *Journal of Neurophysiology* **89**: 1541–66.

Nuñez, A., Amzica, F. and Steriade, M. (1992a) Voltage-dependent fast (20–40 Hz) oscillations in long-axoned neocortical neurons. *Neuroscience* **51**: 7–10.

Nuñez, A., Amzica, F. and Steriade, M. (1992b) Intrinsic and synaptically generated delta (1–4 Hz) rhythms in dorsal lateral geniculate neurons and their modulation by light-induced fast (30–70 Hz) events. *Neuroscience* **51**: 269–84.

Nuñez, A., Curró Dossi, R., Contreras, D. and Steriade, M. (1992c) Intracellular evidence for incompatibility between spindle and delta oscillations in thalamocortical neurons of cat. *Neuroscience* **48**: 75–85.

Nuñez, A., Amzica, F. and Steriade, M. (1993) Electrophysiology of cat association cortical neurons *in vivo*: intrinsic properties and synaptic responses. *Journal of Neurophysiology* **70**: 418–30.

Ojima, H. (1994) Terminal morphology and distribution of corticothalamic fibers originating from layers 5 and 6 of cat primary auditory cortex. *Cerebral Cortex* **4**: 646–63.

Öngür, D. and Price, J. L. (2000) The organization of networks within the orbital and medial prefrontal cortex of rats, monkeys and humans. *Cerebral Cortex* **10**: 206–19.

Otani, S., Daniel, H., Roisin, M. P. and Crepel, F. (2003) Dopaminergic modulation of long-term synaptic plasticity in rat prefrontal neurons. *Cerebral Cortex* **13**: 1251–6.

Packard, M. G. and Teather, L. A. (1998) Amygdala modulation of multiple sensory systems: hippocampus and caudate putamen. *Neurobiology of Learning and Memory* **69**: 163–203.

Packard, M. G., Cahill, L. and McGaugh, J. L. (1994) Amygdala modulation of hippocampal-dependent and caudate nucleus-dependent memory processes. *Proceedings of the National Academy of Sciences USA* **91**: 8477–81.

Pagano, R. R., Gault, M. A. and Gault, F. P. (1964) Amygdala activity: a central measure of arousal. *Electroencephalography and Clinical Neurophysiology* **17**: 255–60.

Palva, J. M., Palva, S. and Kaila, K. (2005) Phase synchrony among neuronal oscillations in the human cortex. *Journal of Neuroscience* **25**: 3962–72.

Panula, P., Pirvola, U., Auvinen, S. and Airaksinen, M. S. (1989) Histamine-immunoreactive nerve fibers in the rat brain. *Neuroscience* **28**: 585–610.

Panula, P., Airaksinen, M. S., Pirvola, U. and Kotilainen, E. (1990) A histamine-containing neuronal system in human brain. *Neuroscience* **34**: 127–32.

Pape, H. C. (1996) Queer current and pacemaker: the hyperpolarization-activated cation current in neurons. *Annual Reviews of Physiology* **58**: 299–327.

Pape, H. C. and Driesang, R. B. (1998) Ionic mechanisms of intrinsic oscillations in neurons of the basolateral amygdaloid complex. *Journal of Neurophysiology* **79**: 217–26.

Pape, H. C. and Mager, R. (1992) Nitric oxide controls oscillatory activity in thalamocortical neurons. *Neuron* **9**: 441–8.

Pape, H. C. and McCormick, D. A. (1995) Electrophysiological and pharmacological properties of interneurons in the cat dorsal lateral geniculate nucleus. *Neuroscience* **68**: 1105–25.

Pape, H. C., Budde, T., Mager, R. and Kisvárday, Z. F. (1994) Prevention of Ca^{2+}-mediated action potentials in GABAergic local circuit neurones of rat thalamus by a transient K^+ current. *Journal of Physiology (London)* **478**: 403–22.

Pape, H. C., Paré, D. and Driesang, R. B. (1998) Two types of intrinsic oscillations in neurons of the lateral and basolateral nuclei of the amygdala. *Journal of Neurophysiology* **79**: 205–16.

Paquet, M. and Smith, Y. (2000) Presynaptic NMDA receptor subunit immunoreactivity in GABAergic terminals in rat brain. *Journal of Comparative Neurology* **423**: 330–47.

Paré, D. and Collins, D. R. (2000) Neuronal correlates of fear in the lateral amygdala: multiple extracellular recordings in conscious cats. *Journal of Neuroscience* **20**: 2701–10.

Paré, D. and Gaudreau, H. (1996) Projection cells and interneurons of the lateral and basolateral amygdala: distinct firing patterns and differential

relation to theta and delta rhythms in conscious cats. *Journal of Neuroscience* **16**: 3334–50.
Paré, D. and Lang, E. J. (1998) Calcium electrogenesis in neocortical pyramidal neurons *in vivo*. *European Journal of Neuroscience* **10**: 3164–70.
Paré, D. and Llinás, R. (1995) Intracellular study of direct entorhinal inputs to field CA1 in the isolated guinea pig brain in vitro. *Hippocampus* **5**: 115–19.
Paré, D. and Smith, Y. (1993a) Distribution of GABA immunoreactivity in the amygdaloid complex of the cat. *Neuroscience* **57**: 1061–76.
Paré, D. and Smith, Y. (1993b) The intercalated cell masses project to the central and medial nuclei of the amygdala in cats. *Neuroscience* **57**: 1077–90.
Paré, D. and Smith, Y. (1994) GABAergic projection from the intercalated cell masses of the amygdala to the basal forebrain in cats. *Journal of Comparative Neurology* **344**: 33–49.
Paré, D. and Smith, Y. (1996) Thalamic collaterals of corticostriatal axons: their termination field and synaptic targets in cats. *Journal of Comparative Neurology* **372**: 551–67.
Paré, D. and Steriade, M. (1990) Control of mamillothalamic axis by brainstem cholinergic laterodorsal tegmental afferents: possible involvement in mnemonic processes. In *Brain Cholinergic Systems*, ed. M. Steriade and D. Biesold, pp. 337–54. Oxford: Oxford University Press.
Paré, D., Steriade, M., Deschênes, M. and Oakson, G. (1987) Physiological properties of anterior thalamic nuclei, a group devoid of inputs from the reticular thalamic nucleus. *Journal of Neurophysiology* **57**: 1669–85.
Paré, D., Smith, Y., Parent, A. and Steriade, M. (1988) Projections of upper brainstem cholinergic and non-cholinergic neurons of cat to intralaminar and reticular thalamic nuclei. *Neuroscience* **25**: 69–88.
Paré, D., Smith, Y., Parent, A. and Steriade, M. (1989) Neuronal activity of identified posterior hypothalamic neurons projecting to the brainstem peribrachial area of the cat. *Neuroscience Letters* **107**: 145–50.
Paré, D., Curró Dossi, R., Datta, S. and Steriade, M. (1990a) Brainstem genesis of reserpine-induced ponto-geniculo-occipital waves: an electrophysiological and morphological investigation. *Experimental Brain Research* **81**: 533–44.
Paré, D., Steriade, M., Deschênes, M. and Bouhassira, D. (1990b) Prolonged enhancement of anterior thalamic synaptic responsiveness by stimulation of a brainstem cholinergic group. *Journal of Neuroscience* **10**: 20–33.
Paré, D., Curró Dossi, R. and Steriade, M. (1991) Three types of inhibitory postsynaptic potentials generated by interneurons in the anterior thalamic complex of cat. *Journal of Neurophysiology* **66**: 1190–204.
Paré, D., Dong. J. and Gaudreau, H. (1995a) Amygdalo-entorhinal relations and their reflection in the hippocampal formation: generation of sharp sleep potentials. *Journal of Neuroscience* **15**: 2482–503.
Paré, D., Pape, H. C. and Dong, J. (1995b) Bursting and oscillating neurons of the cat basolateral amygdaloid complex in vivo: electrophysiological properties and morphological features. *Journal of Neurophysiology* **74**: 1179–91.
Paré, D., Smith, Y. and Paré, J. F. (1995c) Intra-amygdaloid projections of the basolateral and basomedial nuclei in the cat: *Phaseolus vulgaris*-leucoagglutinin anterograde tracing at the light and electron microscopic level. *Neuroscience* **69**: 567–83.
Paré, D., Shink, E., Gaudreau, H., Destexhe, A. and Lang, E. J. (1998a) Impact of spontaneous synaptic activity on the resting properties of cat

neocortical pyramidal neurons in vivo. *Journal of Neurophysiology* **79**: 1450–60.

Paré, D., Lang, E. J. and Destexhe, A. (1998b) Inhibitory control of somatodendritic interactions underlying action potentials in neocortical pyramidal neurons *in vivo*: an intracellular and computational study. *Neuroscience* **84**: 377–402.

Paré, D., Collins, D. R. and Pelletier, J. G. (2002). Amygdala oscillations and the consolidation of emotional memories. *Trends in Cognitive Sciences* **6**: 306–14.

Paré, D., Quirk, G. J. and LeDoux, J. E. (2004) New vistas on amygdala networks in conditioned fear. *Journal of Neurophysiology* **92**: 1–9.

Parent, A., Descarries, L. and Beaudet, A. (1981) Organization of ascending serotonin systems in the adult rat brain. A radioautographic study after intraventricular administration of (^{3}H)5-hydroxytryptamine. *Neuroscience* **6**: 115–38.

Parent, A., Paré, D., Smith, Y., and Steriade, M. (1988) Basal forebrain cholinergic and non-cholinergic projections to the thalamus and brainstem in cats and monkeys. *Journal of Comparative Neurology* **277**: 281–301.

Parent, M. B., Quirarte, G. L., Cahill, L. and McGaugh, J. L. (1995) Spared retention of inhibitory avoidance learning after postraining amygdala lesions. *Behavioral Neuroscience* **109**: 803–7.

Parmentier, R., Ohtsu, H., Djebbara-Hannas, Z. *et al.* (2002) Anatomical, physiological, and pharmacological characteristics of histidine decarboxylase knock-out mice: evidence for the role of brain histamine in behavioral and sleep-wake control. *Journal of Neuroscience* **22**: 7695–711.

Pavlides, C. and Winson, J. (1989) Influences of hippocampal place cell firing in the awake state on the activity of these cells during subsequent sleep episodes. *Journal of Neuroscience* **9**: 2907–18.

Pavlides, C., Greenstein, Y. J., Goudman, M. and Winson, J. (1988) Long-term potentiation in the dentate gyrus is induced preferentially on the positive phase of the theta-rhythm. *Brain Research* **439**: 383–7.

Pavlov, I. P. (1923) 'Innere Hemmung' der bedingten Reflexe und der Schlaf – ein und derselbe Prozess. *Skandinavische Archive für Physiologie* **44**: 42–58.

Pavlov, I. P. (1927) *Conditioned Reflexes: An Investigation of the Physiological Activity of the Cerebral Cortex*. London: Oxford University Press.

Paxinos, G. and Watson, C. (1986) *The Rat Brain in Stereotaxic Coordinates*. New York: Academic Press.

Pedroarena, C. and Llinás, R. (1997) Dendritic calcium conductances generate high-frequency oscillation in thalamocortical neurons. *Proceedings of the National Academy of Sciences USA* **94**: 724–8.

Pelletier, J. G. and Paré, D. (2002) Uniform range of conduction times from the lateral amygdala to distributed perirhinal sites. *Journal of Neurophysiology* **87**: 1213–21.

Pelletier, J. G., Apergis, J. and Paré, D. (2004) Low probability transmission of neocortical and entorhinal impulses through the perirhinal cortex. *Journal of Neurophysiology* **91**: 2079–89.

Pelletier, J. G., Apergis-Schoute, J. and Paré, D. (2005a) Interaction between amygdala and neocortical inputs in the perirhinal cortex. *Journal of Neurophysiology* **94**: 1837–48.

Pelletier, J. G., Likhtik, E., Filali, M. and Paré, D. (2005b) Lasting increases in basolateral amygdala activity after emotional arousal: implications for

facilitated consolidation of emotional memories. *Learning and Memory* **12**: 96–102.

de la Peña, E. and Geijo-Barrientos, E. (1996) Laminar localization, morphology, and physiological properties of pyramidal neurons that have low-threshold calcium current in the guinea-pig medial frontal cortex. *Journal of Neuroscience* **16**: 5301–11.

Pennartz, C. M., Uylings, H. B., Barnes, C. A. and McNaughton, B. L. (2002) Memory reactivation and consolidation during sleep: from cellular mechanisms to human performance. *Progress in Brain Research* **138**: 143–66.

Pennartz, C. M., Lee, E., Verheul, J. *et al.* (2004) The ventral striatum in off-line processing: ensemble reactivation during sleep and modulation by hippocampal ripples. *Journal of Neuroscience* **24**: 6446–56.

Perez-Velazquez, J. L. and Carlen, P. L. (2000) Gap junctions, synchrony and seizures. *Trends in Neurosciences* **23**: 68–74.

Perreault, M. C., Qin, Y., Heggelund, P. and Zhu, J. J. (2003) Postnatal development of GABAergic signalling in the rat lateral geniculate nucleus: presynaptic dendritic mechanisms. *Journal of Physiology (London)* **546**: 137–48.

Petersen, C. C. H., Hahn, T. T. G., Mehta, M., Grinvald, A. and Sakmann, B. (2003) Interaction of sensory responses with spontaneous depolarization in layer 2/3 barrel cortex. *Proceedings of the National Academy of Sciences USA* **100**: 13638–43.

Petrides, M. and Pandya, D. N. (1984) Projections to frontal cortex from posterior parietal region in rhesus monkeys. *Journal of Comparative Neurology* **228**: 105–16.

Petrovich, G. D. and Swanson, L. W. (1997) Projections from the lateral part of the central amygdalar nucleus to the postulated fear conditioning circuit. *Brain Research* **763**: 247–54.

Petsche, H., Stumpf, C. and Gogolak, G. (1962) The significance of the rabbit's septum as a relay station between the midbrain and the hippocampus. I. The control of hippocampus arousal activity by the septum cells. *Electroencephalography and Clinical Neurophysiology* **14**: 202–11.

Petsche, H., Pockberger, H. and Rappelsberger, P. (1984) On the search for the sources of the electroencephalogram. *Neuroscience* **11**: 1–27.

Peyron, C., Tighe, D. K., van der Pol, A. N. *et al.* (1998) Neurons containing hypocretin (orexin) project to multiple neuronal systems. *Journal of Neuroscience* **18**: 9996–10015.

Phelps, E. A. (2004) Human emotion and memory: interactions of the amygdala and hippocampal complex. *Current Opinion in Neurobiology* **14**: 198–202.

Phelps, E. A., Delgado, M. R., Nearing, K. I. and LeDoux, J. E. (2004) Extinction learning in humans: role of the amygdala and vmPFC. *Neuron* **43**: 897–905.

Pickel, V. M., Joh, T. H. and Reis, D. J. (1977) A serotonergic innervation of noradrenergic neurons in nucleus locus coeruleus: demonstration by immunocytochemical localization of the transmitter specific enzymes tyrosine and tryptophan hydroxylase. *Brain Research* **131**: 197–214.

Pickel, V. M., Van, B. E., Chan, J. and Cestari, D. M. (1995) Amygdala efferents form inhibitory-type synapses with a subpopulation of catecholaminergic neurons in the rat nucleus tractus solitarius. *Journal of Comparative Neurology* **362**: 510–23.

Pickel, V. M., Van, B. E., Chan, J. and Cestari, D. M. (1996) GABAergic neurons in rat nuclei of solitary tracts receive inhibitory-type synapses from

amygdaloid efferents lacking detectable GABA-immunoreactivity. *Journal of Neuroscience Research* **44**: 446–58.

Pikkarainen, M., Rönkkö, S., Savander, V., Insausti, R. and Pitkänen, A. (1999) Projections from the lateral, basal, and accessory basal nuclei of the amygdala to the hippocampal formation in rat. *Journal of Comparative Neurology* **403**: 229–60.

Pinault, D., Smith, Y. and Deschênes, M. (1997) Dendrodendritic and axoaxonic synapses in the thalamic reticular nucleus of the adult rat. *Journal of Neuroscience* **17**: 3215–33.

Pinault, D., Leresche, N., Charpier, S. *et al.* (1998) Intracellular recordings in thalamic neurones during spontaneous spike and wave discharges in rats with absence epilepsy. *Journal of Physiology (London)* **509**: 449–56.

Pinto, A. and Sesack, S. R. (2002) Prefrontal cortex projection to the rat amygdala: ultrastructural relationship to dopamine D1 and D2 receptors. *Society for Neuroscience Abstracts* **28**: 587.

Pinto, A., Fuentes, C. and Paré, D. (2006) Feedforward inhibition regulates perirhinal transmission of neocortical inputs to the entorhinal cortex: Ultrastructural study in guinea pigs. *Journal of Comparative Neurology* **495**: 722–34.

Pitkänen, A. (2000) Connectivity of the rat amygdaloid complex. In *The Amygdala: A Functional Analysis*, ed. J. P. Aggleton, pp. 31–115. Oxford: Oxford University Press.

Pitkänen, A. and Amaral, D. G. (1993a) Distribution of calbindin-D28k immunoreactivity in the monkey temporal lobe: the amygdaloid complex. *Journal of Comparative Neurology* **331**: 199–224.

Pitkänen, A. and Amaral, D. G. (1993b) Distribution of parvalbumin-immunoreactive cells and fibers in the monkey temporal lobe: the amygdaloid complex. *Journal of Comparative Neurology* **331**: 14–36.

Pitkänen, A. and Amaral, D. G. (1994) The distribution of GABAergic cells, fibers, and terminals in the monkey amygdaloid complex: an immunohistochemical and in situ hybridization study. *Journal of Neuroscience* **14**: 2200–24.

Pitkänen, A., Stefanacci, L., Farb, C. R. *et al.* (1995) Intrinsic connections of the rat amygdaloid complex: projections originating in the lateral nucleus. *Journal of Comparative Neurology* **356**: 288–310.

Pitkänen, A., Savander, V. and LeDoux, J. E. (1997) Organization of intra-amygdaloid circuitries in the rat: an emerging framework for understanding functions of the amygdala. *Trends in Neurosciences* **20**: 517–23.

Pitkänen, A., Pikkarainen, M., Nurminen, N. and Ylinen, A. (2000) Reciprocal connections between the amygdala and the hippocampal formation, perirhinal cortex, and postrhinal cortex in rat. *Annals of the New York Academy of Sciences* **911**: 369–91.

Pitkänen, A., Kelly, J. L. and Amaral, D. G. (2002) Projections from the lateral, basal, and accessory basal nuclei of the amygdala to the entorhinal cortex in the macaque monkey. *Hippocampus* **12**: 186–205.

Pivik, T. and Foulkes, D. (1968) NREM mentation: relation to personality, orientation time and time of night. *Journal of Consultation Clinical Psychology* **32**: 144–51.

Plihal, W. and Born, J. (1997) Effects of early and late nocturnal sleep on declarative and procedural memory. *Journal of Cognitive Neuroscience* **9**: 534–47.

Plum, F. (1991) Coma and related global disturbances of the human conscious state. In *Cerebral Cortex*, vol. 9 (*Normal and Altered States of Function*), ed. A. Peters and E. G. Jones, pp. 359–425. New York: Plenum.

Poggio, G. F. and Mouncastle, V. B. (1960) A study in the functional contributions of the lemniscal and spinothalamic systems to somatic sensibility: central nervous mechanisms in pain. *Bulletin of the Johns Hopkins Hospital* **106**: 266–316.

Popescu, A. T., Saghyan, A. and Paré, D. (2005) Amygdala activation opens temporal windows of plasticity in the cortico-striatal pathway. *Society for Neuroscience Abstracts* **31**: 651–4.

Power, A. E. (2004) Slow-wave sleep, acetylcholine, and memory consolidation. *Proceedings of the National Academy of Sciences USA* **101**: 1795–6.

Preuss, T. M. and Goldman-Rakic, P. S. (1987) Crossed corticothalamic and thalamocortical connections of macaque prefrontal cortex. *Journal of Comparative Neurology* **257**: 269–81.

Pritzel, M. and Markowitsch, H. J. (1981) Cortico-prefrontal afferents in the guinea pig. *Brain Research Bulletin* **7**: 427–34.

Puil, E., Meiri, H. and Yarom, Y. (1994) Resonant behavior and frequency preferences of thalamic neurons. *Journal of Neurophysiology* **71**: 575–82.

Purpura, D. P. (1970) Operations and processes in thalamic and synaptically related neural subsystems. In *The Neuroscience: Second Study Program*, ed. F. O. Schmitt, pp. 458–470. New York: Rockefeller University Press.

Purpura, D. P., McMurtry, J. G. and Maekawa, K. (1966) Synaptic events in ventrolateral thalamic neurons during suppression of recruiting responses by brain stem reticular stimulation. *Brain Research* **1**: 63–76.

Quirk, G. J., Repa, J. C. and LeDoux, J. E. (1995) Fear conditioning enhances short-latency auditory responses of lateral amygdala neurons: Parallel recordings in the freely behaving rat. *Neuron* **15**: 1029–39.

Quirk, G. J., Russo, G. K., Barron, J. L. and Lebron, K. (2000) The role of ventromedial prefrontal cortex in the recovery of extinguished fear. *Journal of Neuroscience* **20**: 6225–31.

Quirk, G. J., Likhtik, E., Pelletier, J. G. and Paré, D. (2003) Stimulation of medial prefrontal cortex decreases the responsiveness of central amygdala output neurons. *Journal of Neuroscience* **23**: 8800–7.

Raghavachari, S., Kahana, M. J., Rizzuto, D. S. *et al.* (2001) Gating of human theta oscillations by a working memory task. *Journal of Neuroscience* **21**: 3175–83.

Rainnie, D. G., Asprodini, E. K. and Shinnick-Gallagher, G. P. (1991) Inhibitory transmission in the basolateral amygdala. *Journal of Neurophysiology* **66**: 999–1009.

Rainnie, D. G., Asprodini, E. K. and Shinnick-Gallagher, G. P. (1993) Intracellular recordings from morphologically identified neurons of the basolateral amygdala. *Journal of Neurophysiology* **69**: 1350–62.

Ramm, P. and Smith, C. T. (1990) Rates of cerebral protein synthesis are linked to slow wave sleep in the rat. *Physiology and Behavior* **48**: 749–53.

Rao, Z. R., Shiosaka, S. and Tohyama, M. (1987) Origin of cholinergic fibers in the basolateral nucleus of the amygdaloid complex using sensitive double-labeling technique of retrograde biotinized tracer and immunocytochemistry. *Journal für Hirnforschung* **28**: 553–60.

Rash, J. E., Staines, W. A., Yasumura, T. *et al.* (2000) Immunogold evidence that neuronal gap junctions in adult rat brain and spinal cord contain

connexin-36 but not connexin-32 or connexin-43. *Proceedings of the National Academy of Sciences USA* **97**: 7573–8.

Rasler, F. E. (1984) Behavioral and electrophysiological manifestations of bombesin: excessive grooming and elimination of sleep. *Brain Research* **321**: 187–98.

Rasmusson, D. D., Clow, K. and Szerb, J. C. (1994) Modification of neocortical acetylcholine release and electroencephalogram desynchronization due to brainstem stimulation by drugs applied to the basal forebrain. *Neuroscience* **60**: 665–77.

Rasmusson, D. D., Szerb, J. C. and Jordan, J. L. (1996) Differential effects of α-amino-3-hydroxy-5-methyl-4-isoxazole propionic acid and N-methyl-D-aspartate receptor antagonists applied to the basal forebrain on cortical acetylcholine release and EEG desynchronization. *Neuroscience* **72**: 419–27.

Rechtschaffen, A. (1998) Current perspective on the function of sleep. *Perspectives in Biology and Medicine* **41**: 359–90.

Rechtschaffen, A., Verdone, P. and Wheaton, J. (1963) Reports of mental activity during sleep. *Canadian Journal of Psychiatry* **8**: 409–14.

Reinagel, P., Godwin, D., Sherman, S. M. and Koch, C. (1999) Encoding of visual information by LGN bursts. *Journal of Neurophysiology* **81**: 2558–69.

Rempel-Clower, N. L. and Barbas, H. (1998) Topographic organization of connections between the hypothalamus and prefrontal cortex in the rhesus monkey. *Journal of Comparative Neurology* **398**: 393–419.

Repa, J. C., Muller, J., Apergis, J. *et al.* (2001) Two different lateral amygdala cell populations contribute to the initiation and storage of memory. *Nature Neuroscience* **4**: 724–31.

Rescorla, R. A. (2004) Spontaneous recovery. *Learning and Memory* **11**: 501–9.

Ressler, K. J., Rothbaum, B. O., Tannenbaum, L. *et al.* (2004) Cognitive enhancers as adjuncts to psychotherapy: use of D-cycloserine in phobic individuals to facilitate extinction of fear. *Archives of General Psychiatry* **61**: 1136–44.

Ribary, U., Ioannides, A. A., Singh, K. D. *et al.* (1991) Magnetic field tomography of coherent thalamocortical 40-Hz oscillations in humans. *Proceedings of the National Academy of Sciences USA* **88**: 11037–41.

Rice, D. P. and Miller, L. S. (1995) The economic burden of affective disorders. *British Journal of Psychiatry* Suppl. **27**: 34–42.

Richardson, M. P., Strange, B. A. and Dolan, R. J. (2004) Encoding of emotional memories depends on amygdala and hippocampus and their interactions. *Nature Neuroscience* **7**: 278–85.

Riches, I. P., Wilson, F. A. and Brown, M. W. (1991) The effects of visual stimulation and memory on neurons of the hippocampal formation and the neighboring parahippocampal gyrus and inferior temporal cortex of the primate. *Journal of Neuroscience* **11**: 1763–79.

Rinzel, J., Terman, D., Wang, X. J. and Ermentrout, B. (1998) Propagating activity patterns in large-scale inhibitory neuronal networks. *Science* **279**: 1351–5.

Robbins, T. W. and Everitt, B. J. (1995) Arousal systems and attention. In *The Cognitive Neurosciences*, ed. M. S. Gazzaniga, pp. 703–20. Cambridge, MA: MIT Press.

Robinson, T. E. (1980) Hippocampal rhythmic slow activity (RSA; theta): a critical analysis of selected studies and discussion of possible species-differences. *Brain Research* **203**: 69–101.

Roffwarg, H. P., Muzio, J. N. and Dement, W. C. (1966) Ontogenetic development of the human sleep-dream cycle. *Science* **152**: 604–19.

Rogan, M. T. and LeDoux, J. E. (1995) LTP is accompanied by commensurate enhancement of auditory-evoked responses in a fear conditioning circuit. *Neuron* **15**: 127–36.

Rogan, M. T., Stäubli, U. V. and LeDoux, J. E. (1997) Fear conditioning induces associative long-term potentiation in the amygdala. *Nature* **390**: 604–7.

Rolls, E. T., Miyashita, Y., Cahusac, P. M. B. *et al.* (1989) Hippocampal neurons in the monkey with activity related to the place in which a stimulus is shown. *Journal of Neuroscience* **9**: 1835–45.

Rolls, E. T., Cahusac, P., Feigenbaum, J. D. and Miyashita, Y. (1993) Responses of single neurons in the hippocampus of the macaque related to recognition memory. *Experimental Brain Research* **93**: 299–306.

Rolls, E. T., Inoue, K. and Browning, A. (2003) Activity of primate subgenual cingulate cortex neurons is related to sleep. *Journal of Neurophysiology* **90**: 134–42.

Romanski, L. M., Clugnet, M. C., Bordi, F. and LeDoux, J. E. (1993) Somatosensory and auditory convergence in the lateral nucleus of the amygdala. *Behavioral Neuroscience* **107**: 444–50.

Room, P. and Groenewegen, H. J. (1986a) Connections of the parahippocampal cortex. I. Cortical afferents. *Journal of Comparative Neurology* **251**: 415–50.

Room, P. and Groenewegen, H. J. (1986b) Connections of the parahippocampal cortex in the cat. II. Subcortical afferents. *Journal of Comparative Neurology* **251**: 451–73.

Room, P., Russchen, F. T., Groenewegen, H. J. and Lohman, A. H. (1985) Efferent connections of the prelimbic (area 32) and the infralimbic (area 25) cortices: an anterograde tracing study in the cat. *Journal of Comparative Neurology* **242**: 40–55.

Roozendaal, B. (2000) Glucocorticoids and the regulation of memory consolidation. *Psychoneuroendocrinology* **25**: 213–38.

Roozendaal, B. and McGaugh, J. L. (1996a) Amygdaloid nuclei lesions differentially affect glucocorticoid-induced memory enhancement in an inhibitory avoidance task. *Neurobiology of Learning and Memory* **65**: 1–8.

Roozendaal, B. and McGaugh, J. L. (1996b) The memory-modulatory effects of glucocorticoids depend on an intact stria terminalis. *Brain Research* **709**: 243–50.

Ropert, N. and Steriade, M. (1981) Input-output organization of the midbrain reticular core. *Journal of Neurophysiology* **46**: 17–31.

Rosanova, M. and Timofeev, I. (2005) Neuronal mechanisms mediating the variability of somatosensory evoked potentials during sleep oscillations in cats. *Journal of Physiology (London)* **562**: 569–82.

Rose, J. E. and Woolsey, C. N. (1948) The orbitofrontal cortex and its connections with the mediodorsal nucleus in rabbit, sheep and cat. *Publications on Research of Nervous and Mental Disease* **27**: 210–32.

Rosen, J. B., Hitchcock, J. M., Sananes, C. B., Miserendino, M. and Davis, M. (1991) A direct projection from the central nucleus of the amygdala to the acoustic startle pathway: anterograde and retrograde tracing studies. *Behavioral Neuroscience* **105**: 817–25.

Rosene, D. L. and Van Hoesen, G. W. (1977) Hippocampal efferents reach widespread areas of cerebral cortex and amygdala in the rhesus monkey. *Science* **198**: 315–17.

Rosenkranz, J. A. and Grace, A. A. (1999) Modulation of basolateral amygdala neuronal firing and afferent drive by dopamine receptor activation in vivo. *Journal of Neuroscience* **19**: 11027–39.

Rosenkranz, J. A. and Grace, A. A. (2001) Dopamine attenuates prefrontal cortical suppression of sensory inputs to the basolateral amygdala of rats. *Journal of Neuroscience* **21**: 4090–103.

Rosenkranz, J. A. and Grace, A. A. (2002) Dopamine-mediated modulation of odour-evoked amygdala potentials during Pavlovian conditioning. *Nature* **417**: 282–7.

Rossi, G., Macchi, G., Porro, M. *et al.* (1998) Fatal familial insomnia. Genetic, neuropathologic, and biochemical study of a patient from a new Italian kindred. *Neurology* **50**: 688–92.

Roth, M., Shaw, J. and Green, J. (1956) The form, voltage distribution and physiological significance of the K-complex. *Electroencephalography and Clinical Neurophysiology* **8**: 385–402.

Rothbaum, B. O. and Davis, M. (2003) Applying learning principles to the treatment of post-trauma reactions. *Annals of the New York Academy of Sciences* **1008**: 112–21.

Rougeul-Buser, A., Bouyer, J. J., Montaron, M. F. and Buser, P. (1983) Patterns of activities in the ventrobasal thalamus and somatic cortex SI during behavioural immobility in the awake cat: focal waking rhythms. *Experimental Brain Research* Suppl. **7**: 69–87.

Rowell, P. P., Volk, K. A., Li, J. and Bickford, M. E. (2003) Investigations of the cholinergic modulation of GABA release in rat thalamic slices. *Neuroscience* **116**: 447–53.

Roy, J. P., Clercq, M., Steriade, M. and Deschênes, M. (1984) Electrophysiology of neurons of the lateral thalamic nuclei in cat: mechanisms of long-lasting hyperpolarizations. *Journal of Neurophysiology* **51**: 1220–35.

Royer, S. and Paré, D. (2002) Bidirectional synaptic plasticity in intercalated amygdala neurons and the extinction of conditioned fear responses. *Neuroscience* **115**: 455–62.

Royer, S. and Paré, D. (2003) Conservation of total synaptic weights via inverse homo- vs. heterosynaptic LTD and LTP. *Nature* **422**: 518–22.

Royer, S., Martina, M. and Paré, D. (1999) An inhibitory interface gates impulse traffic between the input and output stations of the amygdala. *Journal of Neuroscience* **19**: 10575–83.

Royer, S., Martina, M. and Paré, D. (2000a) Bistable behavior of inhibitory neurons controlling impulse traffic through the amygdala: role of a slowly deinactivating K^+ current. *Journal of Neuroscience* **20**: 9034–9.

Royer, S., Martina, M. and Paré, D. (2000b) Polarized synaptic interactions between intercalated neurons of the amygdala. *Journal of Neurophysiology* **83**: 3509–18.

Ruch-Monachon, M. A., Jalfre, M. and Haefeley, W. (1976) Drugs and PGO waves in the lateral geniculate body of the curarized rat. *Archives Internationales de Pharmacodynamie et Thérapie* **219**: 251–346.

Rudolph, M. and Destexhe, A. (2003) The discharge variability of neocortical neurons during high-conductance states. *Neuroscience* **119**: 855–73.

Rudy, B. and McBain, C. J. (2001) Kv3 channels: voltage-gated K^+ channels designed for high-frequency repetitive firing. *Trends in Neurosciences* **24**: 517–26.

Russchen, F. T. (1982a) Amygdalopetal projections in the cat. I. Cortical afferent connections. A study with retrograde and anterograde tracing techniques. *Journal of Comparative Neurology* **206**: 159–79.

Russchen, F. T. (1982b) Amygdalopetal projections in the cat. II. Subcortical afferent connections. A study with retrograde tracing techniques. *Journal of Comparative Neurology* **207**: 157–76.

Ruth, R. E., Collier, T. J. and Routtenberg, A. (1982) Topography between the entorhinal cortex and the dentate septotemporal axis in rats: I. Medial and intermediate entorhinal projecting cells. *Journal of Comparative Neurology* **209**: 69–78.

Rye, D. B., Saper, C. B., Lee, H. J. and Wainer, B. H. (1987) Pedunculopontine tegmental nucleus of the rat: cytoarchitecture, cytochemistry, and some extrapyramidal connections of the mesopontine tegmentum. *Journal of Comparative Neurology* **259**: 483–528.

Sacchetti, B., Lorenzini, C. A., Baldi, E., Tassoni, G. and Bucherelli, C. (1999) Auditory thalamus, dorsal hippocampus, basolateral amygdala, and perirhinal cortex role in the consolidation of conditioned freezing to context and to acoustic conditioned stimulus in the rat. *Journal of Neuroscience* **19**: 9570–8.

Sainsbury, R. S. (1998) Hippocampal theta: a sensory-inhibition theory of function. *Neuroscience and Biobehavioral Reviews* **22**: 237–41.

Sakai, K. (1985) Anatomical and physiological basis of paradoxical sleep. In *Brain Mechanisms of Sleep*, ed. D. J. McGinty, A. Morrison, R. Drucker-Colin and P. L. Parmeggiani, pp. 111–37. New York: Raven.

Sakai, K. and Crochet, S. (2001) Differentiation of presumed serotonergic dorsal raphe neurons in relation to behavior and wake-sleep states. *Neuroscience* **104**: 1141–55.

Sakai, K. and Jouvet, M. (1980) Brainstem PGO-on cells projecting directly to the cat lateral geniculate nucleus. *Brain Research* **194**: 500–5.

Sakai, K., Salvert, D., Touret, M. and Jouvet, M. (1977a) Afferent connections of the nucleus raphe dorsalis in the cat as visualized by the horseradish peroxidase technique. *Brain Research* **137**: 11–35.

Sakai, K., Touret, M., Salvert, D., Leger, L. and Jouvet, M. (1977b) Afferent projections to the cat locus coeruleus as visualized by the horseradish peroxidase technique. *Brain Research* **119**: 21–41.

Sakai, K., El Mansari, M., Lin, J. S., Zhang, G. and Vanni-Mercier, F. (1990) The posterior hypothalamus in the regulation of wakefulness and paradoxical sleep. In *The Diencephalon and Sleep*, ed. M. Mancia and G. Marini, pp. 171–98. New York: Raven.

Sakakura, H. (1968) Spontaneous and evoked unitary activities of cat lateral geniculate neurons in sleep and wakefulness. *Japanese Journal of Physiology* **18**: 23–42.

Salami, M., Itami, C., Tsumoto, T. and Kimura, F. (2003). Change in conduction velocity by regional myelination yields constant latency irrespective of distance between thalamus and cortex. *Proceedings of the National Academy of Sciences USA* **100**: 6174–9.

Salinas, J. A., Introini-Collison, I. B., Dalmaz, C. and McGaugh, J. L. (1997) Posttraining intraamygdala infusions of oxotremorine and propranolol modulate storage of memory for reductions in reward magnitude. *Neurobiology of Learning and Memory* **68**: 51–9.

Sallanon, M., Denoyer, M., Kitahama, K., Aubert, C., Gay, N. and Jouvet, M. (1989) Long-lasting insomnia induced by preoptic lesions and its transient

reversal by muscimol injection into the posterior hypothalamus in the cat. *Neuroscience* **32**: 669–83.

Salt, T. E. (1989) Gamma-aminobutyric acid and afferent inhibition in the cat and rat ventrobasal thalamus. *Neuroscience* **28**: 17–26.

Samson, R. D. and Paré, D. (2005) Activity-dependent synaptic plasticity in the central nucleus of the amygdala. *Journal of Neuroscience* **25**: 1847–55.

Sanchez, R. and Leonard, C. S. (1996) NMDA-receptor-mediated synaptic currents in guinea pig laterodorsal tegmental neurons in vitro. *Journal of Neurophysiology* **76**: 1101–11.

Sanchez-Vives, M. V. and McCormick, D. A. (1997) Functional properties of perigeniculate inhibition of dorsal lateral geniculate nucleus thalamocortical neurons *in vitro*. *Journal of Neuroscience* **17**: 8880–93.

Sanchez-Vives, M. V. and McCormick, D. A. (2000) Cellular and network mechanisms of rhythmic recurrent activity in neocortex. *Nature Neuroscience* **3**: 1027–34.

Sanchez-Vives, M. V., Bal, T. and McCormick, D. A. (1997) Inhibitory interactions between perigeniculate GABAergic neurons. *Journal of Neuroscience* **17**: 8894–908.

Sanders, M. J., Wiltgen, B. J. and Fanselow, M. S. (2003) The place of the hippocampus in fear conditioning. *European Journal of Pharmacology* **463**: 217–23.

Santini, E., Ge, H., Ren, K., Pena de Ortiz, S. and Quirk, G. J. (2004) Consolidation of fear extinction requires protein synthesis in the medial prefrontal cortex. *Journal of Neuroscience* **24**: 5704–10.

Saper, C. B. (1985) Organization of cerebral cortical afferent systems in the rat. II. Hypothalamocortical projections. *Journal of Comparative Neurology* **237**: 21–46.

Saper, C. B. (1987) Diffuse cortical projection systems: anatomical organization and role in cortical function. In *Handbook of Physiology, The Nervous System*, sect. 1, vol. 5, ed. V. B. Moun castle and F. Plum, pp. 169–210. Bethesda, MD: American Physiological Society.

Saper, C. B., Standaert, D. G., Currie, M. G., Schwartz, D., Geller, D. M. and Needleman, P. (1985) Atriopeptin-immunoreactive neurons in the brain: presence in cardiovascular regulatory areas. *Science* **227**: 1047–9.

Sarter, M. and Bruno, J. P. (2000) Cortical cholinergic inputs mediating arousal, attentional processing and dreaming: differential afferent regulation of the basal forebrain by telencephalic and brainstem afferents. *Neuroscience* **95**: 933–52.

Sarter, M. and Markowitsch, H. J. (1983) Convergence of basolateral amygdaloid and mediodorsal thalamic projections in different areas of the frontal cortex in the rat. *Brain Research Bulletin* **10**: 607–22.

Sarter, M. and Markowitsch, H. J. (1984) Collateral innervation of the medial and lateral prefrontal cortex by amygdaloid, thalamic, and brain-stem neurons. *Journal of Comparative Neurology* **224**: 445–60.

Satoh, K. and Fibiger, H. C. (1986) Cholinergic neurons of the laterodorsal tegmental nucleus: efferent and afferent connections. *Journal of Comparative Neurology* **253**: 277–302.

Saunders, M. G. and Westmoreland, B. F. (1979) The EEG in evaluation of disorders affecting the brain diffusely. In *Current Practice of Clinical Electroencephalography*, ed. D. W. Klass and D. D. Daly, pp. 343–79. New York: Raven Press.

Saunders, R. C. and Rosene, D. L. (1988) A comparison of the efferents of the amygdala and the hippocampal formation in the rhesus monkey: I. Convergence in the entorhinal, prorhinal and perirhinal cortices. *Journal of Comparative Neurology* **271**: 153–84.

Saunders, R. C., Rosene, D. L. and Van Hoesen, G. W. (1988) Comparison of the efferents of the amygdala and the hippocampal formation in the rhesus monkey: II. Reciprocal and non-reciprocal connections. *Journal of Comparative Neurology* **271**: 185–207.

Savander, V., Ledoux, J. E. and Pitkänen, A. (1997) Interamygdaloid projections of the basal and accessory basal nuclei of the rat amygdaloid complex. *Neuroscience* **76**: 725–35.

Scalia, F. and Winans, S. S. (1975) The differential projections of the olfactory bulb and accessory olfactory bulb in mammals. *Journal of Comparative Neurology* **161**: 31–56.

Schafe, G. E., Nadel, N. V., Sullivan, G. M., Harris, A. and LeDoux, J. E. (1999) Memory consolidation for contextual and auditory fear conditioning is dependent on protein synthesis, PKA and MAP kinase. *Learning and Memory* **6**: 97–110.

Schafe, G. E., Nader, K., Blair, H. T. and LeDoux, J. E. (2001) Memory consolidation of Pavlovian fear conditioning: a cellular and molecular perspective. *Trends in Neurosciences* **24**: 540–6.

Scharfman, H. E. (1991) Dentate hilar cells with dendrites in the molecular layer have lower thresholds for synaptic activation by perforant path than granule cells. *Journal of Neuroscience* **11**: 1660–73.

Schiess, M. C., Asprodini, E. K., Rainnie, D. G. and Shinnick-Gallagher, P. (1993) The central nucleus of the rat amygdala: in vitro intracellullar recordings. *Brain Research* **604**: 283–97.

Schiess, M. C., Callahan, P. M. and Zheng, H. (1999) Characterization of the electrophysiological and morphological properties of rat central amygdala neurons in vitro. *Journal of Neuroscience Research* **58**: 663–73.

Schiff, N. D., Ribary, U., Moreno, D. R. *et al.* (2002) Residual cerebral activity and behavioral fragments can remain in the persistently vegetative brain. *Brain* **125**: 1210–34.

Schultz, W. (2002) Getting formal with dopamine and reward. *Neuron* **36**: 241–63.

Schwaber, J. S., Kapp, B. S., Higgins, G. A. and Rapp, P. R. (1982) Amygdaloid and basal forebrain direct connections with the nucleus of the solitary tract and the dorsal motor nucleus. *Journal of Neuroscience* **2**: 1424–38.

Schwindt, P. and Crill, W. (1999) Mechanisms underlying burst and regular spiking evoked by dendritic depolarization in layer 5 cortical pyramidal neurons. *Journal of Neurophysiology* **81**: 1341–54.

Schwindt, P. C., Spain, W. J., Foehring, R. C. *et al.* (1988a) Multiple potassium conductances and their functions in neurons from cat sensorimotor cortex *in vitro*. *Journal of Neurophysiology* **59**: 424–49.

Schwindt, P. C., Spain, W. J., Foehring, R. C., Chubb, M. C. and Crill, W. E. (1988b) Slow conductances in neurons from cat sensorimotor cortex *in vitro* and their role in slow excitability changes. *Journal of Neurophysiology* **59**: 450–67.

Schwindt, P. C., Spain, W. J. and Crill, W. E. (1989) Long-lasting reduction of excitability by a sodium-dependent potassium current in cat neocortical neurons. *Journal of Neurophysiology* **61**: 233–44.

Seamans, J. K., Nogueira, L. and Lavin, A. (2003) Synaptic basis of persistent activity in prefrontal cortex *in vivo* and in organotypic cultures. *Cerebral Cortex* **13**: 1242–50.

Segarra, J. M. (1970) Cerebral vascular disease and behaviour. I. The syndrome of the mesencephalic artery (basilary artery bifurcation). *Archives of Neurology* **22**: 408–18.

Seidemann, E., Meilijson, I., Abeles, M., Bergman, H. and Vaadia, E. (1996) Simultaneously recorded single units in the frontal cortex go through sequences of discrete and stable states in monkeys performing a delayed localization task. *Journal of Neuroscience* **16**: 752–68.

Seidenbecher, T., Laxmi, T. R., Stork, O. and Pape, H. C. (2003) Amygdalar and hippocampal theta rhythm synchronization during fear memory retrieval. *Science* **301**: 846–50.

Sejnowski, T. J. and Destexhe, A. (2000) Why do we sleep? *Brain Research* **886**: 208–23.

Semba, K. (1992) Development of central cholinergic neurons. In *Handbook of Chemical Neuroanatomy*, vol. 10 (*Ontogeny and Transmitters of Peptides in the CNS*), ed. A. Björkland, T. Hökfelt and M. Tohyama, pp. 33–62. Amsterdam: Elsevier.

Semba, K. (2000) Multiple output pathways of the basal forebrain: organization, chemical heterogeneity, and role in vigilance. *Behavioural Brain Research* **115**: 117–41.

Semba, K. (2004) Phylogenetic and ontogenetic aspects of the basal forebrain cholinergic neurons and their innervation of the cerebral cortex. In *Acetylcholine in the Cerebral Cortex* (*Progress in Brain Research*, vol. 145), ed. L. Descarries, K. Krnjevic and M. Steriade, pp. 3–43. Amsterdam: Elsevier.

Seroogy, K. B., Dangaran, K., Lim, S., Haycock, J. W. and Fallon, J. H. (1989) Ventral mesencephalic neurons containing both cholecystokinin- and tyrosine hydroxylase-like immunoreactivities project to forebrain regions. *Journal of Comparative Neurology* **279**: 397–414.

Sesack, S. R., Deutch, A. Y., Roth, R. H. and Bunney, B. S. (1989) Topographical organization of the efferent projections of the medial prefrontal cortex in the rat: an anterograde tract-tracing study with Phaseolus vulgaris leucoagglutinin. *Journal of Comparative Neurology* **290**: 213–42.

Shadlen, M. N. and Movshon, J. A. (1999) Synchrony unbound: a critical evaluation of the temporal binding hypothesis. *Neuron* **24**: 67–77.

Shaffery, J. P., Sinton, C. M., Bissette, G., Roffwarg, H. P. and Marks, G. A. (2002) Rapid eye movement sleep deprivation modifies expression of long-term potentiation in visual cortex of immature rats. *Neuroscience* **110**: 431–43.

Sheer, D. (1984) Focused arousal, 40 Hz, and dysfunction. In *Selfregulation of the Brain and Behavior*, ed. T. Ebert, pp. 64–84. Berlin: Springer.

Shepherd, G. M. (2005) Perception without a thalamus: how does olfaction do it? *Neuron* **46**: 166–8.

Sherin, J. E., Shiromani, P. J., McCarley, R. W. and Saper, C. B. (1996) Activation of ventrolateral preoptic neurons during sleep. *Science* **271**: 216–9.

Sherin, J. E., Elmquist, J. K., Torrealba, F. and Saper, C. B. (1998) Innervation of histaminergic tuberomammillary neurons by GABAergic and galaninergic neurons in the ventrolateral preoptic nucleus of the rat. *Journal of Neuroscience* **18**: 4705–21.

Sherman, S. M. (2001) A wake-up call from the thalamus. *Nature Neuroscience* **4**: 344–6.

Sherrington, C. S. (1955) *Man on his Nature*. New York: Doubleday.

Shi, C. J. and Cassell, M. D. (1999) Perirhinal cortex projections to the amygdaloid complex and hippocampal formation in the rat. *Journal of Comparative Neurology* **406**: 299–328.

Shi, S. H., Hayashi, Y., Petralia, R. S. *et al.* (1999) Rapid spine delivery and redistribution of AMPA receptors after synaptic NMDA receptor activation. *Science* **284**: 1811–16.

Shin, L. M., Orr, S. P., Carson, M. A. *et al.* (2004) Regional cerebral blood flow in the amygdala and medial prefrontal cortex during traumatic imagery in male and female Vietnam veterans with PTSD. *Archives of General Psychiatry* **61**: 168–76.

Shinonaga, Y., Takada, M. and Mizuno, N. (1994) Topographic organization of collateral projections from the basolateral amygdaloid nucleus to both the prefrontal cortex and nucleus accumbens in the rat. *Neuroscience* **58**: 389–97.

Shu, Y., Hasenstaub, A., Badoual, M., Bal, T. and McCormick, D. A. (2003) Barrages of synaptic activity control the gain and sensitivity of cortical neurons. *Journal of Neuroscience* **23**: 10388–401.

Siapas, A. G. and Wilson, M. A. (1998) Coordinated interactions between hippocampal ripples and cortical spindles during slow-wave sleep. *Neuron* **21**: 1123–28.

Siegel, M. and König, P. (2003) A functional gamma-band defined by stimulus-dependent synchronization in area 18 of awake behaving cats. *Journal of Neuroscience* **23**: 4251–60.

Sillito, A., Jones, H. E., Gerstein, G. L. and West, D. C. (1994) Feature-linked synchronization of thalamic relay cell firing induced by feedback from the visual cortex. *Nature* **369**: 479–82.

Silva, L. R., Gutnick, M. J. and Connors, B. W. (1991) Laminar distribution of neuronal membrane properties in neocortex of normal and reeler mouse. *Journal of Neurophysiology* **66**: 2034–40.

Simon, N. R., Mandshanden, I. and Lopes da Silva, F. H. (2000) A MEG study of sleep. *Brain Research* **860**: 64–76.

Singer, W. (1973) The effects of mesencephalic reticular stimulation on intracellular potentials of cat lateral geniculate neurons. *Brain Research* **61**: 35–54.

Singer, W. (1977) Control of thalamic transmission by corticofugal and ascending reticular pathways in the visual system. *Physiological Reviews* **57**: 386–420.

Singer, W. (1990) Role of acetylcholine in use-dependent plasticity of the visual cortex. In *Brain Cholinergic Systems*, ed. M. Steriade and D. Biesold, pp. 314–36. Oxford: Oxford University Press.

Singer, W. (1999) Neuronal synchrony: a versatile code for the definition of relations? *Neuron* **24**: 49–65.

Sirota, A., Csicsvari, J., Buhl, D. and Buzsáki, G. (2003) Communication between neocortex and hippocampus during sleep in rodents. *Proceedings of the National Academy of Sciences USA* **100**: 2065–9.

Slotnick, S. D., Moo, L. R., Kraut, M. A., Lesser, R. P. and Hart Jr., J. (2002) Interactions between thalamic and cortical rhythms during semantic memory recall in human. *Proceedings of the National Academy of Sciences USA* **99**: 6440–3.

Smith, Y. and Paré, D. (1994) Intra-amygdaloid projections of the lateral nucleus in the cat: PHA-L anterograde labeling combined with post-embedding GABA and glutamate immunocytochemistry. *Journal of Comparative Neurology* **342**: 232–48.

Smith, Y., Paré, D., Deschênes, M., Parent, A., and Steriade, M. (1988) Cholinergic and non-cholinergic projections from the upper brainstem core to the visual thalamus in the cat. *Experimental Brain Research* **70**: 166–80.

Smith, Y., Paré, J. F. and Paré, D. (1998) Cat intraamygdaloid inhibitory network: ultrastructural organization of parvalbumin-immunoreactive elements. *Journal of Comparative Neurology* **391**: 164–79.

Smith, Y., Paré, J. F. and Paré, D. (2000) Differential innervation of parvalbumin-immunoreactive interneurons of the basolateral amygdaloid complex by cortical and intrinsic inputs. *Journal of Comparative Neurology* **416**: 496–508.

Snowden, R. J., Treue, S. and Andersen, R. A. (1992) The response of neurons in areas V1 and MT of the alert rhesus monkey to moving random dot patterns. *Experimental Brain Research* **88**: 389–400.

Sobotka, S. and Ringo, J. L. (1993) Investigation of long-term recognition and association memory in unit responses from inferotemporal cortex. *Experimental Brain Research* **96**: 28–38.

Soderling, T. R. and Derkach, V. A. (2000) Postsynaptic protein phosphorylation and LTP. *Trends in Neurosciences* **23**: 75–80.

Soltesz, I. and Crunelli, V. (1992) $GABA_A$ and pre- and post-synaptic $GABA_B$ receptor-mediated responses in the lateral geniculate nucleus. In *Progress in Brain Research*, vol. 90, ed. R. R. Mize, R. E. Marc and A. M. Sillito, pp. 151–69. Amsterdam: Elsevier.

Soltesz, I. and Deschênes, M. (1993) Low- and high-frequency membrane potential oscillations during theta activity in CA1 and CA3 pyramidal neurons of the rat hippocampus under ketamine-xylazine anesthesia. *Journal of Neurophysiology* **70**: 97–116.

Soltesz, I., Lightowler, S., Leresche, N., Jassik-Gerschenfeld, D. and Crunelli, V. (1991) Two inward currents and the transformation of low-frequency oscillations of rat and cat thalamocortical cells. *Journal of Physiology (London)* **441**: 175–97.

Somogyi, P. (1977) A specific 'axo-axonal' interneuron in the visual cortex of the rat. *Brain Research* **136**: 345–50.

Somogyi, P. (1978) The study of Golgi stained cells and the experimental degeneration under the electron microscope: a direct method for the identification in the visual cortex of three successive links in a neuronal chain. *Neuroscience* **3**: 167–80.

Somogyi, P. and Cowey, A. (1981) Combined Golgi and electron microscopic study on the synapses formed by double bouquet cells in the visual cortex of the cat and monkey. *Journal of Comparative Neurology* **195**: 547–66.

Somogyi, P., Kisvárday, Z. F., Martin, K. A.C. and Whitteridge, D. (1983) Synaptic connections of morphologically identified and physiologically characterized large basket cells in the striate cortex of cat. *Neuroscience* **10**: 261–94.

Somogyi, P., Freund, T. F., Hodgson, A. J. *et al.* (1985) Identified axo-axonic cells are immunoreactive for GABA in the hippocampus and visual cortex of cats. *Brain Research* **332**: 143–9.

Somogyi, P., Tamás, G., Lujan, R. and Buhl, E. H. (1998) Salient features of synaptic organisation in the cerebral cortex. *Brain Research Reviews* **26**: 113–35.

Soriano, E., Martinez, A., Fariñas, I. and Frotscher, M. (1993) Chandelier cells in the hippocampal formation of the rat: the entorhinal area and subicular complex. *Journal of Comparative Neurology* **337**: 151–67.

Sorvari, H., Soininen, H., Paljärvi, L., Karkola, K. and Pitkänen, A. (1995). Distribution of parvalbumin-immunoreactive cells and fibers in the human amygdaloid complex. *Journal of Comparative Neurology* **360**: 185–212.

Soury, J. (1899) *Le Système Nerveux Central. Histoire Critique des Théories et des Doctrines*. Paris: Carré et Naud.

Spiegel, E. (1919) Die Kerne im Voderhirn des Sauger. *Arbeiten der Neurologische Institut – Wien Universität* **22**: 418–97.

Spreafico, R., Amadeo, A., Angoscini, P., Panzica, F. and Battaglia, G. (1993) Branching projections from mesopontine nuclei to the nucleus reticularis and related thalamic nuclei: a double labelling study in the rat. *Journal of Comparative Neurology* **336**: 481–92.

Squire, L. R. and Alvarez, P. (1995) Retrograde amnesia and memory consolidation: a neurobiological perspective. *Current Opinions in Neurobiology* **5**: 169–77.

Standaert, D. G., Saper, C. B., Rye, D. B. and Wainer, B. H. (1986) Colocalization of atriopeptin-like immunoreactivity with choline acetyltransferase and substance P-like immunoreactivity in the pedunculopontine and laterodorsal tegmental nuclei in the rat. *Brain Research* **382**: 163–8.

Stanford, L. R., Friedländer, M. J. and Sherman, S. M. (1983) Morphological and physiological properties of geniculate W-cells of the cat: a comparison with X- and Y-cells. *Journal of Neurophysiology* **50**: 582–608.

Stefanacci, L., Suzuki, W. A. and Amaral, D. G. (1996) Organization of connections between the amygdaloid complex and the perirhinal and parahippocampal cortices in macaque monkeys. *Journal of Comparative Neurology* **375**: 552–82.

Steininger, T. L., Gong, H., McGinty, D. and Szymusiak, R. (2001) Subregional organization of preoptic area/anterior hypothalamic projections to arousal-related monoaminergic cell groups. *Journal of Comparative Neurology* **429**: 638–53.

Steriade, M. (1970) Ascending control of thalamic and cortical responsiveness. *International Review of Neurobiology* **12**: 87–144.

Steriade, M. (1976) Cortical inhibition during sleep and waking. In *Mechanisms in Transmission of Signal for Conscious Behavior*, ed. T. Desiraju, pp. 209–48. Amsterdam: Elsevier.

Steriade, M. (1978) Cortical long-axoned cells and putative interneurons during the sleep-waking cycle. *Behavioral and Brain Sciences* **3**: 465–514.

Steriade, M. (1981) Mechanisms underlying cortical activation: neuronal organization and properties of the midbrain reticular core and intralaminar thalamic nuclei. In *Brain Mechanisms and Perceptual Awareness*, ed. O. Pompeiano and C. Ajmone-Marsan, pp. 327–77. New York: Raven.

Steriade, M. (1984) The excitatory-inhibitory response sequence of thalamic and neocortical cells: state-related changes and regulatory systems. In *Dynamic Aspects of Neocortical Function*, ed. G. M. Edelman, W. E. Gall and W. M. Cowan, pp. 107–57. New York: Wiley.

Steriade, M. (1991) Alertness, quiet sleep, dreaming. In *Cerebral Cortex*, vol. 9 (*Normal and Altered States of Function*), ed. A. Peters and E. G. Jones, pp. 279–357. New York: Plenum.

Steriade, M. (1995a) Two channels in the cerebellothalamocortical system. *Journal of Comparative Neurology* **354**: 57–70.

Steriade, M. (1995b) Brain activation, then (1949) and now: coherent fast rhythms in corticothalamic networks. *Archives Italiennes de Biologie* **134**: 5–20.

Steriade, M. (1997a) Synchronized activities of coupled oscillators in the cerebral cortex and thalamus at different levels of vigilance. *Cerebral Cortex* **7**: 583–604.

Steriade, M. (1997b) Thalamic substrates of disturbances in states of vigilance and consciousness in humans. In *Thalamus*, vol. 2 (*Experimental and Clinical Aspects*), ed. M. Steriade, E. G. Jones and D. A. McCormick, pp. 721–42. Oxford: Elsevier.

Steriade, M. (1999) Coherent oscillations and short-term plasticity in corticothalamic networks. *Trends in Neurosciences* **22**: 337–45.

Steriade, M. (2000) Corticothalamic resonance, states of vigilance, and mentation. *Neuroscience* **101**: 243–76.

Steriade, M. (2001a) *The Intact and Sliced Brain*. Cambridge, MA: MIT Press.

Steriade, M. (2001b) Impact of network activities on neuronal properties in corticothalamic systems. *Journal of Neurophysiology* **86**: 1–39.

Steriade, M. (2001c) The GABAergic reticular nucleus: a preferential target of corticothalamic projections. *Proceedings of the National Academy of Sciences USA* **98**: 3625–7.

Steriade, M. (2001d) To burst, or rather, not to burst. *Nature Neuroscience* **4**: 671.

Steriade, M. (2003a) *Neuronal Substrates of Sleep and Epilepsy*. Cambridge: Cambridge University Press.

Steriade, M. (2003b) The corticothalamic system in sleep. *Frontiers in Bioscience* **8**: 878–99.

Steriade, M. (2003c) Presynaptic dendrites of thalamic local-circuit neurons and sculpting inhibition during activated states. *Journal of Physiology (London)* **546**: 1.

Steriade, M. (2004a) Neocortical neuronal classes are flexible entities. *Nature Reviews Neuroscience* **5**: 121–34.

Steriade, M. (2004b). Local gating of information processing through the thalamus. *Neuron* **41**: 493–4.

Steriade, M. (2004c). Slow-wave sleep: serotonin, neuronal plasticity, and seizures. *Archives Italiennes de Biologie* **142**: 359–67.

Steriade, M. (2005a) Cellular substrates of brain rhythms. In *Electroencephalography: Basic Principles, Clinical Applications, and Related Fields* (5th edition), ed. E. Niedermeyer and F. Lopes Da Silva, pp. 31–83. Baltimore, MD: Williams & Wilkins.

Steriade, M. (2005b) Neuronal substrates of spike-wave seizures and hypsarrhythmia in corticothalamic systems. *Advances in Neurology* **27**: 149–54.

Steriade, M. (2006) Brainstem-thalamic neurons implicated in hallucinations. *Behavioral and Brain Sciences*, in press.

Steriade, M. and Amzica F. (1996) Intracortical and corticothalamic coherency of fast spontaneous oscillations. *Proceedings of the National Academy of Sciences USA* **93**: 2533–8.

Steriade, M. and Amzica, F. (1998) Coalescence of sleep rhythms and their chronology in corticothalamic networks. *Sleep Research Online* **1**: 1–10.

Steriade, M. and Buzsáki, G. (1990). Parallel activation of thalamic and cortical neurons by brainstem and basal forebrain cholinergic systems. In *Brain Cholinergic Systems*, ed. M. Steriade and D. Biesold, pp. 3–63. Oxford: Oxford University Press.

Steriade, M. and Contreras, D. (1993) Sleep oscillations in interacting thalamocortical networks. In *Thalamic Networks for Relay and Modulation*, ed. D. Minciacchi, M. Molinari, G. Macchi and E. G. Jones, pp. 385–94. Oxford: Pergamon Press.

Steriade, M. and Contreras, D. (1995) Relations between cortical and thalamic cellular events during transition from sleep pattern to paroxysmal activity. *Journal of Neuroscience* **15**: 623–42.

Steriade, M. and Demetrescu, M. (1960) Unspecific systems of inhibition and facilitation of potentials evoked by intermittent light. *Journal of Neurophysiology* **23**: 602–17.

Steriade, M. and Demetrescu, M. (1967) Simulation of peripheral sensory input by electrical pulse trains applied to specific afferent pathways. *Experimental Neurology* **19**: 265–77.

Steriade, M. and Deschênes, M. (1974) Inhibitory processes and interneuronal apparatus in motor cortex during sleep and waking. II. Recurrent and afferent inhibition of pyramidal tract neurons. *Journal of Neurophysiology* **37**: 1093–113.

Steriade, M. and Deschênes, M. (1984) The thalamus as a neuronal oscillator. *Brain Research Reviews* **8**: 1–63.

Steriade, M. and Deschênes, M. (1987) Inhibitory processes in the thalamus. *Journal of Mind and Behavior* **8**: 559–72.

Steriade, M. and Deschênes, M. (1988) Intrathalamic and brainstem-thalamic networks involved in resting and alert states. In *Cellular Thalamic Mechanisms*, ed. M. Bentivoglio, G. Macchi and R. Spreafico, pp. 37–62. Amsterdam: Elsevier.

Steriade, M. and Glenn, L. L. (1982) Neocortical and caudate projections of intralaminar thalamic neurons and their synaptic excitation from the midbrain reticular core. *Journal of Neurophysiology* **48**: 352–71.

Steriade, M. and Hobson, J. A. (1976) Neuronal activity during the sleep-waking cycle. *Progress in Neurobiology* **6**: 155–376.

Steriade, M. and Llinás, R. R. (1988) The functional states of the thalamus and the associated neuronal interplay. *Physiological Reviews* **68**: 649–742.

Steriade, M. and McCarley, R. W. (2005) *Brain Control of Wakefulness and Sleep* (2nd edition). New York: Springer-Kluwer.

Steriade, M. and Morin, D. (1981) Reticular influences on primary and augmenting responses in the somatosensory cortex. *Brain Research* **205**: 67–80.

Steriade, M. and Timofeev, I. (1997) Short-term plasticity during intrathalamic augmenting responses in decorticated cats. *Journal of Neuroscience* **17**: 3778–95.

Steriade, M. and Timofeev, I. (2001) Corticothalamic operations through prevalent inhibition of thalamocortical neurons. *Thalamus and Related Systems* **1**: 225–36.

Steriade, M. and Timofeev, I. (2003) Neuronal plasticity in thalamocortical networks during sleep and waking oscillations. *Neuron* **37**: 563–76.

Steriade, M., Belekhova, M. and Apostol, V. (1968) Reticular potentiation of cortical flash-evoked afterdischarge. *Brain Research* **11**: 276–80.

Steriade, M., Iosif, G. and Apostol, V. (1969) Responsiveness of thalamic and cortical motor relays during arousal and various stages of sleep. *Journal of Neurophysiology* **32**: 251–65.

Steriade, M., Apostol, V. and Oakson, G. (1971) Control of unitary activities in cerebellothalamic pathway during wakefulness and synchronized sleep. *Journal of Neurophysiology* **34**: 389–413.

Steriade, M., Wyzinski, P. and Apostol, V. (1972) Corticofugal projections governing rhythmic thalamic activity. In *Corticothalamic Projections and Sensorimotor Activities*, ed. T. L. Frigyesi, E. Rinvik and M. D. Yahr, pp. 221–72. New York: Raven Press.

Steriade, M., Deschênes, M. and Oakson, G. (1974a) Inhibitory processes and interneuronal apparatus in motor cortex during sleep and waking. I. Background firing and synaptic responsiveness of pyramidal tract neurons and interneurons. *Journal of Neurophysiology* **37**: 1065–92.

Steriade, M., Deschênes, M., Wyzinski, P. and Hallé, J. P. (1974b) Input-output organization of the motor cortex during sleep and waking. In *Basic Sleep Mechanisms*, ed. O. Petre-Quadens and J. Schlag, pp. 144–200. New York: Academic Press.

Steriade, M., Oakson, G. and Diallo, A. (1977) Reticular influences on lateralis posterior thalamic neurons. *Brain Research* **131**: 55–71.

Steriade, M., Kitsikis, A. and Oakson, G. (1979) Excitatory-inhibitory processes in parietal association neurons during reticular activation and sleep-waking cycle. *Sleep* **1**: 339–55.

Steriade, M., Oakson, G. and Ropert, N. (1982a) Firing rates and patterns of midbrain reticular neurons during steady and transitional states of the sleep-waking cycle. *Experimental Brain Research* **46**: 37–51.

Steriade, M., Parent, A., Ropert, N. and Kitsikis, A. (1982b) Zona incerta and lateral hypothalamic afferents to the midbrain reticular core of the cat – an HRP and electrophysiological study. *Brain Research* **238**: 13–28.

Steriade, M., Parent, A. and Hada, J. (1984a) Thalamic projections of nucleus reticularis thalami of cat: a study using retrograde transport of horseradish peroxidase and double fluorescent tracers. *Journal of Comparative Neurology* **229**: 531–47.

Steriade, M., Sakai, K. and Jouvet, M. (1984b) Bulbothalamic neurons related to thalamocortical activation processes during paradoxical sleep. *Experimental Brain Research* **54**: 463–75.

Steriade, M., Deschênes, M., Domich, L. and Mulle, C. (1985) Abolition of spindle oscillations in thalamic neurons disconnected from nucleus reticularis thalami. *Journal of Neurophysiology* **54**: 1473–97.

Steriade, M., Domich, L. and Oakson, G. (1986) Reticularis thalami neurons revisited: activity changes during shifts in states of vigilance. *Journal of Neuroscience* **6**: 68–81.

Steriade, M., Domich, L., Oakson, G. and Deschênes, M. (1987a) The deafferented reticular thalamic nucleus generates spindle rhythmicity. *Journal of Neurophysiology* **57**: 260–73.

Steriade, M., Parent, A., Paré, D. and Smith, Y. (1987b) Cholinergic and non-cholinergic neurons of cat basal forebrain project to reticular and mediodorsal thalamic nuclei. *Brain Research* **408**: 372–76.

Steriade, M., Paré, D., Parent, A. and Smith, Y. (1988) Projections of cholinergic and non-cholinergic neurons of the brainstem core to relay

and associational thalamic nuclei in the cat and macaque monkey. *Neuroscience* **25**: 47–67.

Steriade, M., Paré, D., Bouhassira, D., Deschênes, M. and Oakson, G. (1989) Phasic activation of lateral geniculate and perigeniculate neurons during sleep with ponto-geniculo-occipital spikes. *Journal of Neuroscience* **9**: 2215–29.

Steriade, M., Datta, S., Paré, D., Oakson, G. and Curró Dossi, R. (1990a) Neuronal activities in brainstem cholinergic nuclei related to tonic activation processes in thalamocortical systems. *Journal of Neuroscience* **10**: 2541–59.

Steriade, M., Jones, E. G. and Llinás, R. R. (1990b) *Thalamic Oscillations and Signaling.* New York: Wiley-Interscience.

Steriade, M., Gloor, P., Llinás, R. R., Lopes da Silva, F. H. and Mesulam, M. M. (1990c) Basic mechanisms of cerebral rhythmic activities. *Electroencephalography and Clinical Neurophysiology* **76**: 481–508.

Steriade, M., Paré, D., Datta, S., Oakson, G. and Curró Dossi, R. (1990d) Different cellular types in mesopontine cholinergic nuclei related to ponto-geniculo-occipital waves. *Journal of Neuroscience* **10**: 2560–79.

Steriade, M., Curró Dossi, R. and Nuñez, A. (1991a) Network modulation of a slow intrinsic oscillation of cat thalamocortical neurons implicated in sleep delta waves: cortical potentiation and brainstem cholinergic suppression. *Journal of Neuroscience* **11**: 3200–17.

Steriade, M., Curró Dossi, R., Paré, D. and Oakson, G. (1991b) Fast oscillations (20–40 Hz) in thalamocortical systems and their potentiation by mesopontine cholinergic nuclei in the cat. *Proceedings of the National Academy of Sciences USA* **88**: 4396–400.

Steriade, M., Amzica, F. and Nuñez, A. (1993a) Cholinergic and noradrenergic modulation of the slow (~0.3 Hz) oscillation in neocortical cells. *Journal of Neurophysiology* **70**: 1384–400.

Steriade, M., Contreras, D., Curró Dossi, R. and Nuñez, A. (1993b) The slow (<1 Hz) oscillation in reticular thalamic and thalamocortical neurons: scenario of sleep rhythm generation in interacting thalamic and neocortical networks. *Journal of Neuroscience* **13**: 3284–99.

Steriade, M., Curró Dossi, R. and Contreras, D. (1993c) Electrophysiological properties of intralaminar thalamocortical cells discharging rhythmic (~40 Hz) spike-bursts at ~1000 Hz during waking and rapid eye movement sleep. *Neuroscience* **56**: 1–9.

Steriade, M., McCormick, D. A. and Sejnowski, T. J. (1993d) Thalamocortical oscillation in the sleeping and aroused brain. *Science* **262**: 679–85.

Steriade, M., Nuñez, A. and Amzica, F. (1993e) A novel slow (<1 Hz) oscillation of neocortical neurons *in vivo*: depolarizing and hyperpolarizing components. *Journal of Neuroscience* **13**: 3252–65.

Steriade, M., Nuñez, A. and Amzica, F. (1993f) Intracellular analysis of relations between the slow (<1 Hz) neocortical oscillation and other sleep rhythms. *Journal of Neuroscience* **13**: 3266–83.

Steriade, M., Amzica, F. and Contreras, D. (1994a) Cortical and thalamic cellular correlates of electroencephalographic burst-suppression. *Electroencephalography and Clinical Neurophysiology* **90**: 1–16.

Steriade, M., Contreras, D. and Amzica, F. (1994b) Synchronized sleep oscillations and their paroxysmal developments. *Trends in Neuroscience* **17**: 199–208.

Steriade, M., Amzica, F. and Contreras, D. (1996a) Synchronization of fast (30–40 Hz) spontaneous cortical rhythms during brain activation. *Journal of Neuroscience* **16**: 392–417.

Steriade, M., Contreras, D., Amzica, F. and Timofeev, I. (1996b) Synchronization of fast (30–40 Hz) spontaneous oscillations in intrathalamic and thalamocortical networks. *Journal of Neuroscience* **16**: 2788–808.

Steriade, M., Jones, E. G. and McCormick, D. A. (1997) *Thalamus*, vol. 1 (*Organisation and Function*). Oxford: Elsevier.

Steriade, M., Timofeev, I., Dürmüller, N. and Grenier, F. (1998a) Dynamic properties of corticothalamic neurons and local cortical interneurons generating fast rhythmic (30–40 Hz) spike bursts. *Journal of Neurophysiology* **79**: 483–90.

Steriade, M., Timofeev, I., Grenier, F. and Dürmüller, N. (1998b) Role of thalamic and cortical neurons in augmenting responses: dual intracellular recordings *in vivo*. *Journal of Neuroscience* **18**: 6425–43.

Steriade, M., Timofeev, I. and Grenier, F. (2001a) Natural waking and sleep states: a view from inside neocortical neurons. *Journal of Neurophysiology* **85**: 1969–85.

Steriade, M., Timofeev, I. and Grenier, F. (2001b) Intrinsic, antidromic and synaptic excitability of cortical neurons during natural waking-sleep cycle. *Society for Neuroscience Abstracts* **27**: 240.

Stickgold, R., James, L. and Hobson, J. A. (2000a) Visual discrimination learning requires sleep after training. *Nature Neuroscience* **3**: 1237–8.

Stickgold, R., Whitbee, D., Schirmer, B., Patel, V. and Hobson, J. A. (2000b) Visual discrimination improvement. A multi-step process occurring during sleep. *Journal of Cognitive Neuroscience* **12**: 246–54.

Stone, V. E., Baron-Cohen, S. and Knight, R. T. (1998) Frontal lobe contributions in theory of the mind. *Journal of Cognitive Neuroscience* **10**: 640–56.

Storm, J. F. (1988) Temporal integration by a slowly inactivating K+ current in hippocampal neurons. *Nature* **336**: 379–81.

Stratford, K. J., Tarczy-Hornoch, K., Martin, K. A.C., Bannister, N. J. and Jack, J. J. B. (1996) Excitatory synaptic inputs to spiny stellate cells in cat visual cortex. *Nature* **382**: 258–60.

Stuart, G. and Sakmann, B. (1994) Active propagation of somatic action potentials into neocortical pyramidal cell dendrites. *Nature* **367**: 69–72.

Stuart, G., Spruston, N., Sakmann, B. and Häusser, M. (1997) Action potential initiation and backpropagation in neurons of the mammalian CNS. *Trends in Neurosciences* **20**: 125–31.

Sugihara, I., Lang, E. J. and Llinás, R. (1993) Uniform olivocerebellar conduction time underlies Purkinje cell complex spike synchronicity in the rat cerebellum. *Journal of Physiology (London)* **470**: 243–71.

Sun, N. and Cassell, M. D. (1993) Intrinsic GABAergic neurons in the rat central extended amygdala. *Journal of Comparative Neurology* **330**: 381–404.

Sutton, R. E., Koob, G. F., Le Moal, M., Rivier, J. and Vale, W. (1982) Corticotropin releasing factor produces behavioral activation in rats. *Nature* **297**: 31–3.

Suzuki, W. A. (1996) The anatomy, physiology and functions of the perirhinal cortex. *Current Opinion in Neurobiology* **6**: 179–86.

Suzuki, W. A. and Porteros, A. (2002) Distribution of calbindin D-28k in the entorhinal, perirhinal, and parahippocampal cortices of the macaque monkey. *Journal of Comparative Neurology* **451**: 392–412.

Suzuki, W. A., Zola-Morgan, S., Squire, L. R. and Amaral, D. G. (1993) Lesions of the perirhinal and parahippocampal cortices in the monkey produce long-lasting memory impairment in the visual and tactual modalities. *Journal of Neuroscience* **13**: 2430–51.

Svoboda, K., Denk, W., Kleinfeld, D. and Tank, D. W. (1997) *In vivo* dendritic calcium dynamics in neocortical neurons. *Nature* **385**: 161–5.

Svoboda, K., Helmchen, F., Denk, W. and Tank, D. W. (1999) Spread of dendritic excitation in layer 2/3 pyramidal neurons in rat barrel cortex *in vivo*. *Nature Neuroscience* **2**: 65–73.

Swadlow, H. A. and Gusev, A. G. (2001) The impact of 'bursting' thalamic impulses at a neocortical synapse. *Nature Neuroscience* **4**: 402–8.

Swanson, L. W. (1992) *Brain Maps: Structure of the Rat Brain*. Amsterdam: Elsevier.

Swanson, L. W. and Hartman, B. K. (1975) The central adrenergic system. An immunofluorescence study of the location of cell bodies and their efferent connections in the rat utilizing dopamine-beta-hydroxylase as a marker. *Journal of Comparative Neurology* **163**: 467–505.

Swanson, L. W. and Petrovich, G. D. (1998) What is the amygdala? *Trends in Neurosciences* **21**: 323–31.

Swanson, L. W., Mogenson, G. J., Simerly, R. B. and Wu, M. (1987) Anatomical and electrophysiological evidence for a projection from the medial preoptic area to the 'mesencephalic and subthalamic locomotor regions' in the rat. *Brain Research* **405**: 108–22.

Szymusiak, R. and McGinty, D. (1986) Sleep-related neuronal discharge in the basal forebrain of cats. *Brain Research* **370**: 82–92.

Szymusiak, R., Steininger, T., Alam, N. and McGinty, D. (2001) Preoptic area sleep-regulating mechanisms. *Archives Italiennes de Biologie* **139**: 77–92.

Takada, M. (1990) The A11 catecholamine cell group: another origin of the dopaminergic innervation of the amygdala. *Neuroscience Letters* **118**: 132–5.

Takagishi, M. and Chiba, T. (1991) Efferent projections of the infralimbic (area 25) region of the medial prefrontal cortex in the rat: an anterograde tracer PHA-L study. *Brain Research* **566**: 26–36.

Takakusaki, K. and Kitai, S. T. (1997) Ionic mechanisms involved in the spontaneous firing of tegmental pedunculopontine nucleus neurons of the rat. *Neuroscience* **78:** 771–94.

Takakusaki, K., Shiroyama, T. and Kitai, S. T. (1997) Two types of cholinergic neurons in he rat tegmental pedunculopontine nucleus: electrophysiological and morphological characterization. *Neuroscience* **79:** 1089–99.

Takeuchi, Y., McLean, J. H. and Hopkins, D. A. (1982) Reciprocal connections between the amygdala and parabrachial nuclei: ultrastructural demonstration by degeneration and axonal transport of horse radish peroxidase in the cat. *Brain Research* **239**: 583–8.

Takeuchi, Y., Matsushima, S., Matsuchima, R. and Hopkins, D. A. (1983) Direct amygdaloid projections to the dorsal motor nucleus of the vagus nerve: a light and electron microscopic study in the rat. *Brain Research* **280**: 143–7.

Takita, M., Izaki, Y., Jay, T. M., Kaneko, H. and Suzuki, S. S. (1999) Induction of stable long-term depression in vivo in the hippocampal-prefrontal cortex pathway. *European Journal of Neuroscience* **11**: 4145–8.

Tamás, G., Buhl, E. H. and Somogyi, P. (1997) Massive autaptic self-innervation of GABAergic neurons in cat visual cortex. *Journal of Neuroscience* **17**: 6352–64.

Tamás, G., Somogyi, P. and Buhl, E. H. (1998) Differentially interconnected networks of GABAergic interneurons in the visual cortex of the cat. *Journal of Neuroscience* **18**: 4255–70.

Tanabe, T., Yarita, H., Iino, M., Ooshima, Y. and Takagi, S. F. (1975a) An olfactory projection area in orbitofrontal cortex of the monkey. *Journal of Neurophysiology* **38**: 1269–83.

Tanabe, T., Iino, M. and Takagi, S. F. (1975b) Discrimination of odors in olfactory bulb, pyriform-amygdaloid areas, and orbitofrontal cortex of the monkey. *Journal of Neurophysiology* **38**: 1284–96.

Tancredi, V., Biagini, G., D'Antuono, M., Louvel, J., Pumain, R. and Avoli, M. (2000) Spindle-like thalamocortical synchronization in a rat brain slice preparation. *Journal of Neurophysiology* **84**: 1093–7.

Tang, A. C., Bartels, A. M. and Sejnowski, T. J. (1997) Effects of cholinergic modulation on responses of neocortical neurons to fluctuating input. *Cerebral Cortex* **7**: 502–9.

Terreberry, R. R. and Neafsey, E. J. (1987) The rat medial frontal cortex projects directly to autonomic regions of the brainstem. *Brain Research Bulletin* **19**: 639–49.

Terzano, M. G., Parrino, L. and Spaggiari, M. C. (1988) The cyclic alternating pattern sequences in the dynamic organization of sleep. *Electroencephalography and Clinical Neurophysiology* **69**: 437–47.

Thierry, A. M., Gioanni, Y., Degenetais, E. and Glowinski, J. (2000) Hippocampo-prefrontal cortex pathway: anatomical and electrophysiological characteristics. *Hippocampus* **10**: 411–19.

Thomson, A. M. (1988a) Inhibitory postsynaptic potentials evoked in thalamic neurons by stimulation of the reticularis nucleus evoke slow spikes in isolated rat brain slices. *Neuroscience* **25**: 491–502.

Thomson, A. M. (1988b) Biphasic responses of thalamic neurons to GABA in isolated rat brain slices. *Neuroscience* **25**: 503–12.

Thomson, A. M. (1997) Activity-dependent properties of synaptic transmission at two classes of connections made by rat neocortical pyramidal neurons *in vitro*. *Journal of Physiology (London)* **502**: 131–47.

Thomson, A. M. and Deuchars, J. (1997) Synaptic interactions in neocortical local circuits: dual intracellular recordings in vitro. *Cerebral Cortex* **7**: 510–22.

Thomson, A. M. and Morris, O. T. (2002) Selectivity in the inter-laminar connections made by neocortical neurones. *Journal of Neurocytology* **31**: 239–46.

Thomson, A. M., West, D. C., Hahn, J. and Deuchars, J. (1996) Single axon IPSPs elicited in pyramidal cells by three classes of interneurons in slices of rat neocortex. *Journal of Physiology (London)* **496**: 81–102.

Thomson, A. M., West, D. C., Wang, Y. and Bannister, A. P. (2002) Synaptic connections and small circuits involving excitatory and inhibitory neurons in layers 2–5 of adult rat and cat neocortex: triple intracellular recordings and biocytin labelling *in vitro*. *Cerebral Cortex* **12**: 936–53.

Tigges, J., Tigges, M., Cross, N. A. *et al.* (1982) Subcortical structures projecting to visual cortical areas in squirrel monkey. *Journal of Comparative Neurology* **209**: 29–40.

Tigges, J., Walker, L. C. and Tigges, M. (1983) Subcortical projections to the occipital lobe and parietal lobes of the chimpanzee brain. *Journal of Comparative Neurology* **220**: 106–15.

Timofeev, I. and Steriade, M. (1996) Low-frequency rhythms in the thalamus of intact-cortex and decorticated cats. *Journal of Neurophysiology* **76**: 4152–68.

Timofeev, I. and Steriade, M. (1997) Fast (mainly 30–100 Hz) oscillations in the cat cerebellothalamic pathway and their synchronization with cortical potentials. *Journal of Physiology (London)* **504**: 153–68.

Timofeev, I. and Steriade, M. (1998) Cellular mechanisms underlying intrathalamic augmenting responses of reticular and relay neurons. *Journal of Neurophysiology* **79**: 2716–29.

Timofeev, I. and Steriade, M. (2004) Neocortical seizures: initiation, development and cessation. *Neuroscience* **123**: 299–336.

Timofeev, I., Contreras, D. and Steriade, M. (1996) Synaptic responsiveness of cortical and thalamic neurons during various phases of slow oscillation in cat. *Journal of Physiology (London)* **494**: 265–78.

Timofeev, I., Grenier, F., Bazhenov, M., Sejnowski, T. J. and Steriade, M. (2000) Origin of slow oscillations in deafferented cortical slabs. *Cerebral Cortex* **10**: 1185–99.

Timofeev, I., Bazhenov, M., Sejnowski, T. J. and Steriade M. (2001a) Contribution of intrinsic and synaptic factors in the desynchronization of thalamic oscillatory activity. *Thalamus and Related Systems* **1**: 53–69.

Timofeev, I., Grenier, F. and Steriade, M. (2001b) Disfacilitation and active inhibition in the neocortex during the natural sleep-wake cycle: an intracellular study. *Proceedings of the National Academy of Sciences USA* **98**: 1924–9.

Timofeev, I., Bazhenov, M., Sejnowski, T. J. and Steriade, M. (2002a). Cortical I_H takes part in the generation of paroxysmal activities. *Proceedings of the National Academy of Sciences USA* **99**: 9533–37.

Timofeev, I., Grenier, F., Bazhenov, M., Houweling, A., Sejnowski, T. J. and Steriade, M. (2002b). Short- and medium-term plasticity associated with augmenting responses in cortical slabs and spindles in intact cortex of cats *in vivo*. *Journal of Physiology (London)* **542**: 583–98.

Tomberg, C. (1999) Cognitive N140 electrogenesis and concomitant 40 Hz synchronization in mid-dorsal prefrontal cortex (area 46) identified in non-averaged human brain potentials. *Neuroscience Letters* **266**: 141–4.

Tomberg, C. and Desmedt, J. E. (1999) The challenge of non-invasive cognitive physiology of the human brain: how to negotiate the irrelevant background noise without spoiling the recorded data through electronic averaging. *Philosophical Transactions of the Royal Society of London* B**354**: 1295–305.

Tömböl, T. and Szafranska-Kosmal, A. (1972) A Golgi study of the amygdaloid complex in the cat. *Acta Neurobiologiae Experimentalis* **32**: 835–48.

Tononi, G. and Cirelli, C. (2001) Some considerations on sleep and neural plasticity. *Archives Italiennes de Biologie* **139**: 221–41.

Tononi, G. and Cirelli, C. (2003) Sleep and synaptic homeostasis. *Brain Research Bulletin* **62**: 143–50.

Toth, T. L. and Crunelli, V. (1992) Computer simulation of the pacemaker oscillations of thalamocortical cells. *NeuroReport* **3**: 65–8.

Toth, T. I., Hughes, S. W. and Crunelli, V. (1998) Analysis and biophysical interpretation of bistable behaviour in thalamocortical neurones. *Neuroscience* **87**: 519–23.

Traub, R. D., Miles, R. and Wong, R. K.S. (1989) Model of the origin of rhythmic population oscillations in the hippocampal slice. *Science* **243**: 1319–25.

Traub, R. D., Buhl, E. H., Glovell, T. and Whittington, M. A. (2003) Fast rhythmic bursting can be induced by in layer 2/3 cortical neurons by enhancing persistent Na^+ conductance and blocking BK channels. *Journal of Neurophysiology* **89**: 909–21.

Traub, R. D., Contreras, D., Cunningham, M. O. *et al.* (2005) Single-column thalamocortical network model exhibiting gamma oscillations, sleep spindles, and epileptogenic bursts. *Journal of Neurophysiology* **93**: 2194–232.

Trulson, M. E. and Jacobs, B. L. (1979) Raphe unit activity in freely moving cats: correlation with level of behavioral arousal. *Brain Research* **163**: 135–50.

Tsatsanis, K. D., Rourke, B. P., Klin, A. *et al.* (2003) Reduced thalamic volume in high-functioning individuals with autism. *Biological Psychiatry* **53**: 121–9.

Tseng, K. Y., Kasanetz, F., Kargieman, L., Riquelne, L. A. and Murer, M. G. (2001) Cortical slow oscillatory activity is reflected in the membrane potential and spike trains of striatal neurons in rats with chronic nigrostriatal lesions. *Journal of Neuroscience* **21**: 6430–9.

Tsvetkov, E., Carlezon, W., Jr., Benes, F. M., Kandel, E. R. and Bolshakov, V. Y. (2002) Fear conditioning occludes LTP-induced presynaptic enhancement of synaptic transmission in the cortical pathway to the lateral amygdala. *Neuron* **34**: 289–300.

Tsvetkov, E., Shin, R. M. and Bolshakov, V. Y. (2004) Glutamate uptake determines pathway specificity of long-term potentiation in the neural circuitry of fear conditioning. *Neuron* **41**: 139–51.

Turner, B. H. and Herkenham, M. (1991) Thalamoamygdaloid projections in the rat: a test of the amygdala's role in sensory processing. *Journal of Comparative Neurology* **313**: 295–325.

Turner, B. H. and Zimmer, J. (1984) The architecture and some of the interconnections of the rat's amygdala and lateral periallocortex. *Journal of Comparative Neurology* **227**: 540–57.

Uchida, S., Maloney, T., March, J. D., Azari, R. and Feinberg, I. (1991) Sigma (12–15 Hz) and delta (0.3–3.0) Hz EEG oscillate reciprocally within NREM sleep. *Brain Research Bulletin* **27**: 93–6.

Ulrich, D. and Huguenard, J. R. (1996) $GABA_B$-receptor-mediated responses in GABAergic projection neurones of rat nucleus reticularis thalami in vitro. *Journal of Physiology (London)* **493**: 845–54.

Uhlrich, D. J., Manning, K. A. and Pienkowski, T. P. (1993) The histaminergic innervation of the lateral geniculate complex in the cat. *Visual Neuroscience* **10**: 225–35.

Uhlrich, D. J., Manning, K. A. and Xue, J. T. (2002) Effects of activation of the histaminergic tuberomammillary nucleus on visual responses of neurons in the dorsal lateral geniculate nucleus. *Journal of Neuroscience* **22**: 1098–107.

Umbriaco, D., Watkins, K. C., Descarries, L., Cozzari, C. and Hartman, B. K. (1994) Ultrastructural and morphometric features of the acetylcholine innervation in adult rat parietal cortex. An electron microscopic study in serial sections. *Journal of Comparative Neurology* **348**: 351–73.

Urbain, N., Gervasoni, D., Soulière, F. *et al.* (2000) Unrelated course of subthalamic nucleus and globus pallidus neuronal activities across vigilance states in the rat. *European Journal of Neuroscience* **12**: 3361–74.

Urbain, N., Rentéro, N., Gervasoni, D., Renaud, B. and Chouvet, G. (2002) The switch of subthalamic neurons from an irregular to a bursting pattern

does not solely depend on their GABAergic inputs in the anesthetic-free rat. *Journal of Neuroscience* **22**: 8665–75.

Ursin, H. and Kaada, B. R. (1960) Functional localization within the amygdaloid complex in the cat. *Electroencephalography and Clinical Neurophysiology* **12**: 1–20.

Uva, L., Gruschke, S., Biella, G., de Curtis, M. and Witter, M. P. (2004) Cytoarchitectonic characterization of the parahippocampal region in guinea pigs. *Journal of Comparative Neurology* **474**: 289–303.

Van Brederode, J. and Spain, W. (1995) Differences in inhibitory synaptic input between layer II–III and layer V neurons of the cat neocortex. *Journal of Neurophysiology* **74**: 1149–66.

Van Hoesen, G. W. and Pandya, D. N. (1975) Some connections of the entorhinal (area 28) and perirhinal (area 35) cortices of the rhesus monkey. I. Temporal lobe afferents. *Brain Research* **95**: 1–24.

Vanni-Mercier, G. and Debilly, G. (1998) A key role for the caudoventral pontine tegmentum in the simultaneous generation of eye saccades in bursts and associated ponto-geniculo-occipital waves during paradoxical sleep in the cat. *Neuroscience* **86**: 571–85.

Veening, J. G., Swanson, L. W. and Sawchenko, P. E. (1984) The organization of projections from the central nucleus of the amygdala to brainstem sites involved in central autonomic regulation: a combined retrograde transport-immunohistochemical study. *Brain Research* **303**: 337–57.

Velayos, J. L., Jimenez-Castellanos, J. Jr. and Reinoso-Suárez, F. (1989) Topographical organization of the projections from the reticular thalamic nucleus to the intralaminar and medial thalamic nuclei in the cat. *Journal of Comparative Neurology* **279**: 457–69.

Venance, L., Rozov, A., Blatow, M., Burnashev, N., Feldmeyer, D. and Monyer, H. (2000) Connexin expression in electrically coupled postnatal rat brain neurons. *Proceedings of the National Academy of Sciences USA* **97**: 10260–5.

Vertes, R. P. (1991) A PHA-L analysis of ascending projections of the dorsal raphe nucleus in the rat. *Journal of Comparative Neurology* **313**: 643–68.

Vertes, R. P. (2004) Differential projections of the infralimbic and prelimbic cortex in the rat. *Synapse* **51**: 32–58.

Vertes, R. P., Fortin, W. J. and Crane, A. M. (1999) Projections of the median raphe nucleus in the rat. *Journal of Comparative Neurology* **407**: 555–82.

Villablanca, J. (1965) The electrocorticogram in the chronic *cerveau isolé* cat. *Electroencephalography and Clinical Neurophysiology* **19**: 576–86.

Villablanca, J. (1974) Role of the thalamus in sleep control: sleep-wakefulness studies of chronic cats without the thalamus: the 'athalamic cat'. In *Basic Sleep Mechanisms*, ed. O. Petre-Quadens and J. Schlag, pp. 51–81. New York: Academic Press.

Vincent, S. R. and Reiner, P. B. (1987) The immunohistochemical localization of choline acetyltransferase in the cat brain. *Brain Research Bulletin* **18**: 371–415.

Vincent, S. R., Satoh, K., Armstrong, D. M. and Fibiger, H. C. (1983) Substance P in the ascending cholinergic reticular system. *Nature* **306**: 688–91.

Vincent, S. R., Satoh, K., Armstrong, D. M. *et al.* (1986) Neuropeptides and NADPH-diaphorase activity in the ascending cholinergic reticular system of the rat. *Neuroscience* **17**: 167–82.

Von der Malsburg, C. (1995) Binding in models of perception and brain function. *Current Opinions in Neurobiology* **5**: 520–6.

Von der Malsburg, C. (1999) The what and why of binding: the modeler's perspective. *Neuron* **24**: 95–104.

Von Krosigk, M., Bal, T. and McCormick, D. A. (1993) Cellular mechanisms of a synchronized oscillation in the thalamus. *Science* **261**: 361–4.

Wainer, B. H. and Mesulam, M.-M. (1990) Ascending cholinergic pathways in the rat brain. In *Brain Cholinergic Systems*, ed. M. Steriade and D. Biesold, pp. 65–119. Oxford: Oxford University Press.

Wainer, B. H., Bolam, J. P., Freund, T. F. *et al.* (1984) Cholinergic synapses in the rat brain: a correlated light and electron microscopic immunohistochemical study employing a monoclonal antibody against choline acetyltransferase. *Brain Research* **308**: 69–76.

Walker, D. L. and Davis, M. (2000) Involvement of NMDA receptors within the amygdala in short- versus long-term memory for fear conditioning as assessed with fear-potentiated startle. *Behavioral Neuroscience* **114**: 1019–33.

Walker, D. L. and Davis, M. (2002) The role of amygdala glutamate receptors in fear learning, fear-potentiated startle, and extinction. *Pharmacology Biochemistry and Behavior* **71**: 379–92.

Walker, D. L., Ressler, K. J., Lu, K. T. and Davis, M. (2002) Facilitation of conditioned fear extinction by systemic administration or intra-amygdala infusions of D-Cycloserine as assessed with fear-potentiated startle in rats. *Journal of Neuroscience* **22**: 2343–51.

Wallace, D. M., Magnuson, D. J. and Gray, T. S. (1989) The amygdalo-brainstem pathway: selective innervation of dopaminergic, noradrenergic and adrenergic cells in the rat. *Neuroscience Letters* **97**: 252–8.

Wallace, D. M., Magnuson, D. J. and Gray, T. S. (1992) Organization of amygdaloid projections to brainstem dopaminergic, noradrenergic, and adrenergic cell groups in the rat. *Brain Research Bulletin* **28**: 447–54.

Wan, H., Warburton, E. C., Zhu, X. O. *et al.* (2004) Benzodiazepine impairment of perirhinal cortical plasticity and recognition memory. *European Journal of Neuroscience* **20**: 2214–24.

Wang, X. J. (1999) Fast burst firing and short-term synaptic plasticity: a model of neocortical chattering neurons. *Neuroscience* **89**: 347–62.

Wang, X. J. and Rinzel, J. (1993) Spindle rhythmicity in the reticularis thalami nucleus: synchronization among mutually inhibitory neurons. *Neuroscience* **53**: 899–904.

Wang, X. J., Tegnér, J., Constantinidis, C. and Goldman-Rakic, P. S. (2004) Division of labor among distinct subtypes of inhibitory neurons in a cortical microcircuit of working memory. *Proceedings of the National Academy of Sciences USA* **101**: 1368–73.

Wang, Z. and McCormick, D. A. (1993) Control of firing mode of corticotectal and corticopontine layer V burst-generating neurons by norepinephrine, acetylcholine and 1*S*, 3*R*-ACPD. *Journal of Neuroscience* **13**: 2199–216.

Warburton, E. C., Koder, T., Cho, K. *et al.* (2003) Cholinergic neurotransmission is essential for perirhinal cortical. *Neuron* **38**: 987–96.

Washburn, M. S. and Moises, H. C. (1992a) Electrophysiological and morphological properties of rat basolateral amygdaloid neurons in vitro. *Journal of Neuroscience* **12**: 4066–79.

Washburn, M. S. and Moises, H. C. (1992b) Inhibitory responses of rat basolateral amygdaloid neurons recorded in vitro. *Neuroscience* **50**: 811–30.

Washburn, M. S. and Moises, H. C. (1992c) Muscarinic responses of rat basolateral amygdaloid neurons recorded in vitro. *Journal of Physiology (London)* **449**: 121–54.

Watanabe, T., Taguchi, Y., Shiosaka, S. *et al.* (1984) Distribution of the histaminergic neuron system in the central nervous system of rats; a fluorescent immunohistochemical analysis with histidine decarboxylase as a marker. *Brain Research* **295**: 13–25.

Webster, H. H. and Jones, B. E. (1988) Neurotoxic lesions of the dorsolateral pontomesencephalic tegmentum cholinergic area in the cat. II. Effects upon sleep-waking states. *Brain Research* **458**: 285–302.

Weese, G. D., Phillips, J. M. and Brown, V. J. (1999) Attentional orienting is impaired by unilateral lesions of the thalamic reticular nucleus in the rat. *Journal of Neuroscience* **19**: 10135–9.

Weisskopf, M. G., Bauer, E. P. and LeDoux, J. E. (1999) L-type voltage-gated calcium channels mediate NMDA-independent associative long-term potentiation at thalamic input synapses to the amygdala. *Journal of Neuroscience* **19**: 10512–19.

Weliky, M. and Katz, L. C. (1999) Correlational structure of spontaneous neuronal activity in the developing lateral geniculate nucleus in vivo. *Science* **285**: 599–604.

Westgaard, F. H., Bonato, P. and Holte, K. A. (2000) Low-frequency oscillations (<0.3 Hz) in the electromyographic (EMG) activity of the human trapezius muscle during sleep. *Journal of Neurophysiology* **88**: 1177–84.

Weyand, T. G., Boudreaux, M. and Guido, W. (2001) Burst and tonic response modes in thalamic neurons during sleep and wakefulness. *Journal of Neurophysiology* **85**: 1107–18.

Whalen, P. J., Rauch, S. L., Etcoff, N. L. *et al.* (1998) Masked presentations of emotional facial expressions modulate amygdala activity without explicit knowledge. *Journal of Neuroscience* **18**: 411–8.

White, E. L. (1989) *Cortical Circuits: Synaptic Organization of the Cerebral Cortex.* Boston, MA: Birkhäuser.

Wiedermann, U. A. and Lüthi, A. (2003) Timing of network synchronization by refractory mechanisms. *Journal of Neurophysiology* **90**: 3902–11.

Wilensky, A. E., Schafe, G. E. and LeDoux, J. E. (1999) Functional inactivation of the amygdala before but not after auditory fear conditioning prevents memory formation. *Journal of Neuroscience* **19**: RC48.

Wilensky, A. E., Schafe, G. E. and LeDoux, J. E. (2000) Functional inactivation of amygdala nuclei during acquisition of Pavlovian fear conditioning. *Society for Neuroscience Abstracts* **26**: 465.

Wilensky, A. E., Schafe, G. E. and LeDoux, J. E. (2001) Does the central nucleus of the amygdala contribute to the consolidation of auditory fear conditioning. *Society for Neuroscience Abstracts* **27**: 187.

Williams, J. A. and Reiner, P. B. (1993) Noradrenaline hyperpolarizes identified rat mesopontine cholinergic neurons *in vitro*. *Journal of Neuroscience* **13**: 3878–83.

Williams, J. A., Comisarow, J., Day, J., Fibiger, H. C. and Reiner, P. B. (1994) State-dependent release of acetylcholine in the rat thalamus measured by *in vivo* microdialysis. *Journal of Neuroscience* **14**: 5236–42.

Williams, J. T., North, R. A., Shefner, S. A., Nishi, S. and Egan, T. M. (1984) Membrane properties of rat locus coeruleus neurones. *Neuroscience* **13**: 137–56.

Williams, S. M. and Goldman-Rakic, P. S. (1998) Widespread origin of the primate mesofrontal dopamine system. *Cerebral Cortex* **8**: 321–45.

Williams, S. R., Toth, T. I., Turner, J. P., Hughes, S. W. and Crunelli, V. (1997) The 'window' component of the low threshold Ca^{2+} current produces

input signal amplification and bistability in cat and rat thalamocortical neurones. *Journal of Physiology (London)* **505**: 689–705.

Wilson, C. J. (1987) Morphology and synaptic connections of crossed corticostriatal neurons in the rat. *Journal of Comparative Neurology* **263**: 567–80.

Wilson, C. J. and Kawaguchi, Y. (1996) The origin of two-state spontaneous membrane potential fluctuations of neostriatal spiny neurons. *Journal of Neuroscience* **16**: 2397–410.

Wilson, F. A. and Rolls, E. T. (1990) Learning and memory is reflected in the response of reinforcement-related neurons in the primate basal forebrain. *Journal of Neuroscience* **10**: 1254–67.

Wilson, M. A. and McNaughton, B. L. (1994) Reactivation of hippocampal ensemble memories during sleep. *Science* **265**: 676–9.

Wilson, M. A., Mascagni, F. and McDonald, A. J. (2002) Sex differences in delta opioid receptor immunoreactivity in rat medial amygdala. *Neuroscience Letters* **328**: 160–4.

Witter, M. P. and Groenewegen, H. J. (1984) Laminar origin and septotemporal distribution of entorhinal and perirhinal projections to the hippocampus in the cat. *Journal of Comparative Neurology* **224**: 371–85.

Witter, M. P. and Groenewegen, H. J. (1986) Connections of the parahippocampal cortex in the cat. IV. Subcortical efferents. *Journal of Comparative Neurology* **251**: 51–77.

Witter, M. P., Room, P., Groenewegen, H. J. and Lohman, A. H.M. (1986) Connections of the parahippocampal cortex in the cat. V. Intrinsic connections: Comments on input/output connections with the hippocampus. *Journal of Comparative Neurology* **252**: 78–94.

Witter, M. P., Groenewegen, H. J., Lopes da Silva, F. H. and Lohman, A. H. M. (1989) Functional organization of the extrinsic and intrinsic circuitry of the parahippocampal region. *Progress in Neurobiology* **33**: 161–253.

Witter, M. P., Wouterlood, F. G., Naber, P. A. and Van Haeften, T. (2000) Anatomical organization of the parahippocampal-hippocampal network. *Annals of the New York Academy of Sciences* **911**: 1–24.

Woody, C. D., Gruen, E. and Wang, X. F. (2003) Electrical properties affecting discharges of units of the mid and posterolateral thalamus of conscious cats. *Neuroscience* **122**: 531–9.

Woolf, N. J., Eckenstein, F. and Butcher, L. L. (1984) Cholinergic systems in the rat brain: I. Projections to the limbic telencephalon. *Brain Research Bulletin* **13**: 751–84.

Woolf, N. J., Hernit, M. C. and Butcher, L. L. (1986) Cholinergic and non-cholinergic projections from the rat basal forebrain. *Neuroscience Letters* **66**: 281–6.

Wouterlood, F. G. (2002) Cell types, local connectivity, microcircuits, and distribution of markers. In *The Parahippocampal Region*, ed. M. P. Witter and F. G. Wouterlood, pp. 61–84. Oxford: Oxford University Press.

Wouterlood, F., Mugnaini, E. and Nederlof, J. (1985) Projection of olfactory lobe efferents to layer I GABA-ergic neurons in the entorhinal area. Combination of anterograde degeneration and immunoelectron microscopy in rat. *Brain Research* **343**: 283–96.

Wouterlood, F. G., Härtig, W., Brückner, G. and Witter, M. P. (1995) Parvalbumin-immunoreactive neurons in the entorhinal cortex of the rat: Localization, morphology, connectivity and ultrastructure. *Journal of Neurocytology* **24**: 135–53.

Wouterlood, F. G., Van, D. J., Van Haeften, T. and Witter, M. P. (2000) Calretinin in the entorhinal cortex of the rat: distribution, morphology, ultrastructure of neurons, and colocalization with gamma-aminobutyric acid and parvalbumin. *Journal of Comparative Neurology* **425**: 177–92.

Wu, J. Y., Guan, L. and Tsau, Y. (1999) Propagating activation during oscillations and evoked responses in neocortical slices. *Journal of Neuroscience* **19**: 5005–15.

Xiang, J. Z. and Brown, M. W. (1998) Differential neuronal encoding of novelty, familiarity and recency in regions of the anterior temporal lobe. *Neuropharmacology* **37**: 657–76.

Xiang, Z., Huguenard, J. R. and Prince, D. A. (1998) Cholinergic switching within neocortical inhibitory networks. *Science* **281**: 985–8.

Xu, L., Tripathy, A., Pasek, D. A. and Meissner, G. (1999) Ruthenium red modifies the cardiac and skeletal muscle Ca^{2+} release channels (ryanodine receptors) by multiple mechanisms. *Journal of Biological Chemistry* **274**: 32680–91.

Yajeya, J., Juan, A. D., Bajo, V. M. *et al.* (1999) Muscarinic activation of a non-selective cationic conductance in pyramidal neurons in rat basolateral amygdala. *Neuroscience* **88**: 159–67.

Yajeya, J., De La Fuente, A., Criado, J. M. *et al.* (2000) Muscarinic agonist carbachol depresses excitatory synaptic transmission in the rat basolateral amygdala in vitro. *Synapse* **38**: 151–60.

Yamada, T., Kameyama, S., Fuchigami, Y. *et al.* (1988) Changes of short latency somatosensory evoked potentials in sleep. *Electroencephalography and Clinical Neurophysiology* **70**: 126–36.

Yang, C. R., Seamans, J. K. and Gorelova, N. (1996) Electrophysiological and morphological properties of layers V–VI principal pyramidal cells in rat prefrontal cortex *in vitro*. *Journal of Neuroscience* **16**: 1904–21.

Yen, C. T., Conley, M., Hendry, S. H.C. and Jones, E. G. (1985) The morphology of physiologically identified GABAergic neurons in the somatic sensory part of the thalamic reticular nucleus in the cat. *Journal of Neuroscience* **5**: 2254–68.

Yingling, C. D. and Skinner, J. E. (1977) Gating of thalamic input to cerebral cortex by nucleus reticularis thalami. In *Attention, Voluntary Contraction and Event-Related Cerebral Potentials*, ed. J. Desmedt, pp. 534–59. Basel: Karger.

Ylinen, A., Bragin, A., Nádasdy, Z. *et al.* (1995) Sharp wave-associated high-frequency oscillation (200 Hz) in the intact hippocampus: network and intracellular mechanisms. *Journal of Neuroscience* **15**: 30–46.

Young, M. P., Tanaka, K. and Yamane, S. (1992) On oscillating neuronal responses in the visual cortex of the monkey. *Journal of Neurophysiology* **67**: 1464–74.

Yu, Y. Q., Xiong, Y., Chan, Y. S. and He, J. (2004) Corticofugal gating of auditory information in the thalamus: an in vivo intracellular recording study. *Journal of Neuroscience* **24**: 3060–9.

Yuste, R. and Tank, D. W. (1996) Dendritic integration in mammalian neurons, a century after Cajal. *Neuron* **16**: 701–16.

Zhang, L. and Jones, E. G. (2004) Corticothalamic inhibition in the thalamic reticular nucleus. *Journal of Neurophysiology* **91**: 759–66.

Zhang, S. J., Huguenard, J. R. and Prince, D. A. (1997) $GABA_A$ receptor-mediated Cl^- currents in rat thalamic reticular and relay neurons. *Journal of Neurophysiology* **78**: 2280–6.

Zhu, J. J. and Heggelund, P. (2001) Muscarinic regulation of dendritic and axonal outputs of rat thalamic interneurons: a new cellular mechanism for uncoupling distal dendrites. *Journal of Neuroscience* **21**: 1148–59.

Zhu, J. J. and Lo, F. S. (1999) Three GABA receptor-mediated postsynaptic potentials in interneurons in the rat lateral geniculate nucleus. *Journal of Neuroscience* **19**: 5721–30.

Zhu, J. J. and Uhlrich, D. J. (1998) Cellular mechanisms underlying two muscarinic receptor-mediated depolarizing responses in relay cells of the rat lateral geniculate nucleus. *Neuroscience* **87**: 767–81.

Zhu J. J., Lytton W. W., Xue, J. T. and Uhlrich D. J. (1999a) An intrinsic oscillation in interneurons of the rat lateral geniculate nucleus. *Journal of Neurophysiology* **81**: 702–11.

Zhu, J. J., Uhlrich, D. J. and Lytton, W. W. (1999b) Burst firing in identified rat geniculate interneurons. *Neuroscience* **91**: 1445–60.

Zhu, J. J., Uhlrich, D. J. and Lytton, W. W. (1999c) Properties of a hyperpolarization-activated cation current in interneurons in the rat lateral geniculate nucleus. *Neuroscience* **92**: 445–57.

Ziakopoulos, Z., Tillett, C. W., Brown, M. W. and Bashir, Z. I. (1999) Input- and layer-dependent synaptic plasticity in the rat perirhinal cortex in vitro. *Neuroscience* **92**: 459–72.

Zola-Morgan, S., Squire, L. R., Amaral, D. G. and Suzuki, W. A. (1989) Lesions of perirhinal and parahippocampal cortex that spare the amygdala and hippocampal formation produce severe memory impairment. *Journal of Neuroscience* **9**: 4355–70.

Index

References to endnotes are indicated thus: 201 n.15